

To update your non-proprietary copy of the SSES DAR, remove and insert the following pages, figures and tables.

REMOVE

INSERT

VOLUME 1

Table 1-3 (Page 1)
Table 1-3 (Page 2)
Table 1-4 (Page 1)
Table 1-4 (Page 4)
Table 1-4 (Page 5)
Table 1-4 (Page 8)
Table 1-4 (Page 12)
Table 1-4 (Page 17)
Table 1-4 (Page 20)
Pages 2-5/2-6
Page 2-7
Page 4-3/4-4
Page 4-5/4-6
Page 4-7/4-8
Page 4-9/4-10
Page 4-11/4-12
Page 4-13/4-14
Page 4-15/4-16
Page 4-17/4-18
Page 4-19/4-20
Page 4-21/4-22
Page 4-23
....
Figure 4-44a
Figure 4-45
Figure 4-53
Figure 4-54

New Table 1-3 (Page 1)
New Table 1-3 (Page 2)
New Table 1-4 (Page 1)
New Table 1-4 (Page 4)
New Table 1-4 (Page 5)
New Table 1-4 (Page 8)
New Table 1-4 (Page 12)
New Table 1-4 (Page 17)
New Table 1-4 (Page 20)
New Page 2-5/2-6
New Page 2-7
New Page 4-3/4-4
New Page 4-5/4-6
New Page 4-7/4-8
New Page 4-9/4-10
New Page 4-11/4-12
New Page 4-13/4-14
New Page 4-15/4-16
New Page 4-17/4-18
New Page 4-19/4-20
New Page 4-21/4-22
New Page 4-23
New Page 4-24
New Figure 4-44a
New Figure 4-45
New Figure 4-53
New Figure 4-54

REMOVE

Figure 4-62 A&B
 Figure 4-62 C&D
 Figure 4-62 E&F

 Page 5-1/5-2
 Page 5-3/5-4
 Page 5-11/5-12
 Page 5-13/5-14
 Table 5-4

 Page 6-7/6-8
 Page 6-9/6-10
 Pages 7-1 to 7-27
 Figures 7-4 to 7-11
 Tables 7-1 to 7-3
 Page 10-1 to 10-15
 Figure 10-1
 Figure 10-2

 Pages 11-5/11-6
 Pages A-1/A-2
 Pages A-3/A-4

 Figures A-4 to A-66
 Pages B-1/B-2
 Pages B-3/B-4

INSERT

New Figure 4-62 A&B
 New Figure 4-62 C&D
 New Figure 4-62 E&F
 New Figure 4-62 I
 New Figure 4-62 J
 New Figure 4-62 K
 New Figure 4-62 m
 New Table 4-22
 New Page 5-1/5-2
 New Page 5-3/5-4
 New Page 5-11/5-12
 New Page 5-13/5-14
 New Table 5-4
 New Table 5-5 (2 pages)
 New Table 5-6
 New Page 6-7/6-8
 New Page 6-9/6-10
 New Pages 7-1 to 7-47
 New Figures 7-4 to 7-26
 New Tables 7-1 to 7-5
 New Pages 10-1 to 10-36
 New Figure 10-1
 New Figure 10-2
 New Figures 10-4 to 10-65
 New Table 10-1
 New Table 10-2
 New Pages 11-5/11-6
 New Pages A-1/A-2
 New Pages A-3/A-4
 New Page A-5
 New Figures A-4 to A-67
 New Pages B-1/B-2
 New Pages B-3/B-4

REMOVE

Page B-5
 Figures B-27 to B-88
 Pages C-1/C-2
 Page C-3
 Figures C-4 to C-10
 Figure E-9
 Figure E-11
 Figures E-12 to E-16
 Figures E-22 to E-38
 Appendix F Tab
 Page F-1

 Page G-1
 Page H-1
 Pages I-1/I-2
 Pages I-5/I-6

 Pages I-9/I-10

 Table I.1 (Page 2)
 Table I.2

INSERT

.....
 New Figures B-27 to B-58
 New Pages C-1/C-2
 New Page C-3
 New Figures C-4 to C-103
 New Figure E-9
 New Figure E-11
 New Figures E-12 to E-16
 New Figures E-21a to E-38a
 New Appendix F Tab
 New Page F-1
 New Table F-1 (2 sheets)
 New Page G-1
 New Page H-1
 New Pages I-1/I-2
 New Page I-5/I-6
 New Pages I-6a/I-6b
 New Page I-9/I-10
 New Figures I-14
 New Figures I-15
 New Table I.1 (Page 2)
 New Table I.2

Remove Appendices A thru I from Volume I and insert into Volume 2.

SSS CONTAINMENT DESIGN PARAMETERS

A. <u>Drywell and Suppression Chamber</u>		<u>Drywell</u>	<u>Suppression Chamber</u>
1.(a)	Internal Design Pressure	53 psig	53 psig
1.(b)	Internal Design Pressure in Combination with other Loads	44 psig	29 psig
2.	External Design Pressure	5 psid	5 psid
3.	Drywell Floor Design Differential Pressure Upward		28 psid
	Downward		28 psid
4.	Design Temperature	340°F	220°F
5.	Drywell Free Volume (Minimum) (including vents) (Normal) (Maximum)	239,337 ft ³ 239,593 ft ³ 239,850 ft ³	
6.	Suppression Chamber Free (Minimum) Volume (Normal) (Maximum)		148,590 ft ³ 153,860 ft ³ 159,130 ft ³
7.	Suppression Chamber Water Volume (Minimum) (Normal) (Maximum)		122,410 ft ³ 126,980 ft ³ 131,550 ft ³
8.	Pool Cross-Section Area Gross (Outside Pedestal) Total Gross (Including Pedestal Water Area) Free (Outside Pedestal) Total Free		5379 ft ² 5679 ft ² 5065 ft ² 5277 ft ²

Table 1-3 (Cont'd)

	<u>Drywell</u>	<u>Suppression Chamber</u>
9. Pool Depth	(Minimum)	22 ft.
	(Normal)	23 ft.
	(Maximum)	24 ft.
B. <u>Vent System</u>		
1. Number of Downcomers		82 (Five capped: see Appendix K) 6
2. Downcomer Outer Diameter		2 ft.
3. Total Downcomer Vent Area		257 ft. ²
4. Downcomer Submergence	(Minimum)	10 ft.
	(Normal)	11 ft.
	(Maximum)	12 ft.
5. Downcomer Loss Factor		2.5
C. <u>Safety Relief Valves</u>		
1. Opening Time		
a. Delay Time (between trip and motion)		0.10 sec.
b. Response Time (close to open)		0.15 sec.

TABLE 1-4

- Review of Susquehanna SES Units 1 & 2 Pool Dynamic Loadings -

-Comparison with NUREG 0487, NUREG 0487-Supplement No. 1, Lead Plant and Generic Long Term Program-

NRC Acceptance Criteria		Lead Plant Position	Generic Long Term	Susquehanna Position	Remarks
NUREG 0487		Supplement No. 1	(Zimmer DAR, Amendment 13)		
I. LOCA RELATED HYDRODYNAMIC LOADS					
A. Submerged Boundary Loads During Vent Clearing. 33 psi overpressure added to local hydrostatic below vent exit (walls and basemat)-linear attenuation to pool surface.	24 PSI overpressure statically applied with hydrostatic pressure to surfaces below vent exit (attenuate to 0 psi at pool surface) for period of vent clearing for plants with (mhL)/ [$(A/A_v) V_{DW}$] ≤ 55. where: \dot{m} = mass flow in vents $\frac{1}{3}$ lb/sec V_{DW} = drywell volume - ft ³ h = enthalpy of air in vent - Btu/lb L = submergence - ft A/A_v = pool area to vent area For plants where (mhL)/[(A/A_v) V_{DW}] > 55, the loading increase over hydrostatic pressure on basemat and submerged walls below vent exit is $p = 24 + 0.27 (mhL) / [(A/A_v) V_{DW}] - 55$ (attenuate to 0 psi at pool surface).	March 20, 1979 letter. 24 psi statically applied to surfaces below vent exit (attenuate to 0 psi at pool surface) for period of vent clearing. Zimmer and LaSalle meet NUREG 0487.	Evaluating impact.	Evaluation indicates 24 PSI overpressure is conservative (see Subsection 4.2.1.2)	
B. Pool Swell Loads.					
1. Pool Swell Analytical Model (PSAM)					
a. Air bubble pressure-use PSAM described in NEDE-21544-P.	(a) No change from NUREG 0487.	(a) Accept NUREG 0487.	(a) Accept NUREG 0487.	(a) Accept NUREG 0487.	
b. Pool swell elevation-Use PSAM described in NEDE-21544-P.	(b) Use PSAM with polytropic exponent of 1.2 to a maximum swell height	(b) Accept NUREG 0487.	(b) Accept NUREG 0487 -Supplement No. 1	(b) Accept NUREG 0487 -Supplement No. 1	

TABLE 1-4

NRC Acceptance Criteria		Lead Plant Position	Generic Long Term	Susquehanna Position	Remarks
NUREG 0487	Supplement No. 1	(Zimmer DAR, Amendment 13)	Program Position		
<p>2, and the total area of the grating. To account for the dynamic nature of the initial loading, the static drag load is increased by a multiplier given by:</p> $F_{SD}/D = 1 + 1 + (0.064Wf)^2$ <p>for $Wf < 2000$ in/sec</p>					
4. Wetwell Air Compression					
a. Wall loads-directly apply the PSAM calculated pressure due to wetwell compression.	(a) No change from NUREG 0487.	(a) Accept 0487.	(a) Accept NUREG 0487.	(a) Accept NUREG 0487.	5
b. Diaphragm upward load-calculate Δ PUP using the correlation: Δ PUP = 8.2 - 44F, for $0 < F \leq 0.13$ Δ PUP = 2.5 psi, for $F > 0.13$ where: $F = \frac{AB \cdot AP \cdot VS}{VD (AV)^2}$	(b) No change from NUREG 0487.	(b) Use Δ PUP = 5.5 PSID.	(b) Same as lead plant.	(b) Same as lead plant.	6
<p>AB = break area AP = net pool area AV = total vent area</p>					

TABLE 1-4

NRC Acceptance Criteria NUREG 0487 Supplement No. 1		Lead Plant Position (Zimmer DAR, Amendment 13)	Generic Long Term Program Position	Susquehanna Position	Remarks
VS = initial wetwell air space volume VD = drywell volume					
5. Asymmetric Load. Apply the maximum air bubble pressure calculated from PSAM and a minimum air bubble pressure (zero increase) in a worst case distribution to the wetwell wall.	Use twice the 10% of maximum bubble pressure statically applied to 1/2 of the submerged boundary (with hydrostatic pressure) proposed in March 16, 1979 letter from GE.	Accept NUREG 0487-Supplement No. 1.	Accept NUREG 0487-Supplement No. 1	Accept NUREG 4087-Supplement No. 1.	5
C. Steam Condensation and Chugging Loads.					
1. Downcomer Lateral Loads.					
a. Single vent loads: (a) No change from NUREG 0487. -A static equivalent load of 8.8 KIPs shall be used provided:	(a) Accept NUREG 0487.	(a) Use single vent dynamic lateral load developed under Task A-13 (NEDE-24106-P). However, extrapolate the 30 Kip and 3 msec impulse to 65 Kips and 3 msec.	(a) Following long term program. Confirmation through plant unique GKM-IIM test data on lateral bracing loads.	See DAR, Subsection 9.6.3 for verification of lateral tip load.	6
(i) the downcomer is 24" in diameter.					
(ii) the downcomer dominant natural frequency is < 7 Hz, submerged.					
(iii) the downcomer is unbraced or braced at or above approx. 8' from the exit.					

TABLE 1-4

NRC Acceptance Criteria NUREG 0487 Supplement No. 1		Lead Plant Position (Zimmer DAR, Amendment 13)	Generic Long Term Program Position	Susquehanna Position	Remarks
b. Medium Steam Flux Loads.	(b) No change from NUREG 0487.	(b) Accept NUREG 0487 with additional plant unique empirical load specification.	(b) Use Condensation Oscillation load specification based on NEDE-24288-P.	(b) Same as (a).	
Sinusoidal pressure fluctuation added to local hydrostatic. Amplitude uniform below vent exit, linear attenuation to pool surface. 7.5 psi peak-to-peak amplitude. 2-7 Hz frequencies. NEDE-21061-P, Rev. 2					
c. Chugging.	(c) No change from NUREG 0487.	(c) Accept NUREG 0487 with additional plant unique empirical load specification.	(c) Use IWECS/MARS acoustic model presented in NEDE-24822-P with sources derived from 4T-C0. Application methodology documented in NEDE-24302-P.	(c) Same as (a).	
-Uniform loading condition - Maximum amplitude uniform below vent exit, linear attenuation to pool surface. +4.8 psi max overpressure, -4.0 psi max underpressure. (Pending resolution of FSI concerns) NEDE-21061-P, Rev. 2.					
-Asymmetric loading condition - Maxi-					

TABLE 1-4

NRC Acceptance Criteria NUREG 0487 Supplement No. 1		Lead Plant Position (Zimmer DAR, Amendment 13)	Generic Long Term Program Position	Susquehanna Position	Remarks
c. Bubble Frequency. (c) 3-11 Hz. T-quencher - a range of bubble frequency of 4-12 Hz is the minimum range that shall be increased if required to include the frequency predicted by the ram-head methodology together with $\pm 50\%$ margin. X-quencher - a range of bubble frequency of 4-12 Hz shall be evaluated.		(c) Plant unique frequency range based on Susquehanna DAR.	(c) Same as lead plant.	(c) Following frequency range documented in Susquehanna DAR.	Additional study performed confirming conservatism of frequency range in Susquehanna DAR (see Subsection 10.2.3).
			X-quencher bubble frequency being developed by Burns & Roe based largely on Caorso test data.		
c. Quencher Arm and Tie Down Loads.					
1. Quencher Arm Loads. Vertical and lateral arm loads are to be developed on the basis of bounding assumptions for air/water discharge from the quencher and conservative combinations of maximum/minimum bubble pressures acting on the quencher per NEDE-21061-P, Rev. 2.	No change from NUREG 0487.	Accept NUREG 0487. Load Specification in SSES DAR Subsection 4.1.2.5 used to verify the conservatism of this approach.	T-quencher arm loads are presented in Susquehanna DAR, Section 4.1.2.5. X-quencher-Accept NUREG 0487.	Following long term program.	

6

5

TABLE 1-4

NRC Acceptance Criteria NUREG 0487 Supplement No. 1		Lead Plant Position (Zimmer DAR, Amendment 13)	Generic Long Term Program Position	Susquehanna Position	Remarks
1. LOCA Air Bubble Loads No change from NUREG 0487.		Documented in plant unique DAR's.	Documented in plant unique DAR's.	Documented in Subsection 4.2.1.7 of SSES DAR.	6
<p>Calculate based on the analytical model of the bubble charging process and drag calculations of NEDE-21471 until the bubbles coalesce. After bubble contact, the pool swell analytical model, together with the drag computation procedure NEDE-21471 shall be used. Use of this methodology shall be subject to the following constraints and modifications:</p> <p>a. A conservative estimate of bubble asymmetry shall be added by increasing accelerations and velocities computed in step 12 of Section 2.2 of NEDE-21730 by 10%. If the alternate steps 5A, 12A and 13A are used the acceleration drag shall be directly</p>		(a) Position documented on page 5.4-8 of Zimmer DAR.	(a) Accept NUREG-0487.	(a) Following the Long Term Program.	5

TABLE 1-4

NRC Acceptance Criteria NUREG 0487 Supplement No. 1		Lead Plant Position (Zimmer DAR, Amendment 13)	Generic Long Term Program Position	Susquehanna Position	Remarks
2. a. SRV ramshead air bubble loads.	(a) No change since NUREG 0487.	(a) Documented on Page 5.4-9 of Zimmer DAR.	(a) N/A	(a) N/A	5
	b. SRV quencher air bubble loads. T-quencher - loads may be computed on the basis of the above ramshead bubble pressure and assuming the bubble to be located at the center of the quencher device having a bubble radius equal to the quencher radius.	(b) Documented on Page 5.4-9 of Zimmer DAR.	(b) T-quencher sub-merged structure methodology is presented in Susquehanna DAR, Section 4.1.3.	(b) Following Long Term Program	
X-quencher - loads may be computed on the basis of the above ramshead methodology using bubble pressure calculated by the methods of NEDE-21061-P, Rev. 2 for the X-quencher.			X-quencher methodology being developed by Burns & Roe.		
C. Steam Condensation Drag Loads.					
Review will be conducted on a plant unique basis.		Documented on Page 5.4-9 of Zimmer DAR.	Plant unique method being developed.	Plant unique methodology documented in DAR Subsection 4.2.2.5.	6

PAF:cvc
34P-B

2.2 DESIGN ASSESSMENT SUMMARY

Design assessment of the SSES structures and components is achieved by analyzing the response of the structures and components to the load combinations explained in Chapter 5. In Chapter 7 predicted stresses and responses (from the loads defined in Chapter 4 and combined as described in Chapter 5) are compared with the applicable code allowable values identified in Chapter 6 and the SSES design will be assessed as adequate by virtue that the design capabilities exceed the stresses or responses resulting from SRV discharge and/or LOCA loads.

2.2.1 Containment Structure and Reactor Building Assessment Summary

2.2.1.1 Containment Structure Assessment Summary

The primary containment walls, base slab, diaphragm slab, reactor pedestal and reactor shield are analyzed for the effects of SRV and LOCA in accordance with Table 5-1. The ANSYS finite element program is used for the dynamic analysis of structures.

Response spectra curves are developed at various locations within the containment structure to assess the adequacy of components. Stress resultants due to dynamic loads are combined with other loads in accordance with Table 5-1 to evaluate rebar and concrete stresses. Design safety margins are defined by comparing the actual concrete and rebar stresses at critical sections with the code allowable values. The assessment methodology of the containment structure is presented in Subsection 7.1.1.1.

The results of the structural assessment of the containment structure are summarized in Appendix A. The results show that the reinforcing bar design stresses and the concrete design stresses are below the allowable stresses.

2.2.1.2 Reactor Building Assessment Summary

The reactor building is assessed for the effects of SRV and LOCA loads in accordance with Table 5-1.

Containment basemat acceleration time histories are used to investigate the reactor building response to the SRV and LOCA loads. Response spectra curves at various reactor building elevations are used to assess the adequacy of components in the reactor building. The assessment methodology of the reactor building is presented in Subsection 7.1.1.2.

The results of the structural assessment of the reactor building are summarized in Appendix E. The results show that the reinforcing bars and concrete design stresses as well as the structural steel design stresses are below the allowable stresses.

2.2.2 Containment Submerged Structures Assessment Summary

Design assessment of the suppression chamber columns includes non-hydrodynamic as well as hydrodynamic loads. Subsection 7.1.2.2 describes the methodology used to evaluate the columns. The results are presented in Figure A-59 and indicate a minimum design margin of 11.4%.

6 The downcomers are dynamically analyzed per Subsection 7.1.4 for the load combinations given in Table 5-3. A summary of the stresses under various load combinations are given in Figure A-66 and indicates that the minimum design margin is 14% when the loads are combined by ABS and 50% when the loads are combined by SRSS.

2 Results from the analysis of the suppression pool liner plate indicate that no structural modifications are required (see Subsection 7.1.3 and 7.2.1.5).

The original downcomer and SRV bracing system has been redesigned so that the downcomers and SRV discharge lines are now supported by separate bracing systems. The SRV discharge lines are supported by bracing connected to the columns, while the downcomers are braced together by a truss system, but no connections exist at the containment or pedestal wall. Subsections 7.1.2.1 and 7.1.2.2 document the evaluation of the downcomer and SRV discharge line bracing systems, respectively.

Figure A-67 presents the SRV support system's maximum stresses and design margins, while Figures A-60 and A-61 show the design margins for the downcomer bracing system members and connections, respectively. All stresses are acceptable.

2.2.3 BOP and NSSS Piping System Assessment Summary

6 All Seismic Category I BOP and NSSS piping are analyzed for the LOCA and SRV hydrodynamic loads and non-hydrodynamic loads per Subsections 7.1.5 and 7.1.6.1.1, respectively. Appendix F gives the stresses and design margins for selected BOP piping systems.

The stress reports for the above evaluation are available for NRC review.

2.2.4 BOP and NSSS Equipment Assessment Summary

All Seismic Category I BOP and NSSS equipment are evaluated for the hydrodynamic and non-hydrodynamic loads per the SSES Seismic Qualification Review Team (SQRT) Program. For each equipment Purchase Order, 4-page SQRT summary forms are prepared documenting the qualification results.

These SQRT summary forms are available for NRC review.

2.2.5 Electrical Raceway System Assessment Summary

Seismic Category I electrical raceway systems in the containment, reactor systems and control building are assessed by the methods contained in Subsection 7.1.8. Loads are combined as shown in Table 5-6. As a result of static and dynamic analysis, it was determined that high stresses resulted in certain members of a few support types. These structural members were strengthened or replaced by stronger members to reduce the stresses below the allowables.

6

2.2.6 HVAC Duct System Assessment Summary

Seismic Category I HVAC duct system in the containment, reactor building and control building are assessed by the methods contained in Subsection 7.1.9. Loads are combined as shown in Table 5-2. As a result of structural analysis, it was found that a few structural members had high stresses but most of the members had adequate margin of safety. The overstressed members were strengthened or replaced by stronger members to ensure an adequate margin of safety.

CHAPTER 4

FIGURES

<u>Number</u>	<u>Title</u>	
4-1	These figures are proprietary and are found in the through proprietary supplement to this DAR.	
4-37		1
4-38	SSES Short Term Suppression Pool Height	
4-39	SSES Short Term Wetwell Pressure	
4-40	SSES Pool Surface Velocity vs Elevation	
4-40a	Poolswell Acceleration Time Histogram	
4-41	Pool Boundary Load During Vent Clearing	2
4-42	This Figure has been Deleted	
4-43	SSES Poolswell Air Bubble Pressure	
4-44	Poolswell Air Bubble Pressure on Suppression Pool Walls Used for SSES Analysis	1
4-44a	Condensation Pressure Forcing Function (Wet & Dry Wells) (This figure has been deleted)	6
4-45	Symmetric and Asymmetric Spatial Loading Specification (This figure has been deleted)	
4-46	SSES Drywell Pressure Response to DBA LOCA	
4-47	SSES Wetwell Pressure Response to DBA LOCA	
4-48	SSES Suppression Pool Temperature Response to DBA LOCA	1
4-49	SSES Drywell Temperature Response to DBA LOCA	
4-50	SSES Suppression Pool Temperature Response to IBA	
4-51	SSES Plant Unique Containment Response to the IBA	2
4-52	Typical Mark II Containment Response to the SBA	
4-53	SSES Components Affected by LOCA Loads	1
4-54	SSES Components Affected by LOCA Loads	

FIGURES (Cont.)

<u>Number</u>	<u>Title</u>
4-55	LOCA Loading History for the SSES Containment Wall and Pedestal
4-56	LOCA Loading History for the SSES Basemat and Liner Plate
1 4-57	LOCA Loading History for the SSES Drywell and Drywell Floor
4-58	LOCA Loading History for the SSES Columns
4-59	LOCA Loading History for the SSES Downcomers
4-60	LOCA Loading History for the SSES Downcomer Bracing System
4-61	LOCA Loading History for SSES Wetwell Piping
6 4-62, a-f	Chugging Pool Boundary Loads (These figures have been deleted)
2 4-62, g&h	Dynamic Downcomer Lateral Loads Due to Chugging
4-62, i-m	Typical Wave Motion Due to Seismic Slosh
6 4-63 thru 4-66	These Figures are Proprietary

CHAPTER 4

TABLES

Number

Title

4-1 thru 4-15	These tables are proprietary and are found in the proprietary supplement to this DAR	
4-16	LOCA Loads Associated with Poolswell	
4-17	SSES Drywell Pressure	2
4-18	SSES Plant Unique Poolswell Code Input Data	
4-19	Input Data for SSES LOCA Transients	
4-20	Component LOCA Load Chart for SSES	
4-21	Wetwell Piping LOCA Loading Situations	
4-22	Seismic SLOSH Wave Height	6

4.0 LOAD DEFINITION

4.1 SAFETY RELIEF VALVE (SRV) DISCHARGE LOAD DEFINITION

See the Proprietary Supplement for this section.

4.2 LOCA LOAD DEFINITION

Subsections 4.2.1, 4.2.2 and 4.2.3 discuss the numerical definition of loads resulting from a LOCA in the SSES containment. The LOCA loads are divided into five groups.

- (1) Short term LOCA loads associated with poolswell (Subsection 4.2.1).
- (2) Condensation oscillations and chugging loads (Subsection 4.2.2).
- (3) Submerged Structures Loads (Subsection 4.2.3)
- (4) Secondary Loads (Subsection 4.2.4).
- (5) Long term LOCA loads (Subsection 4.2.5).

The application of these loads to the various components and structures in the SSES containment is discussed in Subsection 4.2.6.

4.2.1 LOCA LOADS ASSOCIATED WITH POOLSWELL

A description of the LOCA/Poolswell transient is given in Section 3.2.3 of this Design Assessment Report. The LOCA loads associated with poolswell are listed in Table 4-16. A discussion of these loads and their SSES unique values follows.

4.2.1.1 Wetwell/Drywell Pressures during Poolswell

The drywell pressure transient used for the poolswell portion of the LOCA transient (≤ 2.0 sec) is given in Table IV-D-3 of Reference 7. A portion of this table is reproduced herein as Table 4-17. This drywell pressure transient includes the blowdown effects of pipe inventory and reactor subcooling and is the highest possible drywell pressure case for poolswell. This drywell pressure transient is calculated using the method documented in Reference 56.

The short term poolswell wetwell pressure transient resulting from this drywell pressure transient is calculated by applying the poolswell model contained in Reference 8. The equations and assumptions in the poolswell model were coded into a Bechtel computer program and verified against the Class 1, 2 and 3 test cases contained in Reference 9. This verification is documented in Appendix D to this report. Inputs used for the calculation of the SSES plant unique poolswell transient are shown in Table 4-18. The short term wetwell pressure transient calculated with the poolswell code is shown in Figure 4-39. The short term wetwell pressure peak is 56.1 psia (41.4 psig).

Reference 46, Subsection III.B.3.d.2 formulates a methodology for determining the maximum diaphragm uplift P to be used for design assessment. This ΔP is based on following relation:

$$\Delta PUP = 8.2 - 44 \cdot F \text{ (PSI)} \quad 0 < F \leq 0.13$$

$$\Delta PUP = 2.5 \text{ (PSI)} \quad F > 0.13$$

Rev. 2, 5/80

$$F = \frac{AB \cdot AP \cdot VS}{VD \cdot (AV)^2}$$

where: AB = break area;
 AP = net pool area;
 AV = total vent area
 VS = initial wetwell air space volume; and
 VD = drywell volume

For SSES (see Tables 4-18 and 4-19):

AB = 3.53 ft²
 AP = 5065.03 ft²
 AV = 257.52 ft²
 VS = 149,000 ft³
 VD = 239,600 ft³

2 Inserting into the above equation yields:

$$F = 0.168 > 0.13$$

This gives a maximum uplift ΔP of 2.5 PSID. However, as required by NUREG 0808, a more conservative uplift ΔP of 5.5 PSID will be used for design.

4.2.1.2 Submerged Boundary Loads During Vent Clearing

The submerged jet formed by the expulsion of the water leg in the downcomers creates a vent clearing load on the basemat and on the submerged wetwell walls. This loading is defined by Reference 57 as a 24 PSI overpressure statically applied with hydrostatic pressure to surfaces below vent exit with a linear attenuation to zero at pool surface (see Figure 4-41). This load is applied during the vent clearing.

The NRC, in Supplement No. 1 to NUREG-0487, accepts the above 24 PSI overpressure for the vent clearing load for those plants where

$$(\dot{m}hL) / [(A_P / A_V) V_{DW}] \leq 55$$

with: \dot{m} = mass flow in vents - lb/sec
 V_{DW} = drywell volume - ft³
 h = enthalpy of air in vents - btu/lb
 L = submergence - ft
 A_P / A_V = pool area to vent area ratio

6

For SSES, the various parameters are:

\dot{m} = 17,900 lb/sec
 V_{DW} = 239,850 ft³
 h = 194 btu/lb
 L = 12 ft
 A_P / A_V = 5065/257

Substituting into the above gives:

$$[(17,900) (194) (12) (257)] / [(5065) (239,850)] = 8.8$$

Thus, for SSES, the 24 PSI overpressure specified for the air clearing load is acceptable.

6

4.2.1.3 LOCA Jet Loads

During the vent clearing stage induced velocity and acceleration fields are created in the suppression pool producing drag forces on submerged structures. The original methodology employed to predict the drag forces is contained in Reference 12 (often called the Moody jet model) and is an analytical representation of an unsteady water jet discharging into a suppression pool. The jet is made up of constant velocity fluid particles traveling at the speed at which they exited the discharge pipe. The jet front is described as the locus of points which a particle overtakes the one exiting immediately before it. No velocities or accelerations are defined in the fluid external to the jet.

Reference 46, subsection III.D.1.a proposed that velocity and acceleration be predicted throughout the pool using the potential function of a sphere at the jet front. A modification of the load calculated at jet impingement was also required. The Acceptance Criteria was a simple method to determine a bounding jet load for all structures below the downcomer exits.

The Moody jet model was clearly derived for jets with constant or linearly increasing acceleration. However, the vent clearing transients predicted for Mark II plants typically have an acceleration increase greater than linear. Strict application of Reference 12 leads to unrealistic mathematical results. Two interpretations of the results are possible depending upon the time base employed. Examining the jet in "real time" (t in Reference 12) a jet can be seen with two independent fronts traveling at different speeds at different locations which coincide only at the point of jet dissipation. On the other hand, if we use the "exit time" (τ) as a basis the jet reverses and moves backward in both space and "real time" before dissipation. Clearly neither of these observations is of much use in calculating loads on structures.

2

To overcome the difficulties of using this model, an alternative methodology has been formulated. The jet front will be described by the motion of the particle having travelled the farthest at any instant in time. This will be identical to the Moody jet motion for jets with linearly increasing acceleration but will yield a single continuous velocity and acceleration time history even if the acceleration increases more rapidly.

A sphere is then placed at the jet front generating a potential flow described by the following function:

$$\phi = \frac{-3}{8\pi} U_j V \frac{\cos\theta}{r^2}$$

where r and θ are the spherical coordinates from the sphere center to some position in the suppression pool with θ measured

from the jet direction, U_1 is the velocity of the sphere determined by the velocity of the particle having traveled the farthest at the instant in time the drag forces are being computed and V_w is the initial volume of water in the vent.

The local velocity U_∞ , and acceleration, \dot{U}_∞ are then calculated from the above relation by the methods of Reference 14. Once the local velocity and acceleration are known the drag forces are computed from Reference 13 as follows:

$$F_A = \frac{\dot{U}_\infty V \rho}{g_c}$$

$$F_S = \frac{C_D A_x U_\infty^2 \rho}{2g_c}$$

where F_A is the acceleration drag, \dot{U}_∞ is the local acceleration field normal to the structure, V is the acceleration drag volume for flow normal to the structure, ρ is the fluid density, F_S is the standard drag, C_D is the drag coefficient for flow normal to the structure, A_x is the projected structure area normal to U_∞ , and U_∞ is the local velocity field normal to the structure.

When the jet is predicted to dissipate the sphere is traveling at the final jet velocity at the point of maximum jet penetration. This condition is used as the final load calculation point. The final jet velocity is that of the jet front just before the last particle leaving the vent reaches the jet front. The velocity of the last particle is disregarded.

4.2.1.4 Boundary Loads During Poolswell

During the poolswell transient, the high pressure air bubble which forms in the vicinity of the vent exit creates an increase in pressure on all suppression pool boundaries below the vent exit as well as those walls which it is in direct contact. Boundaries which are above the bubble location and up to the point of maximum pool elevation also experience increased pressure loads corresponding to the increased pressure in the wetwell airspace as well as the hydrostatic contribution of the water slug.

Reference 46, Subsection III.B.3.b methodology for specification of these loads uses the Poolswell Analytical Model to determine the maximum values of bubble pressure and wetwell airspace pressure. The analysis takes the maximum pool elevation as 1.5 times the initial submergence. Using this data, a static loading is applied to the containment structure as follows:

1. for the basemat - uniform pressure equal to the maximum bubble pressure superimposed on the hydrostatic load corresponding to a submergence from vent exit to the basemat;

2. for the containment walls below vent exit - maximum bubble pressure plus hydrostatic head corresponding to vertical distance from vent exit;
3. for the containment walls between vent exit and maximum pool elevation-linear variation between maximum bubble pressure and maximum wetwell airspace pressure;
4. for the containment walls above maximum pool elevation - maximum wetwell airspace pressure.

The pressure distribution used for the SSES analysis is shown in Figure 4-44.

4.2.1.5 Poolswell Asymmetric Air Bubble Load

The methodology used in the proceeding subsection assumes that the air flow rate in each downcomer is equal leading to a symmetric loading of the containment boundary. Reference 46 has expressed concern that circumferential variations in the downcomer air flow rate can occur due to drywell air/steam mixture variation that would result in variations in the bubble pressure load on the wetwell wall.

This loading condition is calculated by statically applying the maximum air bubble pressure obtained from the PSAM to 1/2 of the submerged boundary and statically applying 120% of the maximum bubble pressure to the other 1/2 of the submerged boundary. The pressure load on the basemat and wetwell walls below the vent exit is the sum of the air pressure and the hydrostatic pressure. For the portion of the wall above the vent exit, the pressure increase due to the air bubble is linearly attenuated from the bubble pressure at the vent exit to zero at the pool surface. This increase is then added to the local hydrostatic pressure to obtain the total pressure. The time period of application of the load is from the termination of vent clearing until the maximum swell height is reached.

4.2.1.6 Poolswell Impact Load

Any structure located between the initial suppression pool surface (El. 672') and the peak poolswell height (El. 690'-2", see Figure 4-38) is subject to the pool swell impact load. As documented in the response to NRC Question 020.68, the poolswell maximum elevation is determined by the poolswell Analytical Model with a polytropic exponent of 1.2 for wetwell air compression to a maximum swell height which is the greater of 1.5 vent submergence or the elevation corresponding to the drywell floor uplift ΔP determined from the equation documented in Subsection 4.2.1.1 (2.5 PSID). For SSES, using the design drywell floor uplift $\Delta P=2.5$ PSID leads to the greatest poolswell height and yields 1.51 times the initial vent submergence. Since all grating is removable only "small" structures as defined in Reference 10a, Subsection 4.2.5.1 are subject to poolswell impact loads.

Poolswell impact loads of "small" structures are determined as specified in Reference 46, Subsection III.B.3.c.1. An SSES plant-unique velocity vs. elevation curve has been generated with the poolswell model (see Figure 4-40). The velocity curve is conservatively increased by a 1.1 multiplier and used to calculate the impulse per unit area, pulse duration and maximum impact pressure at the component's elevation. The peak pressure is then used to define a versed sine shaped hydrodynamic loading function

$$P(t) = \frac{P_{\max}}{2} (1 - \cos 2\pi t / \tau)$$

where: P = pressure acting on the projected area of the structure;
 P_{\max} = the temporal maximum of pressure acting
on the projected area of the structure;

t = time;

τ = duration of impact

The loading function corresponds to impact on rigid structures. In actuality, the structures being analyzed may be more flexible, resulting in the pressure pulses, during impact, being modified by the motion of the structure. To account for this, the hydrodynamic mass of impact is added to the mass of the impacted structure when performing the structural dynamic analysis.

4.2.1.7 LOCA Air Bubble Submerged Structure Load

During the drywell air purge phase of a LOCA, an expanding bubble is created at the downcomer exits. These rapidly expanding bubbles eventually coalesce into a "blanket" of air which leads to the pool swell phenomena. The bubble charging process creates fluid motion in the suppression pool which causes drag loads on the submerged structures.

The submerged structure drag loads due to air clearing, prior to pool swell, are calculated in the same manner as the drag loads due to CO and chugging presented in Subsection 4.2.2.5. However, the chugging and CO sources are replaced with a source representing the bubble growth prior to pool swell. This source is derived from the original 4T data. All sources are assumed in-phase (87 sources).

4.2.1.8 Poolswell Drag Load

Subsequent to bubble contact all bubbles are assumed to coalesce into a blanket of air and the poolswell drag loads are due the rapidly accelerating upward slug of water and acts in the vertical direction only (except for lift forces which act in the traverse direction to flow). The one dimensional pool swell model is used to predict the vertical flow field. Once the flow field is known the drag forces are calculated by the methods of Reference 13 modified by the methodology presented in Subsection

4.2.3. This load applies to any structure located between the elevation of the vent exit and the peak poolswell height. The duration of the drag load begins when the vent clears except for structures which are originally not submerged. For structures which are not submerged, the drag load duration is based on the slug transient time (Reference 10a, page 4-78, step 3).

4.2.1.9 Poolswell Fallback Load

After the termination of poolswell the slug of water falls under the influence of gravity causing drag forces on structures located between the peak poolswell height and the vent exit. The motion of the water is described by the following equations:

$$H(t) = H_{\max} - gt^2/2$$

$$V_{FB}(t) = gt$$

$$\dot{V}_{FB}(t) = g$$

where g is the acceleration constant, $H(t)$ is the height above initial water level at time t , H_{\max} is the maximum swell height, and t is time starting with $t = 0$ at maximum swell height = H_{\max} . The drag load is then calculated from the methods of Reference 13 modified by Subsection 4.2.3 of the DAR. The loading stops when $H(t)$ has fallen below the structure or when $H(t)$ has returned to normal water level - whichever is calculated to occur first.

4.2.2 Condensation Oscillations and Chugging Loads

Condensation oscillation and chugging loads follow the poolswell loads in time. There are basically three loads in this secondary time period, i.e., from about 4 to 60 seconds after the break. "Condensation oscillation" is broken down into two phenomena, a mixed flow regime and a steam flow regime. The mixed flow regime is a relatively high mass flux phenomenon which occurs during the final period of air purging from the drywell to the wetwell when the mixed flow through the downcomer vents contains some air as well as steam. The steam flow portion of the condensation oscillation phenomena occurs after all the air has been carried over to the wetwell and a relatively high intermediate mass flux of pure steam flow is established.

"Chugging" is a pulsating condensation phenomenon which can occur either following the intermediate mass flux phase of a LOCA, or during the class of smaller postulated pipe breaks that result in steam flow through the vent system into the suppression pool. A necessary condition for chugging to occur is that only pure steam flows from the LOCA vents. Chugging imparts a loading condition to the suppression pool boundary and all submerged structures.

In Revision 2 of the DAR, we stated that the DFFR CO and chugging steam condensation boundary load definition (see Appendix A to Reference 21 and Reference 16) would be compared with the LOCA steam condensation load definition derived from the GKM II-M test data to evaluate the conservatism of the DFFR load. Subsections 9.6.1.1 and 9.6.1.2 document this comparison.

As a result of this comparison and the possible schedule delays associated with licensing SSES based on the DFFR load, PP&L decided on April 1, 1982 to terminate the re-evaluation of SSES based on the DFFR load and re-assess SSES with the GKM II-M load definition. Subsection 9.5.3 documents the GKM II-M load definition. For chugging, both a symmetric and asymmetric load case are considered, while for CO, only a symmetric load case is considered.

For plant evaluation, PP&L does not define a separate CO and chugging load definition, as with the Mark II Owners. Instead, the acceleration response spectra (ARS) generated for the LOCA steam condensation phenomena for combination with the other dynamic loads (i.e., SRV (ADS), seismic, etc.) is the so-called LOCA load, which represents an envelope of the ARS curves generated for both the GKM-II-M CO and chugging load definition, and symmetric and asymmetric load cases (see Subsection 9.6.1.1).

Subsection 7.0 provides the results of the re-evaluation of the SSES plant to the LOCA steam condensation load derived from the GKM-II-M test data.

4.2.2.1 Containment Boundary Loads Due To Condensation Oscillations

This subsection has been deleted.

4.2.2.2 Pool Boundary Loads Due to Chugging

This subsection has been deleted.

4.2.2.3 Downcomer Lateral Loads

The chugging load imparted to the downcomer is taken from Reference 47. This reference specifies two sinusoidal dynamic loads used when evaluating downcomer lateral bracing systems. The durations and amplitudes specified are 3ms, 30 kip and 6 ms, 10 kip (as shown in Figures 4-62G & H).

However, in response to the NRC's concerns with the Mark II single vent lateral load, SSES is re-evaluating the downcomers with an extrapolated single vent lateral load of 65 Kips and 3 msec time duration for faulted conditions. Subsection 9.6.3 verifies the conservatism of this load based on a statistical analysis of the GKM II-M bracing force data at 10^{-5} exceedance probability.

4.2.2.4 Multivent Lateral Loads Due to Chugging

Multivent lateral loads due to chugging are presently being evaluated by the methodology documented in letter report "Method of Applying Mark II Single Vent Dynamic Lateral Load to Mark II Plants with Multiple Vents," transmitted to the NRC on April 9, 1980 under Task A.13.

4.2.2.5 Submerged Structure Loads Due to Condensation Oscillations and Chugging

Condensation Oscillation and chugging induce flows fields in the suppression pool causing drag loads on the submerged structures (i.e., SRV lines, downcomers, etc.). The methodology for calculating these drag loads to be combined with the other design basis loads is presented below.

The force on a submerged structure is the sum of an acceleration force F_A and an unsteady drag force F_D .

$$F_T = F_A + F_D$$

Under certain conditions the pressure gradient is of sufficient magnitude so that the submerged structure force is essentially the acceleration drag force. In order for this to be true, the Strouhal Number must be sufficiently large.

For the SSES submerged structures and the flow fields induced by chugging and CO, the Strouhal Number is sufficiently high that negligible error will be incurred by ignoring the unsteady drag force.

The submerged structure drag force can be approximated by the integral of the pressure field P_ϕ over the structure surface:

$$F = \oint_S P_\phi dS \cdot K$$

where: P_ϕ = determined by the equations for potential flow
 K = hydrodynamic mass factor

6

For a linear isentropic fluid where the velocity is everywhere small compared to the sonic speed c , the equations for potential flow reduce to the acoustic wave equation (Reference 65). Thus, the pressure field also satisfies the acoustic wave equation.

Thus, for calculating the SSES submerged structure drag load due to CO and chugging, the above expression is used, with the pressure P_ϕ , as a function of time and position, calculated by the IWEGS/MARS acoustic model of the SSES suppression pool. The pressure P_ϕ is calculated in an analogous manner as the symmetric wall loads (see Subsection 9.5.3.4.1) for each source, except that the pressures are calculated at the submerged structure surface locations instead of the containment boundary.

For each structure being analyzed (i.e., column) a pressure time history (PTH) is calculated for every 60° increment circumferential around the structure at each elevation corresponding to a nodal point of the structural model. Thus, for each node point elevation, six pressure time histories are calculated. This is repeated for each source. These sets of PTHs, calculated for each source, are then integrated across the structure's surface to give resultant force time histories for structural analysis.

6 The force time histories are then multiplied by a hydrodynamic mass factor, K , of 2 to account for the modification of the flow field due to structure's presence.

4.2.3 Response to NRC Criteria for Loads On Submerged Structure

4.2.3.1 Introduction

In October 1978 the NRC published NUREG-0487, Mark II Containment Lead Plant Program Load Evaluation and Acceptance Criteria. It addresses the load methodologies proposed by the Mark II Lead Plant Program for determining LOCA and SRV hydrodynamic loads. NUREG-0487 was highly critical of the lead plant position for determining submerged structure loads and stipulated very conservative alternative loading criteria. The following subsections will present the NRC submerged structures acceptance criteria and the corresponding Mark II response.

4.2.3.2 NRC Criteria III.D.2.a.1: Bubble Asymmetry

A conservative estimate of asymmetry should be added by increasing acceleration and velocities computed in Step 12 of Section 2.2 of Reference 13 by 10%. If the alternative steps 5A, 12A, and 13A are used, the acceleration drag shall be directly increased by 10% while the standard drag shall be increased by 20%.

Response: These criteria are acceptable.

4.2.3.3 NRC Criteria III.D.2.a.2: Standard Drag In Accelerating Flow

2 The drag coefficients C_D for the standard drag contribution in steps 13, or 13A, 15 of section 2.2 and step 3 of section 2.3 of Reference 13 may not be taken directly from the steady state coefficients of Table 2-3. Modified coefficients C_D from accelerating flow as presented in References 49 and 50 shall be used with transverse forces included, or an upper bound of a factor of three times the standard drag coefficients shall be used for structures with no sharp corners or with streamwise dimensions at least twice the width.

Response:

The three references show that in oscillating flows the standard drag coefficient for cylinders can exceed the steady flow value. Values of C_D in excess of 2.0 were observed while steady state values (for cylinders) never exceed 1.2. The NRC's position is interpreted to mean that neglecting the unsteady effect on standard drag coefficients will be nonconservative in some cases.

A method is presented in Reference 51, Appendix A to account for unsteady effects on standard and acceleration drag during various phases of the LOCA and SRV transients. Also included are methods to estimate transverse forces due to vortex shedding.

Subsequent to reviewing the methodology contained in Appendix A of Reference 51, the NRC in Supplement No. 1 of NUREG-0487, required several modifications to the methodology for determining the unsteady drag coefficients.

A review of the SSES pool swell and fallback drag load calculations indicates that SSES has incorporated these modifications into their calculations. Drag coefficients are not required for calculating the submerged structure drag loads due to air bubble charging prior to pool swell, and the drag loads due to chugging and CO, since these loads are calculated using the pressure time histories at the structure locations (see Subsection 4.2.1.7 and 4.2.2.5).

4.2.3.4 NRC Criteria III.D.2.a.3: Segmentation of Structures

The equivalent uniform flow velocity and acceleration for any structure or structural segment shall be taken as the maximum values "seen" by that structure, not the value at the geometric center.

Response:

For structures submerged in a non-uniform flow field, the velocity and acceleration will be a function of position along the structure. The NRC's criterion is interpreted to mean that the velocity and acceleration should be taken at the end of the segment closest to the disturbing source instead of the geometric center. For certain restrictions on segment length, the error in the calculation of drag using the velocity and acceleration at the geometric center is very small. This is demonstrated for acceleration drag in Reference 51, Appendix B and for standard drag Reference 51, Appendix C. Appendix B also contains a discussion that shows that neglecting end effects in drag calculations is conservative.

4.2.3.5 NRC Criteria III.D.2.a.4: Interference Effects

The computation of drag forces on submerged structures independent of each other (as presented in Reference 13) is adequate for structures sufficiently far from each other so that interference effects are negligible. Interference effects can be expected to be insignificant when two structures are separated by more than three characteristic dimensions of the larger one. For structures closer together than this separation, either detailed analysis of interference effects shall be performed or a conservative multiplication of both the acceleration and standard drag forces by four shall be performed.

Response:

Interference effects can have a significant effect on drag forces. A modification to the calculational procedure is proposed to account for interference. Reference 51, Appendix D describes the proposed method for standard drag with the exception that the free stream velocity used will be that at the structures geometric center in all cases. Reference 51, Appendix E presents the proposed method for acceleration drag.

4.2.3.6 NRC Criteria III.D.2.a.5: Blockage In Downcomer Bracing

A specific example of interference which must be accounted for is the blockage presented to the motion of the water slug during pool swell due to the presence of downcomer bracing systems. If significant blockage relative to the net pool area exists, the standard drag coefficients shall be modified for this effect by conventional methods (Reference 52).

Response:

Blockage effects on the pool swell drag loads produced on the downcomer bracing system were accounted for by using the methods in Reference 87.

4.2.3.7 NRC Criteria III.D.2.a.6: Formula 2-23 of Reference 13

Formula 2-23 of Reference 13 shall be modified by replacing M_H with $\rho_{FB} V_A$ where V_A is obtained from Table 2-1 and 2-2. This is then consistent with the analysis of Reference 14.

Response:

This criteria is acceptable.

4.2.4 Secondary Load

The previous subsections have identified and specified loading methodologies that result in significant containment dynamic loads. In addition, several pool dynamic loads can occur which are considered secondary when compared to the previous loads or because the containment and related equipment response is small when subjected to them. The following subsections identify the secondary loads and the load criteria to be applied to the SSES containment.

4.2.4.1 Downcomer Friction Drag Loads

Friction Drag loads are experienced internally by the downcomers during vent clearing and subsequent air/or steam flow. In addition, the downcomers experience an external drag load during poolswell. Using standard drag force calculation procedures these loads are determined to be 0.6 and .3 KIPS per downcomer, respectively and are not considered in the structural evaluation of the containment.

4.2.4.2 Sonic Waves

Immediately following the postulated instantaneous rupture of a large primary system pipe, a sonic wave front is created at the break location and propagates through the drywell to the vent system. This load has been determined to be negligible and none is specified.

4.2.4.3 Compressive Wave

The compression of the air in the drywell and vent system causes a compressive wave to be generated in the downcomer water legs. This compressive wave then propagates through the pool and causes a differential pressure loading on the submerged structures and on the wetwell wall. This load has been evaluated and is considered negligible.

4.2.4.4 Fallback Loads on Submerged Boundaries

During fallback "water hammer" type loads could exist if the water slug remained intact during this phase. However available test data indicates that this does not occur and the fallback process consists of a relatively gradual settling of the pool water to its initial level as the air bubble "percolates" upward. This is based on visual observations during the EPRI tests (Reference 32) as well as indirect evidence provided by a careful examination of pool bottom pressure forces from the 4T, EPRI, foreign licensee and Marviken tests. Thus these loads are small and will not be considered.

4.2.4.5 Vent Clearing Loads on the Downcomers

The expulsion of the water leg in the downcomers at vent clearing creates a transient water jet in the suppression pool. This jet formation may occur asymmetrically leading to lateral reaction loads on the downcomer. However, this load is bounded by the load specification during chugging and will not be considered for containment analysis.

4.2.4.6 Post Poolswell Waves

Reference 46 indicates the potential for containment loading due to post poolswell waves impinging on the wetwell wall and internal components. Per the response to Question M020.8 documented in Appendix A to Reference 10a, this load is considered negligible when compared to the other design basis loads.

4.2.4.7 Seismic Slosh

Seismic slosh loads are defined as those hydrodynamic loads exerted on the suppression pool walls by water in the suppression pool during a seismic event. Although these loads are expected to be small in comparison with other hydrodynamic loads such as those associated with air/steam SRV discharge and LOCA poolswell

and steam condensation loads, they have been calculated for the SSES containment evaluation, as requested by the NRC in NUREG-0487.

The methodology used to calculate seismic slosh loads for the SSES containment is the SOLA-3D computer code, developed at Los Alamos Scientific Laboratory for multi-dimensional fluid flow analyses, including seismic slosh (Reference 71 and 72). The code has been used for seismic slosh analysis previously, where a toroidal MK I BWR suppression pool was approximated by an annular geometry, and excited by a simulated sinusoidal seismic event. Results of this analysis are reported in Reference 73. It was demonstrated that SOLA-3D could be used to describe suppression pool water motion for a seismic excitation applied to the containment structure.

6 The seismic slosh analysis for SSES suppression pool has been patterned after the annular suppression pool analysis described in Reference 73, with appropriate SSES suppression pool and containment parameters used. The results of calculations are pressure-time histories, caused by water wave motion, to be applied to suppression pool boundaries in manner and location similar to the method used for SRV and LOCA hydrodynamic loads.

Generally, water motion above the quiescent suppression pool surface causes "wave loads" and water motion below causes "inertial loads." The inertia loads will always appear to be larger than the wave loads because the normal hydrostatic load would be included below the water surface. (For example, at 24 ft. submergence in cold water, the hydrostatic head would be slightly more than 10 psi, giving a 10 psi bias to the inertia loads at pool bottom.)

Some numerical results of the calculations are shown in Table 4-22 for the selected locations in the suppression pool. As can be observed, these pressures are small relative to those calculated for the other hydrodynamic loads. Figures 4-62 i, j, k, and m show typical wave motion at the four containment locations in Table 4-22.

4.2.4.8 Thrust Loads

2 Thrust loads are associated with the rapid venting of air and/or steam through the downcomers. To determine this load a momentum balance for the control volume consisting of the drywell, diaphragm floor and vents is taken. Results of the analysis indicates that the load reduces the downward pressure differential on the diaphragm.

4.2.5 Long Term LOCA Load Definition

1 The loss-of-coolant accident causes pressure and temperature transients in the drywell and wetwell due to mass and energy released from the line break. The drywell and wetwell pressure and temperature time histories are required to establish the

structural loading conditions in the containment because they are the basis for other containment hydrodynamic phenomena. The response must be determined for a range of parameters such as leak size, reactor pressure and containment initial conditions. The results of this analysis are containment initial conditions. The results of this analysis are documented in Reference 7.

4.2.5.1 Design Basis Accident (DBA) Transients

The DBA LOCA for SSES is conservatively estimated to be a 3.53 ft² break of the recirculation line (Reference 7). The SSES plant unique inputs for this analysis are shown in Table 4-19. Drywell and wetwell pressure responses are shown in Figures 4-46 and 4-47 (extracted from Reference 7). These transient descriptions do not, however, contain the effects of reactor subcooling. Suppression pool temperature response is shown in Figure 4-48 (Reference 7). This transient description also does not contain the effect of reactor subcooling. Drywell temperature response is shown in Figure 4-49 and similarly does not contain the effects of pipe inventory or reactor subcooling.

4.2.5.2 Intermediate Break Accident (IBA) Transients

The worst-case intermediate break for the Mark II plants is a main steam line break on the order of 0.05 to 0.1 ft². Suppression pool temperature response is shown in Figure 4-50. Drywell temperature and wetwell and drywell pressures for the SSES IBA are shown in Figure 4-51.

4.2.5.3 Small Break Accident (SBA) Transients

At this time plant-unique SBA data for SSES is not available. The wetwell and drywell pressure and temperature transients for a typical Mark II containment are used to estimate SSES containment response to these accidents. These curves are shown in Figure 4-17 (extracted from Reference 10).

4.2.6 LOCA Loading Histories For SSES Containment Components

The various components directly affected by LOCA loads are shown schematically in Figures 4-53 and 4-54. These components may in turn load other components as they respond to the LOCA loads. For example, lateral loads on the downcomer vents produce minor reaction loads in the drywell floor from which the downcomers are supported. The reaction load in the drywell floor is an indirect load resulting from the LOCA and is defined by the appropriate structural model of the downcomer/drywell floor system. Only the direct loading situations are described explicitly here. Table 4-20 is a LOCA load chart for SSES. This chart shows which LOCA loads directly affect the various structures in the SSES containment design. Details of the loading time histories are discussed in the following subsections.

4.2.6.1 LOCA Loads on the Containment Wall and Pedestal

Figure 4-55 shows the LOCA loading history for the SSES containment wall and the RPV pedestal. The wetwell pressure loads apply to the unwetted elevations in the wetwell; and addition of the appropriate hydrostatic pressure is made for loads on the wetted elevations. Condensation oscillation and chugging loads are applied to the wetted elevations in the wetwell only. The poolswell air bubble load applies to the wetwell boundaries as shown in Figure 4.44.

4.2.6.2 LOCA Loads on the Basemat and Liner Plate

Figure 4-56 shows the LOCA loading history for the SSES basemat and liner plate. Wetwell pressures are applied to the wetted and unwetted portions of the liner plate as discussed in Subsection 4.2.6.1. The downcomer water jet impacts the basemat liner plate as does the poolswell air bubble load. Chugging and condensation oscillation loads are applied to the wetted portion of the liner plate.

4.2.6.3 LOCA Loads on the Drywell and Drywell Floor

Figure 4-57 shows the LOCA loading history for the SSES drywell and drywell floor. The drywell floor undergoes a vertically applied, continuously varying differential pressure, the upward component of which is especially prominent during poolswell when the wetwell air space is highly compressed.

4.2.6.4 LOCA Loads on the Columns

Figure 4-58 shows the LOCA loading history for the SSES columns. Poolswell drag and fallback loads are very minor since the column surface is oriented parallel to the pool swell and fallback velocities. The poolswell air bubble, condensation oscillations and chugging will provide loads on the submerged (wetted) portion of the columns.

4.2.6.5 LOCA Loads on the Downcomers

Figure 4-59 shows the LOCA loading history for the SSES downcomers. The downcomer clearing load is a lateral load applied at the downcomer exit (in the same manner as the chugging lateral load) plus a vertical thrust load. Poolswell drag and fallback loads are very minor since the downcomer surfaces are oriented parallel to the pool swell and fallback velocities. The poolswell air bubble load is applied to the submerged portion of the downcomer as are the chugging and condensation oscillation loads.

4.2.6.6 LOCA Loads on the Downcomer Bracing

Figure 4-60 shows the LOCA loading history for the SSES downcomer bracing system. This system is not subject to impact loads since it is submerged at elevation 668'. As a submerged structure it

is subject to poolswell drag, fallback and air bubble loads. Condensation oscillations and chugging at the vent exit will also load the bracing system both through downcomer reaction (indirect load) and directly through the hydrodynamic loading in the suppression pool.

4.2.6.7 LOCA Loads on Wetwell Piping

Figure 4-61 shows the LOCA loading history for piping in the SSES wetwell. Since the wetwell piping occurs at a variety of elevations in the SSES wetwell, sections may be completely submerged, partially submerged, or initially uncovered. Piping may occur parallel to poolswell and fallback velocities as with the main steam safety relief piping. For these reasons there are a number of potential loading situations which arise as shown in Table 4-21. In addition, the poolswell air bubble load applies to the submerged portion of the wetwell piping as do the condensation oscillation and chugging loads.

4.3 ANNULUS PRESSURIZATION

The RPV shield annulus has the recirculation pumps suction lines passing through it (for location in containment see Figure 1-1). The mass and energy release rates from a postulated recirculation line break constitute the most severe transient in the reactor shield annulus. Therefore, this pipe break is selected for analyzing loading of the shield wall and the reactor pressure vessel support skirt for pipe breaks inside the annulus. The reactor shield annulus differential pressure analysis and analytical techniques are presented in Appendices 6A and 6B of the SSES Final Safety Analysis Report (FSAR).

This figure has been deleted

REV. 6, 4/82

SUSQUEHANNA STEAM ELECTRIC STATION UNITS 1 AND 2 DESIGN ASSESSMENT REPORT
--

CONDENSATION PRESSURE FORCING FUNCTIONS
--

FIGURE 4-44 A

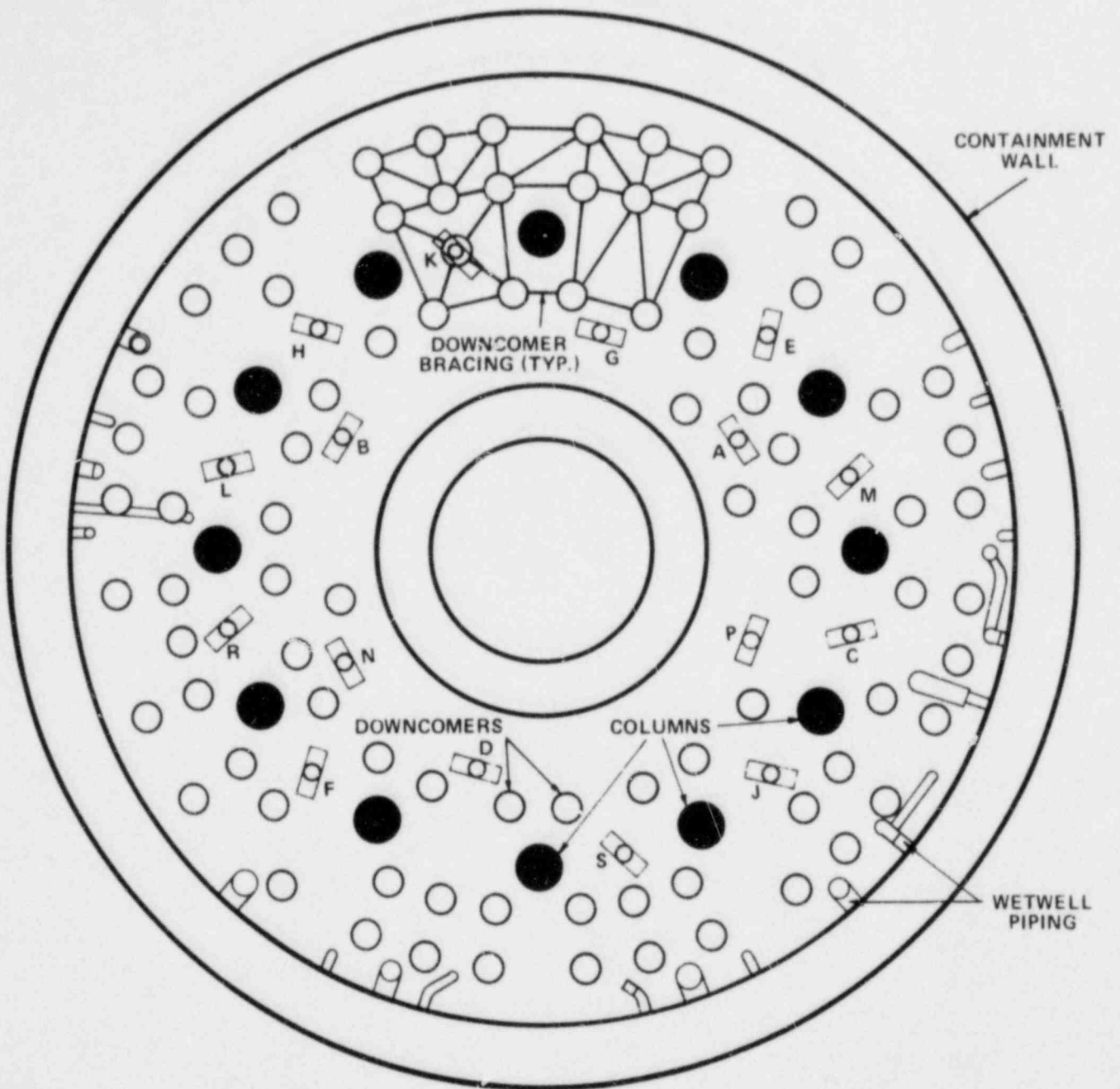
This figure has been deleted

REV. 6, 4/82

**SUSQUEHANNA STEAM ELECTRIC STATION
UNITS 1 AND 2
DESIGN ASSESSMENT REPORT**

**SYMMETRIC AND ASSYMMETRIC
SPATIAL LOADING SPECIFICATION**

FIGURE 4-45



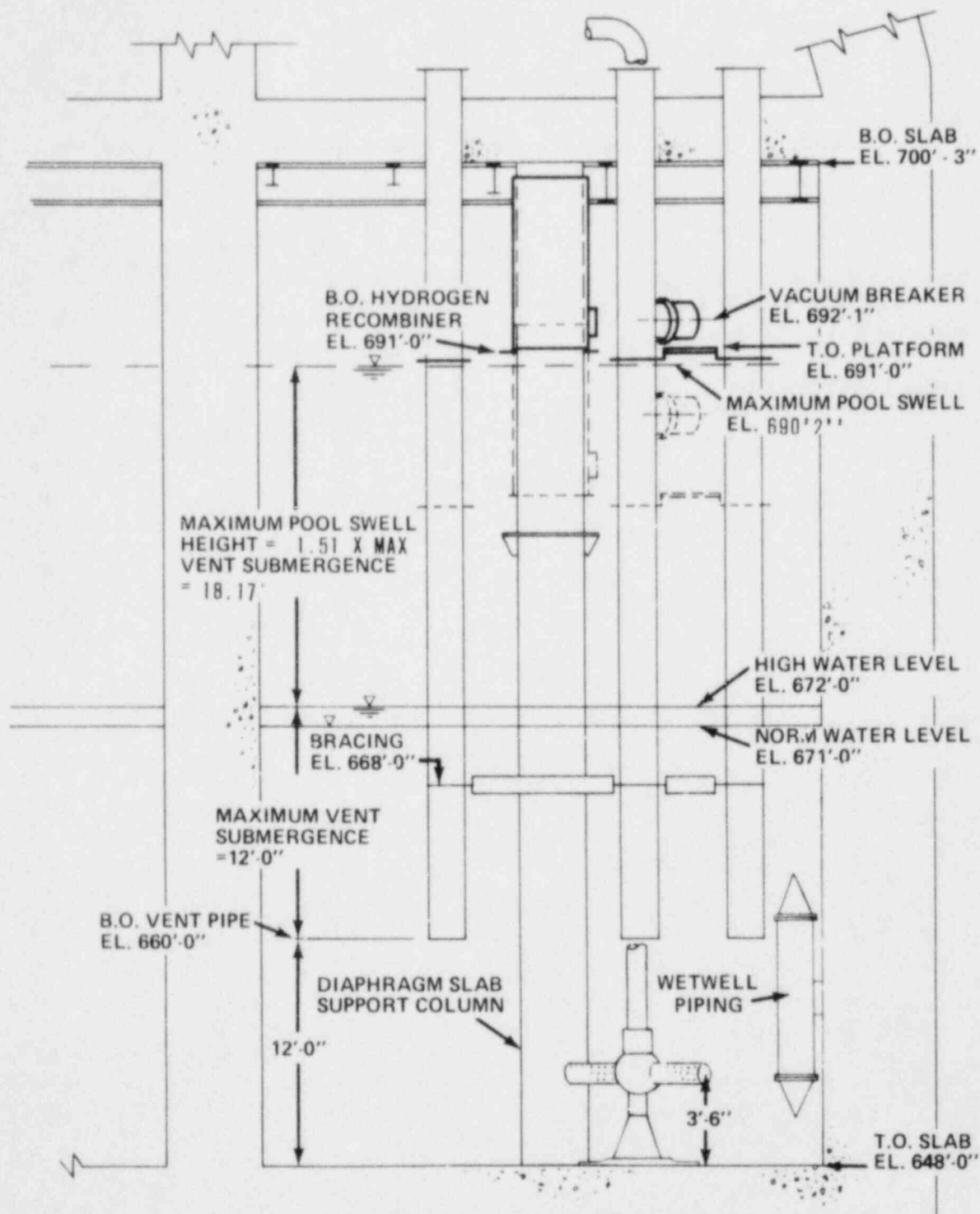
NOTE:
 DOWNCOMER BRACING IS ONLY
 PARTIALLY SHOWN IN THE
 INTEREST OF CLARITY.
 LETTERS INDICATE SRV QUENCHERS

REV. 6, 4/82

SUSQUEHANNA STEAM ELECTRIC STATION
 UNITS 1 AND 2
 DESIGN ASSESSMENT REPORT

SSES COMPONENTS AFFECTED
 BY LOCA LOADS

FIGURE 4-53



REV. 4, 4/82

SUSQUEHANNA STEAM ELECTRIC STATION
UNITS 1 AND 2
DESIGN ASSESSMENT REPORT

SSES COMPONENTS
AFFECTED BY LOCA LOADS

FIGURE 4-54

This figure has been deleted

REV. 6, 4/82

**SUSQUEHANNA STEAM ELECTRIC STATION
UNITS 1 AND 2
DESIGN ASSESSMENT REPORT**

CHUGGING POOL BOUNDARY LOADS

FIGURE 4-62 A & B

This figure has been deleted

REV. 6, 4/82

**SUSQUEHANNA STEAM ELECTRIC STATION
UNITS 1 AND 2
DESIGN ASSESSMENT REPORT**

CHUGGING POOL BOUNDARY LOADS

FIGURE 4-62 C & D

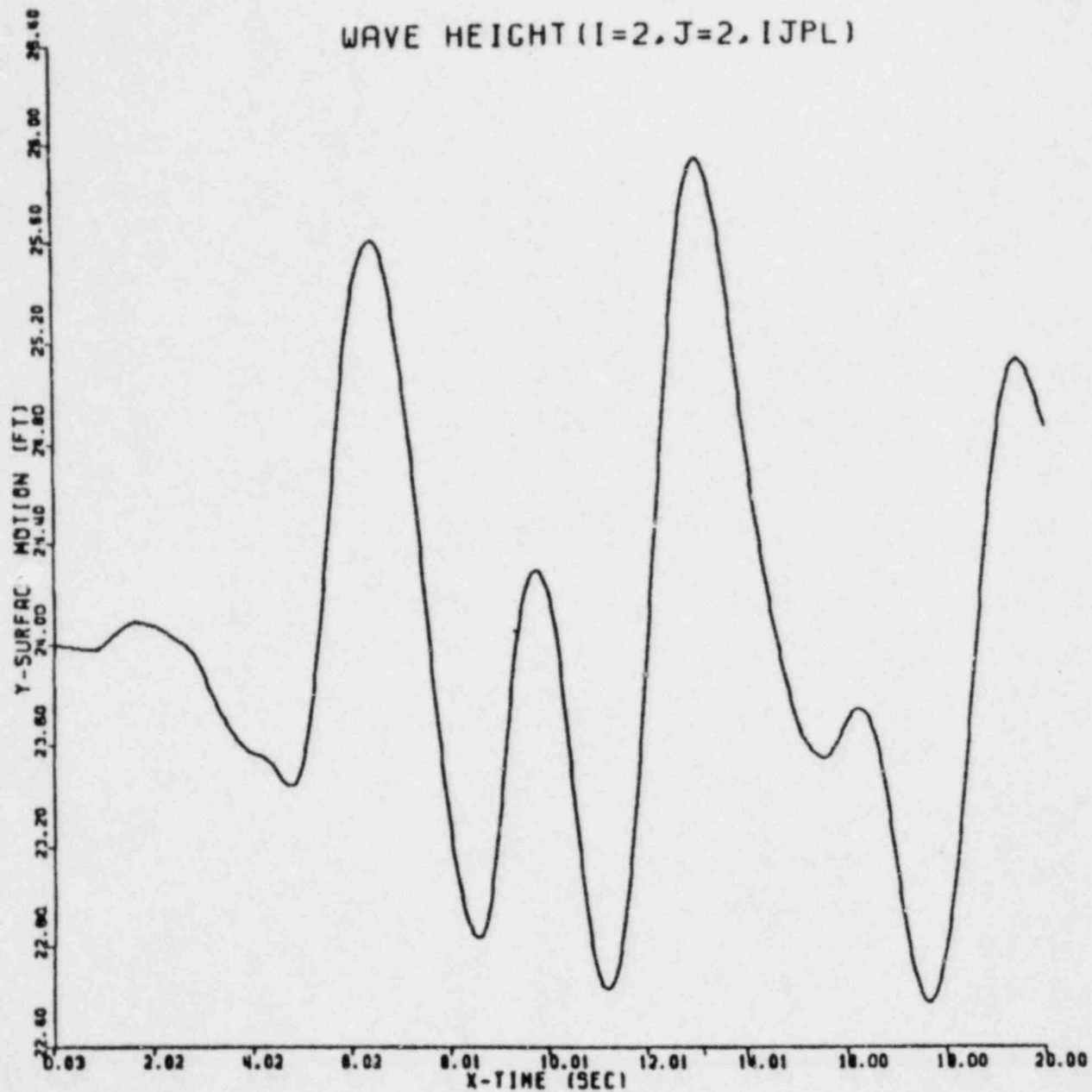
This figure has been deleted

REV. 6, 4/82

**SUSQUEHANNA STEAM ELECTRIC STATION
UNITS 1 AND 2
DESIGN ASSESSMENT REPORT**

CHUGGING POOL BOUNDARY LOADS

FIGURE 4-62 E & F

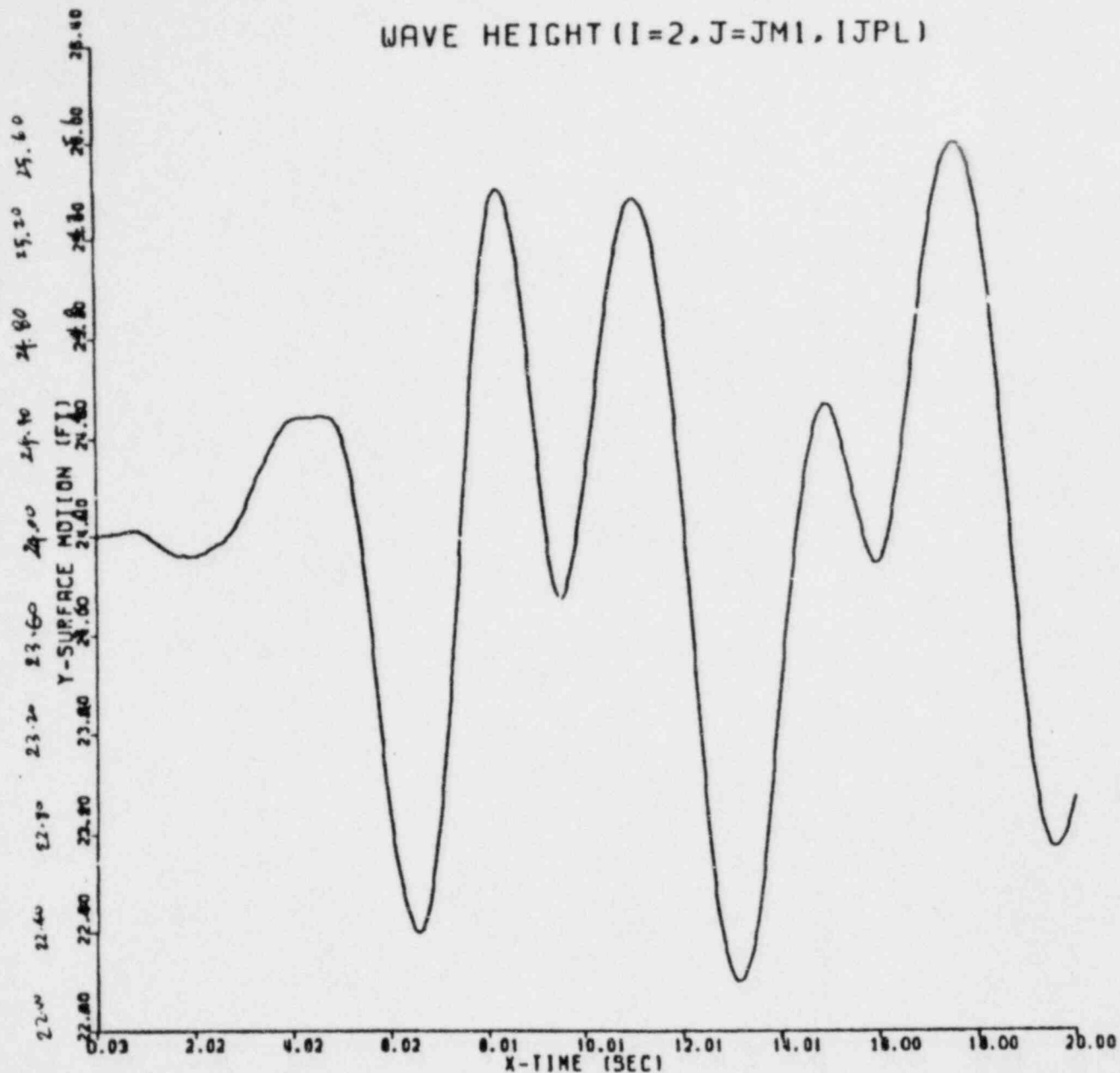


REV. 6, 4/82

SUSQUEHANNA STEAM ELECTRIC STATION
UNITS 1 AND 2
DESIGN ASSESSMENT REPORT

TYPICAL WAVE MOTION DUE
TO SEISMIC SLOSH

FIGURE 4-62i



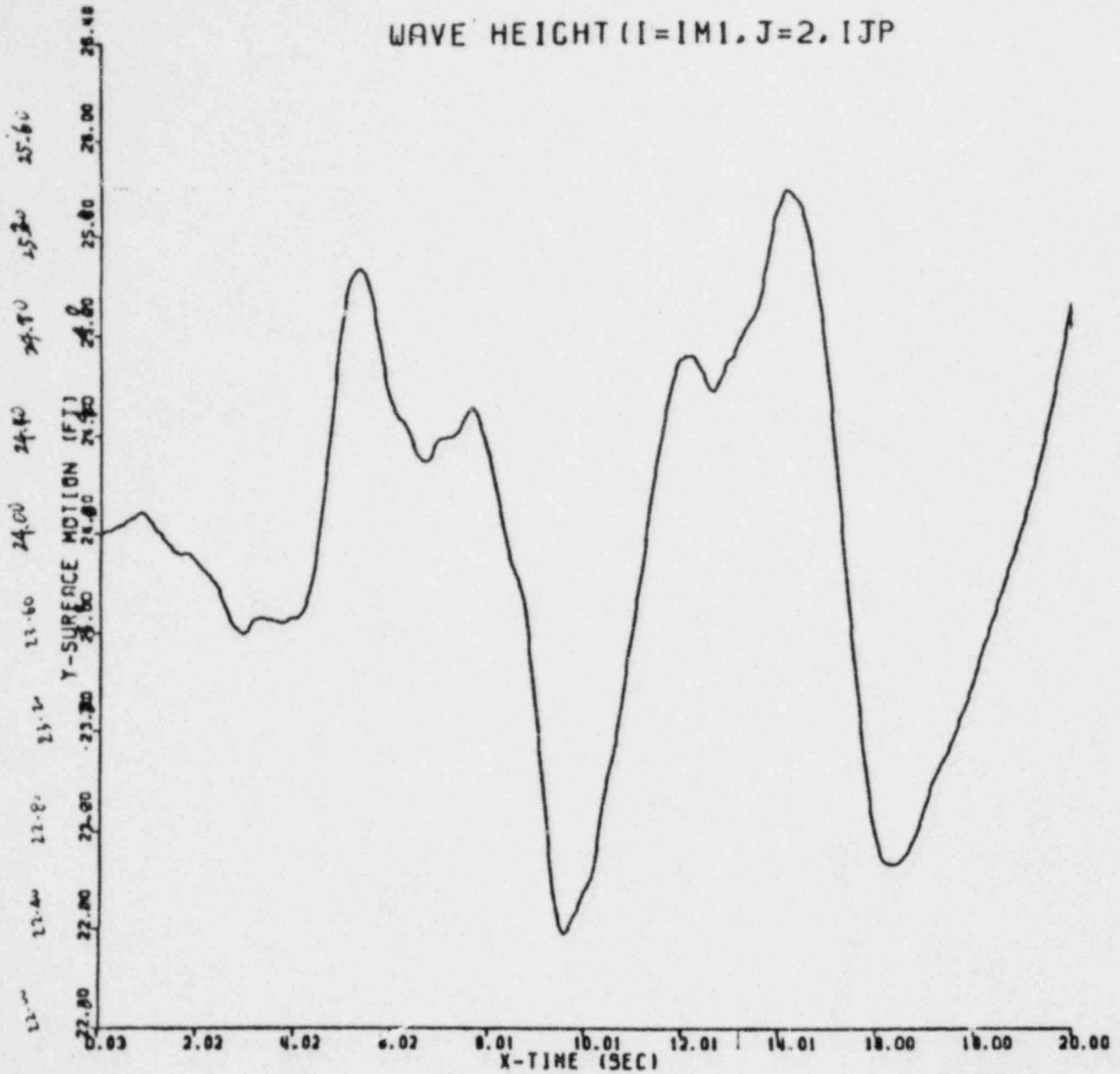
REV. 6, 4/82

SUSQUEHANNA STEAM ELECTRIC STATION
UNITS 1 AND 2
DESIGN ASSESSMENT REPORT

TYPICAL WAVE MOTION
DUE TO SEISMIC SLOSH

FIGURE 4-62J

WAVE HEIGHT (I=1M1, J=2, IJP

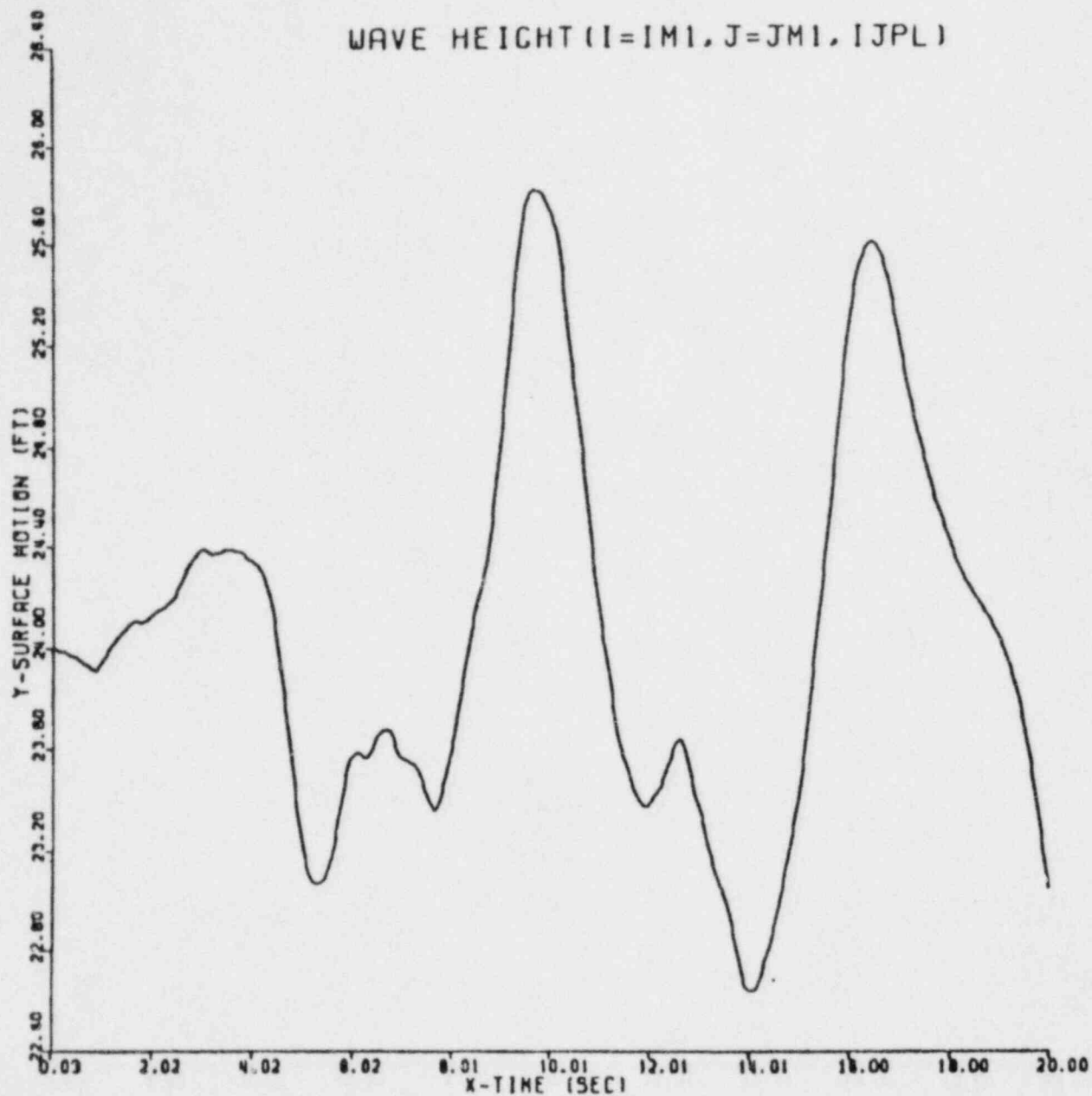


REV. 6, 4/82

SUSQUEHANNA STEAM ELECTRIC STATION
UNITS 1 AND 2
DESIGN ASSESSMENT REPORT

TYPICAL WAVE MOTION
DUE TO SEISMIC SLOSH

FIGURE 4-62K

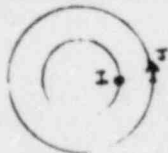
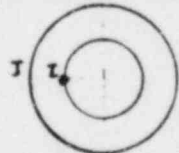
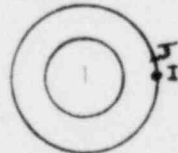
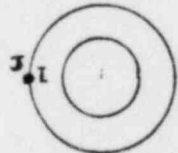


SUSQUEHANNA STEAM ELECTRIC STATION
UNITS 1 AND 2
DESIGN ASSESSMENT REPORT

TYPICAL WAVE MOTION
DUE TO SEISMIC SLOSH

FIGURE 4-62M

Table 4-22
Sloshing Wave Height

Time of Max. Height sec.	HF2, (2,2) I = 2, J = 2 ft.	HF3, (2,17) I = 2, J = 17 ft.	HBK2, (7,2) I = 7, J = 2 ft.	HBK3, (7,17) I = 7, J = 17 ft
14.0			25.40 (1.40)	
9.90				25.80 (1.80)
17.50		25.60 (1.60)		
12.90	25.95 (1.95)			
	 Fig. 4-62i	 Fig. 4-62j	 Fig. 4-62k	 Fig. 4-62m

Note: • = Shows Location

() = Inside bracket is the net wave height from the initial position
24 ft. from the bottom of tank.

I = Mesh numbers on the radius from inside to outside.

J = Circumferential division numbers.

CHAPTER 5

LOAD COMBINATIONS FOR STRUCTURES, PIPING, AND EQUIPMENT

TABLE OF CONTENTS

5.1	CONCRETE CONTAINMENT AND REACTOR BUILDING LOAD COMBINATIONS	
5.2	STRUCTURAL STEEL LOAD COMBINATIONS	
5.3	LINER PLATE LOAD COMBINATIONS	
5.4	DOWNCOMER LOAD COMBINATIONS	
5.5	PIPING, QUENCHER, AND QUENCHER SUPPORT LOAD COMBINATIONS	1
5.5.1	Load Considerations for Piping Inside the Drywell	
5.5.2	Load Considerations for Piping Inside the Wetwell	
5.5.3	Quencher and Quencher Support Load Considerations	
5.5.4	Load Considerations for Piping in the Reactor Building	
5.6	NSSS LOAD COMBINATIONS	
5.7	BALANCE OF PLANT (BOP) EQUIPMENT LOAD COMBINATIONS	6
5.8	ELECTRICAL RACEWAY SYSTEM LOAD COMBINATIONS HVAC	
5.9	DUCT SYSTEM LOAD COMBINATIONS	
5.10	FIGURES	2
5.11	TABLES	

CHAPTER 5

FIGURES

<u>Number</u>	<u>Title</u>
5-1	Piping Stress Diagrams and Tables
5-2	Piping Stress Diagrams and Tables
5-3	Piping Stress Diagrams and Tables
5-4	Piping Stress Diagrams and Tables

CHAPTER 5

TABLES

<u>Number</u>	<u>Title</u>	
5-1	Load Combinations for Containment and Reactor Building Concrete Structures Considering Hydrodynamic Loads	1
5-2	Load Combinations and Allowable Stresses for Structural Steel Components	
5-3	Load Combinations and Allowable Stresses for Downcomers	
5-4	Load Combinations and Allowable Stresses For Balance of Plant (BOP) Equipment	2
5-5	Load Combinations and Allowable Stresses for NSSS Equipment and Piping	
5-6	Load Combinations and Allowable Stresses for the Electrical Raceway System	6

5.0 LOAD COMBINATIONS FOR STRUCTURES, PIPING, AND EQUIPMENT

To verify the adequacy of mechanical and structural design, it is necessary first to define the load combinations to which structures, piping, and equipment may be subjected. In addition to the loads due to pressure, weight, thermal expansion, seismic, and fluid transients, hydrodynamic loads resulting from LOCA and SRV discharge are considered in the design of structures, piping, and equipment in the drywell and suppression pool. This chapter specifies how the LOCA and SRV discharge hydrodynamic loads will be combined with the other loading conditions. For the load combinations discussed in this chapter, seismic and hydrodynamic responses are combined by the methods specified in Reference 10 Subsection 5.2.2 and Reference 10 Section 6.3.

5.6_NSSS_LOAD_COMBINATIONS

The load combinations used for the evaluation of the NSSS piping and equipment are contained in Table 5-5.

5.7 BOP EQUIPMENT LOAD COMBINATIONS

6 | Load combinations for seismic category I equipment located within
2 | the Containment, reactor and control buildings are assessed for
the load combinations shown in Table 5-4.

5.8--ELECTRICAL RACEWAY SYSTEM LOAD COMBINATIONS

The load combinations for evaluating the Electrical Raceway System are given in Table 5-6.

5.9 HVAC DUCT SYSTEM LOAD COMBINATIONS

The load combination for the HVAC duct system are given in Table 5-2.

TABLE 5-4

LOAD COMBINATIONS AND ALLOWABLE STRESSES
FOR BALANCE OF PLANT (BOP) EQUIPMENT

<u>Equation</u>	<u>Condition</u>	<u>Load Combination</u>	<u>Stress Limit</u> 6
1	Normal w/o Temp & pr.	D+L+SRV	F_s
2	Normal w/Temp & pr.	D+L+T+P+SRV	F_s
3	Abnormal/Severe	D+L+T+P+E+SRV+LOCA	$1.5F_s$
4	Abnormal/Extreme	D+L+T+P+E'+SRV+LOCA	$1.5F_s$

where

F_s	=	Allowable stress for normal conditions
D	=	Dead Load
L	=	Live Load
P	=	Pressure loads during operating conditions including pressure gradients and equipment and pipe reactions.
T	=	Thermal effects during normal operating conditions including temperature gradients and equipment and pipe reactions.
E	=	Loads due to operating basis earthquake
E'	=	Loads due to Safe Shutdown earthquake
SRV	=	Loads due to Main Steam Safety relief valve operation
LOCA	=	Loads due to Loss-of-Coolant Accident occurrence.

TABLE 5-5

LOAD COMBINATION AND ACCEPTANCE CRITERIA
FOR ASME CODE CLASS 1, 2 AND 3
NSSS PIPING AND EQUIPMENT

<u>Load Combination</u>	<u>Design Basis</u>	<u>Evaluation Basis</u>	<u>(Service Level)</u>
N + SRV	Upset	Upset	(B)
N + OBE	Upset	Upset	(B)
N + OBE + SRV	Emergency	Upset	(B)
N + SSE + SRV	Faulted	Faulted*	(D)
N + SBA + SRV	Emergency	Emergency**	(C)
N + IBA + SRV	Faulted	Faulted*	(D)
N + SBA + SRV	Emergency	Emergency~	(C)
N + SBA + OBE + SRV	Faulted	Faulted*	(D)
N + IBA + OBE + SRV	Faulted	Faulted*	(D)
N + SBA/IBA + SSE + SRV	Faulted	Faulted*	(D)
N + LOCA** + SSE	Faulted	Faulted*	(D)

LOAD DEFINITION LEGEND

Normal (N)	-	Normal and/or abnormal loads depending on acceptance criteria.
OBE	-	Operational basis earthquake loads.
SSE	-	Safe Shutdown earthquake loads.
SRV	-	Loads associated with Safety Relief Valve ctuation.

LOAD COMBINATION TABLE (Cont.)

LOCA ₁	-	The loss of coolant accident associated with the postulated pipe rupture of large pipes (e.g., main steam, feedwater, recirculation piping).
LOCA ₂	-	Pool swell <u>drag/fallback loads</u> on piping and components located between the main vent discharge outlet and the suppression pool water upper surface.
LOCA ₃	-	Pool swell <u>impact loads</u> on piping and components located above the suppression pool water upper surface.
LOCA ₄	-	Oscillating pressure induced loads on submerged piping and components during condensation oscillations.
LOCA ₅	-	Building motion induced loads from chugging.
LOCA ₆	-	Vertical and horizontal loads on main vent piping.
LOCA ₇	-	Annulus pressurization loads.
SBA	-	The abnormal transients associated with a Small Break Accident.
IBA	-	The abnormal transients associated with an Intermediate Break Accident.

* All ASME Code Class 1, 2, and 3 piping systems which are required to function for safe shutdown under the postulated events shall meet the requirements of NRC's "Interim Technical Position - Functional Capability of Passive Components" - by NEB.

** The most limiting case of load combination among LOCA₁ through LOCA₇ .

TABLE 5-6

LOAD COMBINATIONS AND ALLOWABLE
STRESSES FOR THE ELECTRICAL RACEWAY SYSTEM

<u>Load Combination</u>	<u>Allowable Stresses</u>
1. D+L+SRV	F
2. D+L+E	Note 2
3. D+E'+SRV+LOCA	Note 2

NOTES:

1. For notations, see Table 5-2.
2. For detailed discussion, see Subsection 3.7b.3.1.6.1 of the SSES FSAR.

6.5 PIPING, QUENCHER, AND QUENCHER SUPPORT CAPABILITY
-----ASSESSMENT CRITERIA-----

Piping in the containment and reactor building is analyzed in accordance with Reference 29 Subsections NB3600, NC3600, and ND3600 for the loading described in Subsection 5.5.

The quencher is designed in accordance with Reference 29, Subsection NC3200, for loading discussed in Subsection 5.5.3. The quencher support is designed in accordance with Subsection NF3000 of Reference 29.

6.6 NSSS CAPABILITY ASSESSMENT CRITERIA

6 The capability assessment criteria used for the analysis of NSSS piping systems, reactor pressure vessel (RPV), RPV supports, RPV internal components and floor structure mounted equipment are shown in Table 5-5, Load Combinations and Acceptance Criteria. Table 5-5 is in agreement with a conservative general interpretation of the NRC technical position, "Stress Limits for ASME Class 1, 2 and 3 Components and Component Supports of Safety-Related Systems and Class CS Core Support Structures Under Specific Service Loading Combinations."

Peak response due to related dynamic loads postulated to occur in the same time frame but from different events are combined by the square-root-of-the-sum-of-the-squares method (SRSS). A detailed discussion of this load combination technique is presented in Reference 80.

6.7 BALANCE OF PLANT (BOP) EQUIPMENT CAPABILITY ASSESSMENT CRITERIA

6.7.1.1 Seismic Category I BOP equipment located within the containment, reactor and control building are assessed for load combinations shown in Table 5-4. In these load combinations, seismic and hydrodynamic loads are generally combined using the absolute sum method.

6.7.1.2 However, for the "marginal" cases the responses of the "dynamic" events (Seismic, SRV, LOCA) are combined by the square root of the sum of the squares (SRSS) method before adding these values to the other loads by the absolute sum (ABS) method. The maximum loading effects of both the horizontal and vertical directions are considered as arising from simultaneous excitation in all three principal directions for all combinations involving dynamic loads as detailed in Subsection 7.1.7.4.1.3.

6.7.2 Testing

6.7.2.1 When equipment is qualified by testing, the test motions have simulated the combinations and damping. The equipment have remained operational and functional, before, during and after such tests.

(a)	OBE	alone	-	1/2% damping
(b)	SSE	alone	-	1% damping
(c)	SRV	alone	-	2% damping
(d)	LOCA	alone	-	2% damping
(e)	OBE+SRV+LOCA		-	2% damping
(f)	SSE+SRV+LOCA		-	2% damping

6.7.2.2 Cases (a) and (b) are covered in the PSAR. Cases (c) and (d) are covered in the test evaluation for (e) and (f). Test requirements are depicted by tests response spectrum (TRS) for a given damping value. Equipment is deemed to be qualified if the equipment did not fail or malfunction during the test and the TRS envelope the required response Spectrum (RRS). The RRS for cases (e) and (f) are obtained by combining the response spectrum of the individual components of each event by adding the larger of the horizontal responses to the vertical responses on an absolute sum basis. However, for marginal cases the square root of sum of the squares (SRSS) method is allowed for the individual dynamic events and components.

6.8 ELECTRICAL RACEWAY SYSTEM CAPABILITY ASSESSMENT CRITERIA

The allowable stresses for the Electricl Raceway System are contained in Table 5-6.

CHAPTER 7

DESIGN ASSESSMENT

TABLE OF CONTENTS

7.1 ASSESSMENT METHODOLOGY

7.1.1	Containment and Reactor Building Assessment Methodology	
7.1.1.1	Containment Structure	
7.1.1.1.1	Hydrodynamic Loads	
7.1.1.1.1.1	Structural Models	
7.1.1.1.1.2	Damping	
7.1.1.1.1.3	Fluid-Structure Interactions	
7.1.1.1.1.4	Supplementary Computer Program	2
7.1.1.1.1.5	Load Application	
7.1.1.1.1.5.1	SRV Discharge loads	
7.1.1.1.1.5.2	LOCA Related Loads	
7.1.1.1.1.6	Analysis	
7.1.1.1.1.6.1	Response Spectrum Analysis	
7.1.1.1.1.6.2	Stress Analysis	
7.1.1.1.2	Seismic Loads	
7.1.1.1.3	Static and Thermal Loads	
7.1.1.1.4	Load Combinations	
7.1.1.1.5	Design Assessment	
7.1.1.1.6	Equipment Hatch	
7.1.1.1.6.1	Structural Model	6
7.1.1.1.6.1	Loads and Load Combinations	
7.1.1.1.6.3	Design Assessment	
7.1.1.2	Reactor and Control Building	
7.1.1.2.1	Hydrodynamic Loads	
7.1.1.2.1.1	Structural Model	
7.1.1.2.1.2	Load Application	2
7.1.1.2.1.2.1	SRV Discharge loads	
7.1.1.2.1.2.2	LOCA Related Loads	
7.1.1.2.1.3	Analysis	
7.1.1.2.1.3.1	Response Spectrum Analysis	
7.1.1.2.1.3.2	Stress Analysis	
7.1.1.2.2.2	Seismic Loads	
7.1.1.2.3	Static and Thermal Loads	13
7.1.1.2.4	Load Combinations	
7.1.1.2.5	Design Assessment	2
7.1.2	Structure Steel Assessment Methodology	
7.1.2.1	Downcomer Bracing	
7.1.2.1.1	Bracing System Description	
7.1.2.1.2	Structural Models	
7.1.2.1.3	Loads	
7.1.2.1.3.1	SRV Discharge Loads	
7.1.2.1.3.2	LOCA Related Loads	
7.1.2.1.3.3	Seismic Loads	6
7.1.2.1.3.4	Static & Thermal Loads	
7.1.2.1.4	Load Combinations	
7.1.2.1.5	Design Assessment	
7.1.2.2	SRV Support and Column	

7.1.2.2.1	Description of SRV Support Assemblies and Suppression Chamber Columns
7.1.2.2.2	Structural Models
7.1.2.2.3	Loads
7.1.2.2.3.1	SRV Discharge Loads
7.1.2.2.3.2	LOCA Related Loads
7.1.2.2.3.3	Seismic Load
7.1.2.2.3.4	Static Load
7.1.2.2.3.5	Load Combinations
7.1.2.2.3.6	Design Assessment
7.1.2.3	Openings in Containment Liner
7.1.2.3.1	Equipment Hatch-Personnel Air Lock
7.1.2.3.2	CRD Removal Hatch, etc.
7.1.2.3.3	Refueling Head & Support Skirt
7.1.3	Liner Plate Assessment Methodology
7.1.4	Downcomer Assessment Methodology
7.1.4.1	Downcomer System Description
7.1.4.2	Structural Model
7.1.4.3	Loads and Load Combinations
7.1.4.4	Design Assessment
7.1.4.5	Fatigue Evaluation of Downcomers in Wetwell Airspace
7.1.4.5.1	Loads and Load Combinations Used for Assessment
7.1.4.5.2	Acceptance Criteria
7.1.4.5.3	Method of Analysis
7.1.4.5.4	Results and Design Margins
7.1.5	BOP Piping and SRV System Assessment Methodology
7.1.5.1	Fatigue Evaluation of SRV Discharge Lines in Wetwell Air Volume
7.1.5.1.1	Loads and Load Combinations Used for Assessment
7.1.5.1.2	Acceptance Criteria
7.1.5.1.3	Methods of Analysis
7.1.5.1.4	Results and Design Margins
7.1.6	NSSS Assessment Methodology
7.1.6.1	NSSS Qualification Methods
7.1.6.1.1	NSSS Piping
7.1.6.1.2	Valves
7.1.6.1.3	Reactor Pressure Vessel, Supports and Internal Components
7.1.6.1.4	Floor Structure Mounted Equipment
7.1.6.1.4.1	Qualification Methods
7.1.6.1.4.1.1	Dynamic Analysis
7.1.6.1.4.1.1.1	Methods and Procedures
7.1.6.1.4.1.2	Testing
7.1.6.1.4.1.3	Combined Analysis and Testing
7.1.6.1.4.2	Computer Programs
7.1.7	Balance of Plant (BOP) Equipment Assessment Methodology
7.1.7.1	Hydrodynamic Loads
7.1.7.1.1	SRV Discharge Loads
7.1.7.1.2	LOCA Related Loads
7.1.7.2	Seismic Loads
7.1.7.3	Other Loads
7.1.7.4	Qualification Methods
7.1.7.4.1	Dynamic Analysis
7.1.7.4.1.1	Methods and Procedures

7.1.7.4.1.2	Appropriate Damping Values	2
7.1.7.4.1.3	Three Components of Dynamic Motions	
7.1.7.4.2	Testing	
7.1.7.4.3	Combined Analysis and Testing	
7.1.8	Electrical Raceway System Assessment Methodology	
7.1.8.1	General	
7.1.8.2	Loads	6
7.1.8.2.1	Static Loads	
7.1.8.2.2	Seismic Loads	
7.1.8.2.3	Hydrodynamic Loads	
7.1.8.3	Analytical Methods	
7.1.9	HVAC Duct System Assessment Methodology	
7.2 DESIGN CAPABILITY MARGINS		
7.2.1	Stress Margins	
7.2.1.1	Containment Structure	2
7.2.1.2	Reactor and Control Building	
7.2.1.3	Suppression Chamber Columns	
7.2.1.4	Downcomer Bracing	
7.2.1.5	Liner Plates	
7.2.1.6	Downcomers	
7.2.1.7	Electrical Raceway System	
7.2.1.8	HVAC Duct System	
7.2.1.9	BOP Equipment	
7.2.1.10	NSSS Equipment	6
7.2.1.11	NSSS and BOP Piping	
7.2.2	Acceleration Response Spectra	
7.2.2.1	Containment Structure	2
7.2.2.2	Reactor and Control Building	
7.2.3	Containment Liner Openings	
7.2.3.1	Equipment Hatch - Personnel Airlock	6
7.2.3.2	CRD Removal Hatch, etc.	
7.2.3.3	Refueling Head and Support Skirt	
7.3 FIGURES		
		2

CHAPTER 7

FIGURES

<u>Number</u>	<u>Title</u>
7-1	3-D Containment Finite Element Model (ANSYS MODEL)
2 7-2	Equivalent Modal Damping Ratio vs. Modal Frequency For Structural Stiffness - Proportional - Damping
7-3	Finite Element Soil - Structure Interaction Model
7-4	Containment Response Analysis
7-5	Containment Stress Analysis
7-6	Finite Element Containment Equipment Hatch Model
7-7	Reactor Building Response Analysis
7-8	Reactor Building Stress Analysis
7-9	Downcomer Bracing System - Plan View
7-10	Downcomer Bracing System - Connection Details
7-11	Downcomer Bracing System - Computer Model
7-12	SRV Support System - Plan View
6 7-13	SRV Support System Details
7-14	Finite Element Model of Column
7-15	Finite Element Model of Column
7-16	General Arrangement - Personnel Lock
7-17	Equipment Door Details
7-18	CRD Hatch Details
7-19	Refueling Head Details
7-20	Liner Plate Hydrodynamic Pressure Due to Chugging
7-21	Liner Plate Pressure - Normal Conditions
7-22	Liner Plate Hydrodynamic Pressure Due to Chugging and SRV
7-23	Liner Plate Pressure - Abnormal Condition
7-24	Downcomer with Vacuum Breaker and Detail of Cap

FIGURES (Cont.)

<u>Number</u>	<u>Title</u>
7-25	Downcomer Without Vacuum Breaker
7-26	Location Where Downcomer Fatigue Analysis was Performed

CHAPTER 7

TABLES

Number

Title

3	7-1	Maximum Spectral Accelerations of Containment Due to SRV and LOCA Loads at 1% Damping
	7-2	Maximum Spectral Accelerations of Reactor and Control Buildings Due to SRV and LOCA at 1% Damping
5	7-3	Usage Factor Summary of Downcomers
	7-4	Usage Factor Summary of SRV Discharge Lines
6	7-5	Downcomer and Bracing System Modal Frequencies

7.0--DESIGN ASSESSMENT

Loads on SSES structures, piping, and equipment are defined in Chapter 4. The methods by which these loads are combined are discussed in Chapter 5. The criteria for establishing design capability are stated in Chapter 6.

This chapter describes the assessment of the adequacy of the SSES design by comparing design capabilities with the loadings to which structures, piping, and components are subjected and demonstrating the extent of the design margin. The first section of this chapter discusses the methodology by which design capability and loads are compared. The second section summarizes the results of these comparisons.

7.1--ASSESSMENT METHODOLOGY

7.1.1--Containment and Reactor Building Assessment Methodology

7.1.1.1--Containment Structure

7.1.1.1.1--Hydrodynamic Loads

7.1.1.1.1.1--Structural Models

The dynamic analysis for the structural response of the containment and internal structures due to the SRV discharge loads and LOCA loads is performed using the finite element method. The ANSYS (see Reference 75 and 76) finite element computer program was chosen for the transient dynamic analysis. Figure 7-1 shows the ANSYS finite element model. Beam elements and spar elements are used for the stabilizer truss. Lumped mass elements are used for the RPV internals and suppression pool fluid. Spring-damper elements are used to model the rock foundation. The ANSYS model includes a total of 761 elements and 200 dynamic degrees of freedom.

The soil structure interaction is taken into consideration by modelling the soil using a series of discrete springs and dampers in three directions as shown in Figure 7-1. The properties of the discrete springs and dampers are calculated based on the formulae for lumped parameter foundations found in Reference 33. The validity of this soil model is proven by comparing the results with those of an independent model which represents the soil by finite elements.

7.1.1.1.1.2 Damping

a. Structural Damping

The equations of motion for a discretized structure must include a term to account for viscous damping that is linearly proportional to the velocity. The equations of motion for a damped system are:

$$[M] \{\ddot{r}\} + [C] \{\dot{r}\} + [K] \{r\} = \{R(t)\}$$

where $[C]$ is the viscous damping matrix.

A viscous damping matrix of the form

$$[C] = \alpha [M] + \beta [K] \quad \text{was used (Reference 53).}$$

Where α and β are proportionality constants which relate damping to the velocity of the nodes and the strain rates respectively. This damping matrix leads to the following relation between α and β and the damping ratio of the i th mode C_i :

$$C_i = \alpha / 2\omega_i + \beta \omega_i / 2$$

where ω_i is the natural frequency of the i th mode. For the usual case of only structural damping, $\alpha = 0$ and therefore

$$\beta = \frac{2C_i}{\omega_i}$$

Since only a single value of β is permitted in the ANSYS input, the most dominant natural frequency of the structure is selected for the computation of β (See Reference 54).

A value of β equal to 0.00063 is used in the ANSYS model which corresponds to structural modal damping of approximately 4 percent of critical at 20 Hz which is the most dominant natural frequency of the structure.

Figure 7-2 shows modal damping ratio versus modal frequency for structural stiffness-proportional-damping.

b. Soil Springs and Radiation Damping

The elastic half-space theory as described by Reference 33 (BC-TOP-4A Rev. 3) were used to compute the values of the Spring Constants and dampers in the horizontal and vertical directions (K_H , K_V , C_H & C_V). The following parameters are used to represent the rock foundation:

G = Shear Modulus of foundation medium

= 1.154×10^3 KSI

ν = Poisson's ratio of foundation medium

= 0.3

V_s = Shear wave velocity

= 6180 ft/sec

From which we get the following:

K_H = 3.37×10^6 K/in

C_H = 1.57×10^4 K-sec/in

K_V = 3.96×10^6 K/in

C_V = 2.72×10^4 K-sec/in

The above lumped foundation springs and dampers were then distributed to every node on the basemat according to the tributary area.

7.1.1.1.1.3 Fluid-Structure Interaction

6 For the application of SRV loads described in Section 4.1, a finite element model of the containment was developed in which the suppression pool water was included. The water mass constitutes only one seventh of the total mass of the reinforced concrete structure. The model used considers fluid-structure coupling by lumping the water mass in the suppression pool at each nodal point of the wetted surface. The weighted area approach is considered to determine the fluid mass at each node of the suppression pool.

For the application of the LOCA steam condensation loads, based on the containment wall pressure time histories calculated by the acoustic methodology (see Subsection 9.5.3.4.1 and 9.5.3.4.2), the water mass was excluded. The exclusion of the water-mass is due to the fact that fluid structure interaction was already considered during the pressure time history calculations (Reference 65).

7.1.1.1.1.4 Supplementary Computer Programs

Supplementary computer programs were used for preprocessing and postprocessing of data generated for or by the ANSYS computer program.

A preprocessing program called CHUG was developed to convert the pressure time history forcing functions into concentrated force time - history forcing functions acting at the associated nodes of the ANSYS model. The program writes the nodal forces onto a file for processing by ANSYS.

2 A postprocessor program was developed to calculate the acceleration time history. This program is called DISQ. It reads the structural response displacement time histories generated from ANSYS displacements, scans the maximum displacements and generates the acceleration time histories using the Fast Fourier Transformation method.

Bechtel inhouse computer program MSPEC was used to compute the acceleration response spectrum obtained from DISQ. The program also performs plotting and broadening of the spectrum.

A computer program ENVLP was developed to generate envelopes of a number of spectrum obtained from MSPEC.

Computer program FORCE was developed to scan the maximum absolute stresses generated by ANSYS stress pass. A further explanation of FORCE is found in Subsection 7.1.1.1.6.2.

Verification of CHUG, DISQ, ENVLP and FORCE are available for review.

7.1.1.1.1.5 Load Application

7.1.1.1.1.5.1 SRV Discharge Loads

The SRV loads have been defined in Section 4.1 based on KWU SRV Traces #76, 82 and 35. 6

To obtain the maximum response of the containment due to bubble oscillation, a wide range of frequency content of the forcing function is considered.

The range of frequencies specified by KWU is between 55% and 110% of the frequencies of the three original traces as present in Subsection 4.1.3.5. 2

Based on the natural frequencies and the mode shapes of the primary containment as shown in Appendix B-1, five different frequencies in the range specified are selected in order to obtain the maximum structural response. The five frequency values are considered for each of the three original KWU pressure-time history traces which result in fifteen pressure-time histories to be considered.

As described in Subsection 4.1.3, four pressure distributions depending upon the number of valves actuated are considered; i.e., "All valve, ADS, asymmetric, and single valve". However, the azimuth distribution on the periphery indicates that the all valve case governs the ADS case for the symmetric loading and the asymmetric case governs the single valve case for the asymmetric loading. Therefore, the design assessment is based on only two cases, i.e., "symmetric and asymmetric". 16 2

7.1.1.1.1.5.2 LOCA Related Loads

The LOCA loads are based on LOCA steam condensation tests performed by Kraftwerk Union AG (KWU) at their GKM-II-M test facility. Section 9.0 describes the test facility, test matrix, test results and the GKM-II-M LOCA load definition developed to re-evaluate SSRS for chugging and condensation oscillation. 6

7.1.1.1.1.6 Analyses

7.1.1.1.1.6.1 Response Spectrum Analysis

The structural finite element model of containment as outlined in Subsection 7.1.1.1.1.1 is solved by "Reduced Linear Transient Dynamic Analysis" of the ANSYS computer program. The description of the analysis and the data input are contained in References 75 and 76, respectively. 6

For each set of pressure time histories, based on the analytical procedure in Figure 7-4, acceleration response spectra were generated at 52 dynamic degrees of freedom in the containment. The response spectra of several frequencies, traces, load

conditions and nodal points were enveloped into one set of response spectra curves which represent SRV and LOCA.

The response spectra were generated in two pairs of damping values, the low and the high dampings. The low damping values are 0.5, 1, 2 and 5 percent of critical, and the high damping values are 7, 10, 15 and 20 percent of critical. The peak frequencies of the spectra are broadened by 15% and 20% for low and high damping values, respectively.

Appendix B contains the above response spectra for low damping values at 9 locations.

7.1.1.1.1.6.2--Stress Analysis

The ANSYS computer program (stress pass) is used to compute the force and moment resultants due to SRV and LOCA related loads. A postprocessor program called "FORCE" is developed and used to scan for the maximum absolute values of forces and moments in the azimuth direction.

A multiplier factor for the force and moment resultants due to SRV loads has been established to cover for all the range of frequencies as specified in Subsection 7.1.1.1.5.1. The following procedure is used to establish the multiplier.

A statistical analysis of all the forces and moments obtained from the three traces with varying frequencies in the range specified is performed. Trace number 82 is taken as the base to establish a multiplier factor to cover the other 2 traces and the variation of frequencies since it is observed to develop the highest stresses at most cross-sections. A multiplication factor of 1.7 is established to be applied to the resultant forces and moments from Trace #82 SRV discharge loading.

The forces and moments due to Chugging and Condensation Oscillation (CO) loads are considered. From the response spectra plots of Chugging and CO loads, it was found that KWU Sources 306 and 303 were the controlling cases. Therefore, these two load cases have been analyzed for stresses in containment. The displacement-time histories obtained from the GKM-II-M load definition (see Subsection 9.5.3) are inputted to ANSYS computer model. A post processor program called SCALE was used to scan for the maximum values of forces and moments in the azimuth direction for each load case. For the containment sections shown in Figure A-2, the envelope of force resultants for all the load cases was inputted to the CECAP computer analysis (Refer to Flow Chart, Fig. 7-5, for further information).

7.1.1.1.2--Seismic Loads

Seismic loads constitute a significant loading in the structural assessment. The same seismic loads as those used in the initial building design are used. In that design, a dynamic analysis was made using discrete mathematical idealization of the entire

structure using lumped masses. The resulting axial forces, moments, and shear at various levels due to the Operating Basis Earthquake and the Safe Shutdown Earthquake are used (see section 3.7 of PSAR). The effects of the seismic overturning moment and vertical accelerations are converted into forces at the elements.

As required by NUREG 0487, the effect of sloshing on the containment due to horizontal and vertical SSE is investigated by performing a time-history analysis. As described in Subsection 4.2.4.7, pressure time histories due to seismic slosh were generated for input to the ANSYS model shown in Figure 7-1.

The response spectra generated from the seismic slosh load are presented in Figures B-51 to B-58. By inspection, the peaks are small.

7.1.1.1.3 Static and Thermal Loads

The loads under consideration are the static loads (dead load and accident pressure) and temperature loads (operating and accident temperature) which are all axisymmetrical.

- a. To analyze the above static loads, an inhouse computer program FINEL is used. Moments, axial and shear forces are computed by FINEL in an uncracked axisymmetric finite element containment model.
- b. The operating and accident temperature gradients are computed using ME 620 computer program (Bechtel program). This procedure is discussed in Subsection 3.8.4.1 of the PSAR.
- c. The results from a, b and the dynamic/seismic analysis are combined and applied to a containment element. The element contains data relative to rebar location, direction and quantity and concrete properties. Within that wall element an equilibrium of forces and strains compatibility is established by allowing the concrete to crack in tension. In this way the stresses in the rebar and concrete are determined. The program used for this analysis is called CECAP. For further explanation, see Figure 7-5.

7.1.1.1.4 Load Combinations

All load combinations from 1 through 7a as presented on Table 5-1 have been analyzed. This was done under step c of Subsection 7.1.1.1.3 above. If all the SRV actuation cases and chugging-symmetric and asymmetric-loading along with other loads are to be considered, 41 loading combinations would have to be assessed.

Some of these load combinations have been eliminated by inspection since they are not governing. The five basic load combinations which have been assessed and presented in this report are 1, 4, 4a, 5a and 7a.

The reversible nature of the structural responses due to the pool dynamic loads and seismic loads is taken into account by considering the peak positive and negative magnitudes of the response forces and maximizing the total positive and negative forces and moments governing the design.

Seismic and pool dynamic load effects are combined by summing the peak responses of each load by the absolute sum (ABS) method. This is conservative and the square root sum of squares (SRSS) method is more appropriate since the peak effects of all loads may not occur simultaneously. However, the conservative ABS method is used in the design assessment of the containment and internal concrete structures in order to expedite licensing.

7.1.1.1.5--Design Assessment

2 Material stresses at the critical sections in the primary containment and internal concrete structure are analyzed using the CECAP computer program. Critical sections for bending moment, axial force and shear in three directions are located throughout the containment structure. The liner plate is not considered as a structural element. The CECAP program considers concrete cracking in the analysis of reinforced concrete sections. CECAP uses an iterative technique to obtain stresses considering the redistribution of forces due to cracking and in the process it reduces the thermal stresses due to the relieving effect of concrete cracking. The program is also capable of describing the spiral and transverse reinforcement stresses directly. The input data for the program consists of the uncracked forces, moments and shears calculated by FINEL, ANSYS, and seismic analysis. The loads are then combined in accordance with Table 5-1 with appropriate load factors.

7.1.1.1.6--Equipment Hatch

There are two equipment hatch openings in the containment drywell wall at approximately El. 723 ft. The openings are 180° apart and have a diameter of approximately 12 ft. Concrete and rebar stresses around the local hatch area were assessed.

7.1.1.1.6.1--Structural Model

6 Figure 7-6 shows the STARDYNE finite element model that was developed for analysis of the drywell wall around the hatch opening. The model consists of a section of the drywell wall, diaphragm slab, and wetwell wall with all boundaries at least two hole diameters away from the edge of the opening. All loads can be considered as symmetric about the opening centerline, thus only one half of the opening was modeled. The model uses quadrilateral plate elements with both membrane and bending stiffnesses. Uncracked sections with concrete material properties were used. Loads were applied statically and boundary conditions were chosen to be consistent with the type of loading applied (Ref. BC Topical Report #5).

7.1.1.1.6.2 Loads and Load Combinations

Load combinations are as per Table 5-1. Hydrodynamic loads applied to the model boundaries were taken from the force and moment results of the ANSYS containment model described in Section 7.1.1.1.1. Seismic loads were taken from force and moment results of the containment model as given in Section 7.1.1.1.2. Temperature was considered for the worst case wall gradient.

7.1.1.1.6.3 Design Assessment

Four critical sections around the hatch opening were used for assessment. Moment and force resultants from the STARDYNE model were input to computer program CECAP (CE987) to determine stresses in the concrete and rebar.

7.1.1.2 Reactor and Control Buildings

7.1.1.2.1 Hydrodynamic Loads

7.1.1.2.1.1 Structural Model

The construction of the SSES reactor building is such that no direct coupling with the containment occurs. A 2 in. separation joint is kept between the containment structure and the reactor building at all levels where the two structures abut, except at the base slab where a cold joint exists. This arrangement minimizes the transfer of any direct dynamic response to the reactor building from the containment, where the SRV discharge and LOCA related hydrodynamic loads originate.

The horizontal motions of the containment are considered to be fully transferred to the reactor building through the cold joint at base slab; but the vertical motions are attenuated to account for the transfer through the rock under the two structures. The attenuation has been accounted for by using the weighted average acceleration time histories at different points away from the containment and to the end of the reactor building boundary. The weighted average acceleration is defined as:

$$\bar{a} = \frac{\sum_{i=1}^n A_i \ddot{a}_i}{\sum_{i=1}^n A_i} = \sum_{i=1}^n C_i \ddot{a}_i$$

in which \ddot{a}_i is the individual acceleration. A_i is the free field area on which the acceleration acts and C_i is the weighted average coefficient.

This average time history is applied as an input motion to the reactor building dynamic model. The finite element soil-structure interaction model used for the attenuation study is shown in Figure 7-3.

The mathematical model of the reactor and control buildings consists of lumped masses connected by the linear elastic members. Using the elastic properties of the structural components, the stiffness properties of the model are determined. The detailed description of the model is given in subsection 3.7b.2.1 of the PSAR. The models for North-South, East-West, and Vertical directions are shown in Figures C-1, C-2, and C-3 respectively in Appendix 'C'. These models are the same as those used for the seismic analysis.

7.1.1.2.1.2--Load Application

7.1.1.2.1.2.1--SRV Discharge Loads

2 The axisymmetric and asymmetric SRV discharge loadings used in the reactor building assessment are described in the chapter 4.1 of this report. During the axisymmetric loading, only the gross vertical motion of the base slab is transferred to the reactor building. Therefore, the broadened response spectra curves for axisymmetric loading given in Appendix 'C' are for vertical direction only. However, during the asymmetric loading, gross vertical motion as well as the gross horizontal motion of the base slab are considered in developing the vertical and horizontal response spectra curves for the reactor building. Therefore the broadened response spectra curves for asymmetric loading given in the Appendix 'C' are for both vertical and horizontal directions.

Three different pressure-time history traces (Figures 4-28 through 4-30 of Chapter 4) are used for generating response spectra curves at the base of reactor building over a wide range of frequencies, i.e., 55% to 110% of the original.

7.1.1.2.1.2.2--LOCA Related Loads

6 Loadings associated with Loss of Coolant Accident (LOCA) are briefly described in 7.1.1.1.5.2. The gross vertical and horizontal motions of the Containment base slab due to symmetric and asymmetric load conditions are transferred to the Reactor/Control Building. The vertical motions are attenuated and the horizontal motions are directly transmitted to the Reactor/Control Building foundation.

7.1.1.2.1.3--Analysis

7.1.1.2.1.3.1--Response Spectrum Analysis

6 The response analysis of Reactor/Control buildings was performed in three separate lumped mass models which simulate the E-W, N-S, and vertical responses. The models are shown on Figures C-1, C-2 and C-3. The analytical procedure is presented in the flow chart in Figure 7-7.

Like in the containment, the response spectra of loads from several frequencies, traces, load conditions and nodal points

were enveloped into one set of response spectra curves which represented SRV and LOCA.

The damping values included in generating the acceleration response spectra and broadening of the peak frequencies of the spectra are the same as in the containment structure.

Appendix C contains the acceleration response spectra for low damping values for SRV and LOCA.

7.1.1.2.1.3.2 Stress Analysis

The largest responses at the reactor building base due to all the hydrodynamic loadings are used to obtain forces and moments in the members of the reactor building. The damping values are 2% and 5% for load combinations involving OBE and SSE/LOCA respectively. For the first part of the analysis, the Bechtel Program CE 917 is used to do the modal analysis for the vertical, the East-West and the North-South directions. The results of these analyses are used for input to the Bechtel Program CE 918. Another input, the acceleration response spectra to CE 918 program, is the envelope of the spectra of the gross motion time-histories due to KWU Sources 303, 305, 306, 309 and 314, symmetric and asymmetric load cases. These are obtained from steps 12 and 15 of Figure 7-4. The analysis determines member axial forces, shear forces, and bending moments. The analytical procedure is presented in the flow chart in Figure 7-8. The following load cases are considered.

1. Condensation-Oscillation vertical for 2% and 5% dampings.
- 2a. SRV vertical symmetric and asymmetric for 2% and 5% dampings.
- 2b. SRV North-South asymmetric for 2% and 5% dampings.
- 2c. SRV East-West asymmetric for 2% and 5% dampings. Case 2c involved four separate conditions depending on the positions of the Reactor Building crane.
- 3a. LOCA vertical symmetric and asymmetric for 2% and 5% dampings.
- 3b. LOCA North-South symmetric and asymmetric for 2% and 5% dampings.
- 3c. LOCA East-West symmetric and asymmetric for 2% and 5% dampings.

The combined forces and moments in the members due to LOCA, SRV, and seismic loads for both 2% and 5% damping values in each of the vertical, East-West, and North-South directions were determined (see Figures E-23 thru E-32).

2 The reactor building superstructure steel was analyzed separately using a 3-D finite element lumped mass model. The model is shown in Figure E-21. The bridge crane and crane girders were also modeled. The dynamic analysis was done using the time-history method for seismic loads and response spectrum method for hydrodynamic loads with Bechtel computer program BSAP. Member forces and moments were generated for several different crane and trolley positions. In general, the members experienced their highest stresses when the bridge cranes were positioned such that the maximum possible tributary load is distributed to the columns. The critical case is when bridge crane bumper strikes on one side of the superstructure during SSE or OBE. The results are described in Subsection 7.2.1.2.

The refueling pools and girders were analyzed separately using a 3-D finite element model. The structure contains the surge tanks vault, fuel shipping cask storage pool, spent fuel storage pool, reactor well, and the steam dryer and separator storage pool. For refuelling conditions, all compartments are considered full of water with the exception of the surge tanks vault, which is empty. For operating condition, only the spent fuel storage pool and the fuel shipping cask storage pool are full of water while the remaining compartments are empty. Water mass was lumped at the compartment floors for the dynamic analysis.

6 The dynamic analysis was done using the response spectrum method with the computer program STARDYNE. Static and thermal analyses were also performed on STARDYNE program.

The analysis was performed for critical load combinations which were established by inspection. The results are described in subsection 7.2.1.2.

The box section columns supporting the refueling pool girders were included in the finite element model of the refueling pool analyzed above. The displacements and reactions obtained from the above model were used to assess the structural strength and stability of the columns.

7.1.1.2.2 Seismic Loads

The seismic analysis methodology is discussed in the subsection 3.7b.2.1 of the PSAR.

7.1.1.2.3 Static and Thermal Loads

2 The static loads are discussed in the subsection 3.8.4.4 of the PSAR.

7.1.1.2.4 Load Combinations

All individual loads are combined with the appropriate load factors as shown in Table 5-1.

Steel structures are checked for the load combination listed in Table 5-2.

7.1.1.2.5 Design Assessment

Critical sections for bending moment, axial force and shear in all three directions are located throughout the reactor building. Design capability at the critical sections is determined and then the design capability is compared with the actual forces and moments acting on the sections under all the load combinations. This comparison yields design margins. The design margins are discussed in Section 7.2.1.2

7.1.2 Structural Steel Assessment Methodology

7.1.2.1 Downcomer Bracing

7.1.2.1.1 Bracing System Description

There are 87 downcomers which extend vertically from the diaphragm slab to El. 660'-0" in the wetwell, which is approximately 12 feet below normal water level. The five vacuum breaker downcomers have been capped (see Figure 7-25), however, with regards to the bracing system, these five downcomers still provide vertical and lateral support, since they were capped at the downcomer exits. Downcomers are 24" O.D. pipes with 3/8 inch wall thickness, and are embedded in the diaphragm slab. Downcomers are separated into four independent quadrants. At El. 668'-0" all downcomers within a quadrant are tied together laterally with a bracing system consisting of 6 inch O.D. XX-strong pipes. The bracing members are not connected to either the wetwell wall or pedestal, thus eliminating stresses due to thermal expansion and wetwell wall displacement during hydrodynamic loads. The downcomers support the bracing vertically. The bracing connections consist of 1/2" ring plates and vertical stiffeners. The SRVD lines are not connected to the bracing. Figures 7-9 and 7-10 Sheets 1-3 show a plan view of the bracing system and the bracing connection details, respectively.

7.1.2.1.2 Structural Models

A 3-D STARDYNE finite element model of both the bracing and downcomers was developed for analysis of both the downcomers and bracing. The worst case quadrant of the four was chosen for modeling (3 ADS lines in the vicinity of the quadrant). The chosen quadrant extends from containment radial of 345° to radial of 66.7°. This quadrant consists of 23 downcomers modeled as pipes and having fixed boundary conditions at the diaphragm slab. Bracing members are modeled as pipe elements between downcomers using the actual brace member lengths. Beam connector elements extend from the node at the center line of each downcomer to the end of the brace member. Connector elements have equivalent section properties chosen so as to match stiffnesses determined analytically from the finite element model of the bracing connections described later. A lumped water mass consisting of

two times the downcomer or bracing pipe volume (one time for the virtual mass effect and one time for the contained fluid) is used for nodes below the water level to account for the effect due to fluid-structure interaction. The model consists of 323 nodes, 251 pipe elements, 88 beam elements, and 276 dynamic degrees of freedom for reduced eigenvalue solution (STARDYNE HQR). Total weight considered in the model is 214.5 kips. Figure 7-11 (Sheets 1 & 2) shows the model.

A separate BSAP finite element model was developed for assessment of the bracing connection and downcomer in the vicinity of the connection. Figure 7-11, Sheet 3 shows the model. A section of the downcomer at the brace level is modelled with plate elements. Boundaries of the downcomer were taken sufficiently far away from the connection to eliminate their influence. The connector plates, top partial plates, main ring plates, vertical stiffeners, and top ring plates were modeled with plate elements. (see Figure 7-11, Sheet 3). Brace member forces from the STARDYNE downcomer and bracing analysis were used as input loads for the assessment of the connection shown in Figure 7-10, Sheet 3. The BSAP finite element model was also used to determine the stiffnesses of the connector elements used in STARDYNE.

7.1.2.1.3 Loads

The basis for all hydrodynamic loads considered, is given in Sections 4 and 9.

7.1.2.1.3.1 SRV Discharge Loads

SRV actuation results in fluid pressure loads acting on the containment, downcomers, and bracing. All loads are based on KWU Traces 76, 82, and 35. With respect to the downcomers and bracing, two different types of loads can be defined. One type consists of inertia loading. This is movement of the containment structure due to SRV fluid pressures acting directly on the containment. The response spectrum method is used for analysis of this loading by applying the diaphragm slab spectra (El. 702'-3", see Appendix B) due to SRV to the STARDYNE model.

The second type of loads are described as submerged structure loads. These loads are due to the direct fluid pressures acting on the downcomers and bracing. As described in Subsection 4.1.3.7.3, potential flow theory and the method-of-images were used to calculate the load time histories for each downcomer in the model. These were applied to the STARDYNE model and a linear transient dynamic analysis was performed.

7.1.2.1.3.2 LOCA Related Loads

During a LOCA several types of loads act on the downcomers and bracing. Two of these are inertia and submerged structure loads. These have the same definition as for the SRV case and the analysis is performed in the same manner. This consists of the

response spectra method for inertia load analysis and linear transient dynamic analysis for submerged structure loads.

Subsection 4.2.2.5 describe the methodology for determining the downcomer drag loads due to CO and chugging.

The containment response spectra generated for CO and chugging were determined by the methodology documented in Subsection 9.5.3.

In addition to the above loads, a dynamic lateral load due to chugging at the downcomer tip also occurs. For analyzing multiple downcomers in a quadrant, the generic multi-vent lateral load definition documented in Subsection 4.2.2.4 is used.

In addition, as required by the NRC, a single vent impulse with a 65 kip amplitude and 3 msec duration is applied one time per LOCA event to any single downcomer. This is a low probability event and is only used to show that the downcomer would not fail for one such loading.

For both types of tip loads, several linear transient dynamic analyses were performed. Loads were applied in directions, so as to maximize forces and moments in the downcomers and braces.

Air clearing in the downcomers during a LOCA also produces poolswell drag and fallback loads on the bracing. This load occurs before Chugging and CO and need not be considered in combination with those LOCA loads. Bechtel Nuclear Staff defined the pressure time history loads on the braces and they were analysed locally for these loads (see Subsection 4.2.1.7). An overall equivalent static load on the bracing system was applied to the STARDYNE model.

7.1.2.1.3.3--Seismic Loads

The diaphragm slab response spectra developed for OBE and SSE as described in Subsection 3.8.1.4.1 of the PSAR were used as input to the STARDYNE model to obtain resultant forces in the downcomers and bracing.

In addition to the inertia loading, seismic sloshing in the suppression pool imparts loads on the downcomers and bracing (see Subsection 4.2.4.7). The sloshing frequency is very low and static loads based on the sloshing fluid pressures were applied to the STARDYNE model.

7.1.2.1.3.4--Static and Thermal Loads

The dead load of the downcomers and bracing is considered. The LOCA condition results in the worst temperature loading (Ref. Figure 4-52, Section 4). A maximum temperature of 180°F is used with 65° being taken as the stress free condition.

7.1.2.1.4 Load Combinations

Load combinations and allowable stresses are in accordance with Subsection 5.2. The stochastic loads, i.e., seismic inertia, and the inertia and submerged pressure loads of SRV and chugging are combined by SRSS method. The chugging lateral load is defined as a single impulse and is added by absolute sum method. The seismic sloshing loads are added by absolute sum method due to their low frequency wave. All the static loads are combined by absolute sum method. Poolswell is not combined with other LOCA loads since it precedes them (see Subsection 4.2.1).

7.1.2.1.5 Design Assessment

The results from the three dimensional STARDYNE model of the bracing and downcomers are combined to determine the total stress due to both axial forces and moments. A comparison between the calculated combined stresses and allowables is made and the stress margins are given in Appendix A.

7.1.2.2 SRV Support and Column

7.1.2.2.1 Description of SRV Support Assemblies and Suppression Chamber Columns

In the suppression pool, there are three types of support configurations to laterally brace the SRV discharge lines; two are at El. 666' and the third is at El. 667'. Each type of support assembly consists of two horizontal bracing members and at least one knee brace member. The support assemblies are connected from the SRV discharge lines to the adjacent column (or columns) with 4-inch diameter double extra strong pipes.

The support assemblies restrain the SRV discharge lines in a horizontal direction but not in vertical direction. The general plan of these support assemblies is shown in Figure 7-12 and member connection and the details are shown in Figure 7-13.

The suppression chamber columns are 42 inch diameter pipes with 1-1/4 inch wall thickness. The columns are attached at the diaphragm slab at El. 700' and at the basemat at El. 648'.

7.1.2.2.2 Structural Models

- a. The columns were independently analyzed for static and dynamic loads. The analytical methods used for non-hydrodynamic loads such as dead, live, pressure, temperature, seismic and pipe rupture loads are described in the PSAR, Section 3.8.3.4.5.
- b. For the hydrodynamic SRV loads, the ANSYS computer program was used. For the hydrodynamic LOCA related loads NASTRAN computer program was used. A typical column model is shown in Figure 7-14. The total length of the column is divided into beam elements which are joined at node points. An

effective water mass due to submergence was also considered. Dynamic horizontal forces were applied to the column at the node points below the water. Time-varying forces and moments in the column were calculated for each element.

- c. Another finite element model was developed in which the SRV lines, the SRV support assembly and the column were included. SRV and LOCA related submerged structure loads as well as the inertia effects from the dynamic loads were considered. From this analysis, the SRV discharge pipe's reactions at the support locations were obtained.

The assessment of the columns is based on the combination of loads obtained from a, b, and c above. The assessment of the SRV support assembly is based on loads obtained in paragraph c above. Each of the support types is analyzed separately.

In order to determine the local stresses in the vicinity of the support assembly on the column wall, the column was modeled with the NASTRAN computer program using plate finite elements. The model is shown in Figure 7-15.

7.1.2.2.3 Loads

The support assemblies of the SRV discharge lines are submerged structures. They are subjected to direct pressure loads from air bubble etc., the reactions from the SRV lines due to SRV discharge loads, and the inertia loads due to the building response from dynamic loads. Thermal loads are due to increase in pool temperature during LOCA.

7.1.2.2.3.1 SRV Discharge Loads

The horizontal SRV discharge pressure-time histories are considered as acting on the columns, the SRV discharge pipe and the support assemblies. The vertical SRV discharge pressures are considered as acting on the support assemblies alone.

The reactions from the SRV lines obtained from Subsection 7.1.2.2.2.c are applied to the end of the SRV support members for computation of longitudinal member forces. The direct hydrodynamic pressures due to SRV actuations are applied statically perpendicular to the SRV support members, with a dynamic magnification factors. The SRV hydrodynamic pressures are determined as defined in Subsection 4.1.3.7. This is done for the computation of moments and shear forces in the members.

The inertia forces from building responses due to SRV discharge load are also included by using the response spectra results shown in Appendix B.

Member forces and moments obtained from direct application of SRV discharge pressures, reaction forces of SRV pipe line, and the inertia building responses are combined by absolute sum.

The SRV submerged structure load definition is based on Subsection 4.1.3.7.

7.1.2.2.3.2--LOCA-Related-Loads

During a LOCA, several phenomena cause hydrodynamic loads on the SRV support assemblies. The manner in which the LOCA related loads are applied to the SRV support assemblies is exactly the same as described for the SRV loads in Subsection 7.1.2.2.3.1. The LOCA related loads used for the bracing are used for the SRV support assemblies, except the lateral tip load due to chugging is eliminated.

Among the LOCA related loads, poolswell load and fallback load occur before Chugging and CO and need not be considered in combination with those LOCA loads. The pressure time history loads, due to pool swell, for the SRV assembly supports, were determined by linearly reducing the pressure time history, due to poolswell, for the downcomer bracing, by the ratio of the diameters.

7.1.2.2.3.3--Seismic-Load

The seismic loads on the coupled structure of SRV lines, support assemblies, and columns were obtained by dynamic analysis using the response spectra developed for OBE and SSE as described in Subsection 3.8.1.4.1 of the PSAR.

7.1.2.2.3.4--Static-Load

The dead load, thermal load and bouyancy of the support assemblies were considered.

7.1.2.2.3.5--Load-Combinations

The load combinations and allowable stresses are in accordance with Subsection 5.2. Although the loads on the bracing system under consideration act in a random horizontal directions, each individual load is applied to the system in the worst possible direction to find the maximum resultant forces.

7.1.2.2.3.6--Design-Assessment

The combined stresses due to axial forces and bending moments were determined for all bracing members. Comparison between the resulting calculated stresses and the allowable stresses has been made. Resulting stress margins for the bracing members and their connections are tabulated in Appendix A.

7.1.2.3--Openings-In-Containment-Liner

7.1.2.3.1--Equipment-Hatch-Personnel-Air-Lock

The portion of the equipment hatch-personnel air lock not backed by concrete was reevaluated for additional loads due to

hydrodynamic effects (SRV and LOCA). This reevaluation was performed by Chicago Bridge and Iron Company (CBI) under subcontract from Bechtel. The general arrangement of the personnel lock is shown in Figure 7-16.

The personnel air lock doors are designed to withstand a pressure of 55 psig in the containment vessel. The door mechanism is designed to seal the door against an internal pressure of 5 psig.

For reevaluation, CBI used their computer program E781 for static analysis of shells. The program is based on Reference 77. Equivalent static loads were considered for seismic and hydrodynamic cases using peak spectral accelerations. CBI used the hydrodynamic spectra as given in Appendix C. Design Load combinations given in Table 5-2 were used with modifications for forces on the structure due to thermal expansion of pipes under accident conditions. Stress limits specified in the ASME code were used.

CBI's model was divided into 2 parts:

The first model comprised the 1" thick cylinder and the 3" thick flange extending to the parting joint. An axisymmetrical configuration was used since the shape of the containment vessel at its intersection with the equipment hatch is conical. No restraints at the junction with the containment vessel were considered.

The second model included the 3" thick flange beyond the parting joint, the conical head and a portion of the personnel lock extending from the interior bulk head to an appropriate distance beyond.

At the flange interface, the seismic, SRV, LOCA, jet and pressure loads have a tendency of prying open the door. A meridional force is, therefore, required to permit relatively small radial deflections and rotations at the interface. This force was applied as a restoring force at the parting joint in the form of a meridional force and a transverse shear. Relative displacements were evaluated to assure leaktightness.

The major dead load contribution is in the airlock. Therefore, dead loads and loads from seismic accelerations were applied to the second model as discontinuous loads at the center of gravity of the air lock.

Loads due to SRV, Seismic and LOCA cases were combined by SRSS.

7.1.2.3.2_CBI_Remove_Hatch_Suppression Chamber Access Hatch And Equipment Hatch

These hatches were subcontracted to CBI for design and analysis for additional SRV and LOCA loads. Designs were performed manually in accordance with Bechtel specifications and

appropriate design codes. Details of the CRD removal hatch and equipment hatch are given in Figures 7-17 and 7-18.

7.1.2.3.3 Refuelling Head and Support Skirt

Reevaluation of the refuelling head and support skirt was performed by CBI under subcontract from Bechtel. Figure 7-19 shows the refuelling head.

CBI's program E 781 was used for the static analysis. For dynamic analysis, equivalent pressures from the peak response spectra at El. 778.8 ft. were used. The static and dynamic stresses were then combined as per Table 5-2 of this report. Leak tightness of the flanged joint was investigated for the various loads and suitable pre-stress was recommended to prevent separation of the flange joint components.

7.1.3 Liner Plate Assessment Methodology

PSAR Subsection 3.8.1 provides a description of the liner plate and anchorage system for the containment.

The analysis of the liner plate and anchorages for nonhydrodynamic loads is in accordance with Reference 18.

For the analysis of the liner plate and anchorage for hydrodynamic suction loads, the contributing load on the liner is that due to the net "negative" pressure.

The loads considered for this assessment are KWU Chugging, KWU SRV, hydrostatic pressure and wetwell air pressure.

Figure 7-20 presents the maximum negative pressure due to KWU chugging which were scanned from the symmetric and asymmetric load conditions of Sources 303, 305, 306 and 309. As can be noted from Figure 7-20, Trace 306 gives the maximum negative pressure on all locations.

The maximum negative pressure due to the actuation of all SRV's is -7.8 psi.

The hydrostatic pressure of 24' water gives 10.4 psi pressure on the base slab liner plate.

The wetwell air pressure is 25 psi due to a small break LOCA.

For normal condition the combination of hydrostatic pressure and the actuation of all the SRV's is considered. The distribution of this pressure is shown in Figure 7-21.

For abnormal condition, the combination of KWU chugging, SRV, hydrostatic pressure and wetwell air pressure is considered. The phasing of SRV and chugging events is obtained by aligning the maximum suction peaks. These events are combined by direct addition of pressures as demonstrated in Figure 7-22. The total

net peak pressures for the abnormal condition are tabulated in Figure 7-23. Point 1 in this figure does not lie on pressure boundary and thus, is not critical.

The assessment of liner plate is found in Subsection 7.2.1.5.

7.1.4 Downcomer Assessment Methodology

7.1.4.1 Downcomer System Description

In the wetwell, there are 87 downcomers, 82 of which function as dry well vents during a LOCA. The other 5 provide wetwell to drywell pressure relief through the two vacuum breakers in series mounted on each of them. These five downcomers are capped at the bottom end to protect the vacuum breakers from the cycling due to chugging. Appendix K provides the assessment of capping five of the eighty-seven downcomers as a fix for VB cycling during chugging.

Downcomer layout, location of vacuum breakers and the cap arrangement are shown on Figures 7-9, 7-24 and 7-25, respectively.

7.1.4.2 Structural Model

The downcomers are modeled with the bracing system as described in Subsection 7.1.2.1.2.

The downcomers with the vacuum breakers are included in the STARDYNE model.

An additional 3-D model was developed in which not only the bracing system and downcomers as described in subsection 7.1.2.1.1 were included, but also the vacuum breaker, the vacuum breaker support and a column. This was done in the same quadrant as described in Subsection 7.1.2.1.1.

7.1.4.3 Loads and Load Combinations

Loads affecting the downcomers are the same as those described in Subsection 7.1.2.1.3. Load combinations are given in Table 5-3. The SRSS sum is used for the dynamic loads, except for the chugging lateral and seismic sloshing loads which are added by absolute sums as described in Subsection 7.1.2.1.4.

7.1.4.4 Design Assessment

Reference 30 is used for checking the downcomer stresses due to the load combinations given in Table 5-3.

7.1.4.5 Fatigue Evaluation of Downcomers In Wetwell Air Volume

In an effort to evaluate the steam bypass potential arising from a failure of the downcomers in the wetwell air space, a complete fatigue analysis of the same has been performed. Specifically, the analysis was performed where the downcomers penetrate the diaphragm slab as shown in Figure 7-26. This analysis considered all the cyclic loading acting on the downcomers and is in accordance with the applicable portions of ASME Code. This evaluation is considered supplemental and does not displace the original design basis for these lines as set forth in the appropriate FSAR/DAR sections.

7.1.4.5.1 Loads and Load Combinations used for Assessment

The downcomers are subject to numerous dynamic and hydrodynamic loads from normal, upset, and LOCA-related plant operating conditions. For purposes of fatigue evaluation, the following loads are included: (1) All significant thermal and pressure transients. (2) All cyclic effects due to the hydrodynamic loads including SRV actuations, CO and chugging. (3) Seismic effects. A description of each of these loads is provided in the appropriate DAR sections. The determination of load combinations as well as number and duration of each event is obtained from the applicable sections of DFFR, and FSAR.

7.1.4.5.2 Acceptance Criteria

The design rules, as set forth in the ASME Boiler and Pressure Vessel Code, Section III, Subsection NB were utilized for the fatigue assessment. When required, allowables for fatigue stress evaluation were based on Mill certification reports for downcomers.

7.1.4.5.3 Methods of Analysis

The SRV discharge lines and downcomers in the wetwell air volume, were analyzed for the appropriate load combinations and their associated number of cycles. The combined stresses and corresponding equivalent stress cycles were computed to obtain the fatigue usage factors in accordance with the equations of Subsection NB-3600 of the ASME Code.

7.1.4.5.4 Results and Design Margins

The cumulative usage factors for the various loading conditions for the downcomer (see Figure 7-26) are summarized in Table 7-3.

7.1.5 BOP Piping and SRV Systems Assessment Methodology

The BOP piping and SRV systems were analyzed for the loads discussed in Section 5.5 using Bechtel computer programs ME101 and ME632. These programs are described in FSAR Section 3.9. Static and dynamic analysis of the piping and SRV systems are performed as described in the paragraphs below.

Static analysis techniques are used to determine the stresses due to steady state loads and/or dynamic loads having equivalent static loads. The drag and impact loads are applied as equivalent static loads.

Response spectra at the piping anchors are obtained from the dynamic analysis of the containment subjected to LOCA and SRV loading. Piping systems are then analyzed for these response spectra following the method described in Reference 19.

Time history dynamic analysis of the SRV discharge piping subjected to fluid transient forces in the pipe due to relief valve opening is performed using Bechtel computer code ME632.

7.1.5.1 Fatigue Evaluation of SRV Discharge Lines in Wetwell Air Volume

In an effort to evaluate the steam bypass potential arising from a failure of the SRV discharge line in the wetwell air space, a complete fatigue analysis of the same has been performed. Specifically, structural analyses of all the SRV discharge lines from the diaphragm slab penetration to the quencher was performed. Fatigue evaluation of fluehead penetration, elbows and 3-way restraint attachment to pipe was done. This analysis considered all the cyclic loading acting on the SRV discharge lines and is in accordance with the applicable portions of ASME Code. This evaluation is considered supplemental and does not displace the original design basis for these lines as set forth in the appropriate PSAR/DAR sections.

7.1.5.1.1 Loads and Load Combinations Used for Assessment

The SRV discharge lines are subject to numerous dynamic and hydrodynamic loads from normal, upset, and LOCA-related plant operating conditions. For purposes of fatigue evaluation, the following loads are included: (1) All significant thermal and pressure transients. (2) All cyclic efforts due to the hydrodynamic loads including SRV actuations, CO and chugging and (3) Seismic effects. A description of each of these loads is provided in the appropriate DAR sections. The determination of load combinations as well as number and duration of each event is obtained from the applicable sections of DFFR and PSAR.

7.1.5.1.2 Acceptance Criteria

The design rules, as set forth in the ASME Boiler and Pressure Vessel Code, Section III, Subsection NB were utilized for the fatigue assessment. When required, allowables for fatigue stress evaluation were based on Mill certification reports for SRV discharge lines.

7.1.5.1.3 Methods of Analysis

The SRV discharge lines, in the wetwell air volume, were analyzed for the appropriate load combinations and their associated number

of cycles. The combined stresses and corresponding equivalent stress cycles were computed to obtain the fatigue usage factors in accordance with the equations of Subsection NB-3600 of the ASME Code.

7.1.5.1.4 Results and Design Margins

The cumulative usage factors for fluehead, 3-way restraint attachment to pipe and elbow are summarized in Table 7-4.

7.1.6 NSSS Assessment Methodology

"Safety related" General Electric Company supplied NSSS piping and equipment located within the containment and the reactor and control buildings are subjected to hydrodynamic loads due to SRV and LOCA discharge effects principally originating in the suppression pool of the containment structure. Section 4.1 and 4.2 describe the methodologies used to define these SRV and LOCA loads, respectively. The NSSS piping and equipment are assessed to verify their adequacy to withstand these hydrodynamic loads in combination with seismic and all other applicable loads in accordance with the load combinations given in Table 5-5.

The structural system responses for the SRV and LOCA suppression pool hydrodynamic phenomena are generated by Bechtel Power Corporation using defined forcing functions. These structural system responses are transmitted to General Electric in the form of (1) broadened response spectra and (2) acceleration time-histories at the pedestal to diaphragm floor intersection and the stabilizer elevation.

The response spectra for piping attachment points on the reactor pressure vessel, shield wall and pedestal complex (above the pool area) are generated by General Electric, based upon the acceleration time-histories supplied by Bechtel Power Corporation, using a detailed lumped mass beam model for the reactor pressure vessel internals, including a representation of the structure. For the assessment of the NSSS primary piping (main steam and recirculation) a combination of General Electric and Bechtel developed response spectra are used as input responses for all attachment points of each piping system. For the assessment of the NSSS floor mounted equipment, except the reactor pressure vessel, the broadened response spectra supplied directly by Bechtel are used.

The acceleration time-histories and the detailed reactor pressure vessel and structure lumped mass beam model are used to generate the forces and moments acting on the reactor pressure vessel supports and internal components. These forces and moments are used for the GE assessment of reactor pressure vessel supports and internals.

The structural system response for the LOCA induced annulus pressurization transient asymmetric pressure build up in the annular region between the biological shield wall and the reactor

pressure vessel is based on pressure time-histories supplied by Bechtel. These pressure time-histories are combined with jet reaction, jet impingement and pipe whip restraint loads for the assessment. A time-history analysis is performed resulting in accelerations, forces and moment time-histories as well as response spectra at the piping attachment points on the reactor pressure vessel, shield wall, pedestal, pressure vessel supports and external components (see FSAR Appendices 6A and 6B).

7.1.6.1--NSSS Qualification Methods

7.1.6.1.1--NSSS Piping

The NSSS piping stress analyses are conducted to consider the secondary dynamic responses from: (1) the original design-basis loads including seismic vibratory motions, (2) the structural system feedback loads from the suppression pool hydrodynamic events, and (3) the structural system loads from the LOCA induced annulus pressurization from postulated feedwater, recirculation and main steam pipe breaks.

Lumped mass models are developed by General Electric for the NSSS primary piping systems, main steam and recirculation lines. These lumped mass models include the snubbers, hangers and pipe mounted valves, and represent the major balance of the plant branch piping connected to the main steam and recirculation systems. Amplified response spectrum for all attachment points within the piping system are applied; i.e., distinct acceleration excitations are specified at each piping support and anchor point. The detailed models are analyzed independently to determine the piping system resulting loads (shears and moments) for:

- 1) each design-basis load which includes pressure, temperature, weight, seismic events, etc.,
- 2) the bounding suppression pool hydrodynamic event; and
- 3) the annulus pressurization dynamic effects on the unbroken piping system.

Additionally, the end reaction forces and/or accelerations for the pipe mounted/connected equipment (valves and nozzles) are simultaneously calculated.

The piping stresses from the resulting loads (shears and moments) for each load event are determined and combined in accordance with the load combinations delineated in Table 5-5. These stresses are calculated at geometrical discontinuities and compared to ASME code allowable determined stresses (ASME Boiler and Pressure Vessel Code, Section III-NB-3650) for the appropriate loading condition in order to assure design adequacy. Computer codes used to perform the NSSS piping stress analysis are described in FSAR Section 3.9.1.2.

7.1.6.1.2__Valves

The reaction forces and/or accelerations acting on the pipe mounted equipment when combined in accordance with the required load combinations are compared to the valve allowables to assure design adequacy. The reactor core pressure boundary valves are qualified for operability during seismic and hydrodynamic loading events by both analysis and test. This qualification is unique for each valve.

7.1.6.1.3__Reactor Pressure Vessel, Supports and Internal Components

The bounding load combinations for seismic, hydrodynamic and annulus pressurization forces are established within each acceptance criteria range (upset, emergency and faulted). At the initial analysis step, the loads are conservatively combined using the maximum vertical forces with the maximum horizontal shears and moments from all combinations within each acceptance criteria range. These conservative maximum loads are then compared to generic bounding forces originally used to establish the component design. When the combined calculated forces are less than the design forces, then the component is deemed adequate. When the calculated forces are greater than the design forces, then the increased stresses are compared to the material allowables. When the calculated stresses are below the material allowables, then the design is deemed adequate. If the increased stresses are above the material allowables, then the specific load combination is identified and another stress analysis is conducted using refined methods, if required, to demonstrate the component adequacy.

In certain cases, component test results are combined with analyses to assess component adequacy. Fatigue evaluations of the Reactor Pressure Vessel, supports and internal components are also conducted for SRV cyclic duty loads. The equipment is analyzed for fatigue usage due to SRV load cycles based upon the loading during the SRV events. SRV fatigue usage factors are calculated and combined with all other upset condition usage factors to obtain a cumulative fatigue usage factor.

Computer programs used to conduct RPV component analyses are described in FSAR Section 3.9.1.2.

7.1.6.1.4__Floor Structure Mounted Equipment

7.1.6.1.4.1__Qualification Methods

The adequacy of the design of the equipment is assessed by one of the following:

- a. Dynamic analysis
- b. Testing
- c. Combination of testing and analysis

The choice is based on the practicality of the method depending upon function, type, size, shape, and complexity of the equipment and the reliability of the qualification method.

In general, the requirements outlined in IEEE-344-75, Reference 55, are followed for the qualification of equipment.

7.1.6.1.4.1.1--Dynamic Analysis

7.1.6.1.4.1.1.1--Methods and Procedures

The dynamic analysis of various equipment is classified into three groups according to the relative rigidity of the equipment based on the magnitude of the fundamental natural frequency described below.

- (a) Structurally simple equipment - comprises that equipment which can be adequately represented by a one degree of freedom system
- (b) Structurally rigid equipment - Comprises that equipment whose fundamental frequency is:
 - (i) greater than 33 Hz for the consideration of seismic loads, and,
 - (ii) greater than the high frequency asymptote (ZPA) of the required response spectra (RRS) for the consideration of hydrodynamic loads
- (c) Structurally Complex equipment - Comprises that equipment which cannot be classified as structurally simple or structurally rigid.

The appropriate response spectra for specific equipment are obtained from the response spectra for the floor at which the equipment is located in a building for CBE, SSE and hydrodynamic loads. This includes the vertical as well as both the N-S and E-W horizontal directions. For equipment which is structurally simple, the dynamic loading (either seismic or hydrodynamic) consists of a static load corresponding to the equipment weight times the acceleration selected from the appropriate response spectrum. The acceleration selected corresponds to the equipment's natural frequency, if the equipment's natural frequency is known. If the equipment's natural frequency is not known, the acceleration selected corresponds to the maximum value of the response spectra.

For equipment which is structurally rigid, the seismic load consists of a static load corresponding to the equipment weight times the acceleration at 33 Hz, selected from the appropriate response spectrum and the hydrodynamic loading consist of a static load corresponding to the equipment weight times the accelerations at the ZPA, selected from the appropriate response spectrum.

For the analysis of structurally complex equipment, the equipment is idealized by a mathematical model which adequately predicts the dynamic properties of the equipment and a dynamic analysis is performed using any standard analysis procedure. An acceptable alternative method of analysis is by static coefficient analysis for verifying structural integrity of frame type structures that can be represented by a simple model. No determination of natural frequencies is made and the response of the equipment is assumed to be the peak of the response spectrum. This response is then multiplied by a static coefficient of 1.5 to take into account the effects of both multifrequency excitation and multimode response.

7.1.6.1.4.1.2 Testing

In lieu of performing dynamic analysis, dynamic adequacy is established by providing dynamic test data. Such data must conform to one of the following:

1. Performance data of equipment which has been subjected to equal or greater dynamic loads (considering appropriate frequency range) than those to be experienced under the specified dynamic loading conditions.
2. Test data from comparable equipment previously tested under similar conditions, which has been subjected to equal or greater dynamic loads than those specified.
3. Actual testing of equipment in operating conditions simulating, as closely as possible, the actual installation, the required loadings and load combinations.

A continuous sinusoidal test, sine beat test, or decaying sinusoidal test is used when the applicable floor acceleration spectrum is a narrow band response spectrum. Otherwise, random motion test (or equivalent) with broad frequency content is used.

The equipment to be tested is mounted in a manner that simulates the actual service mounting. Sufficient monitoring devices are used to evaluate the performance of the equipment. With the appropriate test method selected, the equipment is considered to be qualified when the test response spectra (TRS) envelopes the required response spectra (RRS) and the equipment did not malfunction or fail. A new test does not need to be conducted if equipment requires only a very minor modification such as additional bracing or change in switch model, etc., and proper justification is given to show that the modifications do not jeopardize the strength and function of the equipment.

7.1.6.1.4.1.3 Combined Analysis and Testing

There are several instances where the qualification of equipment by analysis alone or testing alone is not practical or adequate because of its size, or its complexity, or large number of similar configurations. In these instances a combination of

analysis and testing is the most practical. The following are general approaches:

- (a) An analysis is conducted on the overall assembly to determine its stress level and the transmissibility of motion from the base of the equipment to the critical components. The critical components are removed from the assembly and subjected to a simulation of the environment on a test table.
- (b) Experimental methods are used to aid in the formulation of the mathematical model for any piece of equipment. Mode shapes and frequencies are determined experimentally and incorporated into a mathematical model of the equipment.

7.1.6.1.4.2--Computer Programs

Computer programs used to conduct equipment analyses are described in PSAR Section 3.9.1.2.

7.1.7--Balance of Plant (BOP) Equipment Assessment Methodology

Seismic Category I BOP equipment located within the containment and the reactor and control buildings are subjected to hydrodynamic loads due to SRV LOCA discharge affects principally originating in the suppression pool of the containment structure. The equipment and equipment support are assessed to verify their adequacy to withstand these hydrodynamic loads in combination with seismic and all other applicable loads in accordance with the load combinations given in Section 5.7.

7.1.7.1--Hydrodynamic loads

7.1.7.1.1--SRV Discharge Loads

Loadings associated with the axisymmetric and asymmetric SRV discharges are described in Chapter 3 and 4 of this report. Acceleration response spectra at the various elevations where the equipment are located have been generated for all appropriate pressure history traces (Figures 4-28 thru 4-30 of Chapter 4) for damping values of 1/2%, 1%, 2% and 5%. These have been enveloped into a single curve for each of the above damping values. Such enveloped curves are generated for each of the N-S, E-W and vertical directions. These curves form the basis for the SRV loads for equipment assessment.

7.1.7.1.2--LOCA Related Loads

Loadings associated with loss-of-coolant accident (LOCA) are described in Section 4.2. Acceleration response spectra at various elevations where the equipment are located have been generated for the above LOCA loads for damping values of 1/2%, 1%, 2% and 5%. These have been enveloped into a single curve for each of the above damping values. Such enveloped curves are generated for each of the N-S, E-W and vertical directions.

These curves form the basis for the LOCA loads for equipment assessment.

7.1.7.2 Seismic Loads

The details of seismic input and seismic loads are discussed in Section 3.7 of PSAR. The effects of both operating basis earthquake (OBE) and safe shutdown earthquake (SSE) are considered. These loads are provided in the form of Acceleration response spectra at each floor for damping values of 1/2%, 1%, 2% and 5% for each of N-S, E-W and vertical directions.

7.1.7.3 Other Loads

In addition to hydrodynamic and seismic loads, other loads such as dead loads, live loads, operating loads, pressure loads, thermal loads, nozzle loads and equipment piping interaction loads, as applicable, are also considered.

7.1.7.4 Qualification Methods

The adequacy of the design of the equipment is assessed by one of the following:

- a. Dynamic analysis
- b. Testing under simulated conditions
- c. Combination of testing and analysis.

The choice is based on the practicality of the method depending upon function, type, size, shape, and complexity of the equipment and the reliability of the qualification method.

In general the requirements outlined in IEEE-344-75, Reference 55, are followed for the qualification of equipment.

7.1.7.4.1 Dynamic Analysis

7.1.7.4.1.1 Methods and Procedures

The dynamic analysis of various equipment is classified into three groups according to the relative rigidity of the equipment based on the magnitude of the fundamental natural frequency described below.

- (a) Structurally simple equipment - comprises of that equipment which can be adequately represented by one degree of freedom system.
- (b) Structurally rigid equipment - Comprises of that equipment whose fundamental frequency is:
 - (i) greater than 33 Hz for the consideration of seismic loads, and,

(ii) greater than 80 Hz for the consideration of hydrodynamic loads.

(c) Structurally Complex equipment - Comprises of that equipment which cannot be classified as structurally simple or structurally rigid.

When the equipment is structurally simple or rigid in one direction but complex in the other, each direction may be classified separately to determine the dynamic loads.

The appropriate response spectra for specific equipment are obtained from the response spectra for the floor at which the equipment is located in a building for OBE, SSE and hydrodynamic loads. This includes the vertical as well as both the N-S and E-W horizontal directions.

For equipment which is structurally simple, the dynamic loading (either seismic or hydrodynamic) consists of a static load corresponding to the equipment weight times the acceleration selected from the appropriate response spectrum. The acceleration selected corresponds to the equipment's natural frequency, if the equipment's natural frequency is known. If the equipment's natural frequency is not known, the acceleration selected corresponds to the maximum value of the response spectra.

For equipment which is structurally rigid the seismic load consists of a static load corresponding to the equipment weight times the acceleration at 33 Hz, selected from the appropriate response spectrum and the hydrodynamic loading consist of a static load corresponding to the equipment weight times the acceleration at 80 Hz., selected from the appropriate response spectrum.

For the analysis of structurally complex equipment, the equipment is idealized by a mathematical model which adequately predicts the dynamic properties of the equipment and a dynamic analysis is performed using any standard analysis procedure. An acceptable alternative method of analysis is by static coefficient analysis for verifying structural integrity of frame type structures such as members physically similar to beams and columns that can be represented by a simple model. No determination of natural frequencies is made and the response of the equipment is assumed to be the peak of the response spectrum at damping values as per Section 7.1.7.4.1.2. This response is then multiplied by a static coefficient of 1.5 to take into account the effects of both multifrequency excitation and multimode response.

7.1.7.4.1.2 Appropriate Damping Values

The following damping values are used for the design assessment:

- 1) Load Combinations involving OBE but not hydrodynamic loads - 1/2%
- 2) Load Combinations involving SSE but not hydrodynamic loads - 1%
- 3) Load Combinations involving hydrodynamic loads, or seismic and hydrodynamic loads - 2%

If the actual damping value of the equipment is different (from test results) then these actual values are used.

7.1.7.4.1.3 Three Components of Dynamic Motions

The responses such as internal forces, stresses and deformations at any point from the three principal orthogonal directions of the dynamic loads are combined as follows:

The response value used is the maximum value obtained by adding the response due to vertical dynamic load with the larger value of the responses due to one of the horizontal corresponding dynamic load by the absolute sum method.

7.1.7.4.2 Testing

In lieu of performing dynamic analysis, dynamic adequacy is established by providing dynamic test data. Such data must conform to one of the following:

1. Performance data of equipment which has been subjected to equal or greater dynamic loads (considering appropriate frequency range) than those to be experienced under the specified dynamic loading conditions.
2. Test data from comparable equipment previously tested under similar conditions, which has been subjected to equal or greater dynamic loads than those specified.
3. Actual testing of equipment to the required load combinations while simulating the actual field installation.

A continuous sinusoidal test, sine beat test, or decaying sinusoidal test is used when the applicable floor acceleration spectrum is a narrow band response spectrum. Otherwise, random motion test (or equivalent) with broad frequency content is used.

The equipment to be tested is mounted in a manner that simulates the actual service mounting. Sufficient monitoring devices are used to evaluate the performance of the equipment. With the appropriate test method selected, the equipment is considered to be qualified when the test response spectra (TRS) envelopes the

required response spectra (RRS) and the equipment did not malfunction or fail. A new test does not need to be conducted if equipment requires only a very minor modifications such as additional bracings or change in switch model etc. and proper justification is given to show that the modifications do not jeopardize the strength and function of the equipment.

7.1.7.4.3--Combined Analysis and Testing

There are several instances where the qualification of equipment by analysis alone or testing alone is not practical or adequate because of its size, or its complexity, or large number of similar configurations. In these instances a combination of analysis and testing is the most practical. The following are general approaches:

- (a) An analysis is conducted on the overall assembly to determine its stress level and the transmissibility of motion from the base of the equipment to the critical components. The critical components are removed from the assembly and subjected to a simulation of the environment on a test table.
- (b) Experimental methods are used to aid in the formulation of the mathematical model for any piece of equipment. Mode shapes and frequencies are determined experimentally and incorporated into a mathematical model of the equipment.

7.1.8--Electrical Raceway System Assessment Methodology

7.1.8.1--General

The PSAR Subsection 3.7b.3.1.6 provides a detailed description of the electrical raceway system design methodology. The analysis and design of supports or Electrical Raceway Systems for non-hydrodynamic loads are in accordance with Reference 3.7b-7 of the PSAR. SRV discharge and LOCA loads are considered similar to seismic loads by using appropriate floor response spectra for the hydrodynamic loads. A damping value of 7% of critical is used for all raceway systems for abnormal/extreme load condition and a damping value of 3% of critical is used for normal load condition involving SRV discharge loading only.

7.1.8.2--Loads

7.1.8.2.1--Static Loads

The static loads are the dead loads and live loads. For cable trays, the weight of the cable is considered to be 45 lbs/ft and a concentrated live load of 200 lb. applicable at any point or cable tray span is used.

7.1.8.2.2 Seismic Loads

The details of the seismic motion input are discussed in Section 3.7 of the PSAR. The effects of the operating basis earthquake (OBE) and the Safe Shutdown earthquake (SSE) are considered.

7.1.8.2.3 Hydrodynamic Loads

The details of the axisymmetric and asymmetric SRV discharge loads, as well as LOCA loads including condensation-oscillation and chugging are discussed Section 4.0

The enveloped acceleration response spectra at each floor for N-S, E-W, and vertical directions have been generated and widened by $\pm 20\%$ for 7% of critical damping and $\pm 15\%$ for lower damping values. These curves form the basis for the hydrodynamic load assessment of the electrical raceway system. Examples of the response spectrum curves for the containment and Reactor and Control buildings are presented in Appendices B and C.

7.1.8.3 Analytical Methods

Cable tray systems are modeled as three dimensional dynamic system consisting of several consecutive supports complete with cable trays and longitudinal and transverse bracing. The cable tray properties are determined from the load deflection tests. Member joints are modeled as spring elements having rotational stiffness with known spring values as determined from the test results.

Composite spectra are developed by enveloping the floor response spectra after broadening by $\pm 20\%$ for critical floors for seismic, SRV and LOCA loading conditions. The design spectrum is obtained by adding these response spectra curves by the absolute sum method. A frequency variation of $\pm 20\%$ is used to further broaden the spectrum at the fundamental frequency of the cable tray system. The composite response spectra curves are obtained for vertical and two horizontal directions.

Modal and response spectrum analyses are performed utilizing "Bechtel Structural Analysis Program" (BSAP) which is a general purpose finite-element computer program. The seismic and hydrodynamic responses are added by the absolute sum method. The total response due to the dynamic loads is calculated by determining absolute sum of vertical response and only the larger response of the two horizontal responses.

Dead and live load stresses are determined from a static analysis of a plane frame model using BSAP computer program and these results are combined with those from the response spectrum analysis. For normal load condition, SRV discharge stresses are proportioned from the response spectrum analysis of SSE plus SRV discharge plus LOCA loads according to their spectral acceleration ratios at the fundamental frequencies. Several

different support types which are widely used have been analyzed by these methods.

An alternative method for analyzing other support types which occur less frequently, uses long hand calculations by a response spectrum analysis technique. The support may be idealized as a single degree of freedom system. In general, the maximum peak spectral accelerations were used in the analysis. In some cases where the stresses are critical, a more refined value for the acceleration response was used corresponding to the computed system fundamental frequency and considering a frequency variation as explained earlier in this section. The vertical and horizontal seismic responses are combined according to Subsection 3.7b.2.6 of the PSAR. The member stresses are kept within the elastic limit.

7.1.9 HVAC Duct System Assessment Methodology

The SRV discharge and LOCA are considered similar to seismic loads by using appropriate floor response spectra generated for the CO, chugging, and SRV loads described in Section 4.0.

A damping value of 5% of critical is used for load combinations involving SSE, SRV discharge and LOCA loads. While a damping value of 3% of critical is used for load combinations involving OBE and/or SRV discharge loads. For a discussion of the seismic and hydrodynamic loads input for HVAC duct system assessment, refer to Subsections 7.1.8.2.2 and 7.1.8.2.3, respectively. The HVAC duct system had been analyzed by the alternative method described in the Subsection 7.1.8.3 by determining the fundamental frequencies of the system in three directions. The inertia forces are determined from the composite spectra to establish member forces and moments due to hydrodynamic as well as seismic loads.

7.2 DESIGN CAPABILITY MARGINS

7.2.1 Stress Margins

Stresses at the critical sections for all of the structures described in Section 7.1, piping and equipment are evaluated for all the loading combinations presented in Section 5.0. The stress margin is defined as

$$(1 - \text{stress ratio}) \times 100$$

$$\text{stress ratio} = \sum C_n \cdot \frac{f_n}{F_n}$$

Where,

f_n = Actual Stress

f_n = Allowable Stress

C_n = Amplification Coefficient

7.2.1.1 Containment Structure

The results from the structural assessment of the containment structure are summarized in Appendix A. Figure A-2 shows the design sections in the basemat, containment walls, reactor pedestal, and the diaphragm slab which were considered in the structural assessment. The tables in Appendix A give the calculated design stresses and margins for load combination Equations 1, 4, 4a, 5, 5a, and 7 (as listed in Table 5-1).

The following observations are made from a review of the structural stresses. The calculated stress level is very low for load combination equation No. 1 (an upset condition) i.e., reinforcing bar stresses are less than 20 ksi. In general, among all the applicable load combinations, the most critical load combination is No. 7a. The maximum reinforcing bar design stress is predicted as 47.24 ksi, which occurs in a wetwell section on the outside face helical bars when using the absolute sum (ABS) method. This gives a minimum stress margin of 12.5% (see Figure A-29).

However, the calculated maximum reinforcing bar design stresses are relatively low in the reactor pressure vessel pedestal, diaphragm slab, and the base slab, as they are less than 18 ksi, 34 ksi, and 45 ksi respectively. The maximum principal concrete compressive stress occurs at the base slab and is calculated as 4280 psi. Thus, all the reinforcing bar design stresses are below the allowable stresses. It should be noted that the allowable stresses on which the margins are based, are related to the minimum specified strength. The actual quality control test results for the reinforcing bars and concrete show the material strengths to be higher than the minimum specified and therefore, the margins are actually greater than calculated.

In general, the concrete stresses were found to be low except at section 27 in the containment basemat (see Figure A-2), where the concrete stress in compression exceeded the maximum allowable stress in five load combinations out of six that were considered in this report. However, under each load combination the concrete is in triaxial compression at Section 27. Under the worst load case, the "hydrostatic" component of the stress is 2830 psi and the "deviatoric" component is only 1392 psi. Because of this large hydrostatic component, the concrete compressive strain is much smaller than the value of 0.003 in/in permitted by the codes. The concrete, therefore, has a very large strain margin before failure will commence. It must also be emphasized that not only the actual strength of the placed concrete is higher than the minimum specified, as indicated in the paragraph above, but that the concrete continues to gain strength after placement. The increase in strength at the end of five years could be as much as 20% over the 90 days strength. Therefore, the locally high compressive stresses in the concrete at Section 27 are deemed acceptable.

7.2.1.2 Reactor and Control Building

The results of the structural assessment of the Reactor and Control Building are summarized in Appendix E. Figures E-1 through E-22 show the design sections in the basemat and the concrete structure composed of floor slabs, shear walls, blockwalls, refueling pool girders, as well as floor structural steel and superstructure steel, which were considered in the structural assessment. The sections selected for assessment were considered to be most critical based on previous seismic calculations. The tables in Appendix E give the calculated design stresses and margins for the critical load combinations equations 1 and 7a of Table 5-1 and equations 1 and 7 Table 5-2. The other load combinations do not govern.

In the case of floor slabs, the calculated stress levels, in general, are very low for slabs above El. 683.0 ft. The governing load combination is equation 1 of Table 5-1 (normal condition) and the reinforcing steel stresses are significantly less than 20 ksi. For slabs below El. 683.0 ft. also, the governing load combination is equation 1 of Table 5-1. The maximum reinforcing steel stress was 49.79 ksi, which occurs in the reactor building slab at El. 645.0 ft. (see Figure E-33). The selected floor sections for the review and assessment are given in Figures E-1 through E-6.

In the case of shear walls, the maximum rebar stress was 43.25 ksi, and the minimum stress margin is 20% (see Figure E-34). The assessed elements are given in Figures E-1, E-3, E-4, E-7, and E-8.

In the blockwalls the calculated maximum reinforcing bar design stress is 30.6 ksi for load combination equation 7a (see Figure E-35). The minimum stress margin for compressive stress in the

concrete is 22%. The blockwall elements reviewed for assessment are shown in Figures E-9 through E-16.

In the case of Reactor Building structural steel (see Figure E-36), load combination Eq. 7 of Table 5-2 generally governs. The maximum bending stress was found to be 31.9 ksi which is less than the allowable value. This stress occurs in a beam at El. 719.1 ft. In the other cases the stress margins are 29% or more. The structural steel elements selected for assessment are given in Figures E-17 through E-20.

A three-dimensional lumped mass model was generated for determining the dynamic response of the Reactor Building Crane Support Structure. This model is shown in Figure E-21. Equation 7, Table 5-2 serves as the governing loading combination. Selected members as given in the model were assessed for structural integrity and stability. The design margins for structure and crane girder are 0% (see Figure E-37). This condition is reached by letting the rails deform in such a way that the crane bumper strikes against one of the rail girders.

The assessment of the Refueling Pool Girder shows that the maximum rebar stress was 51.7 ksi and the design margin is 4% (see Figure E-38). The elements selected for assessment are shown in Figure E-22.

As shown in Figure E-38a, the box section columns supporting the refueling pool were found to have adequate strength for resisting dead, live, and dynamic loads including seismic (OBE, SSE), SRV, and LOCA loads imposed by the refueling girders. Equation 6 was found to be the governing equation for columns. The strength of the box section columns is summarized under elements 41 and 42. The minimum design margin is 38%.

7.2.1.3 SRV Support Assemblies and Suppression Chamber Columns

The stresses at critical sections of the SRV support assemblies and the suppression chamber columns were calculated separately for the load combinations in Table 5.2. The maximum stresses are governed by load combination 7a for both the SRV support assemblies and columns. The results of the SRV support assembly analysis are shown in Figure A-67. The lowest stress margin of SRV support system which includes all bracing members and connections is 21.7%. On the other hand, the maximum stresses in column (42 inch diameter pipe), at the top and bottom bolt anchorages are shown in Figure A-59. The lowest stress margin in the column structure is 11.4%.

7.2.1.4 Downcomer Bracing

Stresses in the bracing members and connections were checked using the load combinations and allowable stresses as given in Table 5-2. Dynamic loads were combined on the basis of the SRSS method. Combined axial and bending stresses were investigated for the most highly loaded members. Equations 1, 3, 4 and 7

govern for the brace members with the design margins as indicated in Figure A-60. For the connections, equations 2 and 7 are critical and the resulting design margins are shown in Figure A-61. All bracing members and connections are adequate.

7.2.1.5 Liner Plate

For the normal load condition, the liner plates do not experience any net negative pressure as can be observed from Figure 7-21.

For the abnormal load condition, the maximum net negative pressure on the pressure boundary portion of the liner plates occurs on the containment wall, at point 8 of Figure 7-23, and is -6.39 psi. Since this is an impulse load of .004 seconds duration and the liner plate is supported every 2 feet, the stress in the liner plate is 12.5 ksi, well below the allowable. There is a margin of 51% for pullout of the embedded T steel sections that support the liner plate.

The liner plates on the base slab are supported by embedded W4x13 structural steel members every 10 feet. The maximum negative net pressure on the base slab occurs at the corner. The magnitude is -5.12 psi. However, due to liner plate connection on the corner between base slab and containment wall, the negative net pressure does not cause a bending problem in the liner plate and no pullout problem on W4x13 sections. The liner plate located away from the corner described above, do not experience negative pressure.

7.2.1.6 Downcomers

A list of downcomer and bracing system modal frequencies and participation factors is given in Table 7-5. The fundamental system mode is at a frequency of 1.8 Hz, which is a cantilever type of mode for all downcomers moving together. Downcomer stresses were checked according to ASME Code Section NB3652 using load combinations in Table 5-3. Stresses and design margins are given in Figure A-66.

7.2.1.7 Electrical Raceway System

It is apparent from the analysis that high stresses are a result of responses due to horizontal inertia loads. During the normal load condition, stresses under SRV discharge are generally low. However, for the abnormal/extreme load condition, certain members required strengthening to relieve high stresses. After implementing these modifications, the resultant stresses do not exceed the allowable stresses in any member of the electrical raceway system supports.

7.2.1.8 HVAC Duct System

Similar to the analysis of the electrical raceway system, the analysis of the HVAC duct system demonstrated that most of the support members have actual stresses lower than the allowable

stresses. However, certain structural members required strengthening to relieve high stresses under the abnormal/extreme load conditions.

7.2.1.9 BOP Equipment

All Seismic Category I BOP equipment are re-assessed for the hydrodynamic and non-hydrodynamic loads (see Subsection 7.1.7) via the SSES Seismic Qualification Review Team (SQRT) program. For each BOP equipment, 4-page SQRT summary forms have been prepared documenting the re-evaluation of that equipment. In some cases, modifications were required to reduce the stresses below the allowables.

In response to SER Open Item #11, the BOP SQRT summary forms requested by the NRC were formally submitted on February 25, 1982 (Reference: PLA-1024). The remaining BOP SQRT summary forms are available for review.

7.2.10 NSSS Equipment

All Seismic Category I NSSS equipment are being evaluated for the load combinations given in Table 5-5 via the SSES SQRT program. For each NSSS equipment, SQRT summary forms are prepared documenting the re-evaluation of that particular equipment.

The NSSS SQRT summary forms requested by the NRC will be formally submitted to the NRC under the SSES SQRT program. All NSSS SQRT summary forms are available for review.

7.2.11 NSSS and BOP Piping

As documented in Subsection 7.1.5 and 7.1.6.1.1, all Seismic Category I BOP and NSSS piping have been analyzed for hydrodynamic and non-hydrodynamic loads per the load combinations given in Subsections 5.5 and 5.6, respectively. As a result of this evaluation, many modifications were required to maintain the stresses below the allowable values. Appendix F provides a summary of the stresses and design margins for selected BOP piping system.

The results of the above evaluation are documented in stress reports, which are available for NRC review.

7.2.2 Acceleration Response Spectra

7.2.2.1 Containment Structure

The method of analysis and load description for the acceleration response spectrum generation are outlined in Subsections 7.1.1.1.6.1. From a review of the acceleration response spectra curves for the containment structure, the maximum spectral accelerations are tabulated for 1% damping of critical. For SRV and LOCA loads, the maximum spectral accelerations are presented in Table 7-1.

7.2.2.2 Reactor and Control Building

The methods of analysis and load application for the computation of the acceleration response spectrum in the reactor and control building are described in Subsections 7.1.1.2.1.1 and 7.1.1.2.1.2. From a review of the acceleration response spectra curves, the maximum spectral accelerations are tabulated for 4% damping of critical. For SRV and LOCA loads, the maximum spectral accelerations are presented in Table 7-2.

7.2.3 Containment Liner Openings

7.2.3.1 Equipment Hatch-Personnel Air Lock

Stresses in the equipment hatch-personnel air lock were all within allowable limits. However, as a result of the new loads, bolt pre-load had to be increased from 65 to 72 kips to maintain acceptable levels of displacement at the flanged joint. The resultant equivalent radial load applied at the bearing on the hinge support results in a minimum safety factor of 3 at ultimate for the roller and race.

7.2.3.2 CRD Removal Hatch, Suppression Chamber Access Hatch and Equipment Hatch

CBI's analysis indicated no stresses in excess of the specified allowable limits for the additional loadings considered.

7.2.3.3 Refueling Head and Support Skirt

The refueling head and flange were found to have no stresses exceeding allowable limits. The only effect of the new loads applied was to increase bolt pre-stress from 161 to 200 kips to maintain leaktightness at the flanged joint. Figure A-33.1 gives the stress margins in the refueling head and the flange.

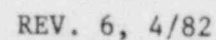
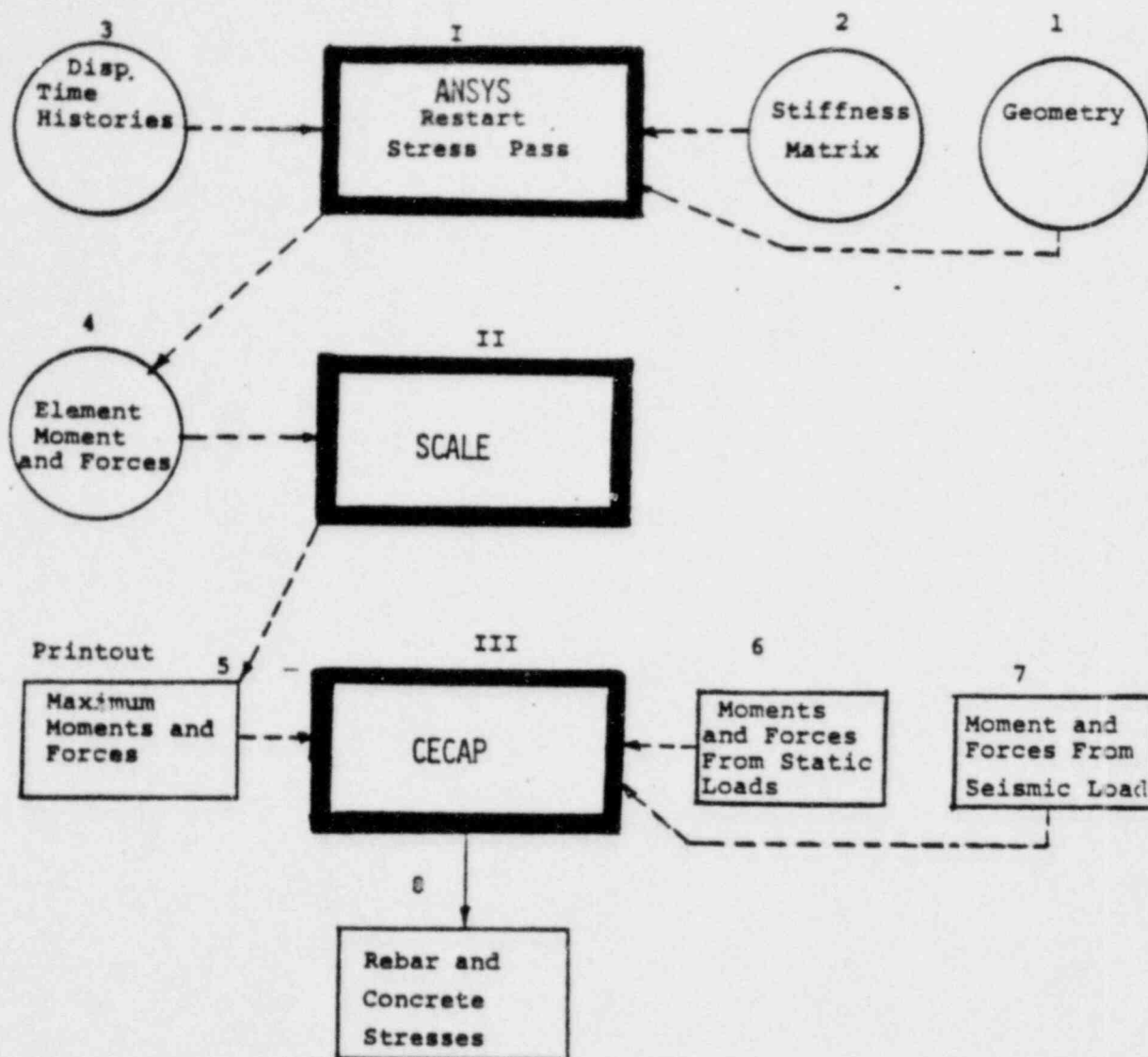


FIGURE 7-4

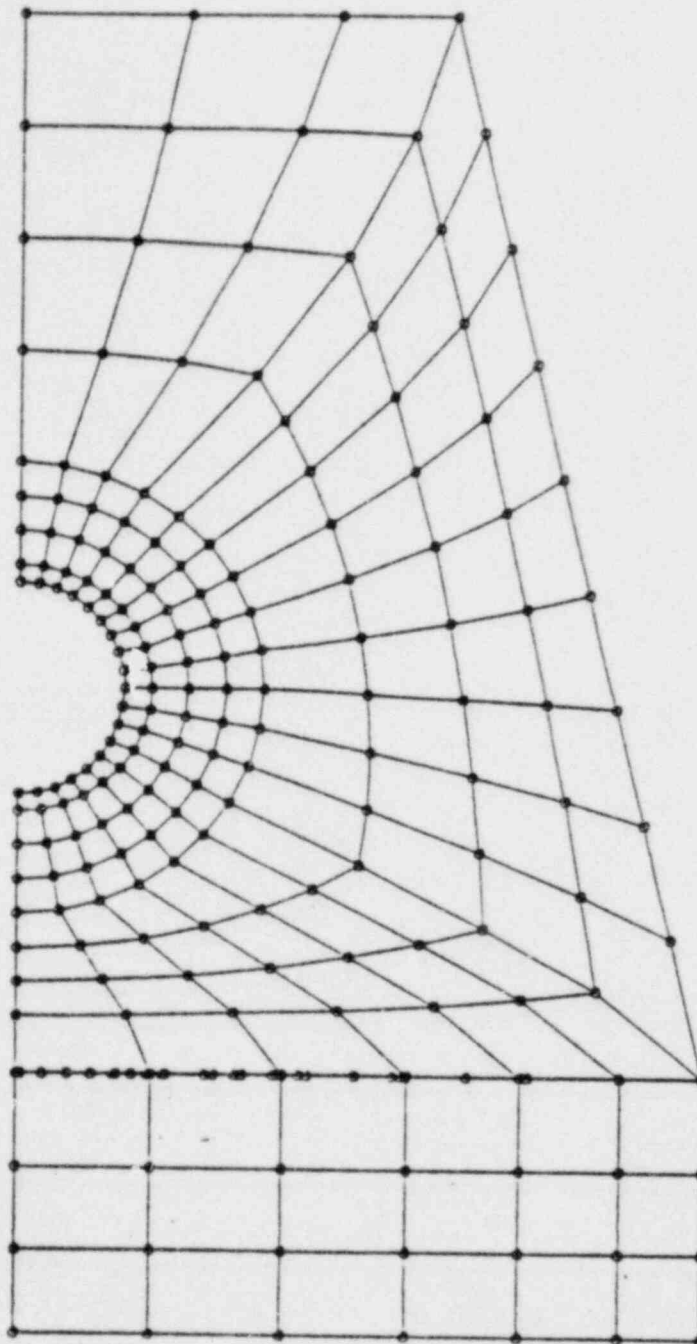


REV. 6, 4/82

SUSQUEHANNA STEAM ELECTRIC STATION
UNITS 1 AND 2
DESIGN ASSESSMENT REPORT

CONTAINMENT STRESS
ANALYSIS

FIGURE 7-5

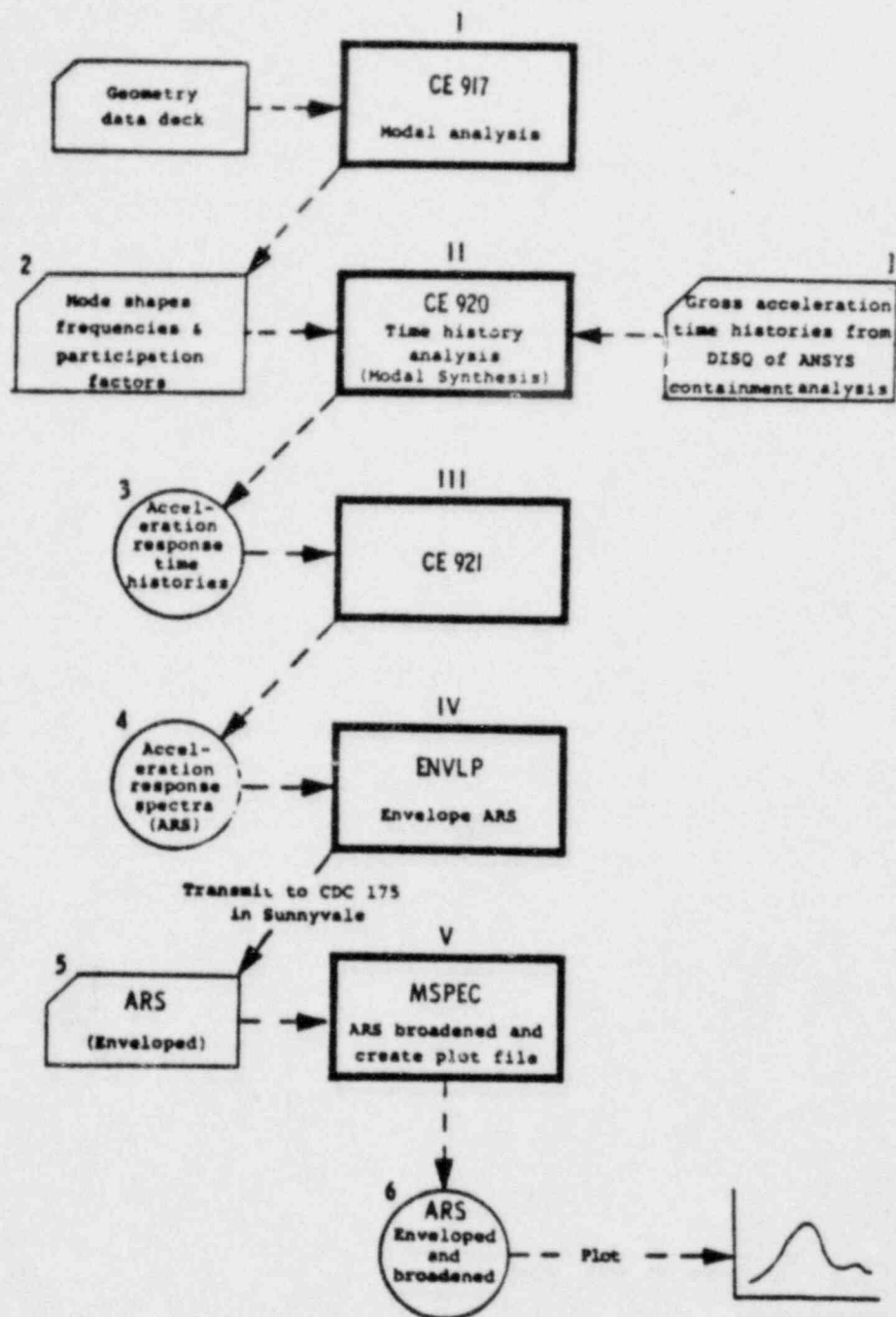


REV. 6, 4/82

SUSQUEHANNA STEAM ELECTRIC STATION
UNITS 1 AND 2
DESIGN ASSESSMENT REPORT

FINITE ELEMENT CONTAINMENT
EQUIPMENT HATCH MODEL

FIGURE 7-6

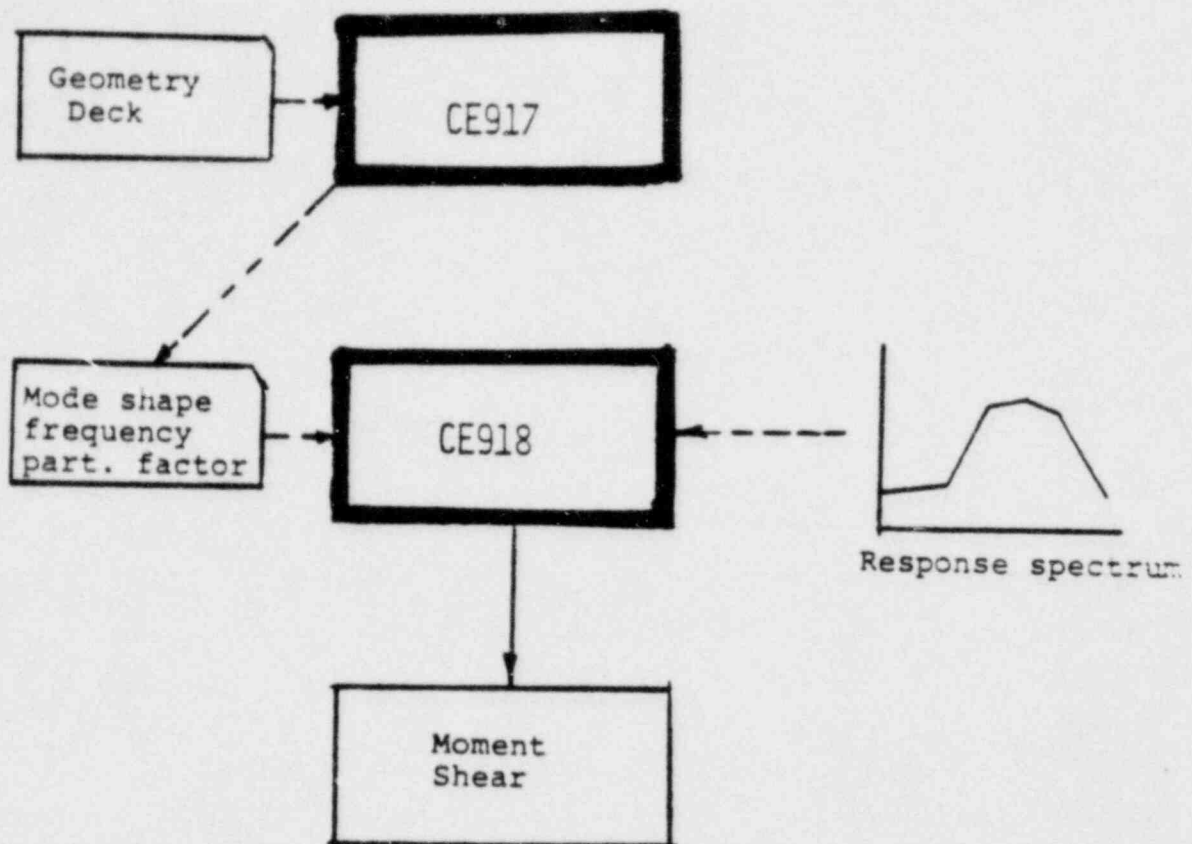


REV. 6, 4/82

SUSQUEHANNA STEAM ELECTRIC STATION
UNITS 1 AND 2
DESIGN ASSESSMENT REPORT

REACTOR BUILDING RESPONSE
ANALYSIS

FIGURE 7-7

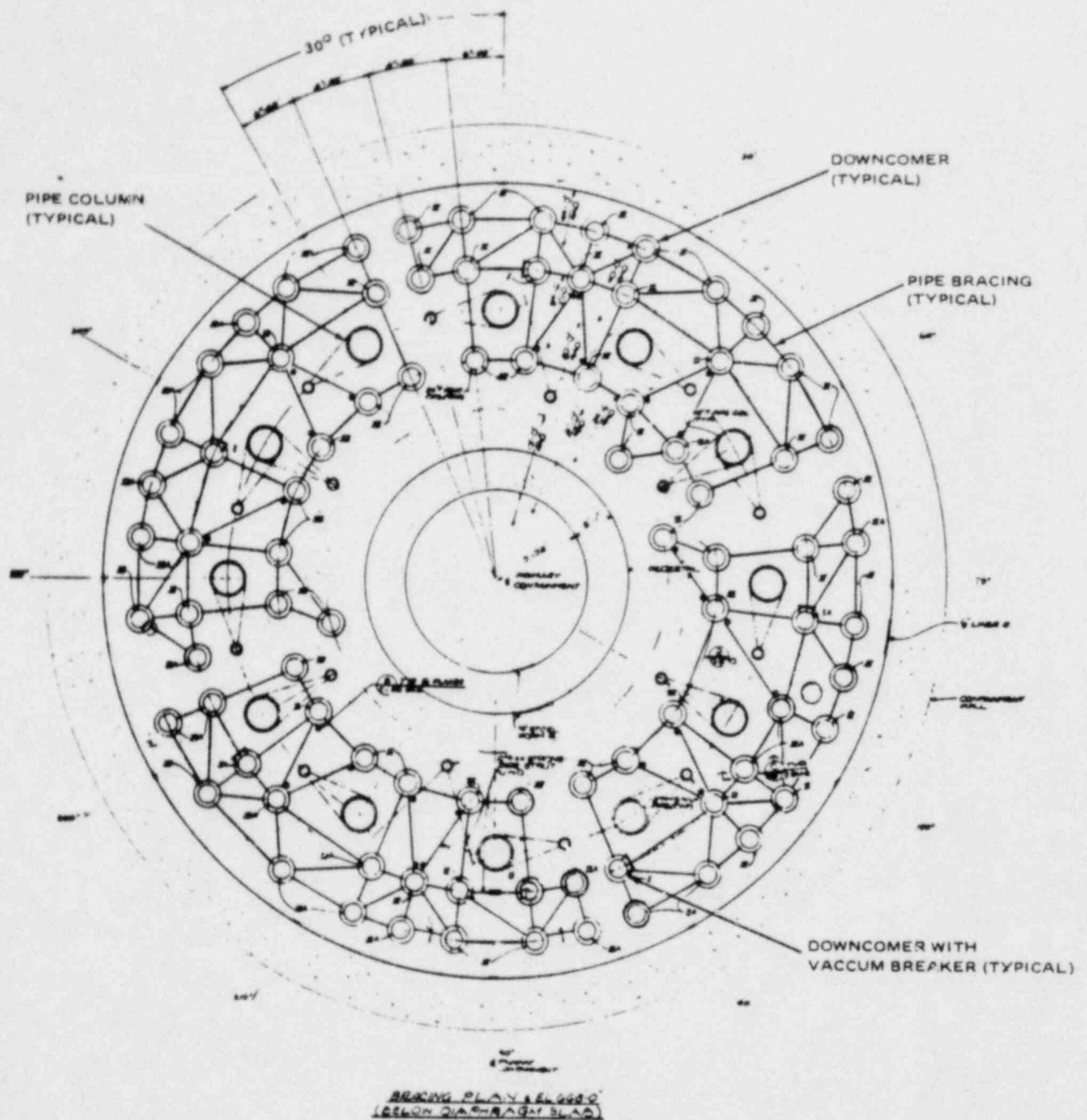


REV. 6, 4/82

SUSQUEHANNA STEAM ELECTRIC STATION
UNITS 1 AND 2
DESIGN ASSESSMENT REPORT

REACTOR BUILDING
STRESS ANALYSIS

FIGURE 7-8

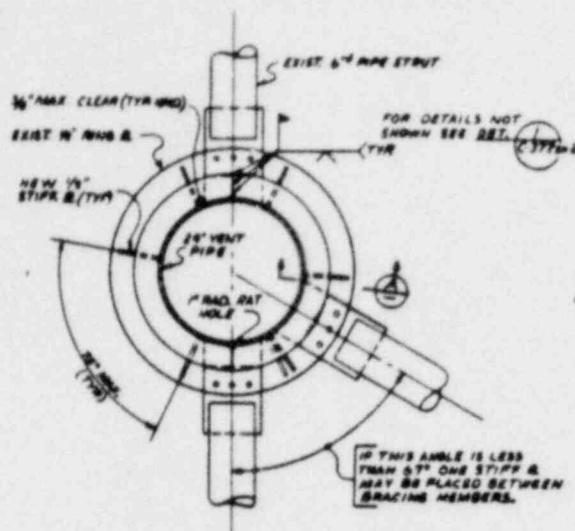


REV. 6, 4/82

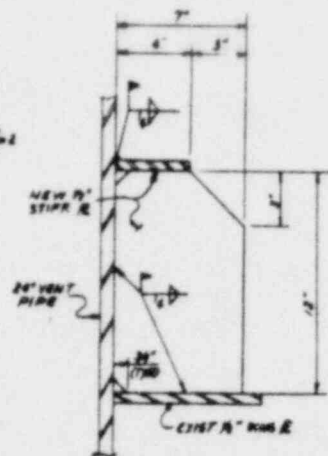
**SUSQUEHANNA STEAM ELECTRIC STATION
UNITS 1 AND 2
DESIGN ASSESSMENT REPORT**

**DOWNCOMER BRACING SYSTEM
PLAN**

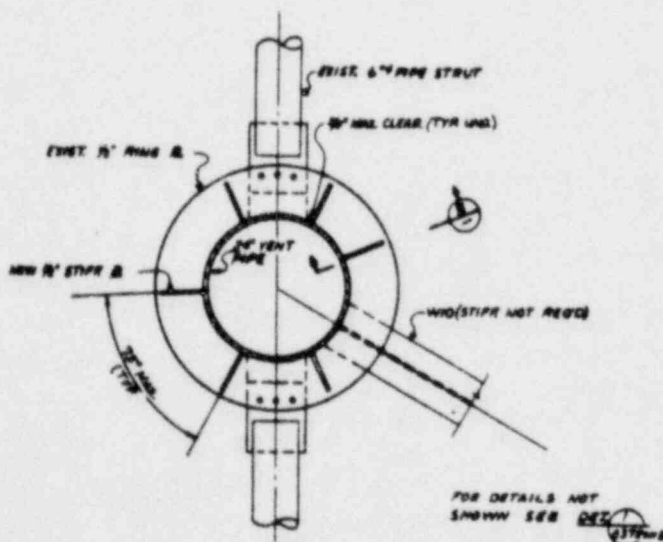
FIGURE 7-9



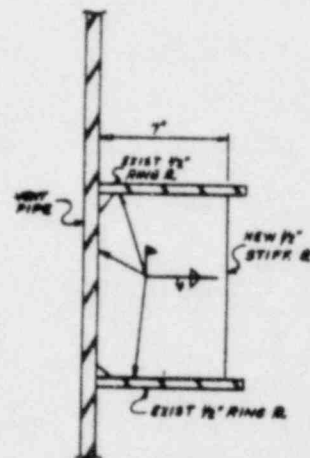
SINGLE RING PLATE
STIFFENER DETAIL



SECTION A
3\"/>



DOUBLE RING PLATE
STIFFENER DETAIL



SECTION B
3\"/>

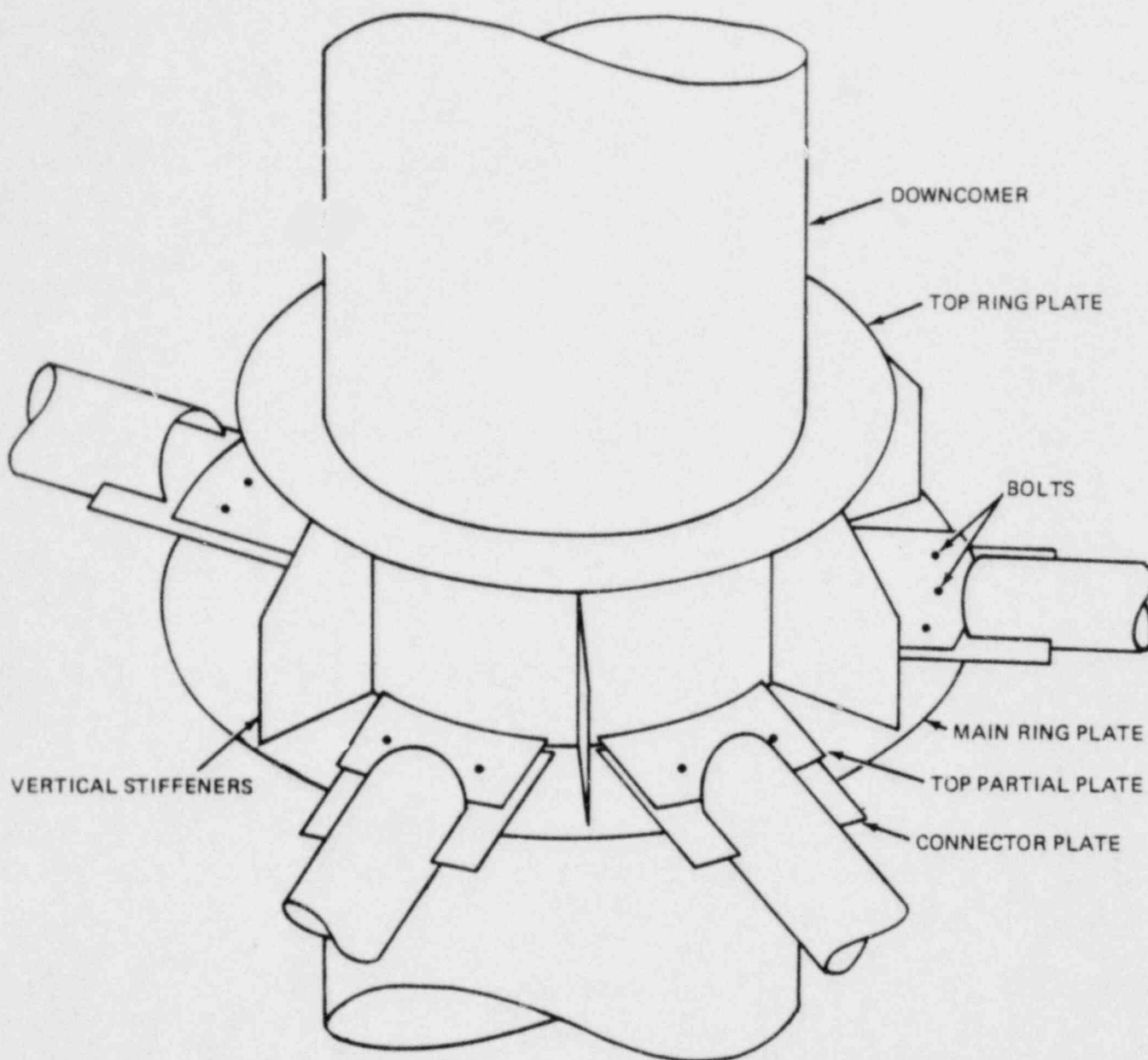
REV. 6, 4/82

SUSQUEHANNA STEAM ELECTRIC STATION
UNITS 1 AND 2
DESIGN ASSESSMENT REPORT

DOWNCOMER BRACING SYSTEM
CONNECTION DETAILS

FIGURE 7-10

(Sheet 2)



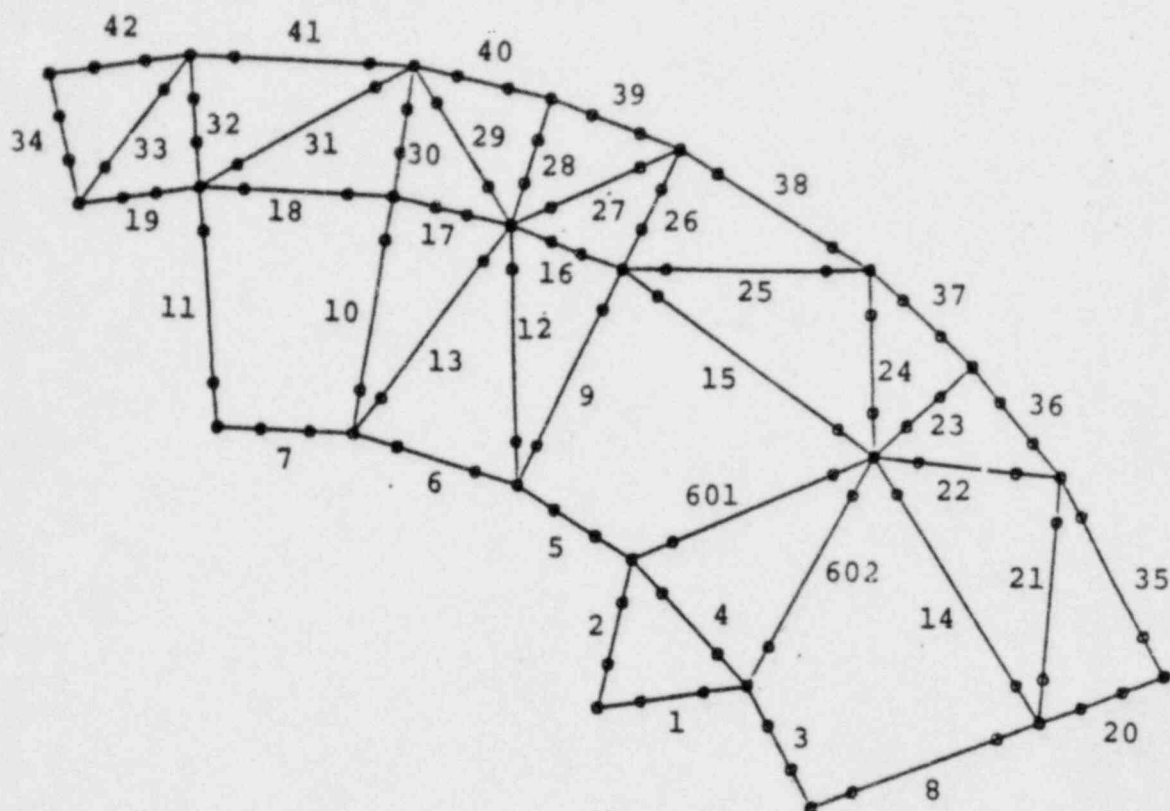
REV. 6, 4/82

SUSQUEHANNA STEAM ELECTRIC STATION
UNITS 1 AND 2
DESIGN ASSESSMENT REPORT

DOWNCOMER BRACING SYSTEM
CONNECTION

FIGURE 7-10

(Sheet 3)



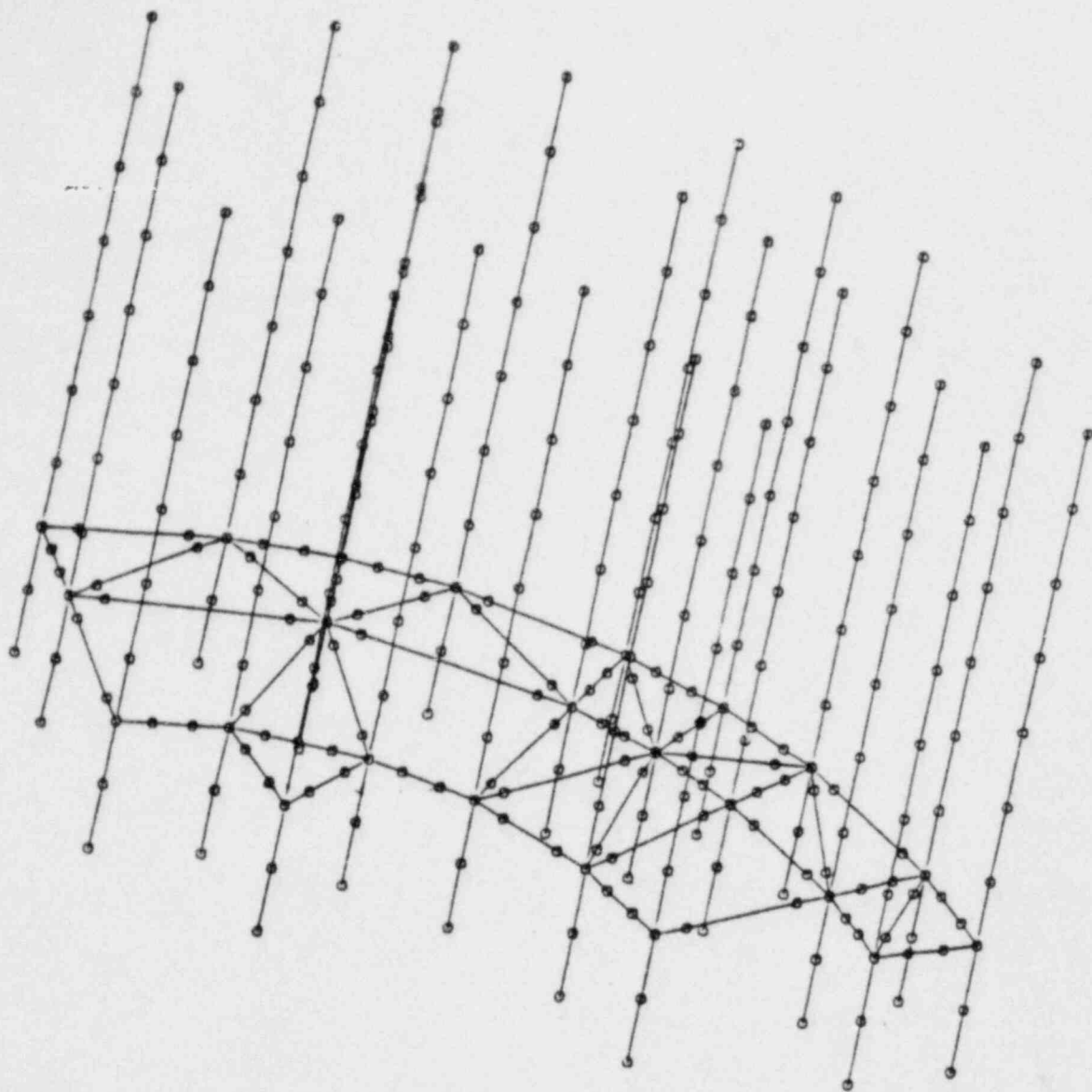
REV. 6, 4/82

SUSQUEHANNA STEAM ELECTRIC STATION
UNITS 1 AND 2
DESIGN ASSESSMENT REPORT

DOWNCOMER BRACING SYSTEM
COMPUTER MODEL

FIGURE 7-11

(Sheet 1)



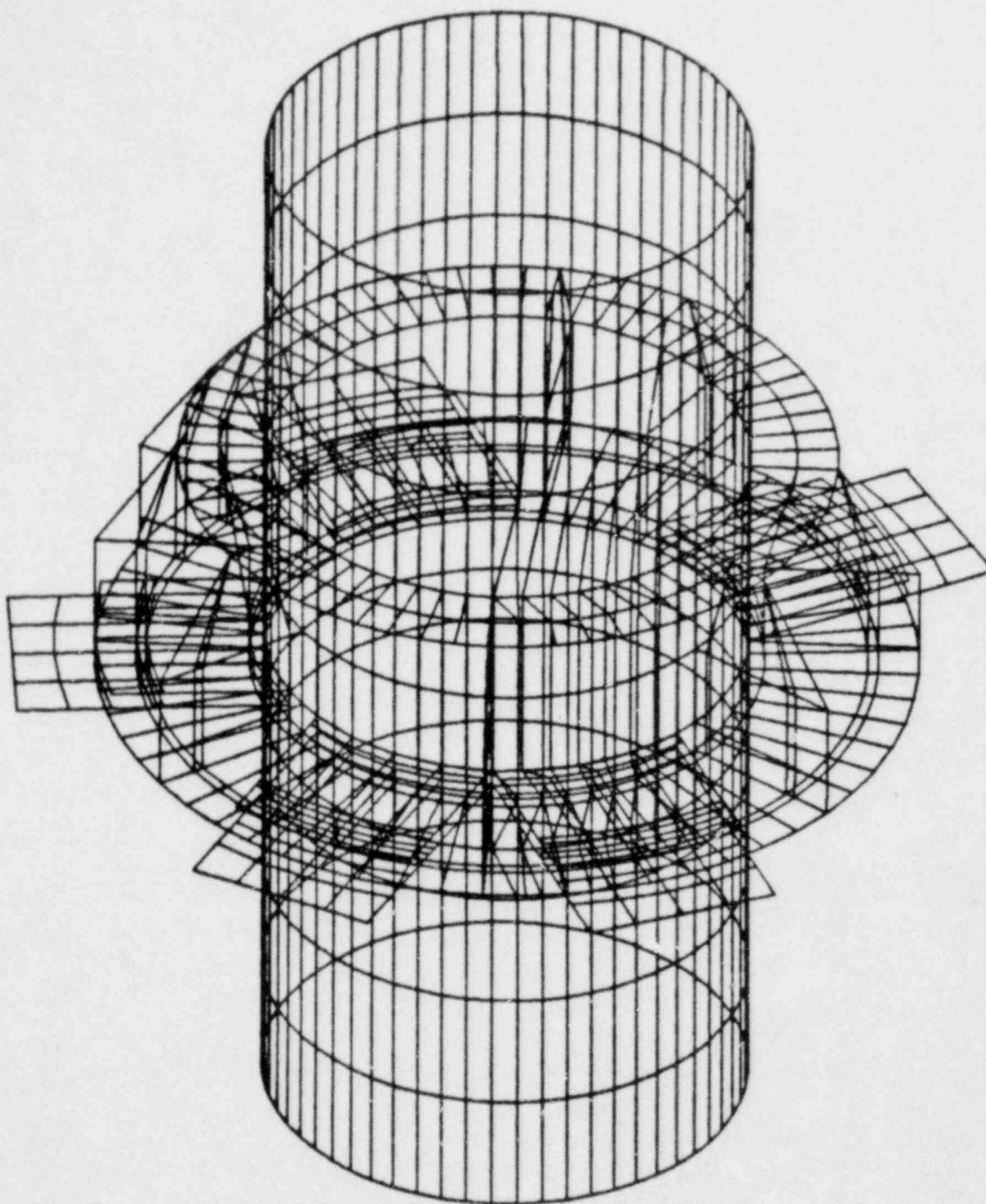
REV. 6, 4/82

**SUSQUEHANNA STEAM ELECTRIC STATION
UNITS 1 AND 2
DESIGN ASSESSMENT REPORT**

**DOWNCOMER BRACING SYSTEM
COMPUTER MODEL**

FIGURE 7-11

(Sheet 2)



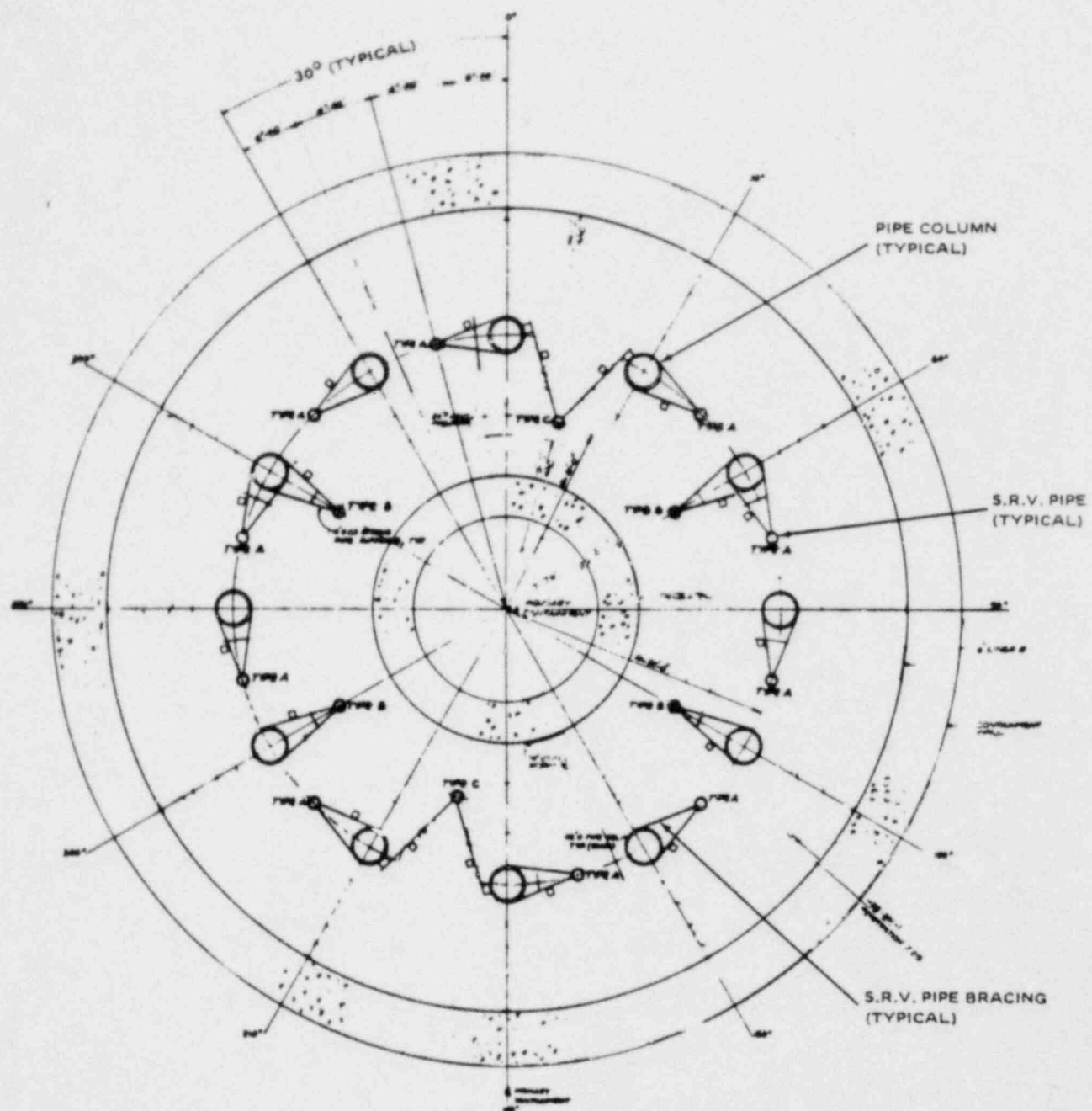
REV. 6, 4/82

SUSQUEHANNA STEAM ELECTRIC STATION
UNITS 1 AND 2
DESIGN ASSESSMENT REPORT

DOWNCOMER BRACING SYSTEM
CONNECTION COMPUTER MODEL

FIGURE 7-11

(Sheet 3)



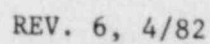
NOTE:
 □ INDICATES KNEE BRACING
 ON THIS SIDE
 TYPES A, B, & C, FOR DETAILS
 SEE DWG C-372 SH. 4
 TYPES A & C @ EL. 66'-0"
 TYPE B @ EL. 66'-0"

REV. 6, 4/82

GUSQUEHANNA STEAM ELECTRIC STATION
 UNITS 1 AND 2
 DESIGN ASSESSMENT REPORT

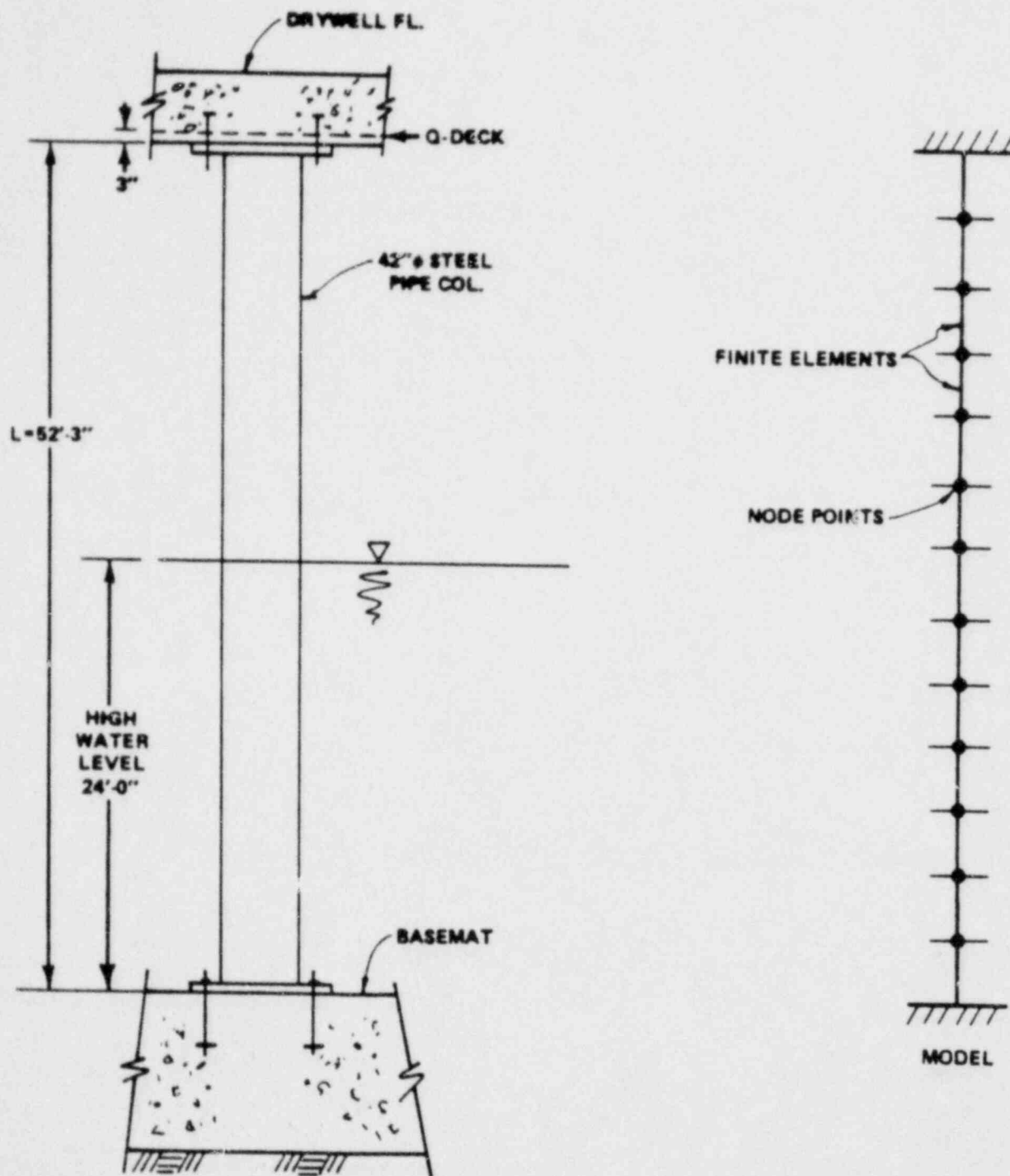
SRV SUPPORT SYSTEM
 PLAN

FIGURE 7-12



SRV SUPPORT SYSTEM DETAILS

FIGURE 7-13

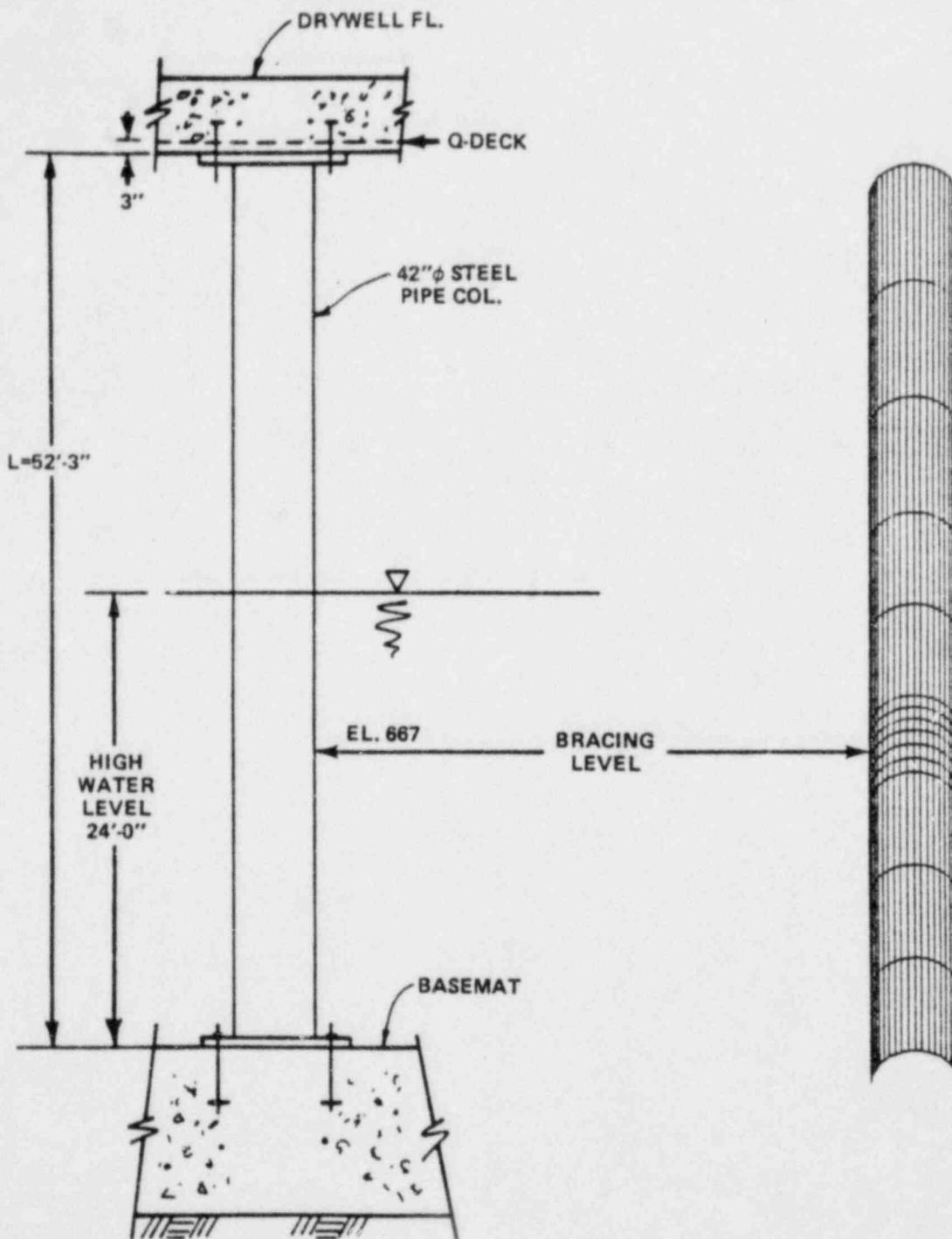


REV. 6, 4/82

SUSQUEHANNA STEAM ELECTRIC STATION
UNITS 1 AND 2
DESIGN ASSESSMENT REPORT

FINITE ELEMENT MODEL OF COLUMN

FIGURE 7-14



REV. 6, 4/82

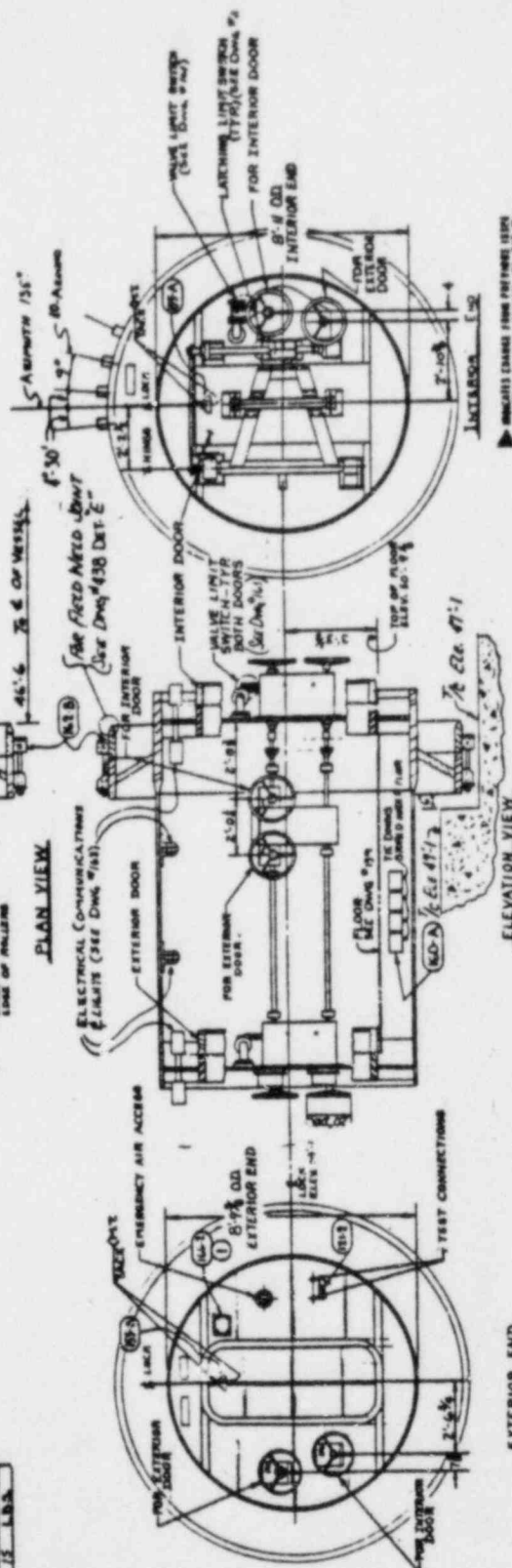
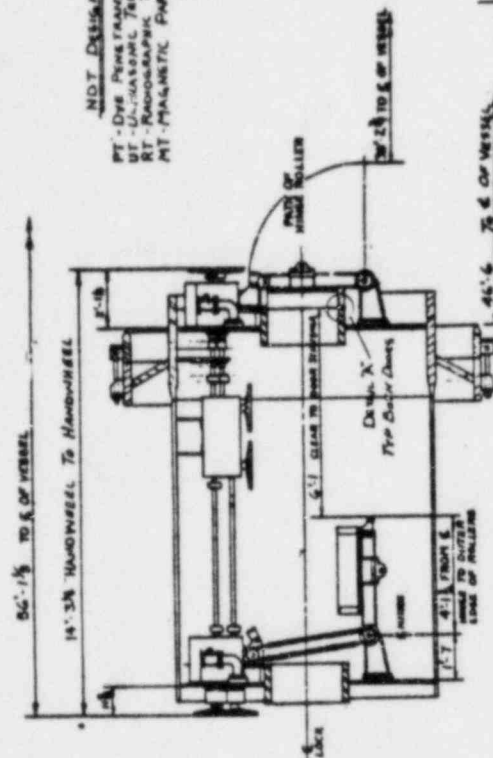
SUSQUEHANNA STEAM ELECTRIC STATION
UNITS 1 AND 2
DESIGN ASSESSMENT REPORT

FINITE ELEMENT MODEL OF COLUMN

FIGURE 7-15

DETAIL "A"

NOT DESIGNATIONS



REV. 6, 4/82

SUSQUEHANNA STEAM ELECTRIC STATION
UNITS 1 AND 2
DESIGN ASSESSMENT REPORT

GENERAL ARRANGEMENT
PERSONNEL LOCK

FIGURE 7-16

100% TISSUE POLYESTER - 6.9 YD. P534

CONSIDERING THE DIFFICULT ECONOMY OF 1932, THE AMERICAN ETHNOLOGICAL SOCIETY WAS NOT ONLY ONE OF THE MOST SUCCESSFUL BUT ALSO ONE OF THE MOST ACTIVE OF THE SOCIETIES OF THE YEAR. THE SOCIETY WAS ORGANIZED IN 1887, AND HAS SINCE THAT TIME BEEN ONE OF THE MOST ACTIVE OF THE SOCIETIES OF THE YEAR. THE SOCIETY WAS ORGANIZED IN 1887, AND HAS SINCE THAT TIME BEEN ONE OF THE MOST ACTIVE OF THE SOCIETIES OF THE YEAR.

[illegible]

THE SHOTS ARE REPORTED TO BE THE STRONGEST EVER FOR LACE VESTS.

ORDERED THAT 5 PAGES BE CONTAINED HEREIN. ONE BE. 64-2

ON 10-10-64. 14-10-64. 10-10-64. 10-10-64.

STATION	ROTATION	OFF POSITION	WAVELENGTH	PHASE DIFFERENCE
1	0°	0°	10.0	0.0
2	15°	15°	10.0	0.0
3	30°	30°	10.0	0.0
4	45°	45°	10.0	0.0
5	60°	60°	10.0	0.0
6	75°	75°	10.0	0.0
7	90°	90°	10.0	0.0
8	105°	105°	10.0	0.0
9	120°	120°	10.0	0.0
10	135°	135°	10.0	0.0
11	150°	150°	10.0	0.0
12	165°	165°	10.0	0.0
13	180°	180°	10.0	0.0
14	195°	195°	10.0	0.0
15	210°	210°	10.0	0.0
16	225°	225°	10.0	0.0
17	240°	240°	10.0	0.0
18	255°	255°	10.0	0.0
19	270°	270°	10.0	0.0
20	285°	285°	10.0	0.0
21	300°	300°	10.0	0.0
22	315°	315°	10.0	0.0
23	330°	330°	10.0	0.0
24	345°	345°	10.0	0.0
25	360°	360°	10.0	0.0

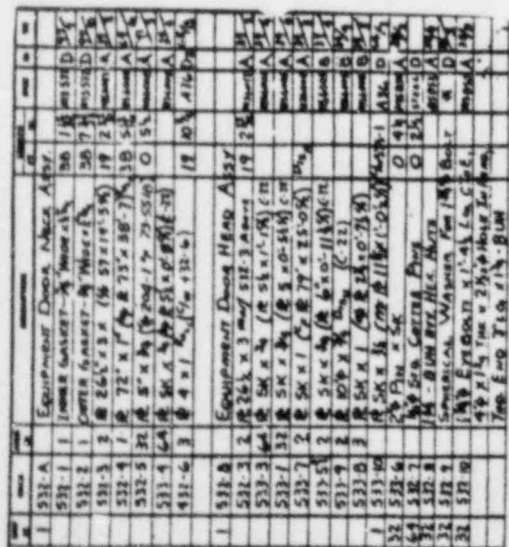
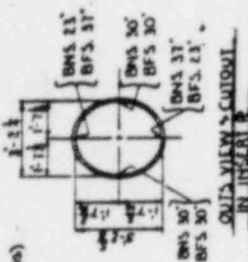


FIGURE 7-17

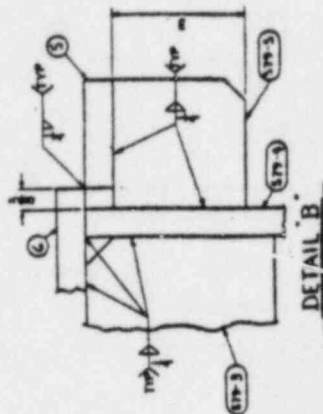
ITEM	DESCRIPTION	QTY	UNIT	ASSEMBLY
578-A	PERMITTING ASS'Y TO BOLT	1	EA	578-A
578-B	GROUP ATTACH TO ASS'Y (SEE 578-B)	1	EA	578-B
578-C	COVER R-45 8" X 8" (SEE 578-C)	1	EA	578-C
578-D	1/4" R-45 8" X 8" (SEE 578-D)	1	EA	578-D
578-E	1/4" R-45 8" X 8" (SEE 578-E)	1	EA	578-E
578-F	1/4" R-45 8" X 8" (SEE 578-F)	1	EA	578-F
578-G	1/4" R-45 8" X 8" (SEE 578-G)	1	EA	578-G
578-H	1/4" R-45 8" X 8" (SEE 578-H)	1	EA	578-H
578-I	1/4" R-45 8" X 8" (SEE 578-I)	1	EA	578-I
578-J	1/4" R-45 8" X 8" (SEE 578-J)	1	EA	578-J
578-K	1/4" R-45 8" X 8" (SEE 578-K)	1	EA	578-K
578-L	1/4" R-45 8" X 8" (SEE 578-L)	1	EA	578-L
578-M	1/4" R-45 8" X 8" (SEE 578-M)	1	EA	578-M
578-N	1/4" R-45 8" X 8" (SEE 578-N)	1	EA	578-N
578-O	1/4" R-45 8" X 8" (SEE 578-O)	1	EA	578-O
578-P	1/4" R-45 8" X 8" (SEE 578-P)	1	EA	578-P
578-Q	1/4" R-45 8" X 8" (SEE 578-Q)	1	EA	578-Q
578-R	1/4" R-45 8" X 8" (SEE 578-R)	1	EA	578-R
578-S	1/4" R-45 8" X 8" (SEE 578-S)	1	EA	578-S
578-T	1/4" R-45 8" X 8" (SEE 578-T)	1	EA	578-T
578-U	1/4" R-45 8" X 8" (SEE 578-U)	1	EA	578-U
578-V	1/4" R-45 8" X 8" (SEE 578-V)	1	EA	578-V
578-W	1/4" R-45 8" X 8" (SEE 578-W)	1	EA	578-W
578-X	1/4" R-45 8" X 8" (SEE 578-X)	1	EA	578-X
578-Y	1/4" R-45 8" X 8" (SEE 578-Y)	1	EA	578-Y
578-Z	1/4" R-45 8" X 8" (SEE 578-Z)	1	EA	578-Z

NOTE: SEE DWG# 607 FOR DETAIL OF INVERT ASS'Y

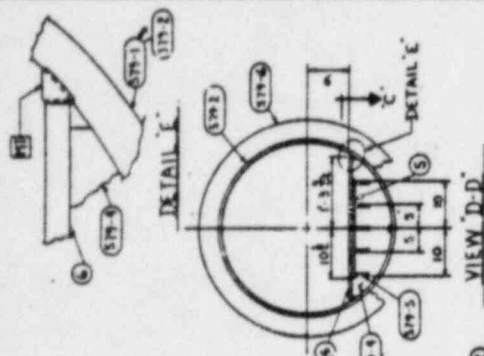
MS-6077 SA 346 6470
MS-572 SALICONE RUBBER
MS-850 SA 193 87
MS-832 SA 194 647
MS-671 SA 316 6460



OUTLINE VIEW - OUTLINE
IN INVERT



DETAIL B



VIEW D-D

DETAIL B

DETAIL C

DETAIL D

DETAIL E

DETAIL F

DETAIL G

DETAIL H

DETAIL I

DETAIL J

DETAIL K

DETAIL L

DETAIL M

DETAIL N

DETAIL O

DETAIL P

DETAIL Q

DETAIL R

DETAIL S

DETAIL T

DETAIL U

DETAIL V

DETAIL W

DETAIL X

DETAIL Y

DETAIL Z

DETAIL AA

DETAIL AB

DETAIL AC

DETAIL AD

DETAIL AE

DETAIL AF

DETAIL AG

DETAIL AH

DETAIL AI

DETAIL AJ

DETAIL AK

DETAIL AL

DETAIL AM

DETAIL AN

DETAIL AO

DETAIL AP

DETAIL AQ

DETAIL AR

DETAIL AS

DETAIL AT

DETAIL AU

DETAIL AV

DETAIL AW

DETAIL AX

DETAIL AY

DETAIL AZ

DETAIL BA

DETAIL BB

DETAIL BC

DETAIL BD

DETAIL BE

DETAIL BF

DETAIL BG

DETAIL BH

DETAIL BI

DETAIL BJ

DETAIL BK

DETAIL BL

DETAIL BM

DETAIL BN

DETAIL BO

DETAIL BP

DETAIL BQ

DETAIL BR

DETAIL BS

DETAIL BT

DETAIL BU

DETAIL BV

DETAIL BW

DETAIL BX

DETAIL BY

DETAIL BZ

DETAIL CA

DETAIL CB

DETAIL CC

DETAIL CD

DETAIL CE

DETAIL CF

DETAIL CG

DETAIL CH

DETAIL CI

DETAIL CJ

DETAIL CK

DETAIL CL

DETAIL CM

DETAIL CN

DETAIL CO

DETAIL CP

DETAIL CQ

DETAIL CR

DETAIL CS

DETAIL CT

DETAIL CU

DETAIL CV

DETAIL CW

DETAIL CX

DETAIL CY

DETAIL CZ

DETAIL DA

DETAIL DB

DETAIL DC

DETAIL DD

DETAIL DE

DETAIL DF

DETAIL DG

DETAIL DH

DETAIL DI

DETAIL DJ

DETAIL DK

DETAIL DL

DETAIL DM

DETAIL DN

DETAIL DO

DETAIL DP

DETAIL DQ

DETAIL DR

DETAIL DS

DETAIL DT

DETAIL DU

DETAIL DV

DETAIL DW

DETAIL DX

DETAIL DY

DETAIL DZ

DETAIL EA

DETAIL EB

DETAIL EC

DETAIL ED

DETAIL EE

DETAIL EF

DETAIL EG

DETAIL EH

DETAIL EI

DETAIL EJ

DETAIL EK

DETAIL EL

DETAIL EM

DETAIL EN

DETAIL EO

DETAIL EP

DETAIL EQ

DETAIL ER

DETAIL ES

DETAIL ET

DETAIL EU

DETAIL EV

DETAIL EW

DETAIL EX

DETAIL EY

DETAIL EZ

DETAIL FA

DETAIL FB

DETAIL FC

DETAIL FD

DETAIL FE

DETAIL FF

DETAIL FG

DETAIL FH

DETAIL FI

DETAIL FJ

DETAIL FK

DETAIL FL

DETAIL FM

DETAIL FN

DETAIL FO

DETAIL FP

DETAIL FQ

DETAIL FR

DETAIL FS

DETAIL FT

DETAIL FU

DETAIL FV

DETAIL FW

DETAIL FX

DETAIL FY

DETAIL FZ

DETAIL GA

DETAIL GB

DETAIL GC

DETAIL GD

DETAIL GE

DETAIL GF

DETAIL GG

DETAIL GH

DETAIL GI

DETAIL GJ

DETAIL GK

DETAIL GL

DETAIL GM

DETAIL GN

DETAIL GO

DETAIL GP

DETAIL GQ

DETAIL GR

DETAIL GS

DETAIL GT

DETAIL GU

DETAIL GV

DETAIL GW

DETAIL GX

DETAIL GY

DETAIL GZ

DETAIL HA

DETAIL HB

DETAIL HC

DETAIL HD

DETAIL HE

DETAIL HF

DETAIL HG

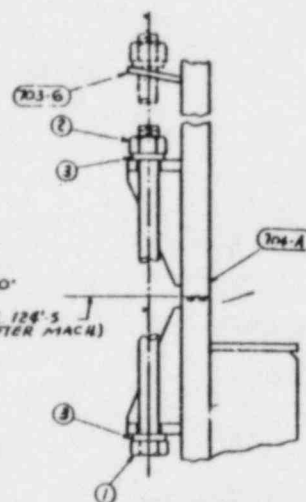
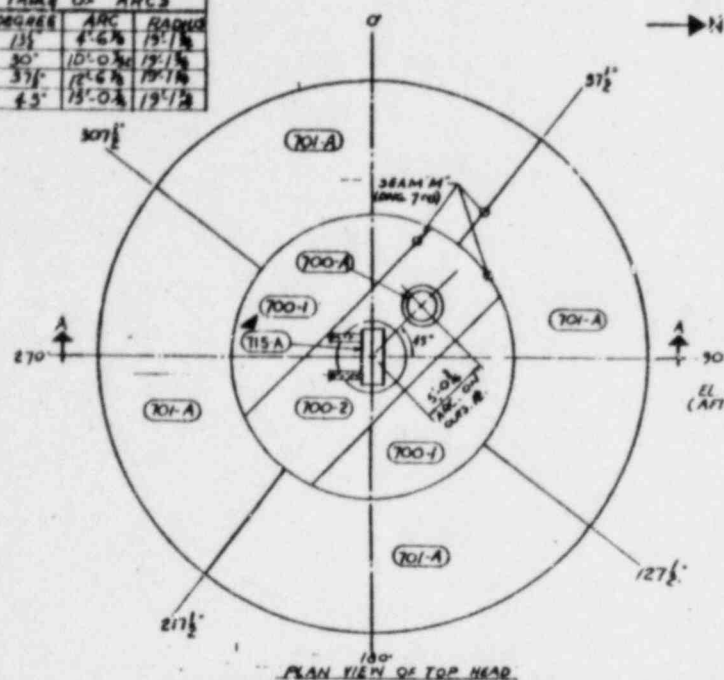
DETAIL HH

DETAIL HI

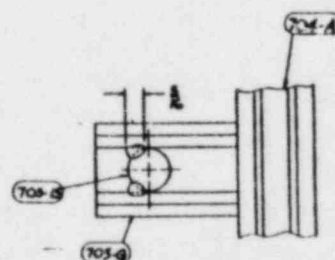
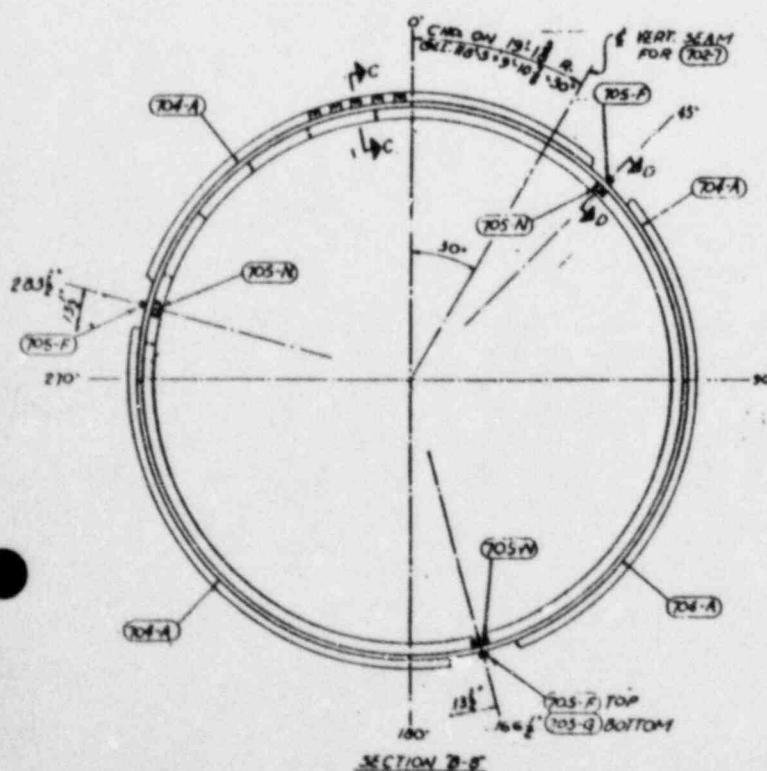
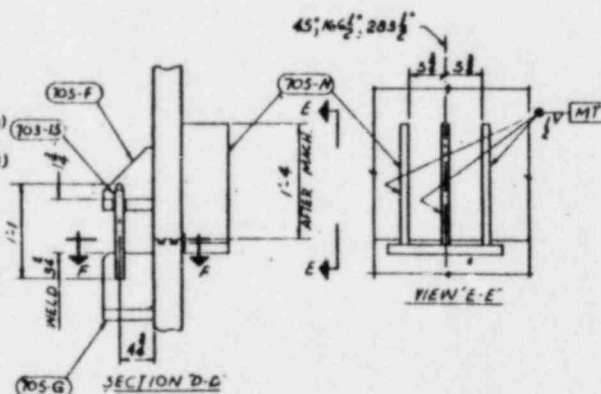
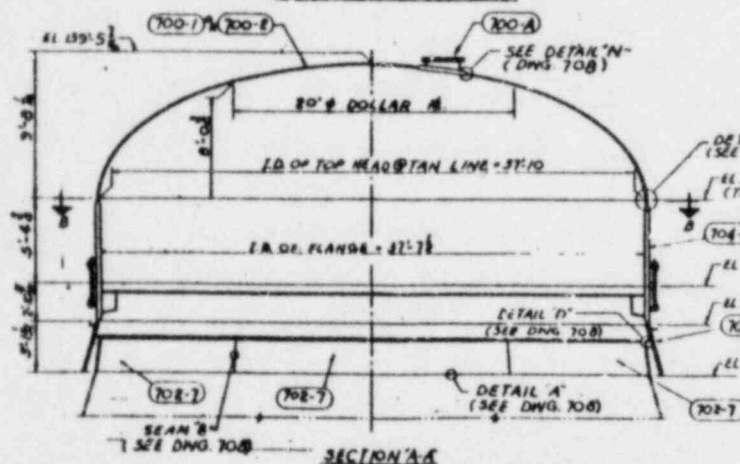
DETAIL HJ

DETAIL HK

DEGREE	ARC	RADIUS
15°	4.6°	15.1°
30°	10.0°	15.1°
37.5°	12.6°	15.1°
45°	15.0°	19.1°



SECTION C-C
~ OPERATIONAL SERVICE ~
BOLT PRELOAD ~ ~~200~~ 200 KIPS
BOLT ELONGATION ~ ~~0.052~~ 0.052 in

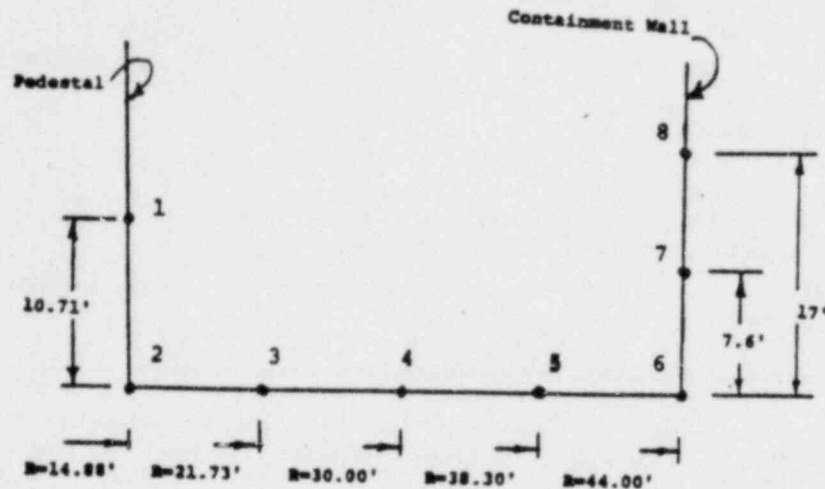


REV. 6, 4/82

**SUSQUEHANNA STEAM ELECTRIC STATION
UNITS 1 AND 2
DESIGN ASSESSMENT REPORT**

REFUELING HEAD DETAILS

FIGURE 7-19



MAXIMUM NEGATIVE PRESSURE FROM KWU 300 SERIES CHUGGING

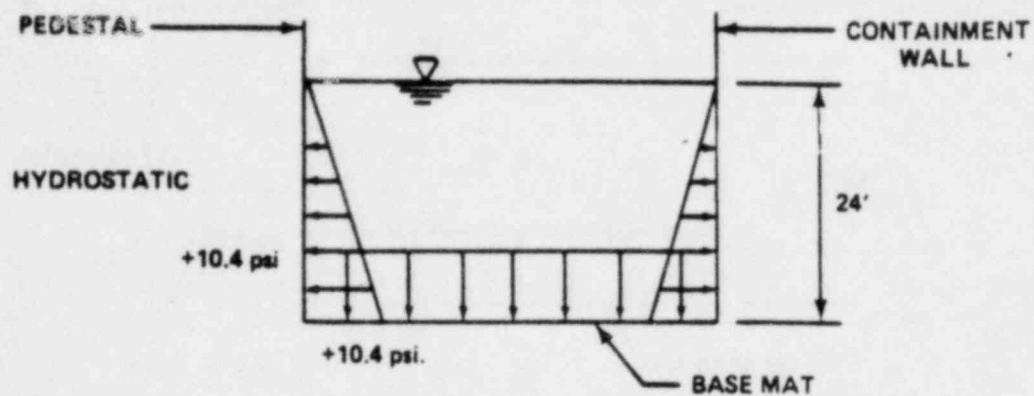
Point No.	Maximum Negative Pressure psi.	Trace No.
1	-62.16	KWU 306
2	-26.42	KWU 306
3	-24.74	KWU 306
4	-26.85	KWU 306
5	-26.69	KWU 306
6	-32.72	kwu 306
7	-28.40	KWU 306
8	-31.39	KWU 306

REV. 6, 4/82

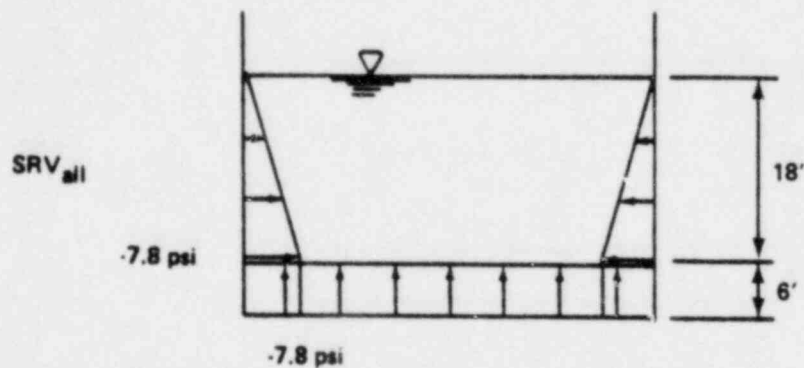
SUSQUEHANNA STEAM ELECTRIC STATION
UNITS 1 AND 2
DESIGN ASSESSMENT REPORT

LINER PLATE HYDRODYNAMIC
PRESSURE DUE TO CHUGGING

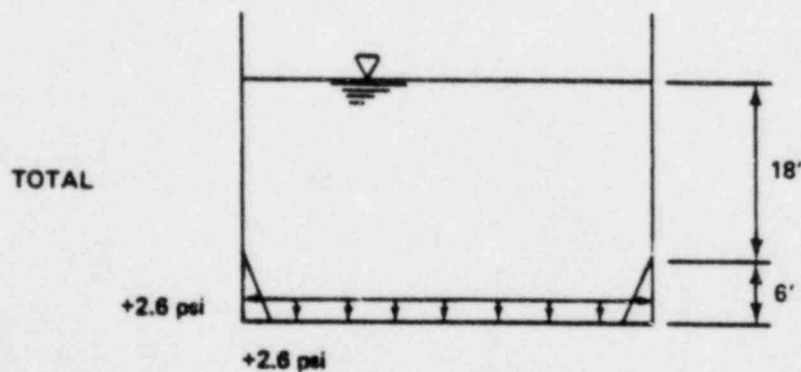
FIGURE 7-20



+



||

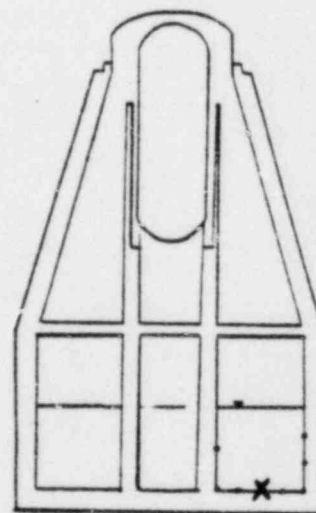
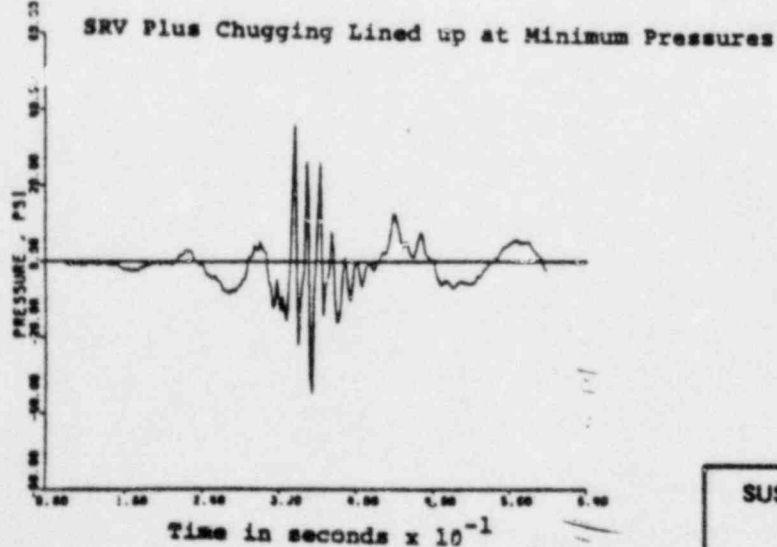
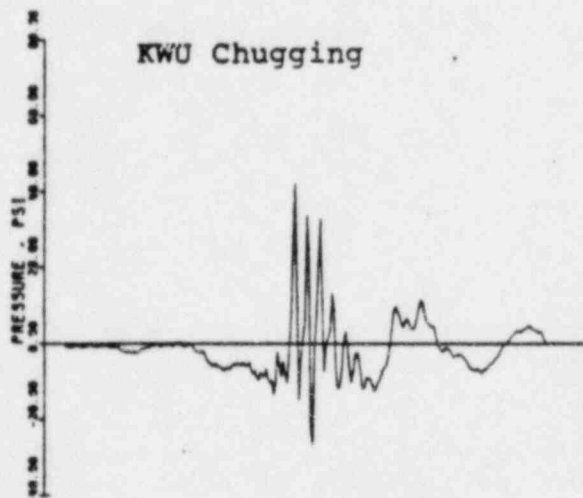
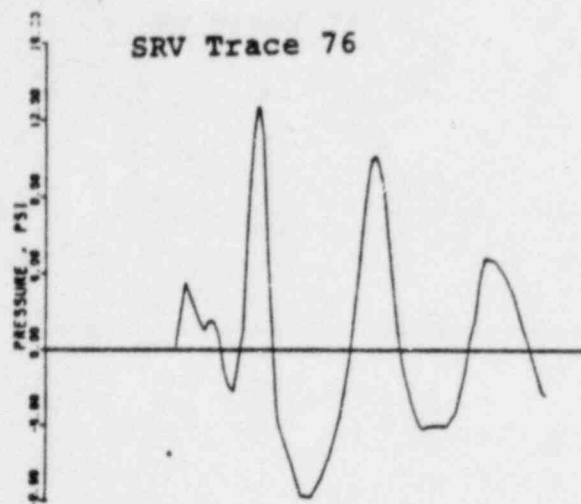


REV. 6, 4/82

SUSQUEHANNA STEAM ELECTRIC STATION
UNITS 1 AND 2
DESIGN ASSESSMENT REPORT

LINER PLATE PRESSURES
NORMAL CONDITION

FIGURE 7-21

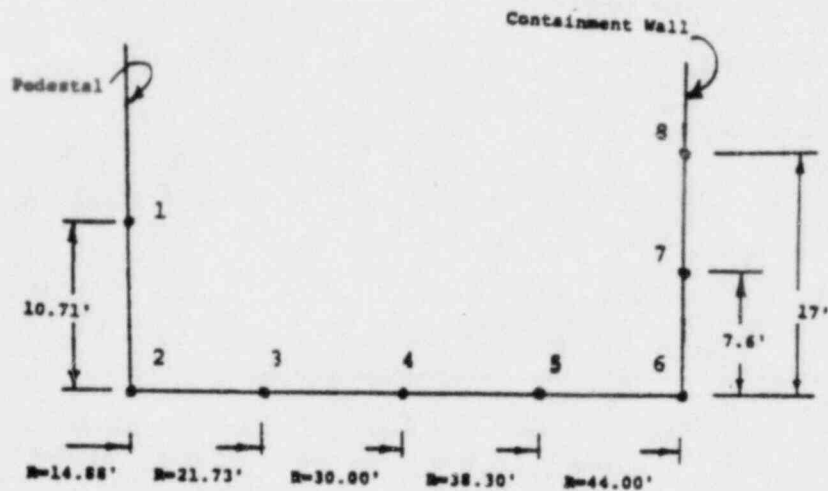


REV. 6, 4/82

SUSQUEHANNA STEAM ELECTRIC STATION
UNITS 1 AND 2
DESIGN ASSESSMENT REPORT

LINER PLATE HYDRODYNAMIC
PRESSURE
DUE TO
CHUGGING AND SRV

FIGURE 7-22



LOAD CASE	POINT IN FIGURE							
	1	2	3	4	5	6	7	8
CHUGGING	-62.16	-26.42	-24.74	-26.85	-26.85	-32.72	-28.40	-31.39
SRV Trace 76	- 5.76	- 7.80	- 7.80	-7.80	- 7.80	- 7.80	- 7.09	- 3.05
Hydrostatic	5.76	10.40	10.40	10.40	10.40	10.40	6.82	3.05
Wetwell pressure due to SBA or IBA*	25.00	25.00	25.00	25.00	25.00	25.00	25.00	25.00
NET PRESSURE	-37.16	1.18	2.86	0.75	0.91	-5.12	-3.69	-6.39

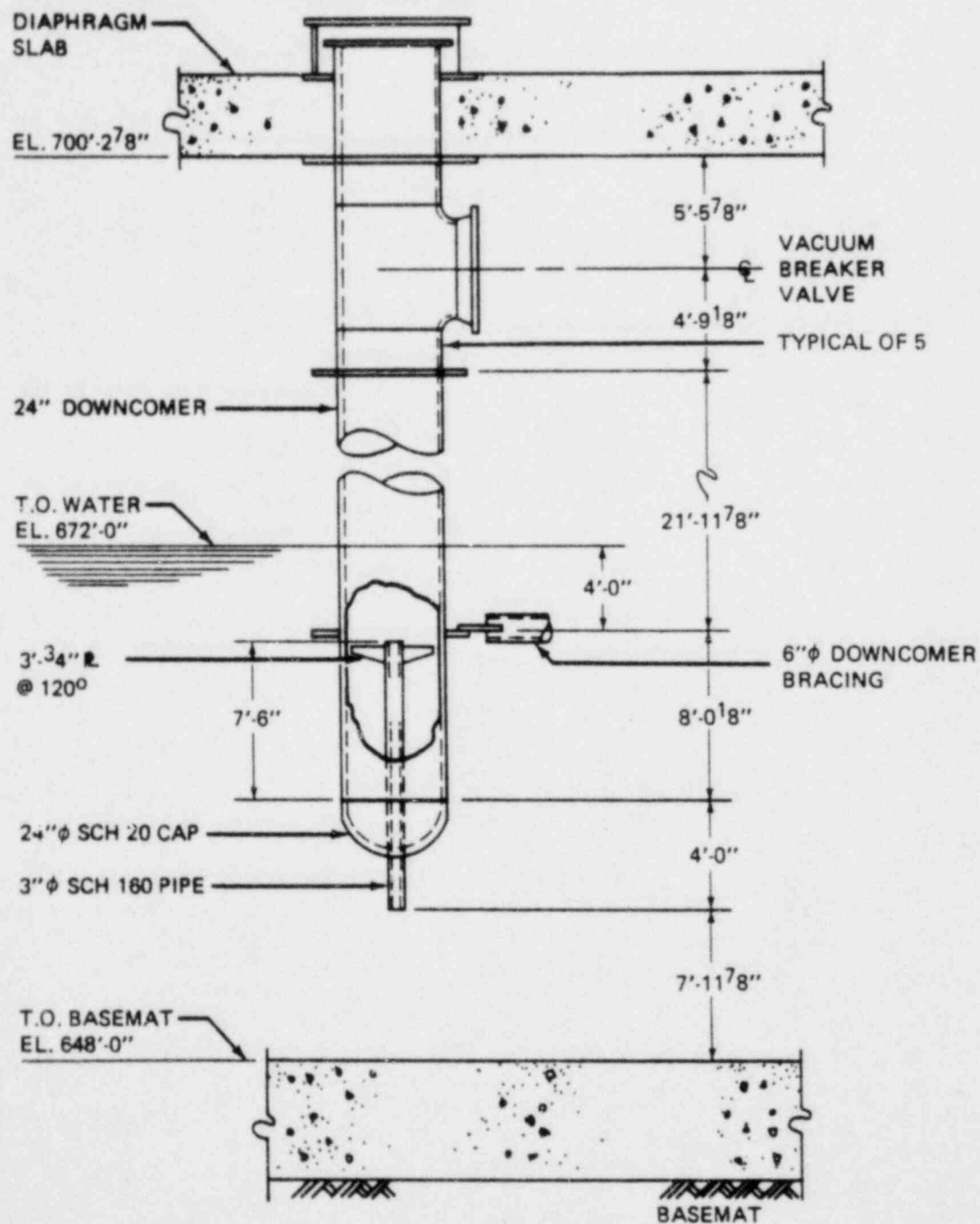
*Wetwell pressure due to DBA is 34 psi.

REV. 6, 4/82

SUSQUEHANNA STEAM ELECTRIC STATION
UNITS 1 AND 2
DESIGN ASSESSMENT REPORT

LINER PLATE PRESSURE
ABNORMAL CONDITION

FIGURE 7-23

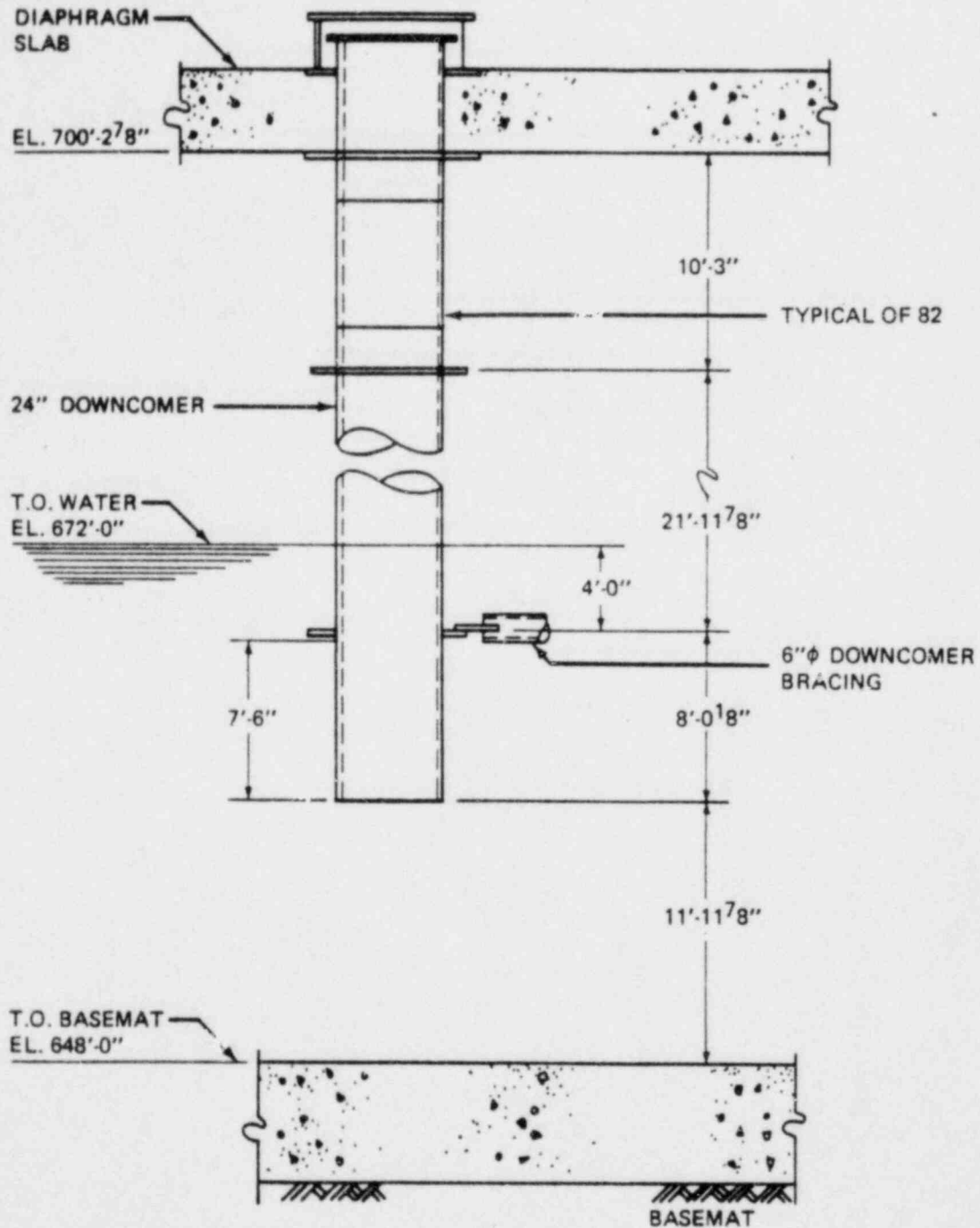


REV. 6, 4/82

SUSQUEHANNA STEAM ELECTRIC STATION
UNITS 1 AND 2
DESIGN ASSESSMENT REPORT

DOWNCOMER WITH
VACUUM BREAKER AND
DETAIL OF CAP

FIGURE 7-24

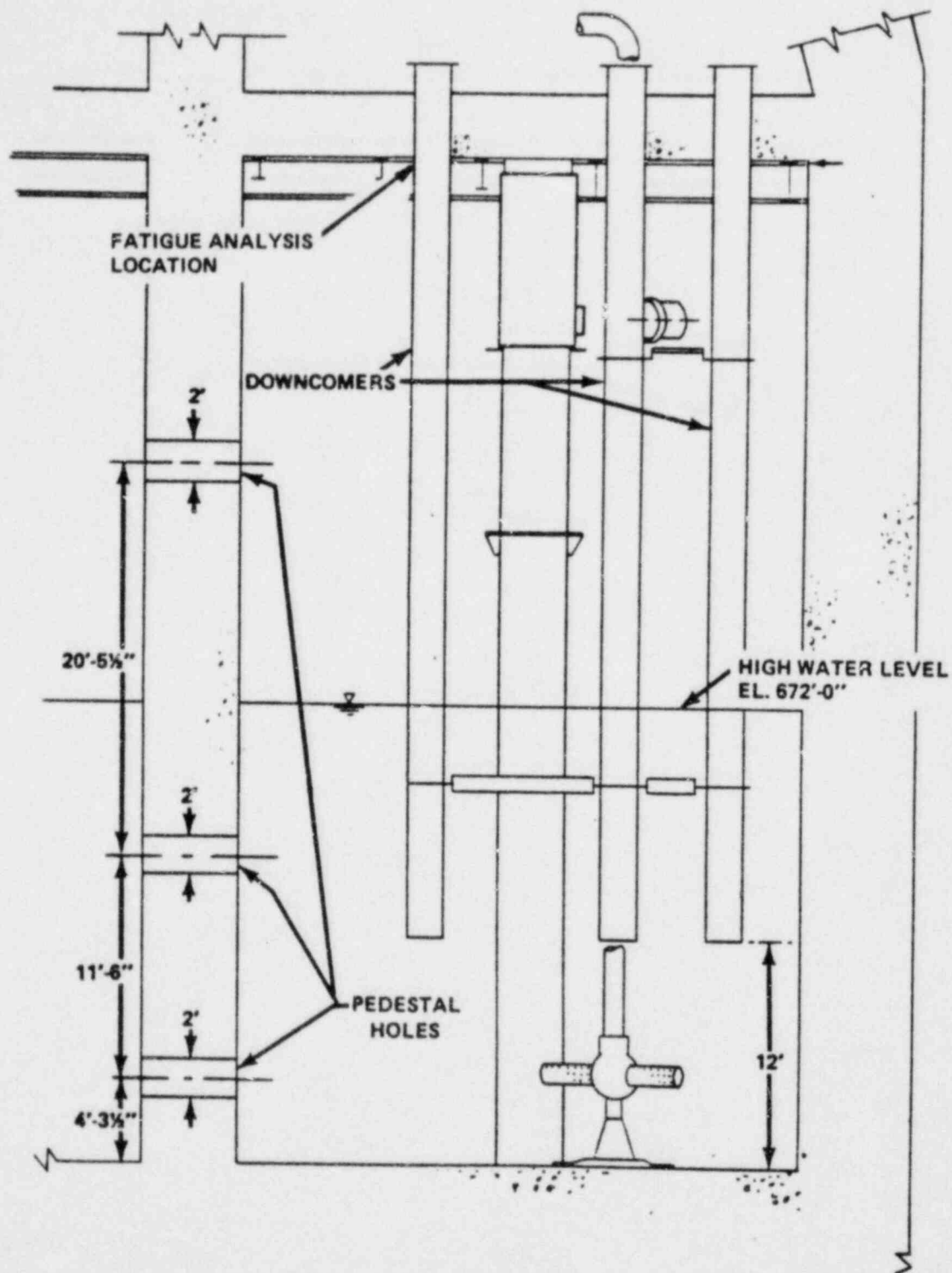


REV. 6, 4/82

SUSQUEHANNA STEAM ELECTRIC STATION
UNITS 1 AND 2
DESIGN ASSESSMENT REPORT

DOWNCOMER WITHOUT
VACUUM BREAKER

FIGURE 7-25



REV. 6, 4/82

SUSQUEHANNA STEAM ELECTRIC STATION
UNITS 1 AND 2
DESIGN ASSESSMENT REPORT

LOCATION WHERE DOWNCOMER
FATIGUE ANALYSIS WAS PERFORMED

FIGURE 7-

Table 7-1
MAXIMUM SPECTRAL ACCELERATIONS OF CONTAINMENT DUE TO SRV AND LOCA
 LOADS AT 1% DAMPING

TYPE OF LOAD		LOAD CASE	DIRECTION	NODE NUMBER	ELEVATION	MAXIMUM SPECTRAL ACCELERATION (g)	STRUCTURAL FREQUENCY Hz
SRV		Axisymmetric	Vertical	841	778'-9-3/4"	1.088	15
			Horizontal	135	672'-0"	1.58	38
		Asymmetric	Vertical	252	702'-3"	0.83	40
			Horizontal	131	672'-0"	0.875	38
L O C A	CHUGGING	Axisymmetric	Vertical	235	702'-3"	1.80	54
			Horizontal	131	672'-0"	8.5	30
		Asymmetric	Vertical	235	702'-3"	1.56	54
			Horizontal	131	672'-0"	7.1	30
	(CO)	Axisymmetric	Vertical	850	731'-3-1/4"	1.0	11
			Horizontal	131	672'-0"	1.97	30

Table 7-2

MAXIMUM SPECTRAL ACCELERATIONS OF REACTOR AND CONTROL BUILDINGS

TYPE OF LOAD	LOAD		NODE		MAXIMUM SPECTRAL ACCELERATION (g)	STRUCTURAL FREQUENCY Hz
	CASE	DIRECTION	NUMBER	ELEVATION		
SRV	Axisymmetric	Vertical	25	697'-0"	1.7	15
		Horizontal	NA	NA	NA	NA
	Asymmetric	Vertical	25	697'-0"	0.35	15
		Horizontal (E-W)	37	683'-0"	0.35	25
L O C A (CO)	CHUGGING	Axisymmetric	Vertical	25	697'-0"	15
			Horizontal	37	683'-0"	25
		Asymmetric	Vertical	25	697'-0"	15
			Horizontal	36	670'-0"	75
	(CO)	Axisymmetric	Vertical	23	870'-0"	11
			Horizontal	37	683'-0"	25
		(E-W)				

Table 7-3

USAGE FACTOR SUMMARY OF DOWNCOMERS

	NORMAL/UPSET CONDITION			EMERGENCY/FAULTED CONDITION		
	$\begin{matrix} + \\ - \end{matrix}$ OBE $\begin{matrix} + \\ - \end{matrix}$ SRV1 $\begin{matrix} + \\ - \end{matrix}$ SRV2	$\begin{matrix} + \\ - \end{matrix}$ SRV1 $\begin{matrix} + \\ - \end{matrix}$ SRV2 $\begin{matrix} + \\ - \end{matrix}$ CHUG	$\begin{matrix} + \\ - \end{matrix}$ SRV1 $\begin{matrix} + \\ - \end{matrix}$ SRV2	<u>SBA</u> *Pressure *Thermal Transient *Steam Flow $\begin{matrix} + \\ - \end{matrix}$ CHUG $\begin{matrix} + \\ - \end{matrix}$ SRV*	<u>IBA or SBA</u> *Pressure *Thermal Transient *Steam Flow $\begin{matrix} + \\ - \end{matrix}$ CHUG $\begin{matrix} + \\ - \end{matrix}$ SRV* $\begin{matrix} + \\ - \end{matrix}$ SSE	<u>DBA</u> *Pressure *Thermal Transient *Steam Flow $\begin{matrix} + \\ - \end{matrix}$ CHUG $\begin{matrix} + \\ - \end{matrix}$ SSE
LOADS						
At diaphragm location	0.0083	0.608	0.774	0.774	0.791	.782

- Notes: 1) SRV* is a combination of direct loads and building response loads.
 2) CHUG is the maximum chugging load (direct load and building response).
 3) The calculation is based on ASME, Section III, 1979 Summer Addendum.
 4) The combination of $\begin{matrix} + \\ - \end{matrix}$ CHUG, $\begin{matrix} + \\ - \end{matrix}$ SRV* and SSE or OBE is by SRSS.
 5) Thermal and pressure loads are combined with 4) by absolute sum.
 6) SRV1 is submerged structure load.
 7) SRV2 is building response load.

TABLE 7-4 MAXIMUM CUMULATIVE USAGE FACTORS
FOR SRV DISCHARGE LINE

COMPONENT	CALCULATED CUMULATIVE USAGE FACTORS	CODE ALLOWABLE CUMULATIVE USAGE FACTORS
Flued Head	0.46	1.0
3-Way Restraint	0.51	1.0
Elbow (Line P)	0.56	1.0

Table 7-5
DOWNCOMERS AND BRACING SYSTEM
MODAL FREQUENCIES

MODE	FREQ. (HZ)	WEIGHT PARTICIPATION FACTORS		
		HORIZ-X	HORIZ-Y	VERTICAL
1	1.84	0.320	1.274	---
2	1.84	-1.278	0.321	---
3	2.53	0.001	-0.013	---
4	6.58	---	0.001	---
5	8.64	0.001	-0.002	---
6	9.95	-0.001	0.001	---
7	13.27	0.004	-0.002	-0.002
8	14.05	-0.001	0.004	-0.002
9	14.55	0.001	-0.001	0.004
10	15.12	0.003	0.002	-0.001
11	15.17	-0.007	---	0.006
12	15.27	0.002	0.001	---
13	15.38	---	0.003	-0.008
14	15.44	-0.001	0.003	-0.007
15	15.46	-0.003	-0.001	0.002
45	15.75	---	0.002	-0.012
46	15.76	-0.004	0.001	0.004
47	17.44	0.010	0.521	---
48	17.44	-0.504	0.006	---
49	17.50	0.023	-0.116	---
50	17.78	0.015	0.126	---
93	45.05	-0.072	0.460	---
94	45.14	-0.416	-0.059	---
95	45.33	-0.005	-0.027	---
96	45.82	0.007	0.256	---

CHAPTER 10
RESPONSES TO NRC QUESTIONS

TABLE OF CONTENTS

10.1	NRC QUESTIONS
10.1.1	IDENTIFICATION OF QUESTIONS UNIQUE TO SSES
10.1.2	IDENTIFICATION OF QUESTIONS PERTAINING TO THE NRC'S REVIEW OF THE DAR
10.1.3	QUESTIONS RECEIVED DURING THE PREPARATION OF THE SAFETY EVALUATION REPORT (SER)
10.2	RESPONSES
10.2.1	QUESTIONS UNIQUE TO SSES AND RESPONSES THERETO
10.2.2	QUESTIONS PERTAINING TO THE NRC'S REVIEW OF THE DAR AND RESPONSE THERETO
10.2.3	QUESTIONS INFORMALLY RECEIVED DURING THE PREPARATION OF THE SAFETY EVALUATION REPORT (SER) AND RESPONSE THERETO
10.3	FIGURES

CHAPTER 10

FIGURES

Number	Title
10-1	This figure has been deleted.
10-2	This figure has been deleted.
10-3	Special relationship of downcomers and pedestal holes
10-4	Transducer locations for the ten vent pipe configuration
10-5	Transducer locations for the six vent pipe configuration
10-6	Transducer locations for the two vent pipe configuration
10-7	Typical pressure time histories from pressure transducers P20, P25 ... 29 and P134
10-8	Typical pressure time histories from pressure transducers P20, P25 ... 29 and P134
10-9	Frequency distribution of measured normalized wall pressures
10-10	Pool wall pressures at three circumferential vent exit locations - 1/6 scale 3 vent geometry
10-11	Pool wall pressures at three circumferential vent exit locations - 1/10 scale 19 vent geometry
10-12	Plan locations of transducers for wetwell
10-13	Locations of pressure transducers for wetwell
10-14	Vent exit elevation pool wall pressures for a chug from JAERI test 0002
10-15	Comparison of probability density of the normalized pressure amplitudes from GKM II-M tests 3 ... 10 and JAERI
10-16	Comparison of probability density of the normalized pressure amplitudes from GKM II-M tests 11 & 12 and JAERI
10-17	Comparison of probability density of the normalized pressure amplitudes from GKM II-M tests 13 ... 20 and JAERI
10-18	Comparison of pressure response spectra of test 21.2 - all valve case - and the SSES load definition
10-19	Comparison of pressure response spectra of test 21.2 - all valve case and one valve case - and the SSES load definition

Figures (Cont.)

<u>Number</u>	<u>Title</u>
10-20	SSES containment response spectra - KWU SRV#76 - Asymmetric direction horizontal
10-21	SSES containment response spectra - KWU SRV#76 - Asymmetric direction vertical
10-22	SSES containment response spectra - KWU SRV#76 - Asymmetric direction horizontal
10-23	SSES containment response spectra - KWU SRV#76 - Asymmetric direction vertical
10-24	SSES containment response spectra - KWU SRV#76 - Asymmetric direction horizontal
10-25	SSES containment response spectra - KWU SRV#76 - Asymmetric direction vertical
10-26	SSES containment response spectra - KWU SRV#76 - Asymmetric direction horizontal
10-17	SSES containment response spectra - KWU SRV#76 - Asymmetric direction vertical
10-28	SSES containment response spectra - KWU SRV#76 - Asymmetric direction horizontal
10-29	SSES containment response spectra - KWU SRV#76 - Asymmetric direction vertical
10-30	SSES containment response spectra - KWU SRV#76 - Asymmetric direction horizontal
10-31	SSES containment response spectra - KWU SRV#76 - Asymmetric direction vertical
10-32	SSES containment response spectra - KWU SRV#76 - Asymmetric direction horizontal
10-33	SSES containment response spectra - KWU SRV#76 - Asymmetric direction vertical
10-34	SSES containment response spectra - KWU SRV#76 - Asymmetric direction horizontal
10-35	SSES containment response spectra - KWU SRV#76 - Asymmetric direction vertical
10-36	SSES containment response spectra - KWU SRV#76 - Asymmetric direction horizontal

FIGURES (Cont.)

Number	Title
10-37	SSES containment response spectra - KWU SRV#76 - Asymmetric direction vertical
10-38	SSES containment response spectra - KWU SRV#76 - Asymmetric direction horizontal
10-39	SSES containment response spectra - KWU SRV#76 - Asymmetric direction vertical
10-40	SSES containment response spectra - KWU SRV#76 - Asymmetric direction horizontal
10-41	SSES containment response spectra - KWU SRV#76 - Asymmetric direction vertical
10-42	LGS containment response spectra - KWU SRV#76 - Asymmetric direction horizontal
10-43	LGS containment response spectra - KWU SRV#76 - Asymmetric direction vertical
10-44	LGS containment response spectra - KWU SRV#76 - Asymmetric direction horizontal
10-45	LGS containment response spectra - KWU SRV#76 - Asymmetric direction vertical
10-46	LGS containment response spectra - KWU SRV#76 - Asymmetric direction horizontal
10-47	LGS containment response spectra - KWU SRV#76 - Asymmetric direction vertical
10-48	LGS containment response spectra - KWU SRV#76 - Asymmetric direction horizontal
10-49	LGS containment response spectra - KWU SRV#76 - Asymmetric direction vertical
10-50	LGS containment response spectra - KWU SRV#76 - Asymmetric direction horizontal
10-51	LGS containment response spectra - KWU SRV#76 - Asymmetric direction vertical
10-52	LGS containment response spectra - KWU SRV#76 - Asymmetric direction horizontal
10-53	LGS containment response spectra - KWU SRV#76 - Asymmetric direction vertical

FIGURES (Cont.)

<u>Number</u>	<u>Title</u>
10-54	LGS containment response spectra - KWU SRV#76 - Asymmetric direction horizontal
10-55	LGS containment response spectra - KWU SRV#76 - Asymmetric direction vertical
10-56	LGS containment response spectra - KWU SRV#76 - Asymmetric direction horizontal
10-57	LGS containment response spectra - KWU SRV#76 - Asymmetric direction vertical
10-58	LGS containment response spectra - KWU SRV#76 - Asymmetric direction horizontal
10-59	LGS containment response spectra - KWU SRV#76 - Asymmetric direction vertical
10-60	LGS containment response spectra - KWU SRV#76 - Asymmetric direction horizontal
10-61	LGS containment response spectra - KWU SRV#76 - Asymmetric direction vertical
10-62	LGS containment response spectra - KWU SRV#76 - Asymmetric direction horizontal
10-63	LGS containment response spectra - KWU SRV#76 - Asymmetric direction vertical
10-64	Reactor Pressure Transient - Case 2.a Without Shutdown Cooling
10-65	Suppression Pool Temperature Transient - Case 2.a Without Shutdown Cooling

CHAPTER 10

TABLES

Number	Title
10-1	Normalized RMS vent static pressure and variance - JAERI data
10-2	Comparison of JAERI/GKM II-M normalized mean variance

10.0--RESPONSES-TO-NRC-QUESTIONS

This chapter will provide responses to those Nuclear Regulatory Commission (NRC) questions which have been designated by Reference 10 (as amended) to be found in the plant-unique Design Assessment Report, to those questions for which the response in Reference 10 is inapplicable, to those questions generated from previous NRC reviews of the plant unique DAR, and those questions received during preparation of the SER. The NRC questions for which responses will be provided are identified in Subsections 10.1.1, 10.1.2, and 10.1.3, and detailed responses to these questions are found in Subsections 10.2.1, 10.2.2 and 10.2.3.

1
12
6

6 | 10.1.1 IDENTIFICATION OF QUESTIONS UNIQUE TO SSES

The below listed questions address concerns unique to SSES.

2 | These questions are answered in detail in Subsection 10.2.1

<u>NRC_Question_Number</u>	<u>Question_Topic</u>
M020.26	Primary and Secondary LOCA Loads
M020.27	Inventory Effects on Blowdown
M020.44	Poolswell Waves and Seismic Slosh
M020.55	SRV Loads on Submerged Structures
M020.58 (1), (2), (3)	Plant Unique Poolswell Calculations
M020.59 (1), (3), (4)	Downcomer Lateral Braces
M020.60	Wetwell Pressure History
M020.61	Poolswell Inside Pedestal
M130.1	Pressure Loading Due to SRV Discharge
M130.2	Load Combination History
M130.4	Soil Modeling
M130.5	Liner and Anchorage Mathematical Model
M130.6	Containment Structural Model-Asymmetric Loads
M130.12	SRV Structural Response

10.1.2 IDENTIFICATION OF QUESTIONS PERTAINING TO THE NRC'S
REVIEW OF THE DAR

16

The below listed questions address concerns generated as a result of the NRC's review of the DAR. These questions are answered in detail in Subsection 10.2.2

2

16

<u>Question Number</u>	<u>Question Topic</u>
1	NUREG-0487 Acceptance Criteria
2	Drywell Pressurization
3	Chugging Loads on Submerged Structures
4	IBA and SBA for Typical Mark II Containment
5	Poolswell Waves and Seismic Slash
6	List of Piping, Equipment, etc., Subject to Pool Dynamic Loads
7	Applicability of the Generic Programs, Tests and Analysis to the SSES Design
8	Time History of Plant Specific Loads
9	Mass and Energy Release
10	"Local" and "Bulk" Pool Temperature
11	Suppression Pool Temperature Monitoring System

2

10.1.3---QUESTIONS RECEIVED DURING THE PREPARATION OF THE
SAFETY EVALUATION REPORT (SER)

The below listed questions were informally received during the NRC's preparation of the SER. These questions are answered in detail in Subsection 10.2.3.

<u>Question Number</u>	<u>Question Topic</u>
1	SSES LOCA Steam Condensation Load Definition (SER Item #27)
2	T-Quencher Frequency Range (SER Item #28)
3	SSES ADS Load Case (SER Item #28)
4	Quencher Bottom Support at Karlstein (SER Item #28)
5	Bending Moment in the Quencher Arm Recorded at Karlstein (SER Item #28)
6	Suppression Pool Temperature Response (SER Item #30)
7	Local to Bulk Temperature Difference for SSES (SER Item #30)
8	Quencher Steam Mass Flux (SER Item #30)

10.2--RESPONSES

10.2.1--QUESTIONS UNIQUE TO SSES AND RESPONSES THERETO

QUESTION MO20.26

The DFFR presents a description of a number of LOCA related hydrodynamic loads without differentiating between primary and secondary loads. Provide this differentiation between the primary and secondary LOCA-related hydrodynamic loads. We recognize that this differentiation may vary from plant to plant. We would designate as a primary load any load that has or will result in a design modification in any Mark II containment since the pool dynamic concerns were identified in our April 1975 generic letters.

RESPONSE MO20.26

The table below shows the LOCA-related hydrodynamic loads on the SSES containment. Those loads which have resulted in containment design modifications are designated as "Primary Loads." These primary loads result from the poolswell transient.

Drywell floor uplift pressures during the wetwell compression phase of poolswell lead to the decision to increase the SSES drywell floor design safety margin for uplift pressures by relocating drywell floor shear ties.

Poolswell impact, drag, and fallback loads resulted in the relocation of equipment in the SSES wetwell to a position above the peak poolswell height. Furthermore, the downcomer bracing system was redesigned.

All other LOCA-related hydrodynamic loads are designated as "Secondary Loads" since no design modification has resulted from their presence.

<u>LOCA Load</u>	<u>"Primary Load"</u>	<u>"Secondary Load"</u>
1. Wetwell/Drywell Pressures (During Poolswell)	X(1)	
2. Poolswell Impact Load	X(2)	
3. Poolswell Drag Load	X(3)	
4. Downcomer Clearing Load		X
5. Downcomer Jet Load		X
6. Poolswell Air Bubble Load		X
7. Poolswell Fallback Load	X(4)	

<u>LOCA_Load</u>	<u>"Primary_Load"</u>	<u>"Secondary_Load"</u>
8. Mixed Flow Condensation Oscillation Load		X
9. Pure Steam Condensation Oscillation Load		X
10. Chugging		X
11. Wetwell/Drywell Pressure and Temperature during DBA LOCA (Long Term)		X
12. Wetwell/Drywell Pressure and Temperature during IBA LOCA (Long Term)		X
13. Wetwell/Drywell Pressure and Temperature during SBA LOCA (Long Term)		X

Footnotes:

- (1) Shear ties changed in drywell floor.
- (2) Equipment moved in wetwell.
- (3) Equipment moved in wetwell. Bracing system redesign.
- (4) Equipment moved in wetwell.

QUESTION_M020.27

The calculated drywell pressure transient typically assumes that the mass flow rate from the recirculation system or steamline is equal to the steady-state critical flow rate based on the critical flow area of the jet pump nozzle or steamline orifice. However, for approximately the first second after the break opening, the rate of mass flow from the break will be greater than the steady-state value. It has been estimated that for a Mark I containment this effect results in a temporary increase in the drywell pressurization rate of about 20 percent above the value based solely on the steady-state critical flow rate. The drywell pressure transient used for the LOCA pool dynamic load evaluation, for each Mark II plant, should include this initially higher blowdown rate due to the additional fluid inventory in the recirculation line.

RESPONSE_M020.27

The drywell pressure transients have been recalculated by GE (Reference 7) with the additional blowdown flow rate produced by the inventory effects included in the analysis. The LOCA loads presented in Section 4.2 have been calculated using these

recalculated drywell pressure transients. Specifically, the drywell pressure transient resulting from the DBA LOCA including the effects of pipe inventory has been used as input to the poolswell model.

QUESTION_M020.44

Table 5-1 and Figures 5-1 through 5-16 in the DFFR provide a listing of the loads and the load combinations to be included in the assessment of specific Mark II plants. This table and these figures do not include loads resulting from pool swell waves following the pool swell process or seismic slosh. We require that an evaluation of these loads be provided for the Mark II containment design.

RESPONSE_M020.44

Subsections 4.2.4.6 and 4.2.4.7 provide our response.

QUESTION_M020.55

The computational method described in DFFR Section 3.4 for calculating SRV loads on submerged structures is not acceptable. It is our position that the Mark II containment applications should commit to one of the following two approaches:

- (1) Design the submerged structures for the full SRV pressure loads acting on one side of the structures; the pressure attenuation law described in Section 3.4.1 of NEDO-21061 for the ramshead and Section A10.3.1 of NEDO-11314-08 for the quencher can be applied for calculating the pressure loads.
- (2) Follow the resolution of GESSAR-238 NI on this issue. The applicant for GESSAR-238 NI has proposed a method presented in the GE report, "Unsteady Drag on Submerged Structures," which is attached to the letter dated March 24, 1976 from G.L. Gyorey to R.L. Tedesco. This report is actively under review.

RESPONSE_M020.55

Loads on submerged structures due to SRV actuation are discussed in Subsection 4.1.3.7.

QUESTION_M020.58

Relating to the pool swell calculations, we require the following information for each Mark II plant:

- (1) Provide a description of and justify all deviations from the DFFR pool swell model. Identify the party responsible for conducting the pool swell calculations (i.e., GE or the A&E). Provide the program input and

results of bench mark calculations to qualify the pool swell computer program.

- (2) Provide the pool swell model input including all initial and boundary conditions. Show that the model input represents conservative values with respect to obtaining maximum pool swell loads. In the case of calculated input, (i.e., drywell pressure response, vent clearing time), the calculational methods should be described and justified. In addition, the party responsible for the calculation (i.e., GE or the A&E) should be identified.
- (3) Pool swell calculations should be conducted for each Mark II plant. The following pool swell results should be provided in graphic form for each plant:
 - (a) Pool surface position versus time
 - (b) Pool surface velocity versus time
 - (c) Pool surface velocity versus position
 - (d) Pressure of the suppression pool air slug and the wetwell air versus time.

RESPONSE_M020.58

- (1) A specific response to this question can be found in Subsection 4.2.1.1. Verification of the SSES poolswell model is provided in Appendix Section D.1.
- (2) Input and discussion of the poolswell model input can be found in Tables 4-17, 4-18, and Section 4.2.1.1.
- (3) The requested graphic results of the SSES poolswell calculation can be found in Figures 4-38, 4-39, 4-40, and 4-43.

QUESTION_M020.59

In the 4T test report NEDE-13442P-01 Section 3.3 the statement is made that for the various Mark II plants a wide diversity exists in the type and location of lateral bracing between downcomers and that the bracing in the 4T tests was designed to minimize the interference with upward flow. Provide the following information for each Mark II plant:

- (1) A description of the downcomer lateral bracing system. This description should include the bracing dimensions, method of attachment to the downcomers and walls, elevation and location relative to the pool surface. A sketch of the bracing system should be provided.
- (2) The basis for calculating the impact or drag load on the bracing system or downcomer flanges. The magnitude and

duration of impact or drag forces on the bracing system or downcomer flanges should also be provided.

- (3) An assessment of the effect of downcomer flanges on vent lateral loads.

2

RESPONSE_M020.59

- (1) Subsection 7.1.2.1 describes the SSES bracing system and the methodology for assessing the adequacy of bracing system.
- (2) The basis for calculating the impact or drag loads on the downcomer bracing system (El. 668') and downcomer stiffener rings (El. 668' and El. 682') is given in Section 4.2. The magnitude and duration of impact or drag forces on the bracing system and downcomer stiffener rings is also given in Section 4.2 .
- (3) This item is not applicable to the SSES design.

6

QUESTION_M020.60

In the 4T test report NEDE-13442P-01 Section 5.4.3.2 the statement is made that an underpressure does occur with respect to the hydrostatic pressure prior to the chug. However, the pressurization of the air space above the pool is such that the overall pressure is still positive at all times during the chug. We require that each Mark II plant provide sufficient information regarding the boundary underpressure, the hydrostatic pressure, the air space and the SRV load pressure to confirm this statement or alternatively provide a bounding calculation applicable to all Mark II plants.

2

RESPONSE_M020.60

This information is provided in Subsection 7.1.3 of the DAR.

QUESTION_M020.61

Significant variations exist in the Mark II plants with regard to the design of the wetwell structures in the region enclosed by the reactor pedestal. These variations occur in the areas of (1) concrete backfill of the pedestal, (2) placement of downcomers, (3) wetwell air space volumes, and (4) location of the diaphragm relative to the pool surface. In addition to variation between plants, for a given plant, variations exist in some of these areas within a given plant. As a result, for a given plant, significant differences in the pool swell phenomena can occur in these two regions. We will require that each plant provide a separate evaluation of pool swell phenomena and loads inside of the reactor pedestal.

RESPONSE_M020.61

The SSES pedestal and wetwell area is shown on Figures 1-1 and 10.3. Due to the absence of downcomers in the pedestal interior, no pool swell would be expected in this region. There are 12 holes in the pedestal, however, eight of which would allow the flow of water from the suppression pool to the pedestal during a LOCA. Some downcomers are near the pedestal flow holes, leading to the possibility that air could be blown through the pedestal holes, which would lead to a greater pedestal pool swell than would be experienced by incompressible water flow alone. One would expect the pedestal pool swell to be much reduced from the suppression pool swell due to its relative separation from the suppression pool and the lack of direct charging from downcomer vents. Indeed, 1/13.3 scale model tests of the SSES pedestal design conducted at the Stanford Research Institute under the sponsorship of EPRI show that the pedestal pool swell is less than 20 percent of the pool swell in the suppression pool (Reference 32). There is no piping or equipment inside the SSES pedestal and, since the pedestal pool swell is very small, the only load involved due to pedestal pool swell would be a small ΔP across the pedestal due to different water levels between the suppression pool and the pedestal interior. This load is considered in the design of the SSES pedestal.

QUESTION M130.1

Provide in Section 5 a description of the pressure loadings on the containment wall, pedestal wall, base mat, and other structural elements in the suppression pool, due to the various combinations of SRV discharges, including the time function and profile for each combination. If this information is not generic, each affected utility should submit the information as described above.

RESPONSE M130.1

Chapter 4 describes the pressure loadings and time histories due to SRV discharge and other hydrodynamic loads.

QUESTION M130.2

In DFFR Section 5.2 it is stated that the load combination histories are presented in the form of bar charts as shown on Figures 5-1 through 5-16. It is not indicated how these load combination histories are used. In particular, it is not clear whether only loads represented by concurrent bars will be combined, and it should be noted that depending on the dynamic properties of the structures and the rise time and duration of the loads, a structure may respond to two or more given loads at the same time even though these loads occur at different times. Also, although condensation oscillations are depicted as bars on the bar charts, the procedure for the analysis of structures due to these loads has not been presented. Accordingly, the description of the method should include consideration of such conditions. Also, for condensation oscillation loads and for SRV oscillatory loads, include low cycle fatigue analysis.

RESPONSE_M130.2

The loads will be combined according to Section 5.0. Section 7.0 describes the assessment methodology and results for the re-assessment of SSES for the hydrodynamic and non-hydrodynamic loads.

QUESTION_M130.4

Through the use of figures, describe in detail the soil modelling as indicated in DFFR Subsection 5.4.3 and describe the solid finite elements which you intend to use for the soil.

RESPONSE_M130.4

Soil modelling is explained in Subsection 7.1.1.1.

QUESTION_M130.5

Describe the mathematical model which you will use for the liner and the anchorage system in the analysis as described in DFFR Subsection 5.6.3.

RESPONSE_M130.5

The mathematical model which will be used for analysis of the liner and the anchorage for hydrodynamic suction pressures is described in Subsection 7.1.3.

QUESTION_M130.6

In DFFR Subsection 5.1.1.1 it was stated that the SRV discharge could cause axisymmetric or asymmetric loads on the containment. In Subsection 5.4.1 an axisymmetric finite element computer program is recommended for dynamic analysis of structures due to SRV loads, and no mention is made of the analysis for asymmetric loads. Describe the structural analysis procedure used to consider asymmetric pool dynamic loads on structures and through the use of figures, describe in more detail the structural model which you intend to use.

RESPONSE_M130.6

The dynamic analyses and models used are explained in Chapter 7.

QUESTION_M130.12

Reference is made in DFFR Subsection 5.4.3 to studies of structural response to SRV load. Provide citations for this reference and where such studies are not readily available, copies are requested.

RESPONSE_M130.12

Studies mentioned in DFFR Subsection 5.4.3 are the results of analysis completed for a specific plant at the time of writing of the DFFR. Reference to the studies was intended to indicate the need for considering strain dependent soil properties. For the SSES analysis, Reference 33 is used to determine the soil constants in the analysis.

10.2.2 QUESTIONS PERTAINING TO THE NRC'S REVIEW OF THE DAR AND RESPONSE THERETO

6

QUESTION 1

The LOCA and SRV related pool dynamic loads that are currently acceptable to us are discussed in NUREG-0487. Table IV-1 of NUREG-0487 summarizes these Mark II pool dynamic loads. By letter, dated February 2, 1979, you indicated on Table IV-1 the LOCA related dynamic loads acceptable to the staff that will be adopted for SSES. Revise the DAR to incorporate this information and provide the same information for the SRV related pool dynamic loads. For both the SRV and LOCA loads indicate the alternative criteria that will be used for each item for which an exemption is proposed and provide references that discuss these alternative criteria.

RESPONSE

See response to Question 021.69 contained in Volume 16 of the SSES FSAR and Table 1-4 of the DAR.

2

QUESTION 2

Subsection 4.2.1.1 of the DAR state that the drywell pressure transient used for the pool swell portion of LOCA is based on the methodology described in NEDO-21061. Subsection III.B.3.a.6 of NUREG-0487 requires that a comparison similar to those presented in reference 1* be made if the model used is different from the model described in NEDM-10320. We require the model prior to completion of review of the pool swell calculations.

*Reference (1) Letter "Response to NRC Request for Additional Information (Round 3 Questions," to J. P. Stolz (NRC-DPM) from L. J. Sobon (GE), dated June 30, 1978.

RESPONSE

See response to Question 021.70 contained in the SSES FSAR.

QUESTION 3

Subsection 4.2.2.2 of the DAR states that the chugging loads on submerged structures and imparted on the downcomers will be evaluated later. Provide the present status of these evaluations and the schedule for your submission of the completed evaluation.

6

RESPONSE

See response to Question 021.71 in the SSES FSAR.

2

QUESTION 4

Statements are made in Subsections 4.2.3.2 and 4.2.3.3 of the DAR that plant unique data of the Susquehanna SES intermediate break

accident (IBA) and small break accident (SBA) are estimated from curves for a typical Mark II containment. Discuss the applicability of these analyses (e.g., power level, initial conditions, downcomer configuration, etc.) to Susquehanna SES.

RESPONSE

See response to Question 021.72 contained in the SSES PSAR.

QUESTION_5

Provide the information previously requested in 020.44 regarding loads resulting from pool swell waves following the pool swell process or seismic slosh. Discuss the analytical model and assumptions used to perform these analyses.

RESPONSE

See response to Question 021.73 contained in the SSES PSAR.

QUESTION_6

Provide a list and drawing to identify all piping, equipment instrumentation and structures in containment that may be subjected to pool dynamic loads. In addition, provide drawings to show the location of access galleys in the wetwell, the vent vacuum breaker configuration, wetwell grating, vent bracing configuration, vent configuration in the pedestal region of wetwell and large horizontal structures in the pool swell zone.

RESPONSE

See response to Question 021.74 contained in the SSES PSAR.

QUESTION_7

Discuss the applicability of the generic supporting programs, tests and analyses to Susquehanna SES design (i.e., PSI concerns, downcomer stiffeners, downcomer diameter, etc.).

RESPONSE

See response to Question 021.75 contained in the SSES PSAR.

QUESTION_8

Provide the time history of plant specific loads and assessment of responses of plant structures, piping, equipment and components to pool dynamic loads. Identify any significant plant modifications resulting from pool dynamic loads considerations.

RESPONSE

See response to Question 021.76 contained in the SSES PSAR.

QUESTION_9

Provide figures showing reactor pressure, quencher mass flux and suppression pool temperature versus time for the following events:

- (1) a stuck-open SRV during power operation assuming reactor scram at 10 minutes after pool temperature reaches 110°F and all RHR systems operable;
- (2) same as event (1) above except that only one RHR train available;
- (3) a stuck-open SRV during hot standby condition assuming 120°F pool temperature initially and only one RHR train available;
- (4) the Automatic Depressurization System (ADS) activated following a small line break assuming an initial pool temperature of 120°F and only one RHR train available; and
- (5) the primary system is isolated and depressurizing at a rate of 100°F per hour with an initial pool temperature of 120°F and only one RHR train available.

Provide parameters such as service water temperature, RHR heat exchanger capability, and initial pool mass for the analysis.

RESPONSE

See response to Question 021.77 contained in the SSES PSAR.

QUESTION_10

With regard to the pool temperature limit, provide the following additional information:

- (1) Definition of the "local" and "bulk" pool temperature and their application to the actual containment and to the scaled test facilities, if any; and
- (2) The data base that support any assumed difference between the local and the bulk temperatures.

RESPONSE

See response to Question 021.78 contained in the SSES PSAR.

QUESTION_11

For the suppression pool temperature monitoring system, provide the following additional information:

- (1) Type, number and location of temperature instrumentation that will be installed in the pool; and

- (2) Discussion and justification of the sampling or averaging technique that will be applied to arrive at a definitive pool temperature.

RESPONSE

See response to Question 021.79 contained in the SSES PSAR.

10.2.3 Questions Received During the Preparation of the Safety
-----Evaluation Report and Response Thereto-----

QUESTION 1

With regard to the SSES LOCA steam condensation load definition, provide the following additional information:

- (1) Justification for the interchangeability of the GKM II-M temporal chug strength probability distribution with the spacial variation of chug strengths at SSES.
- (2) Justification for not considering CO & SRV(ADS).
- (3) Comparison of the CO measured at 4T-CO with the CO observed at GKM II-M.

RESPONSE 1

- (1) The SSES LOCA steam condensation load definition assumes that the chugs occurring simultaneously at different vent pipes of SSES have different intensities and follow the same distribution of chug amplitudes in time as in the GKM II-M single vent facility. This assumption forms the basis for two key elements of the LOCA load definition.

The first element assumes that the average of simultaneously occurring chugs at different vents in SSES is equivalent to the average of consecutive GKM II-M chugs. Thus, as documented in Subsection 9.5.3.1.2, the random amplitude chugs at SSES were replaced with the same chug at every vent which represents the average of consecutive GKM II-M chugs or "mean value" chug.

The second element assumes that the chug amplitude or strength at the individual SSES vents are random variables which have the same probability distribution as the distribution of chug amplitudes at GKM II-M. The GKM II-M probability distribution was then applied statistically to an analytical model of the SSES suppression pool to calculate the symmetric and asymmetric amplitude factors. These factors were then applied to the selected mean value chugs to achieve the desired exceedance probability prior to transportation to SSES for containment analysis (see Subsections 9.5.3.4.1 and 9.5.3.4.2).

These two elements infer that the multi-vent facility is composed of many "single cells" whose chug strengths vary stochastically and independently of each other. The random nature of chugging is explained qualitatively by looking at the actual bubble collapsing mechanism. The most plausible mechanism for bubble collapse at the individual vents appears to be the convection in the pool. This means that bubble collapses at individual vents are triggered by the local turbulent convection at each vent. Thus due to the

stochastic nature of turbulence, the time at which rapid condensation and hence bubble collapse is triggered varies from vent to vent. This implies that the size of the bubble formed before collapse starts, will also vary from vent to vent. Therefore, the chug strength will vary from vent to vent. Since, the GKM II-M tests were designed to be prototypical of SSES (i.e., same initial pool temperature, same steam flow, etc.), this random variation is expected to be similar for both the GKM II-M single vent facility and the SSES plant.

Additional qualitative data verifying the random nature of chugging is provided by numerous multi-vent test programs. Specifically, the KWU multi-vent concrete cell tests in Karlstein, Creare subscale multi-vent tests and JAERI full scale multi-vent tests provide multi-vent data of the chugging phenomena.

The Karlstein facility investigated the chugging phenomena for 2, 6, and 10 vents at subscale. Each vent in the concrete cell was instrumented with a pressure transducer in such a way that it was indicative of the chug strength for its respective vent. Figures 10-4, 10-5, and 10-6 illustrate these vent transducers and the remaining transducers for the 10, 6, and 2 vent facilities, respectively.

Figures 10-7 and 10-8 show typical pressure time histories for the pressure transducers mounted near the vent pipes for the six vent configuration. These pressure transducers were all exposed to a steam environment and clearly indicate that the chug strengths differ by up to a factor of 10.

In addition, Figure 10-9 shows that the distribution of relative frequencies of the measured wall pressures becomes narrower as the number of vent pipes increases from 2 to 6 to 10. Again, the variation in chug strengths results in a lower global pressure amplitude with increasing number of vents.

This variation in chug strengths was also observed in the Creare subscale multi-vent test program. This observation was obtained by examining the pool wall pressures measured at the three different circumferential locations at the vent exit. All test geometries had three transducers located 120° apart circumferentially at the vent exit elevation. In the multi-vent geometrics, each of these pressure transducers was located close to a particular vent. Therefore, the amplitude of the POP measured at each circumferential location reflects to a large extent the chug strength at the vent closest to it (since pressure amplitude varies inversely with the distance between the vent and wall pressure measurement location). For example, only if the chug strengths at all vents were identical, would the peak over-pressure (POP) measured at each of these three circumferential locations be identical.

Figure 10-10 shows the pool wall pressures at the three circumferential vent exit locations in the 1/6 scale 3 vent geometry. The steam mass flux was 8 lbm/sec ft² and as determined from the vent static pressures over 80% of the chugs shown had all three vents participating. This figure shows that the POP's at the three locations are different for individual chugs. Therefore, it can be concluded that the chug strength varies from vent to vent.

Similar data from the 1/10 scale 19 vent geometry at a steam mass flux of 8 lbm/sec ft² are shown in Figure 10-11. Again, from vent static pressure data for vents closest to each circumferential wall pressure measurement location, it was determined that all three vents participated in the chugs shown. The POP's at the three different circumferential locations are seen as being different for individual chugs. Note that the variation of chug strength from vent to vent is expected to be stochastic to a large extent. Therefore, it is expected that for some chugs, the chug strength at the three vents would be similar.

Additional proof that the chug strengths in a multi-vent facility behave stochastically is given by the JAERI multi-vent test data. There are several pool wall pressure transducers that are located near the exits of different vents in the JAERI facility. Specifically, transducers WWPF-202, 302, 602, and 702 are located at the vent exit elevation next to vents 2, 3, 4, and 7, respectively (see Figure 10-12 and 10-13). The pressure amplitudes measured by these transducers reflect the chug strengths at vents closest to them.

The variation of chug strengths at individual vents is shown in Figure 10-14. The pool wall pressures at the vent exit elevation for a chug occur at 62.5 seconds in JAERI test 0002. In this chug event, a high amplitude chug occurred at vent 7 as indicated by the large pressure spike at WWPF702. The other vents had relatively smaller chugs. Keep in mind that the variation of chug strengths from vent to vent is stochastic in nature and that not all pool chugs will exhibit the large variation seen in Figure 10-14. Nonetheless, varying degrees of variation in chug strengths from vent to vent were found in all the chugs from Tests 0002, 2101, and 3102 for which expanded time traces are available.

So far, we have stated that chugging is stochastic in nature, and as such the chug strengths are expected to vary, even though the same thermodynamic conditions exist at each vent (i.e., steam air content, mass flux, bulk pool temperature, etc.). As presented above, this phenomena has been observed in numerous multi-vent test facilities. However, we have not quantitatively verified our assumption of the interchangeability of the temporal chug strength variations at GKM II-M with the spacially varying chug strengths at SSFS. Again, the Creare subscale multi-vent test data and

JAERI test data provide information verifying the conservatism of this assumption. Each will be presented below.

As previously stated, one element of our LOCA load definition replaces the random amplitude chugs at SSES with the same chug at every vent, which is representative of the mean value data at GKM II-M. The Creare test data coupled with the accepted acoustic methodology provides verification of this assumption. Creare has acoustically modeled the 1/10-scale single and multi-vent geometries and they have derived a source which represents the mean value chug in the 1/10-scale single vent geometry.

They then placed this mean value chug source at each vent location of their acoustic model for the 1/10-scale 3, 7, and 19 vent geometries. For each of the three multi-vent geometries, the pressure time history at the pool bottom elevation (same as the transducer location at this elevation in the test geometries) was computed for 20 chug events. Each chug event involved selecting start times for individual vents randomly within a 20 msec time window. The multi-vent multiplier was then computed based on the mean POP at the pool bottom elevation for the 20 computed chugs. The predicted multi-vent multipliers compared quite favorably with the measured values. Subsection A 5.2.2 of Reference 66 gives a detailed description of the analysis and results. Thus, for subscale multi-vent geometries, the first element of our LOCA load definition is verified.

Final quantitative justification for our key assumption is provided by comparing the available JAERI full-scale multi-vent data with the GKM II-M single vent data.

There are two sets of JAERI data available that can be used to infer chug strengths at individual vents in a given multi-vent chug event. The first set is the pool wall pressure data from the pool wall transducers located at the vent exit elevation. In the JAERI test geometry, there were four pool wall pressure transducers-WWPF 202, 302, 602, and 702-located such that each of these transducers is very near the exits of four individual vents. Therefore, the pressure data from a given transducer reflects the chug strength at the vent closest to that transducer.

As previously stated, the data from these wall pressure transducers were used to qualitatively show that the chug strengths vary significantly from vent to vent in a JAERI multi-vent chug event. Unfortunately, since a pool transducer "sees" pressures due to chugs at all vents to varying extents, the data from such transducers are not suitable for quantitative evaluation of vent to vent chug strength variations.

The other set of JAERI data that provides a measure of chug strengths at the individual vents are the vent static pressure measurements. Five of the seven vents in the JAERI test facility are instrumented with vent exit static pressure transducers.

The vent static pressure is a direct measure of the "vent component" of the chug-induced pool wall pressure. Further, due to desynchronization in a multi-vent geometry, the "vent component" is the dominant component of the chug induced pool pressures observed in multi-vent chugging. Therefore, the spatial (vent to vent) variation of the vent static pressures in the JAERI multi-vent geometry should provide a reliable estimate of the vent to vent chug strength variation in a multi-vent geometry.

Individual vent exit static pressures of 1.125 sec periods are available for 38 chug events from six JAERI tests, eight chugs from Test 0002, seven chugs from Test 0003, six chugs from Test 0004, five chugs from Test 1101, five chugs from Test 1201, and seven chugs from Test 2101. These chugs were selected from periods of high amplitude chugging in each test. Therefore, this data base covers the worst chugging regions observed in these JAERI tests.

The individual vent exit static pressures for a given pool chug event were processed in the following manner. First, the rms pressure P_i was computed for each vent static pressure trace. Next, the average rms pressure \bar{P} was computed. For example, if vent static pressures were available for all the five instrumented vents, the average rms vent static pressure for that chug is:

$$\bar{P} = \frac{P_1 + P_2 + P_3 + P_4 + P_5}{5}$$

Since we are interested in the relative variation in chug strengths between individual vents, the individual rms vent static pressures were normalized by the average rms pressure \bar{P} .

The normalized individual rms vent static pressure \bar{P}_i for the 38 chugs analyzed are given in Table 10-1. Also shown are the values of the normalized variances for the individual vent rms pressures for individual chug events. Note that due to instrumentation malfunctions, for all except one JAERI test, vent exit static pressure data are not available for all five instrumented vents.

Due to small number of vents (at most five) for which vent static pressure data are available, it is difficult to draw meaningful statistical inferences for vent to vent chug strength variations from any one individual pool chug event.

Therefore, it is necessary to make an assumption that allows the use of the data from all 38 chug events such that meaningful statistical inferences can be drawn. This assumption is that the normalized statistical distribution of chug strengths from vent to vent is independent of blowdown conditions. That is, the normalized vent to vent chug strength for all 38 chug events are samples selected from the same statistical population. Note that this is precisely the same assumption made in analyzing the temporal statistical properties of the GKM II-M single vent data (see Subsection 9.5.3.2.1).

The GKM II-M data that provides a direct measure of the vent component of the chug strength are the pool wall pressure data band pass filtered between 0.5-13 Hz. In this frequency range, the pool wall pressures measured are due to the vent pressure oscillations produced by \pm chug (see Subsection 9.4.2.1.2).

As described in Subsection 9.5.3.2.1, the pressure amplitudes of individual chugs were normalized by the sliding mean value over a given time interval. In this way, a normalized data base reflecting the temporal variations of chug strengths was obtained for all the GKM II-M tests. Note that again implicit in this procedure is the assumption that the statistics of the variation of the normalized chug strengths is independent of system conditions. As previously mentioned, this assumption was also used for combining the JAERI data for 38 pool chug events into a single statistical data base.

The histograms of the normalized chug strengths for the various GKM II-M tests are given in Figures 9-181, 9-182, and 9-183.

At this point, we now have a normalized vent to vent chug strength variation data base from the JAERI multi-vent tests and a corresponding normalized chug to chug strength variation data base from the GKM II-M single vent tests. Table 10-2 shows the variance for the JAERI and GKM II-M data bases. The variance for the JAERI data base is the average value of the individual variances shown in Table 10-1 for each of the 38 chug events. The variance of the GKM II-M data was calculated for the 0.5-13 Hz band passed data plotted in Figures 9-181, 9-182, and 9-183. It is seen that the average variance from the JAERI tests is virtually identical to the variance from the GKM II-M Full MSL tests* and is somewhat greater than the variances from the 1/3 and 1/6 MSL GKM II-M tests. This implies that the variation of vent to vent chug strengths in the JAERI multi-vent tests is equal to or greater than the chug to chug strength variation observed in the GKM II-M single vent tests.

Figures 10-15 through 10-17 show the comparison of the probability density histograms of the JAERI data and the low

* The full MSL break chug strength statistics were used to develop the SSSES probabilistic amplitude factors.

band passed GKM II-M Full MSL, 1/3 MSL and 1/6 MSL data, respectively. Again, the JAERI and GKM II-M data histograms are quite similar.

From the above comparisons it can be again concluded that the assumption that the vent to vent variation in chug strengths in a single vent geometry is equivalent to the vent to vent chug strength variation in a multi-vent geometry, used in developing the SSES chugging load definition from the GKM II-M single vent test data is quite reasonable.

Additional verification of the conservatism of the SSES LOCA load definition is provided by comparing the wall loads at JAERI calculated with the SSES LOCA load definition with the available JAERI wall load data (see Subsection 9.5.3.5.1). Figures 9-268 and 9-269 show that the SSES LOCA load definition bounds the available JAERI data by a substantial margin. Please note that the wall loads calculated by the SSES LOCA load definition do not include the symmetric amplitude factor and thus represent "mean value" chugs.

- (2) The Mark II Owners have specified two different CO loads for containment analysis. The first CO load (CO 1) corresponds to the CO occurring at the beginning of a postulated LOCA and the second CO load (CO 2) corresponds to the reduced CO load occurring later in the blowdown. For containment analysis, the Owners combine the reduced CO 2 load with loads due to SRV (ADS), on the basis that ADS occurs later in a LOCA justifying a reduced CO load for the combination CO & SRV (ADS).

However, SSES combines the so-called LOCA loads with SRV (ADS) for containment analysis. The LOCA load comprises the envelop of the responses due to both chugging and CO. Thus, the SSES load combination LOCA & SRV (ADS) considers both CO and chugging and is more conservative than the Owner's combination of a reduced CO load (CO 2) with SRV (ADS).

- (3) The SSES LOCA load definition selected one CO pressure time history (PTH No. 14) from GKM II-M as representative and bounding of the CO at GKM II-M (see Figure 9-177a & b). Subsequently, this CO PTH was sourced and applied in-phase to the IWEGS/MARS acoustic model for containment analysis.

Figure 9-264 represents the enveloping PSD of PTH No. 14. Figure 2-1 of Reference 70 presents the envelop for PSD values observed for CO in the 4T-CO tests. These two figures indicate that the PSD of PTH No. 14 from GKM II-M compares favorably with the enveloping PSD of the CO in 4T-CO.

QUESTION 2

The dominant frequency for the Karlstein T-Quencher Test 21.2 appears to be 8.0 Hz instead of the 6.8 Hz reported in Table 8-10 of the DAR. Using the multipliers from Figure 8-174 and this 8.0

Hz frequency, we get a transposed frequency of 10.6 Hz. This value falls outside of the specified frequency range. A Fourier analysis indicates an exceedance of approximately 70% at this 10.6 Hz frequency. Please provide justification for the existing load specification frequency range.

RESPONSE 2

As can be seen in Figure 8-188, Test 21.2 does not show a clearly predominant frequency. We have interpreted 6.5 Hz as the predominant frequency because of the maximum peak occurring in the PSD at that frequency; however, a second peak, only slightly lower than the 6.5 Hz peak, can be seen in that PSD at approximately 8.0 Hz.

To investigate further the significance of Test 21.2 to the acceptability of the Susquehanna T-Quencher load specification, KWU performed a pressure response spectra comparison of the load specification and Test 21.2.

The method of "weighted traces" presented to the NRC in the June 13, 1980 Lead Plant Meeting and documented in the KWU Report R - 141/141/79 is used for this comparison. Figure 10-18 shows that the Susquehanna load specification bounds the measured pressure time history of Karlstein Test 21.2 representing the all valve case.

Assuming a maximum predominant frequency in Test 21.2 of 8 Hz and transferring the measured data of Test 21.2 to the all-valve and single-valve load case we get the comparison shown in Figure 10-19. The pressure response spectra of the Susquehanna load specifications is slightly exceeded by the pressure spectra from Test 21.2 in the frequency range between 10 Hz and 11 Hz. This slight exceedance is only related to the single-valve load case and is considered insignificant to the total load specification and in relation to the total data base from Karlstein.

In addition, the term "dominant frequency" is highly subjective and sensitive to the method chosen for determining the dominant frequency. Originally, KWU determined the dominant frequency range for the three SSES design traces (KKB Traces #35, 76 and 82) to be 6.5 to 8.0 Hz (see SSES DAR, page 8P-101). This frequency range was based on a PSD analysis of the three traces. However, for these non-stationary SRV traces, the PSD analysis is sensitive to the time segment chosen for analysis. Using a particular time duration may give one dominant frequency while another may give a slightly different dominant frequency.

Subsequently, Bechtel has taken the design traces and performed their own analysis to determine the dominant frequency. They calculated a dominant frequency range of 6.45 to 8.69 Hz for the three traces. This frequency range was based on the inverse of the peak-to-peak oscillation time period for the first two peaks. This was done for both negative and positive peak-to-peak periods.

Furthermore, Sargent & Lundy have determined the dominant frequency range of the three traces to be 5.8 to 8.9 Hz. As can be seen, the dominant frequency varies according to who performs the analysis and the methodology selected.

For containment analysis, the KWU methodology requires that time scale multipliers be applied to the three design traces. They range from 0.9 (time contraction or frequency expansion) to 1.8 (time expansion or frequency contraction). When these multipliers are applied to the three design traces, specified frequency ranges of 3.3 to 8.9 Hz, 3.6 to 9.7 Hz and 3.8 to 9.9 Hz are obtained by using the above dominant frequency ranges from the original traces. Thus, the specified frequency range varies depending on the interpretation of the "dominant frequency".

However, regardless of the interpreted dominant frequency range, the same three traces and time expansion and contraction factors are used for containment analysis. Thus, one's opinion of what the dominant frequency range is for the three traces is not as important as the time factors chosen for actually applying the traces to the containment boundary.

With this in mind, Figures 10-20 thru 10-41 illustrate the response spectra generated by KWU Trace #76 for SSES. The trace was frequency expanded and contracted by 110% and 55%, respectively, to give a specified frequency ranges of 3.3 to 8.9 Hz, 3.6 to 9.7 Hz or 3.8 to 9.9 Hz, again, depending on the interpretation of the "dominant frequency".

Figures 10-42 thru 10-63 show the response spectra generated by KWU Trace #76 for the Limerick Generating Station (LGS). The LGS structural model is essentially identical to the SSES model. However, these spectra reflect the use of frequency expansion and contraction factors of 125% and 55%, respectively. This gives specified frequency ranges of 3.3 to 10 Hz, 3.6 to 10.9 Hz or 3.8 to 11 Hz. Thus, depending on the dominant frequency, these spectra reflect the use of the NRC's upper bound dominant frequency of 11 Hz, as required by Supplement No. 1 to NUREG-0487.

A node by node comparison of the two spectra shows that the expanded spectral input used for LGS has negligible effect on the total response contributed by all modes. Thus, this supports the conclusion that an extension of the upper frequency multiplier would have no significant impact on the SSES response spectra analysis.

QUESTION 3

The Karlstein tests run with depressed water legs to simulate the ADS load case utilized the longest discharge line length for SSES. Is this line length prototypical of the SSES ADS line lengths? If not, what is the magnitude of the difference between the SSES ADS line lengths and the test line length? If not

prototypical, is the data from the ADS tests acceptable for transportation to SSES with regards to frequency content?

RESPONSE_3

Tests 10.3, 11.1, 12.1, and 13.1 are considered representative for the ADS actuation load case. These tests were all performed with the long discharge line. No tests with a short discharge line and a depressed initial water level (representing ADS conditions) were performed. These long line tests represent a bounding condition, in that the longest discharge line with depressed initial water level contains the largest possible initial air mass and will therefore produce the lowest possible pressure oscillation frequency.

To check whether the frequencies expected from short line ADS actuation fall within our specified frequency range we will transpose the test results from Test 11.1 to short line conditions.

Table 8B on page 8P-105 of the Susquehanna DAR shows the average frequencies measured during the Karlstein tests. A portion of that table is shown below:

Measured Frequencies (Hz)		
Long	Clean Conditions	(3.5) *-4
Line	Real Conditions	5
Short	Clean Conditions	5
Line	Real Conditions	6.5

*Tests with low amplitude

This data indicates a ratio of approximately 1.3 exists between the frequencies measured in long line tests and short line tests.

Subsection 8.5.3.3.4.6 of the Susquehanna DAR provides the comparison of the T-Quencher ADS load specification with the Karlstein test results. When the measured frequency for Test 11.1 was adjusted to account for back pressure and water surface area effects the measured 3 Hz frequency was raised to 5.7 Hz. To check the short line ADS load case we will adjust this 5.7 Hz by the 1.3 ratio obtained above. This produces a predominant frequency for the ADS - short line conditions of

$$V = 5.7 \times 1.3 = 7.4 \text{ Hz}$$

This frequency lies within the specified frequency range.

QUESTION_4

Was the quencher bottom support used at Karlstein prototypical of the supports at Susquehanna SES?

RESPONSE_4

The bottom support used in Karlstein is prototypical but not identical of those used at Susquehanna. The T-Quencher installed in the Karlstein test tank had the same distance between the bottom of the support and the quencher mid-plane as those quenchers installed at Susquehanna. Therefore, the thermo-hydraulic loading on the quencher supports are the same for the Karlstein test tank and Susquehanna. From a structural point of view, the bottom support used at Karlstein is not identical to those used at Susquehanna in that the supports in the plant are stiffer.

QUESTION_5

In three instances, the bending moment in the quencher arm recorded at Karlstein exceeds the specified bending moment. Is the specified bending moment in the quencher arm conservative? Why?

RESPONSE_5

As shown in Figure 8-153 the measured bending moments transposed to the weld of the quencher arm exceed the specified moment in 3 out of a total of 99 cases during vent cleaning. The total load specification for the quencher arm is made up of three components:

- a) internal pressure
- b) bending moment
- c) temperature gradient

The following table lists the specified and maximum measured values for each of the load components.

<u>Condition</u>	<u>Specified Value</u>	<u>Maximum Measured Value</u>
Steady State Pressure	22 bars	13 bars
Internal Temperature	219° C	191.6° C
Bending Moment	65 kNm	85 kNm

As can be seen, the specified values exceed the measured maximum values except for the referenced bending moments noted above.

As a result of this exceedance, a stress analysis, identical to the one performed for the specified values, was completed using the above maximum measured values. This analysis shows that the total stress due to the specified loads bounds the total stress due to the maximum measured loads. In addition, a fatigue evaluation of the arm weld was performed using the maximum measured data. The results indicate the weld has a usage factor less than unity, and thus is acceptable.

QUESTION 6

Explain why a single failure will not disable both the RHR shutdown cooling function and one RHR loop in the suppression pool cooling mode.

RESPONSE 6

A single failure can indeed disable the RHR shutdown cooling function and one RHR loop in the suppression pool cooling mode under the following assumptions. Both units are operating at full power when a complete long-term loss of offsite power (LOOP) occurs. This leads to main steam line isolation and reactor scram. Following the LOOP all four (4) diesel generators should start to supply power to the ESS busses, however, it is assumed that the diesel generator OG501C does not start (single failure). OG501C supplies power to the ESS busses 1A203 and 2A203*, to the RHR pumps 1C and 2C*, and to the RHR service water pump 1A. Loss of OG501C means that the inboard shutdown cooling isolation valves on both units, 1F009 and 2F009*, lose power to their operators, thus disabling the RHR shutdown cooling mode. Since these valves are located inside the primary containment, it is conservatively assumed that they will not be manually reopened. Only the "B" loop and the corresponding RHRSW loop of the RHR system (in both units) would be readily available for suppression pool cooling, using e.g., RHR pumps 1B and 2D*. The "A" loop of one unit could be made available by manually operating four (4) valves (close F048A, open F024A, HV-1210A and HV-1215A) and using RHRSW pump 2A* and either RHR pump 1A or 2A*. However, a simultaneous operation of RHR pumps 1A and 2A* is prohibited by electrical interlocks. Thus one of the units would have only one RHR loop available in the suppression pool cooling mode without the possibility to switch to shutdown cooling.

This case has not been considered in the transients submitted as part of Appendix I of the DAR and may be more limiting. However, a similar but more conservative case was analyzed as part of a sensitivity study and resulted in a maximum pool temperature of 203°F. The assumptions for this case are identical to case 2.a (Appendix I, DAR) except that shutdown cooling is not initiated. For this case, the curves for reactor pressure vs. time and suppression pool temperature vs. time are found in Figures 10-64 and 10-65, respectively.

* Indicates Unit #2 component.

As mentioned above, this case is similar, but more conservative than the case under consideration. The major difference is that reactor water make-up would not be from the feedwater/condensate system but from HPCI (at reactor pressures above approximately 300 psia) and core spray (at reactor pressures below approximately 300 psia), which both take suction from the condensate storage tank and/or the suppression pool. Thus, water much colder than feedwater would be used for make-up.

This contributes to the reactor depressurization and leads to less steam being dumped into the suppression pool. The peak suppression pool temperature for this case will therefore be lower than that shown in Figures 10-65.

To confirm a temperature of less than 203°F we have initiated an additional analysis case, whose results are contained in Appendix I (Figures I-14 and I-15).

QUESTION 7

How will PP&L use the LaSalle in-plant test data to establish the local to bulk ΔT for Susquehanna SES?

RESPONSE 7

The following table gives a comparison of suppression pool geometries for LaSalle and Susquehanna SES:

	<u>LaSalle</u>	<u>Susquehanna</u>
Suppression Pool I.D.	86'-8"	88'
Pedestal O.D.	30'	29'-9"
Suppression Pool Volume (Normal Water Level)	142,160 ft ³	126,980 ft ³
No. of Quenchers	18	16
Pool Volume/Quencher	7898 ft ³	7936 ft ³
Quencher Submergence (Normal Water Level)	21.5 ft	19.5 ft
Height of Quencher Center- Line Above Base Mat	5 ft	3.5 ft

Based on the similarity between Susquehanna and LaSalle the local to bulk ΔT established from LaSalle inplant tests is also applicable to Susquehanna. In addition, PP&L is continuing to fund the development of computer codes (like Bechtel's KFIX) for the prediction of SRV discharge induced suppression pool mixing processes. The calculated temperature distributions will be compared to existing (Caorso) and future (LaSalle or Zimmer) in-plant test data.

Following satisfactory qualification of the computer codes they can then be used to establish local to bulk temperature differences without test.

QUESTION_8

What are the reactor pressures that correspond to quencher steam mass fluxes of 42 lbm/ft²s and 94 lbm/ft²s?

RESPONSE_8

The reactor pressures are 163 psia and 369 psia respectively.

This figure has been deleted.

REV. 6, 4/82

SUSQUEHANNA STEAM ELECTRIC STATION
UNITS 1 AND 2
DESIGN ASSESSMENT REPORT

DOWNCOMER
BRACING SYSTEM

FIGURE 10-1

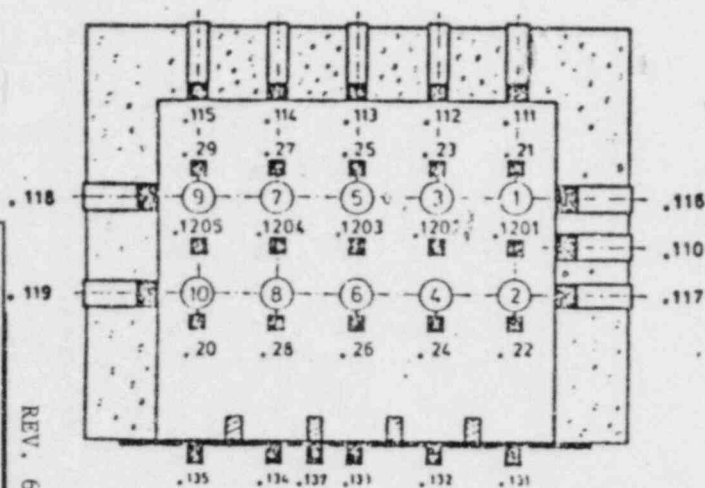
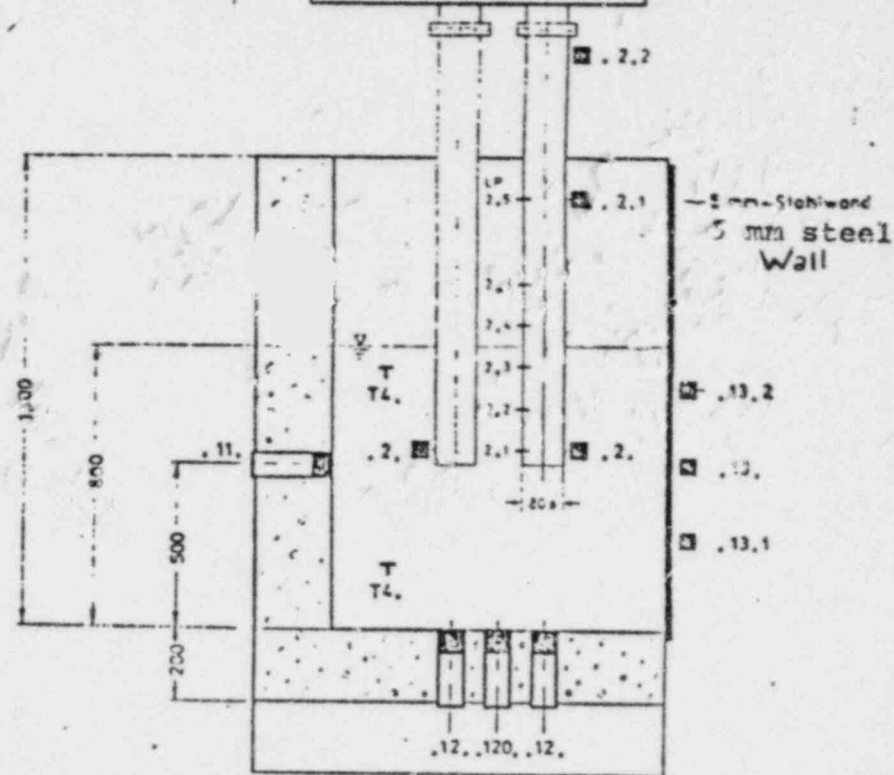
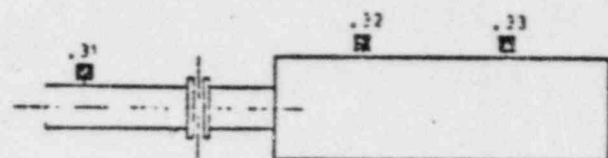
This figure has been deleted.

REV. 6, 4/82

SUSQUEHANNA STEAM ELECTRIC STATION
UNITS 1 AND 2
DESIGN ASSESSMENT REPORT

DOWNCOMER
BRACING DETAILS

FIGURE 10-2



Concrete cells 3 and 4

Diagram of measuring points

REV. 6, 4/82

SUSQUEHANNA STEAM ELECTRIC STATION
UNITS 1 AND 2

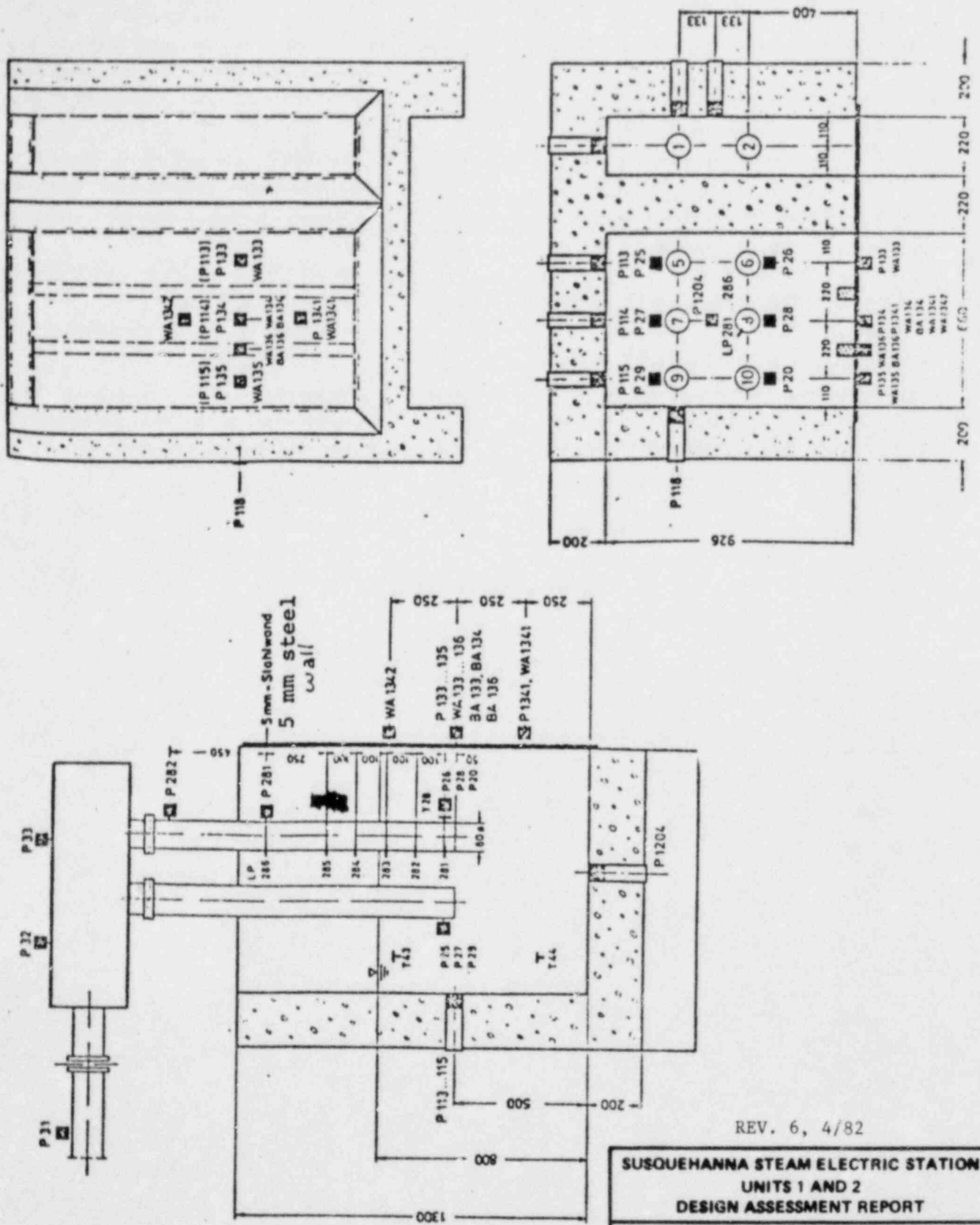
DESIGN ASSESSMENT REPORT

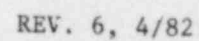
TRANSDUCER LOCATIONS

FOR THE TEN VENT PIPE

CONFIGURATION

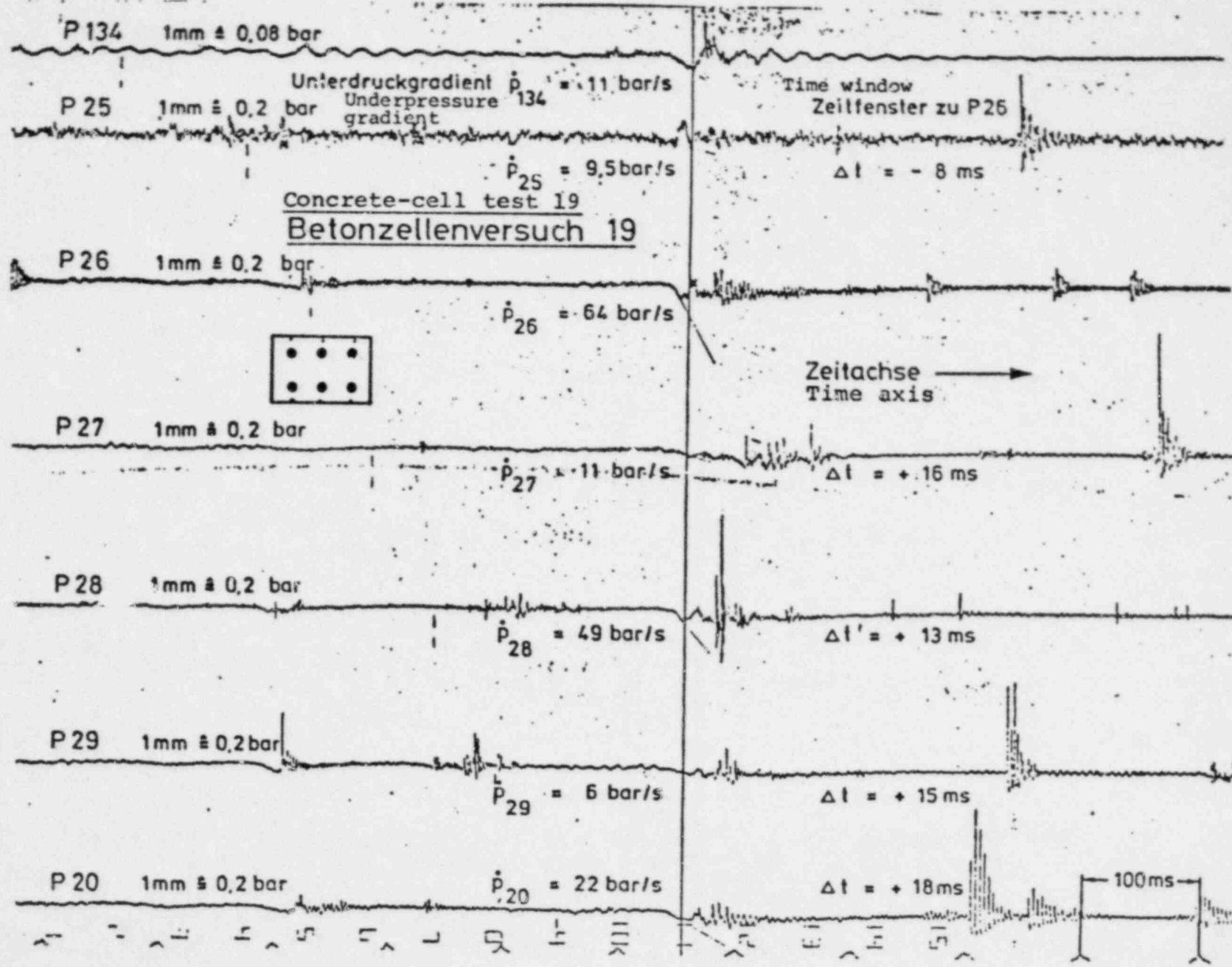
FIGURE 13-4





TRANSDUCER LOCATIONS
FOR THE TWO VENT PIPE
CONFIGURATION

FIGURE 10-6

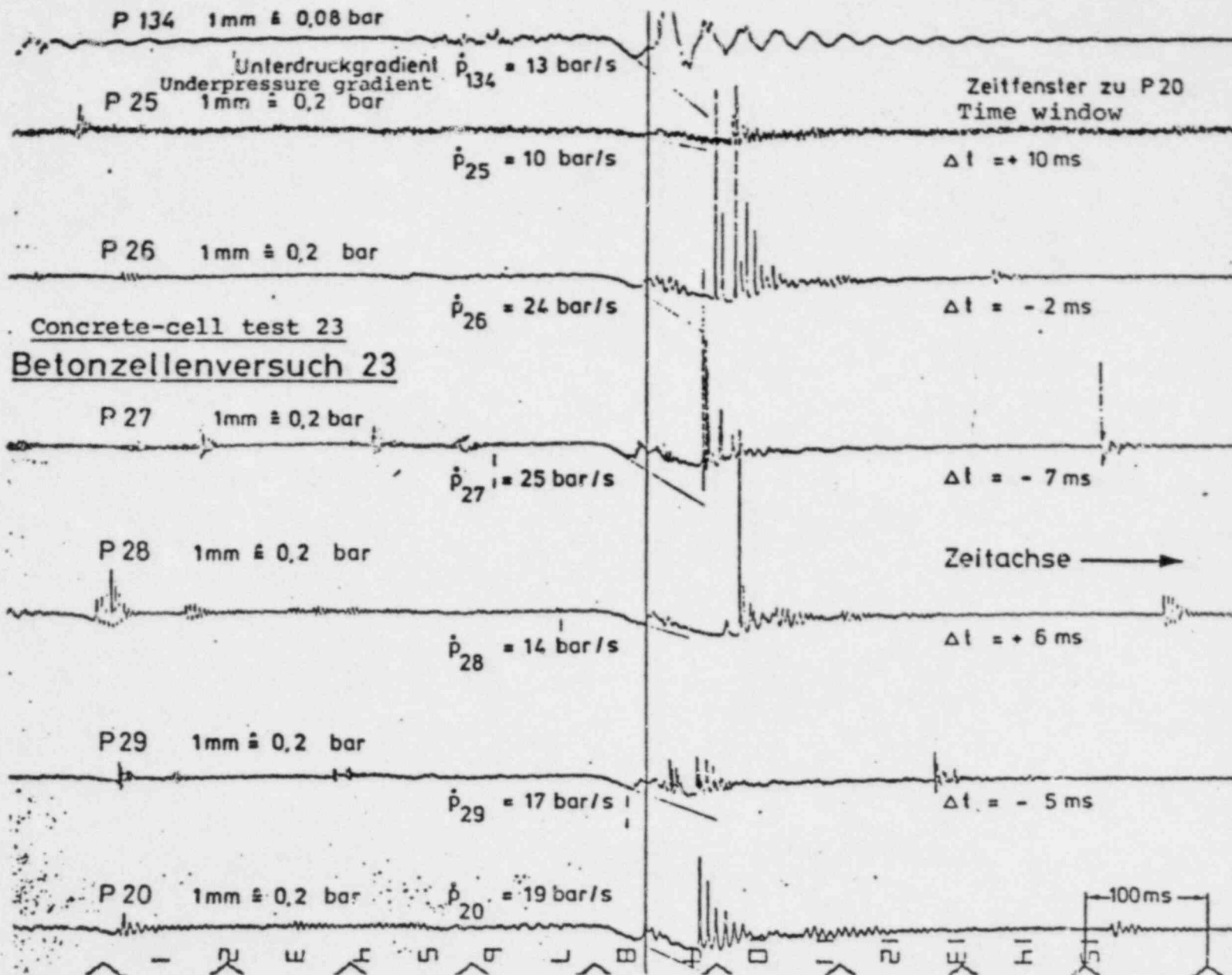


SUSUEHANNA STEAM ELECTRIC STATION
UNITS 1 AND 2
DESIGN ASSESSMENT REPORT

TYPICAL PRESSURE TIME
HISTORIES FROM PRESSURE
TRANSDUCERS P20, P25, 29 & P134

FIGURE 10-7

REV. 6, 4/82

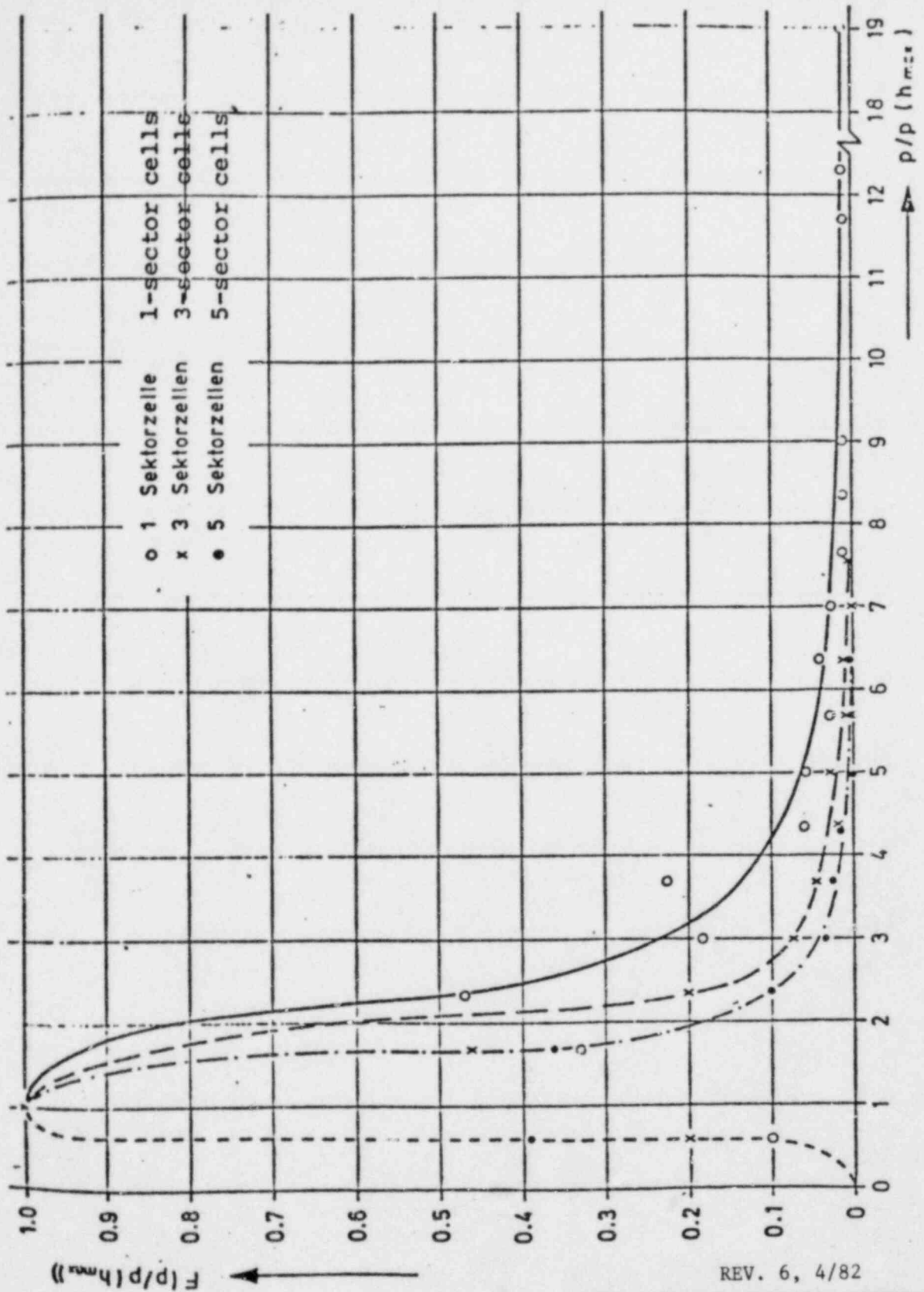


REV. 6, 4/82

SUSQUEHANNA STEAM ELECTRIC STATION
UNITS 1 AND 2
DESIGN ASSESSMENT REPORT

TYPICAL PRESSURE TIME
HISTORIES FROM PRESSURE
TRANSDUCERS P20, P25, P26, P27, P28, P29, P134

FIGURE 10-8

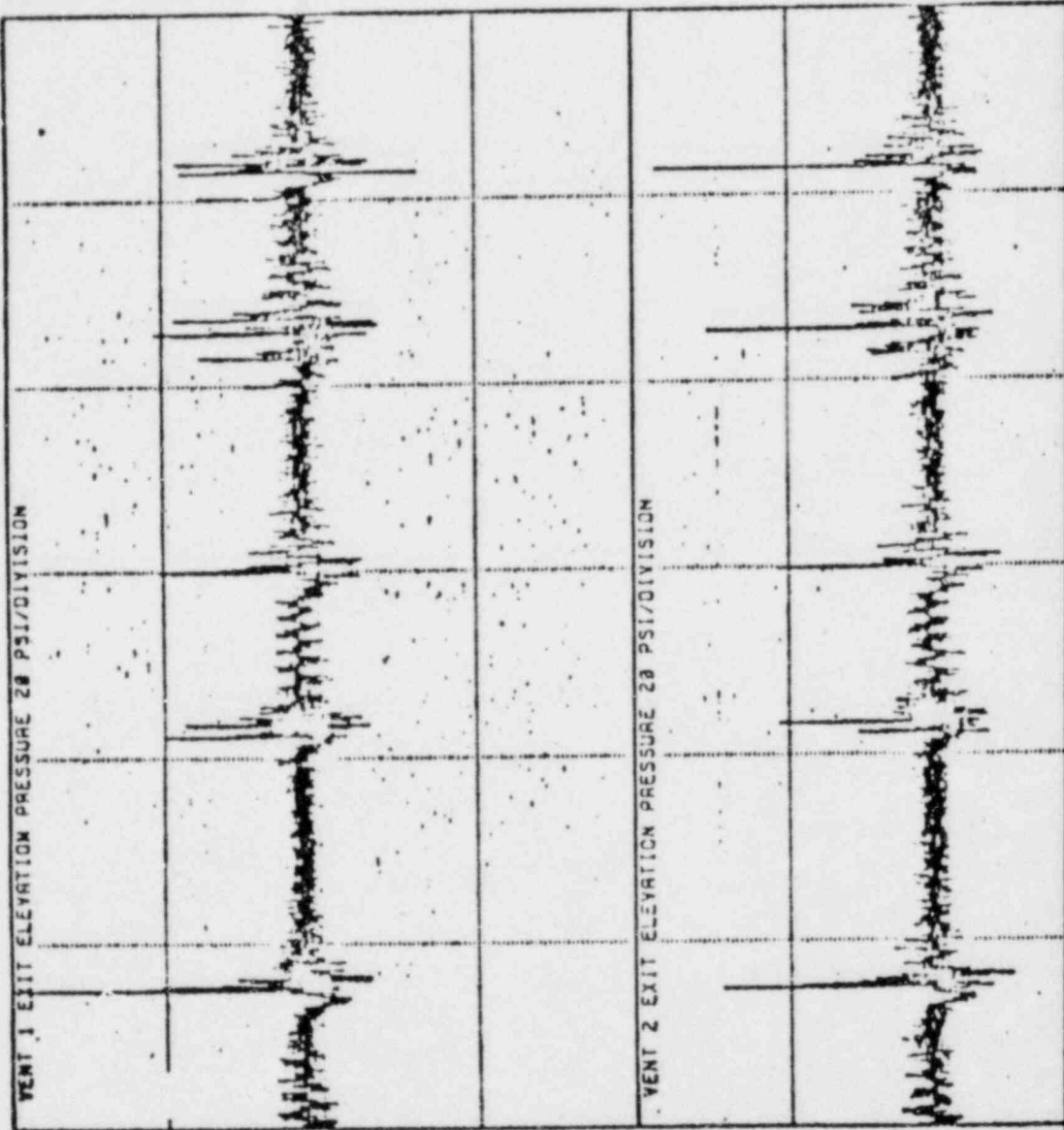


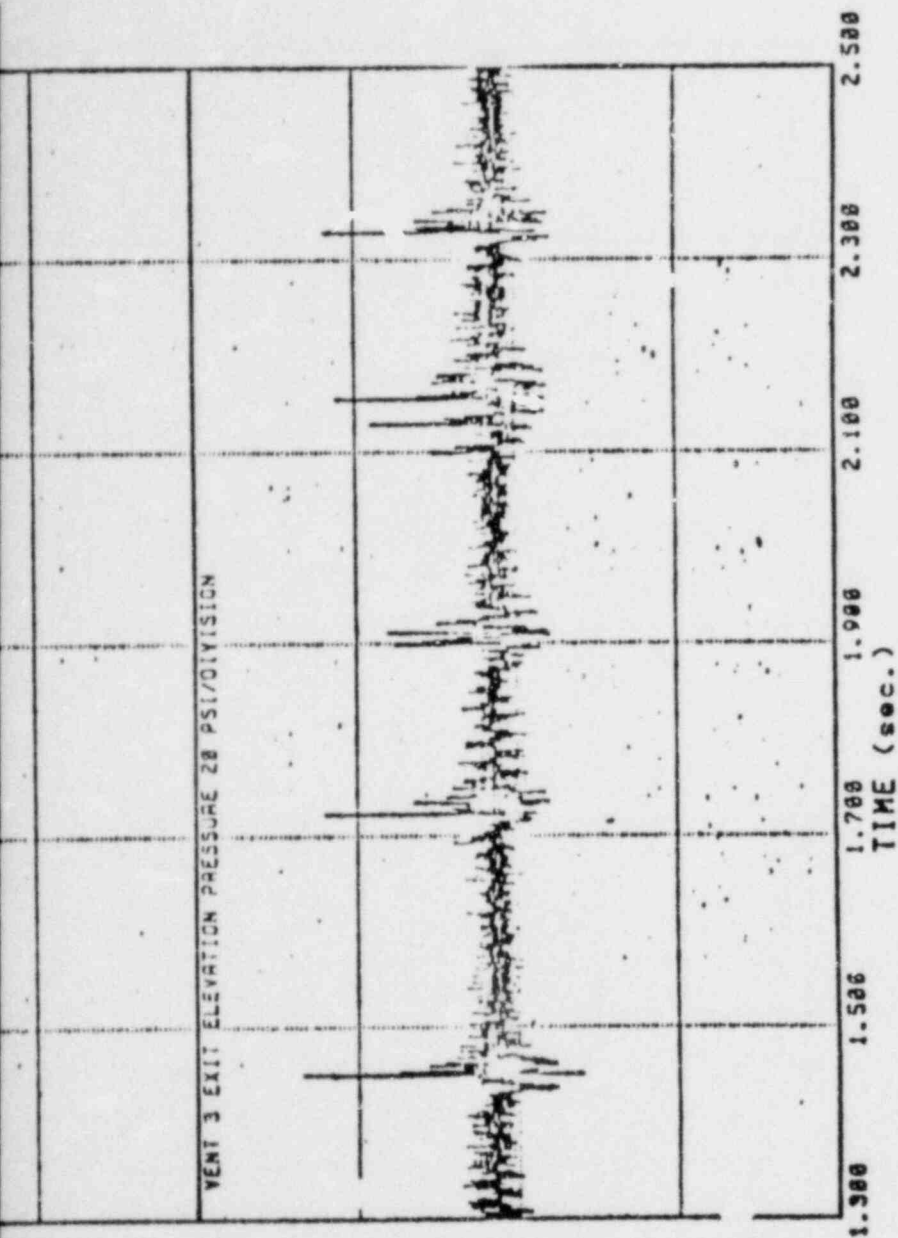
REV. 6, 4/82

**SUSQUEHANNA STEAM ELECTRIC STATION
UNITS 1 AND 2
DESIGN ASSESSMENT REPORT**

**FREQUENCY DISTRIBUTION OF
MEASURED NORMALIZED
WALL PRESSURES**

FIGURE 10-9





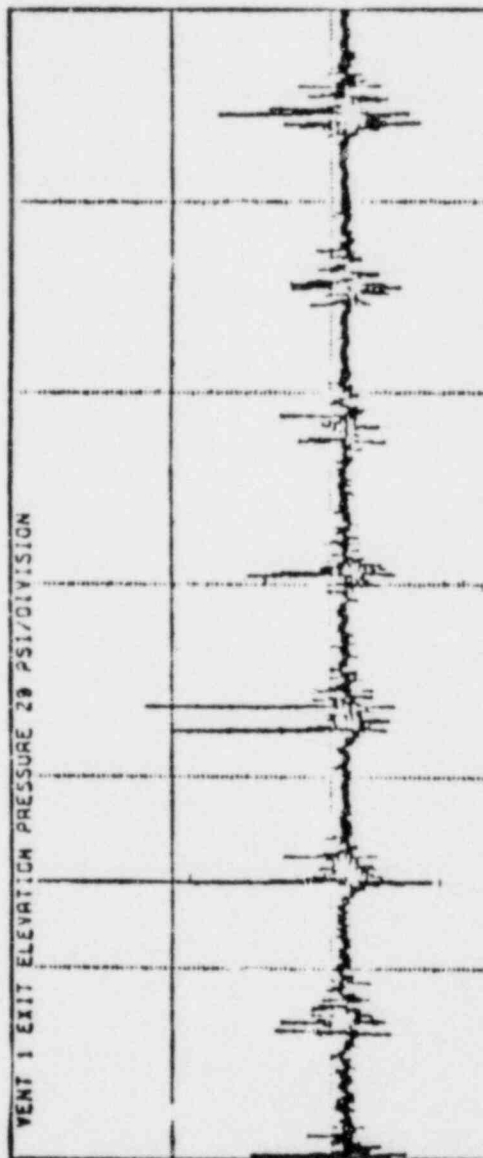
REV. 6, 4/82

**SUSQUEHANNA STEAM ELECTRIC STATION
UNITS 1 AND 2
DESIGN ASSESSMENT REPORT**

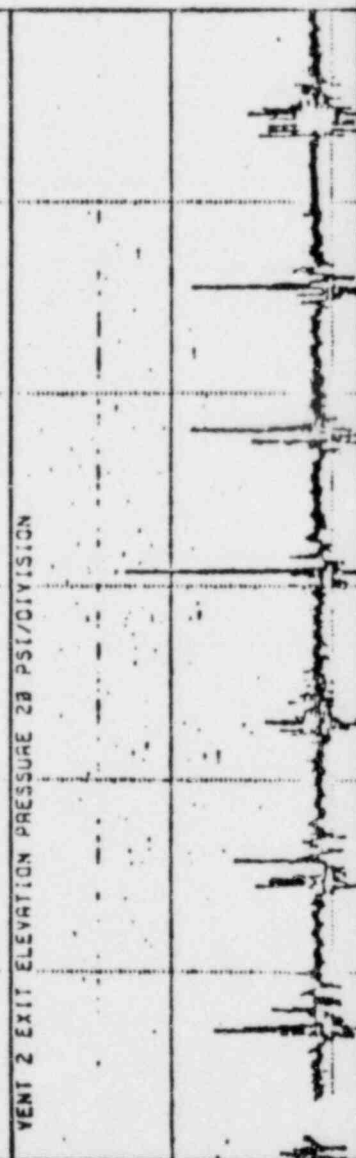
POOL WALL PRESSURES AT THREE
CIRCUMFERENTIAL VENT EXIT
LOCATIONS-1/ (SCALE 3 VENT
GEOMETRY

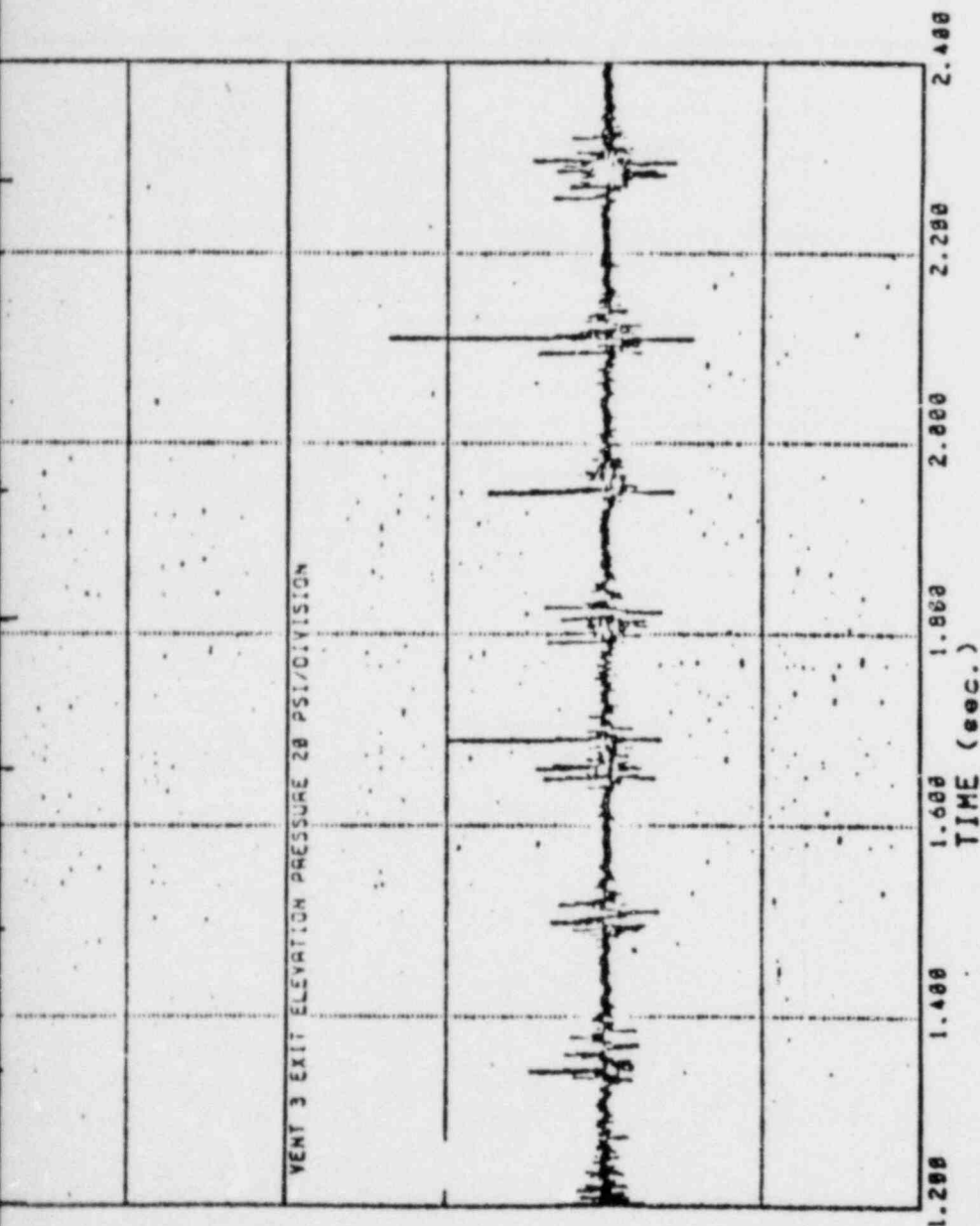
FIGURE 10-10

VENT 1 EXIT ELEVATION PRESSURE 20 PSI/DIVISION



VENT 2 EXIT ELEVATION PRESSURE 20 PSI/DIVISION



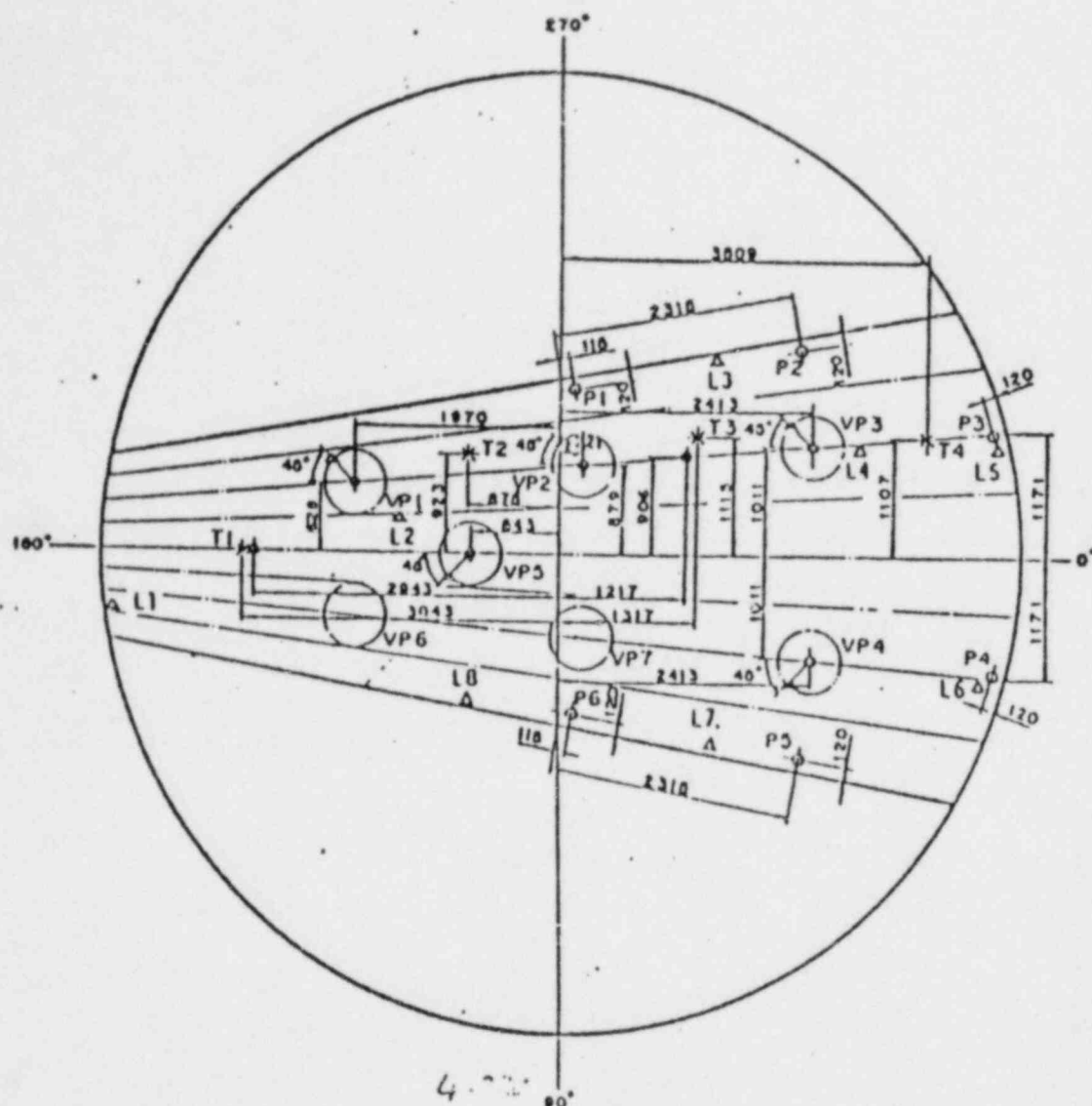


REV. 6, 4/82

**SUSQUEHANNA STEAM ELECTRIC STATION
UNITS 1 AND 2
DESIGN ASSESSMENT REPORT**

COOL WALL PRESSURES AT THREE
CIRCUMFERENTIAL VENT EXIT
LOCATIONS-1/10 SCALE 10
VENT GEOMETRY

FIGURE 10-11



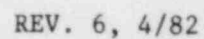
Δ: Water level
 ○: Pressure
 ○: Pressure on
 wetwell bottom
 floor
 X: Temperature
 VP: Vent pipe

REV. 6, 4/82

SUSQUEHANNA STEAM ELECTRIC STATION
 UNITS 1 AND 2
 DESIGN ASSESSMENT REPORT

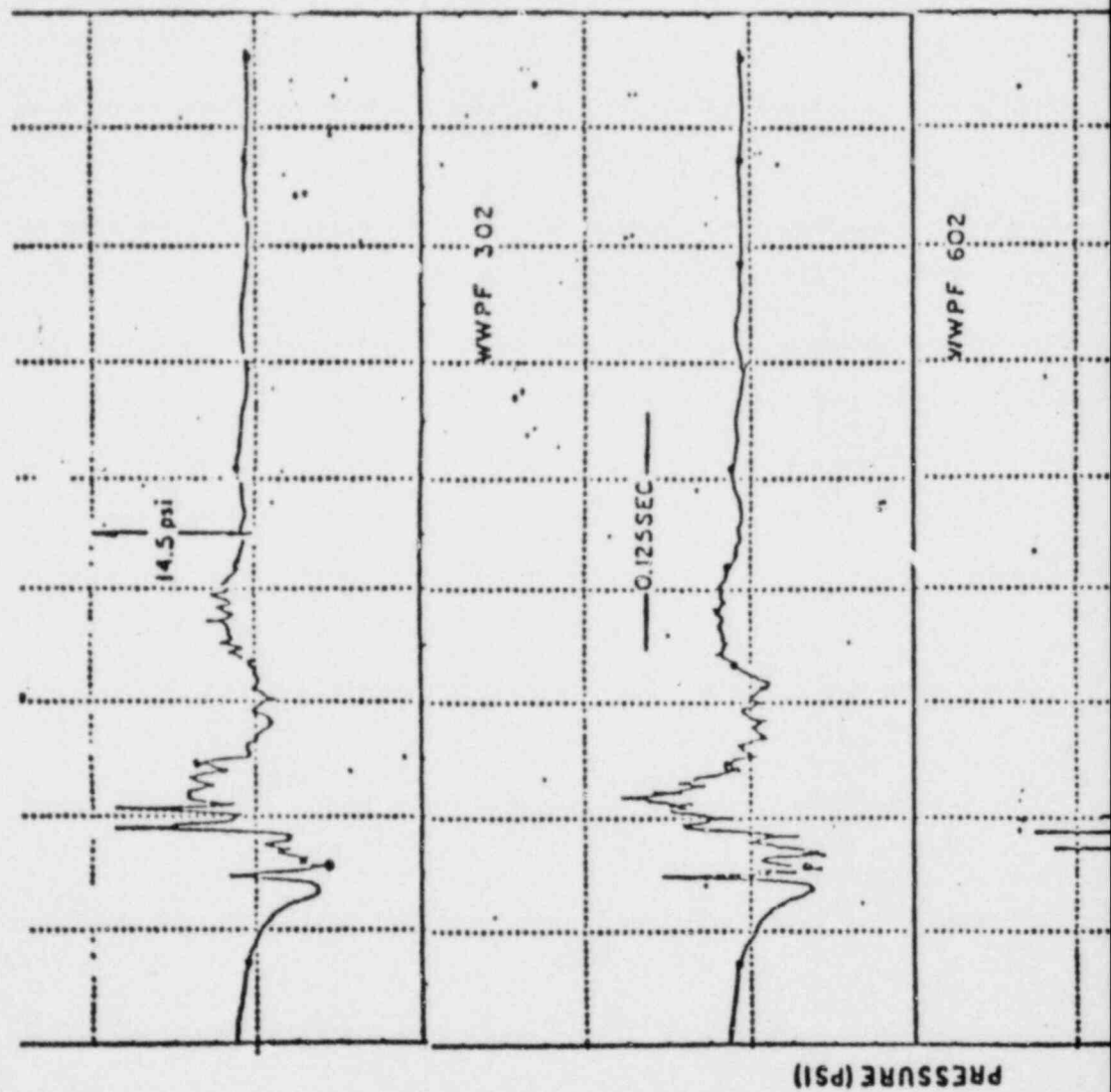
PLAN LOCATIONS OF
 TRANSDUCERS FOR WETWELL

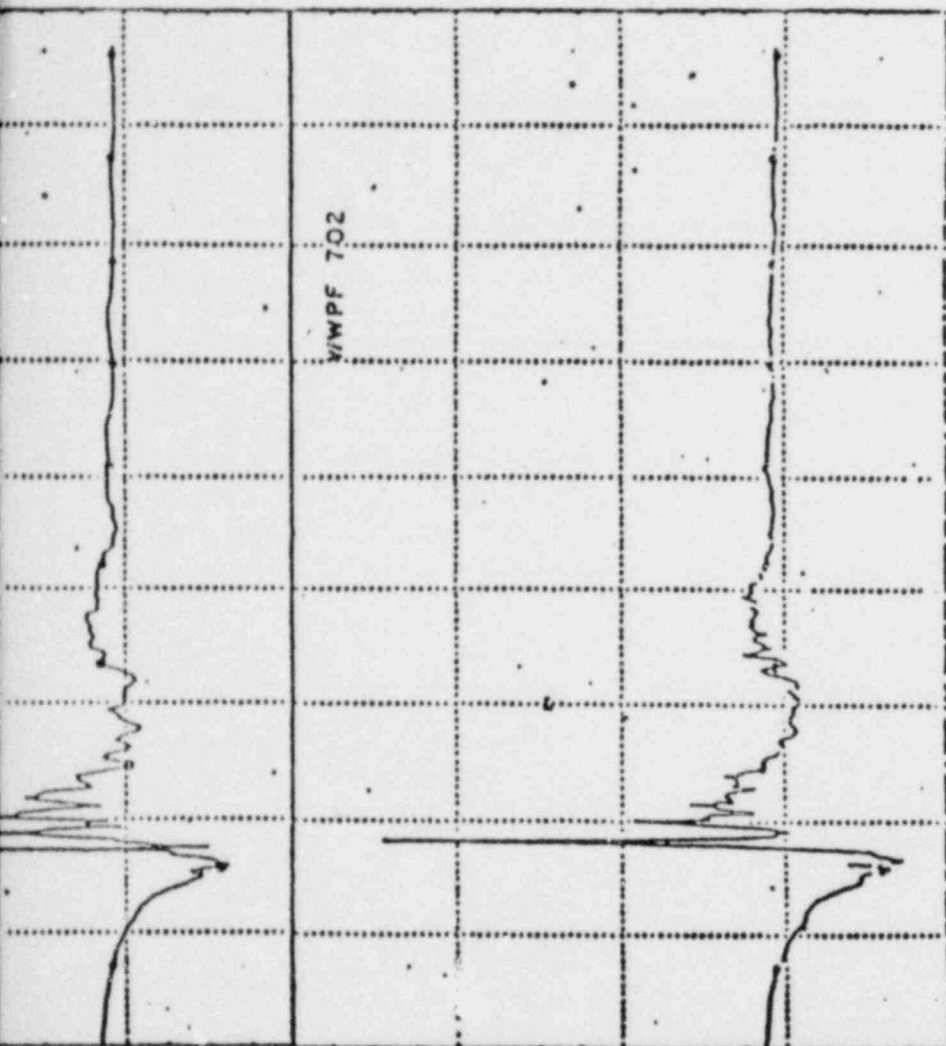
FIGURE 10-12



LOCATIONS OF PRESSURE
TRANSDUCERS FOR WETWELL

FIGURE 10-13





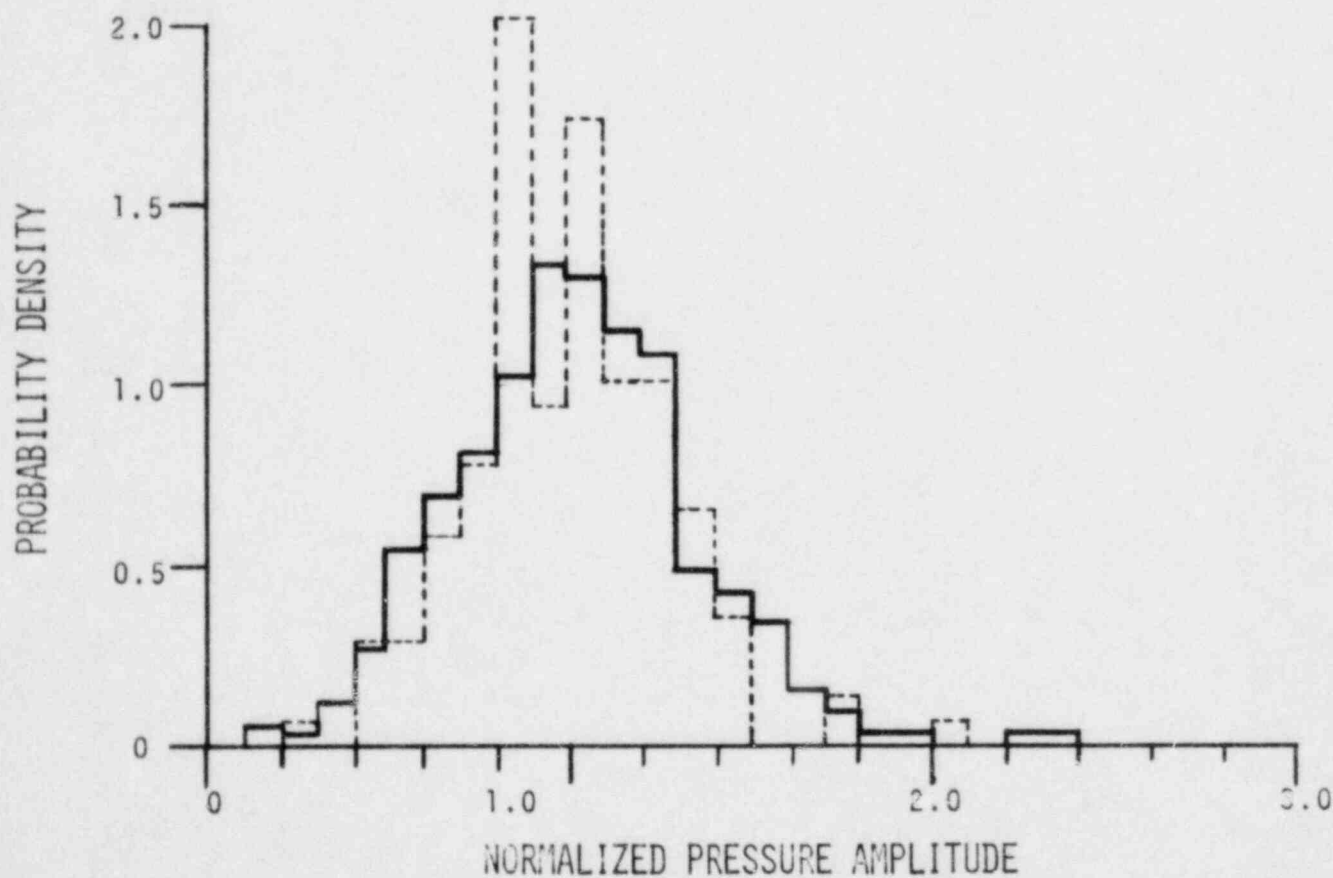
REV. 6, 4/82

**SUSQUEHANNA STEAM ELECTRIC STATION
UNITS 1 AND 2
DESIGN ASSESSMENT REPORT**

VENT EXIT ELEVATION POOL
WALL PRESSURES FOR A CHUG
FROM JAERI TEST 0002

FIGURE 10-14

— GKMIIM MSL TESTS
 TESTS NO. 3-10(0.5-13HZ)
 - - - - JAERI TESTS

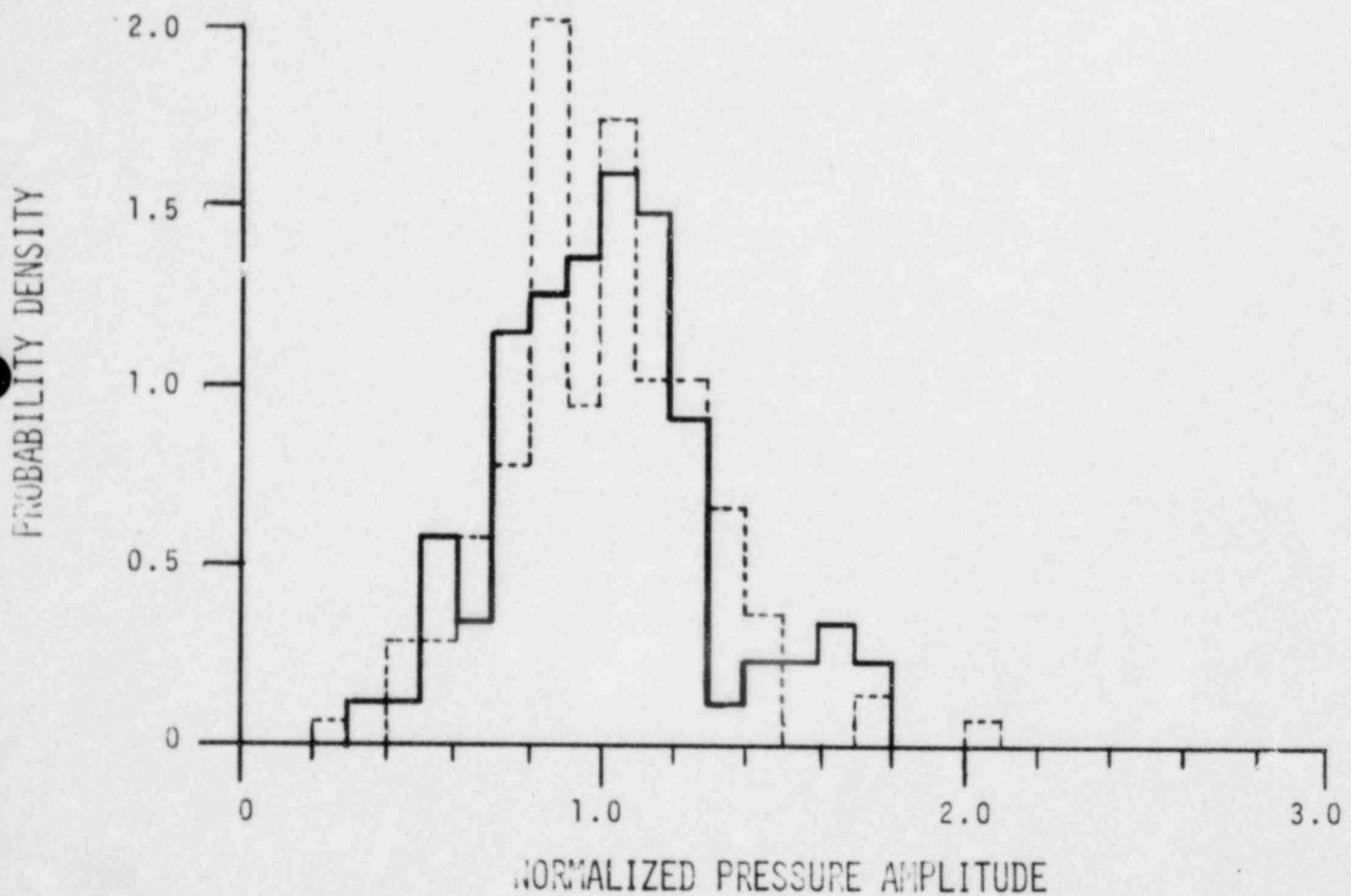


REV. 6, 4/82

SUSQUEHANNA STEAM ELECTRIC STATION
UNITS 1 AND 2
DESIGN ASSESSMENT REPORT

COMPARISON OF PROBABILITY
 DENSITY OF THE NORMALIZED
 PRESSURE AMPLITUDES FROM
 GKM II-M TESTS 3, 10 & JAERI
 FIGURE 10-15

— GKMIIM1/MSL TESTS
 TESTS NO. 11,12(0.5-13HZ)
 - - - - - JAERI TESTS



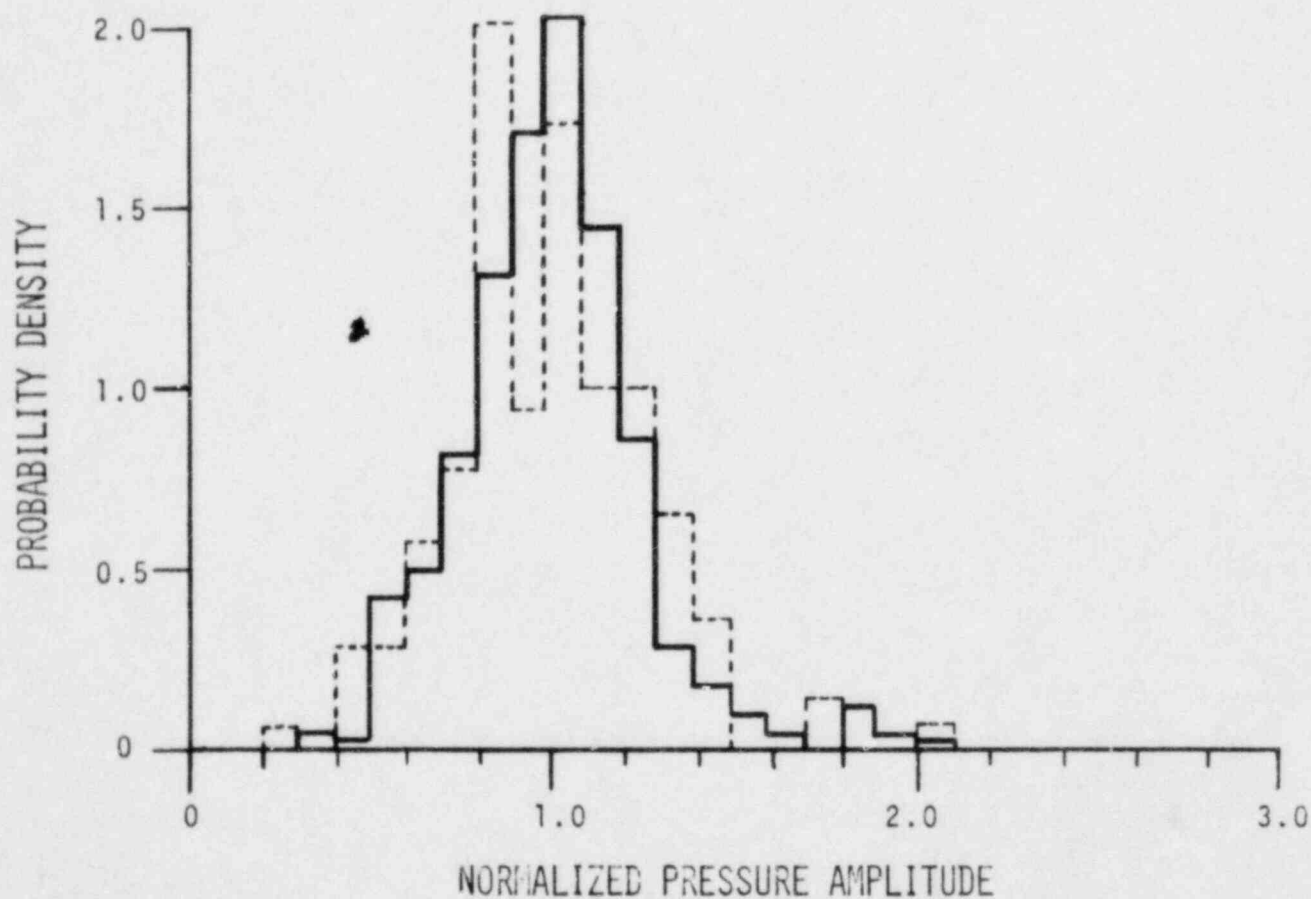
REV. 6, 4/82

SUSQUEHANNA STEAM ELECTRIC STATION
UNITS 1 AND 2
DESIGN ASSESSMENT REPORT

COMPARISON OF PROBABILITY
 DENSITY OF THE NORMALIZED
 PRESSURE AMPLITUDES FROM
 GKMIIM1-M TESTS 11 & 12
 & JAERI

FIGURE 10-16

— GKMIIM1/6MSL TESTS
 TEST NO. 13-20(0.5-13HZ)
 - - - - JAERI TESTS

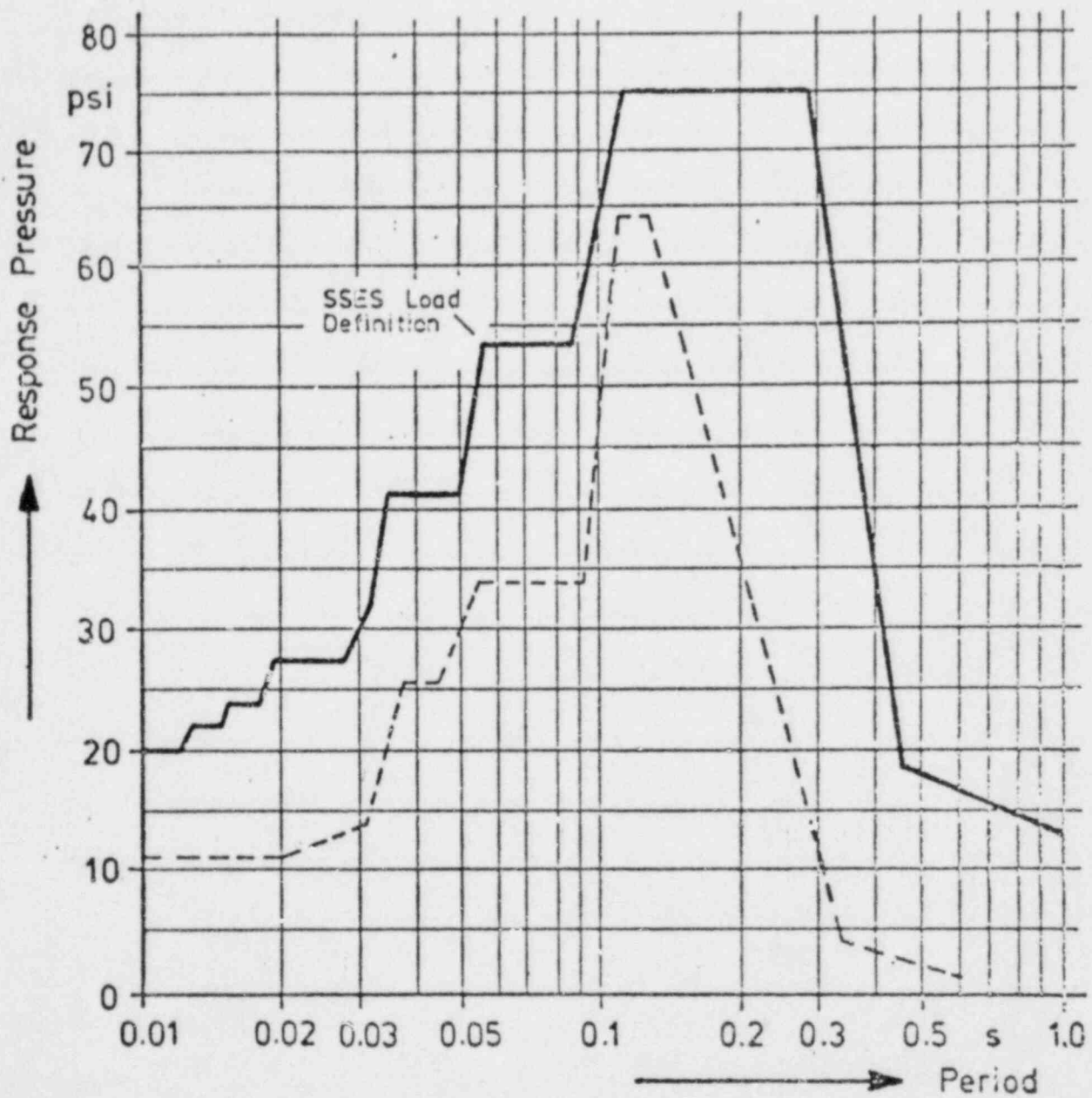


REV. 6, 4/82

SUSQUEHANNA STEAM ELECTRIC STATION
 UNITS 1 AND 2
 DESIGN ASSESSMENT REPORT

COMPARISON OF PROBABILITY
 DENSITY OF THE NORMALIZED
 PRESSURE AMPLITUDES FROM
 GKMIIM TESTS 13, 20 & JAERI

FIGURE 10-17

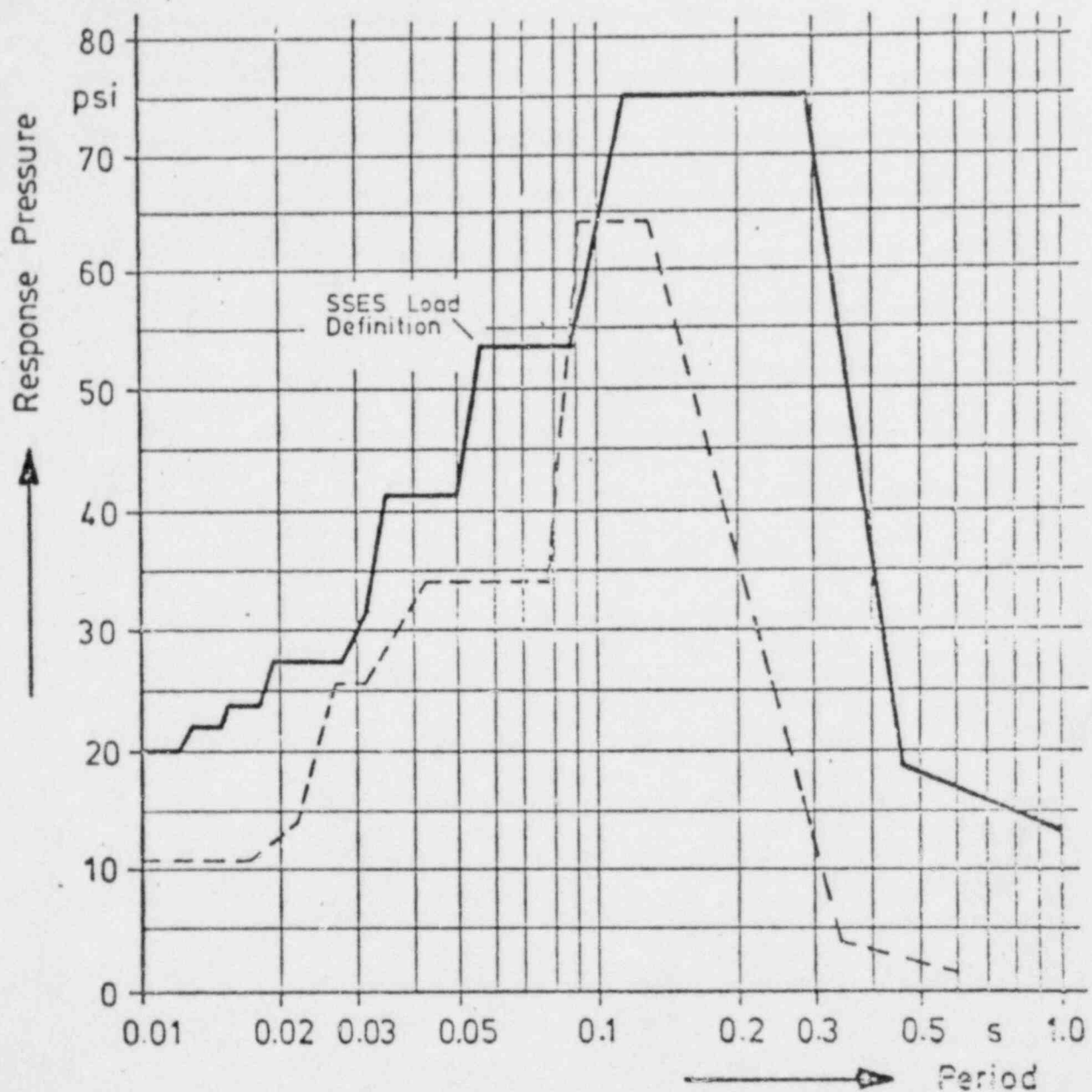


REV. 6, 4/82

**SUSQUEHANNA STEAM ELECTRIC STATION
UNITS 1 AND 2
DESIGN ASSESSMENT REPORT**

COMPARISON OF PRESSURE
RESPONSE SPECTRA OF TEST
21.2 -ALL VALVE CASE-AND THE
SSSES LOAD DEFINITION

FIGURE 10-18

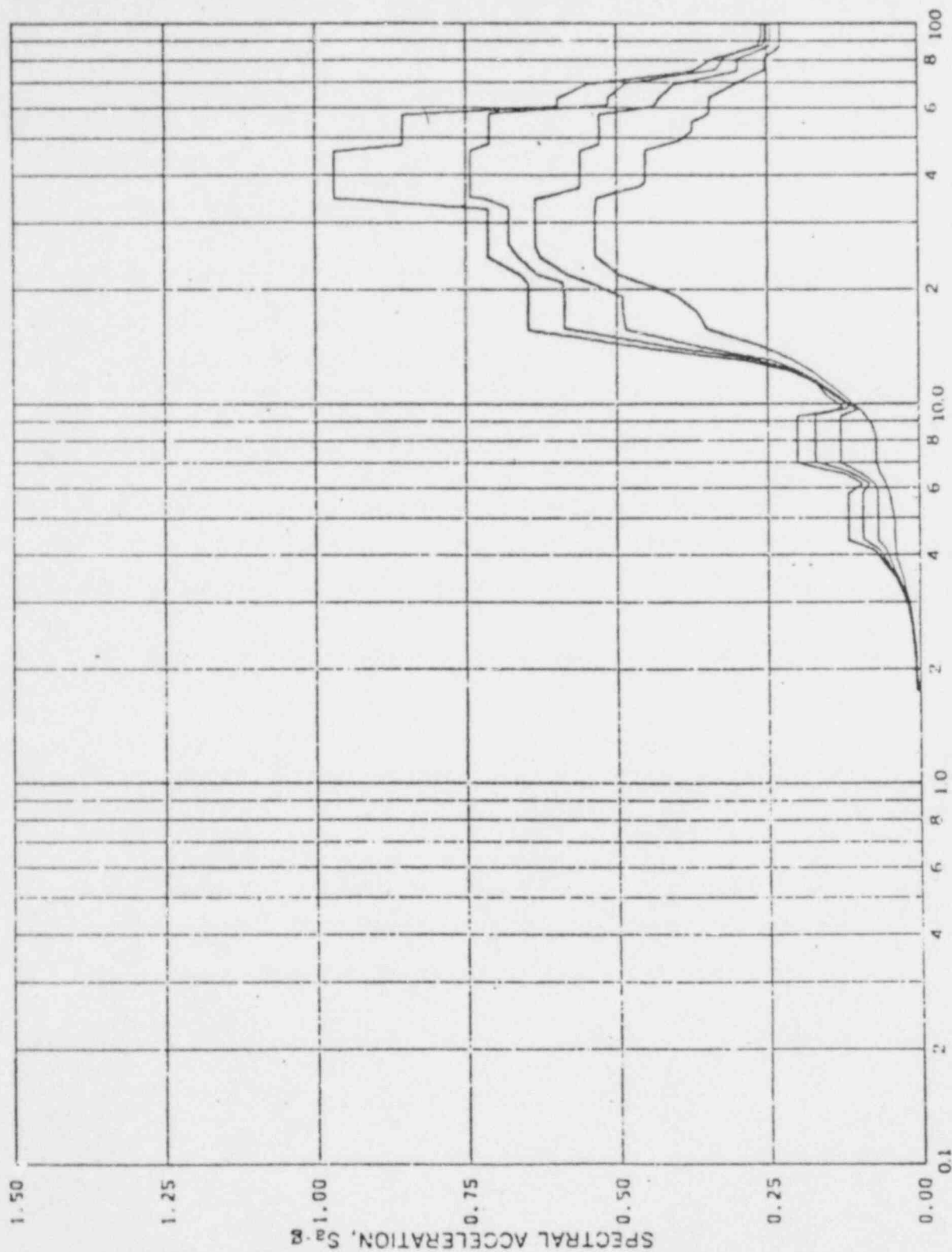


REV. 6, 4/82

**SUSQUEHANNA STEAM ELECTRIC STATION
UNITS 1 AND 2
DESIGN ASSESSMENT REPORT**

COMPARISON OF PRESSURE
RESPONSE SPECTRE OF TEST 21.2
ALL VALVE CASE AND ONE VALVE
CASE AND THE SSES LOAD DEFINITION

FIGURE 10-19



FREQUENCY-CPS

Acceleration Spectra for CONTAINMENT SHELL

Load Case: SUSQUEHANNA KWU-SRV #76 ASYMM.

Node 131, Direction X, Elev 672'-0"

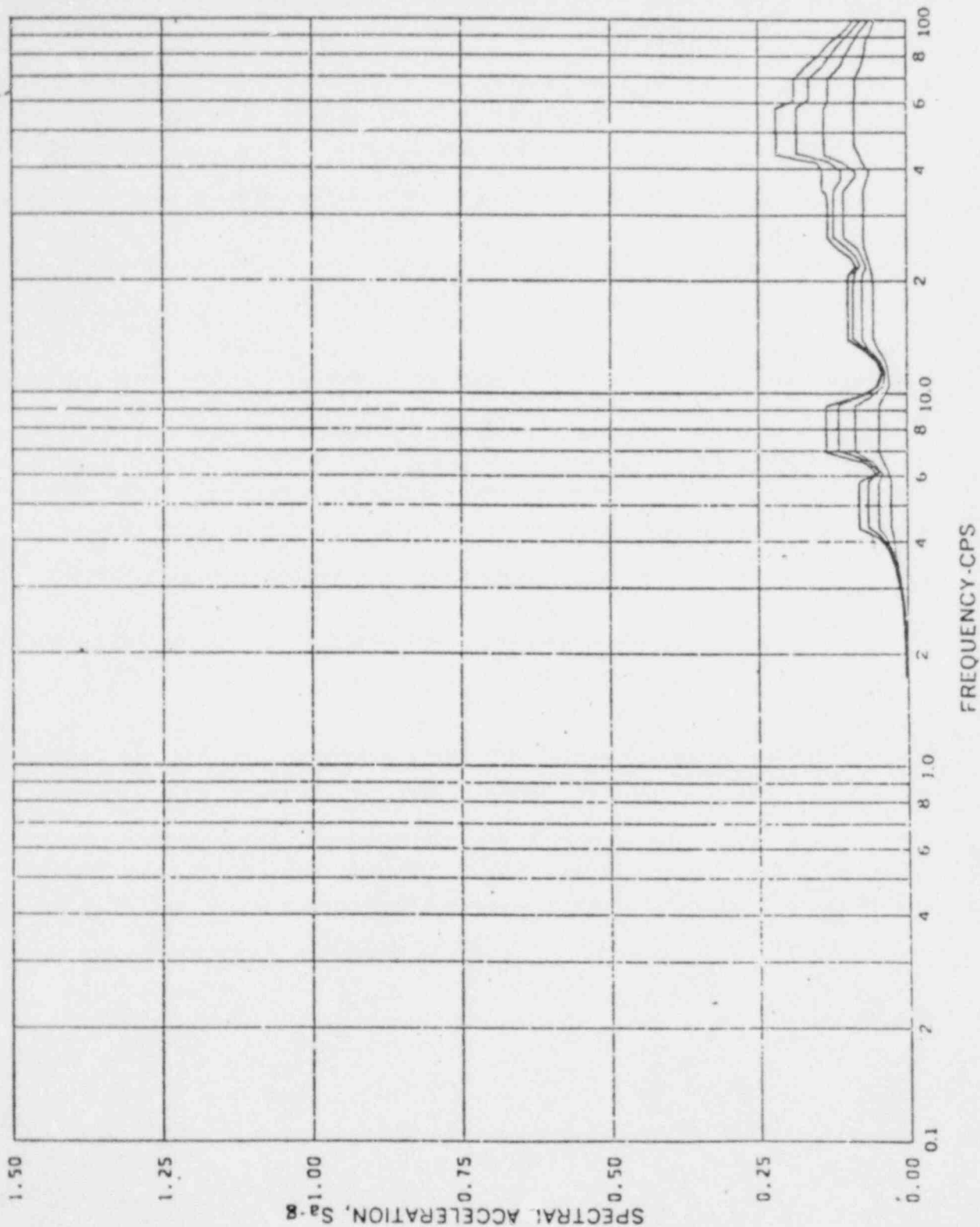
Damping: 0.005, 0.01, 0.02, 0.05

REV. 6, 4/82

**SUSQUEHANNA STEAM ELECTRIC STATION
UNITS 1 AND 2
DESIGN ASSESSMENT REPORT**

SSS CONTAINMENT RESPONSE
SPECTRA KWV SRV #76
ASYMMETRIC - DIRECTION
HORIZ ONTAL

FIGURE 10-20



Acceleration Spectra for CONTAINMENT SHELL

Load Case: Susquehanna KWU-SRV #76 ASYMM.

Node 131, Direction Z, Elev 672'-0"

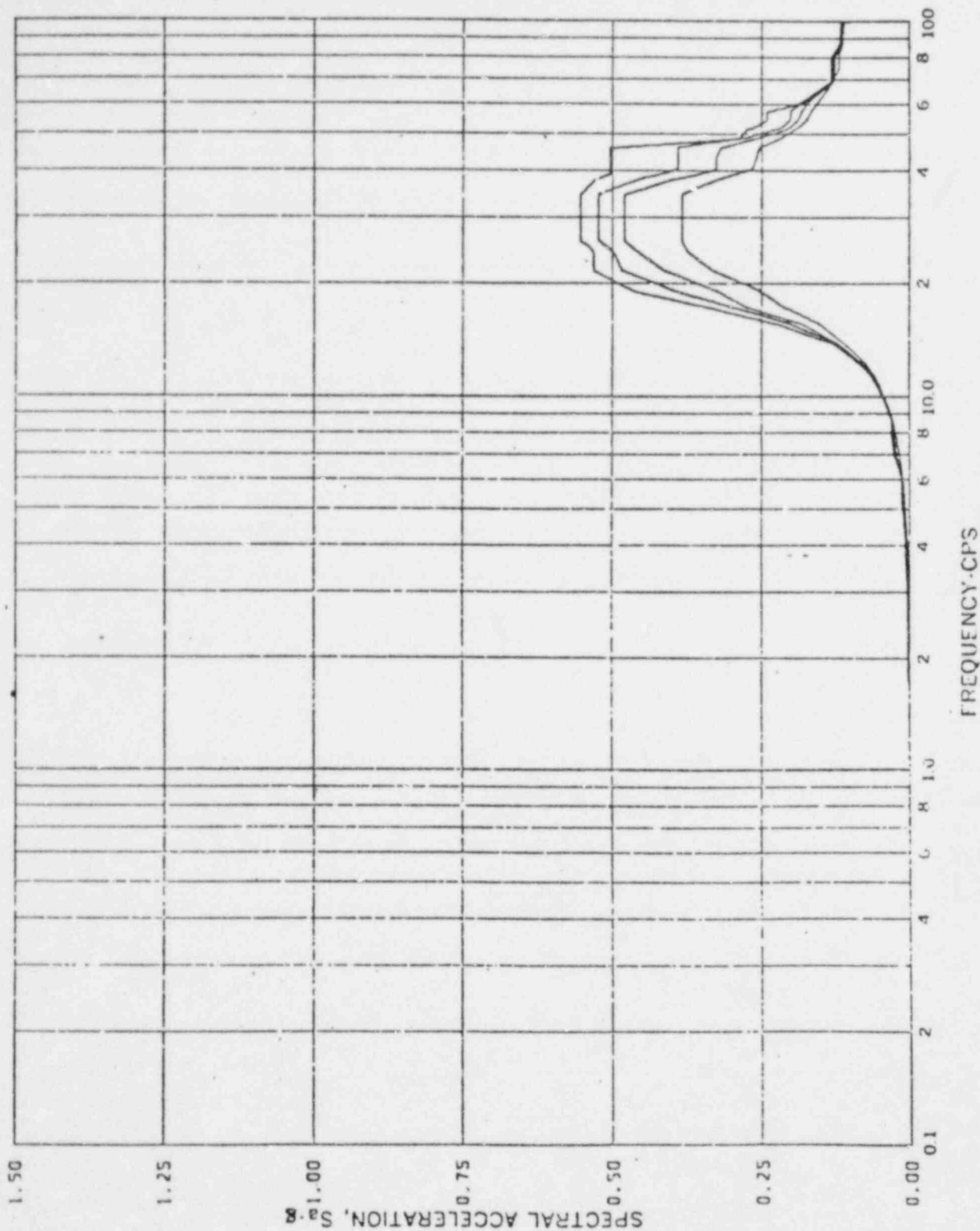
Damping: 0.005, 0.01, 0.02, 0.05

REV. 6, 4/82

**SUSQUEHANNA STEAM ELECTRIC STATION
UNITS 1 AND 2
DESIGN ASSESSMENT REPORT**

SSS CONTAINMENT RESPONSE
SPECTRA KWU SRV #76 -
ASYMMETRIC- DIRECTION
VERTICAL

FIGURE 10-21



FREQUENCY-CPS

Acceleration Spectra for CONTAINMENT SHELL

Load Case: Susquehanna KWU-SRV #76 ASYMM.

Node 135, Direction Y, Elev 672'-0"

Damping: 0.005, 0.01, 0.02, 0.05

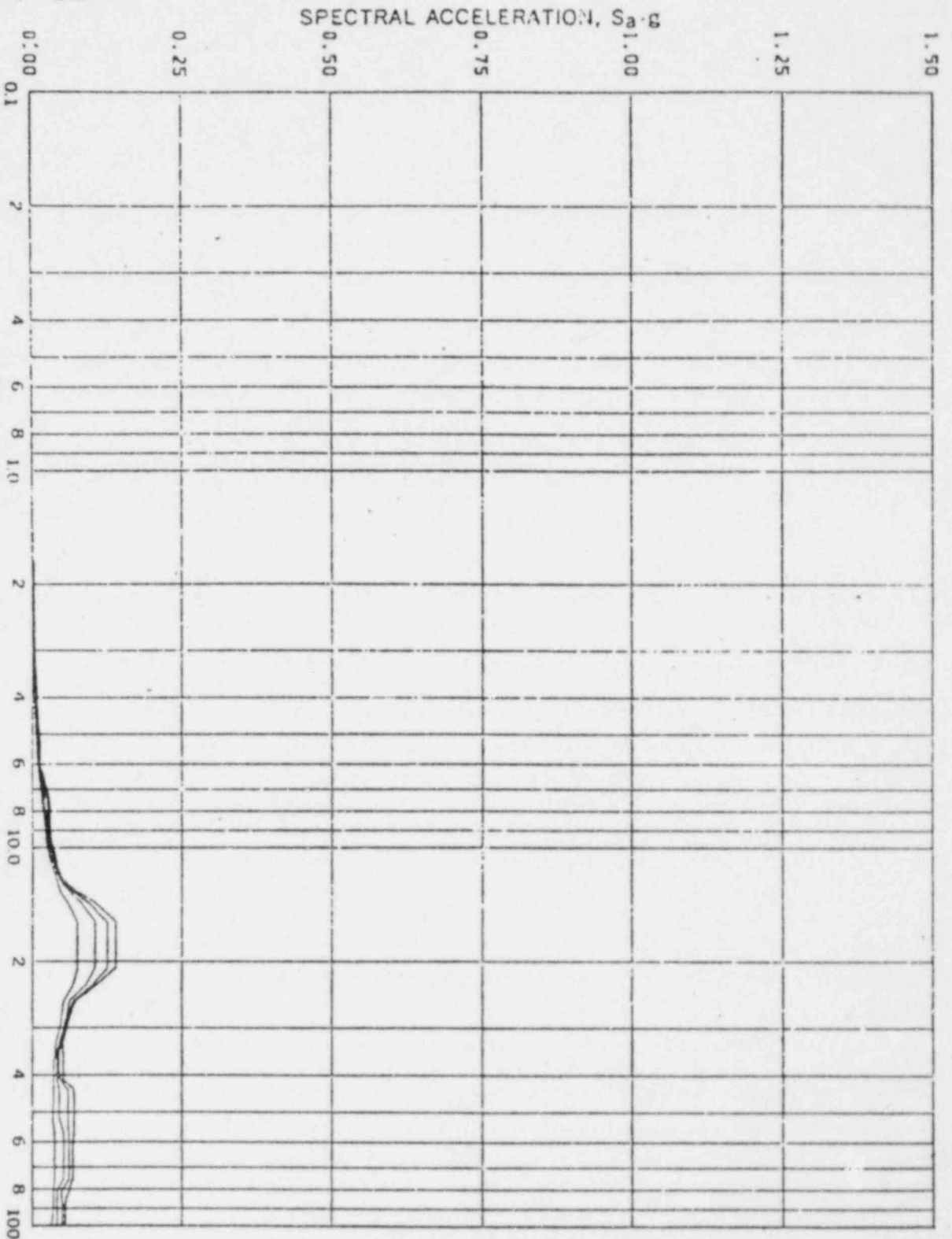
REV. 6, 4/82

**SUSQUEHANNA STEAM ELECTRIC STATION
UNITS 1 AND 2
DESIGN ASSESSMENT REPORT**

SSES CONTAINMENT RESPONSE
SPECTRA KWU SRV #76
ASYMMETRIC - DIRECTION
HORIZONTAL

FIGURE 10-22

REV. 6, 4/82



FREQUENCY - CPS

Acceleration Spectra for CONTAINMENT SHELL.

Load Case: Susquehanna KMW-SRV #76 ASYMM.

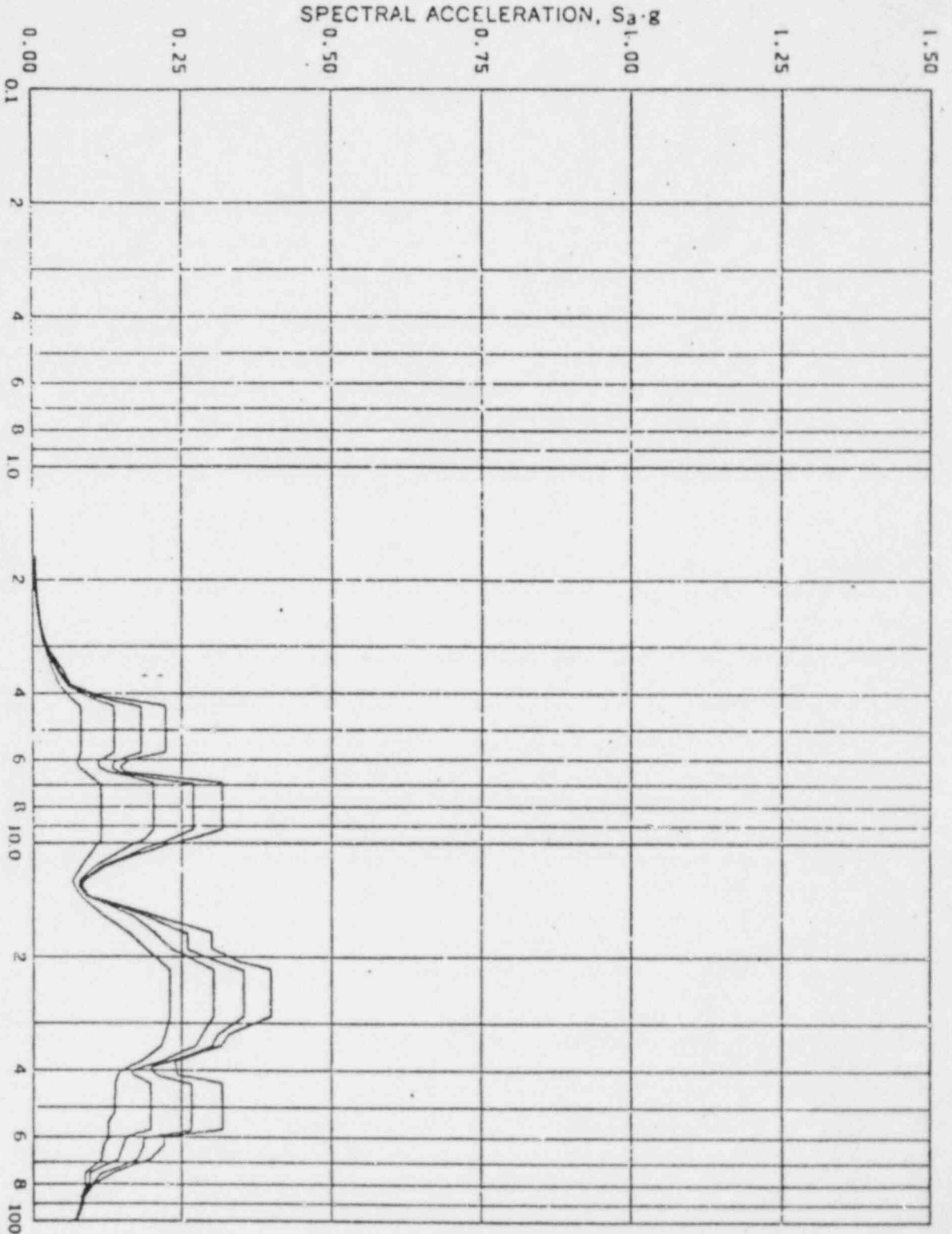
Node 135, Direction 2, Elev 672'-0"

Damping: 0.005, 0.01, 0.02, 0.05

SUSQUEHANNA STEAM ELECTRIC STATION
UNITS 1 AND 2
DESIGN ASSESSMENT REPORT

SSES CONTAINMENT RESPONSE
SPECTRA KWU SRV # 76
ASYMMETRIC - DIRECTION
HORIZONTAL
10-24
FIGURE

REV. 6, 4/82



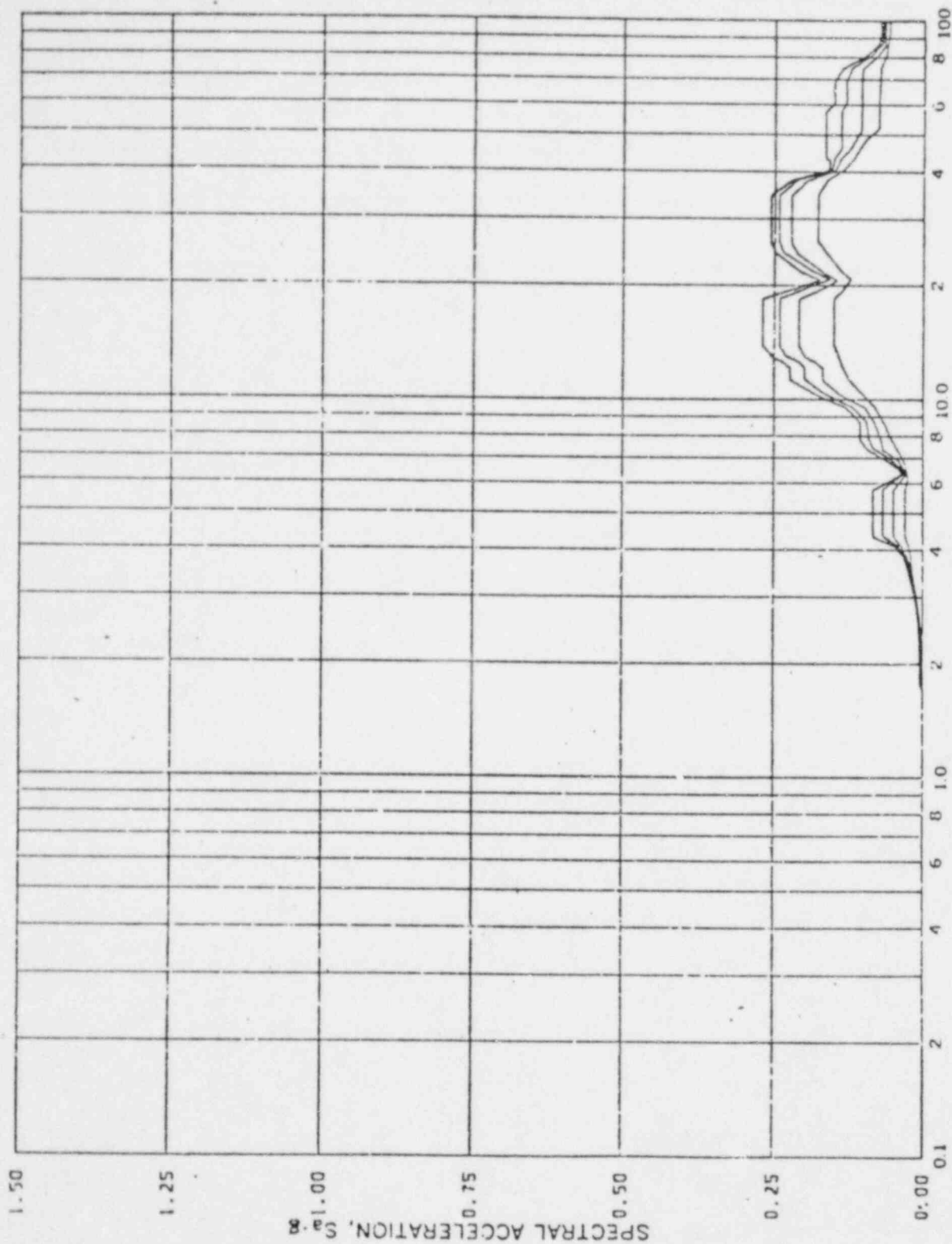
FREQUENCY - CPS

Acceleration Spectra for PEDESTAL

Load Case: Susquehanna KWU-SRV # 76 ASYMM.

Node 211, Direction X, Elev 702'-3"

Damping: 0.005, 0.01, 0.02, 0.05



FREQUENCY-CPS

Acceleration Spectra for PEDESTAL

Load Case: Susquehanna KWU-SRV #76 ASYMM.

Node 211, Direction Z, Elev 702'-3"

Damping: 0.005, 0.01, 0.02, 0.05

REV. 6, 4/82

**SUSQUEHANNA STEAM ELECTRIC STATION
UNITS 1 AND 2
DESIGN ASSESSMENT REPORT**

SSS CONTAINMENT RESPONSE
SPECTRA KWU SRV #76
ASYMMETRIC - DIRECTION
VERTICAL

FIGURE

10-25

SUSQUEHANNA STEAM ELECTRIC STATION
UNITS 1 AND 2
DESIGN ASSESSMENT REPORT

SSES CONTAINMENT RESPONSE
SPECTRA - KWU SRV #76
ASYMMETRIC - DIRECTION
HORIZONTAL
FIGURE 10-26

REV. 6, 4/82

SPECTRAL ACCELERATION, $S_a \cdot g$



FREQUENCY-CPS

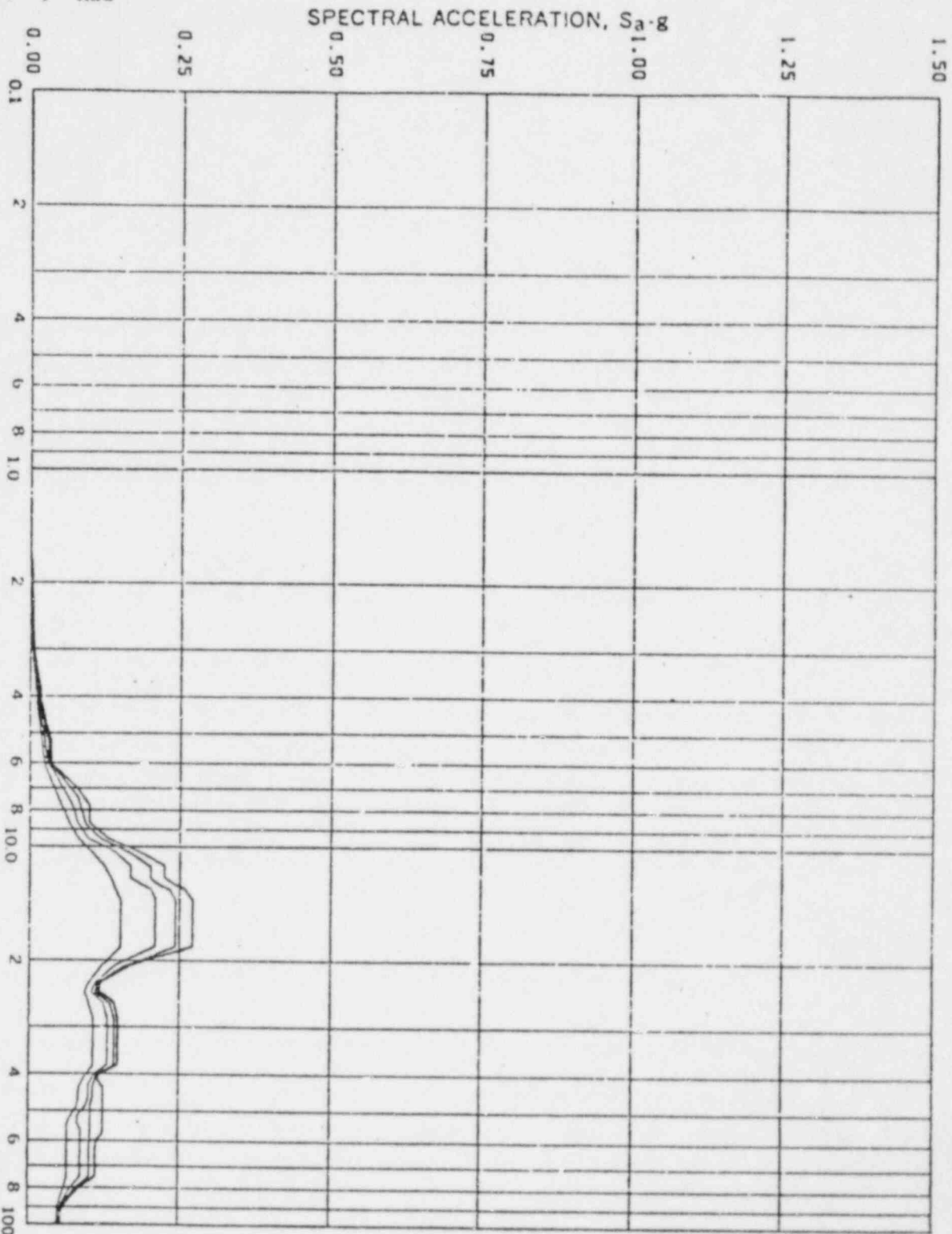
Acceleration Spectra for PEDESTAL

Load Case: Susquehanna KWU-SRV #76 ASYMM.

Mode 215, Direction Y, Elev 702'-3"

Damping: 0.005, 0.01, 0.02, 0.05

REV. 6, 4/82



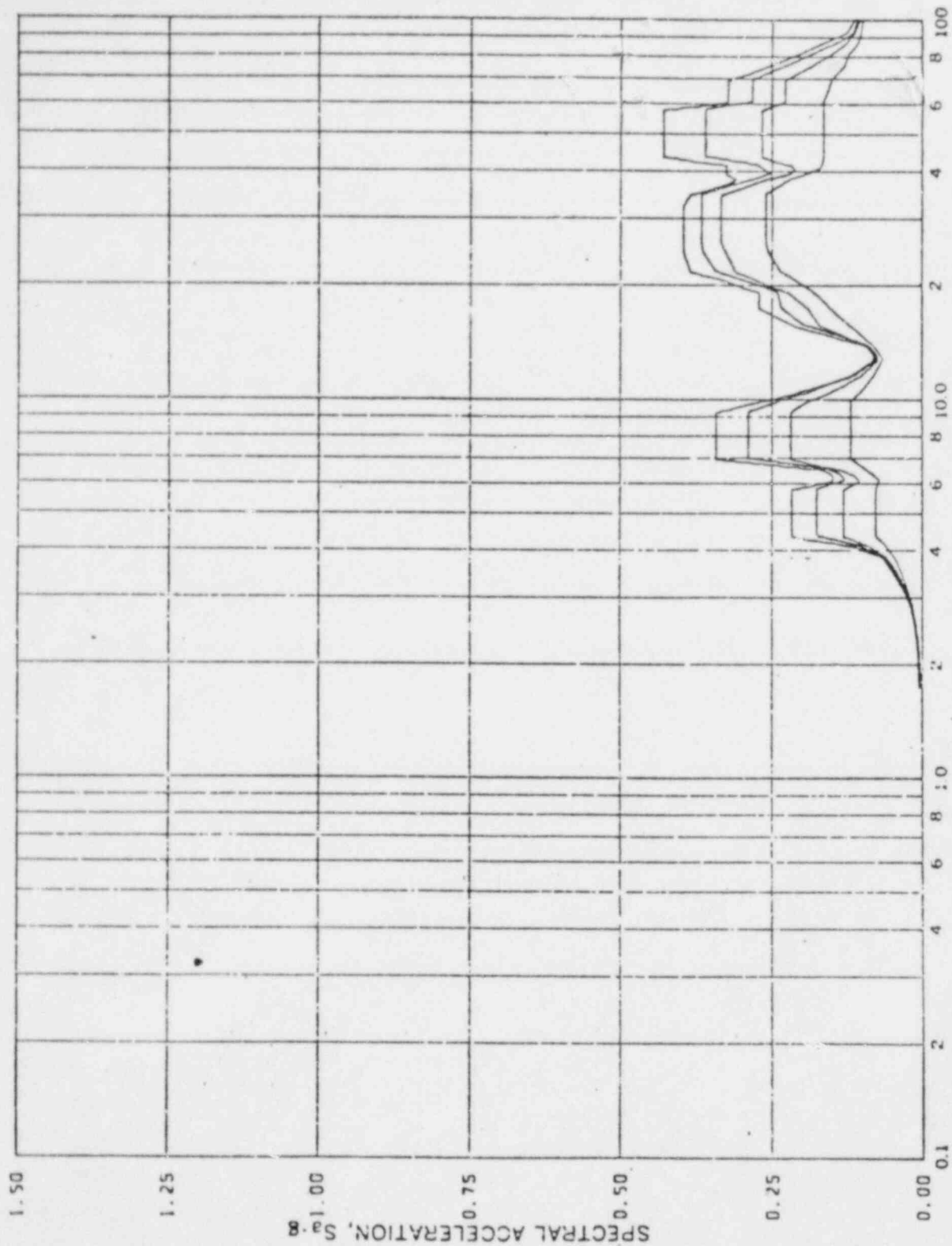
FREQUENCY-CPS

Acceleration Spectra for PEDESTAL

Load Case: Susquehanna KWU-SRV #76 ASYMM.

Node 215, Direction Z, Elev 702'-3"

Damping: 0.005, 0.01, 0.02, 0.05



Acceleration Spectra for CONTAINMENT SHELL

Load Case: SUSQUEHANNA KWU-SRV #76 ASYMM.

Node 291, Direction: X, Elev 702'-3"

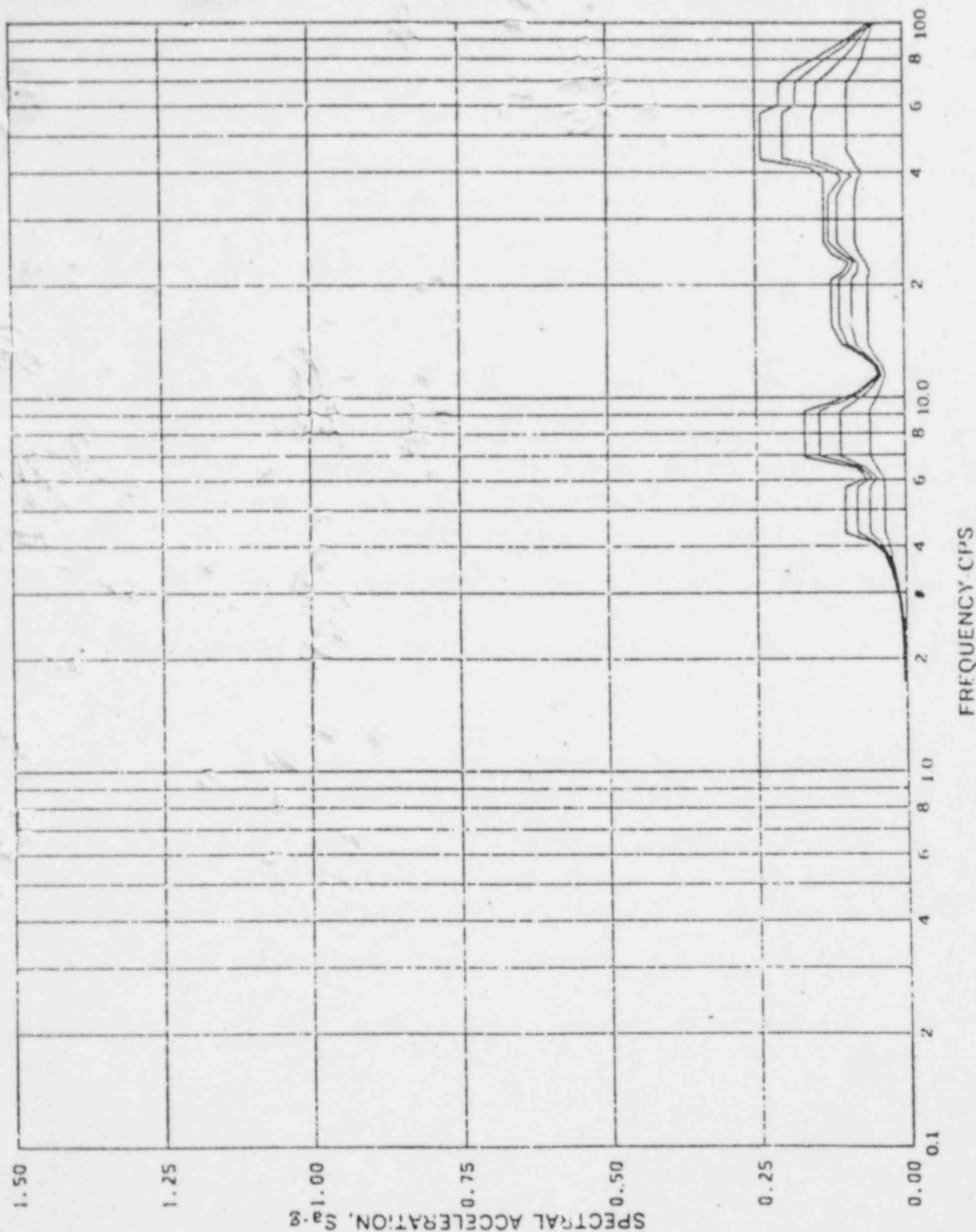
Damping: 0.005, 0.01, 0.02, 0.05

REV. 6, 4/82

**SUSQUEHANNA STEAM ELECTRIC STATION
UNITS 1 AND 2
DESIGN ASSESSMENT REPORT**

SSS CONTAINMENT RESPONSE
SPECTRA - KWU SRV #76
ASYMMETRIC - DIRECTION
HORIZONTAL

FIGURE 10-28



FREQUENCY - CPS

Acceleration Spectra for CONTAINMENT SHELL

Load Case: SUSQUEHANNA KWU-SRV #76 ASYMM.

Mode 291, Direction Z, Elev 702'-3"

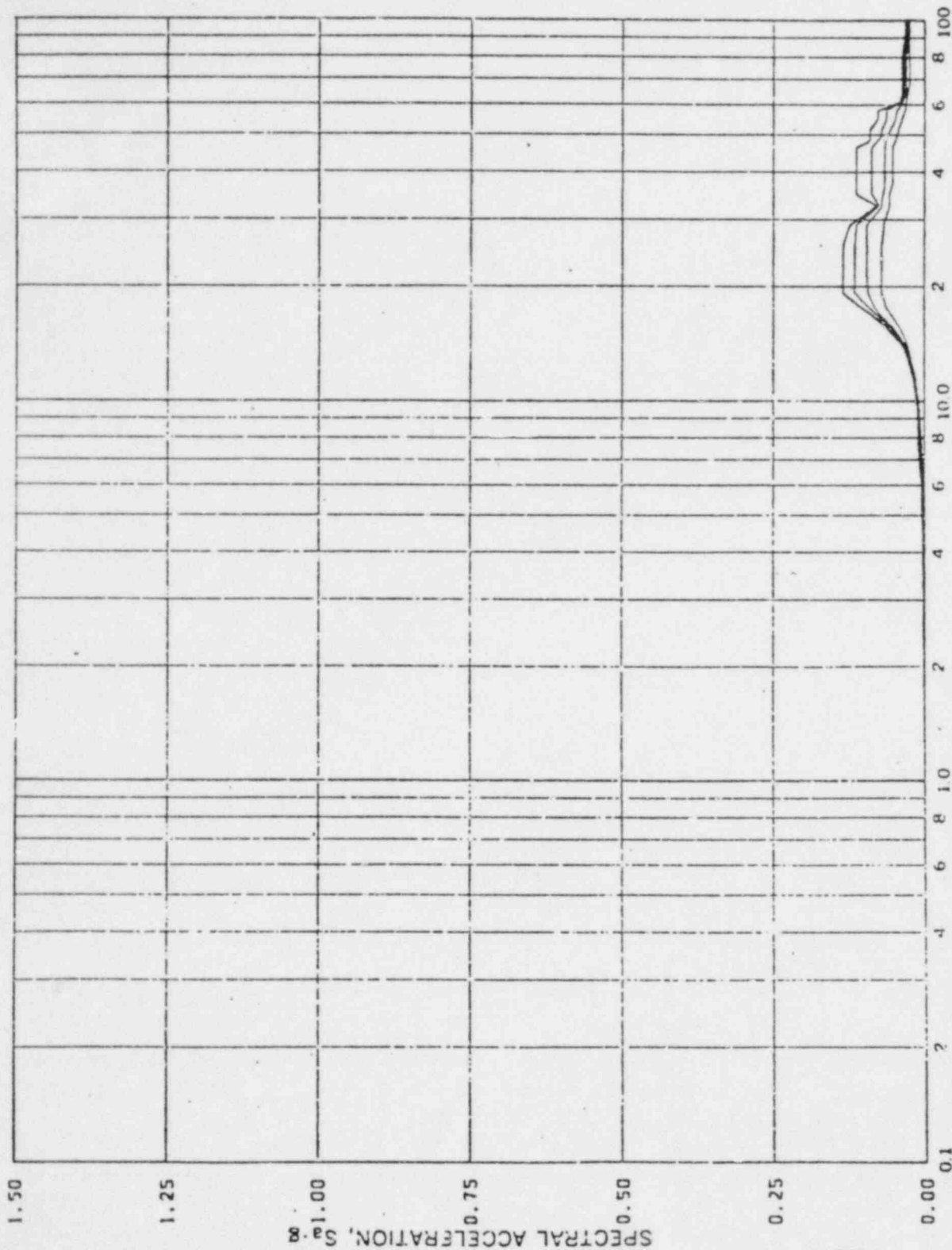
Damping: 0.005, 0.01, 0.02, 0.05

REV. 6, 4/82

**SUSQUEHANNA STEAM ELECTRIC STATION
UNITS 1 AND 2
DESIGN ASSESSMENT REPORT**

SSS CONTAINMENT RESPONSE
SPECTRA - KWU SRV #76
ASYMMETRIC -DIRECTION
VERTICAL

FIGURE 10-29



FREQUENCY-CPS

Acceleration Spectra for CONTAINMENT SHELL

Load Case: Susquehanna KWU-SRV #76 ASYMM.

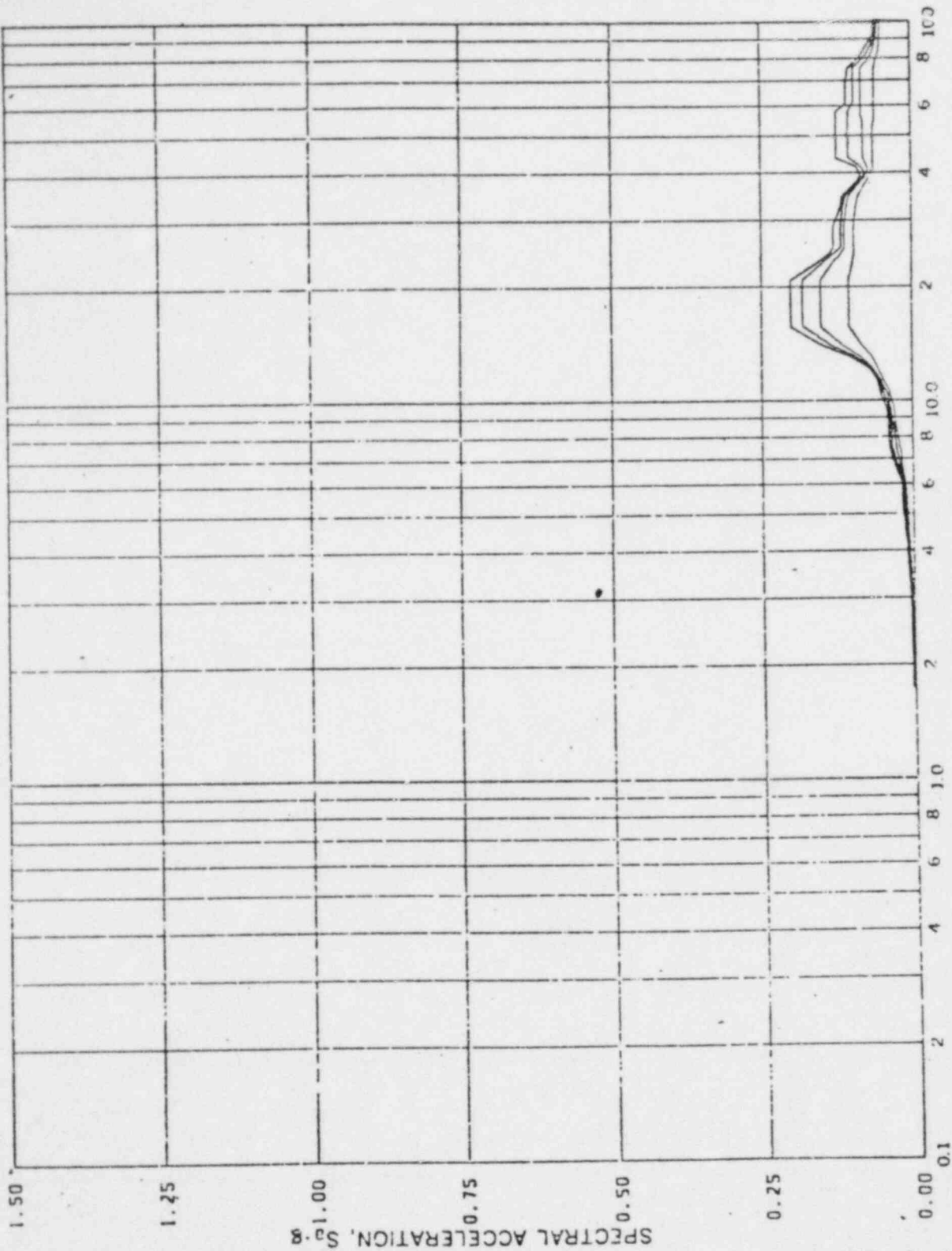
Node 295, Direction Y, Elev 202'-3"

Damping: 0.005, 0.01, 0.02, 0.05

REV. 6, 4/82

**SUSQUEHANNA STEAM ELECTRIC STATION
UNITS 1 AND 2
DESIGN ASSESSMENT REPORT**

SSS CONTAINMENT RESPONSE
SPECTRA- KWU SRV #76
ASYMMETRIC - DIRECTION
HORIZONTAL
FIGURE 10-30



FREQUENCY-CPS

Acceleration Spectra for CONTAINMENT SHELL

Load Case: SUSQUEHANNA KWU-SRV #76 ASYMM.

Node 295, Direction Z, Elev 702'-3"

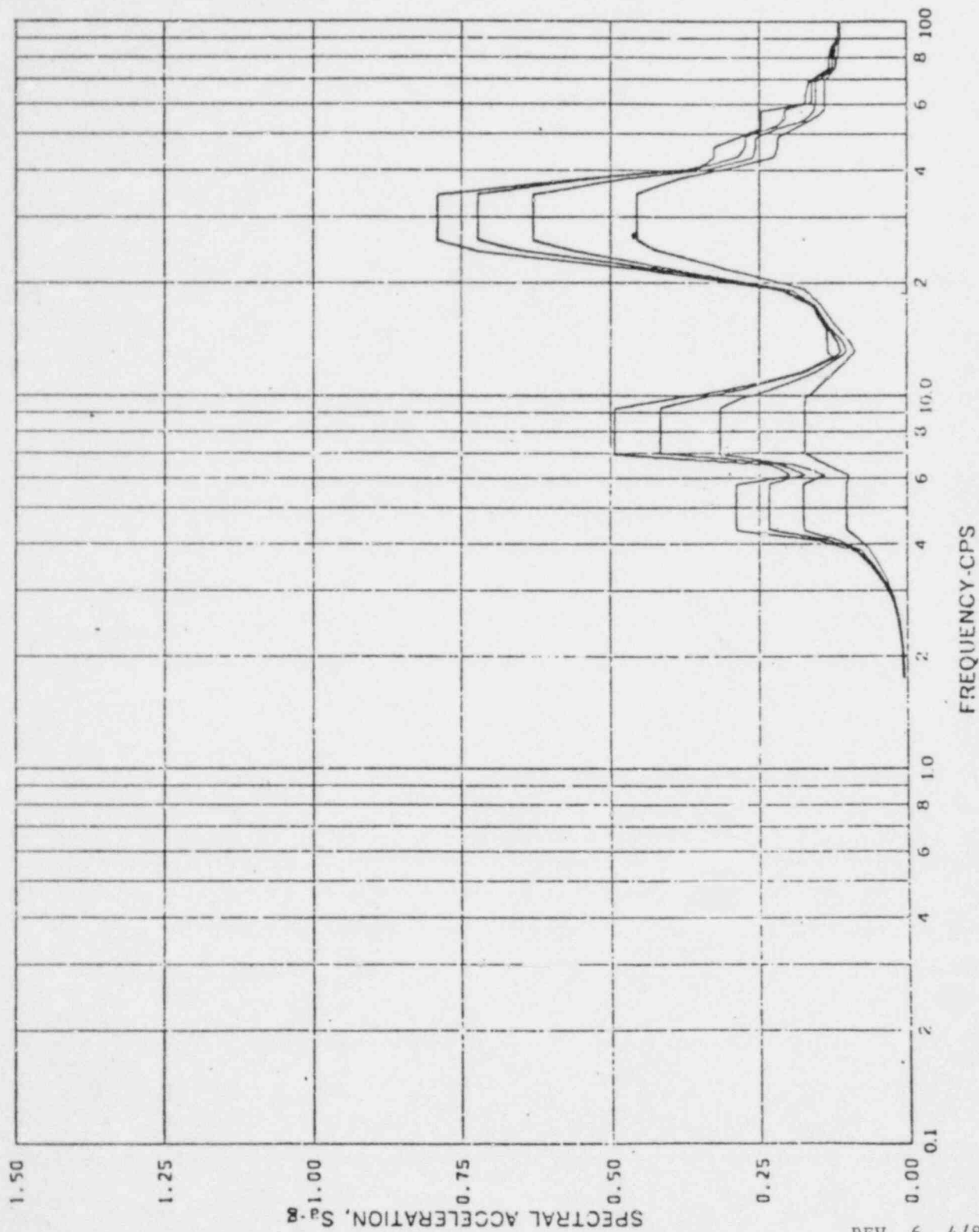
Damping: 0.005, 0.01, 0.02, 0.05

REV. 6, 4/82

**SUSQUEHANNA STEAM ELECTRIC STATION
UNITS 1 AND 2
DESIGN ASSESSMENT REPORT**

SSES CONTAINMENT RESPONSE
SPECTRA - KWU SRV #76
ASYMMETRIC - DIRECTION
VERTICAL

FIGURE 10-31



FREQUENCY-CPS

Acceleration Spectra for CONTAINMENT SHELL

Load Case: SUSQUEHANNA KWU-SRV #76 ASYMM.

Node 331, Direction X, Elev 730'-8-1/2"

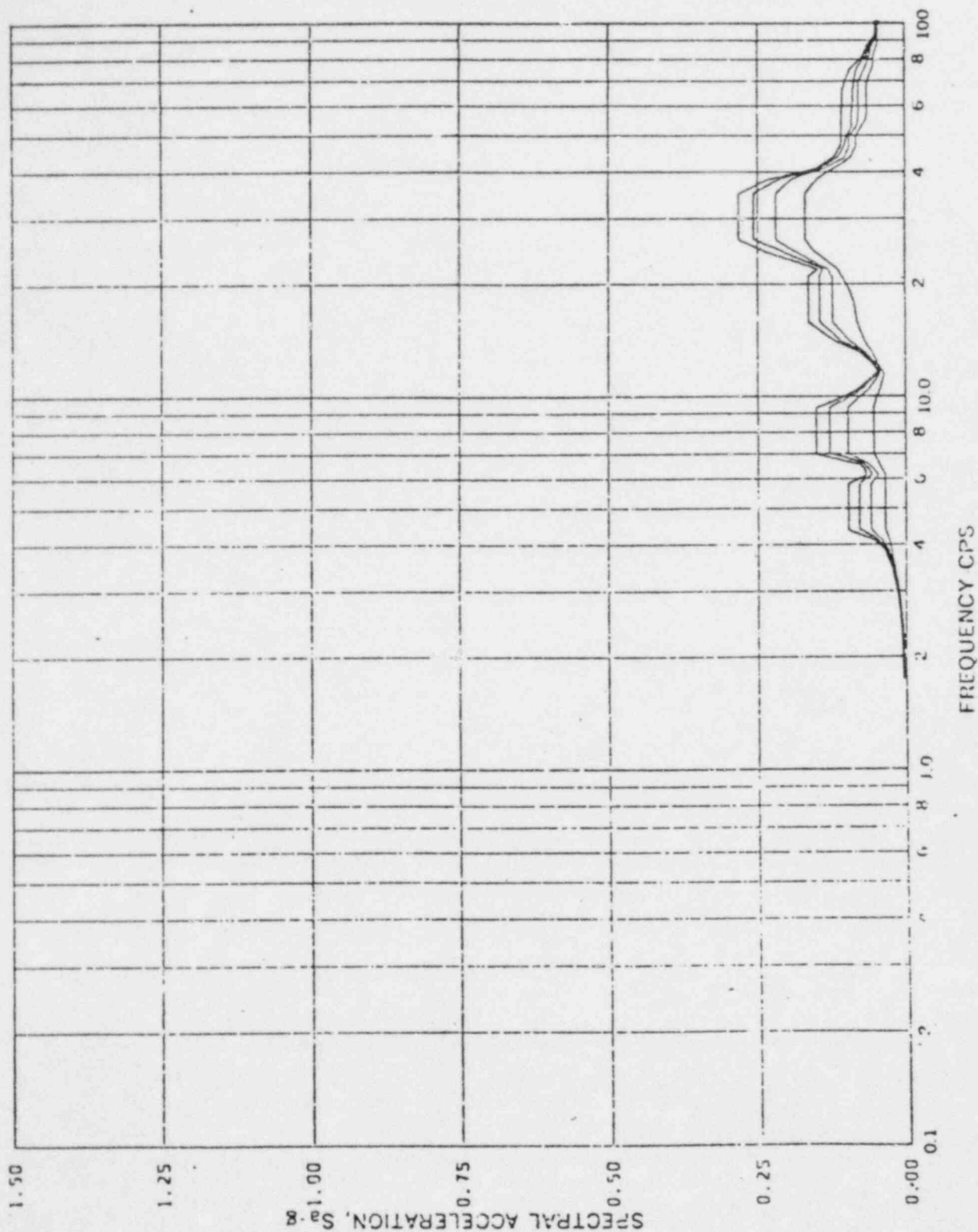
Damping: 0.005, 0.01, 0.02, 0.05

REV. 6, 4/82

**SUSQUEHANNA STEAM ELECTRIC STATION
UNITS 1 AND 2
DESIGN ASSESSMENT REPORT**

SSS CONTAINMENT RESPONSE
SPECTRA - KWU SRV #76
ASYMMETRIC - DIRECTION
HORIZONTAL

FIGURE 10-32



FREQUENCY CPS

Acceleration Spectra for CONTAINMENT SHELL

Load Case: Susquehanna KWU-SRV #76 ASYMM.

Node 331, Direction Z, Elev 730'-8-1/2"

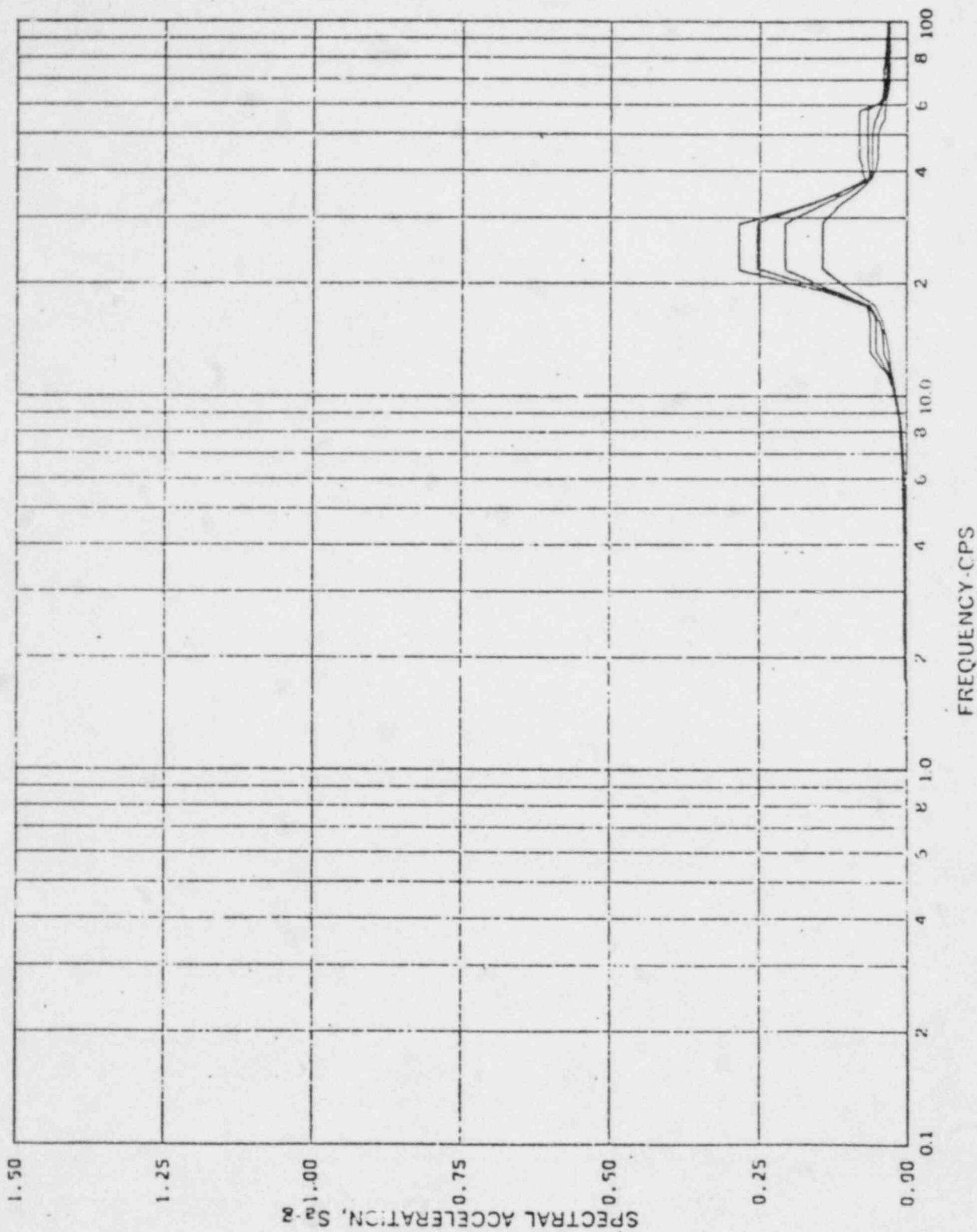
Damping: 0.005, 0.01, 0.02, 0.05

REV. 6, 4/82

**SUSQUEHANNA STEAM ELECTRIC STATION
UNITS 1 AND 2
DESIGN ASSESSMENT REPORT**

SSS CONTAINMENT RESPONSE
SPECTRA - KWU SRV #76
ASYMMETRIC - DIRECTION
VERTICAL

FIGURE 10-33



Acceleration Spectra for CONTAINMENT SHELL

Load Case: Susquehanna KWU-SRV #76 ASYMM.

Node 335, Direction Y, Elev 730'-8-1/2"

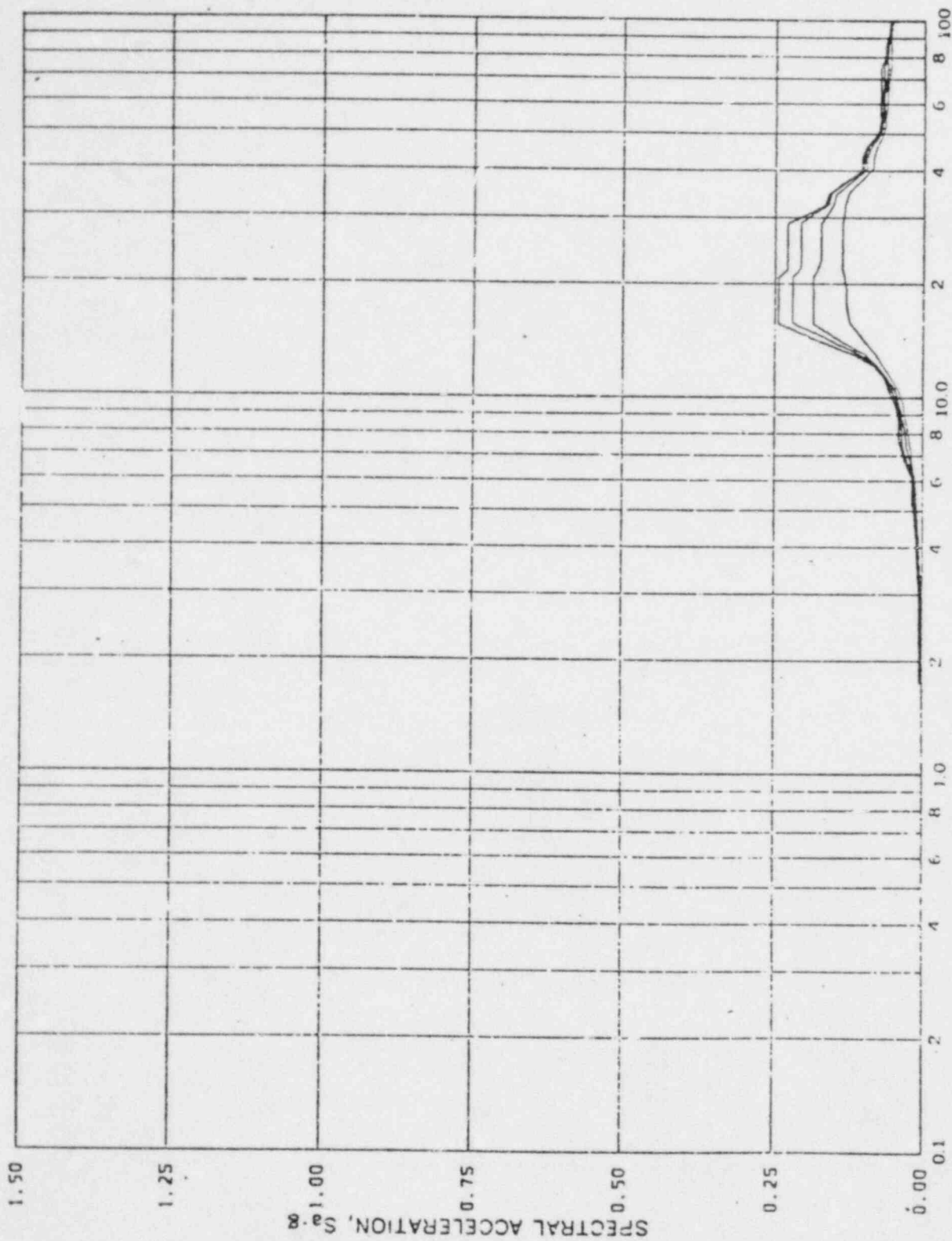
Damping: 0.005, 0.01, 0.02, 0.05

REV. 6, 4/82

**SUSQUEHANNA STEAM ELECTRIC STATION
UNITS 1 AND 2
DESIGN ASSESSMENT REPORT**

SSES CONTAINMENT RESPONSE
SPECTRA - KWU SRV # 76
ASYMMETRIC - DIRECTION
HORIZONTAL

FIGURE 10-34



FREQUENCY-CPS

Acceleration Spectra for CONTAINMENT SHELL

Load Case: SUSQUEHANNA KWU-SRV #76 ASYMM.

Node 335, Direction Z, Elev 740'-8-1/2"

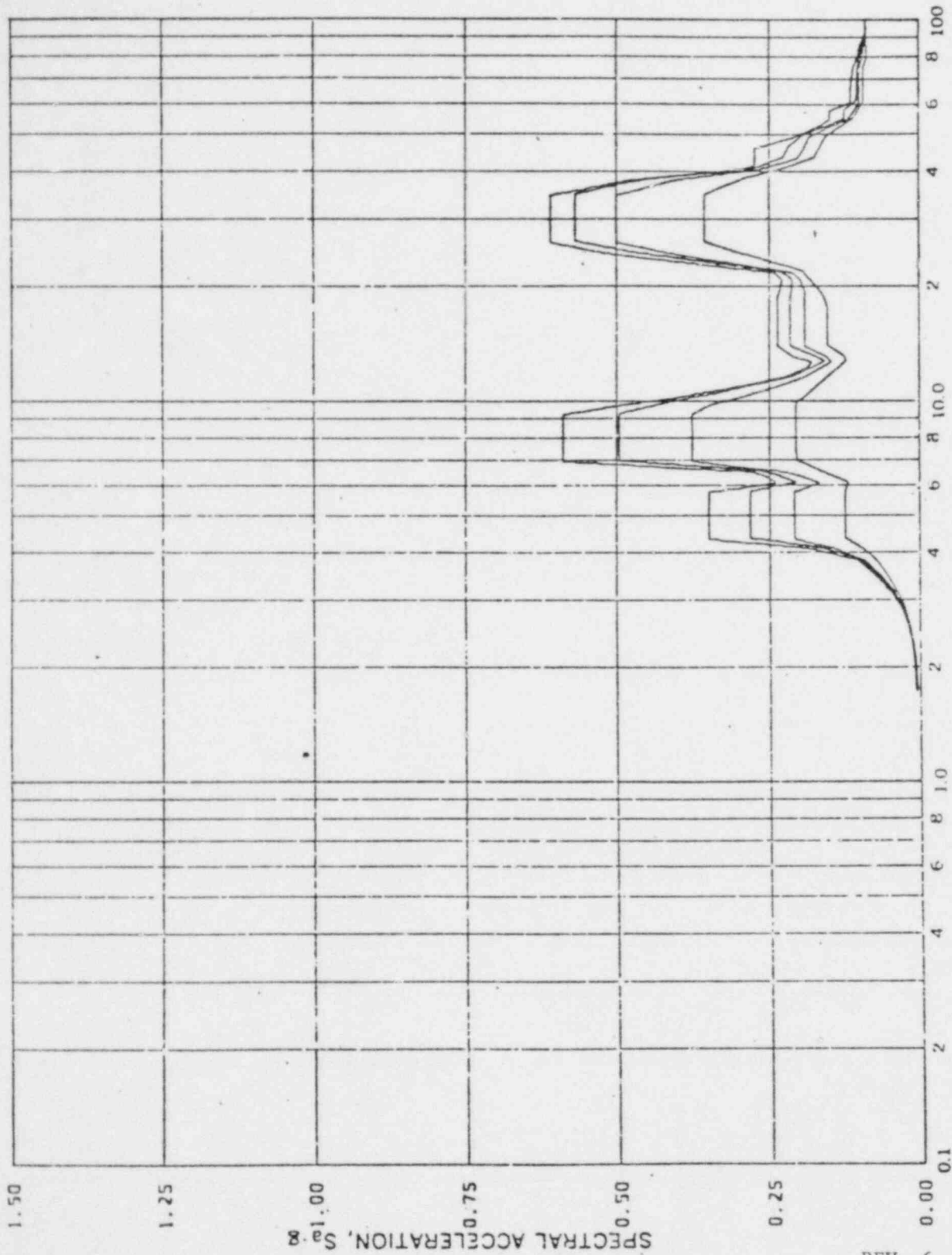
Damping: 0.005, 0.01, 0.02, 0.05

REV. 6, 4/82

**SUSQUEHANNA STEAM ELECTRIC STATION
UNITS 1 AND 2
DESIGN ASSESSMENT REPORT**

SSS CONTAINMENT RESPONSE
SPECTRA - KWU SRV #76
ASYMMETRIC - DIRECTION
VERTICAL

FIGURE 10-35



FREQUENCY-CPS

Acceleration Spectra for CONTAINMENT SHELL

Load Case: Susquehanna KWU-SRV #76 ASYMM.

Node 371, Direction X, Elev 750'-1-1/2"

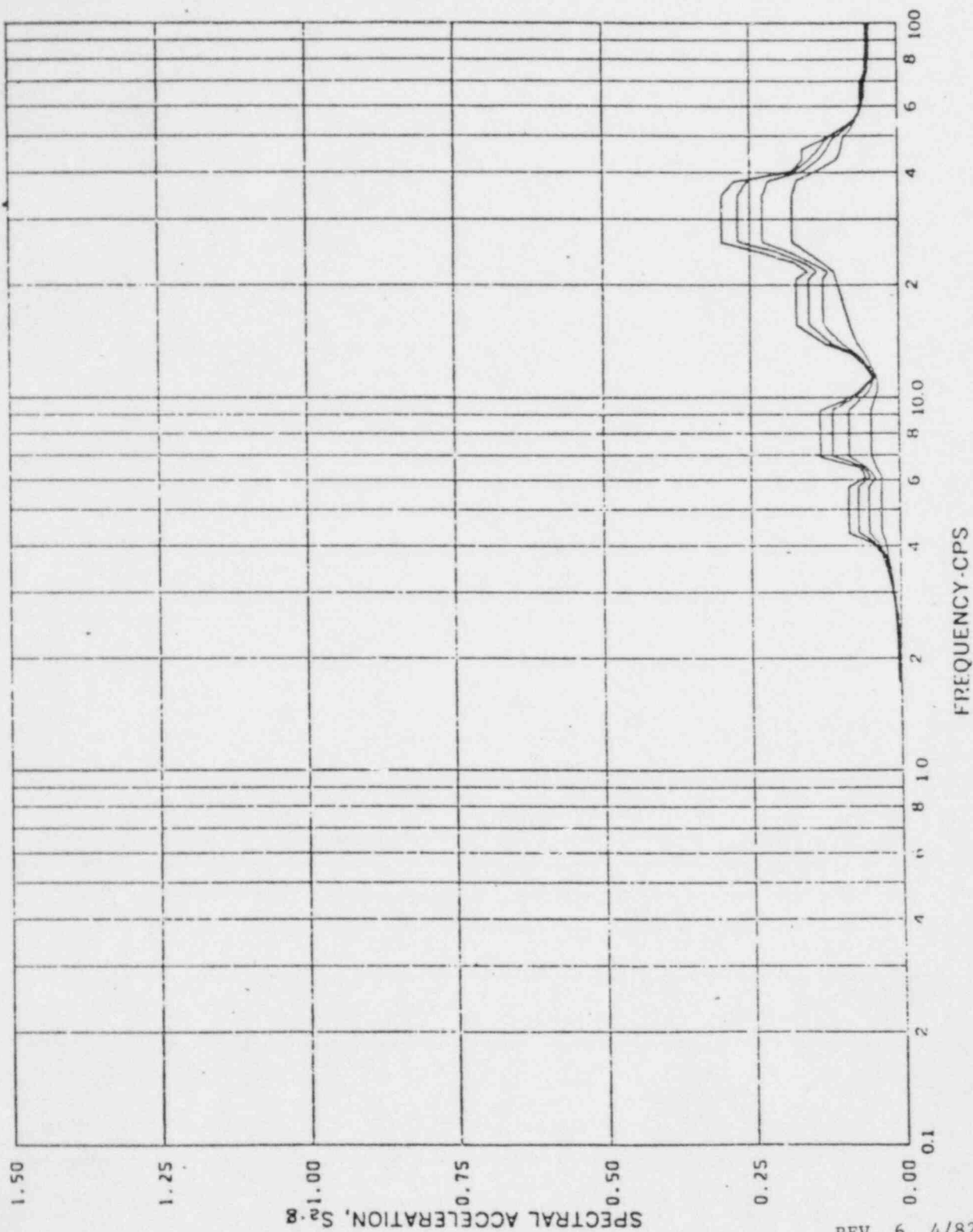
Damping: 0.005, 0.01, 0.02, 0.05

REV. 6, 4/82

**SUSQUEHANNA STEAM ELECTRIC STATION
UNITS 1 AND 2
DESIGN ASSESSMENT REPORT**

SSES CONTAINMENT RESPONSE
SPECTRA KWU SRV #76
ASYMMETRIC - DIRECTION
HORIZONTAL

FIGURE 10-36



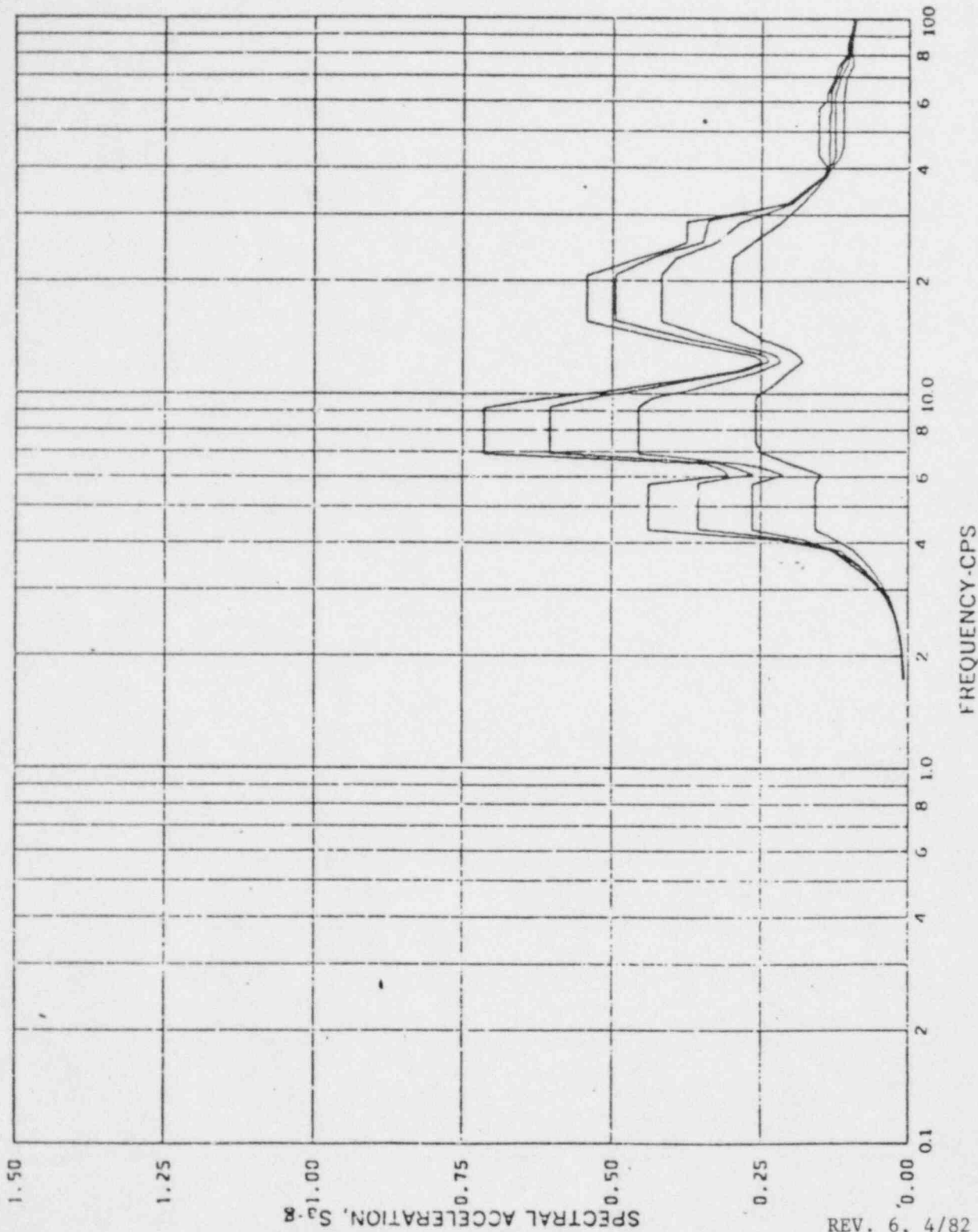
REV. 6, 4/82

**SUSQUEHANNA STEAM ELECTRIC STATION
UNITS 1 AND 2
DESIGN ASSESSMENT REPORT**

SSS CONTAINMENT RESPONSE
SPECTRA KWU SRV #76
ASYMMETRIC - DIRECTION
VERTICAL

FIGURE 10-37

Acceleration Spectra for CONTAINMENT SHELL
Load Case: Susquehanna KWU-SRV #76 ASYMM.
Mode 371, Direction Z, Elev 750'-1-1/2"
Damping: 0.005, 0.01, 0.02, 0.05

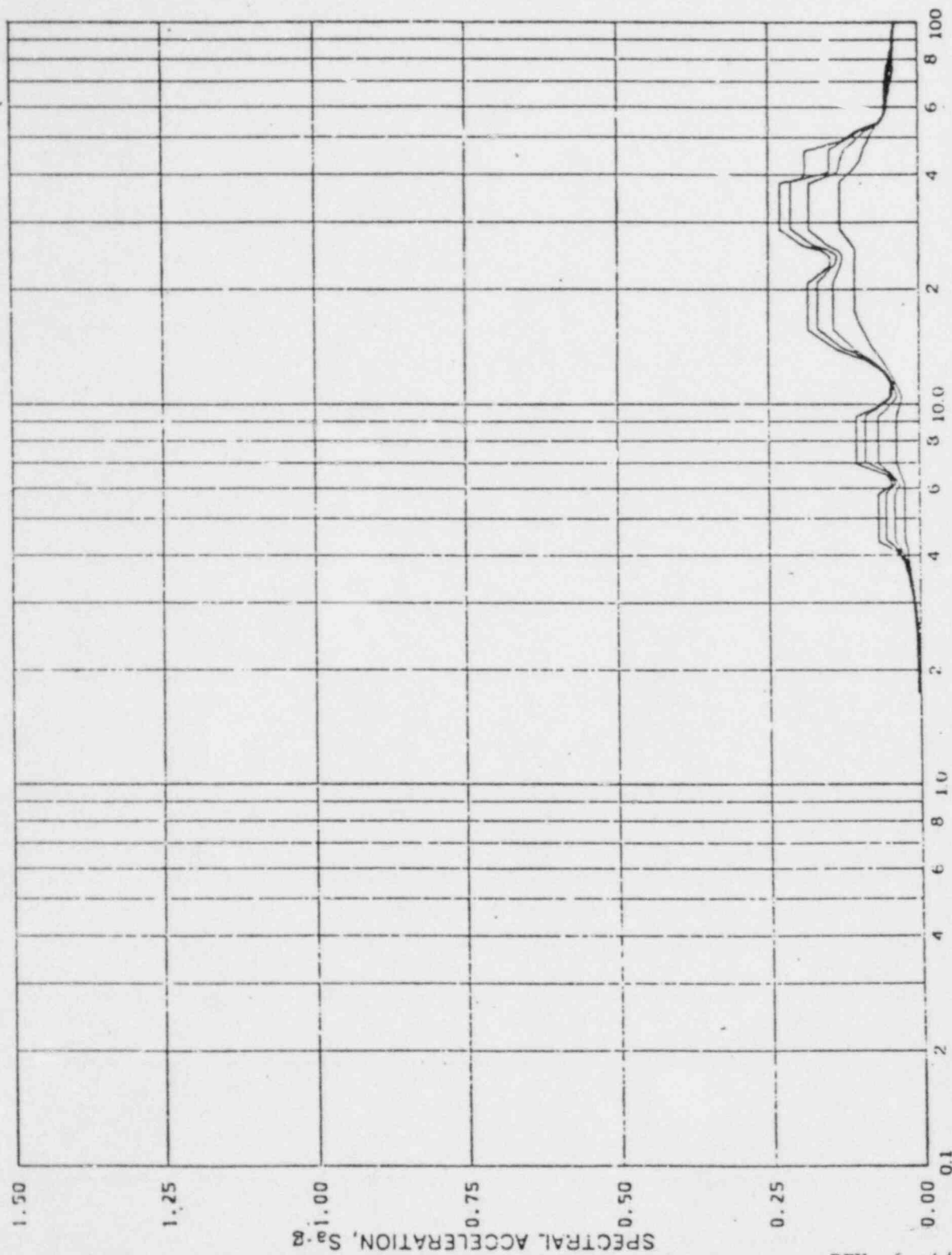


Acceleration Spectra for CONTAINMENT SHELL
 Load Case: Susquehanna KWU-SRV #76 ASYMM.
 Node 411, Direction X, Elev 778'-9-3/4"
 Damping: 0.005, 0.01, 0.02, 0.05

REV. 6, 4/82

**SUSQUEHANNA STEAM ELECTRIC STATION
 UNITS 1 AND 2
 DESIGN ASSESSMENT REPORT**

SSES CONTAINMENT RESPONSE
 SPECTRA KWU SRV #76
 ASYMMETRIC - DIRECTION
 HORIZONTAL
 FIGURE 10-38



FREQUENCY-CPS

Acceleration Spectra for CONTAINMENT SHELL

Load Case: Susquehanna KWU-SRV #76 ASYMM.

Node 411, Direction Z, Elev 778'-9-3/4"

Damping: 0.005, 0.01, 0.02, 0.05

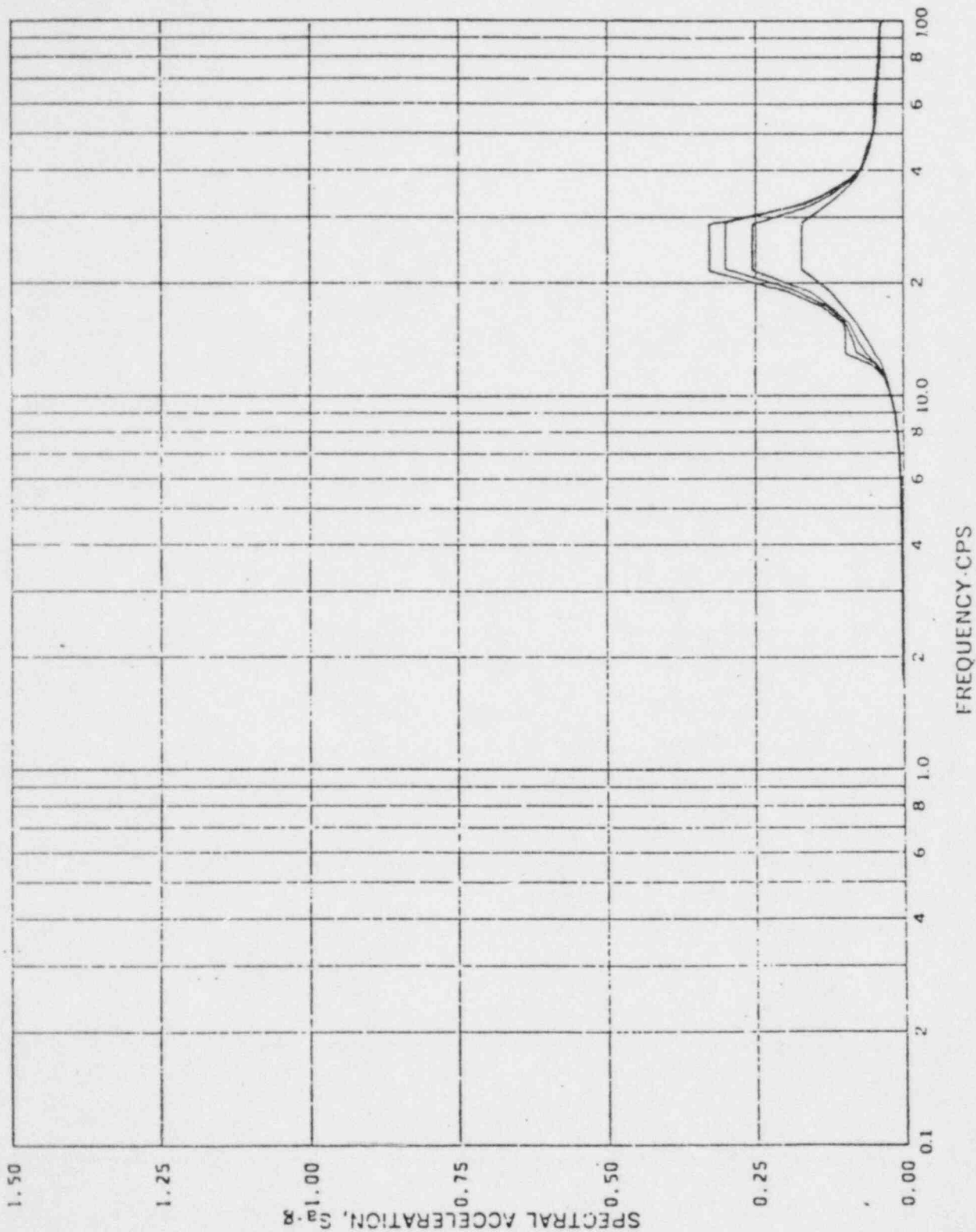
REV. 6, 4/82

**SUSQUEHANNA STEAM ELECTRIC STATION
UNITS 1 AND 2
DESIGN ASSESSMENT REPORT**

SSS CONTAINMENT RESPONSE
SPECTRA - KWU SRV # 76
ASYMMETRIC - DIRECTION
VERTICAL

FIGURE

10-39



FREQUENCY CPS

Acceleration Spectra for CONTAINMENT SHELL

Load Case: SUSQUEHANNA KWU-SRV #76 ASYMM.

Node 415, Direction Y, Elev 778'-9-3/4"

Damping: 0.005, 0.01, 0.02, 0.05

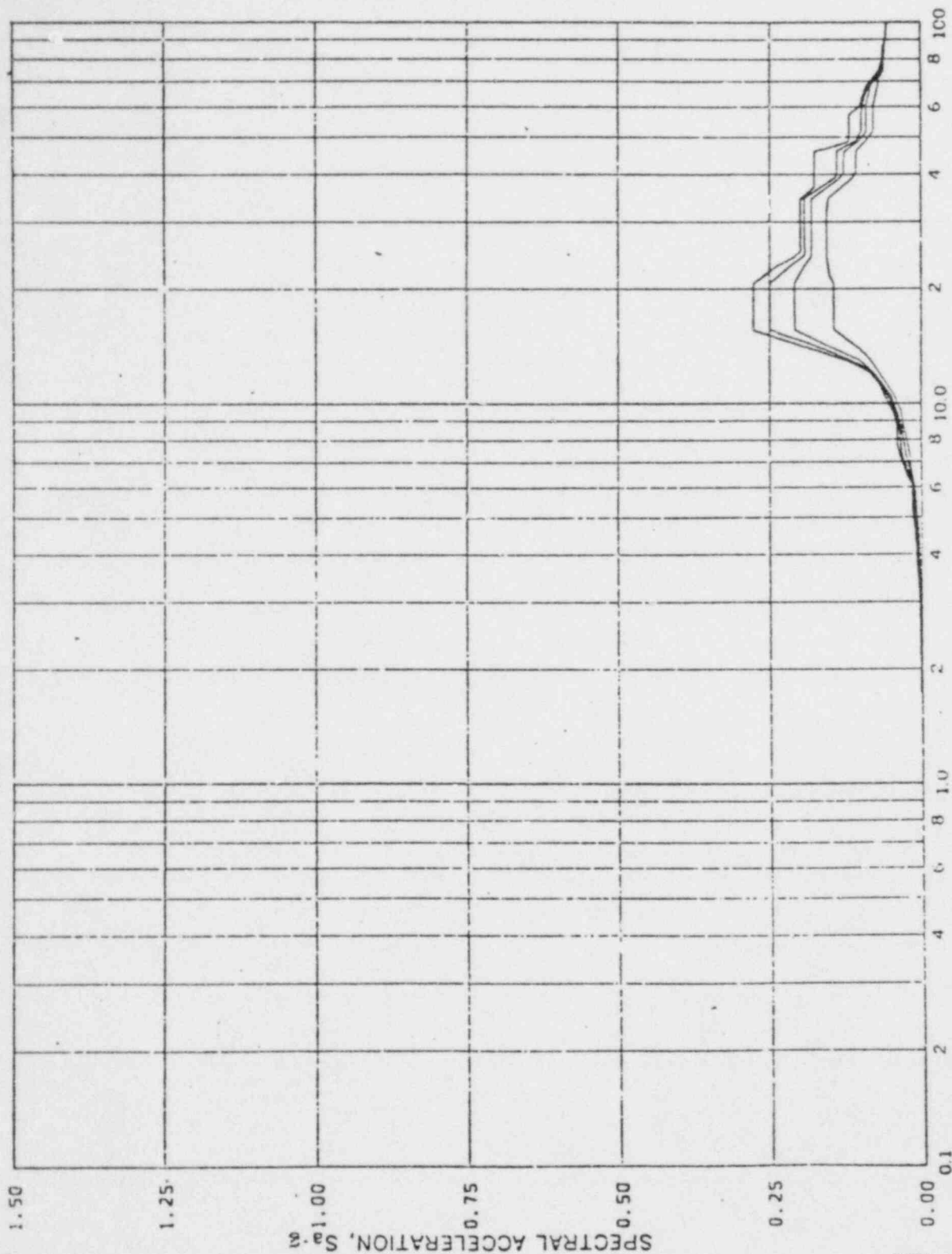
REV. 6, 4/82

**SUSQUEHANNA STEAM ELECTRIC STATION
UNITS 1 AND 2
DESIGN ASSESSMENT REPORT**

SSES CONTAINMENT RESPONSE
SPECTRA KWU SRV #76
ASYMMETRIC - DIRECTION
HORIZONTAL

FIGURE

10-40



FREQUENCY-CPS

Acceleration Spectra for CONTAINMENT SHELL

Load Case: Susquehanna KWU-SRV #76 ASYMM.

Node 415, Direction Z, Elev 778'-9-3/4"

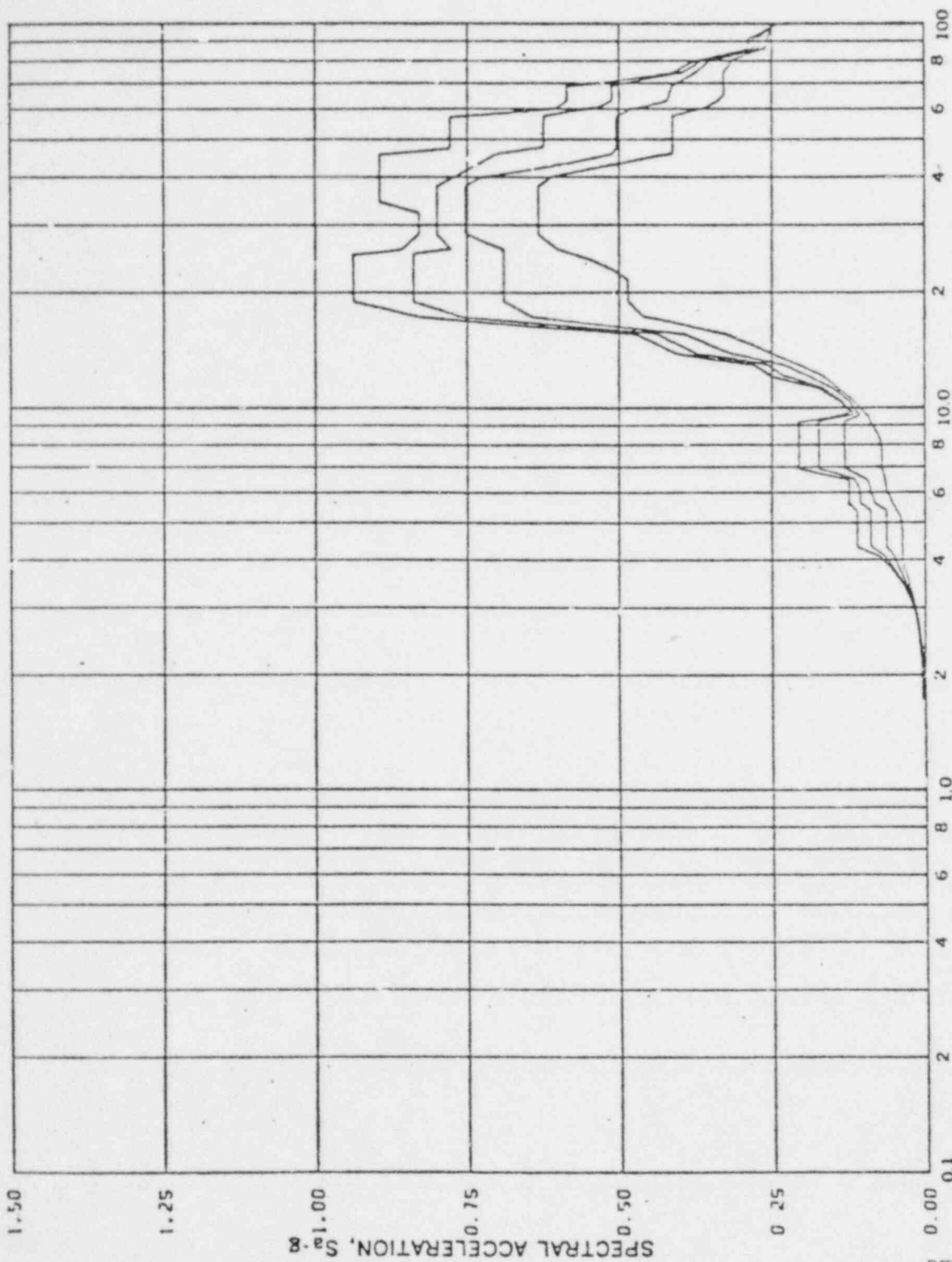
Damping: 0.005, 0.01, 0.02, 0.05

REV. 6, 4/82

**SUSQUEHANNA STEAM ELECTRIC STATION
UNITS 1 AND 2
DESIGN ASSESSMENT REPORT**

SSS CONTAINMENT RESPONSE
SPECTRA KWU SRV # 76
ASYMMETRIC - DIRECTION
VERTICAL

FIGURE 10-41



FREQUENCY-CPS

Limerick Generation Station, Acceleration Spectra for WETWELL

Load Case: SRV - ASYMMETRIC - TRACE 76

Node: 131 Direction: HORIZ Elev: 205'-11" Angle: 0°

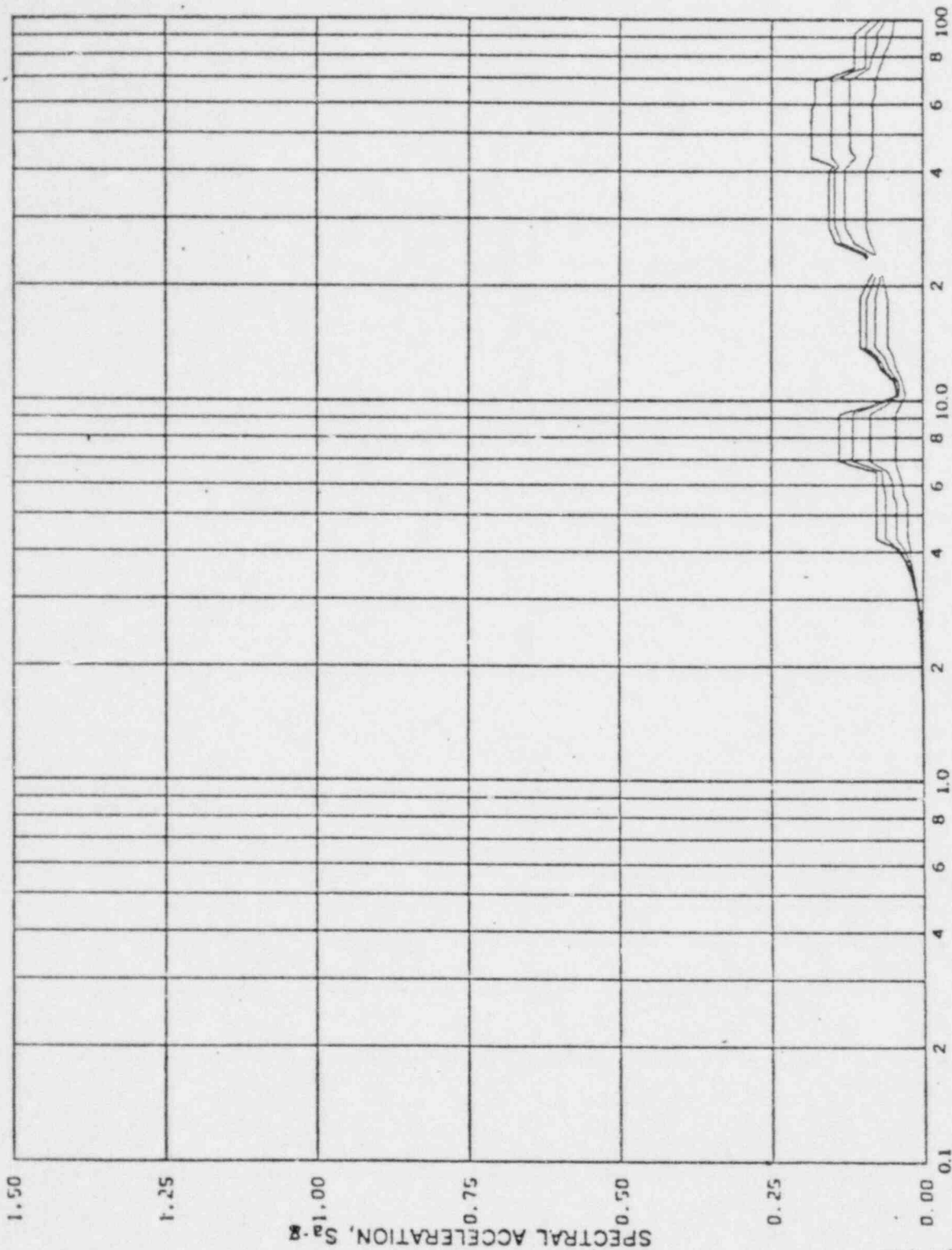
Damping: 0.005, 0.01, 0.02, 0.05 By: PC Date: 5-5-80 Check: KLM Date: 5/6/80

REV. 6, 4/82

**SUSQUEHANNA STEAM ELECTRIC STATION
UNITS 1 AND 2
DESIGN ASSESSMENT REPORT**

LGS CONTAINMENT RESPONSE
SPECTRA-KEWU SRV # 76
ASYMMETRIC - DIRECTION
HORIZONTAL

FIGURE 10-42



FREQUENCY-CPS

Limerick Generation Station, Acceleration Spectra for WETWELL

Load Case: SRV - ASYMMETRIC - TRACE 76

Node: 131 Direction: VERT Elev: 205'-11" Angle: 0°

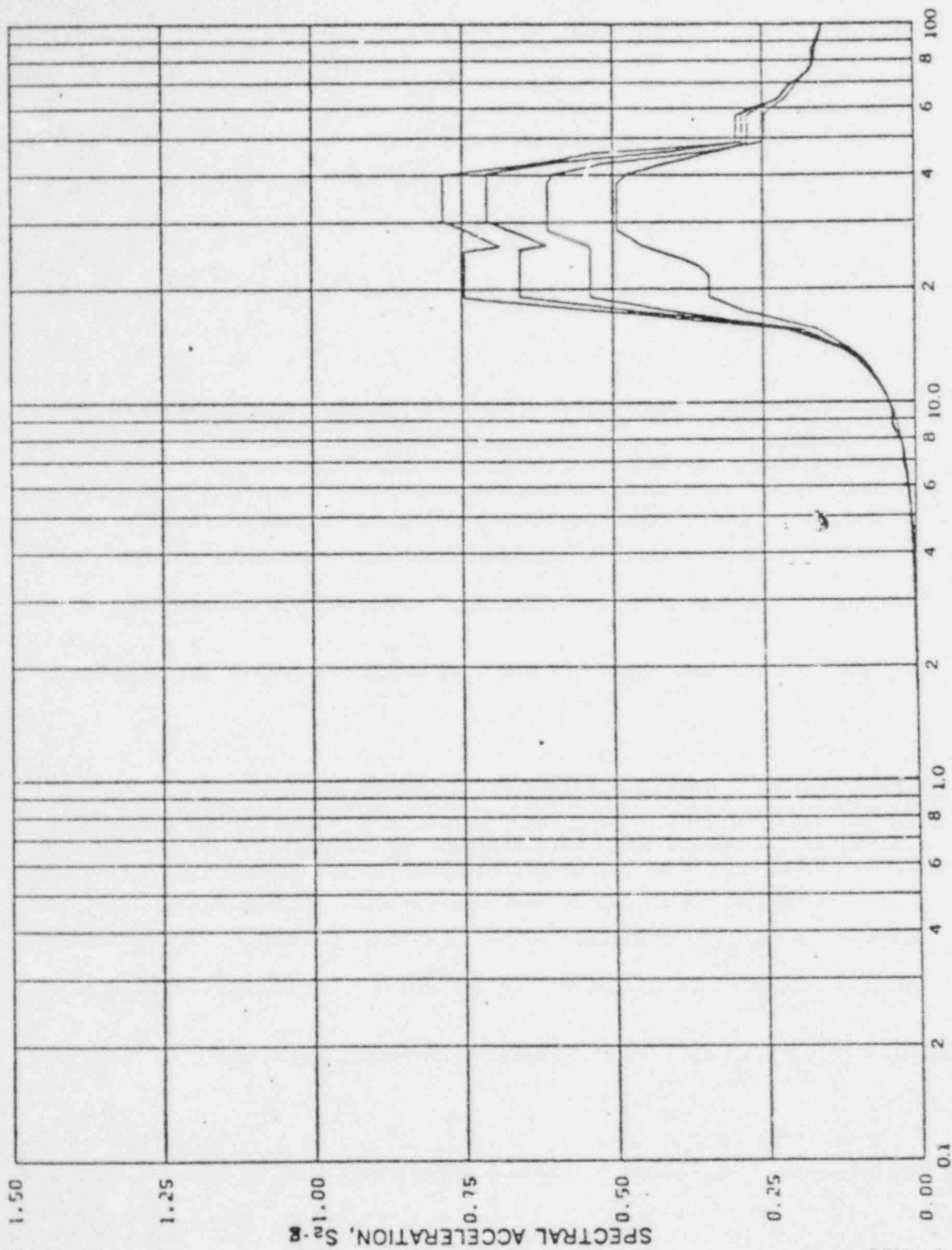
Damping: 0.005, 0.01, 0.02, 0.05 By: PL Date: 5-5-80 Check: KW Date: 5/6/80

REV. 6, 4/82

**SUSQUEHANNA STEAM ELECTRIC STATION
UNITS 1 AND 2
DESIGN ASSESSMENT REPORT**

LGS CONTAINMENT RESPONSE
SPECTRA-KWU SRV #76
ASYMMETRIC - DIRECTION
VERTICAL

FIGURE 10-43



REV. 6, 4/82

**SUSQUEHANNA STEAM ELECTRIC STATION
UNITS 1 AND 2
DESIGN ASSESSMENT REPORT**

LGS CONTAINMENT RESPONSE
SPECTRA - KWJ SRV #76
ASYMMETRIC - DIRECTION
HORIZONTAL

FIGURE 10-44

FREQUENCY - CPS

Limerick Generation Station, Acceleration Spectra for WETWELL

Load Case: SRV - ASYMMETRIC - TRACE 76

Node: 135 Direction: HORIZ Elev: 205'-11" Angle: 90°

Damping: 0.005, 0.01, 0.02, 0.05 By: PC Date: 5-5-80 Check: LM Date: 5/6/80

SUSQUEHANNA STEAM ELECTRIC STATION

UNITS 1 AND 2

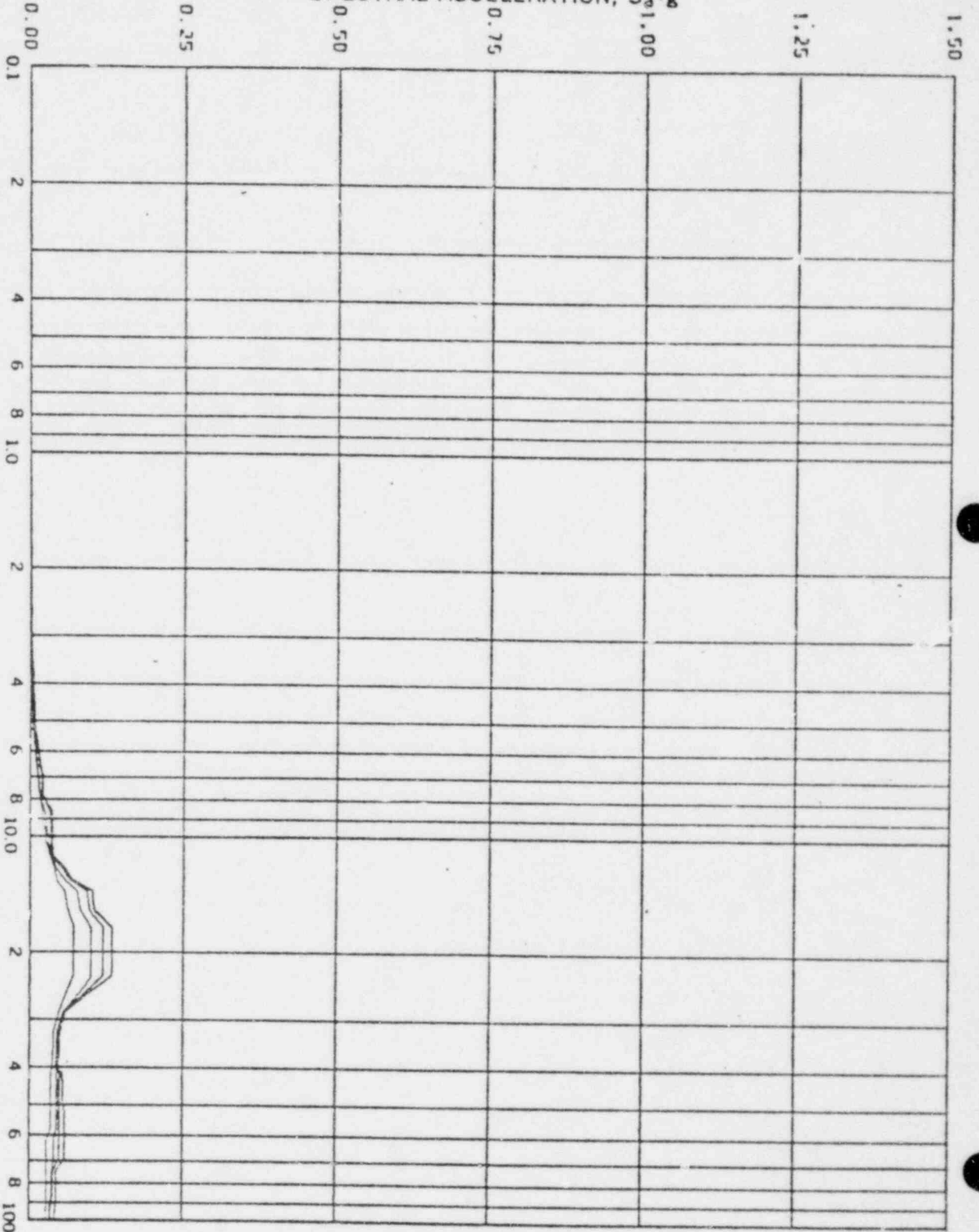
DESIGN ASSESSMENT REPORT

LGS CONTAINMENT RESPONSE
SPECTRA - KWU SRV # 76
ASYMMETRIC - DIRECTION
VERTICAL

FIGURE 0-45

REV. 6, 4/82

SPECTRAL ACCELERATION, $S_a \cdot g$



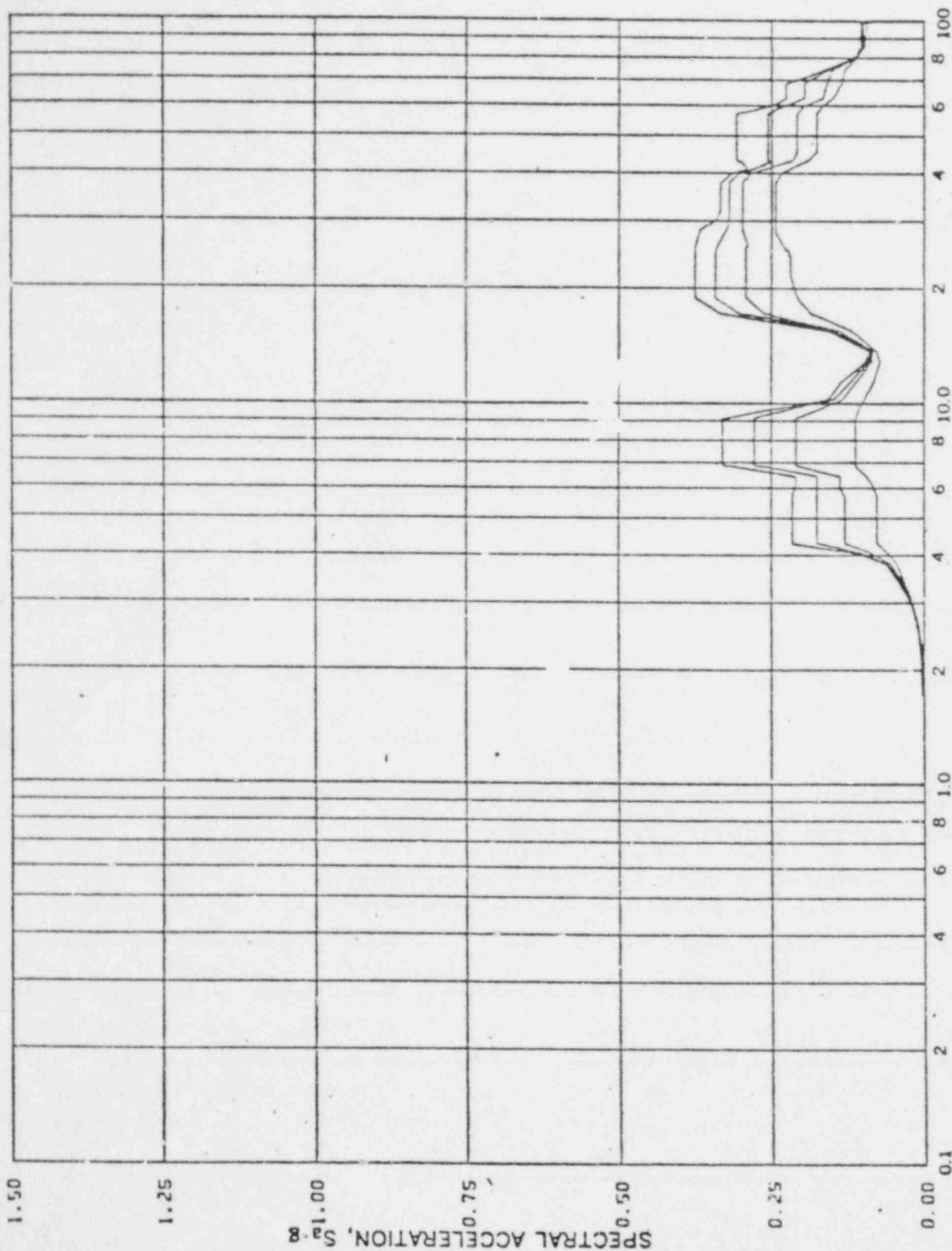
FREQUENCY-CPS

Limerick Generation Station, Acceleration Spectra for METWELL

Load Case: SRV - ASYMMETRIC - TRACE 76

Node: 135 Direction: VERT Elev: 205' - 11" Angle: 90°

Damping: 0.005, 0.01, 0.02, 0.05 By: PC Date: 5-5-80 Check: Klu Date: 5/6/80



FREQUENCY-CPS

Limerick Generation Station, Acceleration Spectra for PEDESTAL

Load Case: SRV - ASYMMETRIC - TRACE 76

Node: 211 Direction: HORIZ Elev: 236'-2" Angle: 0°

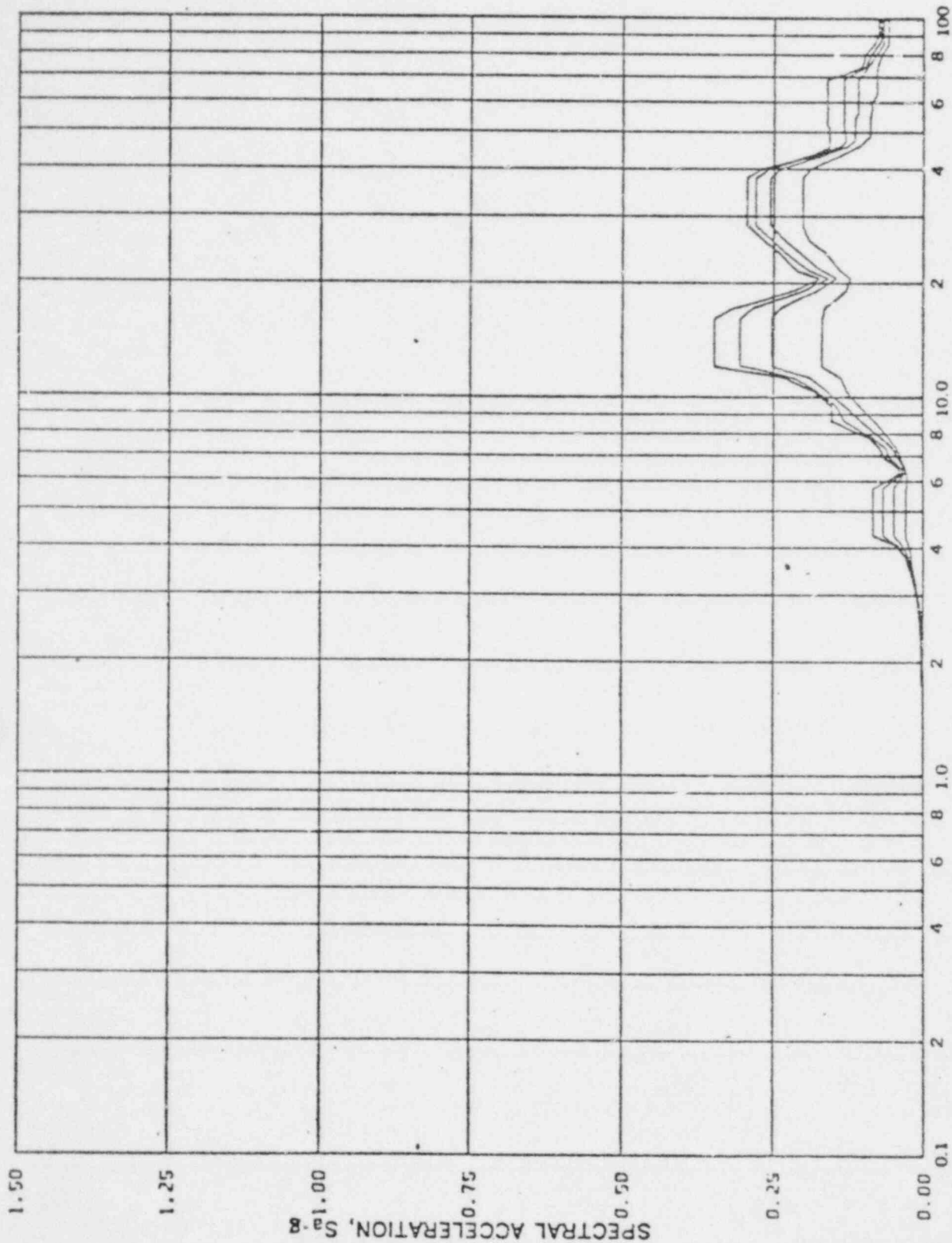
Damping: 0.005, 0.01, 0.02, 0.05 By: PC Date: 5-5-80 Check: KW Date: 5/6/80

REV. 6, 4/82

**SUSQUEHANNA STEAM ELECTRIC STATION
UNITS 1 AND 2
DESIGN ASSESSMENT REPORT**

LGS CONTAINMENT RESPONSE
SPECTRA - KWU SRV #76
ASYMMETRIC - DIRECTION
HORIZONTAL

FIGURE 10-46



FREQUENCY-CPS

Limerick Generation Station, Acceleration Spectra for PEDESTAL

Load Case: SRV - ASYMMETRIC - TRACE 76

Node: 211 Direction: VERT Elev: 236'-2" Angle: 0°

Damping: 0.005, 0.01, 0.02, 0.05 By: PL Date: 5-80 Check: 5/6/80

REV. 6, 4/82

**SUSQUEHANNA STEAM ELECTRIC STATION
UNITS 1 AND 2
DESIGN ASSESSMENT REPORT**

LGS CONTAINMENT RESPONSE
SPECTRA - KWU SRV #76
ASYMMETRIC - DIRECTION
VERTICAL

FIGURE 10-47

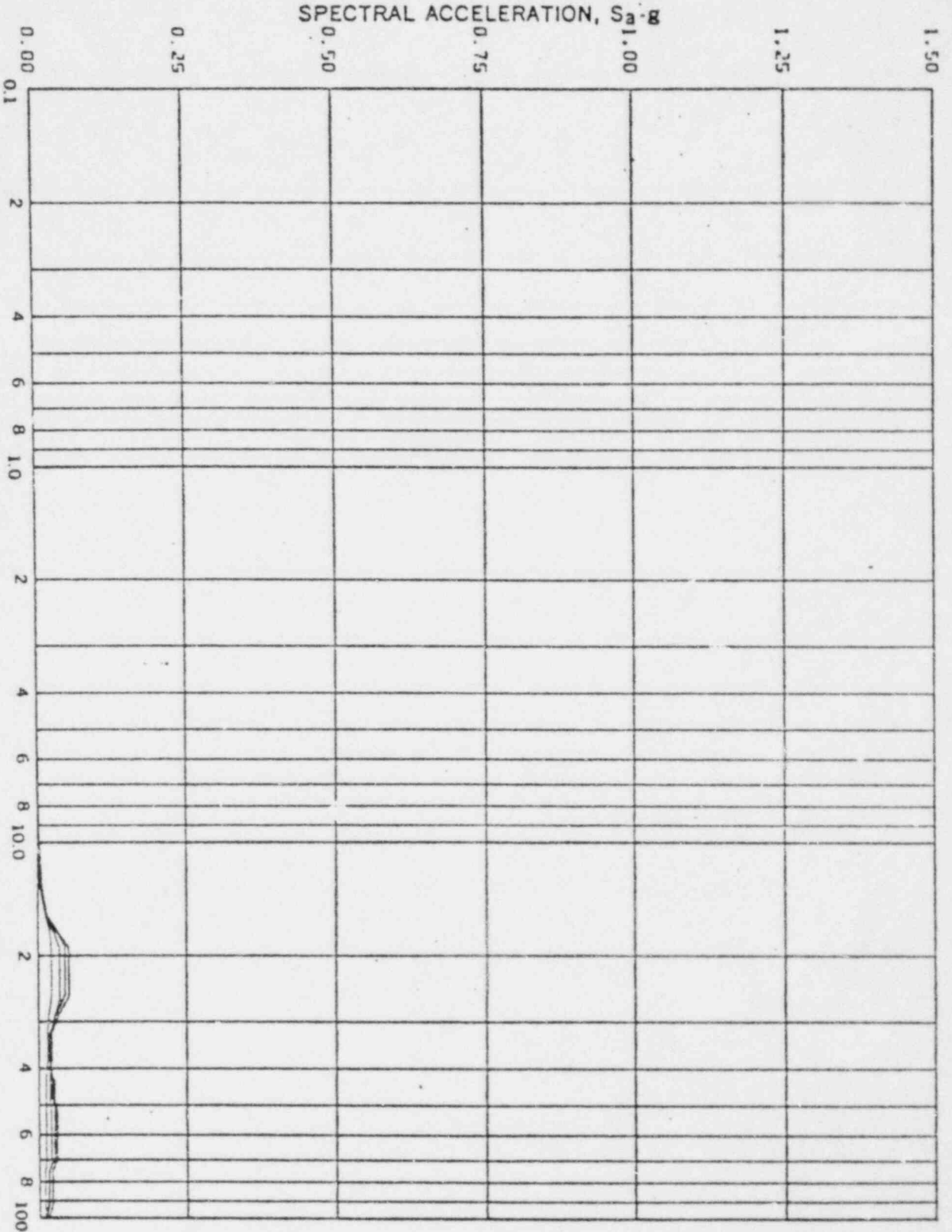
SUSQUEHANNA STEAM ELECTRIC STATION

UNITS 1 AND 2

DESIGN ASSESSMENT REPORT

LGS CONTAINMENT RESPONSE
SPECTRA - KWU SRV #76
ASYMMETRIC - DIRECTION
HORIZONTAL
FIGURE 10-48

REV. 6, 4/82



FREQUENCY-CPS

Limerick Generation Station, Acceleration Spectra for PEDESTAL

Load Case: SRV - ASYMMETRIC - TRACE 76

Node: 215 Direction: HORIZ Elev: 236'-2" Angle: 90°

Damping: 0.005, 0.01, 0.02, 0.05 By: R Date: 5-5-80 Check: M Date: 5/6/80



FREQUENCY-CPS

Limerick Generation Station, Acceleration Spectra for PEDESTAL

Load Case: SRV - ASYMMETRIC - TRACE 76

Node: 215 Direction: VERT Elev: 236'-2" Angle: 90°

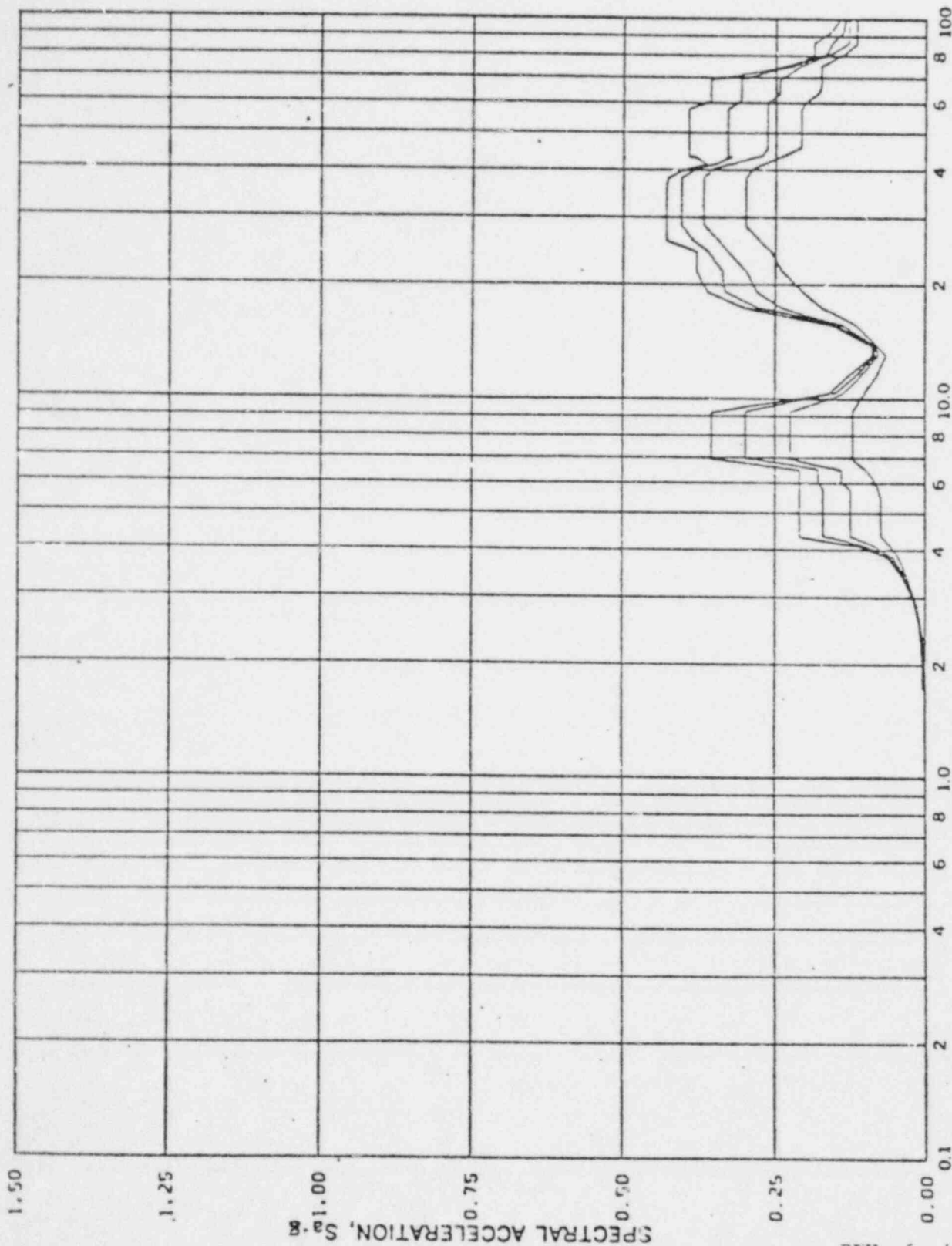
Damping: 0.005, 0.01, 0.02, 0.05 By: PC Date: 5-5-80 Check: KW Date: 5/6/80

RE7. 6, 4/82

SUSQUEHANNA STEAM ELECTRIC STATION UNITS 1 AND 2 DESIGN ASSESSMENT REPORT

LGS CONTAINMENT RESPONSE
SPECTRA - KWU SRV #76
ASYMMETRIC - DIRECTION
VERTICAL

FIGURE 10-49



FREQUENCY-CPS

Limerick Generation Station, Acceleration Spectra for WETWELL

Load Case: SRV - ASYMMETRIC - TRACE 76

Node: 291 Direction: HORIZ Elev: 236'-2" Angle: 0°

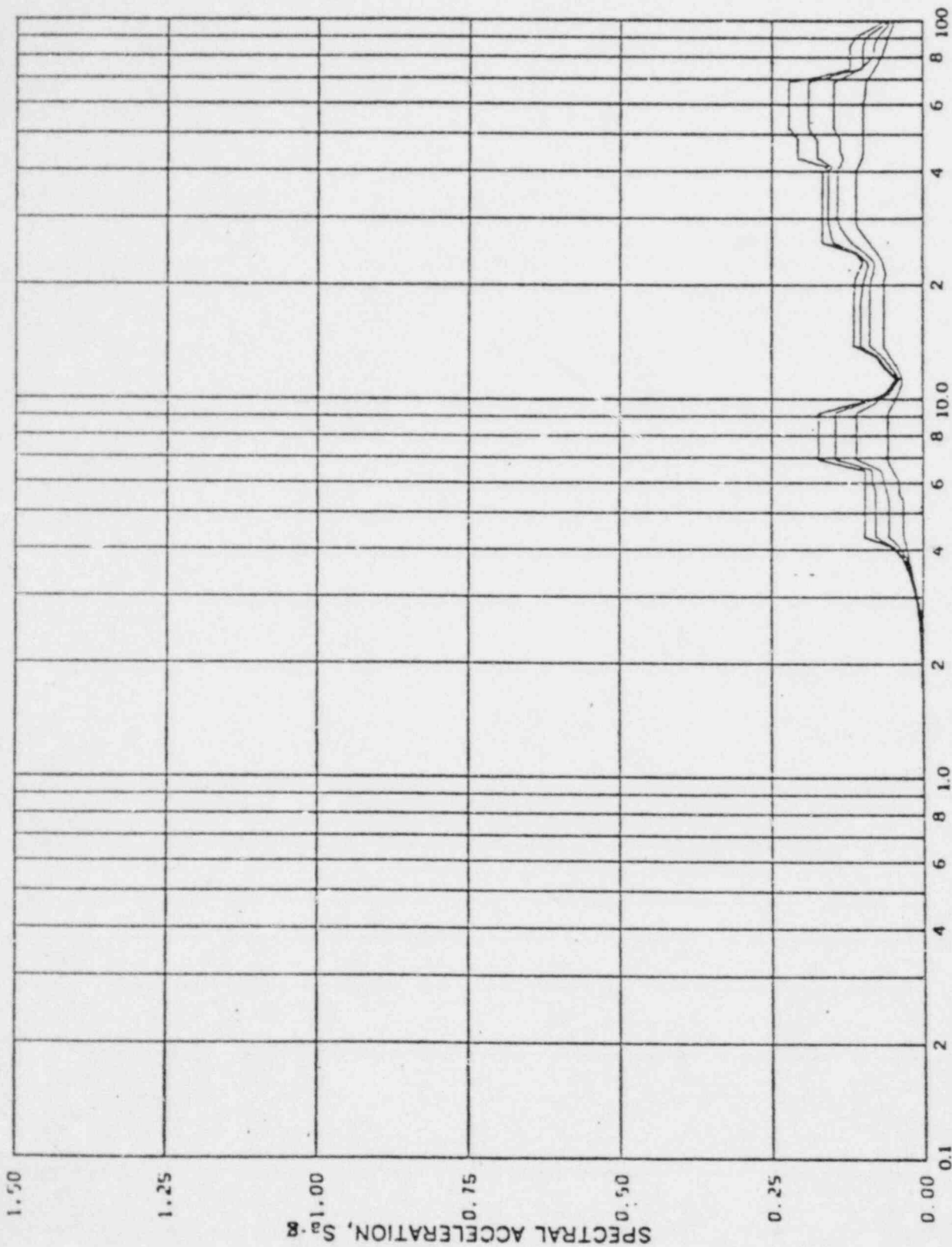
Damping: 0.005, 0.01, 0.02, 0.05 By: RL Date: 5-5-80 Check: KLW Date: 5/6/80

REV. 6, 4/82

**SUSQUEHANNA STEAM ELECTRIC STATION
UNITS 1 AND 2
DESIGN ASSESSMENT REPORT**

LGS CONTAINMENT RESPONSE
SPECTRA - KWU SRV #76
ASYMMETRIC - DIRECTION
HORIZONTAL

FIGURE 10-50



FREQUENCY - CPS

Limerick Generation Station, Acceleration Spectra for WETWELL

Load Case: SRV - ASYMMETRIC - TRACE 76

Node: 291 Direction: VERT Elev: 236'-2" Angle: 0°

Damping: 0.005, 0.01, 0.02, 0.05 By: PC Date: 5-5-80 Check: KW Date: 5/6/80

REV. 6, 4/82

**SUSQUEHANNA STEAM ELECTRIC STATION
UNITS 1 AND 2
DESIGN ASSESSMENT REPORT**

LGS CONTAINMENT RESPONSE
SPECTRA - KWU SRV #76
ASYMMETRIC - DIRECTION
VERTICAL

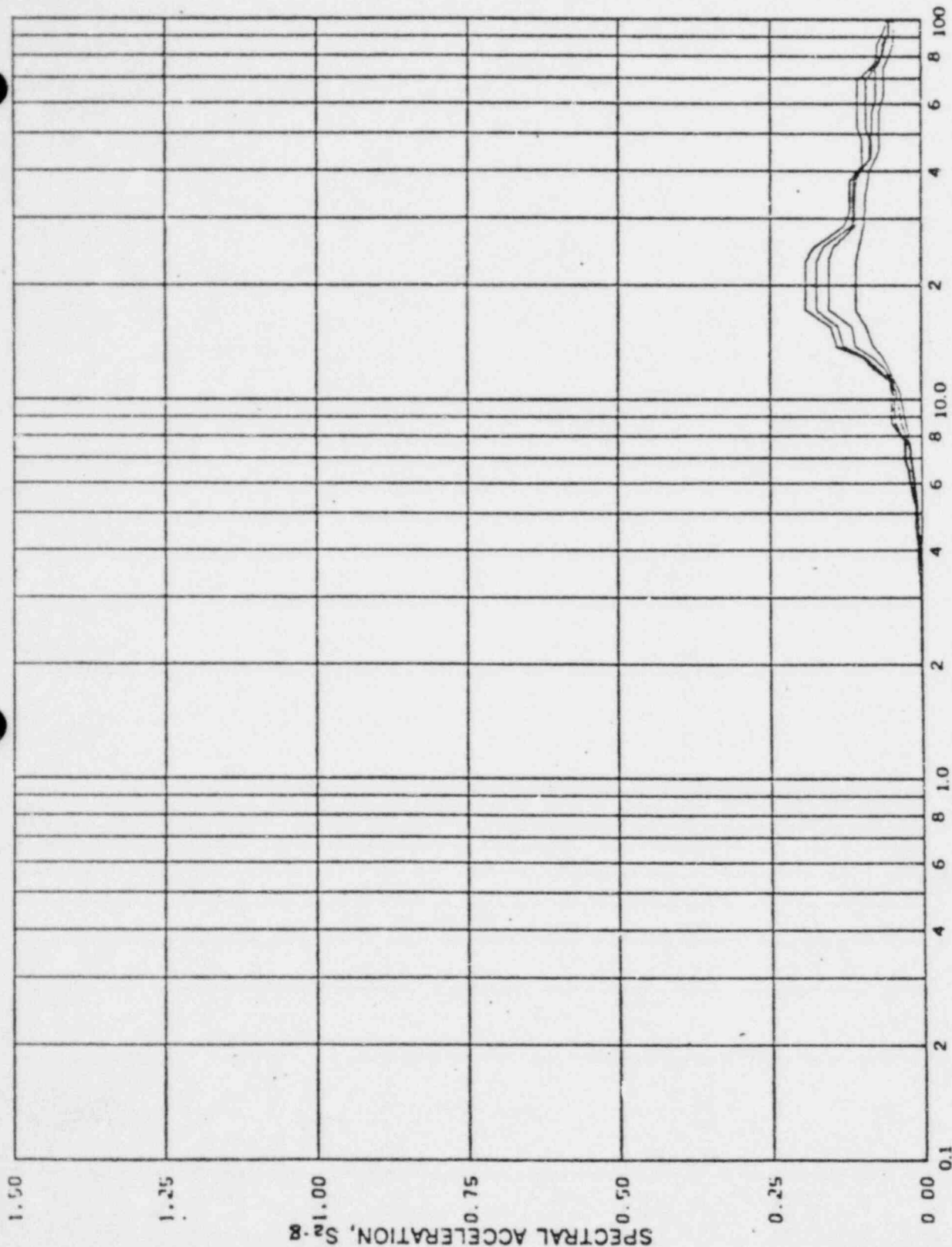
FIGURE 10-51



Limerick Generation Station, Acceleration Spectra for WETWELL
 Load Case: SRV - ASYMMETRIC - TRACE 76
 Node: 295 Direction: HORIZ Elev: 236'-2" Angle: 90°
 Damping: 0.005, 0.01, 0.02, 0.05 By: PC Date: 5-5-80 Check: WJL Date: 5/6/80

REV. 6, 4/82

SUSQUEHANNA STEAM ELECTRIC STATION UNITS 1 AND 2 DESIGN ASSESSMENT REPORT
LGS CONTAINMENT RESPONSE SPECTRA - KWU SRV #76 ASYMMETRIC - DIRECTION HORIZONTAL
FIGURE 10-52



FREQUENCY-CPS

Limerick Generation Station, Acceleration Spectra for WETWELL

Load Case: SRV - ASYMMETRIC - TRACE 76

Node: 295 Direction: VERT Elev: 236'-2" Angle: 90°

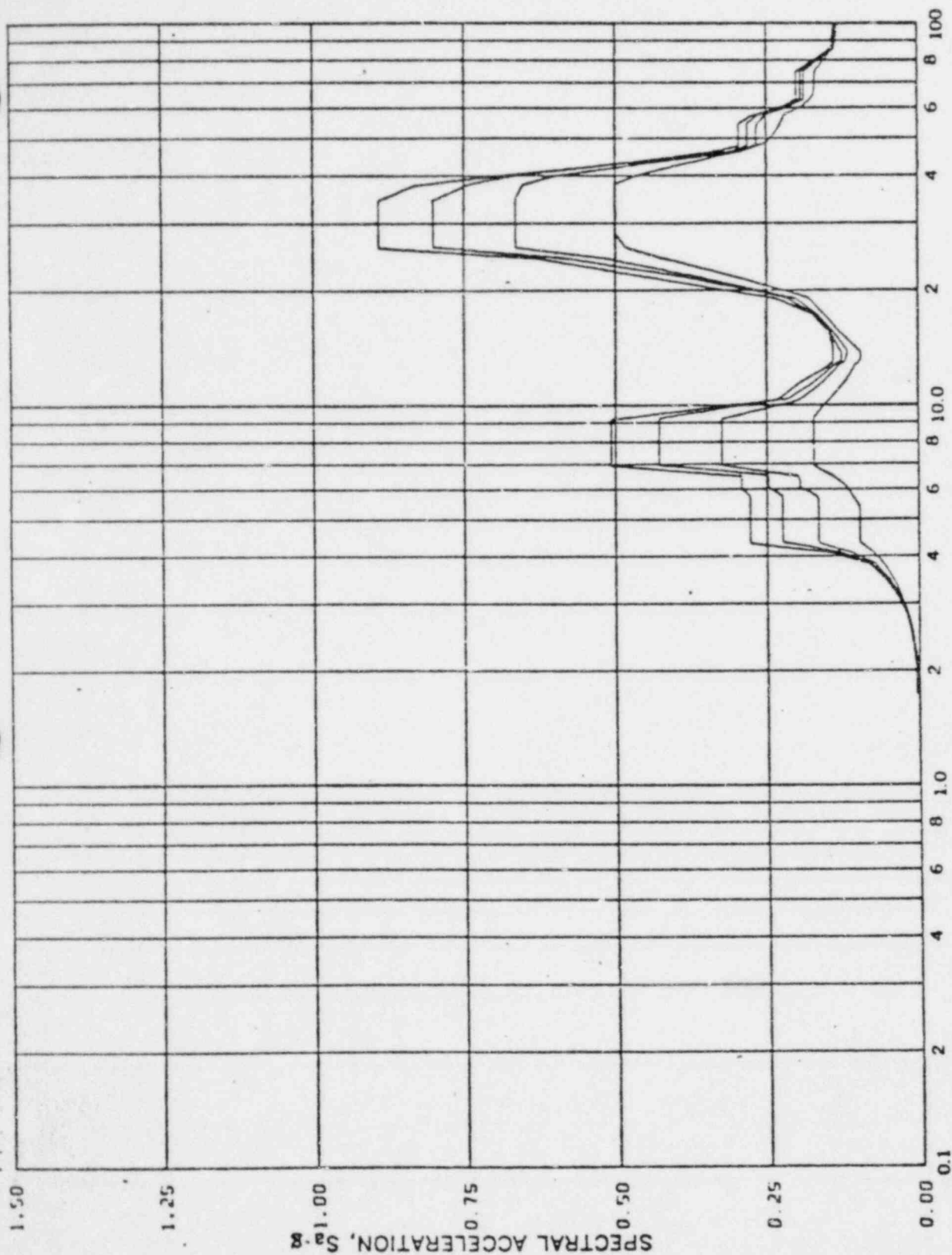
Damping: 0.005, 0.01, 0.02, 0.05 By: PC Date: 5-5-80 Check: WU Date: 5/6/80

REV. 6, 4/82

**SUSQUEHANNA STEAM ELECTRIC STATION
UNITS 1 AND 2
DESIGN ASSESSMENT REPORT**

LGS CONTAINMENT RESPONSE
SPECTRA - KWU SRV # 76
ASYMMETRIC - DIRECTION
VERTICAL

FIGURE 10-53

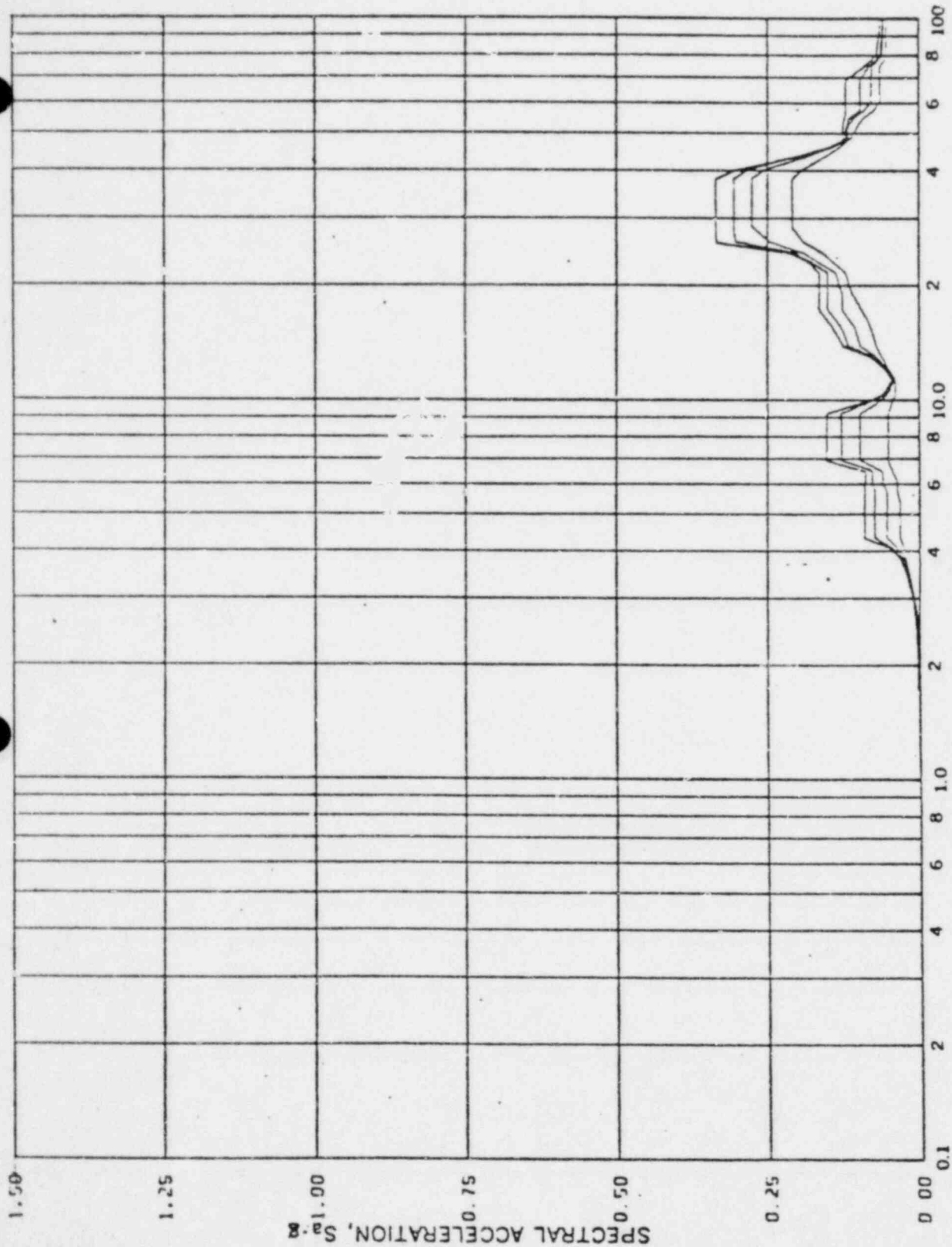


REV. 6, 4/82

**SUSQUEHANNA STEAM ELECTRIC STATION
UNITS 1 AND 2
DESIGN ASSESSMENT REPORT**

LGS CONTAINMENT RESPONSE
SPECTRA - KWU SRV # 76
ASYMMETRIC - DIRECTION
HORIZONTAL

FIGURE 10-54



FREQUENCY-CPS

Limerick Generation Station, Acceleration Spectra for DRYWELL

Load Case: SRV - ASYMMETRIC - TRACE 76

Node: 331 Direction: VERT Elev: 264'-6" Angle: 0°

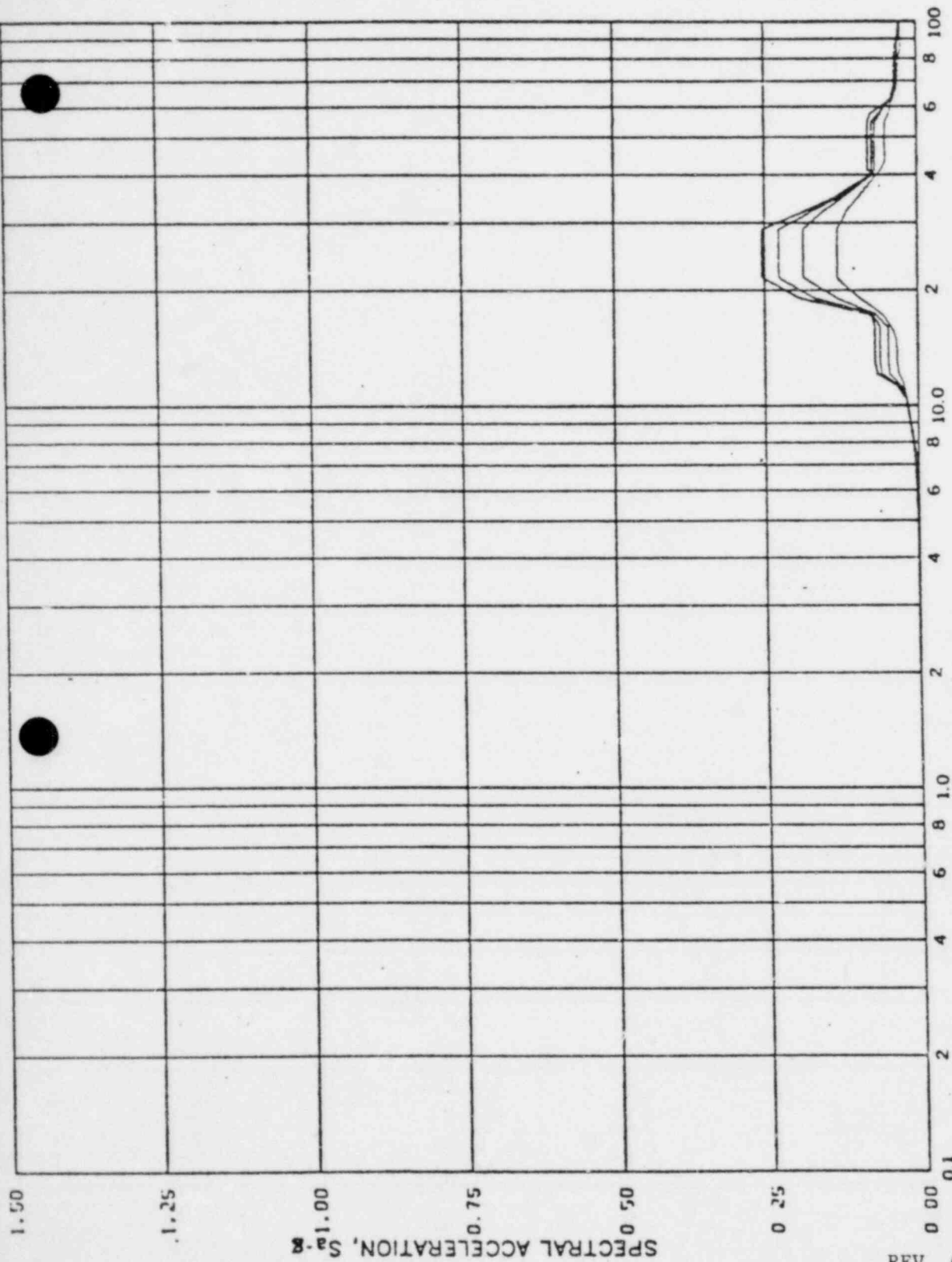
Damping: 0.005, 0.01, 0.02, 0.05 By: PL Date: 5-5-80 Check: KW Date: 5/6/80

REV. 6, 4/82

**SUSQUEHANNA STEAM ELECTRIC STATION
UNITS 1 AND 2
DESIGN ASSESSMENT REPORT**

LGS CONTAINMENT RESPONSE
SPECTRA - KWU SRV # 76
ASYMMETRIC - DIRECTION
VERTICAL

FIGURE 10-55



REV. 6, 4/82

**SUSQUEHANNA STEAM ELECTRIC STATION
UNITS 1 AND 2
DESIGN ASSESSMENT REPORT**

LGS CONTAINMENT RESPONSE
SPECTRA - KWU SRV # 76
ASYMMETRIC - DIRECTION
HORIZONTAL

FIGURE 10-56

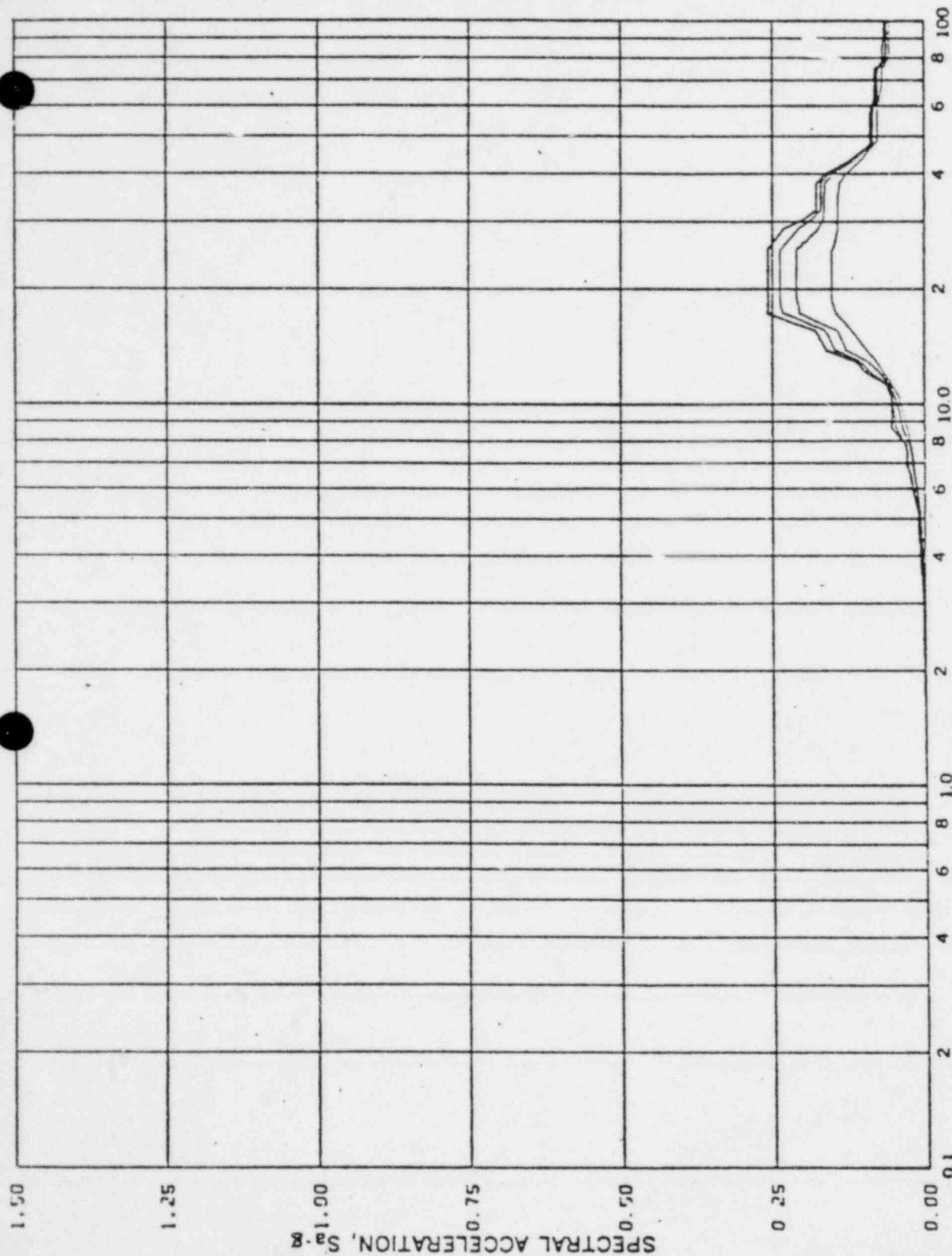
FREQUENCY-CPS

Limerick Generation Station, Acceleration Spectra for DRYWELL

Load Case: SRV - ASYMMETRIC - TRACE 76

Node: 335 Direction: HORIZ Elev: 264'-6" Angle: 90°

Damping: 0.005, 0.01, 0.02, 0.05 By: PL Date: 5-5-80 Check: KLW Date: 5/6/80



FREQUENCY-CPS

Limerick Generation Station, Acceleration Spectra for DRYWELL

Load Case: SRV - ASYMMETRIC - TRACE 76

Node: 335 Direction: VERT Elev: 264'-6" Angle: 90°

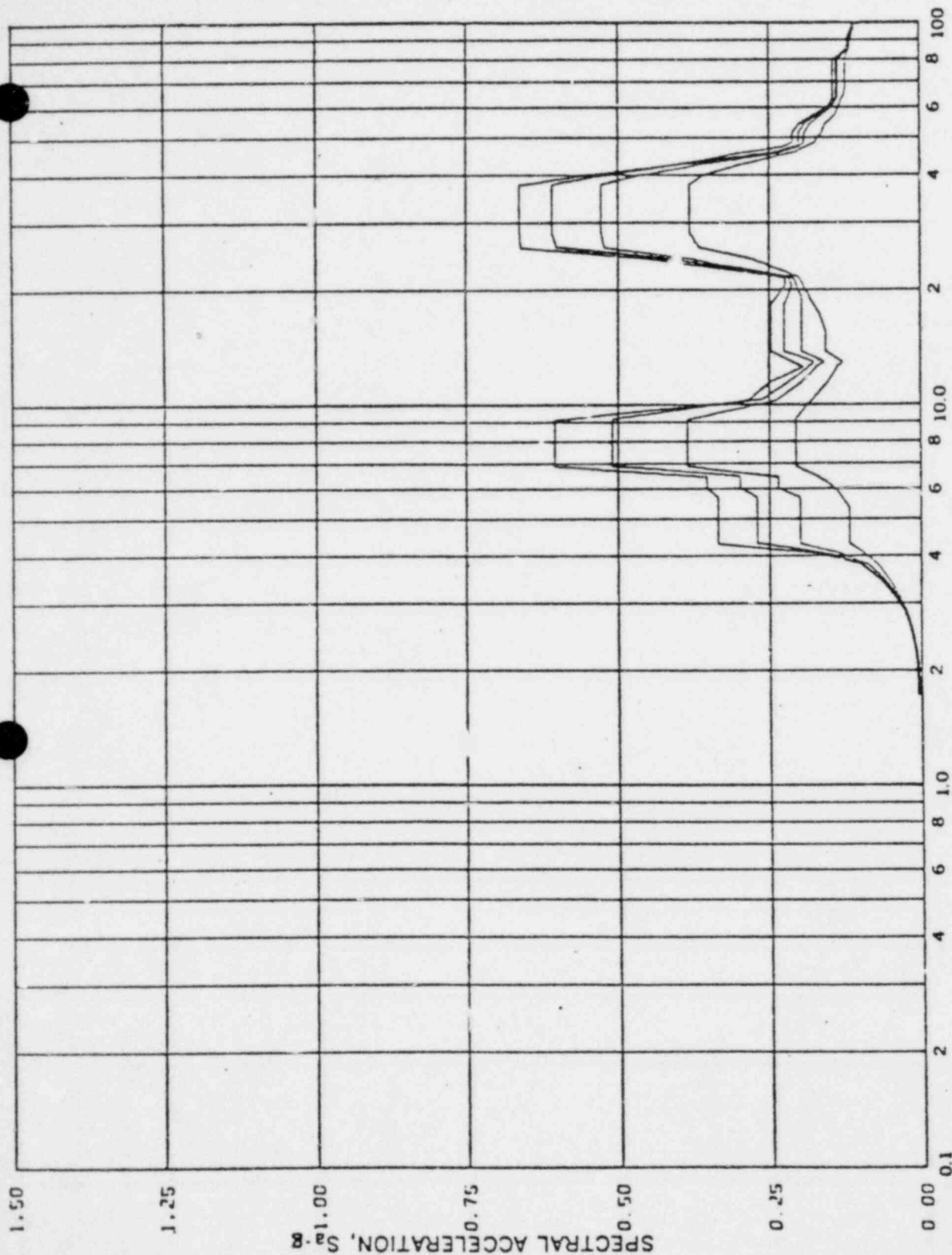
Damping: 0.005, 0.01, 0.02, 0.05 By: PC Date: 5-5-80 Check: VJW Date: 5/6/80

REV. 6, 4/82

**SUSQUEHANNA STEAM ELECTRIC STATION
UNITS 1 AND 2
DESIGN ASSESSMENT REPORT**

LGS CONTAINMENT RESPONSE
SPECTRA - KWU SRV # 76
ASYMMETRIC - DIRECTION
VERTICAL

FIGURE 10-57



FREQUENCY-CPS

Limerick Generation Station, Acceleration Spectra for DRYWELL

Load Case: SRV - ASYMMETRIC - TRACE 76

Node: 371 Direction: HORIZ Elev: 283'-11" Angle: 0°

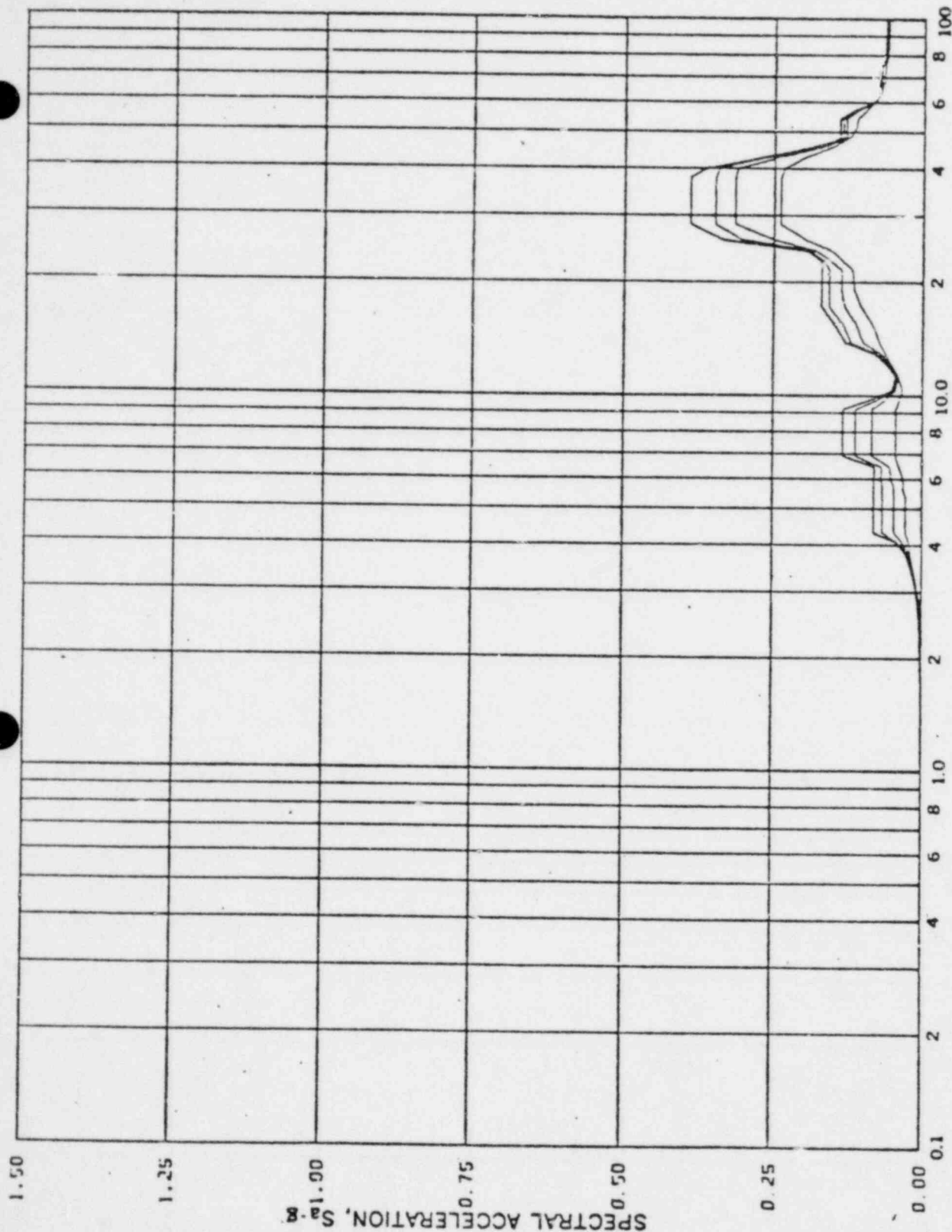
Damping: 0.005, 0.01, 0.02, 0.05 By: PC Date: 5-5-80 Check: Wm Date: 5/6/80

REV. 6, 4/82

**SUSQUEHANNA STEAM ELECTRIC STATION
UNITS 1 AND 2
DESIGN ASSESSMENT REPORT**

LGS CONTAINMENT RESPONSE
SPECTRA - KWU SRV # 76
ASYMMETRIC - DIRECTION
HORIZONTAL

FIGURE 10-58



FREQUENCY-CPS

Limerick Generation Station, Acceleration Spectra for DRYWELL

Load Case: SRV - ASYMMETRIC - TRACE 76

Node: 371 Direction: VERT Elev: 283'-11" Angle: 0°

Damping: 0.005, 0.01, 0.02, 0.05 By: fl Date: 5-5-80 Check: Kur Date: 5/6/80

REV. 6, 4/82

**SUSQUEHANNA STEAM ELECTRIC STATION
UNITS 1 AND 2
DESIGN ASSESSMENT REPORT**

LGS CONTAINMENT RESPONSE
SPECTRA - KWU SRV #76
ASYMMETRIC - DIRECTION
VERTICAL

FIGURE 10-59

SUSQUEHANNA STEAM ELECTRIC STATION

UNITS 1 AND 2

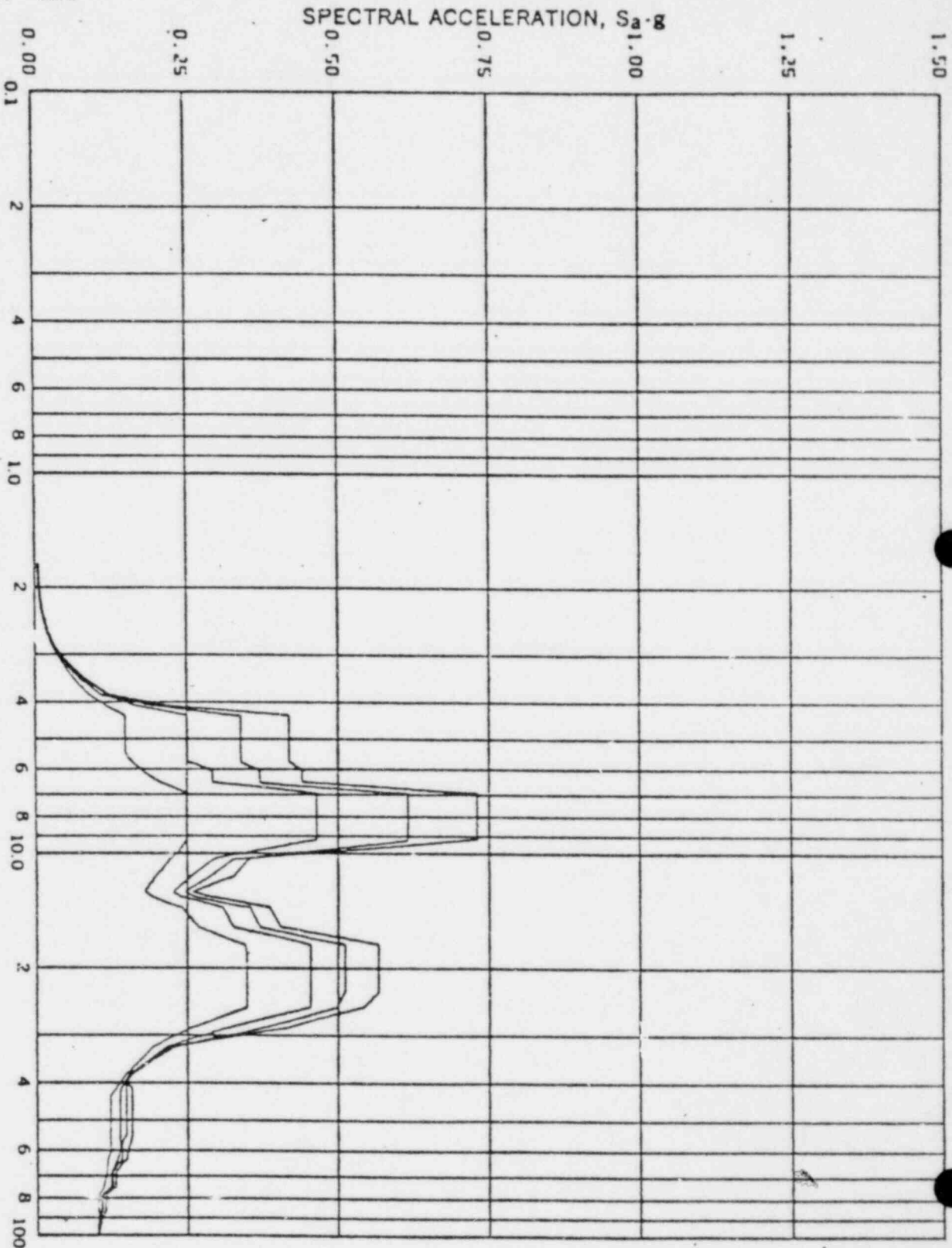
DESIGN ASSESSMENT REPORT

LGS CONTAINMENT RESPONSE
SPECTRA - KWU SRV # 76
ASYMMETRIC - DIRECTION
HORIZONTAL

10-60

FIGURE

REV. 6, 4/82



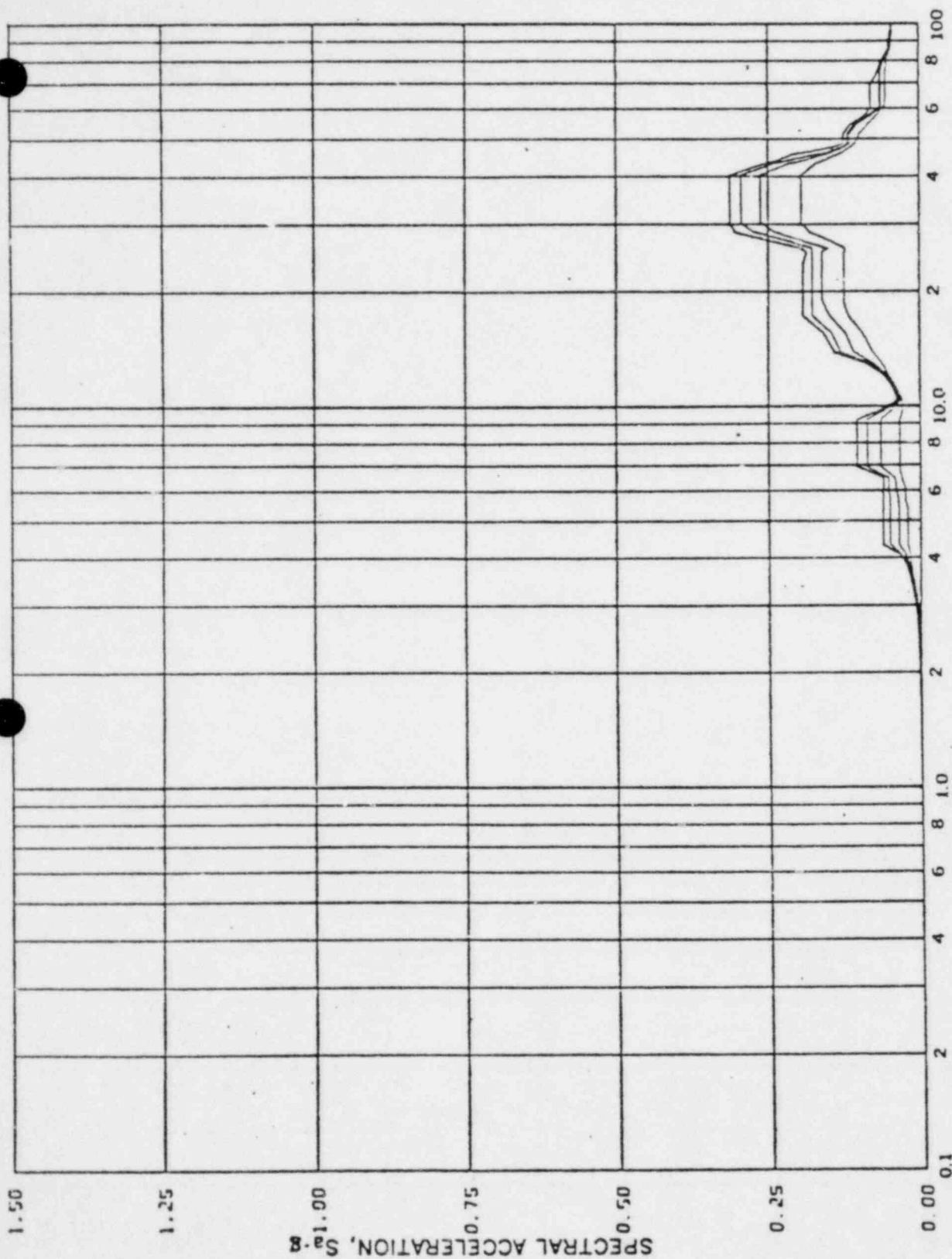
FREQUENCY-CPS

Limerick Generation Station, Acceleration Spectra for DRYWELL

Load Case: SRV - ASYMMETRIC - TRACE 76

Node: 411 Direction: HORIZ Elev: 312'-7" Angle: 0°

Damping: 0.005, 0.01, 0.02, 0.05 By: R Date: 5-5-80 Check: W Date: 5/4/80



FREQUENCY-CPS

Limerick Generation Station, Acceleration Spectra for DRYWELL

Load Case: SRV - ASYMMETRIC - TRACE 76

Node: 411 Direction: VERT Elev: 312'-7" Angle: 0°

Damping: 0.005, 0.01, 0.02, 0.05 By: PC Date: 5-5-80 Check: VW Date: 5/6/80

REV. 6, 4/82

SUSQUEHANNA STEAM ELECTRIC STATION UNITS 1 AND 2 DESIGN ASSESSMENT REPORT

LGS CONTAINMENT RESPONSE
SPECTRA - KWU SRV # 76
ASYMMETRIC - DIRECTION
VERTICAL

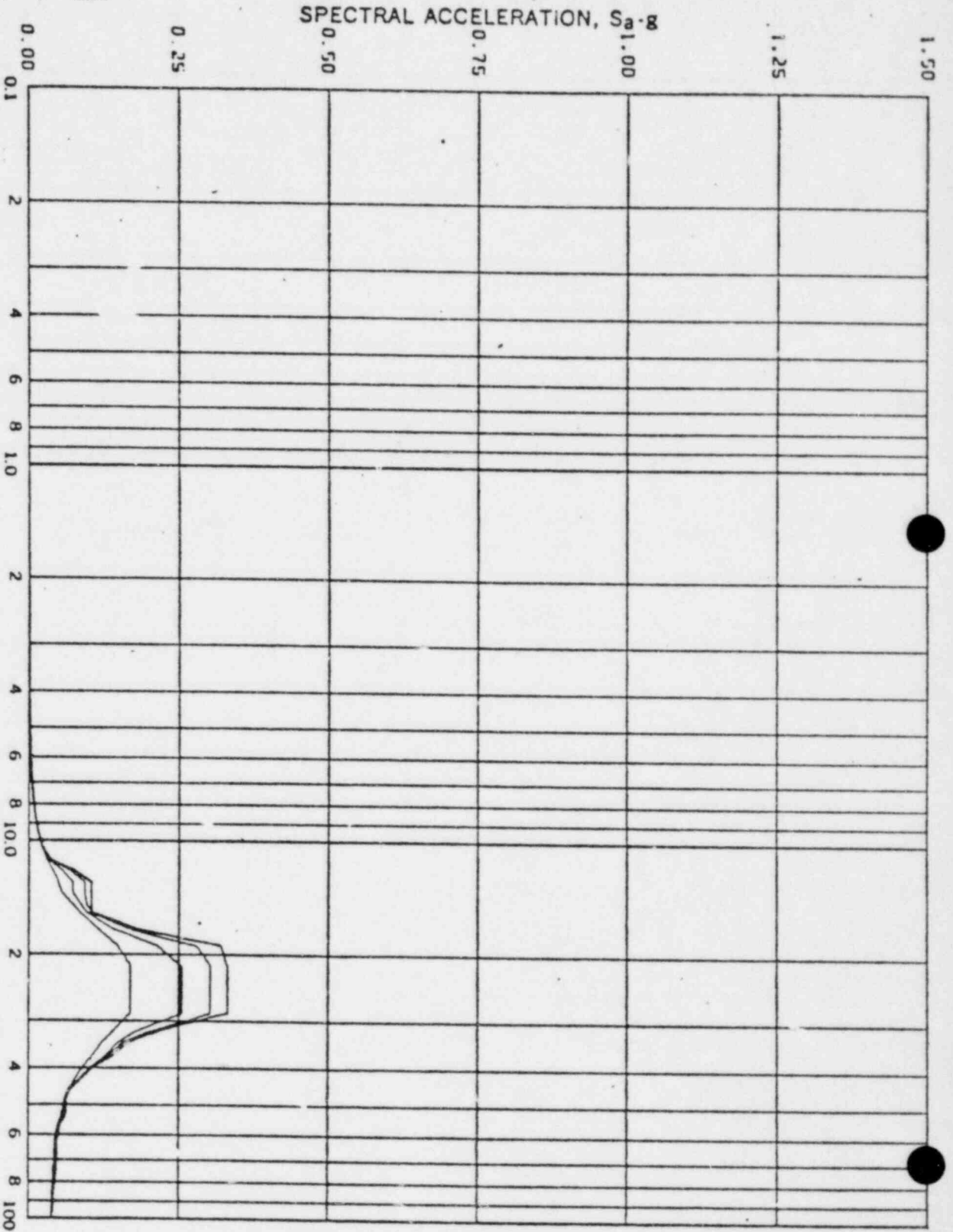
FIGURE 10-61

SUSQUEHANNA STEAM ELECTRIC STATION
UNITS 1 AND 2
DESIGN ASSESSMENT REPORT

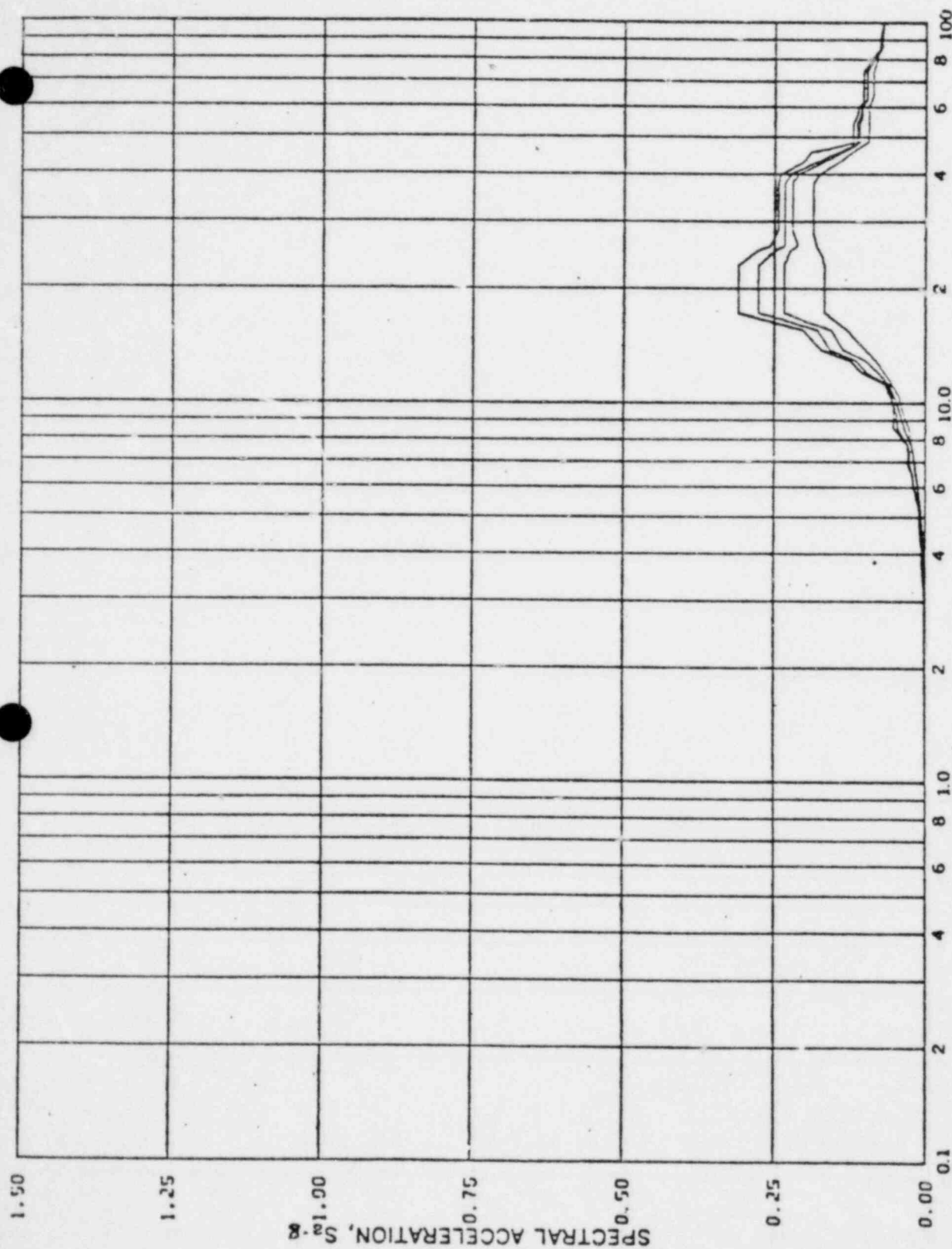
LGS CONTAINMENT RESPONSE
SPECTRA - KWU SRV # 76
ASYMMETRIC - DIRECTION
HORIZONTAL

FIGURE 10-62

REV. 6, 4/82



Limerick Generation Station, Acceleration Spectra for DRYWELL
Load Case: SRV - ASYMMETRIC - TRACE 76
Node: 415 Direction: HORIZ Elev: 312'-7" Angle: 90°
Damping: 0.005, 0.01, 0.02, 0.05 By: R Date: 5-5-80 Check: KW Date: 5/6/80



FREQUENCY-CPS

Limerick Generation Station, Acceleration Spectra for DRYWELL

Load Case: SRV - ASYMMETRIC - TRACE 76

Node: 415 Direction: VERT Elev: 312'-7" Angle: 90°

Damping: 0.005, 0.01, 0.02, 0.05 By: pc Date: 5-5-80 Check: blw Date: 5/6/80

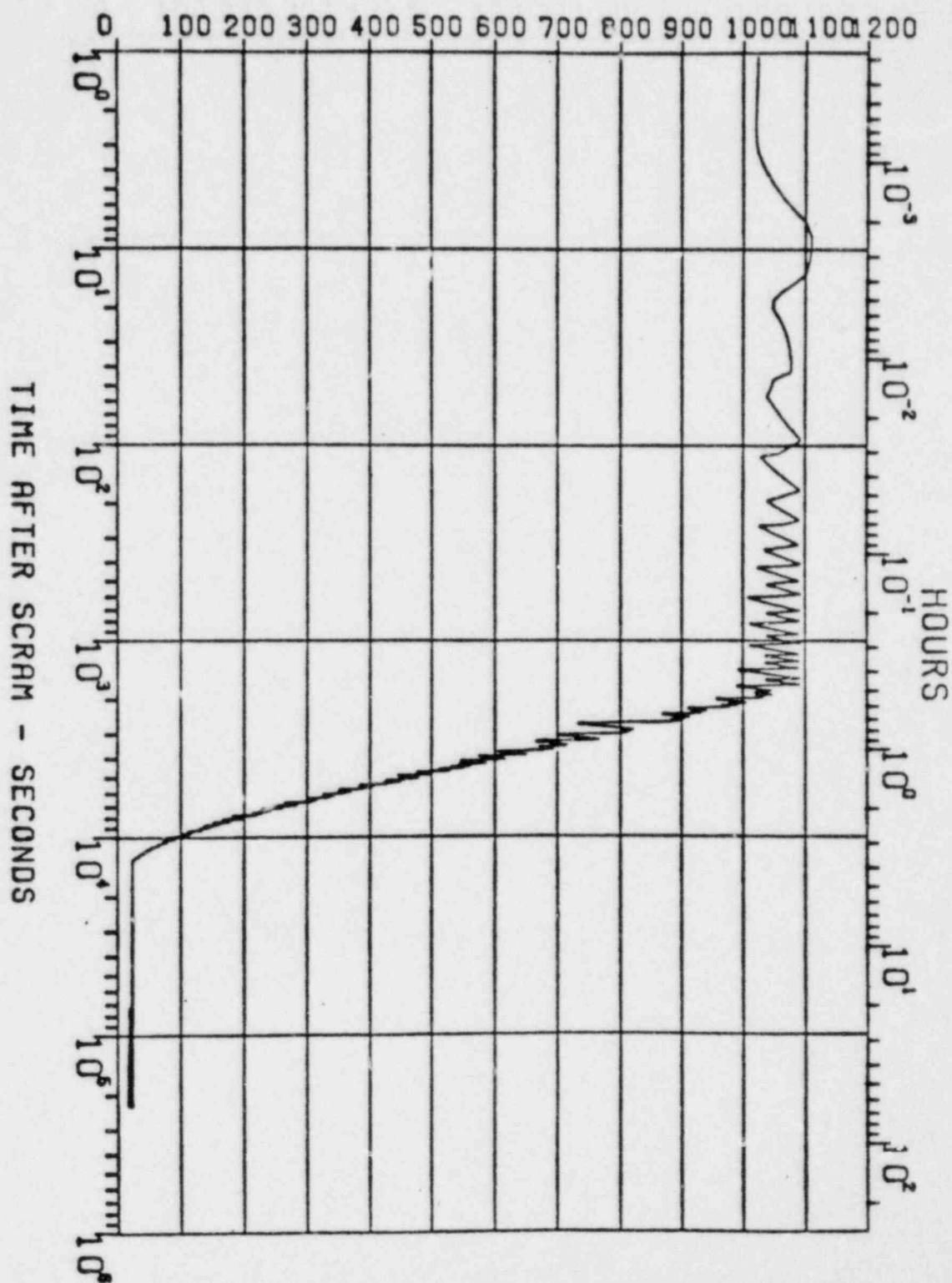
REV. 6, 4/82

**SUSQUEHANNA STEAM ELECTRIC STATION
UNITS 1 AND 2
DESIGN ASSESSMENT REPORT**

LGS CONTAINMENT RESPONSE
SPECTRA - KWU SRV # 76
ASYMMETRIC - DIRECTION
VERTICAL

FIGURE 10 - 63

REACTOR VESSEL PRESSURE PSIA

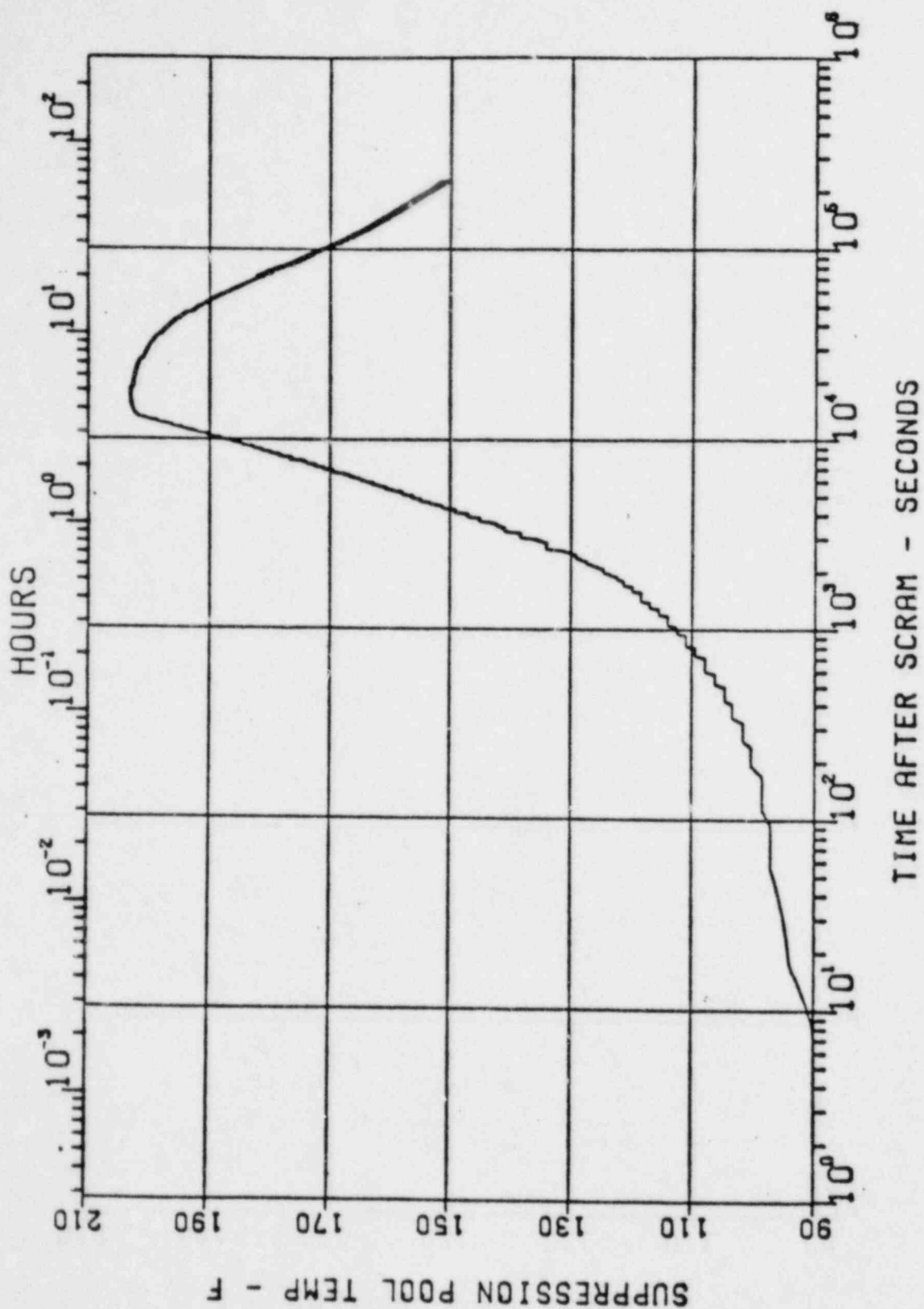


REV. 6, 4/82

SUSQUEHANNA STEAM ELECTRIC STATION
UNITS 1 AND 2
DESIGN ASSESSMENT REPORT

REACTOR PRESSURE
TRANSIENT - CASE 2.A
WITHOUT SHUTDOWN COOLING

FIGURE 10-64



REV. 6, 4/82

SUSQUEHANNA STEAM ELECTRIC STATION
UNITS 1 AND 2
DESIGN ASSESSMENT REPORT

REACTOR PRESSURE
TEMPERATURE TRANSIENT-CASE
2.A WITHOUT SHUTDOWN COOLING
FIGURE 10-65

TABLE 10-1
JAERI DATA

JAERI TEST	CLOG START TIME (sec)	NORMALIZED RMS VENT STATIC PRESSURE					VAR. σ^2
		VENT 1	VENT 2	VENT 3	VENT 4	VENT 5	
0002	58.65	-	0.88	-	1.13	0.99	.015
	62.37	-	0.87	-	1.38	0.75	.114
	66.35	-	1.17	-	1.03	0.81	.033
	72.65	-	0.99	-	1.29	0.72	.083
	74.65	-	0.72	-	1.29	0.98	.080
	76.75	-	0.85	-	1.06	1.09	.018
	78.80	-	0.85	-	1.09	1.06	.016
	80.25	-	0.90	-	1.03	1.07	.007
0003	82.27	-	1.10	-	1.01	0.89	.011
	84.10	-	0.83	-	1.07	1.10	.021
	85.98	-	0.61	-	1.36	1.04	.141
	87.85	-	1.16	-	1.13	0.71	.064
	89.90	-	0.64	-	1.05	1.31	.144
	91.45	-	0.54	-	1.50	0.97	.232
	96.85	-	1.12	-	1.01	0.83	.014
0004	39.50	-	0.95	-	1.44	0.61	.173
	40.65	-	0.86	-	1.34	0.79	.089
	43.00	-	0.47	-	1.77	0.76	.461
	45.20	-	0.41	-	1.35	1.23	.264
	49.00	-	0.44	-	1.75	0.81	.453
	53.05	-	0.68	-	1.29	1.03	.094
1101	40.40	0.81	0.86	-	1.36	0.97	.061
	42.02	0.91	0.78	-	1.21	1.10	.036
	44.20	1.34	0.68	-	1.01	0.96	.075
	46.25	0.77	0.49	-	1.24	1.50	.207
	48.80	0.89	0.54	-	1.42	1.14	.140
1201	47.60	0.86	1.00	-	1.15	1.00	.013
	49.40	1.11	1.35	-	0.72	0.82	.081
	51.20	1.08	0.93	-	1.23	0.75	.042
	53.00	1.31	0.65	-	1.15	0.90	.084
	54.90	1.22	0.60	-	1.27	0.91	.097
2101	35.80	1.14	0.84	0.84	0.90	1.28	.040
	39.75	1.13	1.17	0.89	0.99	0.82	.023
	42.00	1.07	0.67	0.98	0.89	1.40	.071
	43.85	0.89	1.07	1.23	1.22	0.60	.072
	46.10	2.08	0.56	0.29	1.20	0.88	.478
	48.15	0.87	0.82	1.10	1.30	0.90	.039
	100.10	0.96	0.71	0.93	1.18	1.21	.041

TABLE 10-2
JAERI/GKMIIM COMPARISON

DATA BASE	NORMALIZED MEAN VARIANCE
JAERI DATA	0.108
GKMIIM MSL DATA (0.5-13 Hz)	0.107
GKMIIM 1/3 MSL DATA (0.5-13 Hz)	0.083
GKMIIM 1/6 MSL DATA (0.5-13Hz)	0.064

55. "IEEE Recommended Practices for Seismic Qualification of Class 1E Equipment For Nuclear Power Generating Stations," IEEE Std. 344-1975.
56. A. J. James, "The General Electric Pressure Suppression Containment Analytical Model," GE, July 1971.
57. Letter MPN-080-79, L. J. Sobon (GE) to J. F. Stolz (NRC), Subject: Vent Clearing Pool Boundary Loads for Mark II Plants, 3/20/79.
58. P. W. Huber, A. A. Sonin, W. G. Anderson, "Considerations in Small-scale Modeling of Poolswell in BWR Containments," NUREG-CR-1143, July 1979, Contract No. NRC-04-77-011.
59. C. K. Chun, "Suppression Pool Dynamics," NUREG-0264, Contract No. AT (49-24)-0342.
60. R. L. Kiang and P. R. Jeuck, "A Study of Pool Swell Dynamics In a Mark II Single Cell Model," EPRI, Draft Report. 2
61. Conrath, R. and Hilbert, D., "Methoden der Mathematischen Physik I (Methods of Mathematical Physics I)," Springer-Verlag, Berlin, Heidelberg, New York, 1968.
62. Antony-Spies, P., "Theory of the Excitation of Eigenmodes of a Water-Filled Tank by a Collapsing Steam Bubble" (translated by Ad-Ex), Technical Report KWU/R14/77, September, 1977.
63. MARC-CDC, User Information Manual, Control Data Corporation, 1976.
64. Koch, E. and Sobottka, H., "KKP 1/KKI - Estimate of the Mitigating Values of the Dynamic Loads on the Pressure Suppression System During Air-Free Condensation at the Vent Pipes", Technical Report KWU/R113/3593, December 1975.
65. "Mark II Improved Chugging Methodology", NEDE-24822-P, General Electric Company, May 1980.
66. "Single and Multivent Chugging Final Report", NEDE-24300-P, General Electric Company, December 1980.
67. Mark II Owners Group, "Assumptions for use in Analyzing Mark II BWR Suppression Pool Temperature Transients Involving Safety/Relief Valve Discharge," Revision 1, December 1980. 5
68. Everstine, G. C., "A Nastran Implementation of the Doubly Asymptotic Approximation for Underwater Shock Response", Nastran Users's Experiences, NASA TMX 3428, pp 207-228, October 1976.

5

69. MacNeal, R. H., Citerley, R., and Chaigiu, M., "A New Method for Analyzing Fluid-Structure Interaction using M.S.C./Nastran", Trans. 5th Int. Conf. on Structural Mechanics in Reactor Technology, Paper B4/9, August 1979.

70. Mach II Generic Condensation Oscillation Load Definition Report, NEDE-24288-P, General Electric Company, November 1980.

71. C. W. Hirt, B. D. Nichols, N.C. Romero, "SOLA: A Numerical Solution Algorithm for Transient Fluid Flows," LA-5852, April 1975.

72. B. D. Nichols, C. W. Hirt, R. S. Hotchkiss, "SOLA-VOP: A Solution Algorithm for Transient Fluid Flow with Multiple Free Boundaries," LA-8355, August 1980.

73. C. W. Hirt, B. D. Nichols, L. R. Stein, "Multidimensional Analysis for Pressure Suppression Systems," LA-UR-79-1305, April 1979.

74. Zimmer Nuclear Power Station - Unit, Attachment 1., Amendment 99, Submittal of Revision 61 to the PSAR, September 28, 1979.

6

75. "ANSYS Engineering Analysis System Theoretical Manual," November 1, 1977 by Swanson Analysis Systems, Inc.

76. "ANSYS Engineering Analysis Systems Users Manual" August 1, 1978 by Swanson Analysis Systems, Inc.

77. A. Kalmins "Analysis of Shells of Revolution Subjected to Symmetrical and Non-Symmetrical Loads", Journal of Applied Mechanics, September 1964.

78. Abrahamson, G. R., and Hashemi, A., "SSES In-Plant Tests to Measure Submerged Structure Loads and Pool Frequencies," SRI Report to PP&L, April 1980.

79. "Mark II Containment Lead Plant Program Load Evaluation and Acceptance Criteria," NUREG-0487 Supplement No. 1, USNRC, September 1980.

80. General Electric report NEDO-24310, "Technical Bases for the Use of the Square Root of the Sum of the Squares (SRSS) Method of Combining Dynamic Loads for Mark II Plants," July 1977.

APPENDIX A

CONTAINMENT DESIGN ASSESSMENT

TABLE OF CONTENTS

A.1	CONTAINMENT STRUCTURAL DESIGN ASSESSMENT
A.2	CONTAINMENT SUBMERGED STRUCTURES DESIGN ASSESSMENT
A.3	FIGURES

APPENDIX A

FIGURES

<u>Number</u>	<u>Title</u>
A-1	Concrete and Reinforcement Stress Elements
A-2	Typical Section Showing Section Location
A-3	Reinforced Bar Arrangement
2 A-4 thru A-9	Containment Stresses and Margins - Equation 1
A-10 thru A-15	Containment Stresses and Margins - Equation 4 - Absolute Method
A-16 thru A-21	Containment Stresses and Margins - Equation 4A - Absolute Method
6 A-21.1 thru A-21.6	Containment Stresses and Margins - Equation 5 - Absolute Method
2 A-22 thru A-27	Containment Stresses and Margins - Equation 5A - Absolute Method
A-28 thru A-33	Containment Stresses and Margins - Equation 7A - Absolute Method
A-33.1	Stress Margins for Refueling Head and Support Skirt
A-34 thru A-39	Containment Stresses and Margins - Equation 4 - SRSS Method (Deleted)
6 A-40 thru A-45	Containment Stresses and Margins - Equation 4A - SRSS Method (Deleted)
A-46 thru A-51	Containment Stresses and Margins - Equation 5A - SRSS Method (Deleted)
A-52 thru A-57	Containment Stresses and Margins - Equation 7A - SRSS Method (Deleted)
A-58	Suppression Chamber Columns - Mode Shapes
2 A-59	Suppression Chamber Columns - Stress Summary
A-60	Downcomer Bracing System - Stress Summary
A-61	Downcomer Bracing System - Connections
6 A-62 & A-63	Downcomers - Mode Shapes - I (Deleted)
A-64 & A-65	Downcomers - Mode Shapes - II (Deleted)

APPENDIX A

FIGURES (Cont.)

<u>Number</u>	<u>Title</u>	
A-66	Downcomers - Stress Summary and Design Margins	2
A-67	SRV Support Assemblies - Stress Summary	6

APPENDIX A

Containment Design Assessment

2 | This appendix indicates the containment elements and cross-sections where stresses are determined and contains a tabulation of the predicted stresses, allowable stresses, and design margins for each loading combination considered. The structural assessment of the containment is covered in Section A.1; the submerged structures are assessed in Section A.2.

A.1 CONTAINMENT STRUCTURAL DESIGN ASSESSMENT

6 | Six load combinations, out of Table 5-1, are tabulated covering all the critical sections in the containment concrete structures. The emphasis is placed on the reinforcing bar stresses. Generally, load combination equation 7a appears to be the most critical for most of the elements. This load combination also includes the seismic loads. These seismic loads are obtained from the results of the flexible base seismic model described in Section 3.7b.2 of the PSAR.

2 | The tabulated stresses are shown for the critical load combinations by adding the dynamic loads by the absolute sum method. The concrete shield wall is not a part of the structural system and therefore values for the section 12 and 13 are not included in the following tables.

A.2 CONTAINMENT SUBMERGED STRUCTURES DESIGN ASSESSMENT

The stress summaries for the suppression chamber columns, the downcomer bracing, and the downcomers are covered in Figures A-59 through A-67. In addition, the mode shapes for the columns are shown on Figure A-58.

| 2
| 6

CECAP OUTPUT

LOAD COMBINATION EQN. 1 = 1.4D + 1.5 SRV (ASYM) - Absolute Sum

STRESSES IN KSI

DRYWELL WALL

SECTION NUMBER	EL. FT.	INSIDE FACE REBAR*		OUTSIDE FACE REBAR*				SHEAR TIES	PRINCIPAL CONC. STRESS
		VERT.	HOOP	VERT.	HOOP	SPIRAL 1	SPIRAL 2		
1	787	0.032	-0.083	-0.130	0.34	0.183	0.024	-0.360	
2	787	-0.072	-0.052	-0.121	0.078	0.017	-0.061	-0.172	
3	745	-0.270	-0.055	-0.421	0.113	-0.123	-0.185	-0.111	
4	724	-0.320	0.019	-0.470	0.130	-0.140	-0.202	-0.183	
5	710	-0.601	0.01	-0.512	0.942	0.251	0.178	-0.376	

* Allowable Reinforcing Steel Stress = 54 KSI

Minimum Stress Margin = 98%

REV. 6, 4/82

**SUSQUEHANNA STEAM ELECTRIC STATION
UNITS 1 AND 2
DESIGN ASSESSMENT REPORT**

**CONTAINMENT MARGINS
DRYWELL WALL**

FIGURE A-4

CECAP OUTPUT

LOAD COMBINATION EQN. 1 = 1.4D + 1.5 SRV (ASYM) - Absolute Sum

STRESSES IN KSI

WETWELL WALL

SECTION NUMBER	EL. FT.	INSIDE FACE REBAR*		OUTSIDE FACE REBAR*				SHEAR TIES	PRINCIPAL CONC. STRESS
		VERT.	HOOP	VERT.	HOOP	SPIRAL 1	SPIRAL 2		
6	695	-0.840	1.78	-0.375	2.00	0.953	0.671	-0.388	
7	672	-1.09	9.51	-0.725	5.44	2.39	2.32	-0.112	
8	672	-1.07	9.82	-0.767	5.74	3.42	1.55	-0.122	
9	672	-1.01	9.49	-0.737	5.45	2.39	2.33	-0.119	
10	660	-1.41	9.79	-0.514	6.39	3.11	2.77	-0.054	
11	650	-1.27	2.48	-0.70	2.71	1.43	0.584	0.096	

* Allowable Reinforcing Steel Stress = 54 KSI

Minimum Stress Margin = 81.8%

REV. 6, 4/82

SUSQUEHANNA STEAM ELECTRIC STATION
UNITS 1 AND 2
DESIGN ASSESSMENT REPORT

CONTAINMENT MARGINS
WETWELL WALL

FIGURE A-5

CECAP OUTPUT

LOAD COMBINATION EQN. 1 = 1.4D + 1.5 SRV (ASYM) - Absolute Sum

STRESSES IN XSI

RPV PEDESTAL

SECTION NUMBER	EL. FT.	INSIDE FACE REBAR*		OUTSIDE FACE REBAR*				SHEAR TIES	PRINCIPAL CONC. STRESS
		VERT.	HOOP	VERT.	HOOP	SPIRAL 1	SPIRAL 2		
14	725	-1.49	2.18	-2.08	2.82	-	-	0.358	
15	704	-0.33	1.97	-1.51	0.37	-	-	0.007	

* Allowable Reinforcing Steel Stress = 54 KSI

Minimum Stress Margin = 94.8%

REV. 6, 4/82

SUSQUEHANNA STEAM ELECTRIC STATION
UNITS 1 AND 2
DESIGN ASSESSMENT REPORT

CONTAINMENT MARGINS
RPV PEDESTAL

FIGURE A-6

CECAP OUTPUT

LOAD COMBINATION EQN. 1 = 1.4D + 1.5 SRV (ASYM) - Absolute Sum

STRESSES IN KSI

RPV PEDESTAL

SECTION NUMBER	EL. FT.	INSIDE FACE REBAR*		OUTSIDE FACE REBAR*				SHEAR TIES	PRINCIPAL CONC. STRESS
		VERT.	HOOP	VERT.	HOOP	SPIRAL 1	SPIRAL 2		
16	695	-0.808	1.04	- 1.28	0.796	-	-	-0.01	
17	666	-0.801	2.76	- 1.95	5.56	-	-	0.116	
18	666	-0.976	3.66	- 1.79	4.64	-	-	0.117	
19	651	-0.882	- .005	- 2.24	0.344	-	-	0.241	
20	651	-1.13	0.05	- 2.16	0.333	-	-	0.230	

* Allowable Reinforcing Steel Stress = 54 KSI

Minimum Stress Margin = 89.7%

REV. 6, 4/82

**SUSQUEHANNA STEAM ELECTRIC STATION
UNITS 1 AND 2
DESIGN ASSESSMENT REPORT**

**CONTAINMENT MARGINS
RPV PEDESTAL**

FIGURE A-7

CECAP OUTPUT

LOAD COMBINATION EQN. 1 = 1.4D + 1.5 SRV (ASYM) - Absolute Sum

STRESSES IN KSI

DIAPHRAGM SLAB

SECTION NUMBER	RADIUS FT.	EL. FT.	TOP FACE REBAR *		BOTTOM FACE REBAR*		SHEAR TIES
			RADIAL	TANGENTIAL	RADIAL	TANGENTIAL	
21	8	702	2.39	1.74	1.92	2.04	- .383
22	17	702	1.08	3.16	2.83	5.32	5.50
23	17	702	.833	2.68	3.05	4.54	6.68
24	26	702	2.11	3.64	3.85	6.53	- .133
25	34	702	4.40	4.07	3.39	5.32	- .189

* Allowable Reinforcing Steel Stress = 54 KSI

Minimum Stress Margin = 87.6%

REV. 6, 4/82

SUSQUEHANNA STEAM ELECTRIC STATION
UNITS 1 AND 2
DESIGN ASSESSMENT REPORT

CONTAINMENT MARGINS
DIAPHRAGM SLAB

FIGURE A-8

CECAP OUTPUT

LOAD COMBINATION EQN. 1 = $1.4D + 1.5 SRV$ (ASYM) - Absolute Sum

STRESSES IN KSI

BASE SLAB

SECTION NUMBER	RADIUS FT.	EL. FT.	TOP FACE REBAR *		BOTTOM FACE REBAR*		SHEAR TIES
			RADIAL	TANGENTIAL	RADIAL	TANGENTIAL	
26	8	644	*** - .234	** .143	1.11	1.57	-0.049
27	17	644	** 4.12	*** 5.54	6.64	7.27	5.39
28	26	644	** 10.94	*** 10.97	1.98	.362	.01
29	34	644	7.46	6.81	3.64	4.17	2.67
30	43	644	19.58	6.33	9.83	6.21	5.95

* Allowable Reinforcing Steel Stress = 54 KSI

** North - South Bars

*** East - West Bars

Minimum Stress Margin for this Load Combination = 63.7%

REV. 6, 4/82

SUSQUEHANNA STEAM ELECTRIC STATION
UNITS 1 AND 2
DESIGN ASSESSMENT REPORT

CONTAINMENT MARGINS
BASE SLAB

FIGURE A-9

CECAP OUTPUT

LOAD COMBINATION EQN. 4 - Absolute Sum

STRESSES IN KSI

DRYWELL WALL

SECTION NUMBER	EL. FT.	INSIDE FACE REBAR*		OUTSIDE FACE REBAR*				SHEAR TIES	PRINCIPAL CONC. STRESS **
		VERT.	HOOP	VERT.	HOOP	SPIRAL 1	SPIRAL 2		
1	787	4.14	-0.25	20.59	21.43	21.06	20.96	2.08	- 2.97
2	787	3.73	-0.16	20.18	21.09	20.80	20.47	1.85	- 2.95
3	745	4.12	7.66	28.54	29.41	29.06	28.88	2.18	- 2.52
4	724	2.54	4.41	36.17	30.28	33.26	33.18	3.20	- 2.17
5	710	8.87	4.24	14.72	21.11	18.10	17.73	7.93	- 2.14

* Allowable Reinforcing Steel Stress = 54 KSI

** Allowable Concrete Compressive Stress = -3.4 KSI

Minimum Stress Margin = 33%

REV. 6, 4/82

SUSQUEHANNA STEAM ELECTRIC STATION
UNITS 1 AND 2
DESIGN ASSESSMENT REPORT

CONTAINMENT MARGINS
DRYWELL WALL

FIGURE A-10

CECAP OUTPUT.

LOAD COMBINATION EQN. 4 - Absolute Sum

STRESSES IN KSI

WETWELL WALL

SECTION NUMBER	EL. FT.	INSIDE FACE REBAR*		OUTSIDE FACE REBAR*				SHEAR TIES	PRINCIPAL CONC. STRESS **
		VERT.	HOOP	VERT.	HOOP	SPIRAL 1	SPIRAL 2		
6	695	9.75	17.50	4.36	24.58	14.82	14.11	5.39	- 0.28
7	672	5.41	21.49	29.23	31.28	32.73	27.78	4.17	- 1.61
8	672	5.04	22.02	27.90	31.81	35.83	23.88	5.10	- 1.66
9	672	5.19	21.14	29.08	30.93	31.49	28.51	4.22	- 1.62
10	660	3.56	15.68	32.84	26.06	30.92	27.98	2.69	- 1.97
11	650	9.05	3.80	8.53	11.88	11.99	8.43	14.36	- 1.29

* Allowable Reinforcing Steel Stress = 54 KSI

** Allowable Concrete Compressive Stress = -3.4 KSI

Minimum Stress Margin = 33.6%

REV. 6, 4/82

SUSQUEHANNA STEAM ELECTRIC STATION
UNITS 1 AND 2
DESIGN ASSESSMENT REPORT

CONTAINMENT MARGINS
WETWELL WALL

FIGURE A-11

CECAP OUTPUT

LOAD COMBINATION EQN. 4 - Absolute Sum

STRESSES IN KSI

RPV PEDESTAL

SECTION NUMBER	EL. FT.	INSIDE FACE REBAR*		OUTSIDE FACE REBAR*				SHEAR TIES	PRINCIPAL CONC. STRESS **
		VERT.	HOOP	VERT.	HOOP	SPIRAL 1	SPIRAL 2		
14	725	-1.50	-1.06	-0.21	4.27	-	-	0.46	- 0.25
15	704	1.22	-0.48	0.31	-3.19	-	-	5.91	- 0.48

* Allowable Reinforcing Steel Stress = 54 KSI

** Allowable Concrete Compressive Stress = -3.4 KSI

Minimum Stress Margin = 89%

REV. 6, 4/82

SUSQUEHANNA STEAM ELECTRIC STATION
UNITS 1 AND 2
DESIGN ASSESSMENT REPORT

CONTAINMENT MARGINS
RPV PEDESTAL

FIGURE A-12

CECAP OUTPUT

LOAD COMBINATION EQN. 4 - Absolute Sum

STRESSES IN KSI

RPV PEDESTAL

SECTION NUMBER	EL. FT.	INSIDE FACE REBAR*		OUTSIDE FACE REBAR*				SHEAR TIES	PRINCIPAL CONC. STRESS **
		VERT.	HOOP	VERT.	HOOP	SPIRAL 1	SPIRAL 2		
16	695	-0.78	10.04	-1.07	9.49	-	-	1.65	- 0.16
17	666	-0.97	15.93	-0.66	6.02	-	-	5.89	- 0.22
18	666	-0.89	17.16	-0.98	2.14	-	-	0.23	- 0.16
19	651	-0.49	-1.65	-0.56	-2.08	-	-	0.62	- 0.30
20	651	-0.42	-1.67	-0.75	-2.04	-	-	0.64	- 0.31

* Allowable Reinforcing Steel Stress = 54 KSI

** Allowable Concrete Compressive Stress = -3.4 KSI

Minimum Stress Margin = 68.2%

REV. 6, 4/82

SUSQUEHANNA STEAM ELECTRIC STATION
UNITS 1 AND 2
DESIGN ASSESSMENT REPORT

CONTAINMENT MARGINS
RPV PEDESTAL

FIGURE A-13

CECAP OUTPUT

LOAD COMBINATION EQN. 4 - Absolute Sum

STRESSES IN KSI

DIAPHRAGM SLAB

SECTION NUMBER	RADIUS FT.	EL. FT.	TOP FACE REBAR *		BOTTOM FACE REBAR*		SHEAR TIES	PRINCIPAL CONC. STRESS **
			RADIAL	TANGENTIAL	RADIAL	TANGENTIAL		
21	8	702	2.50	3.66	8.49	8.39	4.95	- 0.20
22	17	702	0.25	0.80	13.54	19.19	2.02	- 1.02
23	17	702	1.09	1.83	11.92	15.76	2.29	- 0.58
24	26	702	2.82	3.32	18.21	22.38	1.55	- 0.36
25	34	702	9.96	8.00	16.19	17.92	1.61	- 0.14

* Allowable Reinforcing Steel Stress = 54 KSI

** Allowable Concrete Compressive Stress = -3.4 KSI

Minimum Stress Margin = 58.5%

REV. 6, 4/82

SUSQUEHANNA STEAM ELECTRIC STATION
UNITS 1 AND 2
DESIGN ASSESSMENT REPORT

CONTAINMENT MARGINS
DIAPHRAGM SLAB

FIGURE A-14

CECAP OUTPUT

LOAD COMBINATION EQN. 4 - Absolute Sum

STRESSES IN KSI

BASE SLAB

SECTION NUMBER	RADIUS FT.	EL. FT.	TOP FACE REBAR *		BOTTOM FACE REBAR*		SHEAR TIES	PRINCIPAL CONC. STRESS \$
			RADIAL	TANGENTIAL	RADIAL	TANGENTIAL		
26	8	644	*** - 0.11	** - 4.00	9.81	12.04	37.66	- 2.09
27	17	644	* - 8.76	*** - 8.83	19.26	18.45	0.19	- 3.85†
28	26	644	** - 5.82	*** - 5.90	18.44	15.40	1.29	- 2.60
29	34	644	- 0.75	- 4.03	13.94	21.73	2.92	- 2.14
30	43	644	12.45	- 1.51	23.23	15.79	1.21	- 1.27

* Allowable Reinforcing Steel Stress = 54 KSI

** North - South Bars

*** East - West Bars

\$ Allowable Concrete Compressive Stress = -3.4 KSI

† Maximum Concrete Strain = -0.00083

Minimum Stress Margin = 30.2%

REV. 6, 4/82

3USQUEHANNA STEAM ELECTRIC STATION
UNITS 1 AND 2
DESIGN ASSESSMENT REPORT

CONTAINMENT MARGINS
BASE SLAB

FIGURE A-15

CECAP OUTPUT

LOAD COMBINATION EQN. 4A - Absolute Sum

STRESSES IN KSI

DRYWELL WALL

SECTION NUMBER	EL. FT.	INSIDE FACE REBAR*		OUTSIDE FACE REBAR*				SHEAR TIES	PRINCIPAL CONC. STRESS **
		VERT.	HOOP	VERT.	HOOP	SPIRAL 1	SPIRAL 2		
1	787	3.74	1.25	19.52	21.95	20.76	20.71	2.09	- 2.61
2	787	3.93	2.19	17.34	20.53	18.99	18.88	2.36	- 2.39
3	745	2.93	9.91	23.45	29.28	26.48	26.25	2.20	- 2.31
4	724	3.55	11.98	26.53	28.68	27.61	27.61	2.31	- 2.22
5	710	7.36	5.67	2.87	22.15	12.62	12.40	3.60	- 1.76

* Allowable Reinforcing Steel Stress = 54 KSI

** Allowable Concrete Compressive Stress = -3.4 KSI

Minimum Stress Margin = 45.7%

REV. 6, 4/82

SUSQUEHANNA STEAM ELECTRIC STATION
UNITS 1 AND 2
DESIGN ASSESSMENT REPORT

CONTAINMENT MARGINS
DRYWELL WALL

FIGURE A-16

CECAP OUTPUT

LOAD COMBINATION EQN. 4A - Absolute Sum

STRESSES IN KSI

WETWELL WALL

SECTION NUMBER	EL. FT.	INSIDE FACE REBAR*		OUTSIDE FACE REBAR*				SHEAR TIES	PRINCIPAL CONC. STRESS **
		VERT.	HOOP	VERT.	HOOP	SPIRAL 1	SPIRAL 2		
6	695	2.79	15.29	8.32	23.38	16.50	15.19	2.93	- 1.23
7	672	0.18	21.23	21.61	33.87	28.84	26.63	2.84	- 2.05
8	672	-0.20	18.84	18.44	31.95	29.64	20.75	2.15	- 2.00
9	672	-0.05	17.19	19.03	30.06	25.05	24.03	1.94	- 2.02
10	660	-0.66	16.62	25.74	28.99	28.83	25.91	2.33	- 2.39
11	650	3.30	2.85	4.74	12.08	10.25	6.57	10.88	- 1.60

* Allowable Reinforcing Steel Stress = 54 KSI

** Allowable Concrete Compressive Stress = -3.4 KSI

Minimum Stress Margin = 37.2%

REV. 6, 4/82

SUSQUEHANNA STEAM ELECTRIC STATION
UNITS 1 AND 2
DESIGN ASSESSMENT REPORT

CONTAINMENT MARGINS
WETWELL WALL

FIGURE A-17

CECAP OUTPUT

LOAD COMBINATION EQN. 4A - Absolute Sum

STRESSES IN KSI

RPV PEDESTAL

SECTION NUMBER	EL. FT.	INSIDE FACE REBAR*		OUTSIDE FACE REBAR*				SHEAR TIES	PRINCIPAL CONC. STRESS **
		VERT.	HOOP	VERT.	HOOP	SPIRAL 1	SPIRAL 2		
14	725	-2.33	-0.54	-1.43	4.12	-	-	0.62	- 0.34
15	704	-2.24	-0.31	-1.25	-2.35	-	-	0.89	- 0.37

* Allowable Reinforcing Steel Stress = 54 KSI

** Allowable Concrete Compressive Stress = -3.4 KSI

Minimum Stress Margin = 92.3%

REV. 6, 4/82

SUSQUEHANNA STEAM ELECTRIC STATION
UNITS 1 AND 2
DESIGN ASSESSMENT REPORT

CONTAINMENT MARGINS
RPV PEDESTAL

FIGURE A-18

CECAP OUTPUT—

LOAD COMBINATION EQN. 4A - Absolute Sum

STRESSES IN KSI

RPV PEDESTAL

SECTION NUMBER	EL. FT.	INSIDE FACE REBAR*		OUTSIDE FACE REBAR*				SHEAR TIES	PRINCIPAL CONC. STRESS **
		VERT.	HOOP	VERT.	HOOP	SPIRAL 1	SPIRAL 2		
16	695	-2.14	2.43	-3.32	2.39	-	-	0.75	- 0.45
17	666	-2.94	14.24	-3.18	5.36	-	-	7.22	- 0.45
18	666	-2.49	13.93	-3.29	2.47	-	-	4.57	- 0.50
19	651	-2.46	-0.78	-3.30	-1.51	-	-	1.06	- 0.51
20	651	-2.40	-0.84	-3.63	-1.45	-	-	1.10	- 0.56

* Allowable Reinforcing Steel Stress = 54 KSI

** Allowable Concrete Compressive Stress = -3.4 KSI

Minimum Stress Margin = 73.6%

REV. 6, 4/82

SUSQUEHANNA STEAM ELECTRIC STATION
UNITS 1 AND 2
DESIGN ASSESSMENT REPORT

CONTAINMENT MARGINS
RPV PEDESTAL

FIGURE A-19

CECAP OUTPUT

LOAD COMBINATION EQN. 4A - Absolute Sum

STRESSES IN KSI

DIAPHRAGM SLAB

SECTION NUMBER	RADIUS FT.	EL. FT.	TOP FACE REBAR *		BOTTOM FACE REBAR*		SHEAR TIES	PRINCIPAL CONC. STRESS **
			RADIAL	TANGENTIAL	RADIAL	TANGENTIAL		
21	8	702	5.47	5.44	9.96	9.57	5.63	- 0.17
22	17	702	1.21	3.33	14.79	20.83	2.76	- 0.84
23	17	702	3.07	4.77	12.42	16.86	4.38	- 0.51
24	26	702	2.45	6.87	25.15	28.50	1.42	- 0.51
25	34	702	12.43	10.04	21.36	23.12	3.81	- 0.16

* Allowable Reinforcing Steel Stress = 54 KSI

** Allowable Concrete Compressive Stress = -3.4 KSI

Minimum Stress Margin = 47.2%

REV. 6, 4/82

SUSQUEHANNA STEAM ELECTRIC STATION
UNITS 1 AND 2
DESIGN ASSESSMENT REPORT

CONTAINMENT MARGINS
DIAPHRAGM SLAB

FIGURE A-20

CECAP OUTPUT

LOAD COMBINATION EQN. 4A - Absolute Sum

STRESSES IN KSI

BASE SLAB

SECTION NUMBER	RADIUS FT.	EL. FT.	TOP FACE REBAR *		BOTTOM FACE REBAR*		SHEAR TIES	PRINCIPAL CONC. STRESS \$
			RADIAL	TANGENTIAL	RADIAL	TANGENTIAL		
26	8	644	*** 11.51	** 0.78	14.23	13.93	44.77	- 1.36
27	17	644	** - 7.82	*** - 8.99	16.73	18.51	0.39	- 3.66†
28	26	644	** - 6.31	*** - 6.39	17.92	13.65	1.22	- 2.73
29	34	644	- 2.51	- 6.23	13.67	20.49	2.27	- 2.53
30	43	644	18.06	- 3.39	25.87	17.12	3.53	- 1.61

* Allowable Reinforcing Steel Stress = 54 KSI

** North - South Bars

*** East - West Bars

\$ Allowable Concrete Compressive Stress = -3.4 KSI

† Maximum Concrete Strain = -0.00078

Minimum Stress Margin = 17.0%

REV. 6, 4/82

SUSQUEHANNA STEAM ELECTRIC STATION
UNITS 1 AND 2
DESIGN ASSESSMENT REPORT

CONTAINMENT MARGINS
BASE SLAB

FIGURE A-21

CECAP OUTPUT

LOAD COMBINATION EQN. 5 - Absolute Sum

STRESSES IN KSI

DRYWELL WALL

SECTION NUMBER	EL. FT.	INSIDE FACE REBAR*		OUTSIDE FACE REBAR*				SHEAR TIES	PRINCIPAL CONC. STRESS **
		VERT.	HOOP	VERT.	HOOP	SPIRAL 1	SPIRAL 2		
1	787	3.39	-0.66	19.84	20.84	22.62	18.06	2.07	- 3.04
2	787	3.39	-0.57	19.85	20.42	22.24	18.03	2.14	- 3.01
3	745	5.01	7.12	27.59	26.00	33.77	19.82	2.19	- 2.35
4	724	6.74	9.03	33.90	26.23	39.46	20.67	2.28	- 2.20
5	710	9.58	4.15	20.30	19.02	26.57	12.76	9.38	- 2.12

* Allowable Reinforcing Steel Stress = 54 KSI

** Allowable Concrete Compressive Stress = -3.4 KSI

Minimum Stress Margin = 26.9%

REV. 6, 4/82

SUSQUEHANNA STEAM ELECTRIC STATION
UNITS 1 AND 2
DESIGN ASSESSMENT REPORT

CONTAINMENT MARGINS
DRYWELL WALL

FIGURE A-21.1

CECAP OUTPUT

LOAD COMBINATION EQN. 5 - Absolute Sum

STRESSES IN KSI

WETWELL WALL

SECTION NUMBER	EL. FT.	INSIDE FACE REBAR*		OUTSIDE FACE REBAR*				SHEAR TIES	PRINCIPAL CONC. STRESS **
		VERT.	HOOP	VERT.	HOOP	SPIRAL 1	SPIRAL 2		
6	695	9.13	17.44	16.74	21.13	31.31	6.55	7.12	- 0.84
7	672	8.12	19.00	30.87	28.79	42.39	17.28	4.99	- 1.50
8	672	7.85	18.28	28.79	28.06	47.26	9.59	5.11	- 1.53
9	672	11.05	21.44	24.21	28.06	39.59	12.69	8.94	- 1.17
10	660	6.31	15.45	34.44	25.26	42.39	17.32	2.28	- 1.63
11	650	12.08	3.58	13.77	11.82	23.17	2.41	16.28	- 1.42

* Allowable Reinforcing Steel Stress = 54 KSI

** Allowable Concrete Compressive Stress = -3.4 KSI

Minimum Stress Margin = 12.5%

REV. 6, 4/82

SUSQUEHANNA STEAM ELECTRIC STATION
UNITS 1 AND 2
DESIGN ASSESSMENT REPORT

CONTAINMENT ASSESSMENT
WETWELL WALL

FIGURE A-21.2

CECAP OUTPUT

LOAD COMBINATION EQN. 5 - Absolute Sum

STRESSES IN KSI

RPV PEDESTAL

SECTION NUMBER	EL. FT.	INSIDE FACE REBAR*		OUTSIDE FACE REBAR*				SHEAR TIES	PRINCIPAL CONC. STRESS **
		VERT.	HOOP	VERT.	HOOP	SPIRAL 1	SPIRAL 2		
14	725	-0.20	-2.70	2.43	10.24	-	-	1.10	- 0.51
15	704	10.55	-0.24	8.61	-3.16	-	-	14.34	- 0.50

* Allowable Reinforcing Steel Stress = 54 KSI

** Allowable Concrete Compressive Stress = -3.4 KSI

Minimum Stress Margin = 81.0%

REV. 6, 4/82

SUSQUEHANNA STEAM ELECTRIC STATION
UNITS 1 AND 2
DESIGN ASSESSMENT REPORT

CONTAINMENT MARGINS
RPV PEDESTAL

FIGURE A-21.3

CECAP OUTPUT

LOAD COMBINATION EQN. 5 - Absolute Sum

STRESSES IN KSI

RPV PEDESTAL

SECTION NUMBER	EL. FT.	INSIDE FACE REBAR*		OUTSIDE FACE REBAR*				SHEAR TIES	PRINCIPAL CONC. STRESS **
		VERT.	HOOP	VERT.	HOOP	SPIRAL 1	SPIRAL 2		
16	695	1.28	10.22	0.80	9.72	-	-	3.36	- 0.09
17	666	-0.36	15.90	-0.13	4.56	-	-	3.29	- 0.23
18	666	-0.27	16.55	-0.29	4.41	-	-	3.32	- 0.24
19	651	0.22	-1.60	0.08	-2.04	-	-	1.31	- 0.29
20	651	0.72	-1.68	0.23	-2.09	-	-	2.45	- 0.31

* Allowable Reinforcing Steel Stress = 54 KSI

** Allowable Concrete Compressive Stress = -3.4 KSI

Minimum Stress Margin = 69.3%

REV. 6, 4/82

SUSQUEHANNA STEAM ELECTRIC STATION
UNITS 1 AND 2
DESIGN ASSESSMENT REPORT

CONTAINMENT MARGINS
RPV PEDESTAL

FIGURE A-21.4

CECAP OUTPUT

LOAD COMBINATION EQN. 5 - Absolute Sum

STRESSES IN KSI

DIAPHRAGM SLAB

SECTION NUMBER	RADIUS FT.	EL. FT.	TOP FACE REBAR *		BOTTOM FACE REBAR*		SHEAR TIES	PRINCIPAL CONC. STRESS \$
			RADIAL	TANGENTIAL	RADIAL	TANGENTIAL		
21	8	702	0.76	2.96	11.72	8.52	3.74	- 0.41
22	17	702	- 0.50	0.63	17.48	20.61	2.23	- 1.33
23	17	702	- 0.27	0.98	16.41	19.25	2.04	- 1.15
24	26	702	0.85	1.60	24.52	26.77	1.77	- 1.15
25	34	702	2.05	1.15	26.94	21.41	1.48	- 0.99

* Allowable Reinforcing Steel Stress = 54 KSI

\$ Allowable Concrete Compressive Stress = -3.4 KSI

Minimum Stress Margin = 50.1%

REV. 6, 4/82

SUSQUEHANNA STEAM ELECTRIC STATION
UNITS 1 AND 2
DESIGN ASSESSMENT REPORT

CONTAINMENT MARGINS
DIAPHRAGM SLAB

FIGURE A-21.5

CECAP OUTPUT

LOAD COMBINATION EQN. 5 - Absolute Sum

STRESSES IN KSI

BASE SLAB

SECTION NUMBER	RADIUS FT.	EL. FT.	TOP FACE REBAR *		BOTTOM FACE REBAR*		SHEAR TIES	PRINCIPAL CONC. STRESS \$
			RADIAL	TANGENTIAL	RADIAL	TANGENTIAL		
26	8	644	*** - 0.75	** - 4.08	9.16	8.63	34.03	- 2.02
27	17	644	** - 9.25	*** - 9.26	20.47	18.34	0.19	- 3.98†
28	26	644	** - 5.75	*** - 5.76	20.59	17.94	1.32	- 2.65
29	34	644	- 0.64	- 4.66	12.97	20.58	3.35	- 2.21
30	43	644	12.47	- 2.53	22.24	16.08	1.21	- 1.42

* Allowable Reinforcing Steel Stress = 54 KSI

** North - South Bars

*** East - West Bars

\$ Allowable Concrete Compressive Stress = -3.4 KSI

† Maximum Concrete Strain = -0.00086

Minimum Stress Margin = 37%

REV. 6, 4/82

SUSQUEHANNA STEAM ELECTRIC STATION
UNITS 1 AND 2
DESIGN ASSESSMENT REPORT

CONTAINMENT MARGINS
BASE SLAB

FIGURE A-21.6

CECAP OUTPUT

LOAD COMBINATION EQN. 5A - Absolute Sum

STRESSES IN KSI

DRYWELL WALL

SECTION NUMBER	EL. FT.	INSIDE FACE REBAR*		OUTSIDE FACE REBAR*				SHEAR TIES	PRINCIPAL CONC. STRESS **
		VERT.	HOOP	VERT.	HOOP	SPIRAL 1	SPIRAL 2		
1	787	3.11	0.41	18.88	21.49	22.67	17.70	2.07	- 2.75
2	787	3.56	1.14	16.97	20.26	20.98	16.25	2.23	- 2.56
3	745	1.73	8.70	21.46	27.90	31.50	17.86	2.11	- 2.48
4	724	4.77	11.32	29.52	28.69	38.08	20.14	2.31	- 2.15
5	710	7.13	4.81	14.27	19.72	24.04	9.96	7.36	- 1.96

* Allowable Reinforcing Steel Stress = 54 KSI

** Allowable Concrete Compressive Stress = -3.4 KSI

Minimum Stress Margin = 29.4%

REV. 6, 4/82

SUQUEHANNA STEAM ELECTRIC STATION
UNITS 1 AND 2
DESIGN ASSESSMENT REPORT

CONTAINMENT MARGINS
DRYWELL WALL

FIGURE A-22

CECAP OUTPUT

LOAD COMBINATION EQN. 5A - Absolute Sum

STRESSES IN KSI

WETWELL WALL

SECTION NUMBER	EL. FT.	INSIDE FACE REBAR*		OUTSIDE FACE REBAR*				SHEAR TIES	PRINCIPAL CONC. STRESS **
		VERT.	HOOP	VERT.	HOOP	SPIRAL 1	SPIRAL 2		
6	695	2.54	22.66	12.44	28.25	31.50	9.20	3.0	- 1.45
7	672	0.31	26.65	21.82	36.85	41.67	16.99	3.49	- 2.08
8	672	0.23	23.70	19.30	32.98	43.50	8.79	2.64	- 1.98
9	672	0.10	23.86	19.16	33.18	39.05	13.29	2.36	- 1.97
10	660	-0.45	24.14	26.22	34.37	44.77	15.82	2.91	- 2.29
11	650	3.44	6.68	6.85	16.95	21.71	2.09	11.97	- 1.55

* Allowable Reinforcing Steel Stress = 54 KSI

** Allowable Concrete Compressive Stress = -3.4 KSI

Minimum Stress Margin = 17.0%

REV. 6, 4/82

SUSQUEHANNA STEAM ELECTRIC STATION
UNITS 1 AND 2
DESIGN ASSESSMENT REPORT

CONTAINMENT MARGINS
WETWELL WALL

FIGURE A-23

CECAP OUTPUT

LOAD COMBINATION EQN. 5A - Absolute Sum

STRESSES IN KSI

RPV PEDESTAL

SECTION NUMBER	EL. FT.	INSIDE FACE REBAR*		OUTSIDE FACE REBAR*				SHEAR TIES	PRINCIPAL CONC. STRESS **
		VERT.	HOOP	VERT.	HOOP	SPIRAL 1	SPIRAL 2		
14	725	-1.61	-0.65	-0.65	5.31	-	-	0.95	- 0.26
15	704	-0.93	-0.58	0.15	-2.64	-	-	3.00	- 0.38

* Allowable Reinforcing Steel Stress = 54 KSI

** Allowable Concrete Compressive Stress = -3.4 KSI

Minimum Stress Margins = 90.1%

REV. 6, 4/82

SUSQUEHANNA STEAM ELECTRIC STATION
UNITS 1 AND 2
DESIGN ASSESSMENT REPORT

CONTAINMENT MARGINS
RPV PEDESTAL

FIGURE A-24

CECAP OUTPUT

LOAD COMBINATION EQN. 5A - Absolute Sum

STRESSES IN KSI

RPV PEDESTAL

SECTION NUMBER	EL. FT.	INSIDE FACE REBAR*		OUTSIDE FACE REBAR*				SHEAR TIES	PRINCIPAL CONC. STRESS **
		VERT.	HOOP	VERT.	HOOP	SPIRAL 1	SPIRAL 2		
16	695	-1.42	2.74	-2.49	2.85	-	-	0.65	- 0.34
17	666	-2.24	14.84	-2.17	5.96	-	-	6.57	- 0.32
18	666	-2.00	13.60	-2.52	2.43	-	-	4.05	- 0.39
19	651	-1.66	-0.88	-2.30	-1.64	-	-	0.84	- 0.38
20	651	-1.59	-0.94	-2.66	1.58	-	-	0.88	- 0.44

* Allowable Reinforcing Steel Stress = 54 KSI

** Allowable Concrete Compressive Stress = -3.4 KSI

Minimum Stress Margin = 72.5%

REV. 6, 4/82

SUSQUEHANNA STEAM ELECTRIC STATION
UNITS 1 AND 2
DESIGN ASSESSMENT REPORT

CONTAINMENT MARGINS
RPV PEDESTAL

FIGURE A-25

CECAP OUTPUT

LOAD COMBINATION EQN. 5A - Absolute Sum

STRESSES IN KSI

DIAPHRAGM SLAB

SECTION NUMBER	RADIUS FT.	EL. FT.	TOP FACE REBAR *		BOTTOM FACE REBAR*		SHEAR TIES	PRINCIPAL CONC. STRESS **
			RADIAL	TANGENTIAL	RADIAL	TANGENTIAL		
21	8	702	2.46	4.47	12.16	9.07	2.90	- 0.18
22	17	702	- 0.45	2.41	18.27	20.77	2.04	- 1.21
23	17	702	0.10	2.65	17.62	20.57	1.93	- 1.08
24	26	702	- 0.51	6.89	33.51	27.12	1.30	- 1.33
25	34	702	2.29	2.65	32.04	25.41	1.41	- 1.06

* Allowable Reinforcing Steel Stress = 54 KSI

** Allowable Concrete Compressive Stress = -3.4 KSI

Minimum Stress Margin = 37.9%

REV. 6, 4/82

SUSQUEHANNA STEAM ELECTRIC STATION
UNITS 1 AND 2
DESIGN ASSESSMENT REPORT

CONTAINMENT MARGINS
DIAPHRAGM SLAB

FIGURE A-26

CECAP OUTPUT

LOAD COMBINATION EQN. 5A - Absolute Sum

STRESSES IN KSI

BASE SLAB

SECTION NUMBER	RADIUS FT.	EL. FT.	TOP FACE REBAR *		BOTTOM FACE REBAR*		SHEAR TIES	PRINCIPAL CONC. STRESS \$
			RADIAL	TANGENTIAL	RADIAL	TANGENTIAL		
26	8	644	*** - 6.31	** - 8.00	19.12	18.62	33.80	- 3.08
27	17	644	** - 8.34	*** - 8.29	17.43	18.34	0.21	- 3.70†
28	26	644	** - 5.84	*** - 6.49	19.28	15.59	1.27	- 2.74
29	34	644	- 2.62	- 5.76	14.10	20.50	2.43	- 2.49
30	43	644	18.05	- 3.06	27.51	15.17	5.42	- 1.61

* Allowable Reinforcing Steel Stress = 54 KSI

** North - South Bars

*** East - West Bars

\$ Allowable Concrete Compressive Stress = -3.4 KSI

† Maximum Concrete Strain = -0.00078

Minimum Stress Margin = 37.4%

REV. 6, 4/82

SUSQUEHANNA STEAM ELECTRIC STATION
UNITS 1 AND 2
DESIGN ASSESSMENT REPORT

CONTAINMENT MARGINS
BASE SLAB

FIGURE A-27

CECAP OUTPUT

LOAD COMBINATION EQN. 7A - Absolute Sum

STRESSES IN KSI

DRYWELL WALL

SECTION NUMBER	EL. FT.	INSIDE FACE REBAR*		OUTSIDE FACE REBAR*				SHEAR TIES	PRINCIPAL CONC. STRESS **
		VERT.	HOOP	VERT.	HOOP	SPIRAL 1	SPIRAL 2		
1	787	4.19	1.66	16.13	16.86	18.63	14.35	2.00	- 2.34
2	787	3.86	1.46	17.29	17.05	19.50	14.83	1.98	- 2.40
3	745	3.56	6.70	26.4	28.54	35.71	19.23	2.19	- 2.43
4	724	5.08	9.55	30.20	27.72	40.58	17.33	2.28	- 2.19
5	710	6.86	4.73	16.45	19.09	26.94	8.60	7.74	- 1.99

* Allowable Reinforcing Steel Stress = 54 KSI

** Allowable Concrete Compressive Stress = -3.4 KSI

Minimum Stress Margin = 24.8%

REV. 6, 4/82

SUSQUEHANNA STEAM ELECTRIC STATION
UNITS 1 AND 2
DESIGN ASSESSMENT REPORT

CONTAINMENT MARGINS
DRYWELL WALL

FIGURE A-28

CECAP OUTPUT

LOAD COMBINATION EQN. 7A - Absolute Sum

STRESSES IN KSI

WETWELL WALL

SECTION NUMBER	EL. FT.	INSIDE FACE REBAR*		OUTSIDE FACE REBAR*				SHEAR TIES	PRINCIPAL CONC. STRESS **
		VERT.	HOOP	VERT.	HOOP	SPIRAL 1	SPIRAL 2		
6	695	4.79	15.13	16.45	22.43	34.95	3.93	4.09	- 1.26
7	672	3.62	18.05	25.25	29.38	42.84	11.79	3.51	- 2.88
8	672	3.04	15.65	22.60	27.01	43.18	6.44	2.25	- 1.76
9	672	3.09	14.81	23.38	26.21	39.03	10.55	2.14	- 1.78
10	660	2.39	14.88	32.18	27.20	47.24	12.14	2.59	- 2.18
11	650	6.33	2.14	11.48	13.65	23.33	1.79	14.03	- 2.42

* Allowable Reinforcing Steel Stress = 54 KSI

** Allowable Concrete Compressive Stress = -3.4 KSI

Minimum Stress Margin = 12.5%

REV. 6, 4/82

SUSQUEHANNA STEAM ELECTRIC STATION
UNITS 1 AND 2
DESIGN ASSESSMENT REPORT

CONTAINMENT MARGINS
WETWELL WALL

FIGURE A-29

CECAP OUTPUT

LOAD COMBINATION EQN. 7A - Absolute Sum

STRESSES IN KSI

RPV PEDESTAL

SECTION NUMBER	EL. FT.	INSIDE FACE REBAR*		OUTSIDE FACE REBAR*				SHEAR TIES	PRINCIPAL CONC. STRESS **
		VERT.	HOOP	VERT.	HOOP	SPIRAL 1	SPIRAL 2		
14	725	-1.37	-0.28	-0.20	5.63	-	-	1.44	- 0.24
15	704	-0.81	-0.83	0.32	-2.84	-	-	0.88	- 0.41

* Allowable Reinforcing Steel Stress = 54 KSI

** Allowable Concrete Compressive Stress = -3.4 KSI

Minimum Stress Margin = 89.5%

REV. 6, 4/82

SUSQUEHANNA STEAM ELECTRIC STATION
UNITS 1 AND 2
DESIGN ASSESSMENT REPORT

CONTAINMENT MARGINS
RPV PEDESTAL

FIGURE A-30

CECAP OUTPUT

LOAD COMBINATION EQN. 7A - Absolute Sum

STRESSES IN KSI

RPV PEDESTAL

SECTION NUMBER	EL. FT.	INSIDE FACE REBAR*		OUTSIDE FACE REBAR*				SHEAR TIES	PRINCIPAL CONC. STRESS **
		VERT.	HOOP	VERT.	HOOP	SPIRAL 1	SPIRAL 2		
16	695	-0.86	2.69	-1.87	2.80	-	-	0.57	- 0.61
17	666	-1.94	14.77	-1.92	5.72	-	-	6.76	- 0.72
18	666	-1.69	13.79	-2.21	2.32	-	-	4.10	- 0.35
19	651	-1.13	-0.95	-2.16	-1.65	-	-	0.76	- 0.38
20	651	-1.29	-0.96	-2.26	-1.63	-	-	0.79	- 0.39

* Allowable Reinforcing Steel Stress = 54 KSI

** Allowable Concrete Compressive Stress = -3.4 KSI

Minimum Stress Margin = 72.6%

REV. 6, 4/82

SUSQUEHANNA STEAM ELECTRIC STATION
UNITS 1 AND 2
DESIGN ASSESSMENT REPORT

CONTAINMENT MARGINS
RPV PEDESTAL

FIGURE A-31

CECAP OUTPUT

LOAD COMBINATION EQN. 7A - Absolute Sum

STRESSES IN KSI

DIAPHRAGM SLAB

SECTION NUMBER	RADIUS FT.	EL. FT.	TOP FACE REBAR *		BOTTOM FACE REBAR*		SHEAR TIES	PRINCIPAL CONC. STRESS **
			RADIAL	TANGENTIAL	RADIAL	TANGENTIAL		
21	8	702	1.53	4.18	13.80	9.17	2.76	- 0.33
22	17	702	- 0.44	2.32	17.43	19.58	1.88	- 1.16
23	17	702	- 0.39	2.29	17.33	18.81	2.06	- 1.14
24	26	702	0.76	2.85	29.96	30.60	1.40	- 1.30
25	34	702	2.37	2.06	31.58	23.84	1.39	- 1.06

* Allowable Reinforcing Steel Stress = 54 KSI

** Allowable Concrete Compressive Stress = -3.4 KSI

Minimum Stress Margin = 41.5%

REV. 6, 4/82

SUSQUEHANNA STEAM ELECTRIC STATION
UNITS 1 AND 2
DESIGN ASSESSMENT REPORT

CONTAINMENT MARGINS
DIAPHRAGM SLAB

FIGURE A-32

CECAP OUTPUT

LOAD COMBINATION EQN. 7A - Absolute Sum

STRESSES IN KSI

BASE SLAB

SECTION NUMBER	RADIUS FT.	EL. FT.	TOP FACE REBAR *		BOTTOM FACE REBAR*		SHEAR TIES	PRINCIPAL CONC. STRESS \$
			RADIAL	TANGENTIAL	RADIAL	TANGENTIAL		
26	8	644	*** -11.44	** - 5.28	13.61	13.09	42.25	- 1.44
27	17	644	** -10.40	*** - 9.56	22.34	16.88	0.27	- 4.28†
28	26	644	** - 6.58	*** - 6.49	19.07	15.64	1.30	- 2.84
29	34	644	- 2.52	- 6.24	13.83	20.05	2.45	- 2.54
30	43	644	17.96	- 3.37	27.41	14.91	5.23	- 2.43

* Allowable Reinforcing Steel Stress = 54 KSI

** North - South Bars

***East - West Bars

\$ Allowable Concrete Compressive Stress = -3.4 KSI

† Maximum Concrete Strain = -0.00092

Minimum Stress Margin = 19.9%

REV. 6, 4/82

SUSQUEHANNA STEAM ELECTRIC STATION
UNITS 1 AND 2
DESIGN ASSESSMENT REPORT

CONTAINMENT MARGINS
BASE SLAB

FIGURE A-33

ITEM	MAXIMUM STRESS	ALLOWABLE STRESS	GOVERNING EQUATION	STRESS MARGIN
Membrane	14.0 Ksi	19.3 Ksi	3	27.3
Surface	31.8 Ksi	57.9 Ksi	3	45.1
Bolts	33.0 Ksi	41.3 Ksi	*	7.8
Leak Tightness	1.9 Kips/in	2.2 Kips/in	6	10.8

* For 200 Kips Bolt Pre-load to Assure Leak Tightness

REV. 6, 4/82

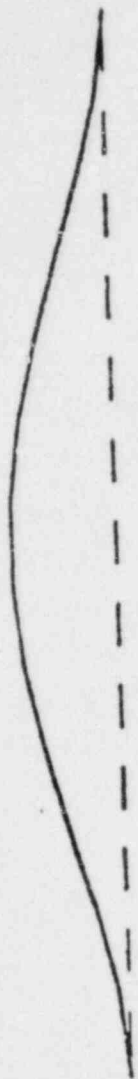
SUSQUEHANNA STEAM ELECTRIC STATION
UNITS 1 AND 2
DESIGN ASSESSMENT REPORT

STRESS MARGIN FOR REFUELING
HEAD AND SUPPORT SKIRT
FIGURE A-33.1

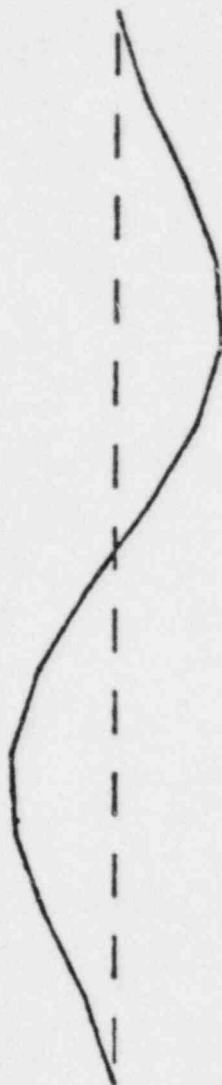
CECAP OUTPUT
SRSS METHOD

Figures A-34 thru A-57

Deleted



MODE 1
f=24 HZ



MODE 2
f=62 HZ



MODE 3
f=112 HZ

REV. 6, 4/82

SUSQUEHANNA STEAM ELECTRIC STATION
UNITS 1 AND 2
DESIGN ASSESSMENT REPORT

SUPPRESSION CHAMBER COLUMNS
MODE SHAPES

FIGURE A-58

SUPPRESSION CHAMBER COLUMNS

COLUMN	MAXIMUM AXIAL STRESS (KSI)	ALLOWABLE AXIAL STRESS (KSI)	MAXIMUM FLEXURAL STRESS (KSI)	ALLOWABLE FLEXURAL STRESS (KSI)	COMBINED STRESS RATIO	MARGIN %
42"dia pipe(shell element)	8.56	31.49	20.99	34.2	0.886	11.4
Top Anchorage	20.96	30.0	-	-	0.698	30.2
Bottom Anchorage	-	-	-	-	-	41.0

Note: These stress margins are based on load combination 7 of Table 5-2 which is the critical load combination.

REV. 6, 4/82

DOWNCOMER BRACING SYSTEM - STRESS SUMMARY

BRACING MEMBER DESIGN MARGINS FOR
CRITICAL MEMBERS AND GOVERNING LOAD COMBINATIONS

MEMBER*	EQN. 1 %	EQN. 3 %	EQN. 4 %	EQN. 7 %
5	68	73	76	4
6	72	80	82	12
7	63	75	77	12
18	69	78	79	14

Ref. DAR Table 5-2 for Load Combinations.

* For member number see Fig. 7-11

REV. 6, 4/82

SUSQUEHANNA STEAM ELECTRIC STATION
UNITS 1 AND 2
DESIGN ASSESSMENT REPORT

DOWNCOMER BRACING SYSTEM
STRESS SUMMARY

FIGURE A-60

DOWNCOMER RING STRESSES AND MARGINS

CONNECTION COMPONENT	MAXIMUM STRESS (KSI)		STRESS MARGIN (%)	
	EQ. 2	EQ. 7	EQ. 2	EQ. 7
Main Ring Plate	14.1 (21.4)	31.5 (32.4)	34	2.8
Connector Plate	6.1 (21.4)	10.5 (32.4)	71.4	67.6
Top Partial Plate	11.2 (21.4)	16.7 (32.4)	47.6	48.5
Top Ring Plate	2.8 (21.4)	5.0 (32.4)	87.1	84.5
Bolts	13.1 (22.5)	15.4 (33.8)	41.8	54.4

- NOTE: 1. Numbers in Parenthesis Represent the Maximum Allowable Stress Limit.
2. Load Combination Equations are From Table S-2.

REV. 6, 4/82

SUSQUEHANNA STEAM ELECTRIC STATION
UNITS 1 AND 2
DESIGN ASSESSMENT REPORT

DOWNCOMER RING STRESSES
AND MARGINS

FIGURE A-61

DOWN COMER MODE SHAPES
FIGURES A-62 THROUGH A-65
DELETED

DOWNCOMER - STRESS SUMMARY AND DESIGN MARGINS

LOAD COMBINATION	CONDITION	ALLOWABLE STRESS (KSI)	ABSOLUTE SUM STRESS (KSI)	DESIGN MARGIN ABS. SUM (%)	SRSS SUM STRESS (KSI)	DESIGN MARGIN SRSS (%)
Equation 1	Upset	30.0	14.6	51	14.6	51
Equation 2	Emergency	45.0	27.0	40	19.2	57
Equation 3	Emergency	45.0	38.9	14	22.5	50
Equation 4	Faulted	60.0	30.6	49	21.9	64
Equation 5	Faulted	60.0	39.5	34	22.5	63
Equation 6	Faulted	60.0	44.3	26	25.8	57
Equation 7	Faulted	60.0	32.1	46	22.4	63

NOTE: Load combinations from DAR Table 5-3 and Stresses checked per ASME Code NB 3652.

REV. 6, 4/82

SUSQUEHANNA STEAM ELECTRIC STATION
UNITS 1 AND 2
DESIGN ASSESSMENT REPORT

DOWNCOMERS

STRESS SUMMARY

FIGURE A-66

SRV SUPPORT ASSEMBLIES
(MAXIMUM STRESSES AND STRESS MARGINS FOR TYPICAL ASSEMBLIES)

			MAXIMUM	ALLOWABLE		
	MAXIMUM	ALLOWABLE	FLEXURAL	FLEXURAL	COMBINED	
	AXIAL STRESS	AXIAL STRESS	STRESS	STRESS	STRESS	STRESS
Bracing Member	(KSI)	(KSI)	(KSI)	(KSI)	RATIO	MARGIN %
Type A Horizontal Member	5.65	28.65	10.78	31.5	0.530	47.0
Type A Knee Member	6.53	27.66	11.92	31.5	0.614	38.6
Type B Horizontal Member	6.34	27.66	14.89	31.5	0.702	29.8
Type B Knee Member	7.32	26.52	15.98	31.5	0.783	21.7
Type C Horizontal Member	4.14	25.65	12.91	31.5	0.571	42.9
Type C Knee Member	4.78	23.87	13.49	31.5	0.629	37.1

Note: The stress margins are based on load combination 7 of Table 5-2, which is the critical load combination.

REV. 6, 4/82

SUSQUEHANNA STEAM ELECTRIC STATION
UNITS 1 AND 2
DESIGN ASSESSMENT REPORT

SRV SUPPORT ASSEMBLIES
STRESS

FIGURE A-67

APPENDIX B
CONTAINMENT MODE SHAPES AND RESPONSE SPECTRA

TABLE OF CONTENTS

- B.1 Containment Mode Shapes
- B.2 Containment Response Spectra
- B.3 Figures

3

APPENDIX B

FIGURES

Number

Title

B-1	Model for Containment Response Spectra
B-2	Containment Modes and Frequencies
B-3 thru B-17	Containment Mode Shapes - Modes 1 through 15

Containment Response Spectra

B-18	KWU-SRV-#76 Axisy. Direction Y
3 B-19 thru B-21	KWU-SRV-#76 Axisy. Direction Z
B-22 thru B-24	KWU-SRV-#76 Asymm. Direction X
B-25	KWU-SRV-#76 Asymm. Direction Y
B-26	KWU-SRV-#76 Asymm. Direction Z
B-27	KWU-Chuqqinq-#303 Axisym Direction Y
B-28 thru B-30	KWU-Chuqqinq-#303 Axisym Direction Z
B-31 thru B-33	KWU-Chuqqinq-#303 Axisym. Direction X
B-34	KWU-Chuqqinq-#303 Asym. Direction Z
6 B-35	KWU-Chuqqinq-#306 Axisym. Direction Y
B-36 thru B-38	KWU-Chuqqinq-#306 Axisym. Direction Z
B-39	KWU-Chuqqinq-#306 Axisym. Direction X
B-40 thru B-41	KWU-Chuqqinq-#306 Asym. Direction X
B-42	KWU-Chuqqinq-#306 Asym. Direction Z

APPENDIX B

FIGURES (Cont.)

<u>Number</u>	<u>Title</u>
B-43	KWU-Condensation Oscillation-#314 Direction Y
B-44 thru B-46	KWU-Condensation Oscillation-#314 Direction Z
B-47 thru B-49	KWU-Condensation Oscillation-#314 Direction X
B-50	KWU-Condensation Oscillation-#314 Direction Z
B-51 thru B-54	Seismic Sloshing-Direction X
B-55 thru B-58	Seismic Sloshing-Direction Z

B.1 CONTAINMENT MODE SHAPES

The containment model is shown as Figure B-1. While, Figure B-2 shows containment frequencies from the model analysis with water mass included as discussed in Subsection 7.1.1.1.1.3. Containment mode shapes are shown in Figures B-3 through B-17, covering mode shapes 1 through 15.

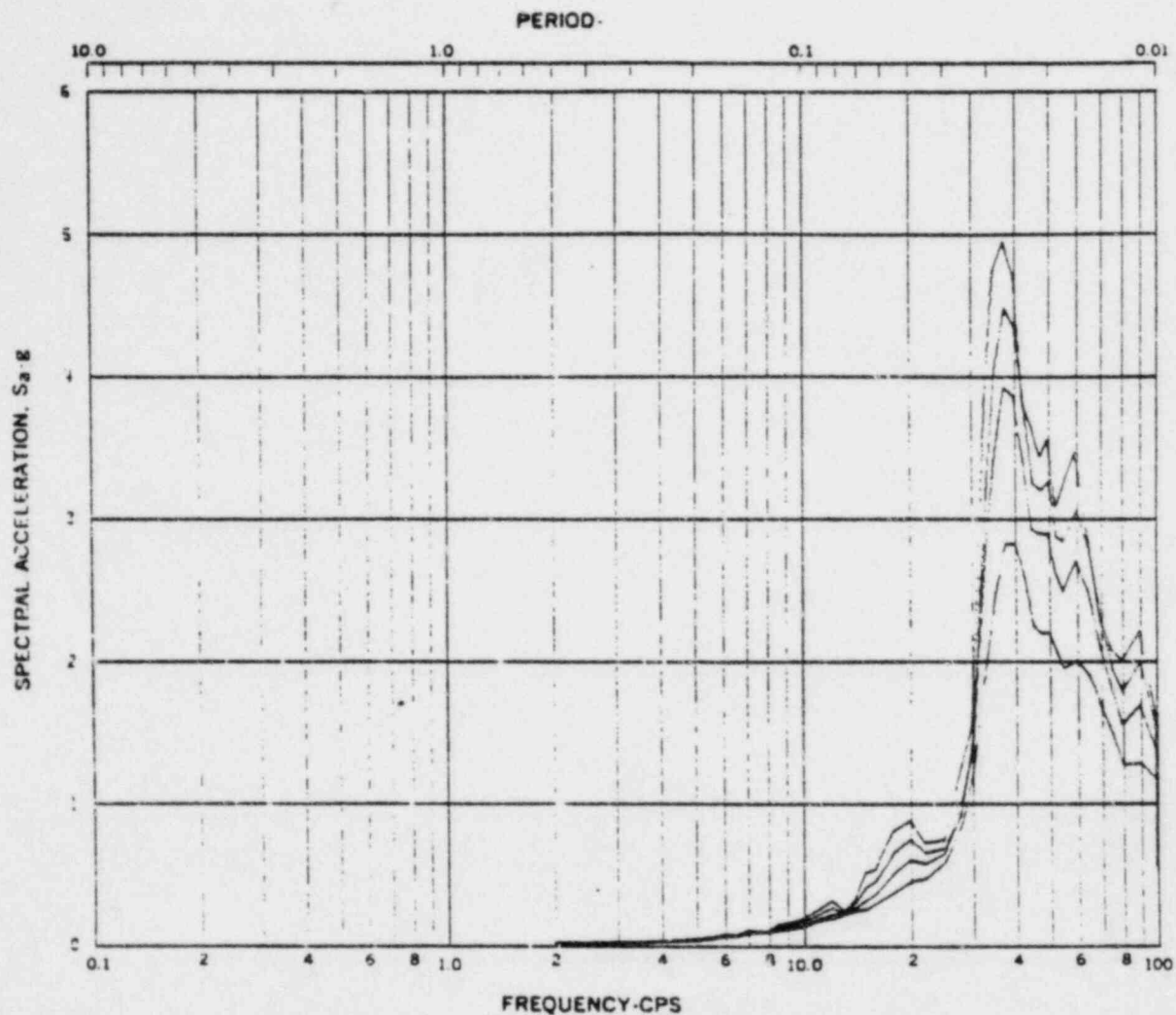
B.2 CONTAINMENT RESPONSE SPECTRA

This appendix shows examples of the horizontal and vertical response spectra curves of the containment structure due to LOCA and SRV loading. Four spectral damping values, i.e., 0.005, 0.01, 0.02, and 0.05 are shown on each group of curves. The structural model of the containment is shown on Figure B-1. The modal frequencies and mode shapes are shown on Figures B-2 to B-17. The response spectrum curves shown on B-18 to B-58 are submitted as representative examples of the containment structure response spectra caused by SRV actuation, CO, chugging and seismic slosh.

The SRV load (generated by KWU) consists of 3 traces and each trace consists of 5 frequencies. The asymmetric and axisymmetric load cases are considered (see Subsection 7.1.1.1.1.5.1).

The LOCA load case consists of chugging and condensation oscillation loads, each of which contain 3 frequencies. Asymmetric and axisymmetric load cases are considered for chugging, and only axisymmetric load case is considered for condensation oscillation (See section 7.1.1.1.1.5.2).

The seismic slosh response spectra were generated for the load methodology described in Subsection 4.2.4.7.



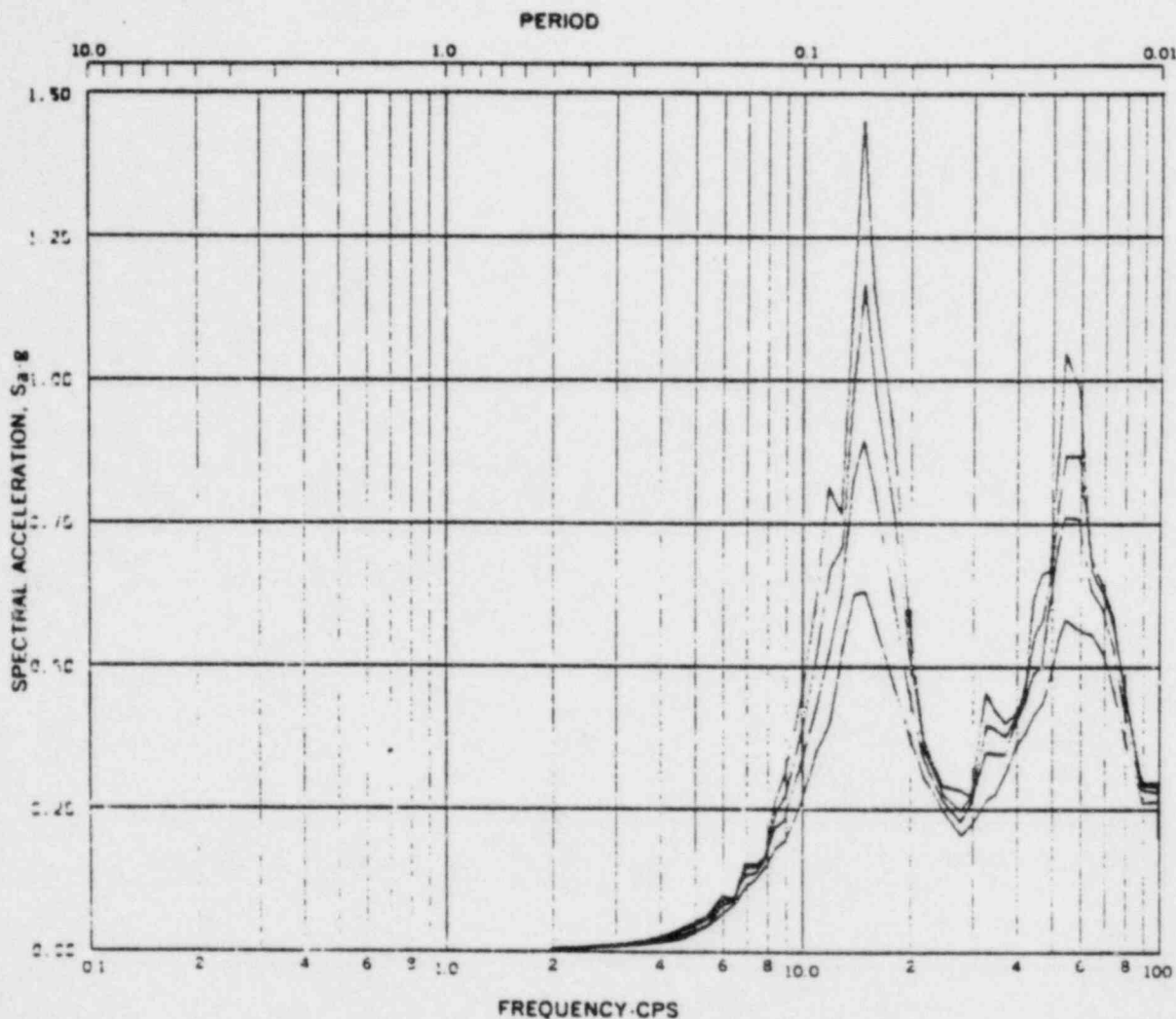
Acceleration Spectra for CONTAINMENT SHELL
 Load Case: Susquehanna KWU 303 SYMM.
 Mode 135, Direction Y, Elev 672'-0"
 Damping: 0.005, 0.01, 0.02, 0.05

REV. 6, 4/82

**SUSQUEHANNA STEAM ELECTRIC STATION
 UNITS 1 AND 2
 DESIGN ASSESSMENT REPORT**

**CONTAINMENT RESPONSE SPECTRA
 KWU-CHUGGING-#303
 AXISYM. DIRECTION 'Y'**

FIGURE B-27



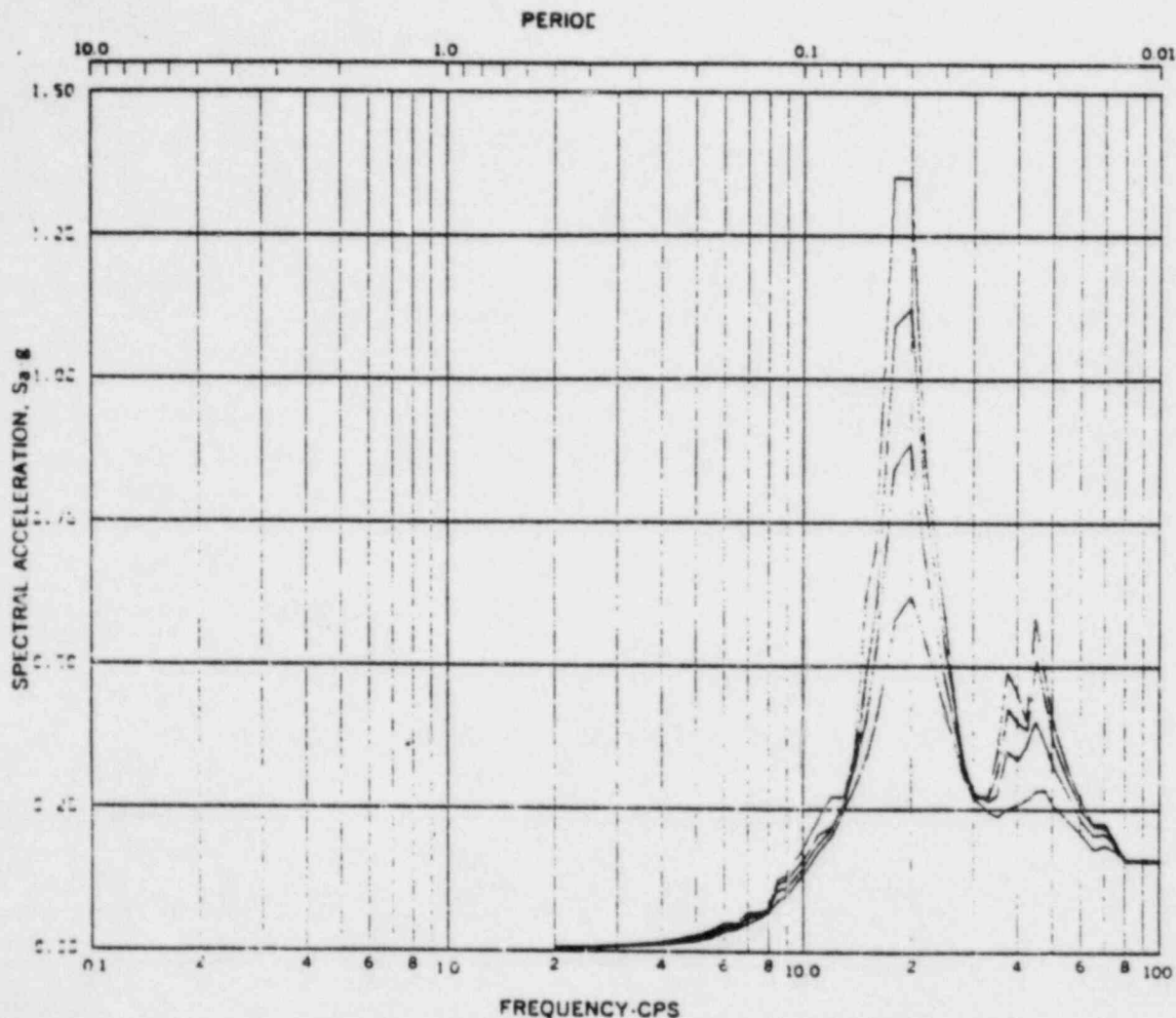
Acceleration Spectra for PEDESTAL
 Load Case: SEISMIC KWU 303 SYMM.
 Mode 215, Direction W, Elev 702'-3"
 Damping: 0.005, 0.01, 0.02, 0.05

REV. 6, 4/82

BUSQUEHANNA STEAM ELECTRIC STATION
 UNITS 1 AND 2
 DESIGN ASSESSMENT REPORT

CONTAINMENT RESPONSE SPECTRA
 KWU-CHUGGING-#303
 AXISYM. DIRECTION 'Z'

FIGURE B-28



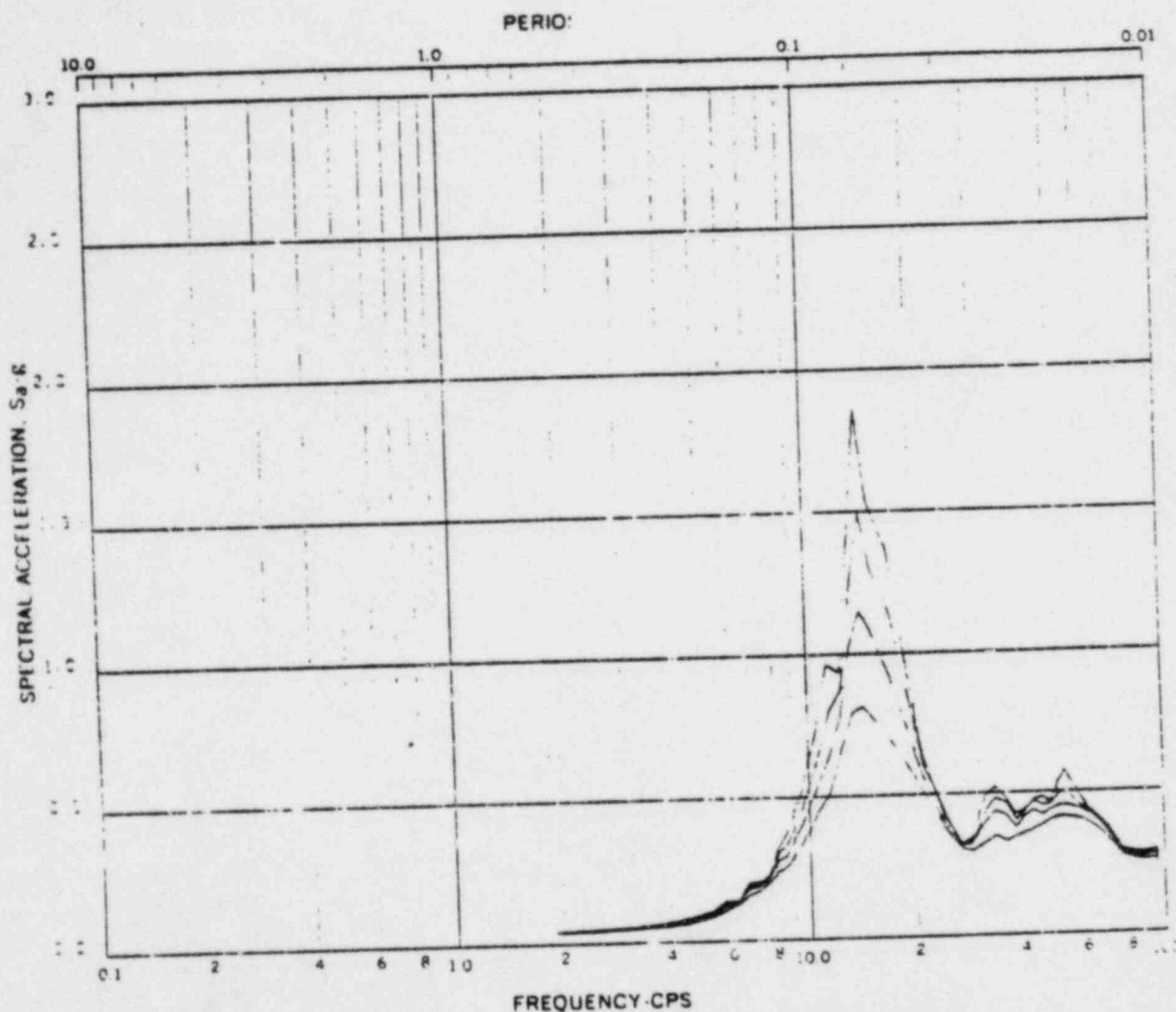
FREQUENCY-CPS
 Acceleration Spectra for CONTAINMENT SHELL
 Load Case: Susquehanna KWU 303 SYMM.
 Mode 415, Direction 2, Elav 778' - 9-3/4"
 Damping: 0.005, 0.01, 0.02, 0.05

REV. 6, 4/82

SUSQUEHANNA STEAM ELECTRIC STATION
UNITS 1 AND 2
DESIGN ASSESSMENT REPORT

CONTAINMENT RESPONSE SPECTRA
 KWU-CHUGGING-#303
 AXISYM. DIRECTION 'Z'

FIGURE B-29



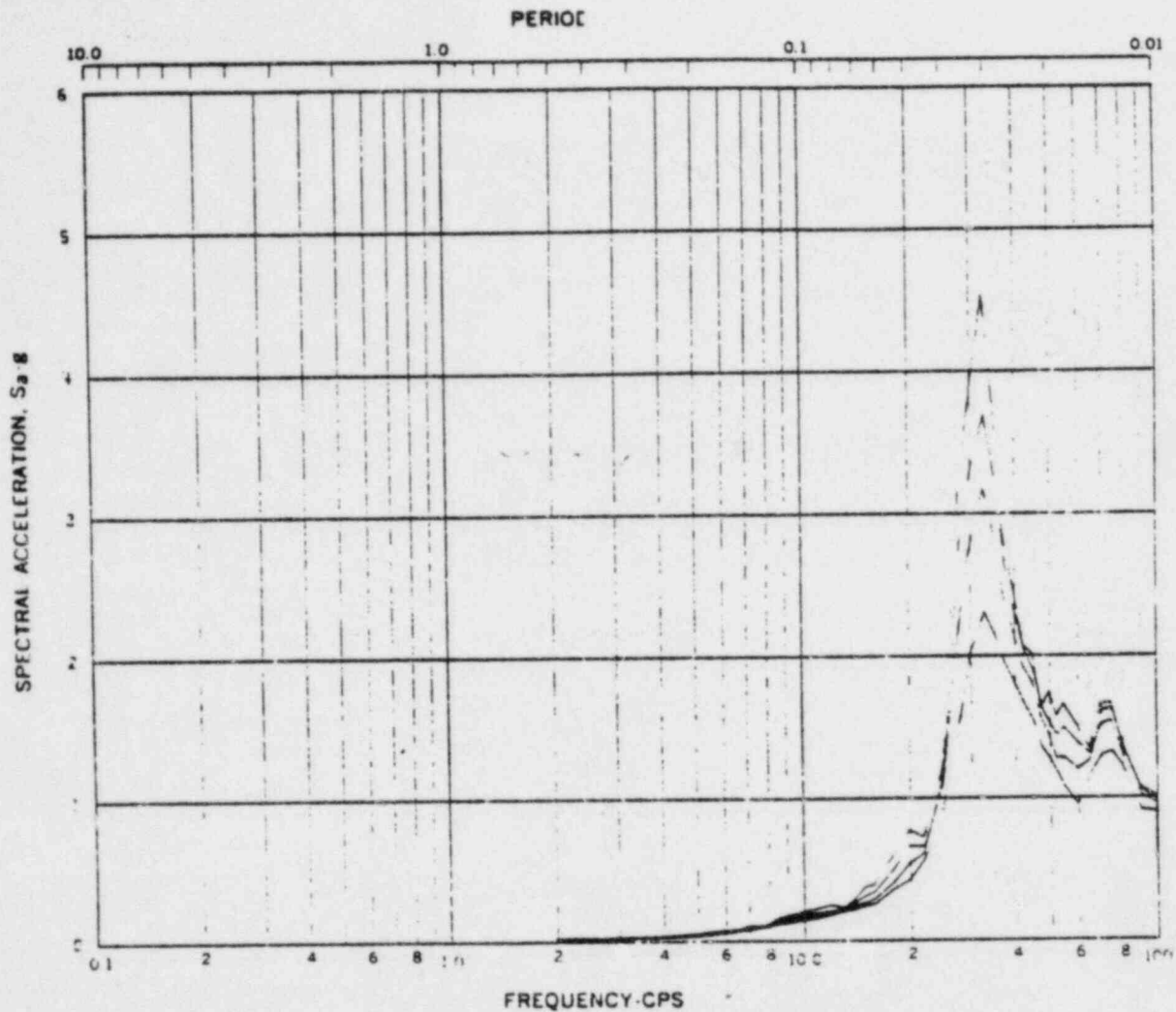
Acceleration Spectra for PEDESTAL
 Load Case: Seismicity KWU 303 SYMM.
 Node 535, Direction S, Elev 729' - 9-3/4"
 Damping: 0.005, 0.01, 0.02, 0.05

REV. 6, 4/82

SUSQUEHANNA STEAM ELECTRIC STATION
UNITS 1 AND 2
DESIGN ASSESSMENT REPORT

CONTAINMENT RESPONSE SPECTRA
 KWU-CHUGGING-#303
 AXISYM. DIRECTION 'Z'

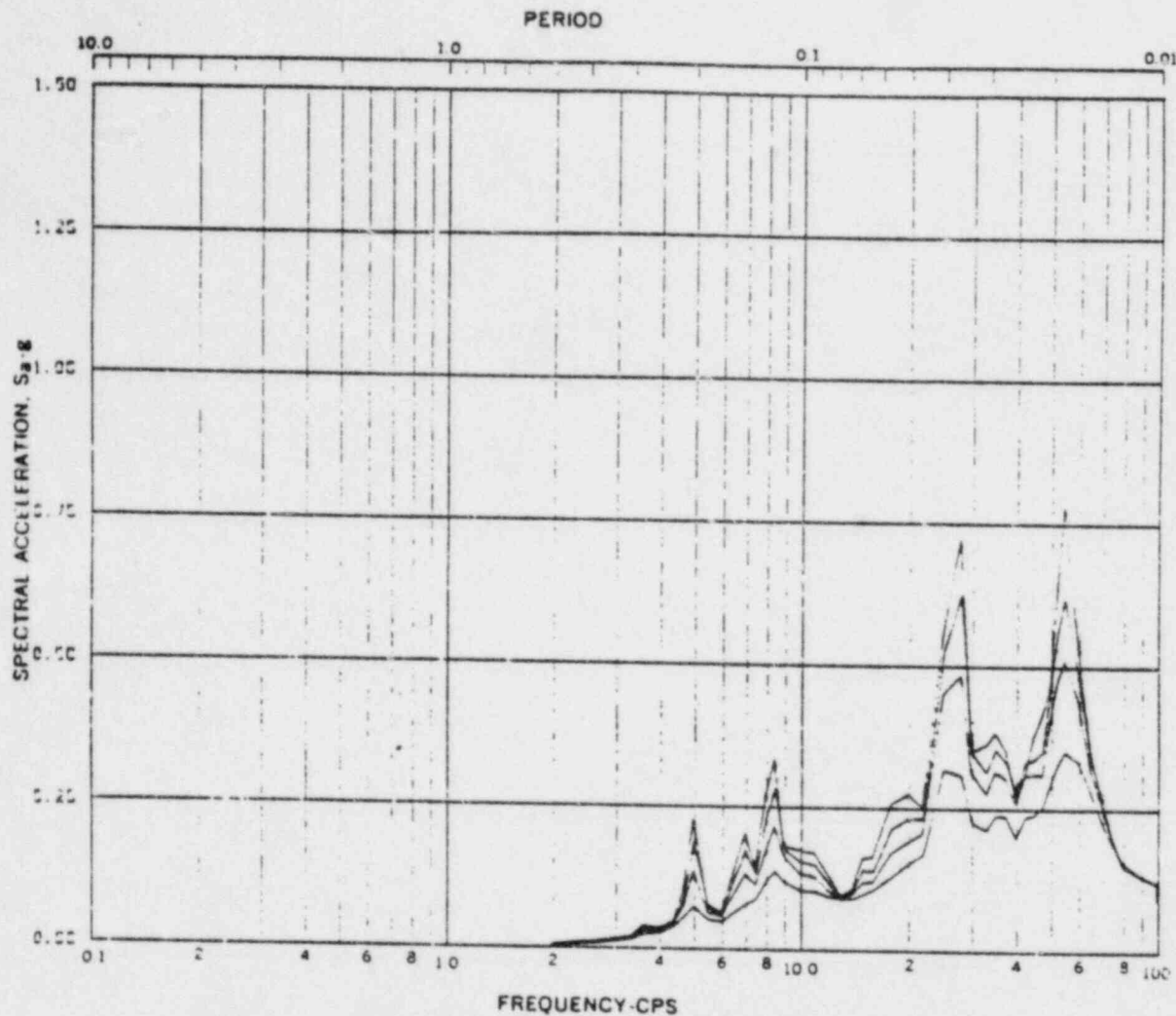
FIGURE B-30



Acceleration Spectra for CONTAINMENT SHELL
 Load Case: Earthquake KWU 303 SYMM.
 Mode 131, Direction X, Elev 672'-0"
 Damping: 0.005, 0.01, 0.02, 0.05

REV. 6, 4/82

SUSQUEHANNA STEAM ELECTRIC STATION UNITS 1 AND 2 DESIGN ASSESSMENT REPORT
CONTAINMENT RESPONSE SPECTRA KWU-CHUGGING-#303 AXISYM. DIRECTION 'X'
FIGURE B-31



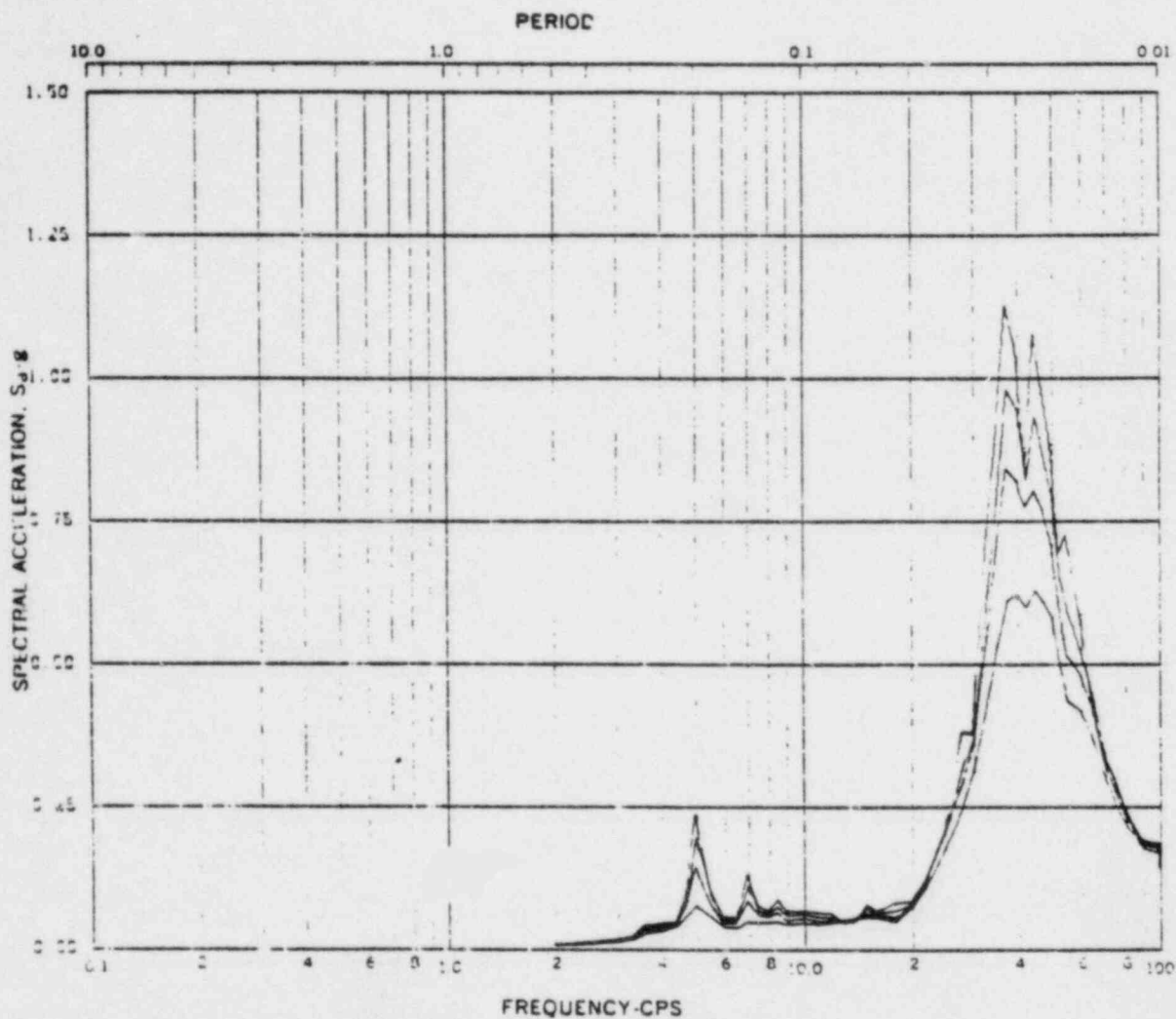
Accelerations: Spectra for CONTAINMENT SHELL
 Load Case: Susquehanna KWU 303 ASYM.
 Mode 411, Direction X, Elev 778' - 9-3/4"
 Damping: 0.005, 0.01, 0.02, 0.05

REV. 6, 4/82

SUSQUEHANNA STEAM ELECTRIC STATION
 UNITS 1 AND 2
 DESIGN ASSESSMENT REPORT

CONTAINMENT RESPONSE SPECTRA
 KWU-CHUGGING-#303
 ASYM. DIRECTION 'X'

FIGURE B-32



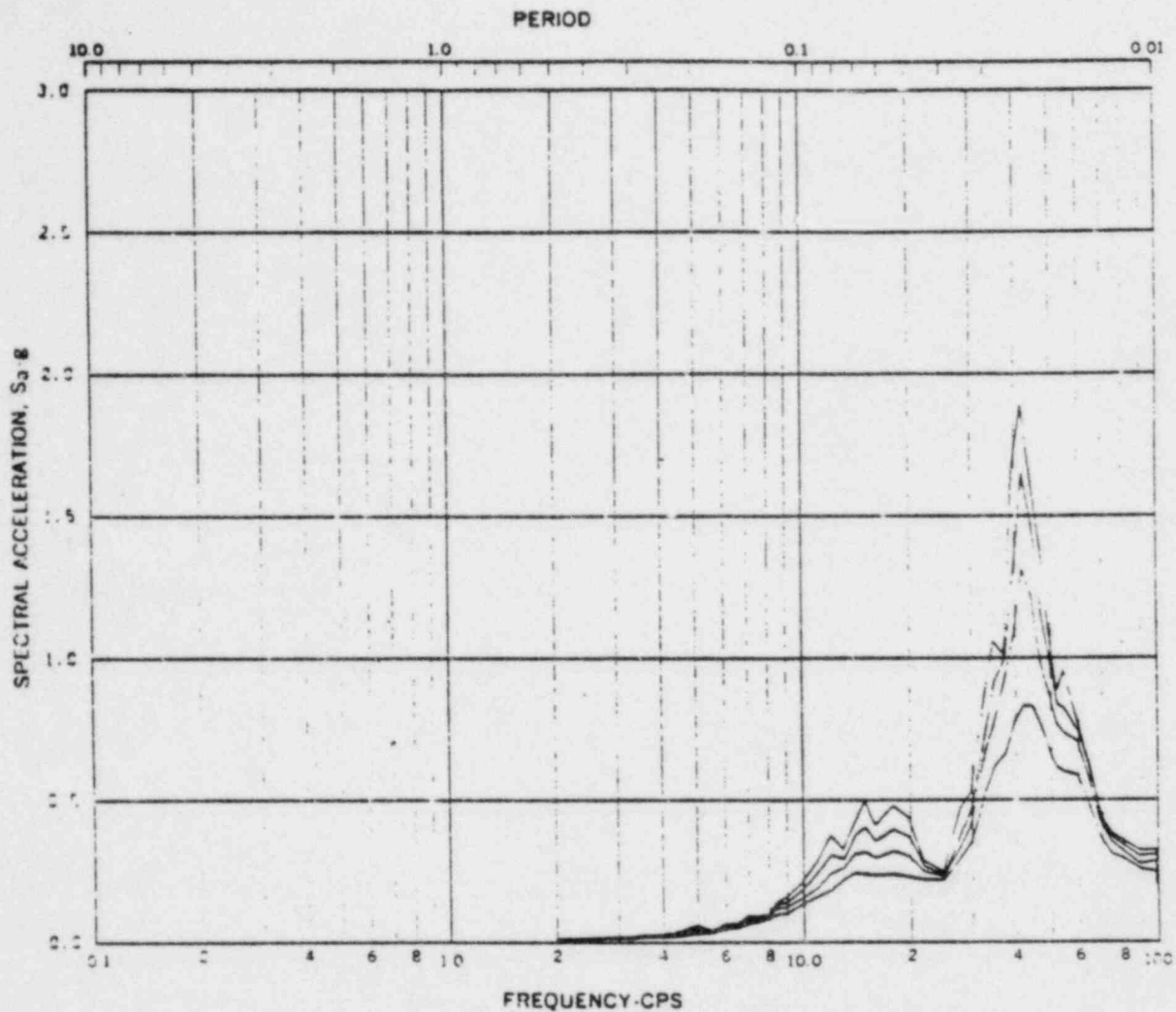
Acceleration Spectra for PEDESTAL
 Load Case: Susquehanna KWU 303 ASYM.
 Mode 531, Direction X, Elev 729' - 9-3/4"
 Damping: 0.005, 0.01, 0.02, 0.05

REV. 6, 4/82

**SUSQUEHANNA STEAM ELECTRIC STATION
 UNITS 1 AND 2
 DESIGN ASSESSMENT REPORT**

CONTAINMENT RESPONSE SPECTRA
 KWU-CHUGGING-#303
 ASYM. DIRECTION 'X'

FIGURE B-33



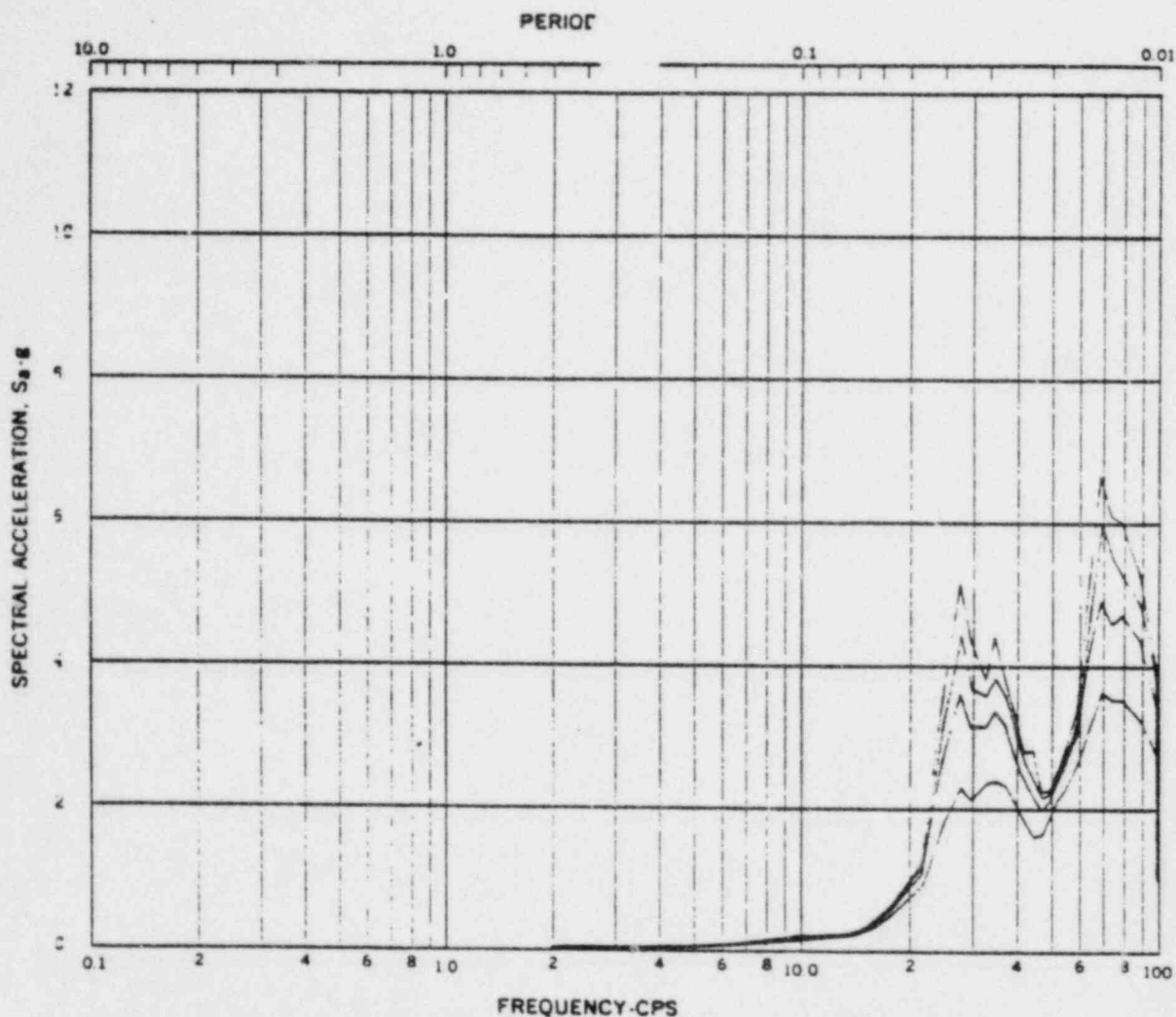
Acceleration Spectra for DIAPHRAGM SLAB
 Load Case: Seismicity KWU 303 ASYM.
 Mode 252*, Direction X, Elev 702'-3"
 Damping: 0.005, 0.01, 0.02, 0.05

REV. 6, 4/82

**SUSQUEHANNA STEAM ELECTRIC STATION
 UNITS 1 AND 2
 DESIGN ASSESSMENT REPORT**

**CONTAINMENT RESPONSE SPECTRA
 KWU-CHUGGING-#303
 ASYM. DIRECTION 'Z'**

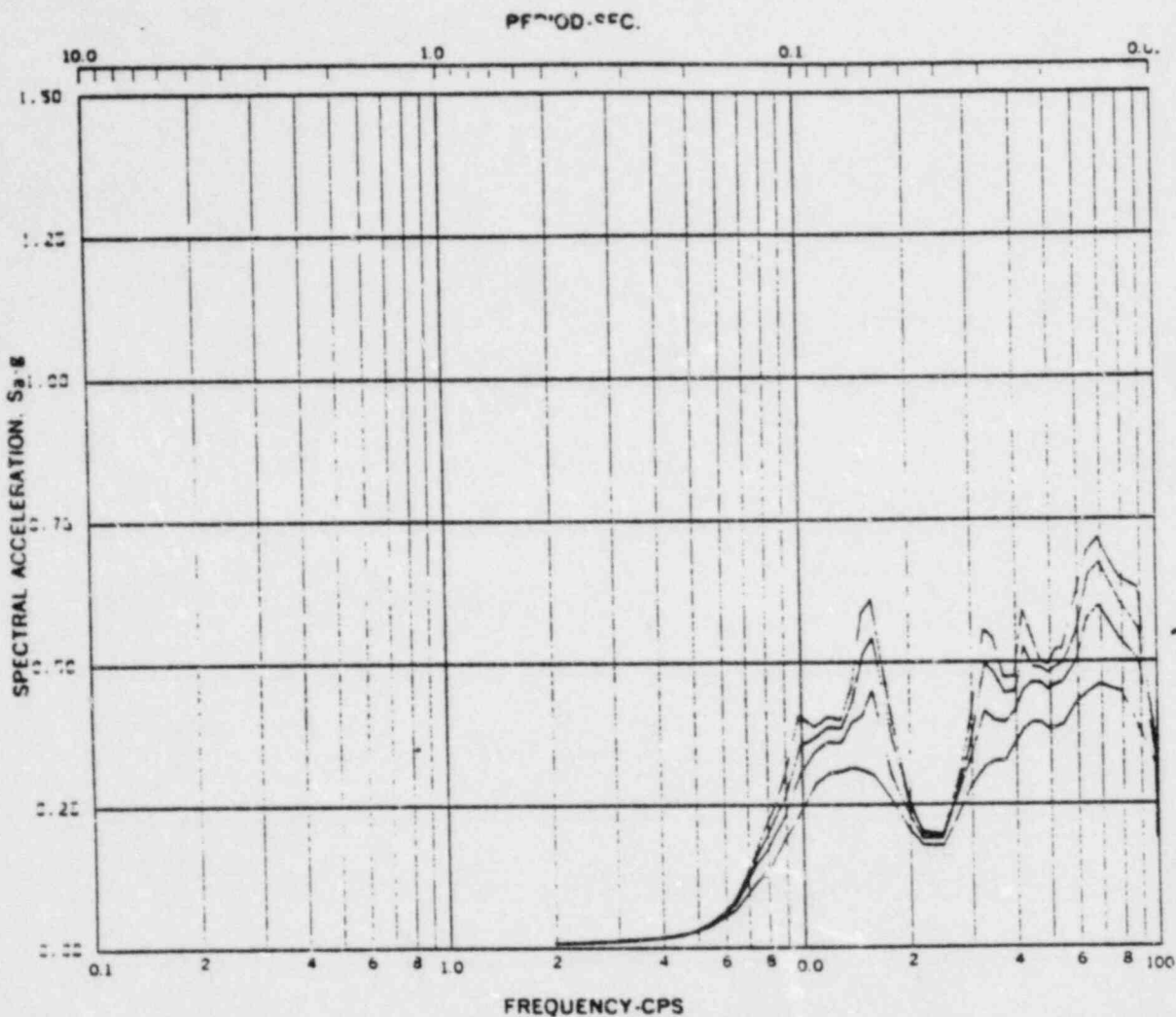
FIGURE B-34



FREQUENCY-CPS
 Acceleration Spectra for CONTAINMENT SHELL
 Load Case: Susquehanna KWU 306 SYMM.
 Mode 135, Direction Y, Elav 672'-0"
 Damping: 0.005, 0.01, 0.02, 0.05

REV. 6, 4/82

SUSQUEHANNA STEAM ELECTRIC STATION UNITS 1 AND 2 DESIGN ASSESSMENT REPORT
CONTAINMENT RESPONSE SPECTRA KWU-CHUGGING-#306 AXISYM. DIRECTION 'Y'
FIGURE B-35



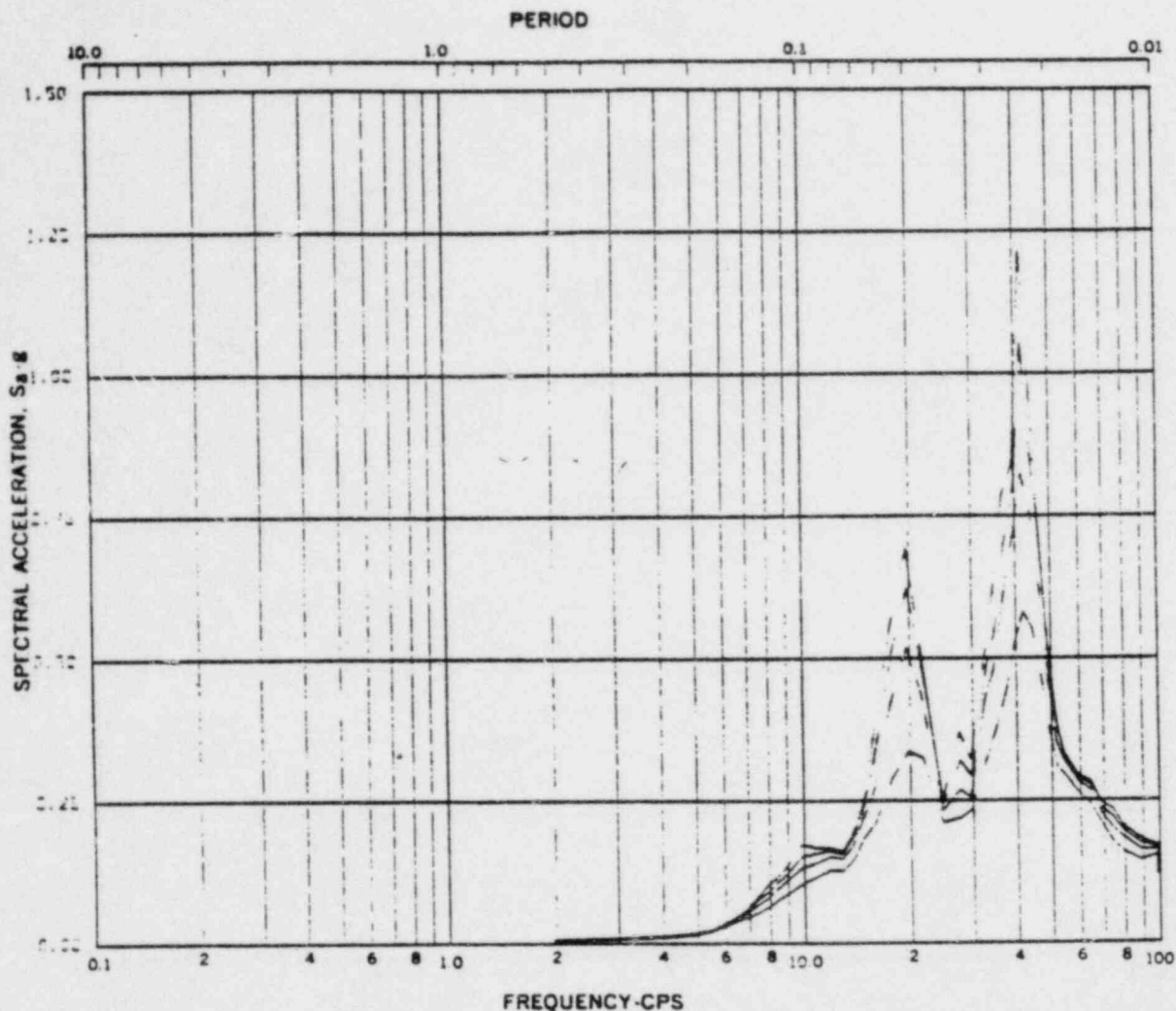
Acceleration Spectra for PEDESTAL
 Load Case: SUSQUEHANNA KWU 306 SMM.
 Mode 215, Direction W, Elev 702'-3"
 Damping: 0.005, 0.01, 0.02, 0.05

REV. 6, 4/82

**SUSQUEHANNA STEAM ELECTRIC STATION
 UNITS 1 AND 2
 DESIGN ASSESSMENT REPORT**

**CONTAINMENT RESPONSE SPECTRA
 KWU-CHUGGING-#306
 AXISYM. DIRECTION 'Z'**

FIGURE B-36



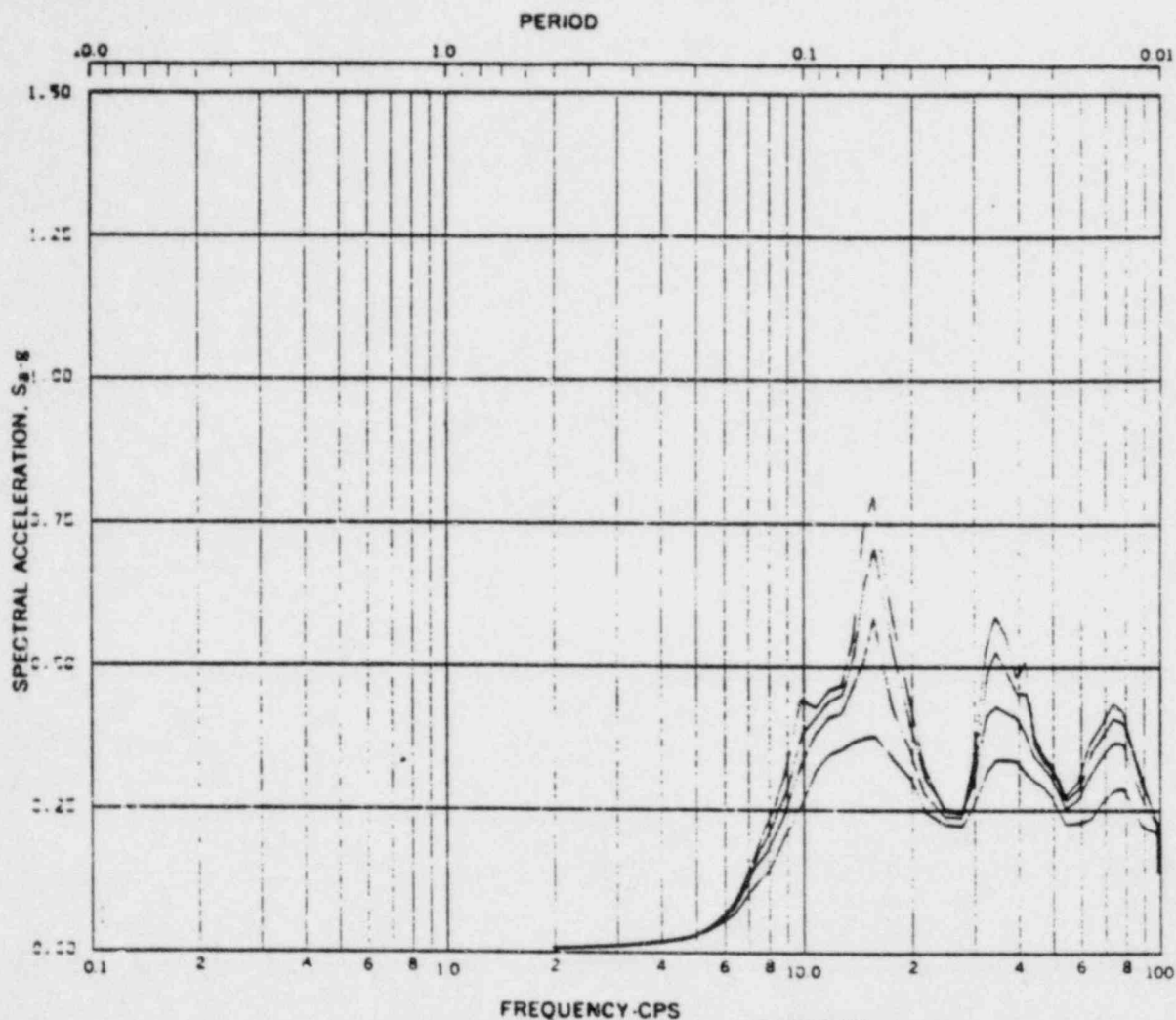
Acceleration Spectra for CONTAINMENT SHELL
 Load Case: Susquehanna KWU 306 SYM.
 Mode 415, Direction X, Elev 778' - 9-3/4"
 Damping: 0.005, 0.01, 0.02, 0.05

REV. 6, 4/82

**SUSQUEHANNA STEAM ELECTRIC STATION
 UNITS 1 AND 2
 DESIGN ASSESSMENT REPORT**

**CONTAINMENT RESPONSE SPECTRA
 KWU-CHUGGING-#306
 AXISYM. DIRECTION 'Z'**

FIGURE B-37

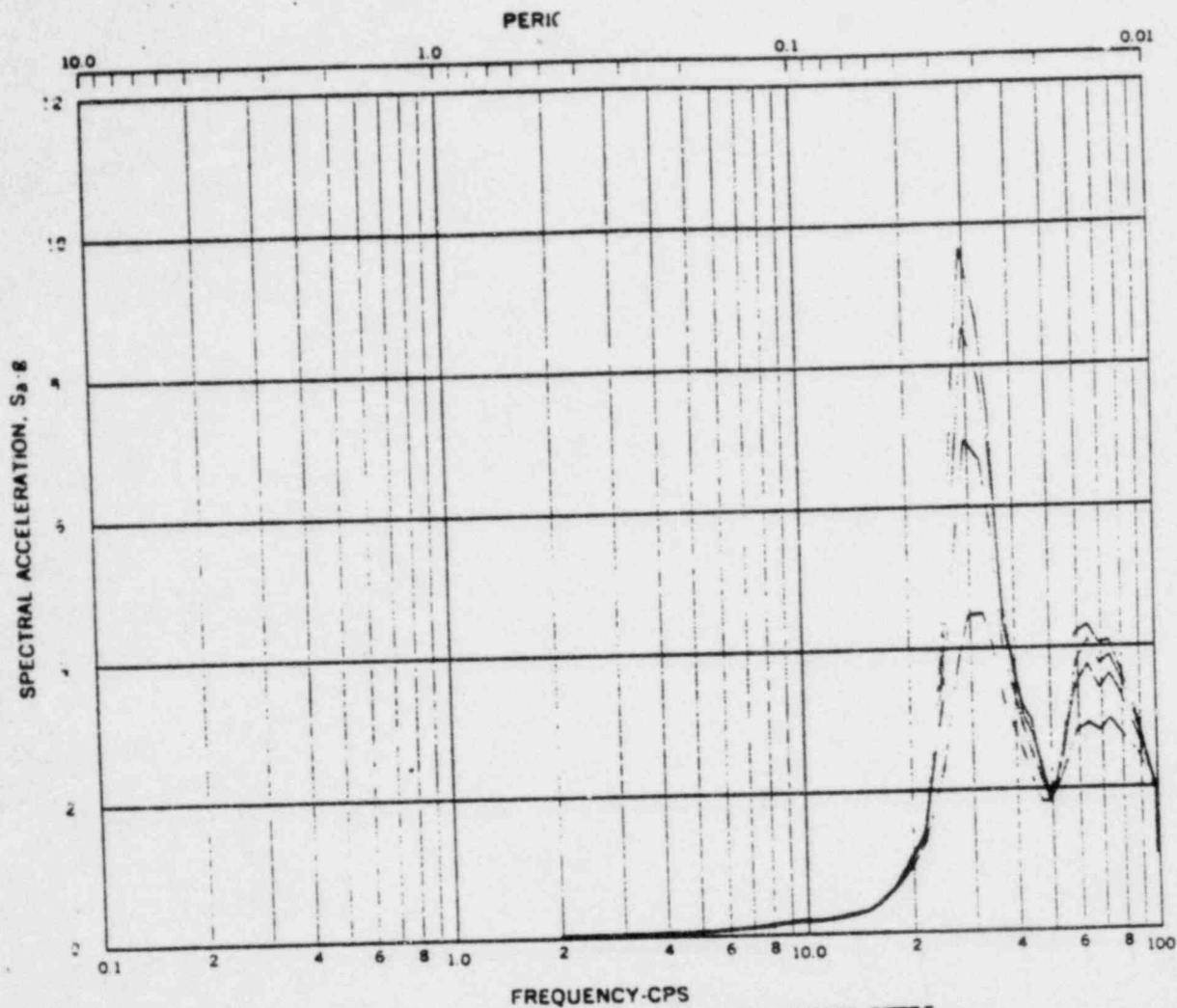


Acceleration Spectra for PEDESTAL
 Load Case: SUSQUEHANNA KWU 306 SYM.
 Mode 535, Direction X, Elev 729' - 9-3/4"
 Damping: 0.005, 0.01, 0.02, 0.05

REV. 6, 4/82

SUSQUEHANNA STEAM ELECTRIC STATION
UNITS 1 AND 2
DESIGN ASSESSMENT REPORT

CONTAINMENT RESPONSE SPECTRA
KWU-CHUGGING-#306
AXISYM. DIRECTION "Z"
FIGURE B-38



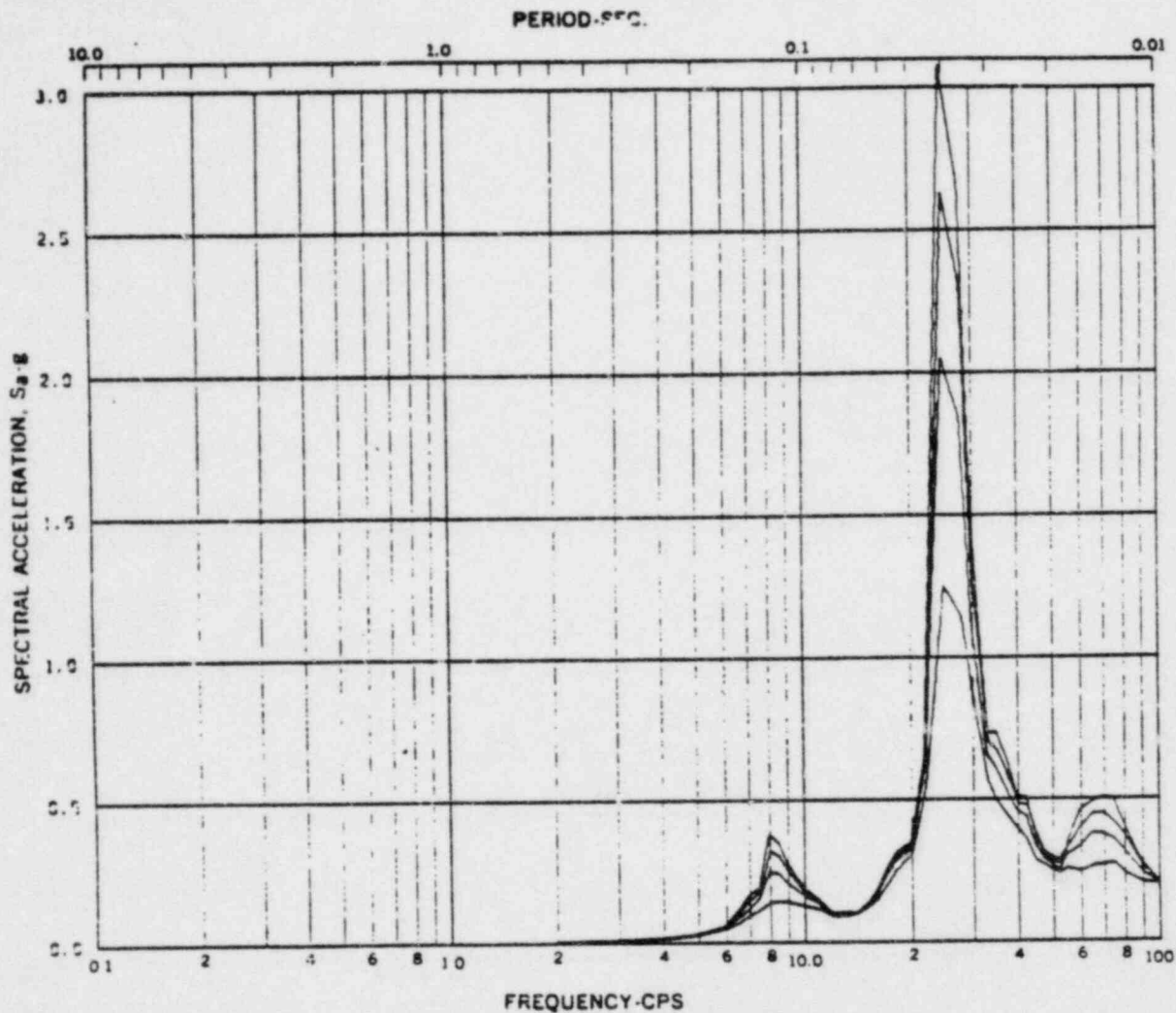
Acceleration Spectra for CONTAINMENT SHELL
 Load Case: KWU 306 SYMM.
 Mode 131, Direction X, Elev 672'-0"
 Damping: 0.005, 0.01, 0.02, 0.05

REV. 6, 4/82

SUSQUEHANNA STEAM ELECTRIC STATION
UNITS 1 AND 2
DESIGN ASSESSMENT REPORT

CONTAINMENT RESPONSE SPECTRA
 KWU-CHUGGING-#306
 AXISYM. DIRECTION 'X'

FIGURE B-39



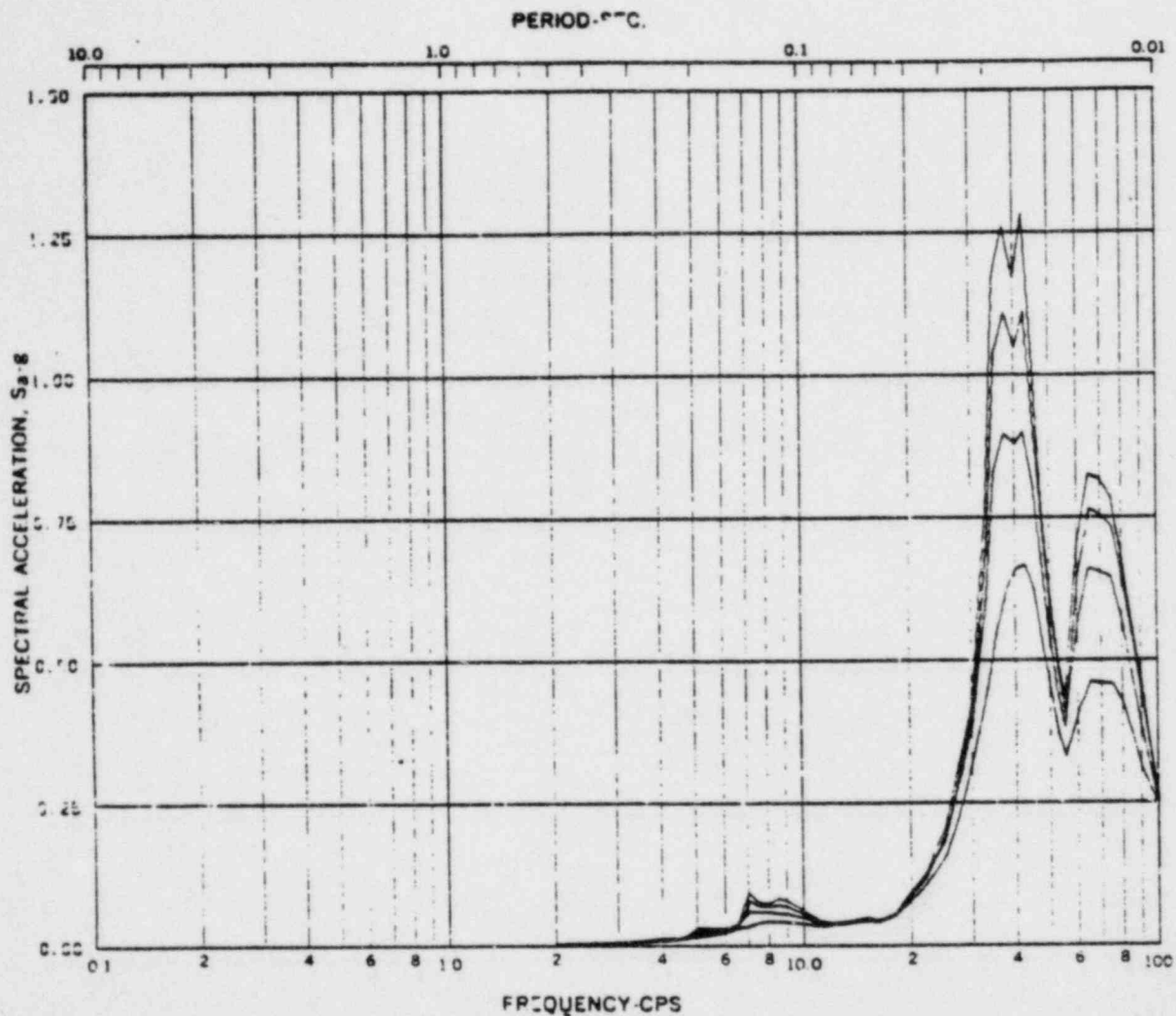
Acceleration Spectra for CONTAINMENT SHELL
 Load Case: Seismicity KWU 306 ASYMM.
 Mode 411, Direction X, Elev 778' - 9-3/4"
 Damping: 0.005, 0.01, 0.02, 0.05

REV. 6, 4/82

BUSQUEHANNA STEAM ELECTRIC STATION
UNITS 1 AND 2
DESIGN ASSESSMENT REPORT

CONTAINMENT RESPONSE SPECTRA
 KWU-CHUGGING-#306
 ASYM. DIRECTION 'X'

FIGURE B-40



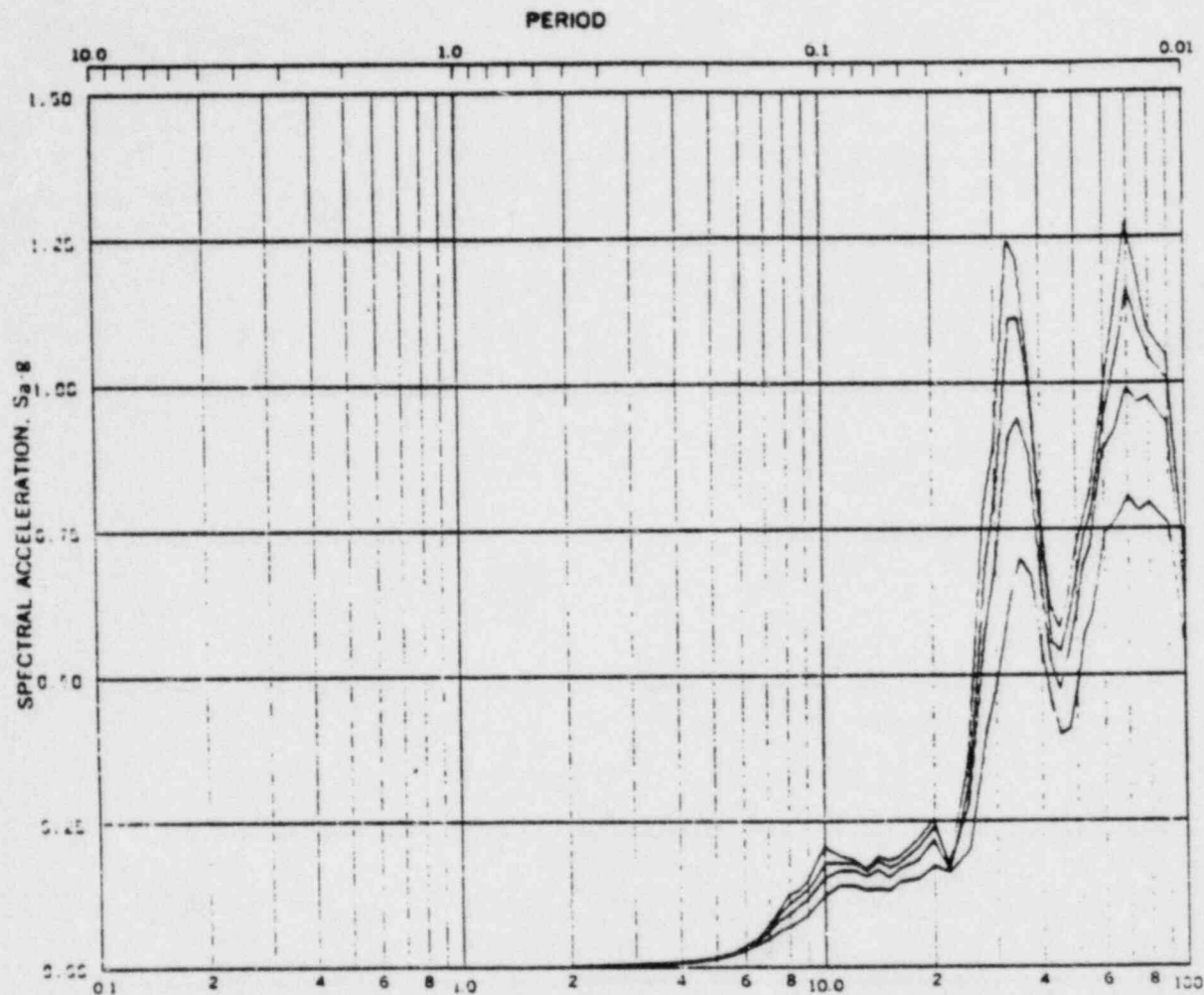
Acceleration Spectra for PEDESTAL
 Load Case: SUSQUEHANNA KWU 306 ASYMM.
 Mode 531, Direction X, Elev 729' - 9-3/4"
 Damping: 0.005, 0.01, 0.02, 0.05

REV. 6, 4/82

**SUSQUEHANNA STEAM ELECTRIC STATION
 UNITS 1 AND 2
 DESIGN ASSESSMENT REPORT**

**CONTAINMENT RESPONSE SPECTRA
 KWU-CHUGGING-#306
 ASYM. DIRECTION 'X'**

FIGURE B-41



FREQUENCY-CPS

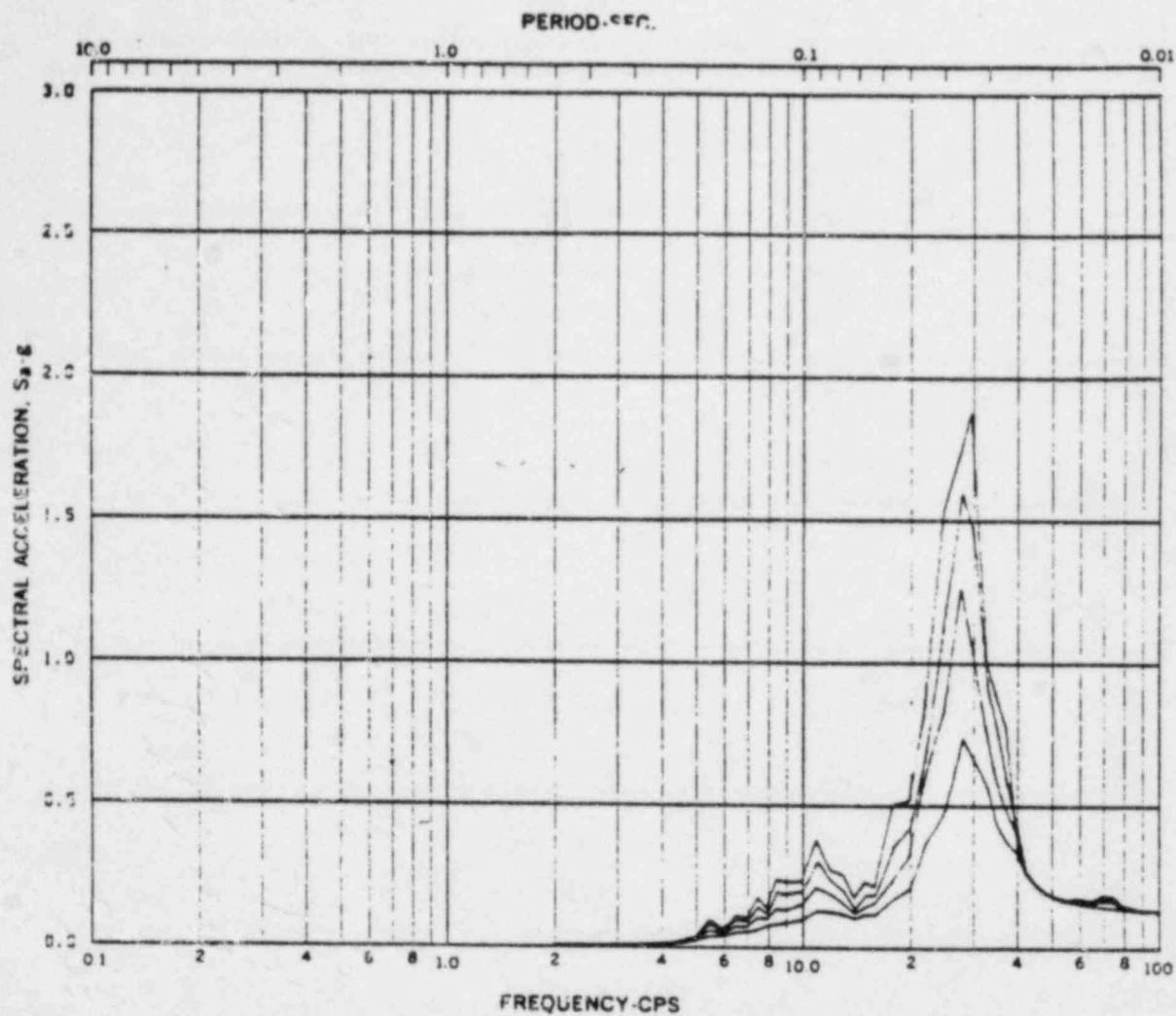
Acceleration Spectra for DIAPHRAGM SLAB
 Load Case: ASYM. KWU 306 ASYM.
 Node 252*, Direction X, Elev 702'-3"
 Damping: 0.005, 0.01, 0.02, 0.05

REV. 6, 4/82

**BUSQUEHANNA STEAM ELECTRIC STATION
 UNITS 1 AND 2
 DESIGN ASSESSMENT REPORT**

**CONTAINMENT RESPONSE SPECTRA
 KWU-CHUGGING-#306
 ASYM. DIRECTION 'Z'**

FIGURE B-42



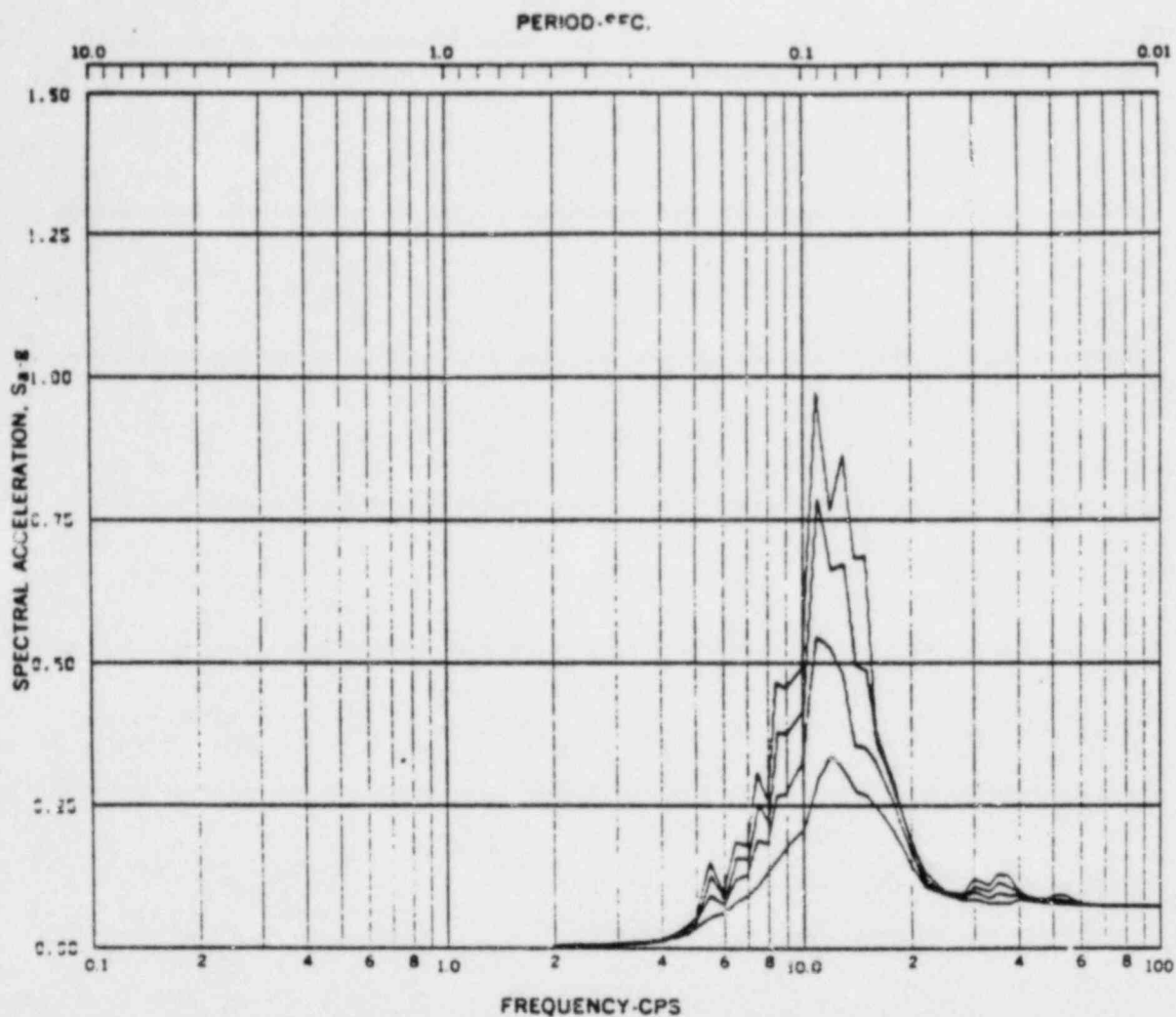
Acceleration Spectra for CONTAINMENT SHELL
 Load Case: Seismicity KWU 314 C.O.
 Mode 135, Direction Y, Elev 672'-0"
 Damping: 0.005, 0.01, 0.02, 0.05

REV. 6, 4/82

SUSQUEHANNA STEAM ELECTRIC STATION
UNITS 1 AND 2
DESIGN ASSESSMENT REPORT

CONTAINMENT RESPONSE SPECTRA
 KWU-COND. OSCIL.-#314
 DIRECTION 'Y'

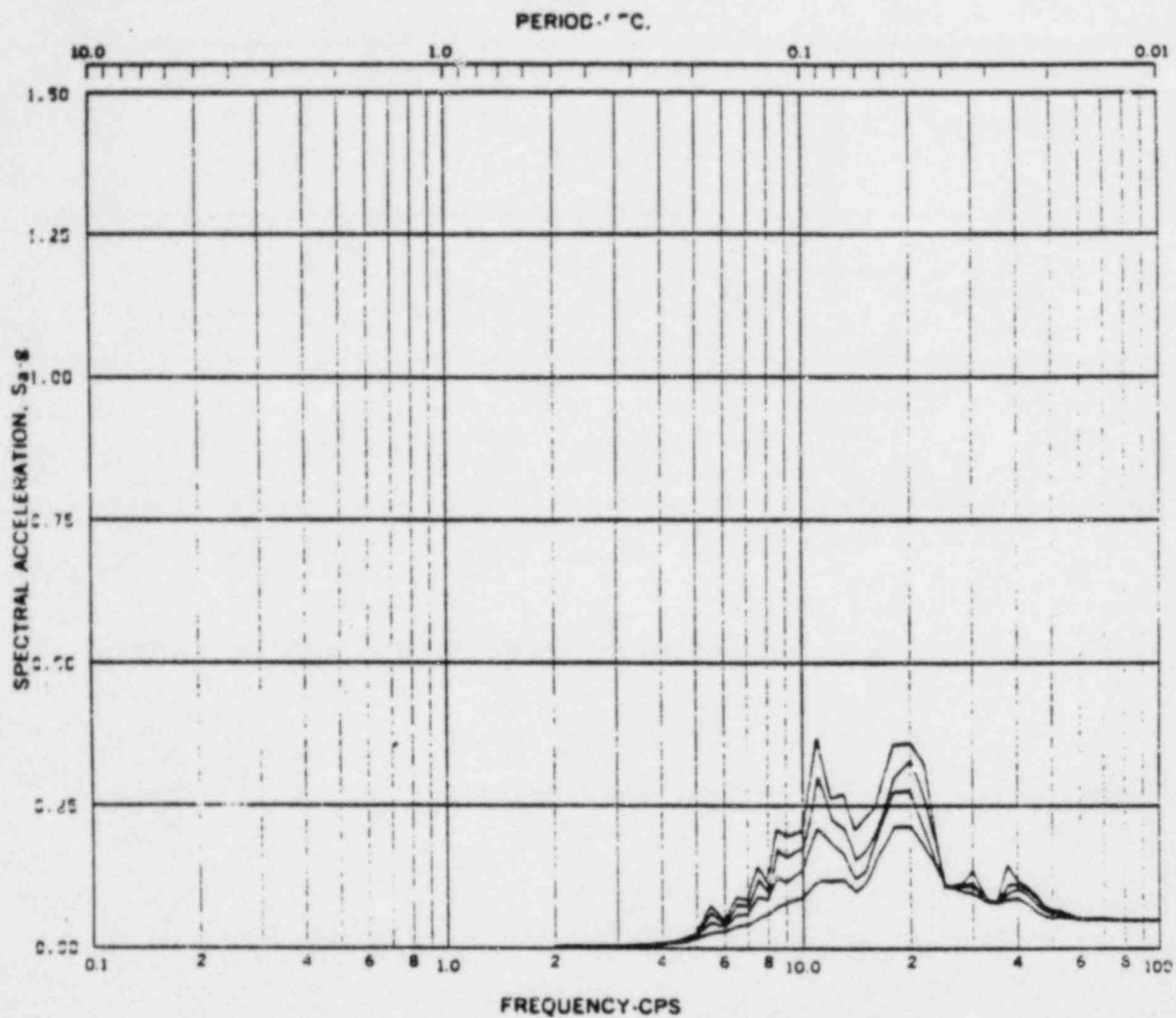
FIGURE B-43



Acceleration Spectra for PEDESTAL
 Load Case: Seismicity KWU 314 C.O.
 Mode 215, Direction W, Elev 702'-3"
 Damping: 0.005, 0.01, 0.02, 0.05

REV. 6, 4/82

SUSQUEHANNA STEAM ELECTRIC STATION UNITS 1 AND 2 DESIGN ASSESSMENT REPORT
CONTAINMENT RESPONSE SPECTRA KWU-COND. OSCIL.-#314 DIRECTION 'Z'
FIGURE B-24



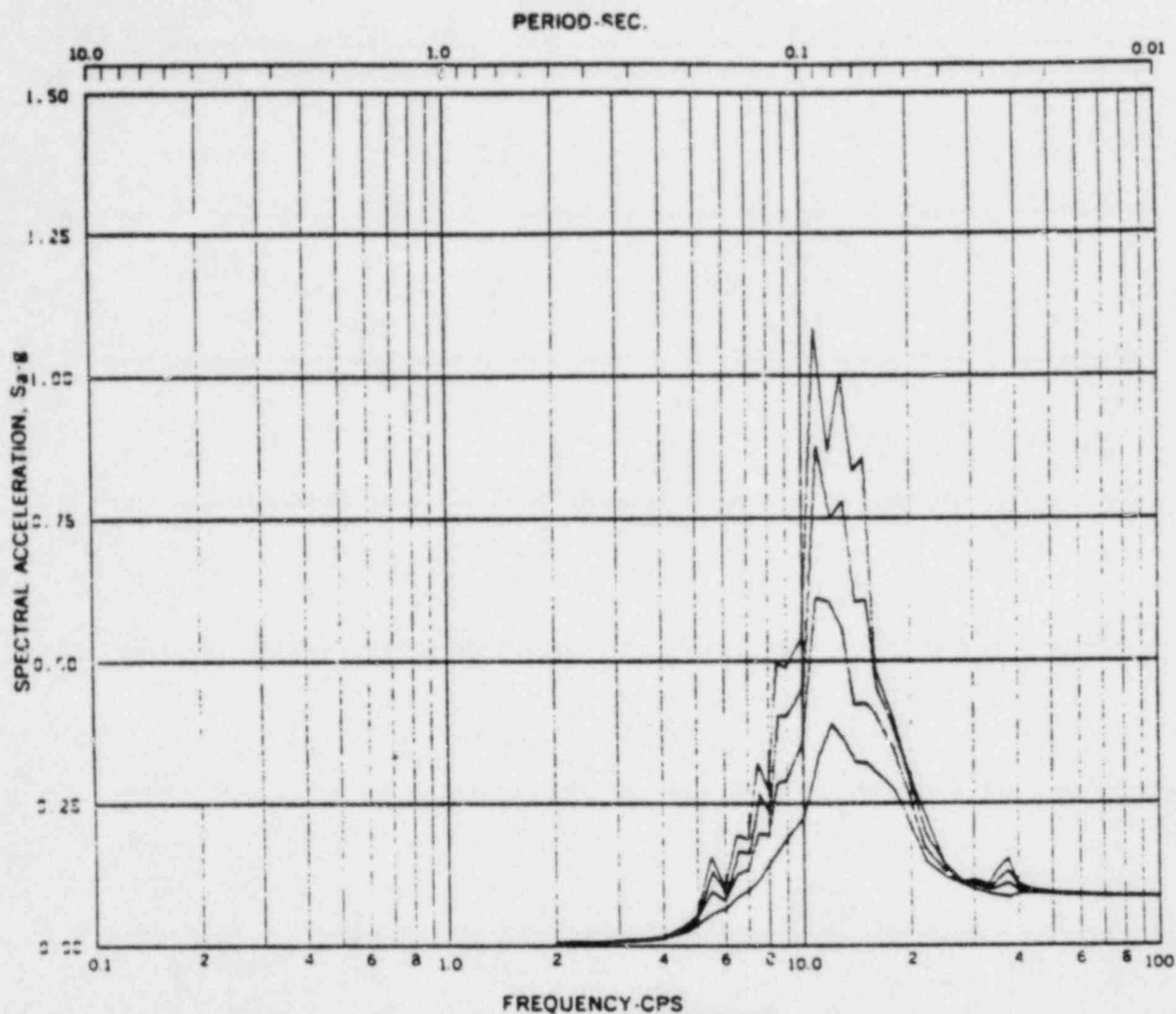
Acceleration Spectra for CONTAINMENT SHELL
 Load Case: BUSQUEHANNA KWU 314 C.O.
 Mode 415, Direction z, Elev 778' - 9-3/4"
 Damping: 0.005, 0.01, 0.02, 0.05

REV. 6, 4/82

BUSQUEHANNA STEAM ELECTRIC STATION
 UNITS 1 AND 2
 DESIGN ASSESSMENT REPORT

CONTAINMENT RESPONSE SPECTRA
 KWU-COND. OSCIL.-#314
 DIRECTION 'Z'

FIGURE B-45



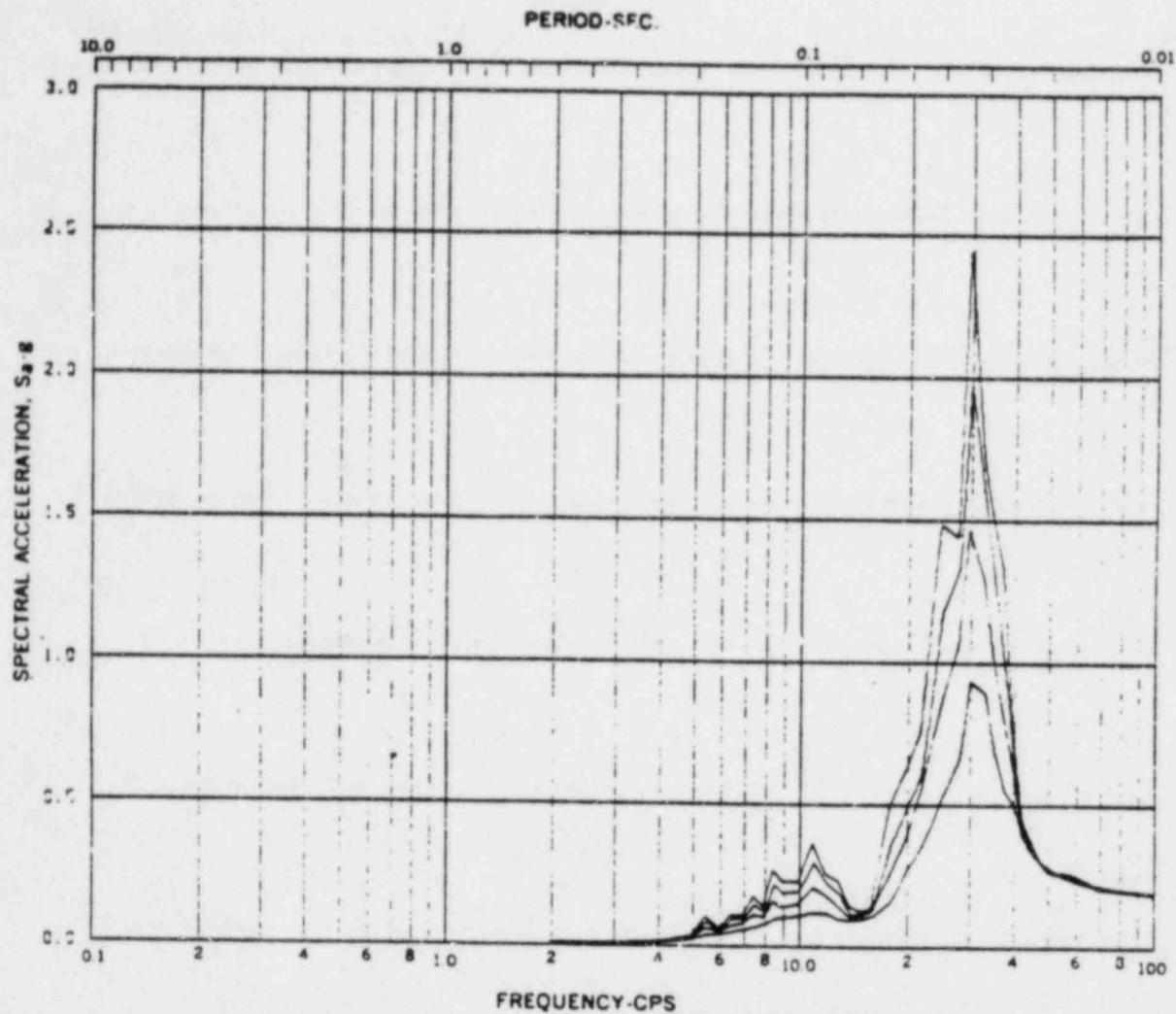
Acceleration Spectra for PEDESTAL
 Load Case: SUSQUEHANNA KWU 314 C.O.
 Mode 535, Direction X, Elev 729' - 9-3/4"
 Damping: 0.005, 0.01, 0.02, 0.05

REV. 6, 4/82

SUSQUEHANNA STEAM ELECTRIC STATION
UNITS 1 AND 2
DESIGN ASSESSMENT REPORT

CONTAINMENT RESPONSE SPECTRA
 KWU-COND. OSCIL.-#314
 DIRECTION 'Z'

FIGURE B-46



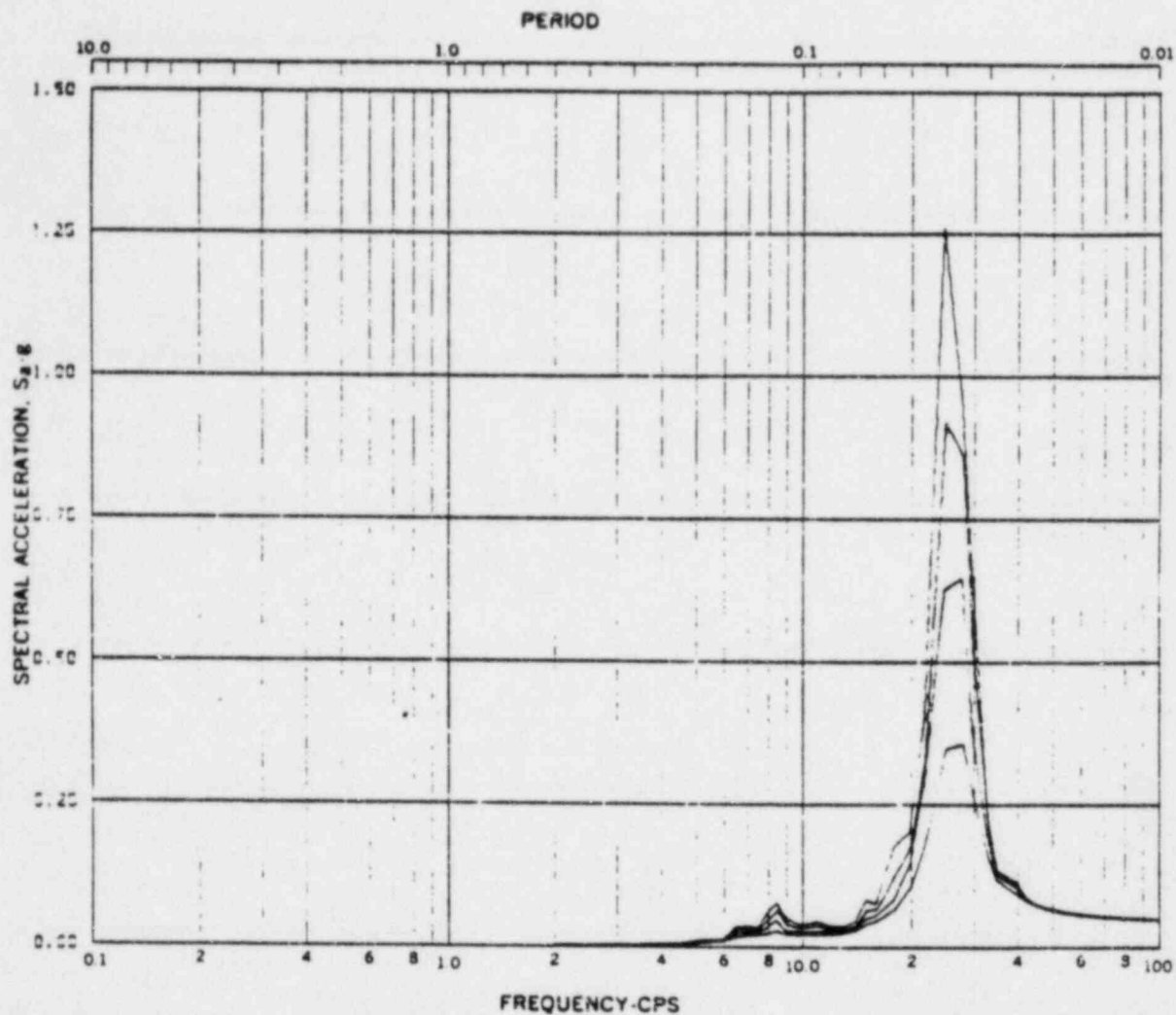
Acceleration Spectra for CONTAINMENT SHELL
 Load Case: Seismicity KWU 314 C.O.
 Mode 131, Direction X, Elev 672'-0"
 Damping: 0.005, 0.01, 0.02, 0.05

REV. 6, 4/82

SUSQUEHANNA STEAM ELECTRIC STATION
UNITS 1 AND 2
DESIGN ASSESSMENT REPORT

CONTAINMENT RESPONSE SPECTRA
 KWU-COND. OSCIL.-#314
 DIRECTION 'X'

FIGURE B-47



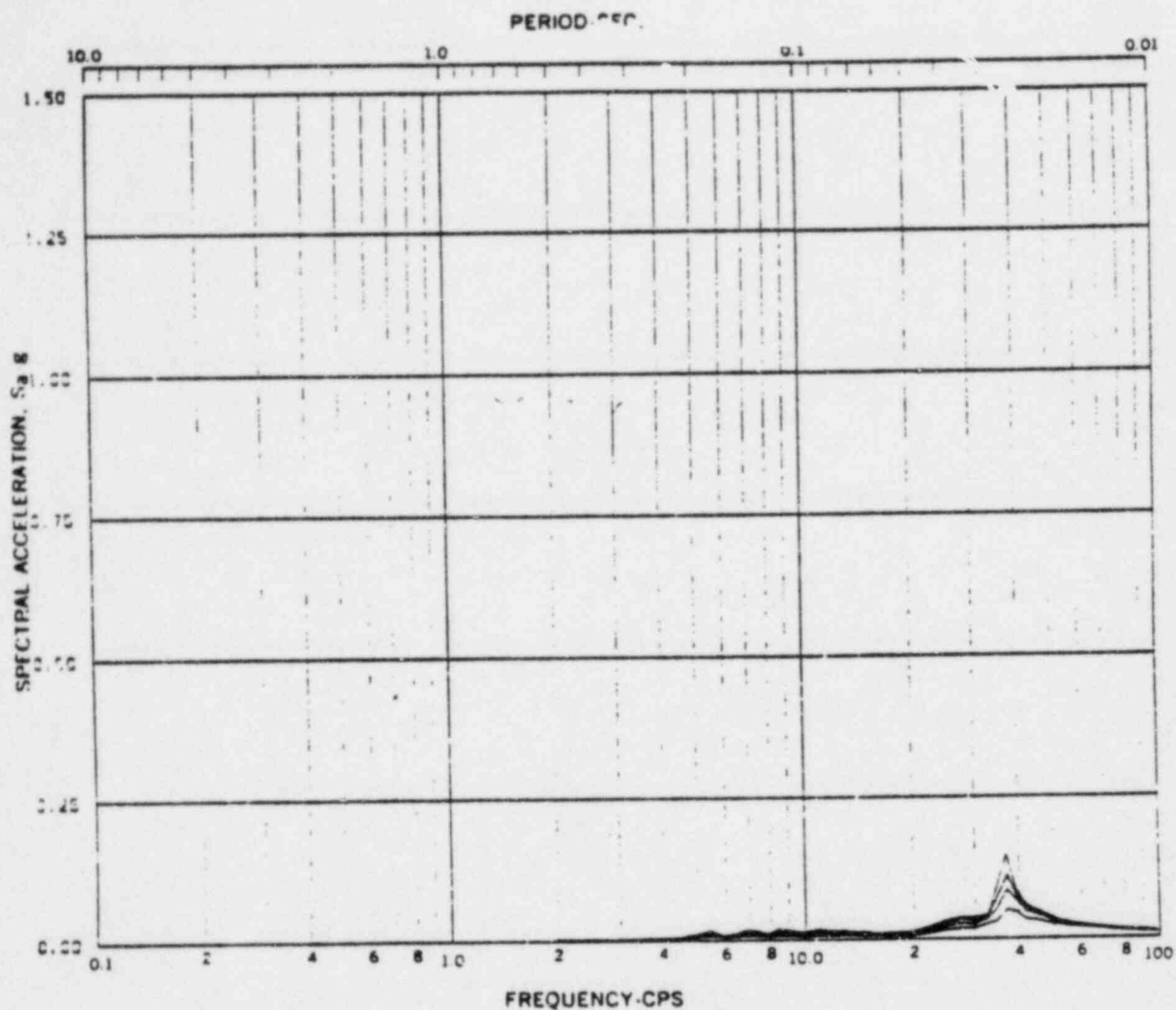
Acceleration Spectra for CONTAINMENT SHELL
 Load Case: Seismicity KWU 314 C.O.
 Mode 411, Direction X, Elev 778' - 9-3/4"
 Damping: 0.005, 0.01, 0.02, 0.05

REV. 6, 4/82

SUSQUEHANNA STEAM ELECTRIC STATION
UNITS 1 AND 2
DESIGN ASSESSMENT REPORT

CONTAINMENT RESPONSE SPECTRA
 KWU-COND. OSCIL.-#314
 DIRECTION 'X'

FIGURE B-48



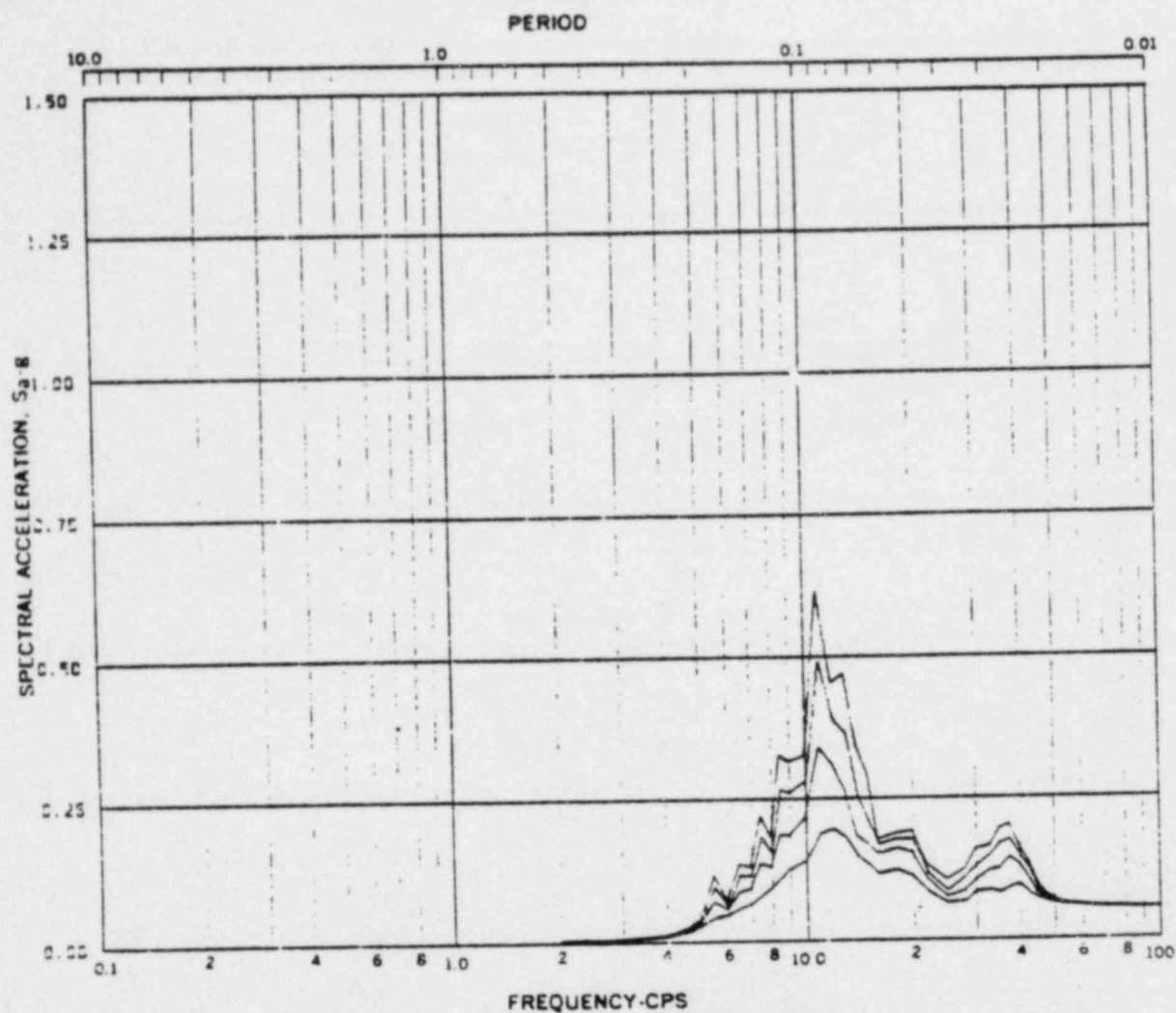
Acceleration Spectra for PEDESTAL
 Load Case: Susquehanna KWU 314 C.O.
 Mode 531, Direction X, Elev 729' - 9-3/4"
 Damping: 0.056, 0.01, 0.02, 0.05

REV. 6, 4/82

SUSQUEHANNA STEAM ELECTRIC STATION
 UNITS 1 AND 2
 DESIGN ASSESSMENT REPORT

CONTAINMENT RESPONSE SPECTRA
 KWU-COND. OSCIL. #314
 DIRECTION 'X'

FIGURE B-49



Acceleration Spectra for DIAPHRAGM SLAB
 Load Case: SEISMIC KWU 314 COO.
 Mode 752*, Direction X, Elev 702'-3"
 Damping: 0.005, 0.01, 0.02, 0.05

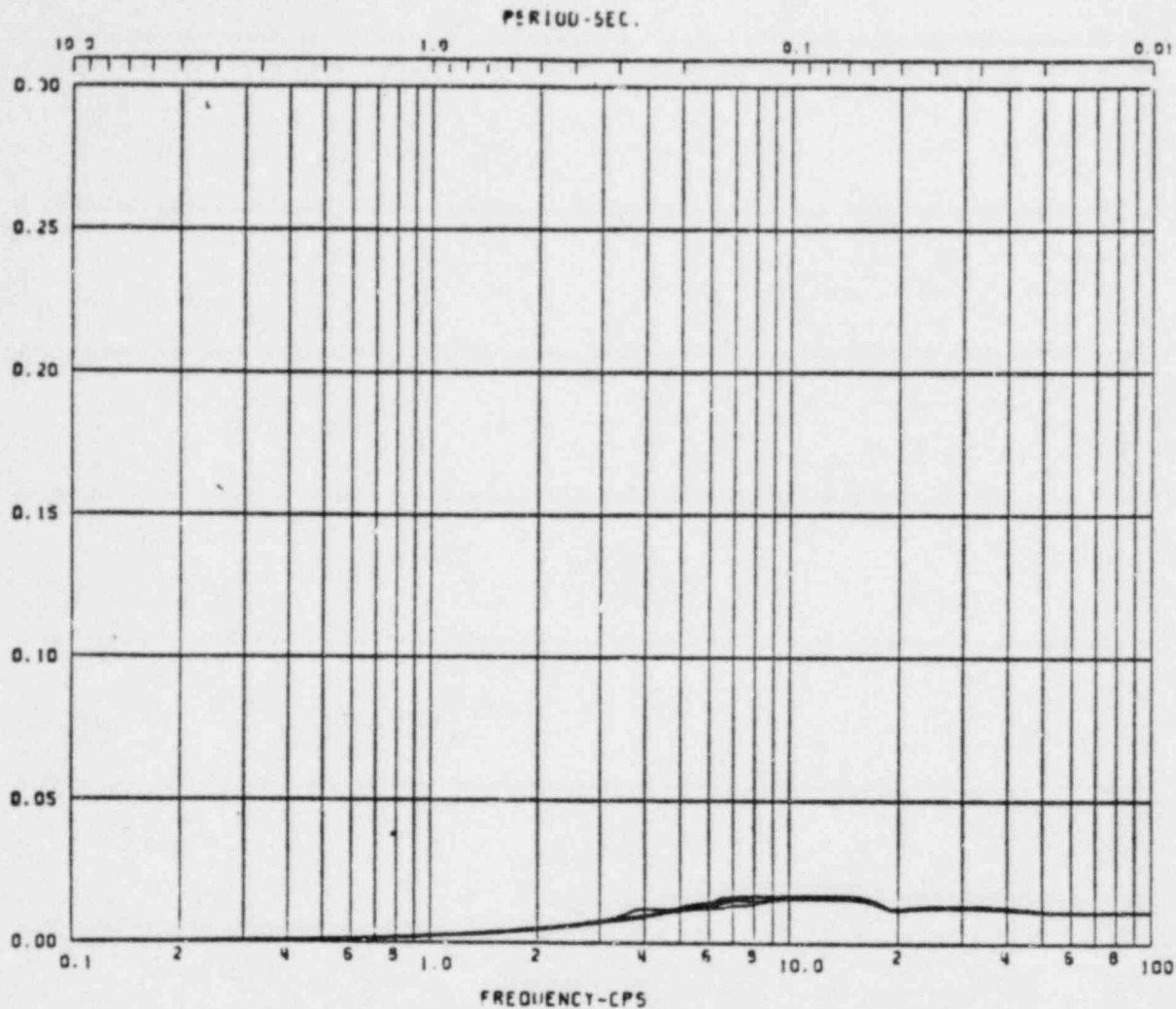
REV. 6, 4/82

BUSQUEHANNA STEAM ELECTRIC STATION
UNITS 1 AND 2
DESIGN ASSESSMENT REPORT

CONTAINMENT RESPONSE SPECTRA
 KWU-COND. OSCIL.-#314
 DIRECTION 'Z'

FIGURE B-50

SPECTRAL ACCELERATION, SA-C



Acceleration Spectra for CONTAINMENT SHELL
Seismic Slosh
Load Case: Susquehanna
Node 131, Direction X, Elev 672'-0"
Damping: 0.005, 0.01, 0.02, 0.05

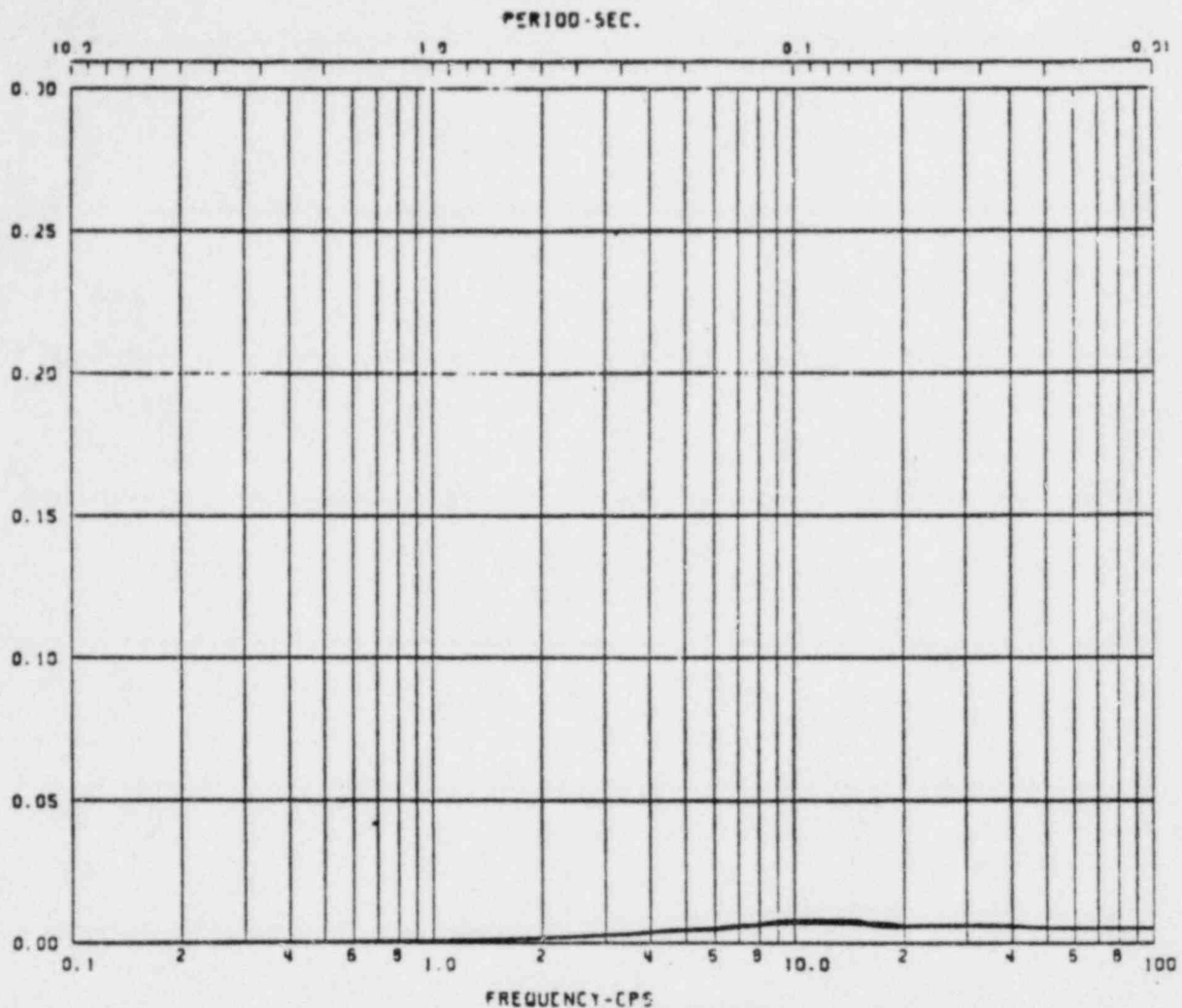
REV. 6, 4/82

**SUSQUEHANNA STEAM ELECTRIC STATION
UNITS 1 AND 2
DESIGN ASSESSMENT REPORT**

**CONTAINMENT RESPONSE SPECTRA
SEISMIC SLOSHING
DIRECTION 'X'**

FIGURE B-51

SPECTRAL ACCELERATION, SA-C



Acceleration Spectra for CONTAINMENT SHELL
 Load Case: Susquehanna Seismic Sloss
 Node 135, Direction X, Elev 672'-0"
 Damping: 0.005, 0.01, 0.02, 0.05

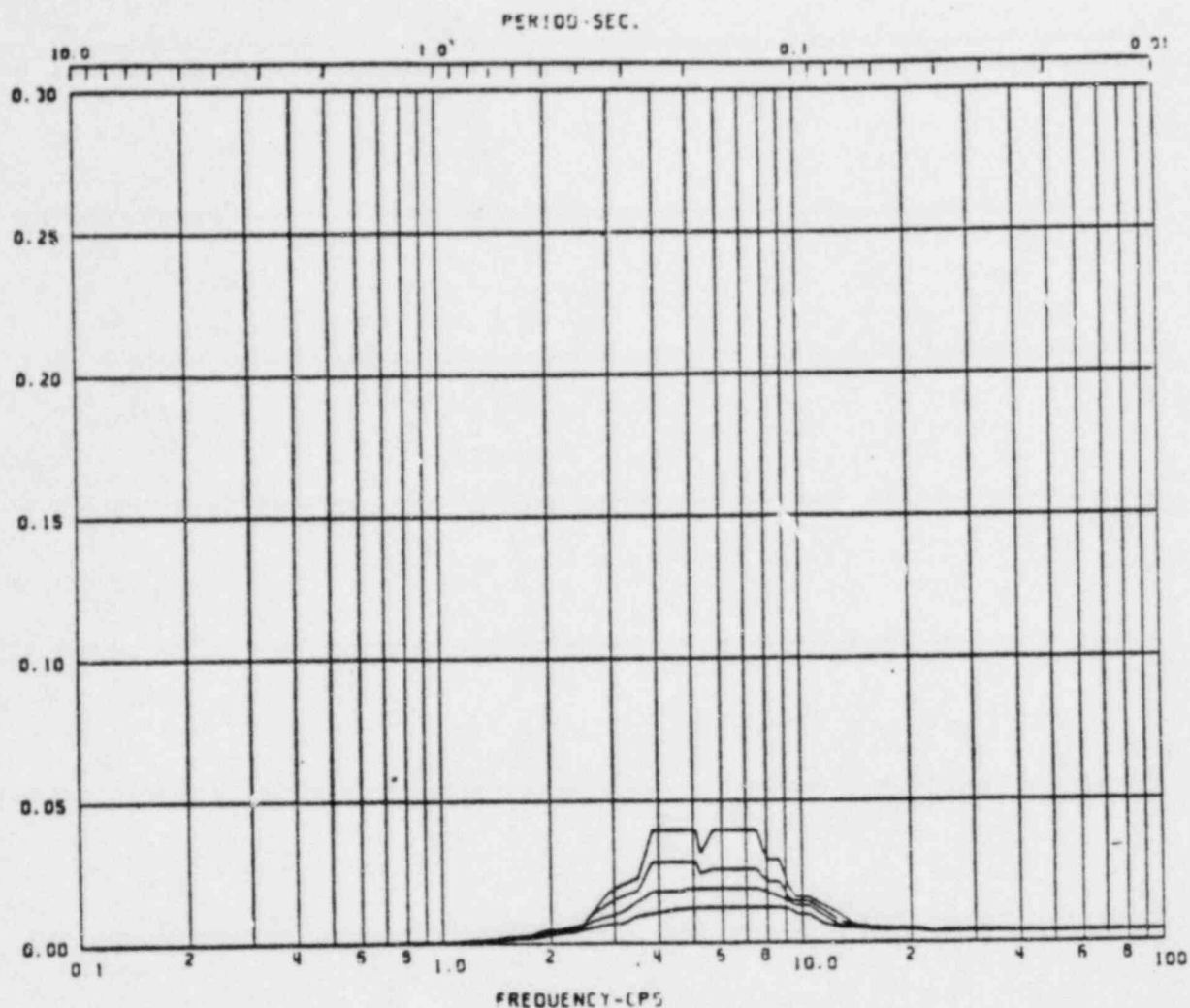
REV. 6, 4/82

**SUSQUEHANNA STEAM ELECTRIC STATION
 UNITS 1 AND 2
 DESIGN ASSESSMENT REPORT**

**CONTAINMENT RESPONSE SPECTRA
 SEISMIC SLOSHING
 DIRECTION 'X'**

FIGURE B-52

SPECTRAL ACCELERATION, SA-C



Acceleration Spectra for CONTAINMENT SHELL
Load Case: Susquehanna Seismic Slosh
Mode 411, Direction X, Elev 778' - 9-3/4"
Damping: 0.005, 0.01, 0.02, 0.05

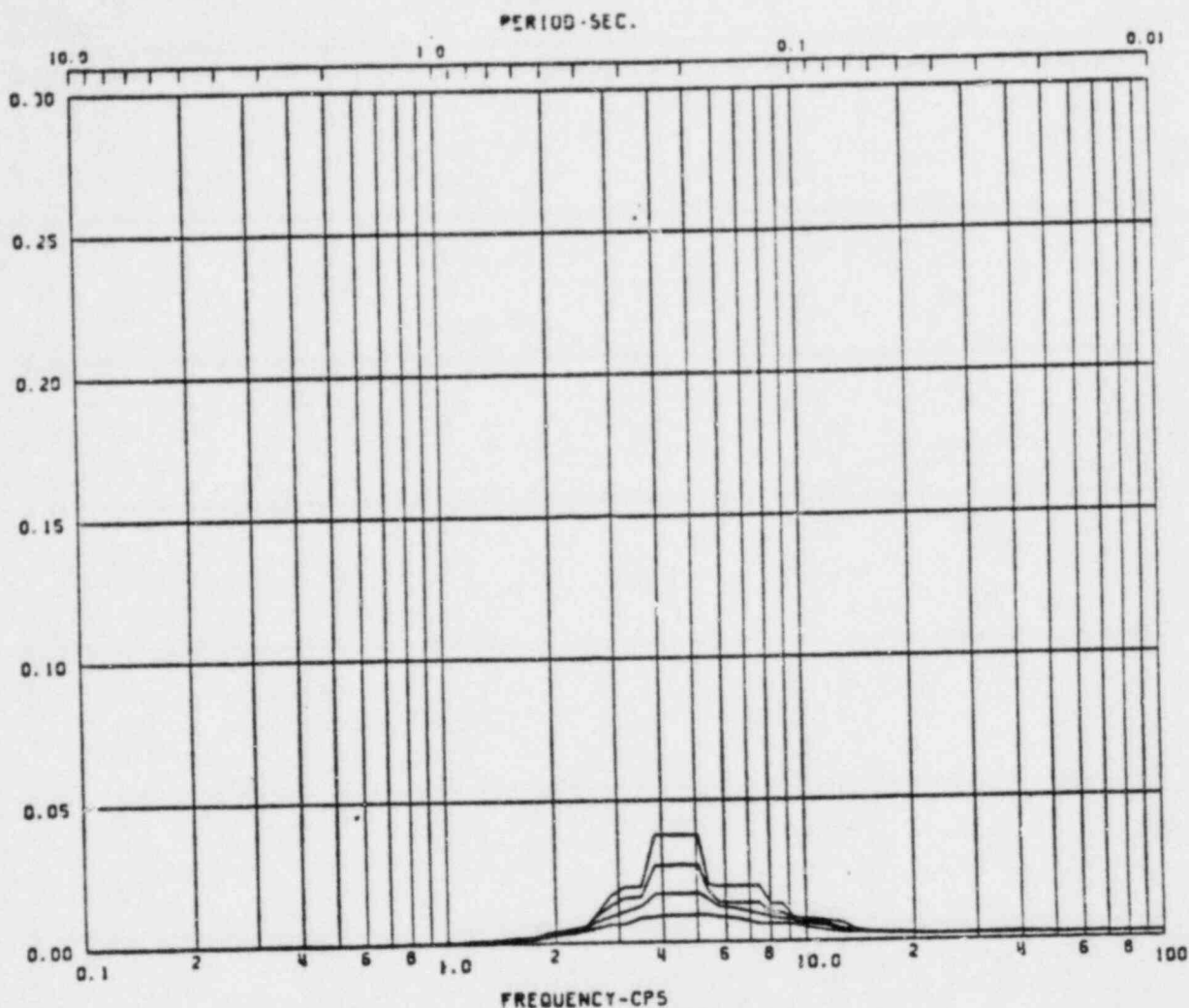
REV. 6, 4/82

BUSQUEHANNA STEAM ELECTRIC STATION
UNITS 1 AND 2
DESIGN ASSESSMENT REPORT

CONTAINMENT RESPONSE SPECTRA
SEISMIC SLOSHING
DIRECTION 'X'

FIGURE B-53

SPECTRAL ACCELERATION, SA-C



Acceleration Spectra for PEDESTAL
 Load Case: Susquehanna Seismic Slosh
 Mode 531, Direction X, Elev 729'-9-3/4"
 Damping: 0.005, 0.01, 0.02, 0.05

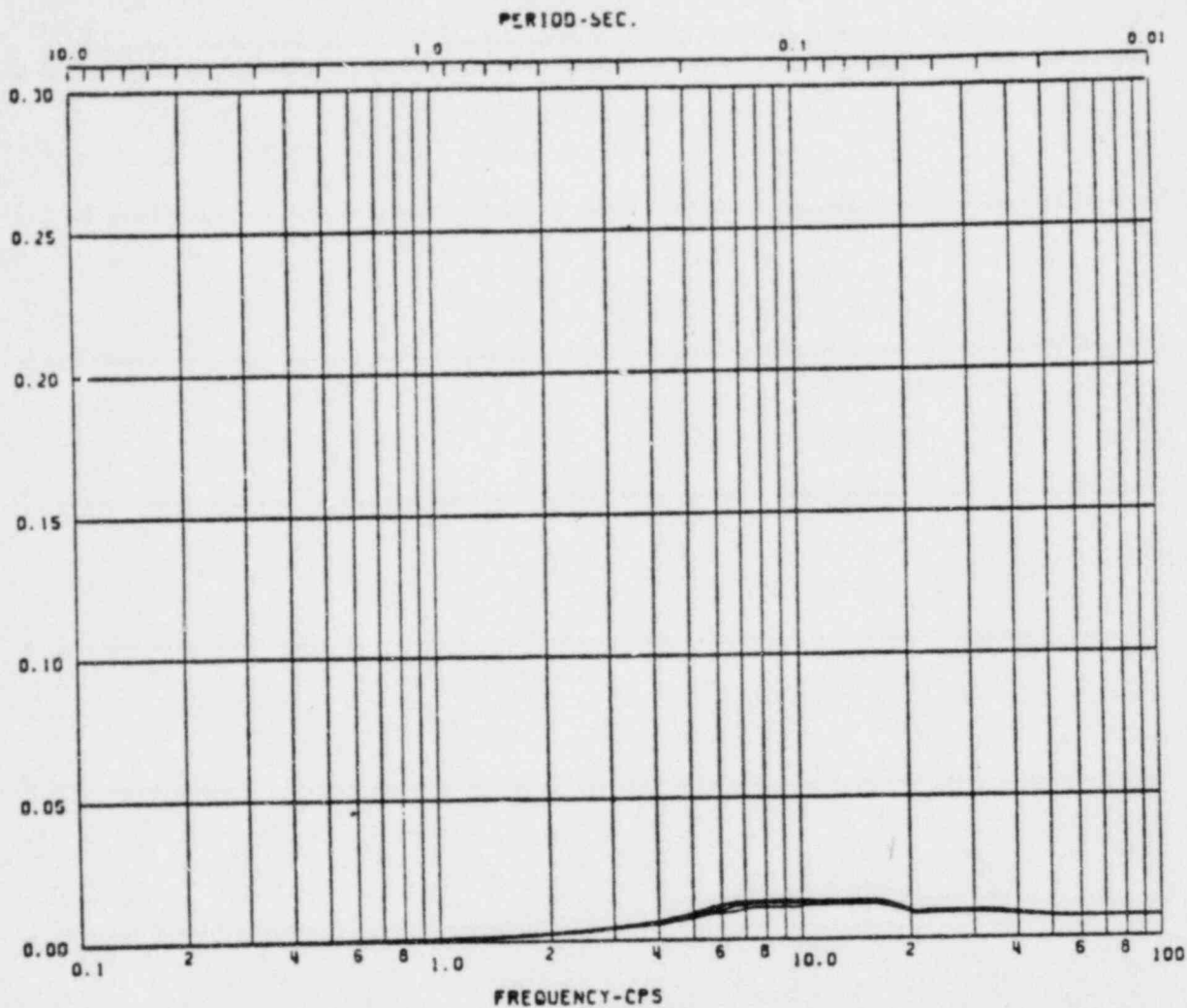
REV. 6, 4/82

BUSQUEHANNA STEAM ELECTRIC STATION
 UNITS 1 AND 2
 DESIGN ASSESSMENT REPORT

CONTAINMENT RESPONSE SPECTRA
 SEISMIC SLOSHING
 DIRECTION 'X'

FIGURE B-54

SPECTRAL ACCELERATION, SA-C



Acceleration Spectra for PEDESTAL
 Load Case: Seismic SLOSH
 Node 215, Direction Z, Elev 702'-3"
 Damping: 0.005, 0.01, 0.02, 0.05

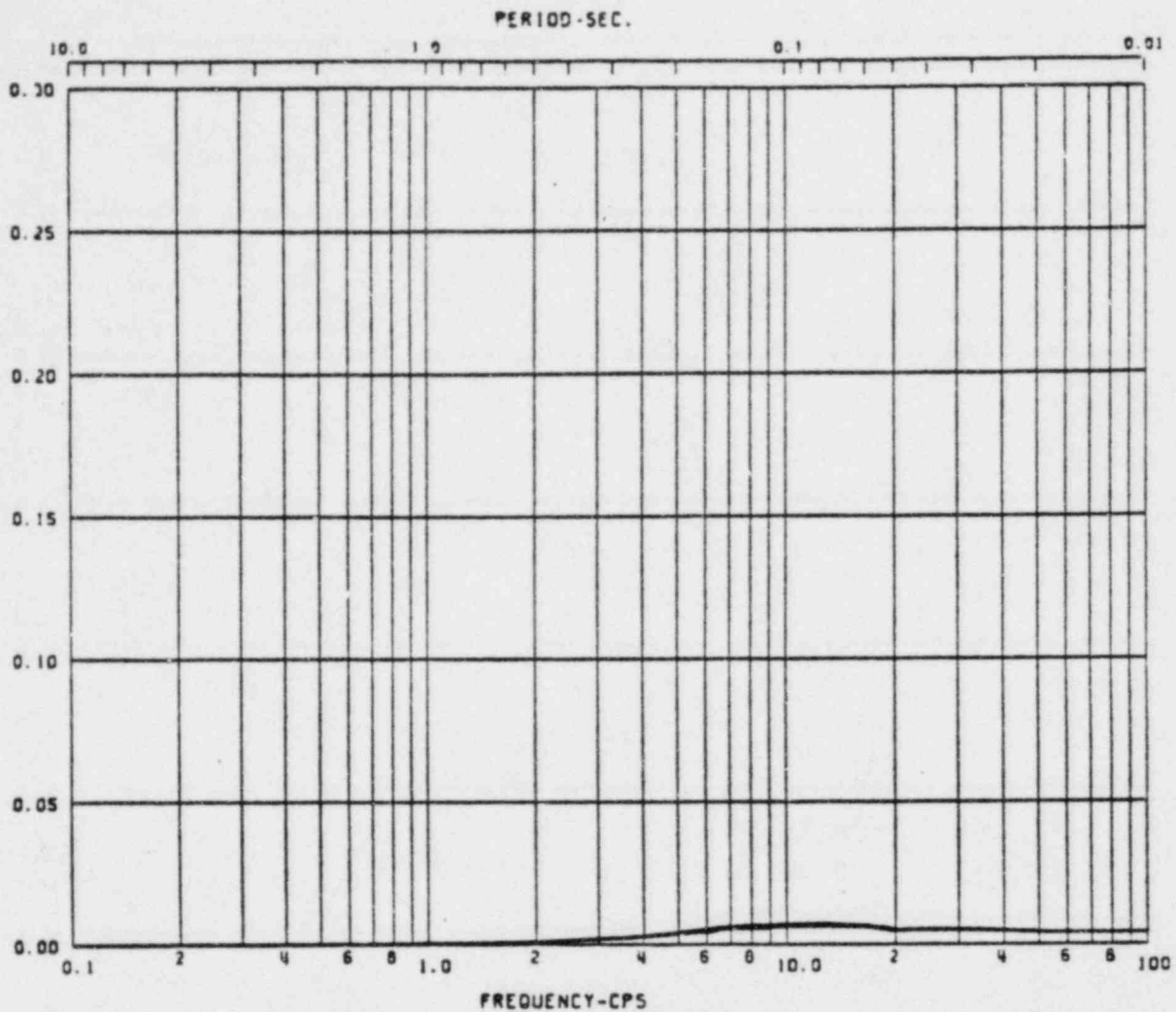
REV. 6, 4/82

BUSQUEHANNA STEAM ELECTRIC STATION
 UNITS 1 AND 2
 DESIGN ASSESSMENT REPORT

CONTAINMENT RESPONSE SPECTRA
 SEISMIC SLOSHING
 DIRECTION 'Z'

FIGURE B-55

SPECTRAL ACCELERATION, SA-C



Acceleration Spectra for CONTAINMENT SHELL
Load Case: SUSQUEHANNA Seismic Slosh
Node 415, Direction Z, Elev 778' - 9-3/4"
Damping: 0.005, 0.01, 0.02, 0.05

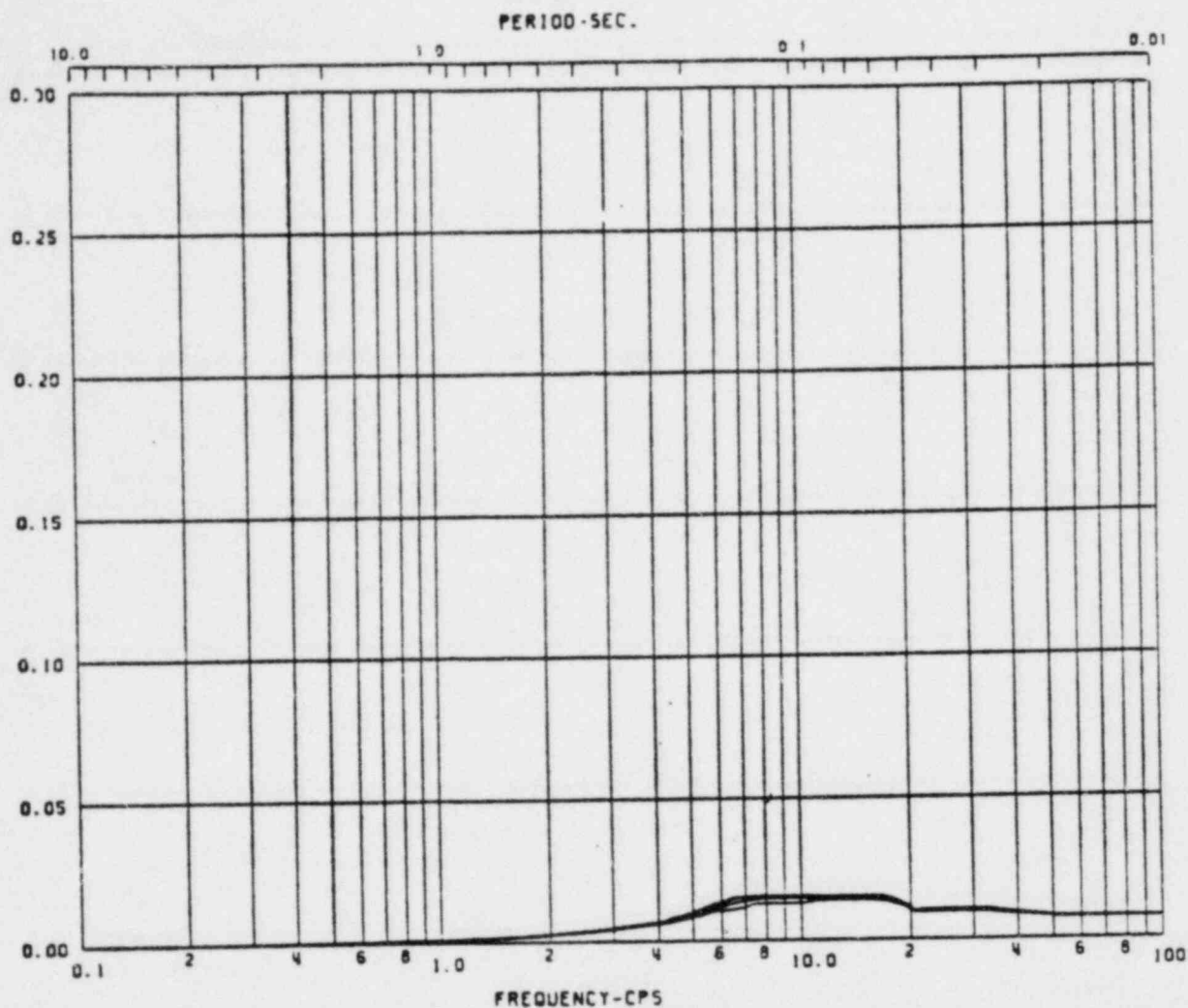
REV. 6, 4/82

SUSQUEHANNA STEAM ELECTRIC STATION
UNITS 1 AND 2
DESIGN ASSESSMENT REPORT

CONTAINMENT RESPONSE SPECTRA
SEISMIC SLOSHING
DIRECTION 'Z'

FIGURE B-56

SPECTRAL ACCELERATION, SA-C



Acceleration Spectra for PEDESTAL
Load Case: Seismic SLOSH
Node 535, Direction Z, Elev 729'-9-3/4"
Damping: 0.005, 0.01, 0.02, 0.05

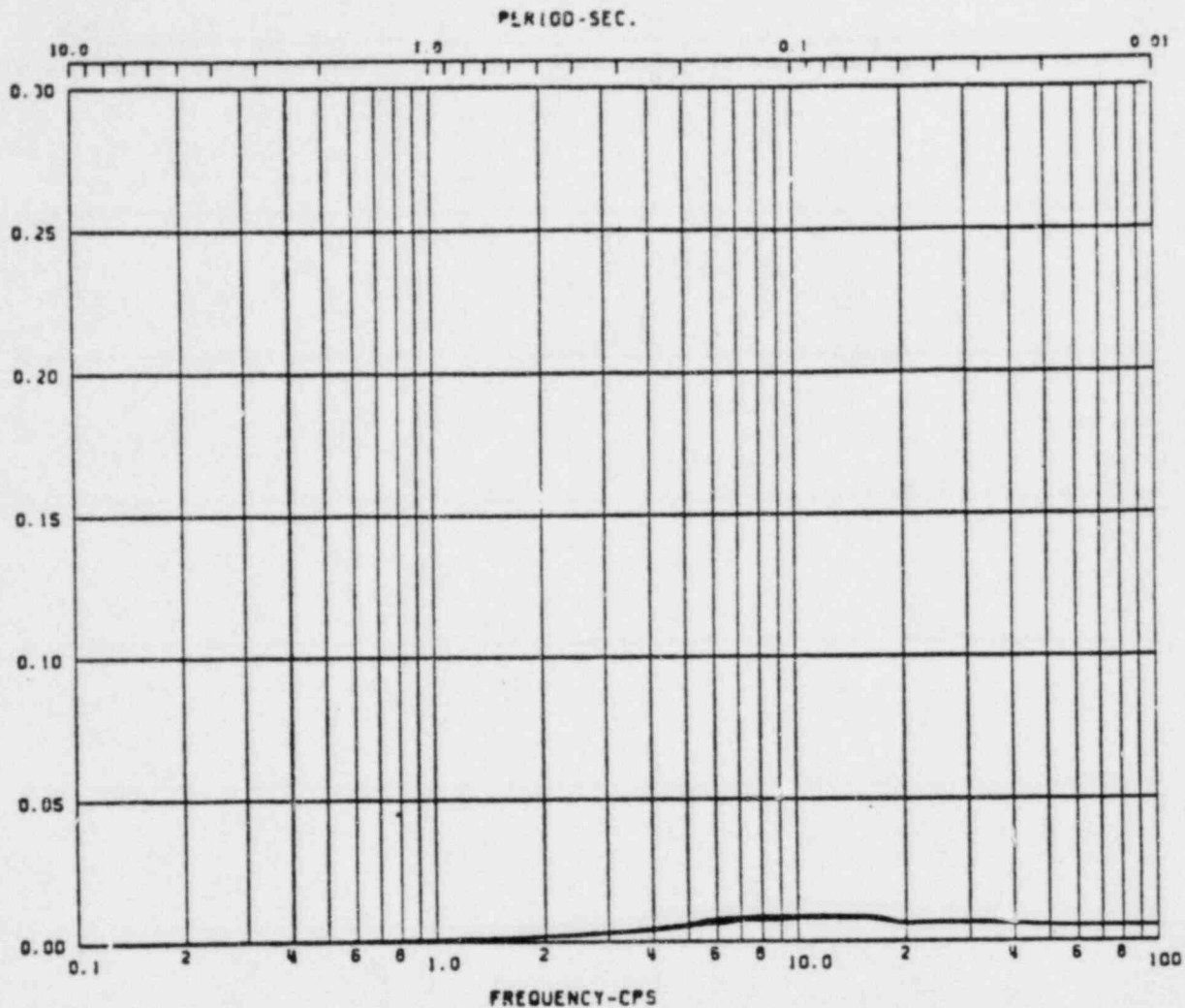
REV. 6, 4/82

**BUSQUEHANNA STEAM ELECTRIC STATION
UNITS 1 AND 2
DESIGN ASSESSMENT REPORT**

**CONTAINMENT RESPONSE SPECTRA
SEISMIC SLOSHING
DIRECTION 'Z'**

FIGURE B-57

SPECTRAL ACCELERATION, SA-C



Acceleration Spectra for DIAPHRAGM SLAB
Load Case: Susquehanna Seismic Slosh
Node 252, Direction Z, Elev 702'-3"
Damping: 0.005, 0.01, 0.02, 0.05

REV. 6, 4/82

SUSQUEHANNA STEAM ELECTRIC STATION
UNITS 1 AND 2
DESIGN ASSESSMENT REPORT

CONTAINMENT RESPONSE SPECTRA
SEISMIC SLOSHING
DIRECTION 'Z'

FIGURE B-58

APPENDIX C
REACTOR BUILDING RESPONSE SPECTRA
DUE TO LOCA AND SRV

APPENDIX C

FIGURES

Number	Title
C-1	Model for Reactor Building Response Spectra, North-South
C-2	Model for Reactor Building Response Spectra, East-West
C-3	Model for Reactor Building
C-4 thru C-20	Reactor Building Response Spectra-KWU SRV Vertical Direction
C-21 thru C-37	Reactor Building Response Spectra-KWU SRV East-West Direction
C-38 thru C-54	Reactor Building Response Spectra-KWU LOCA Vertical Direction
C-55 thru C-71	Reactor Building Response Spectra-KWU LOCA East-West Direction
C-72 thru C-87	Reactor Building Response Spectra-KWU LOCA North-South Direction
C-88 thru C-103	Reactor Building Response Spectra-KWU SRV North-South Direction

APPENDIX C

REACTOR RESPONSE SPECTRA DUE TO LOCA AND SRV

This appendix shows the reactor building models and examples of the horizontal and vertical response spectra curves of the reactor building due to LOCA and SRV loading. Four spectral damping values (i.e. 0.005, 0.01, 0.02 and 0.05) are shown on each group of curves.

The mathematical models of the reactor building are shown in Figures C-1, C-2 and C-3. The broadened acceleration response spectra shown in C-4 to C-103 are submitted as representative examples of the reactor building structure response spectra. These response spectra are also taken at critical locations of the reactor building structure. The loads under consideration are SRV and LOCA.

The SRV load (generated by KWU) consists of 3 traces and each trace consists of 5 frequencies. The asymmetric and axisymmetric load cases are considered. They are generated in the North-South, East-West and Vertical directions.

The LOCA load case consists of chugging and condensation oscillation loads. Each of the chugging and condensation oscillation loads contain 3 frequencies. Axisymmetric load cases are considered for both chugging and CO, while the asymmetric load is only considered for chugging. The response spectra are generated in the North-South, East-West and Vertical directions from an envelope of the chugging and CO spectra. They are also broadened by $\pm 15\%$ at peak frequencies to account for uncertainties in the modelling and material properties.

3

6

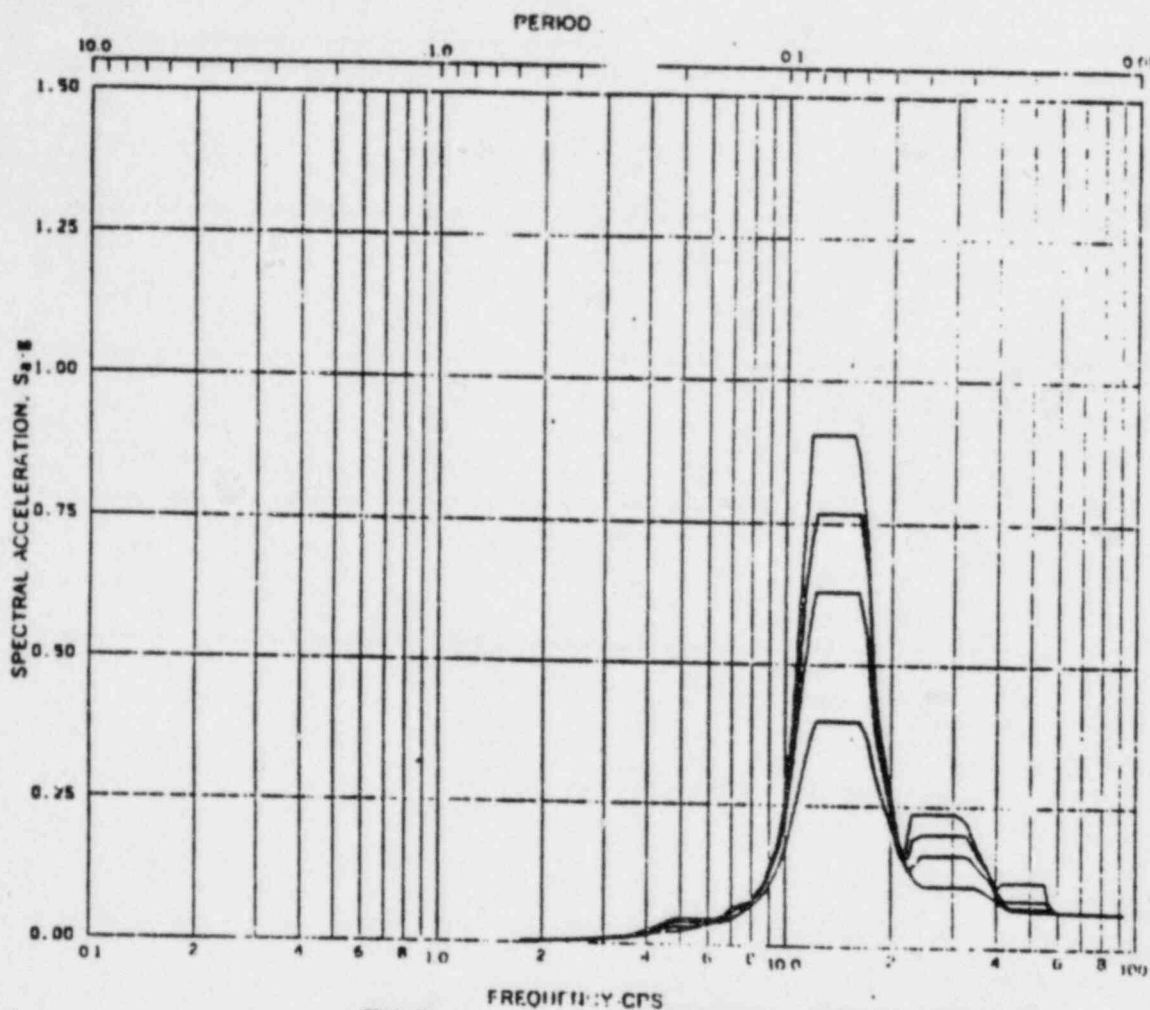


Fig. BV1-3 Acceleration Spectra for REACTOR & CONTROL BLDGS.
 Load Case: Susquehanna SRV
 Mode -, Direction VERT, Elev 670'-0"
 Damping: 0.005, 0.01, 0.02, 0.06

REV. 6, 4/82

**SUSQUEHANNA STEAM ELECTRIC STATION
 UNITS 1 AND 2
 DESIGN ASSESSMENT REPORT**

**REACTOR/CONTROL BUILDING
 RESPONSE SPECTRA**

**KWU-SRV
 FIGURE C-4**

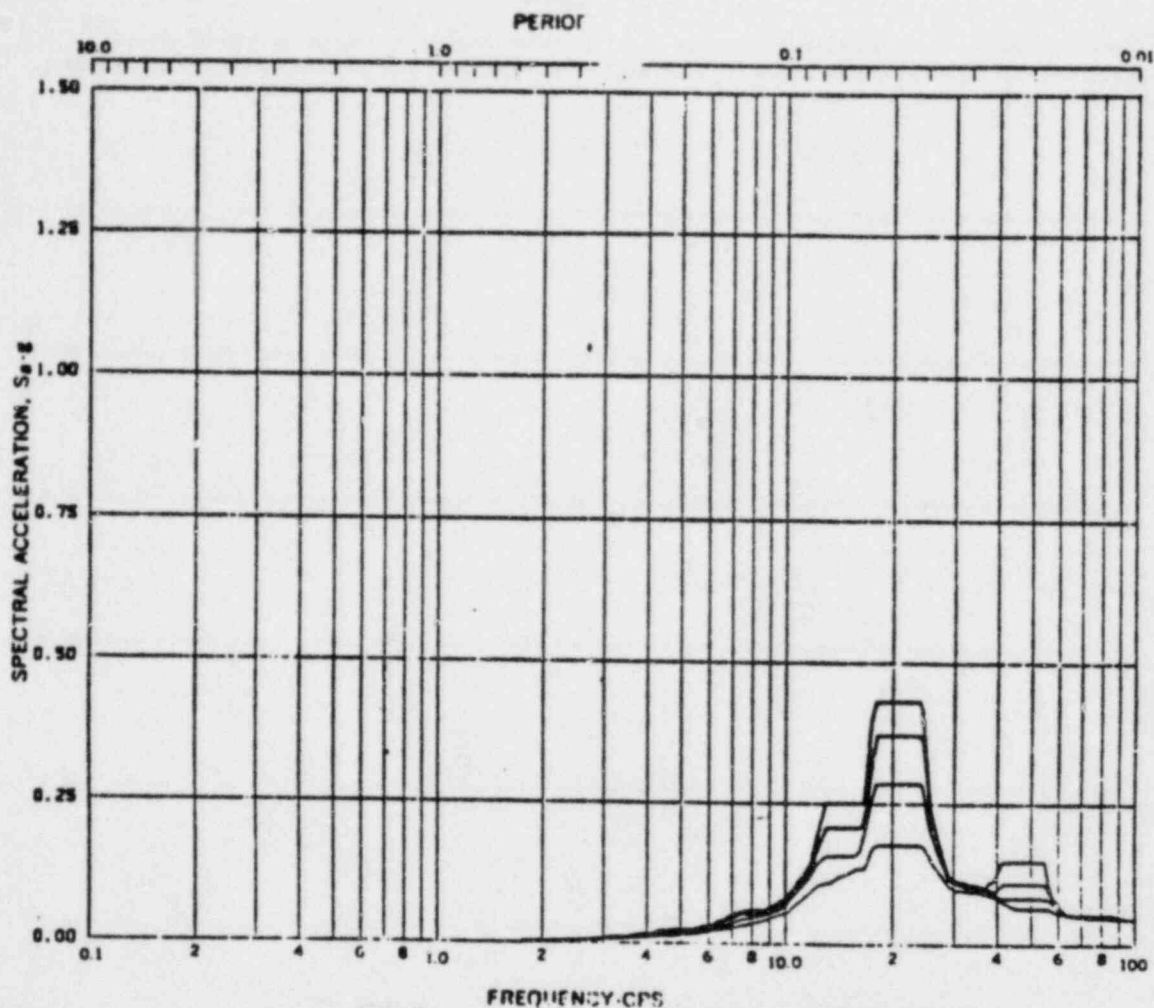


Fig. BV2-3 Acceleration Spectra for REACTOR & CONTROL BLDGS.
 Load Case: Susquehanna SRV
 Node -, Direction VERT, Elev 676'-0"
 Damping: 0.005, 0.01, 0.02, 0.05

REV. 6, 4/82

SUSQUEHANNA STEAM ELECTRIC STATION UNITS 1 AND 2 DESIGN ASSESSMENT REPORT
REACTOR/CONTROL BUILDING RESPONSE SPECTRA
KWU-SRV FIGURE C- 5

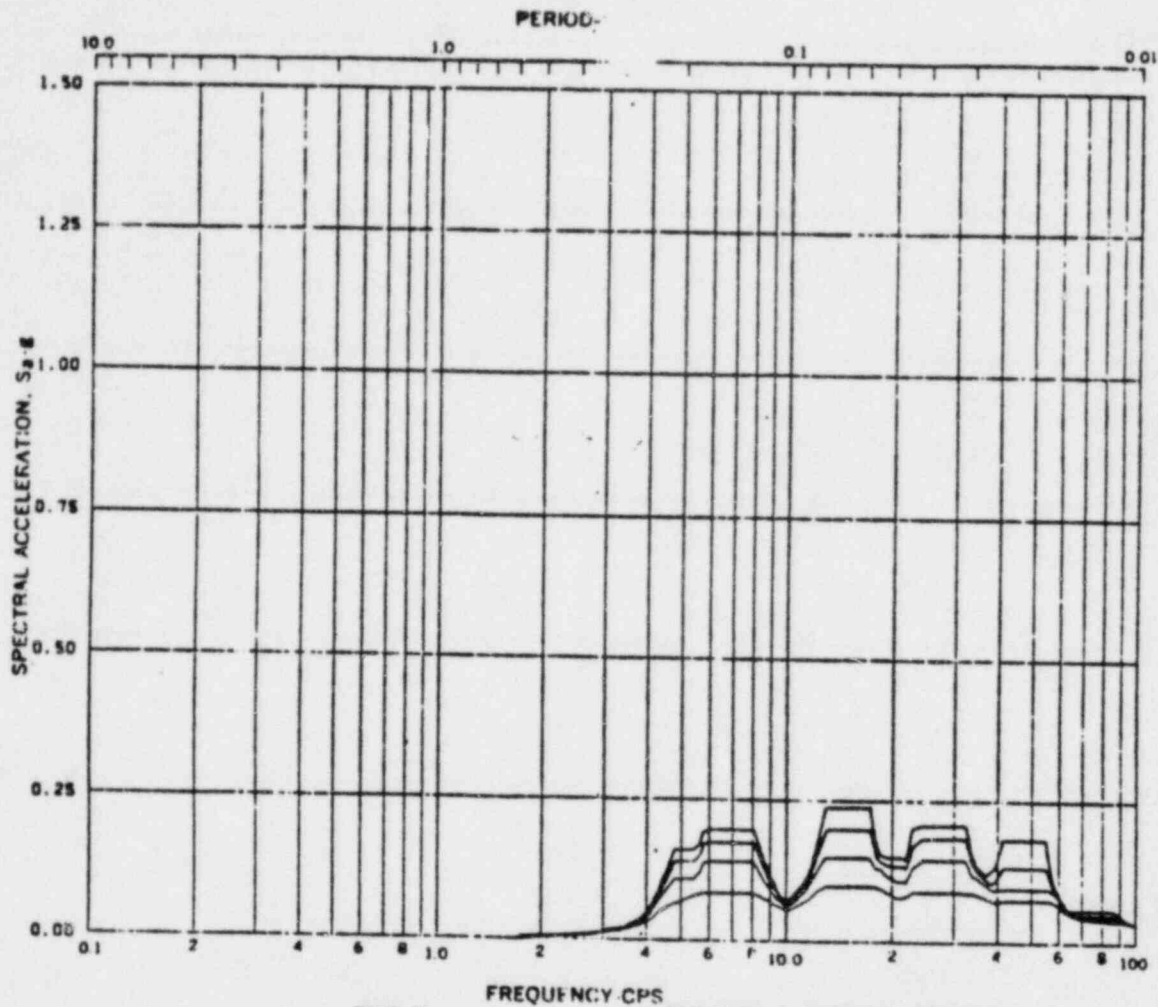


Fig. BV3-3 Acceleration Spectra for REACTOR & CONTROL BLDGS.
 Load Case: Susquehanna SRV
 Mode --- Direction VERT Elev 583'-0"
 Damping: 0.005, 0.01, 0.02, 0.05

REV. 6, 4/82

**SUSQUEHANNA STEAM ELECTRIC STATION
 UNITS 1 AND 2
 DESIGN ASSESSMENT REPORT**

**REACTOR/CONTROL BUILDING
 RESPONSE SPECTRA**

KWU-SRV

FIGURE C-6

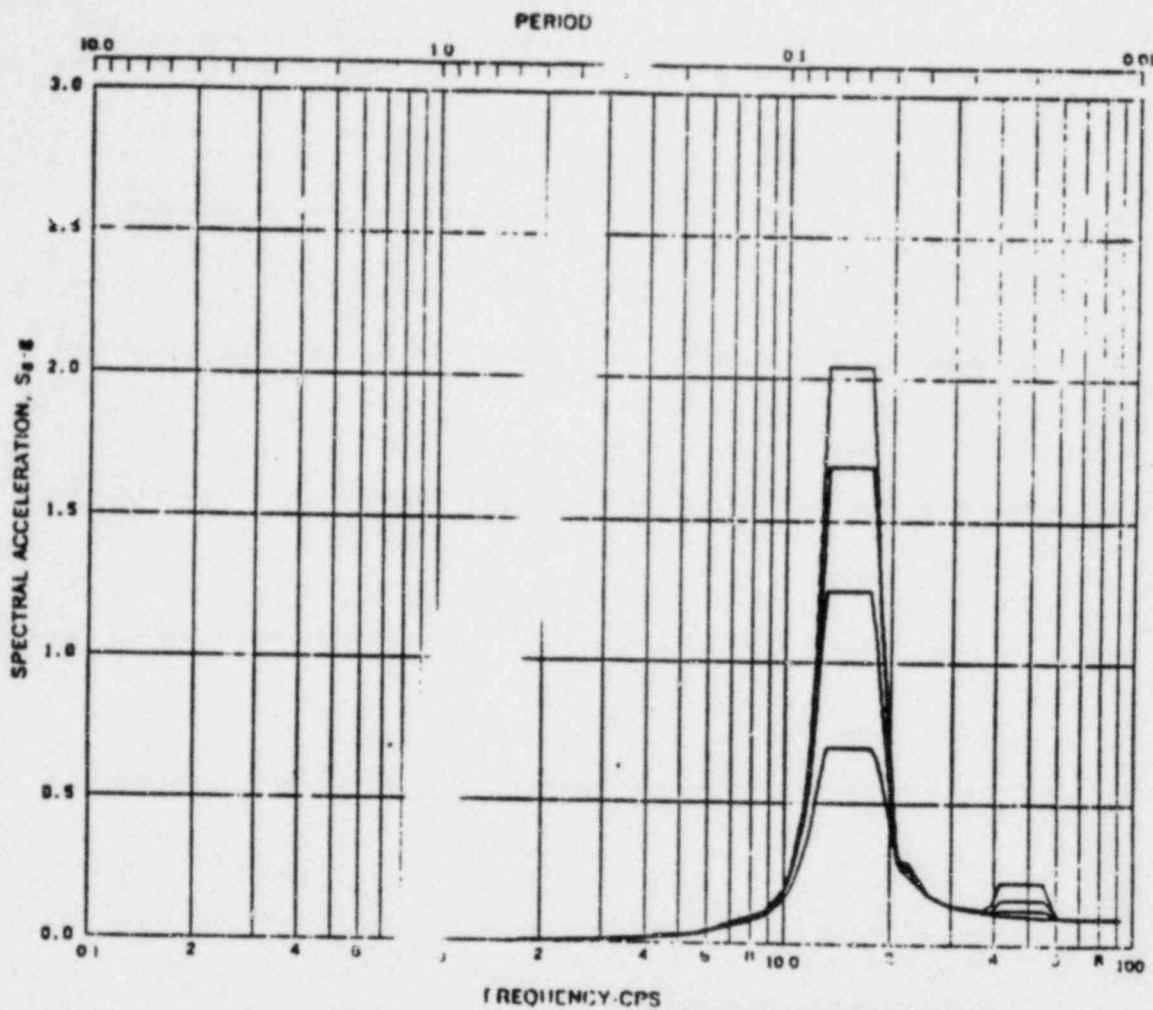


Fig. RV.4

Acceleration Spectra for REACTOR & CONTROL BLDGS.

Lead Case: Busquehanna SRV

Mode -, Direction VERT, Elev 697'-0"

Damping: 0.005, 0.01, 0.02, 0.05

REV. 6, 4/82

**BUSQUEHANNA STEAM ELECTRIC STATION
UNITS 1 AND 2
DESIGN ASSESSMENT REPORT**

**REACTOR/CONTROL BUILDING
RESPONSE SPECTRA**

KWU-SRV

FIGURE C- 7

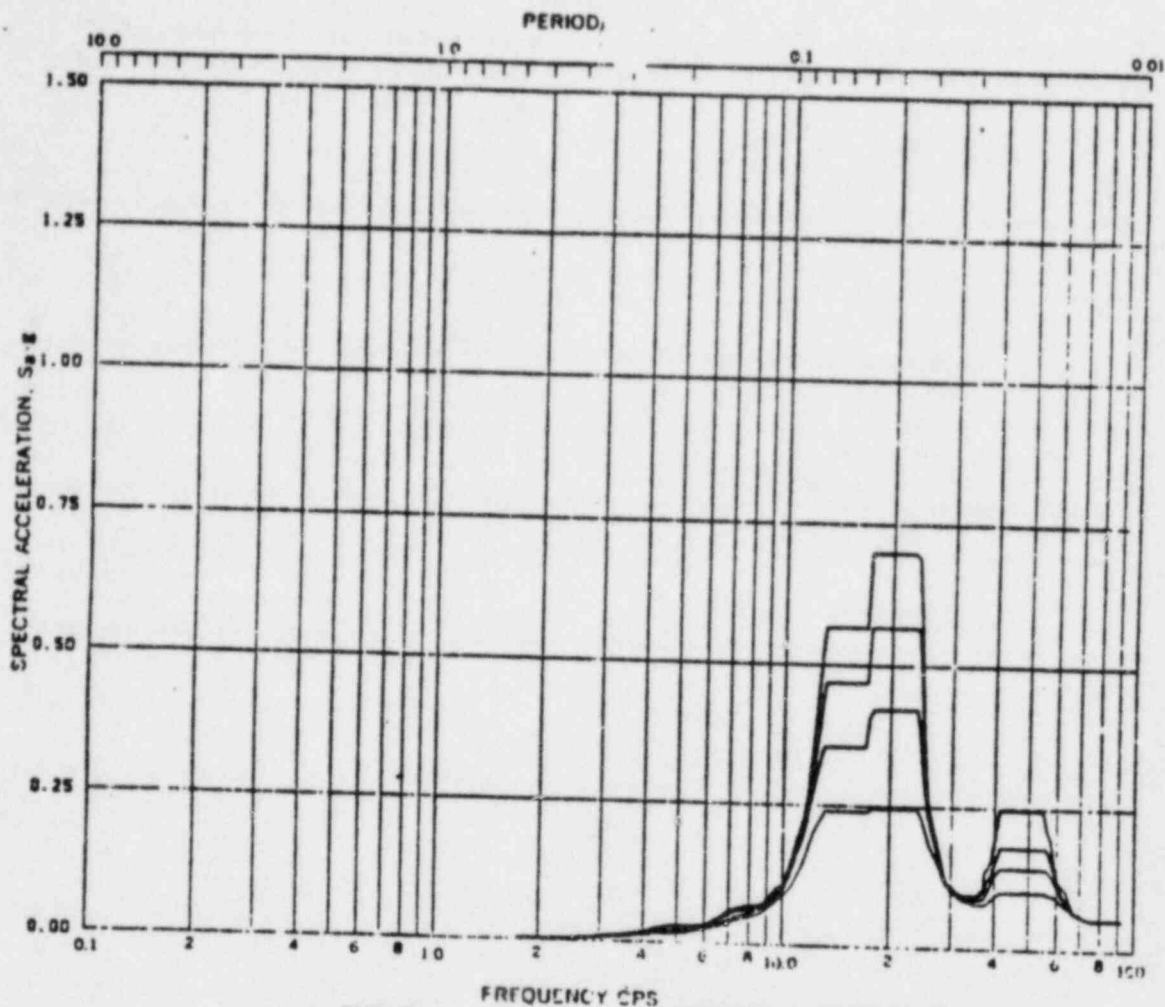


Fig. BV5-3 Acceleration Spectra for REACTOR & CONTROL BLDGS.
 Load Case: Susquehanna SRV
 Mode -, Direction VERT., Elev 709'-0"
 Damping: 0.005, 0.01, 0.02, 0.05

REV. 6, 4/82

**SUSQUEHANNA STEAM ELECTRIC STATION
 UNITS 1 AND 2
 DESIGN ASSESSMENT REPORT**

**REACTOR/CONTROL BUILDING
 RESPONSE SPECTRA**

KWU-SRV
 FIGURE C- 8

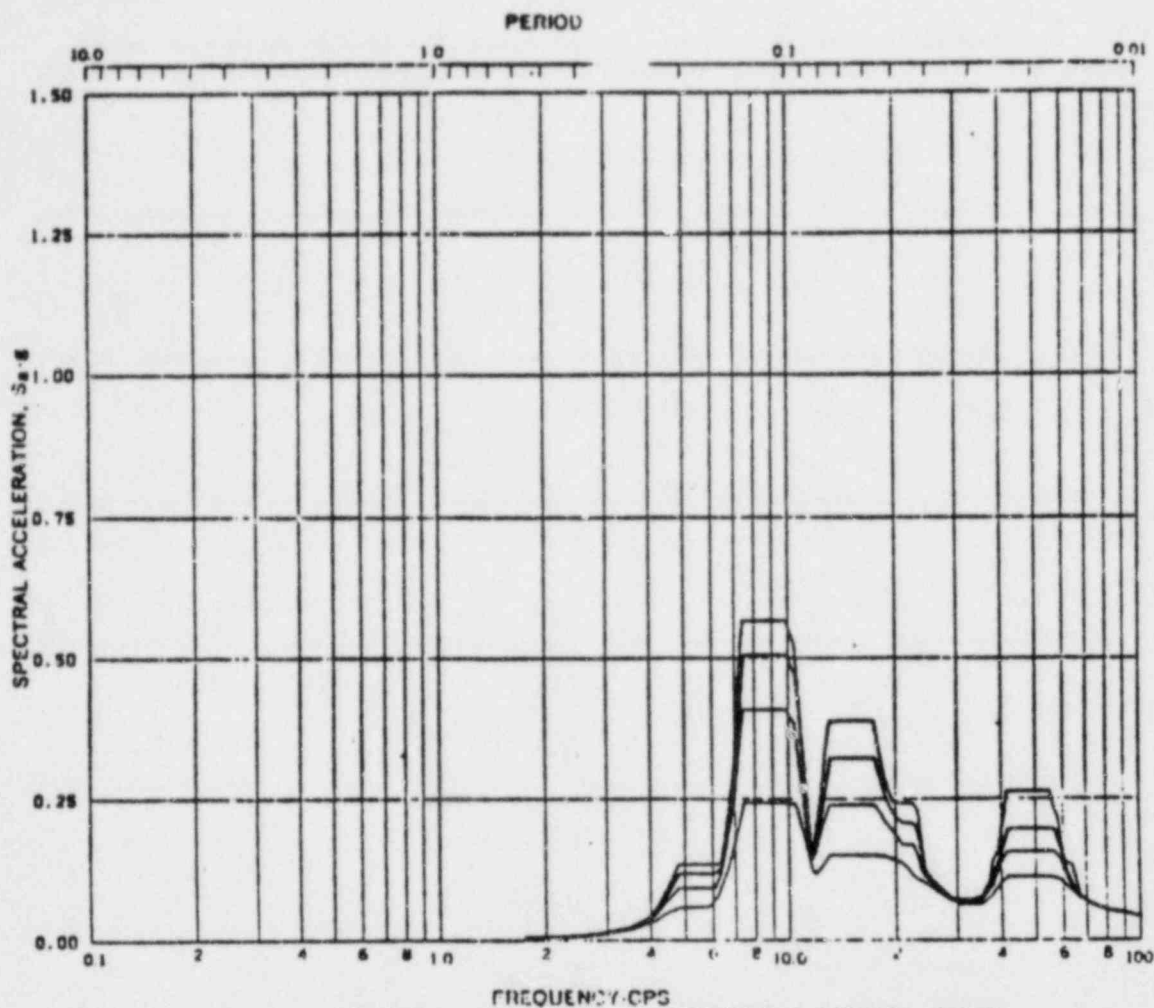


Fig. BV6-3 Acceleration Spectra for REACTOR & CONTROL BLDGS.
 Load Case: Susquehanna SRV
 Mode -, Direction VERT, Elev 719'-1"
 Damping: 0.005, 0.01, 0.02, 0.05

REV. 6, 4/82

**SUSQUEHANNA STEAM ELECTRIC STATION
 UNITS 1 AND 2
 DESIGN ASSESSMENT REPORT**

**REACTOR/CONTROL BUILDING
 RESPONSE SPECTRA**

KWU-SRV

FIGURE C- 9

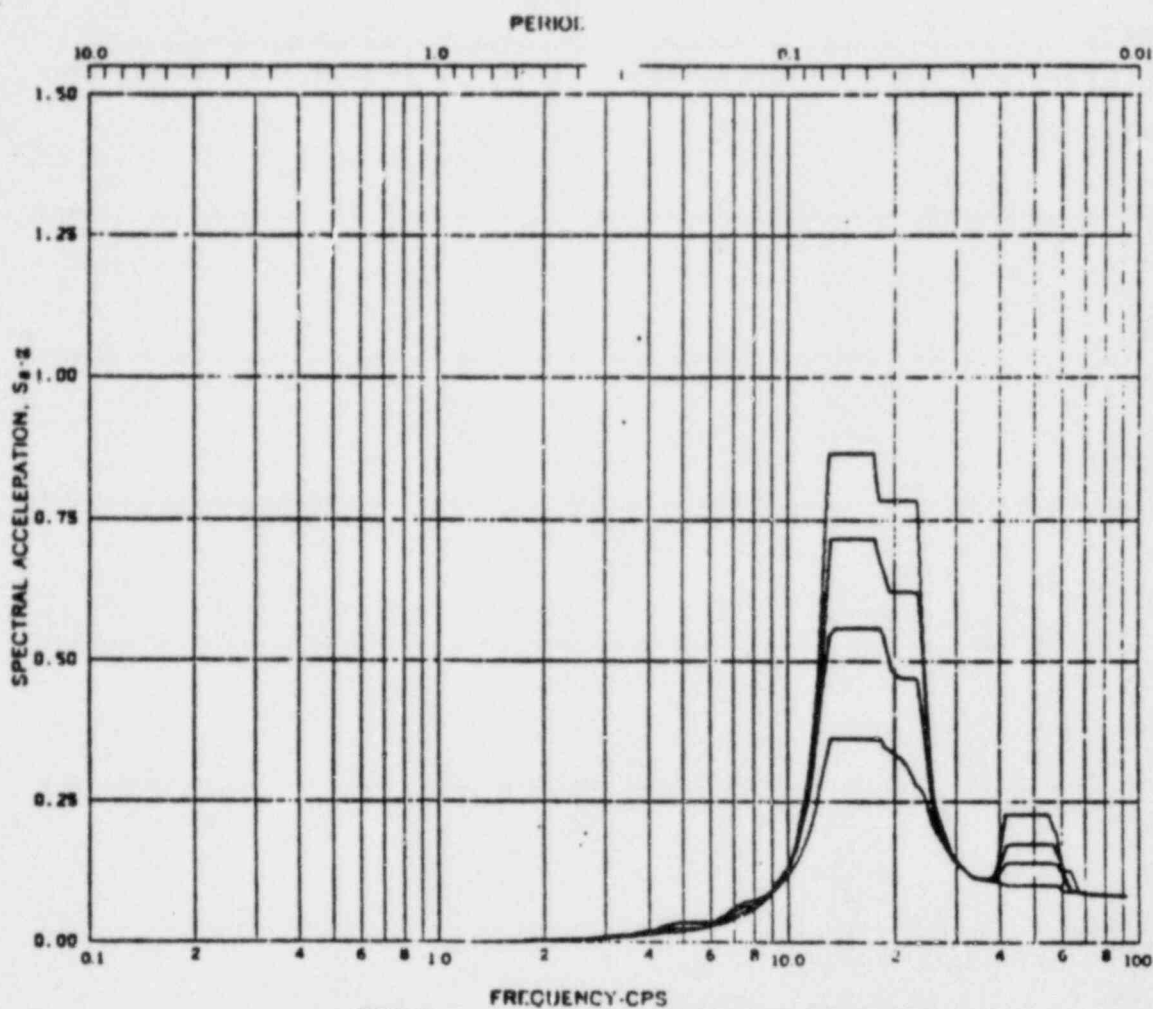


Fig. BV7-3 Acceleration Spectra for REACTOR & CONTROL BLDGS.
 Load Case: Susquehanna SRV
 Node -, Direction VERT., Elev 728'-0"
 Damping: 0.006, 0.01, 0.02, 0.05

REV. 6, 4/82

**SUSQUEHANNA STEAM ELECTRIC STATION
 UNITS 1 AND 2
 DESIGN ASSESSMENT REPORT**

**REACTOR/CONTROL BUILDING
 RESPONSE SPECTRA**

**KWU-SRV
 FIGURE C-10**

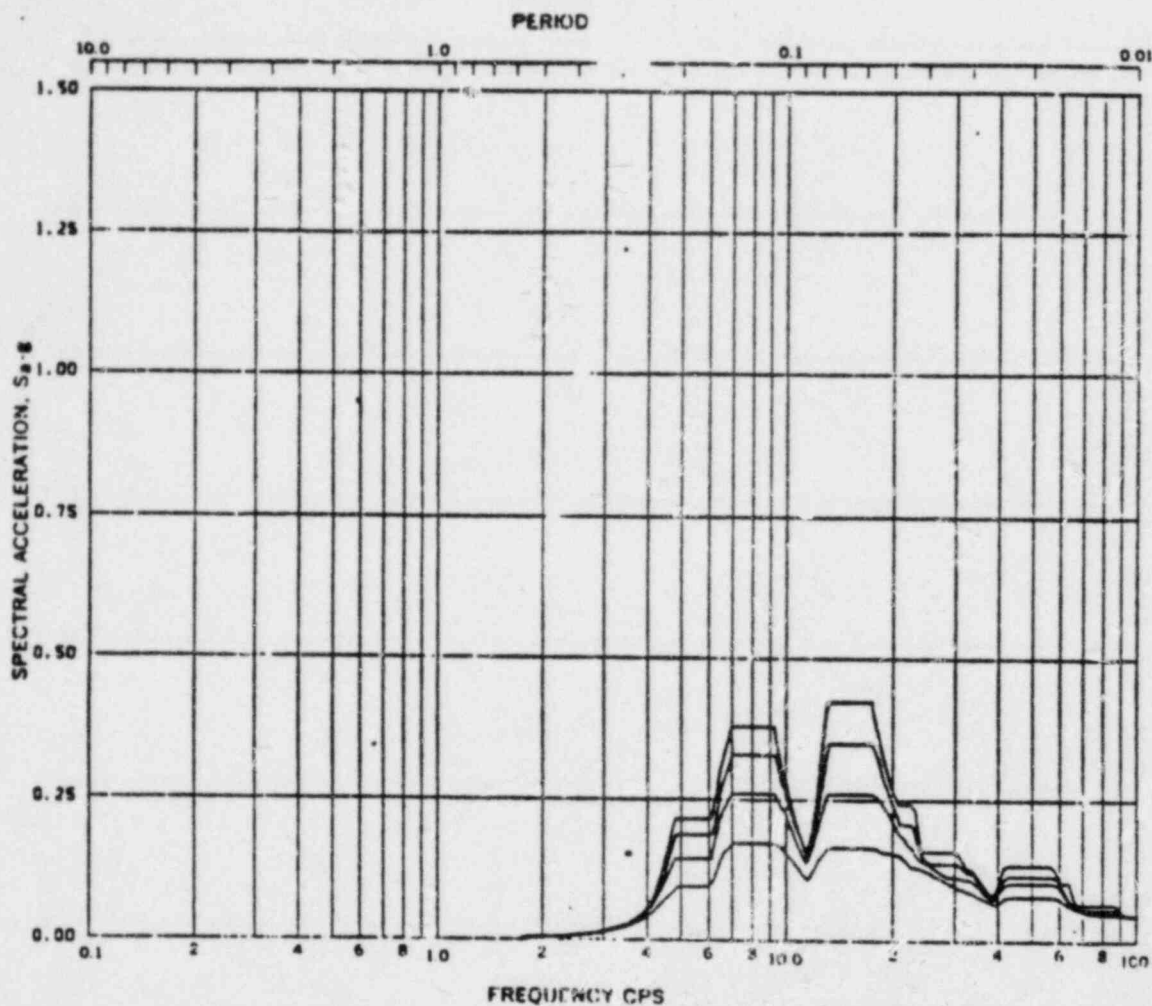


Fig. BVR-3 Acceleration Spectra for REACTOR & CONTROL BLDGS.
 Load Case: Superswelling SRV
 Mode -, Direction VERT, Elev 749'-1"
 Damping: 0.005, 0.01, 0.02, 0.05

REV. 6, 4/82

SUSQUEHANNA STEAM ELECTRIC STATION UNITS 1 AND 2 DESIGN ASSESSMENT REPORT
REACTOR/CONTROL BUILDING RESPONSE SPECTRA
KWU-SRV FIGURE C-11

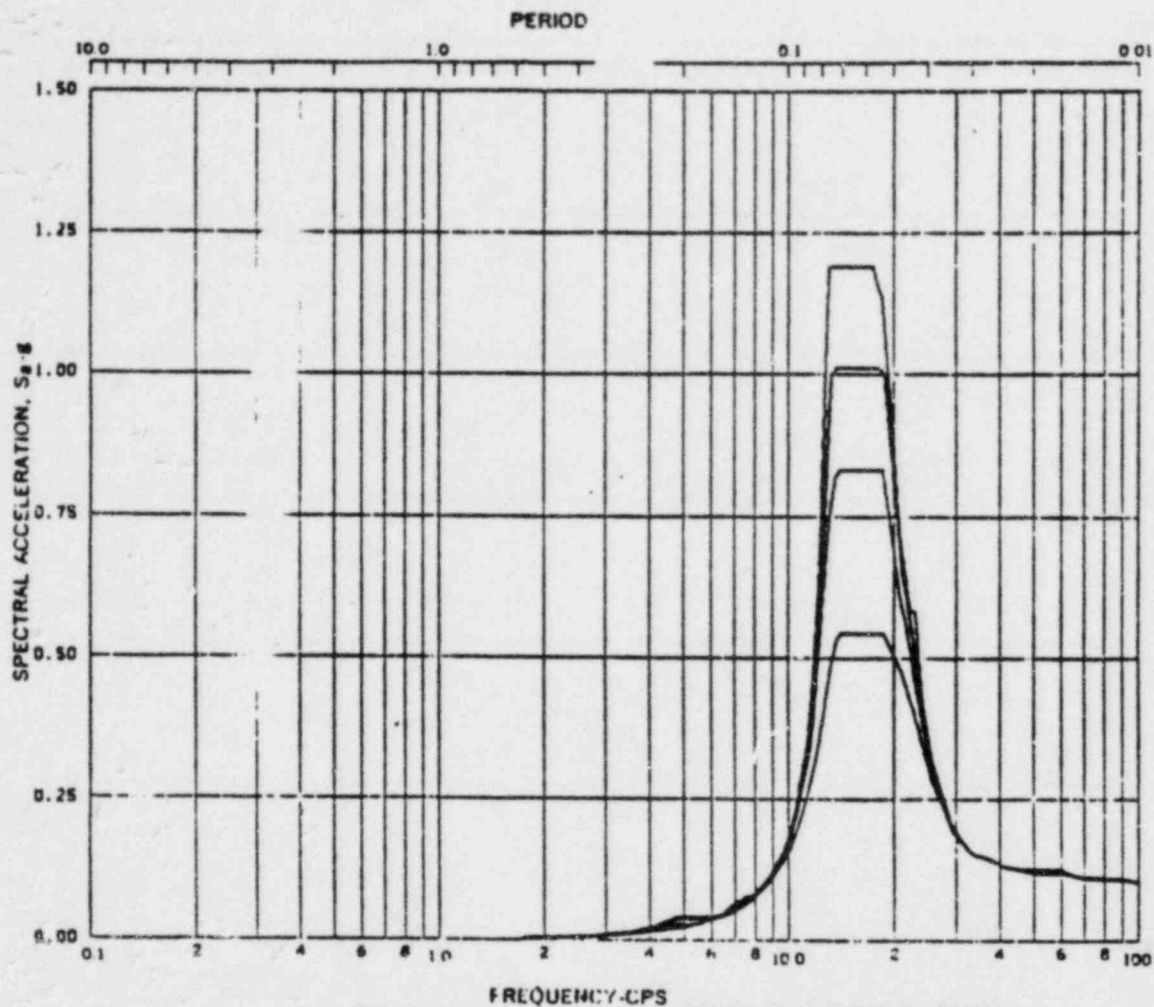


Fig. BV9-3 Acceleration Spectra for REACTOR & CONTROL BLDGS.
 Load Case: Susquehanna SRV
 Mode -, Direction VERT., Elev 753'-0"
 Damping: 0.005, 0.01, 0.02, 0.05

REV. 6, 4/82

**SUSQUEHANNA STEAM ELECTRIC STATION
 UNITS 1 AND 2
 DESIGN ASSESSMENT REPORT**

**REACTOR/CONTROL BUILDING
 RESPONSE SPECTRA**

**KWU-SRV
 FIGURE C-12**

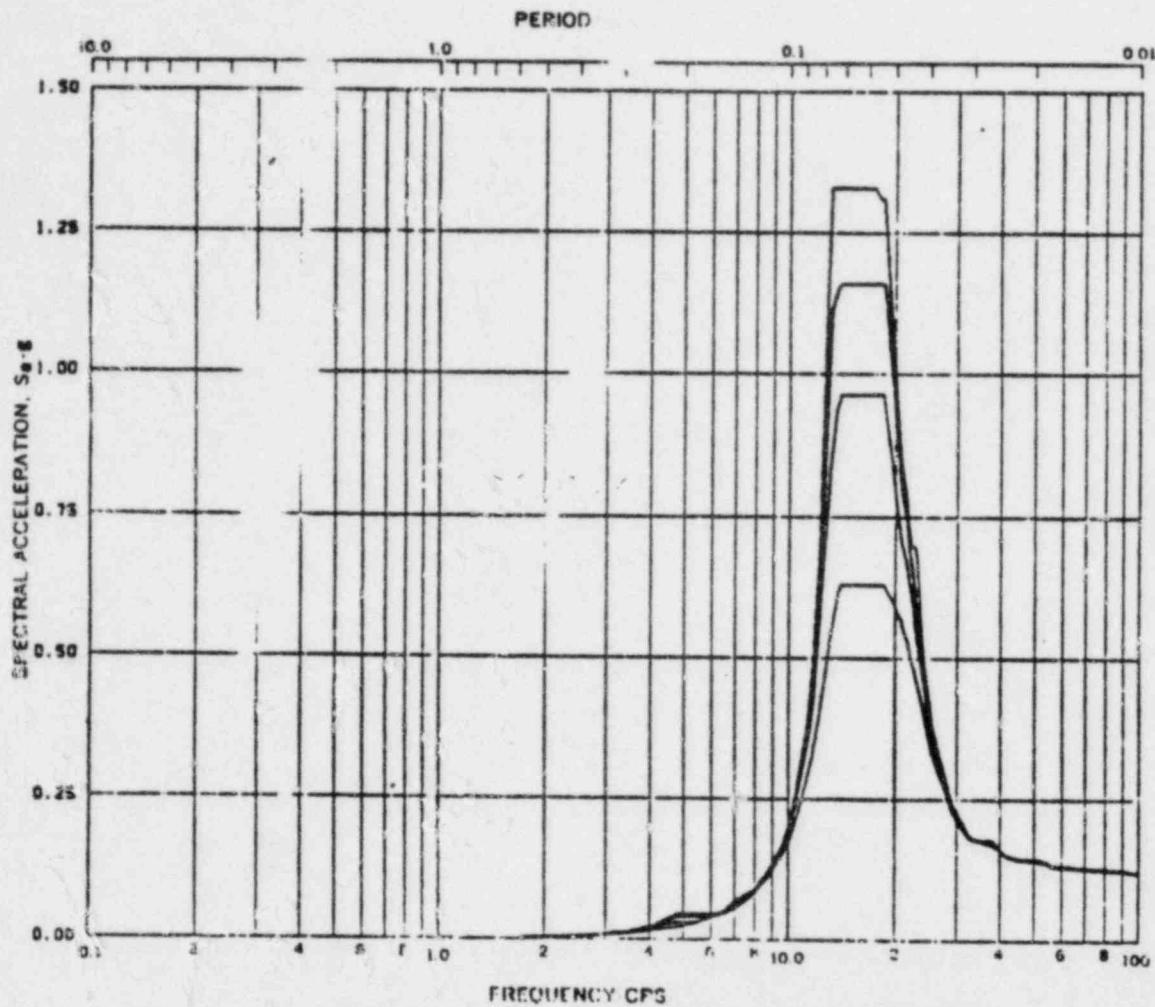


Fig. BV10-2 Acceleration Spectra for REACTOR & CONTROL BLDGS.
 Load Case: Susquehanna SRV
 Mode -, Direction VERT., Elev 771'-0"
 Damping: 0.005, 0.01, 0.02, 0.05

REV. 6, 4/82

SUSQUEHANNA STEAM ELECTRIC STATION UNITS 1 AND 2 DESIGN ASSESSMENT REPORT
REACTOR/CONTROL BUILDING RESPONSE SPECTRA
KWU-SRV FIGURE C-13

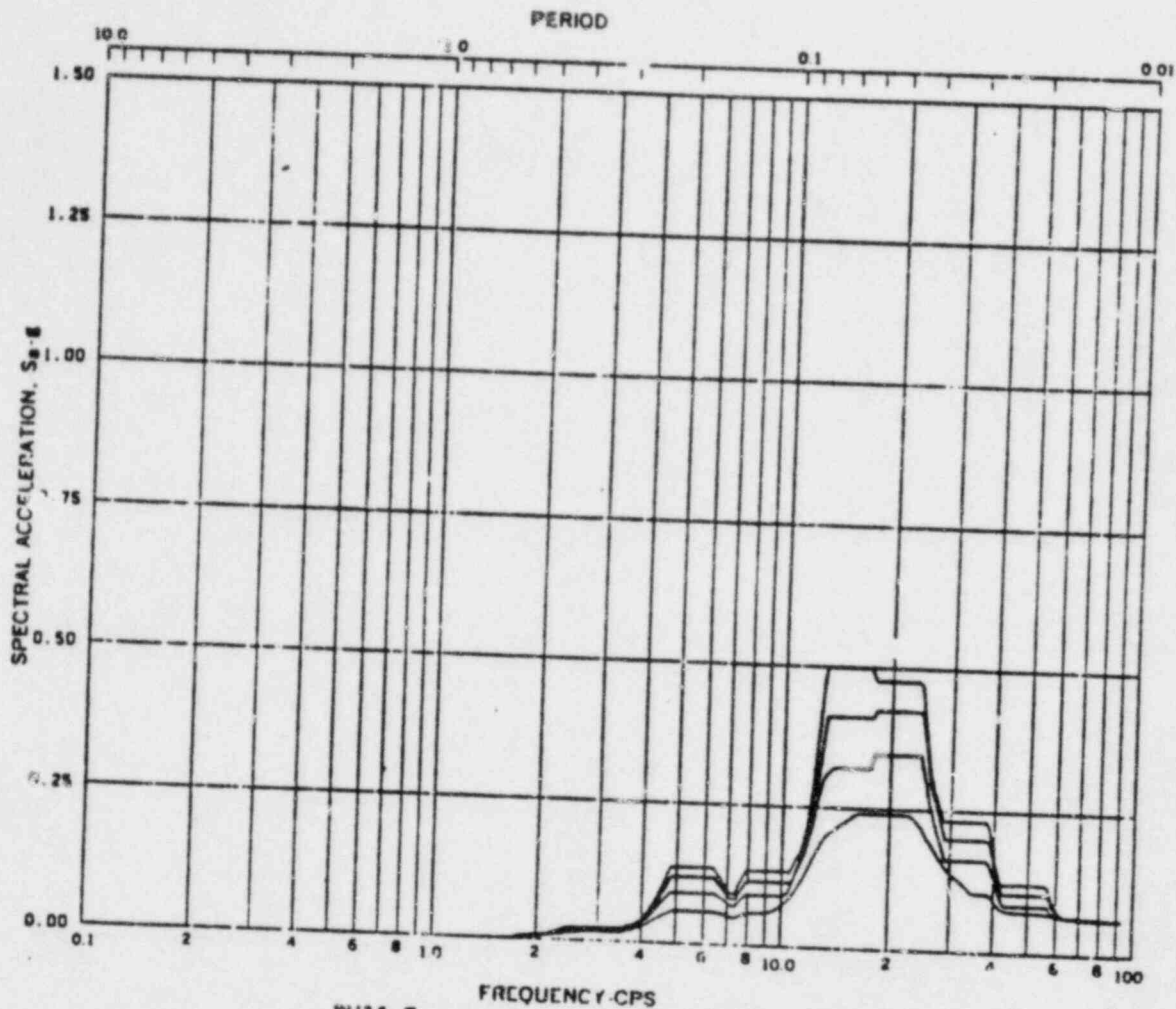


Fig. BV11-3 Acceleration Spectra for REACTOR & CONTROL BLDGS.
 Load Case: Susquehanna SRV
 Mode -, Direction VERT, Elev 779'-1"
 Damping: 0.005, 0.01, 0.02, 0.05

REV. 6, 4/82

SUSQUEHANNA STEAM ELECTRIC STATION
 UNITS 1 AND 2
 DESIGN ASSESSMENT REPORT

REACTOR/CONTROL BUILDING
 RESPONSE SPECTRA

KWU-SRV
 FIGURE C-14

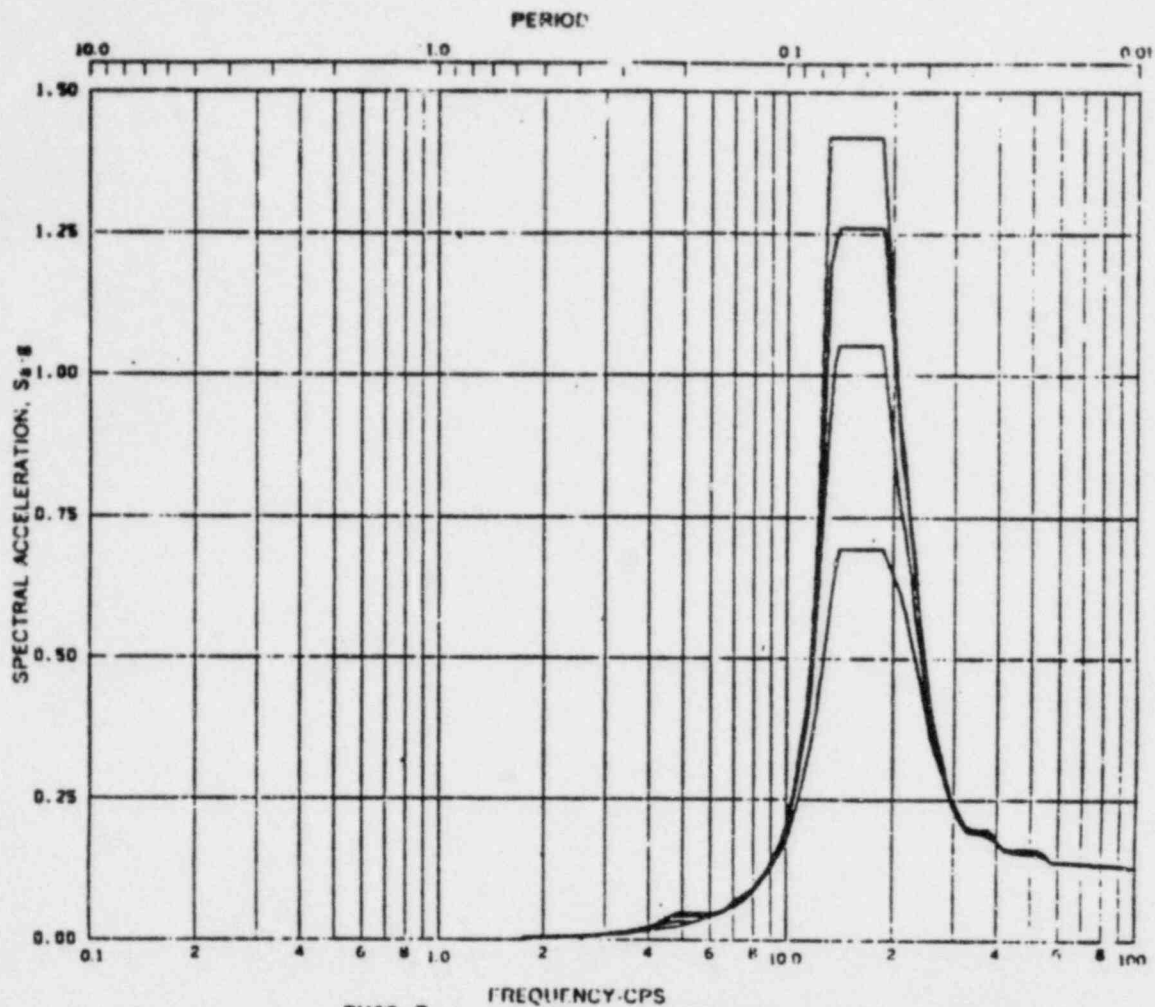


Fig. BV12-3 Acceleration Spectra for REACTOR & CONTROL BLDGS.
 Load Case: Susquehanna SRV
 Mode -, Direction VERT, Elev 783'-0"
 Damping: 0.005, 0.01, 0.02, 0.05

REV. 6, 4/82

**SUSQUEHANNA STEAM ELECTRIC STATION
 UNITS 1 AND 2
 DESIGN ASSESSMENT REPORT**

**REACTOR/CONTROL BUILDING
 RESPONSE SPECTRA**

**KWU-SRV
 FIGURE C- 15**

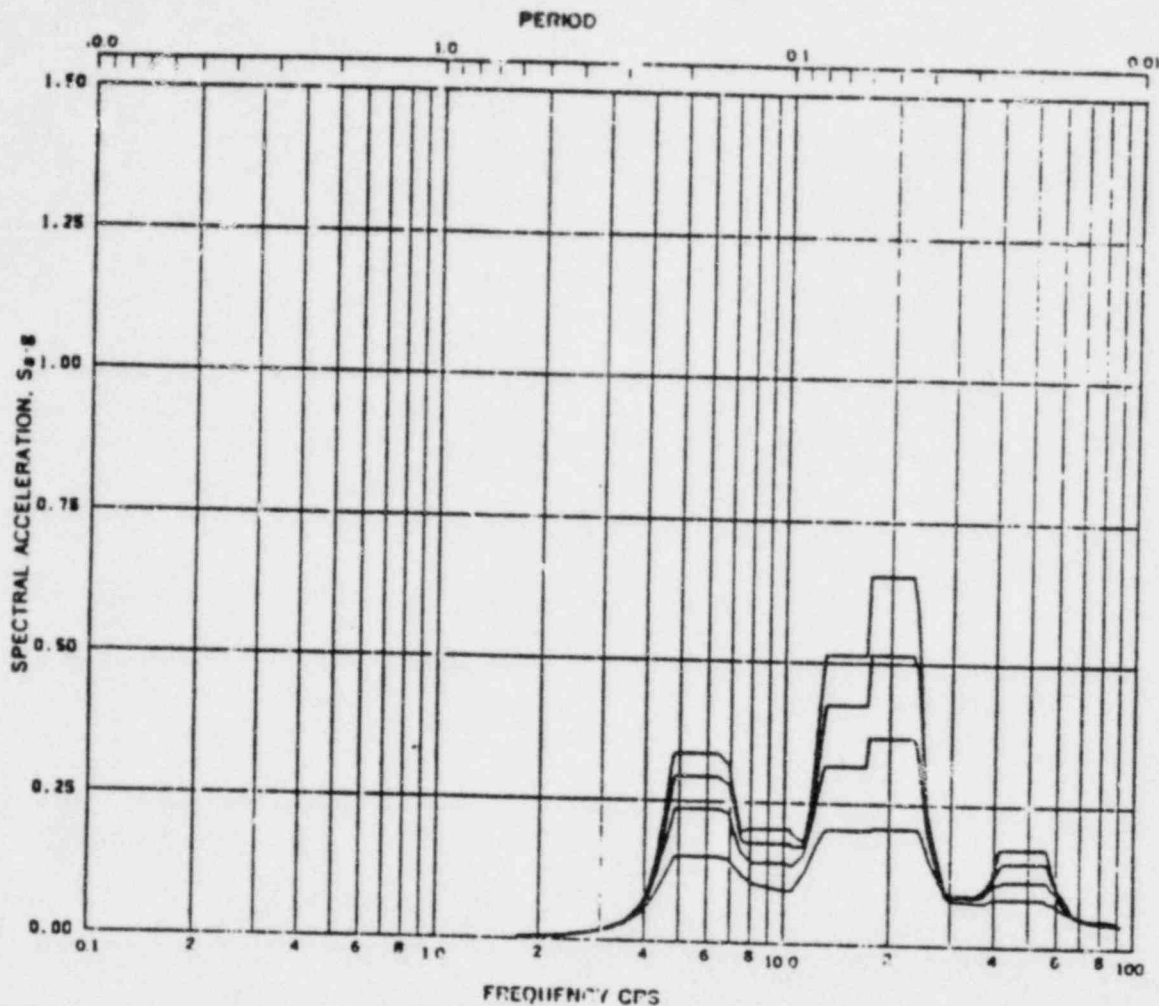


Fig. BV13-3 Acceleration Spectra for REACTOR & CONTROL BLDGS.
 Load Case: Susquehanna SRV
 Mode -, Direction VERT, Elev 799'-1"
 Damping: 0.005, 0.01, 0.02, 0.05

REV. 6, 4/82

**SUSQUEHANNA STEAM ELECTRIC STATION
 UNITS 1 AND 2
 DESIGN ASSESSMENT REPORT**

**REACTOR/CONTROL BUILDING
 RESPONSE SPECTRA**

KWU-SRV
 FIGURE C- 16

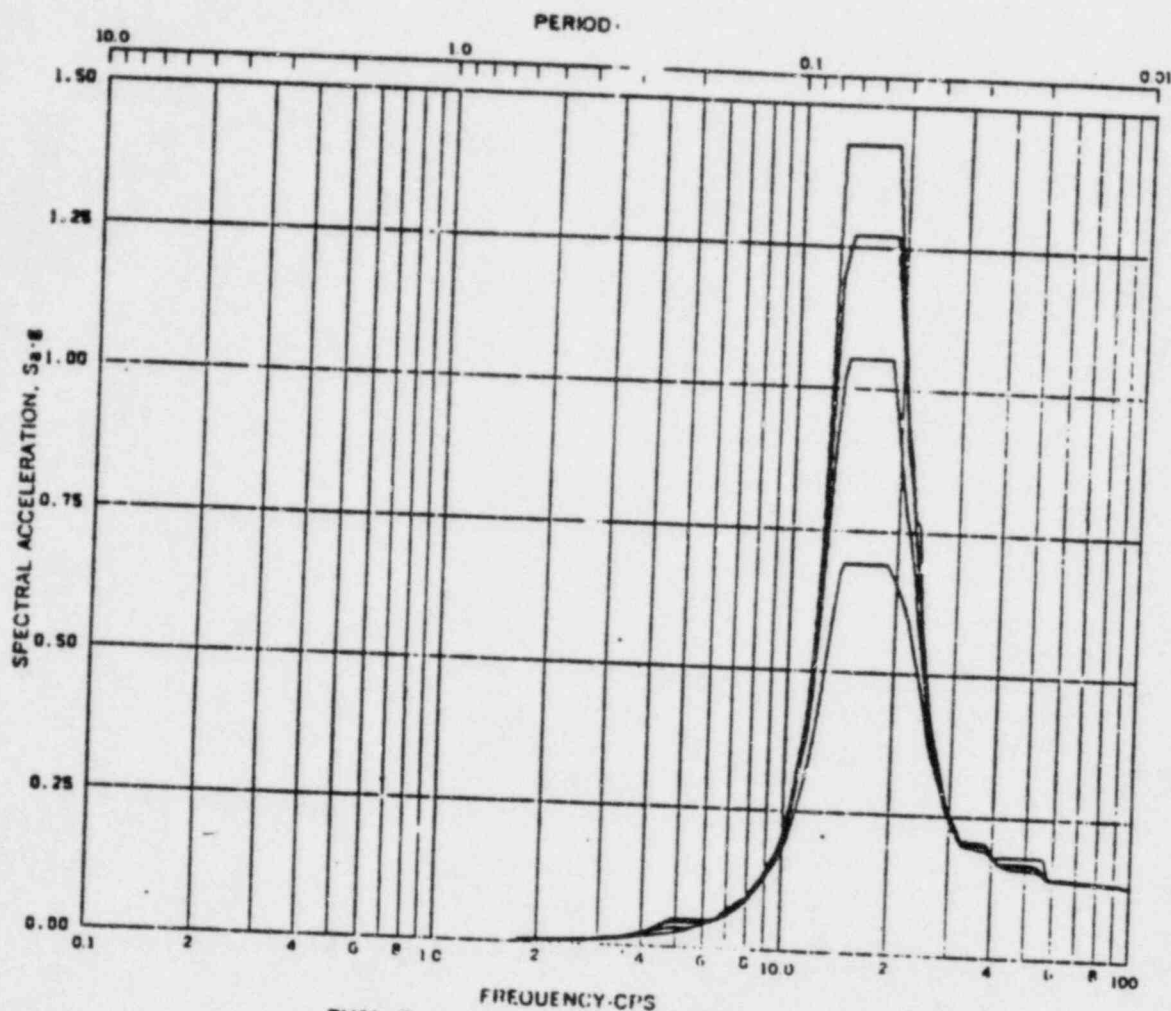


Fig. BV14-3 Acceleration Spectra for REACTOR & CONTROL BLDGS.
 Load Case: Susquehanna SRV
 Mode -, Direction VERT., Elev 806'-0"
 Damping: 0.005, 0.01, 0.02, 0.05

REV. 6, 4/82

SUSQUEHANNA STEAM ELECTRIC STATION
 UNITS 1 AND 2
 DESIGN ASSESSMENT REPORT

REACTOR/CONTROL BUILDING
 RESPONSE SPECTRA

KWU-SRV

FIGURE C-17

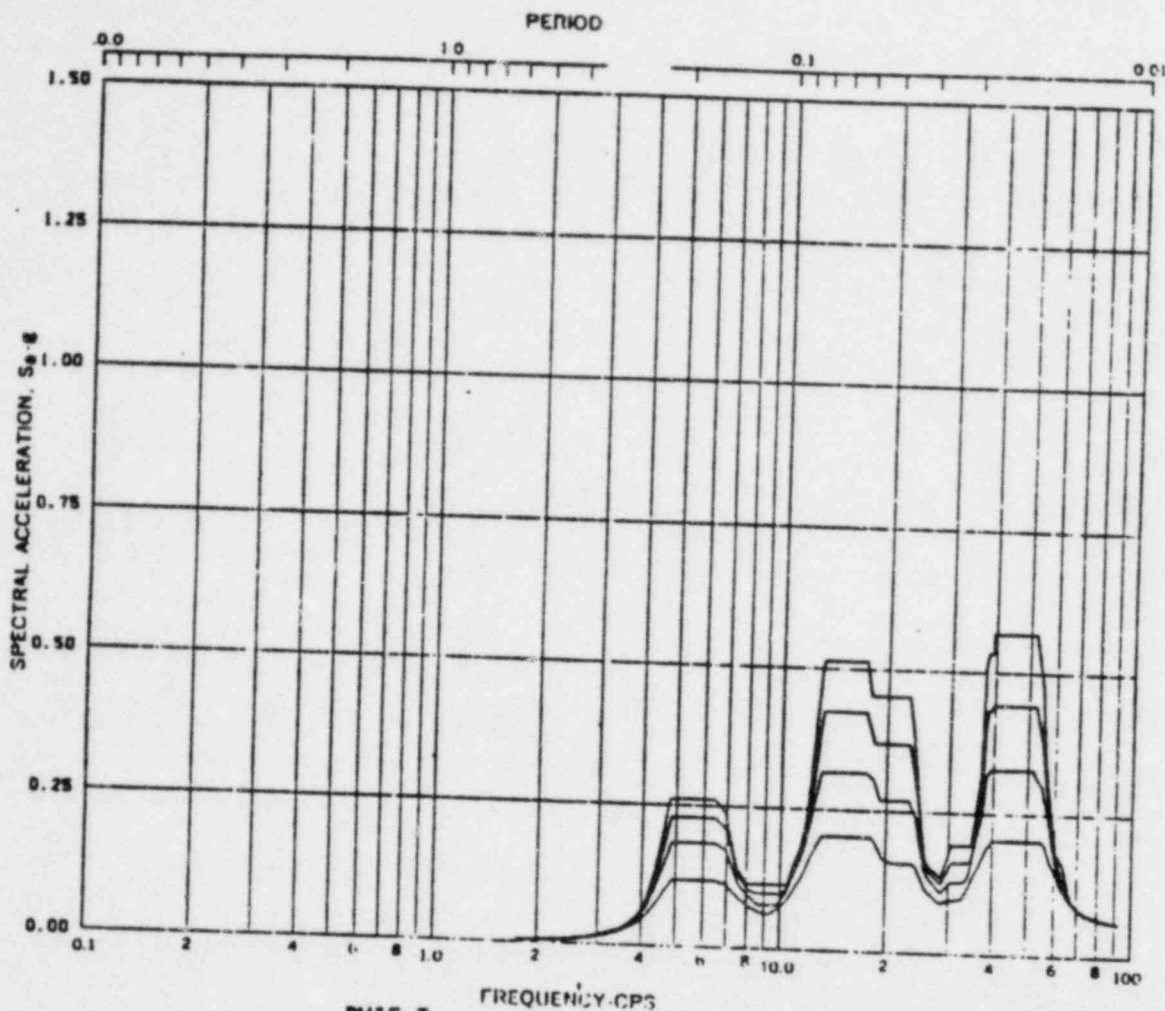


Fig. BV15-3 Acceleration Spectra for REACTOR & CONTROL BLDGS.
 Load Case: Susquehanna SRV
 Mode -, Direction VERT, Elev 818'-1"
 Damping: 0.005, 0.01, 0.02, 0.05

REV. 6, 4/82

**SUSQUEHANNA STEAM ELECTRIC STATION
 UNITS 1 AND 2
 DESIGN ASSESSMENT REPORT**

**REACTOR/CONTROL BUILDING
 RESPONSE SPECTRA**

KWU-SRV

FIGURE (18

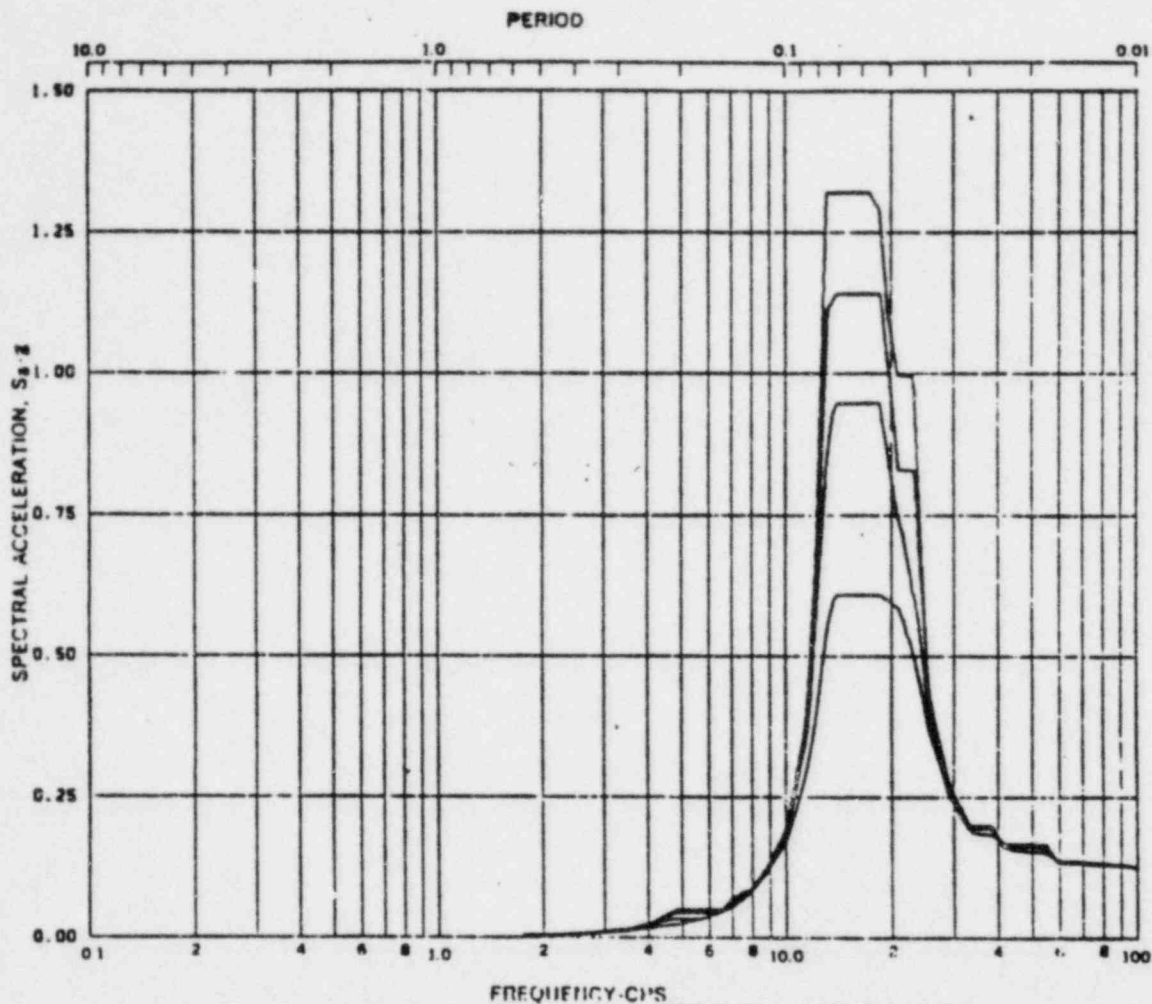


Fig. BV16-3 Acceleration Spectra for REACTOR & CONTROL BLDGS.
 Load Case: Susquehanna SRV
 Node -, Direction VERT., Elev 825'-0"
 Damping: 0.005, 0.01, 0.02, 0.05

REV. 6, 4/82

**SUSQUEHANNA STEAM ELECTRIC STATION
 UNITS 1 AND 2
 DESIGN ASSESSMENT REPORT**

**REACTOR/CONTROL BUILDING
 RESPONSE SPECTRA**

**KWU-SRV
 FIGURE C- 19**

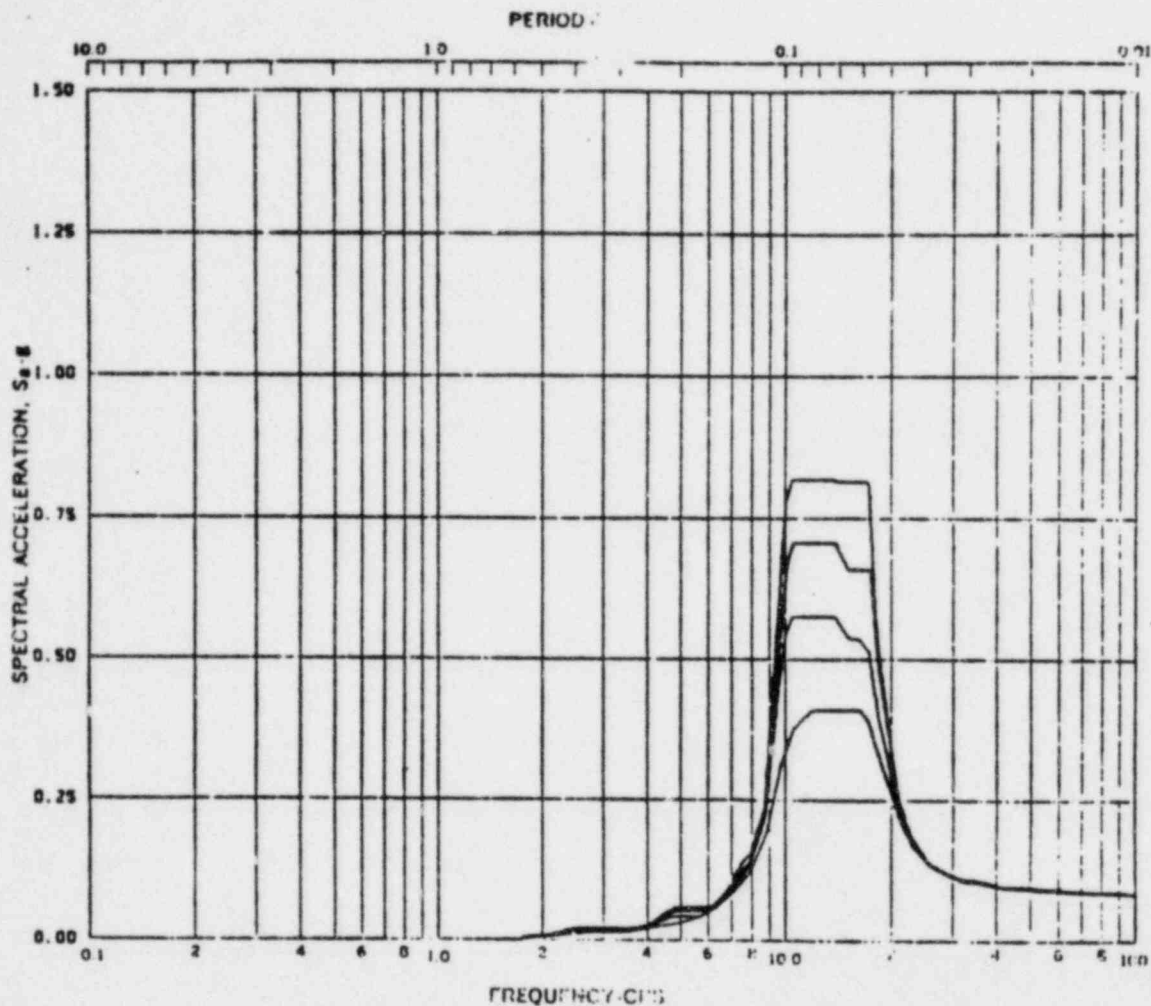


Fig. BV17-3 Acceleration Spectra for REACTOR & CONTROL BLDGS.
 Load Case: Susquehanna SRV
 Mode -, Direction VERT., Elev 870'-0"
 Damping: 0.005, 0.01, 0.02, 0.05

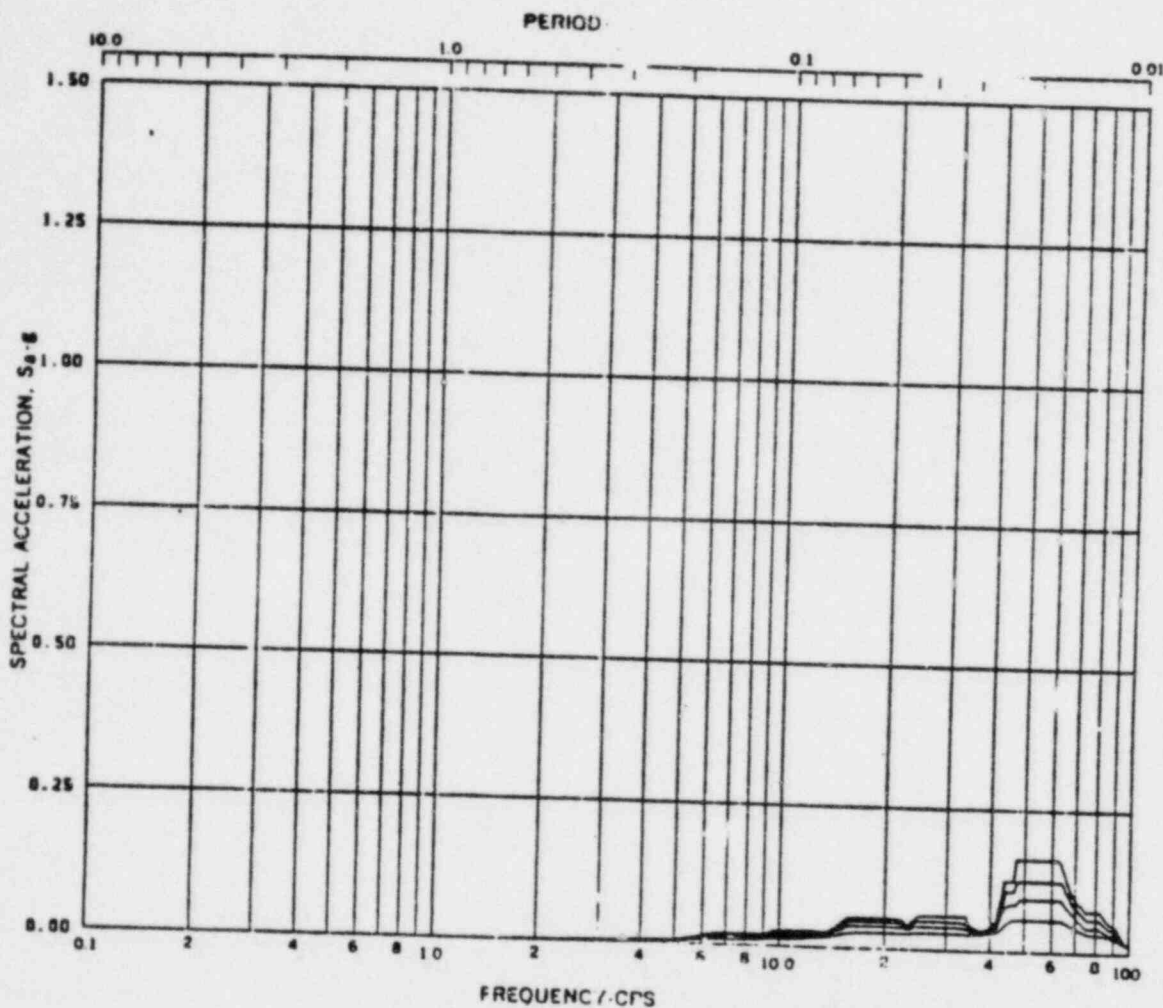
REV. 6, 4/82

**SUSQUEHANNA STEAM ELECTRIC STATION
 UNITS 1 AND 2
 DESIGN ASSESSMENT REPORT**

**REACTOR/CONTROL BUILDING
 RESPONSE SPECTRA**

KWU-SRV

FIGURE C- 20



— Acceleration Spectra for REACTOR & CONTROL BLDGS.
 Load Case: Susquehanna SRV
 Mode —, Direction E-W, Elev 656'-0"
 Damping: 0.005, 0.01, 0.02, 0.05

REV. 6, 4/82

SUSQUEHANNA STEAM ELECTRIC STATION
UNITS 1 AND 2
DESIGN ASSESSMENT REPORT

REACTOR/CONTROL BUILDING
RESPONSE SPECTRA

KWU-SRV
FIGURE C- 21

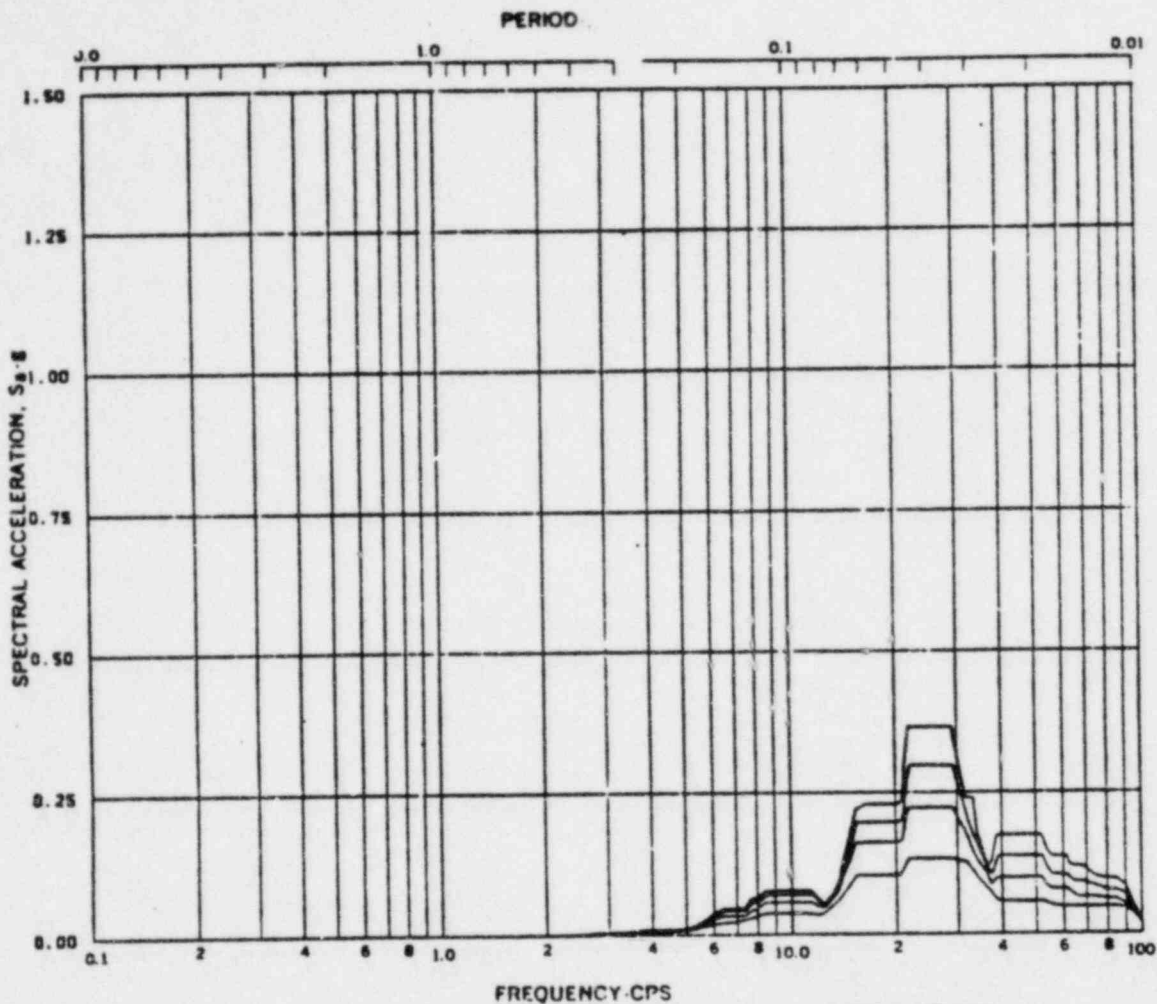


Fig. BE2-3 Acceleration Spectra for REACTOR & CONTROL BLDGS.
 Load Case: Susquehanna SRV
 Mode -, Direction E-W, Elev 670'-0"
 Damping: 0.005, 0.01, 0.02, 0.05

REV. 6, 4/82

**SUSQUEHANNA STEAM ELECTRIC STATION
 UNITS 1 AND 2
 DESIGN ASSESSMENT REPORT**

**REACTOR/CONTROL BUILDING
 RESPONSE SPECTRA**

KWU-SRV
 FIGURE C- 22

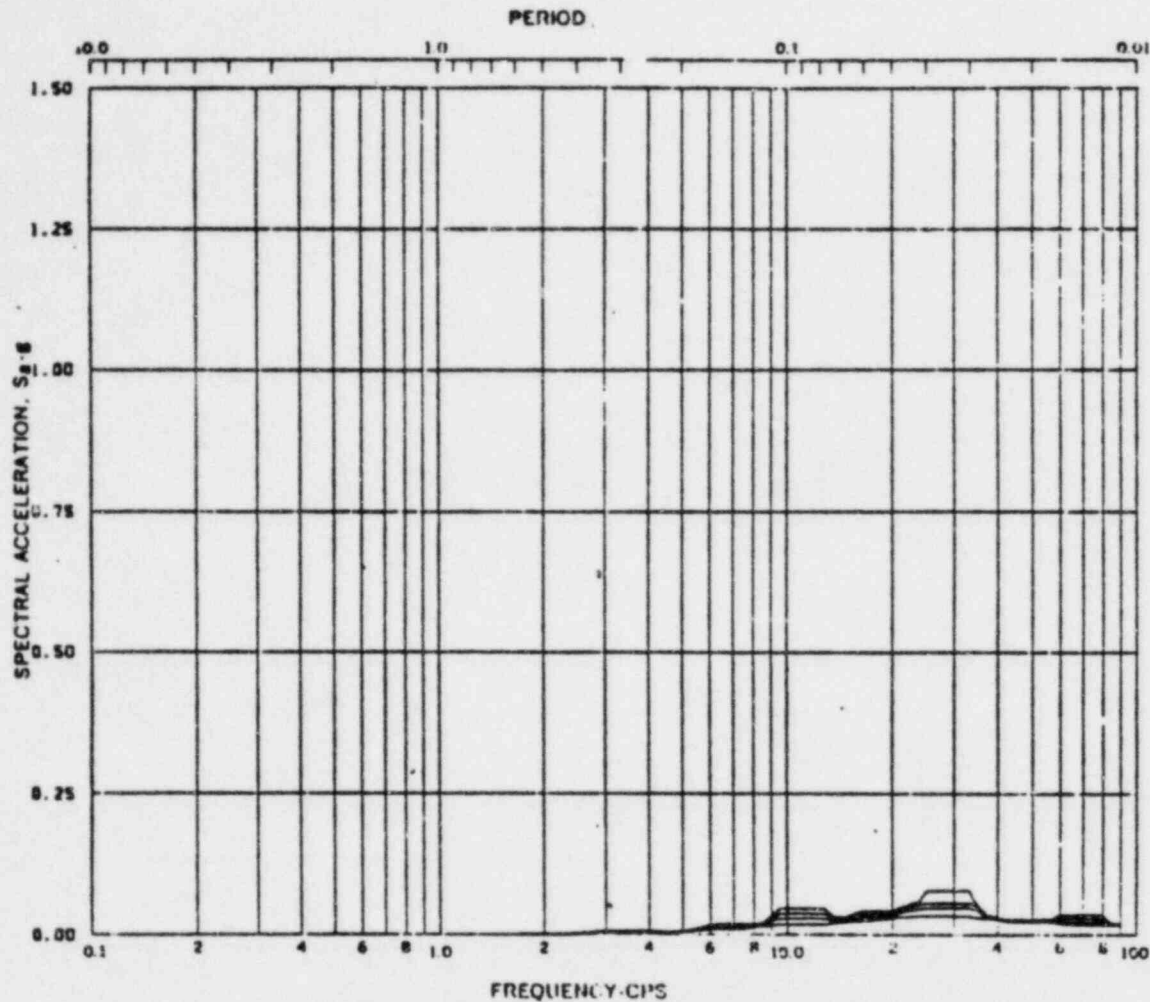


Fig. BE3-3 Acceleration Spectra for REACTOR & CONTROL BLDGS.
 Load Case: Susquehanna SRV
 Mode -, Direction E-W, Elev 676'-0"
 Damping: 0.005, 0.01, 0.02, 0.05

REV. 6, 4/82

**SUSQUEHANNA STEAM ELECTRIC STATION
 UNITS 1 AND 2
 DESIGN ASSESSMENT REPORT**

**REACTOR/CONTROL BUILDING
 RESPONSE SPECTRA**

KWU-SRV

FIGURE C- 23

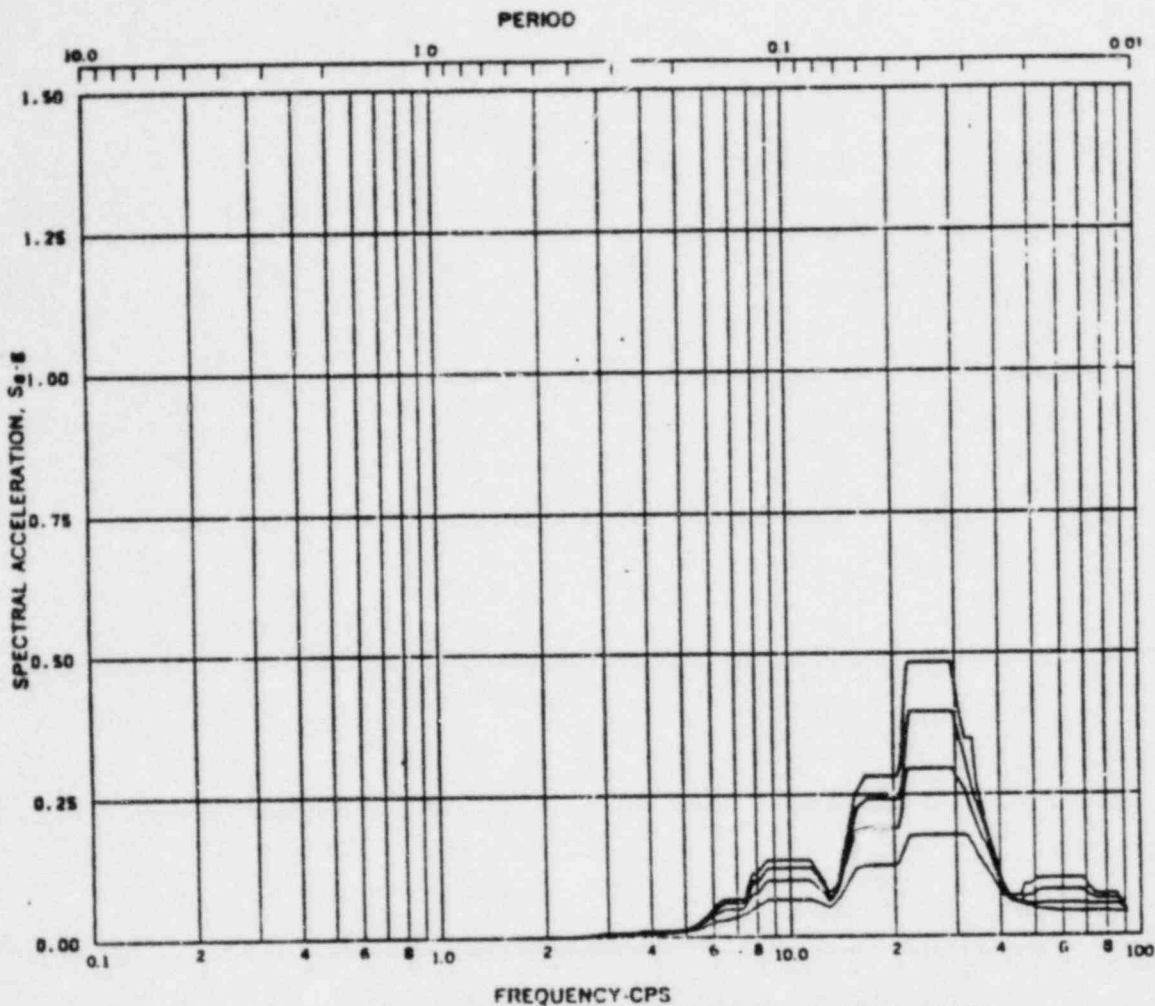


Fig. BF4-3 Acceleration Spectra for REACTOR & CONTROL BLDGS.
 Load Case: Susannah SRV
 Mode -, Direction F-W, Elev 683'-0"
 Damping: 0.005, 0.01, 0.02, 0.05

REV. 6, 4/82

**BUSQUEHANNA STEAM ELECTRIC STATION
 UNITS 1 AND 2
 DESIGN ASSESSMENT REPORT**

**REACTOR/CONTROL BUILDING
 RESPONSE SPECTRA**

KWU-SRV

FIGURE C- 24

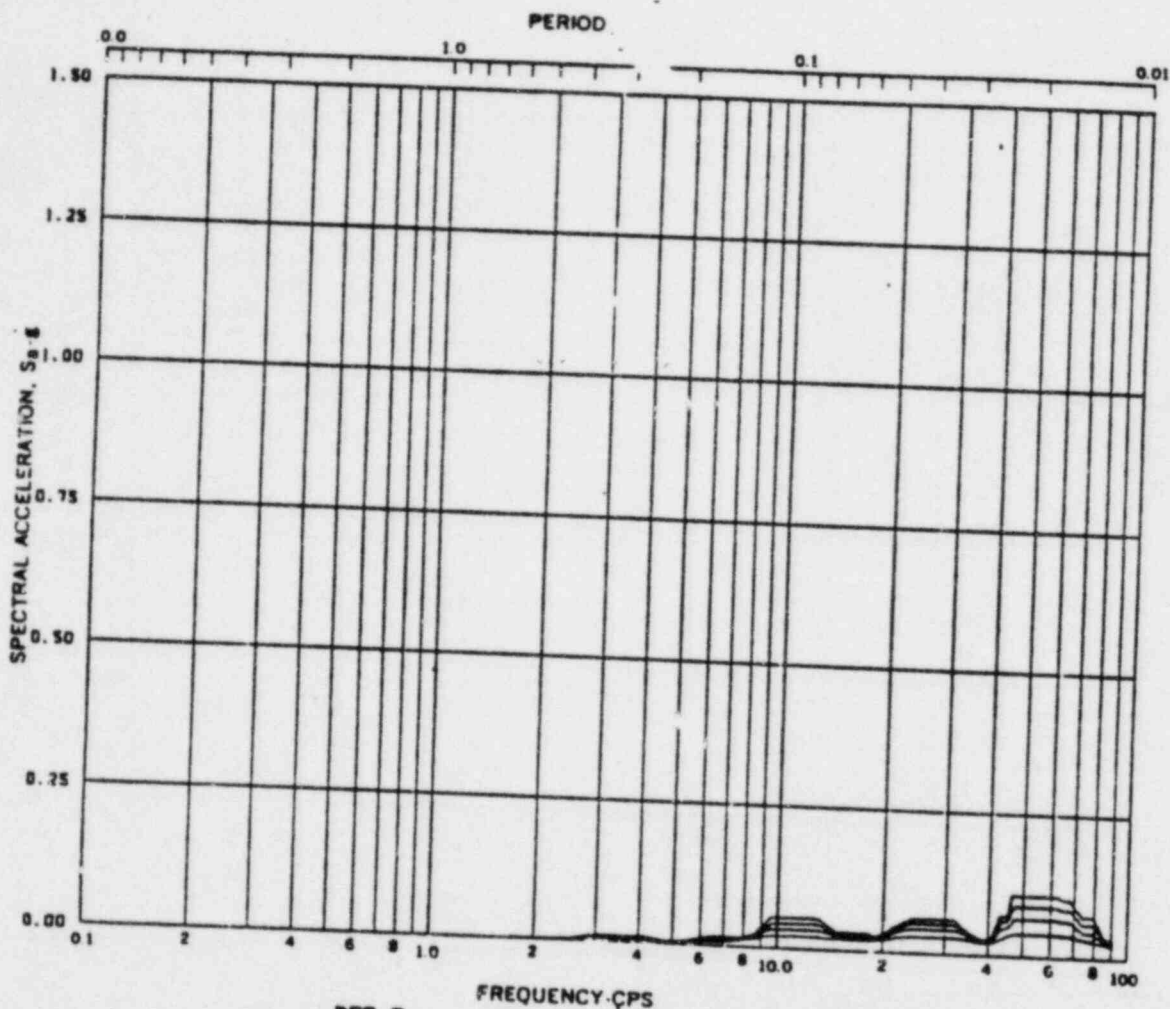


Fig. BE5-3 Acceleration Spectra for REACTOR & CONTROL BLDGS.
 Load Case: Susquehanna SRV
 Mode -, Direction E-W, Elev 697'-0"
 Damping: 0.005, 0.01, 0.02, 0.05

REV. 6, 4/82

**SUSQUEHANNA STEAM ELECTRIC STATION
 UNITS 1 AND 2
 DESIGN ASSESSMENT REPORT**

**REACTOR/CONTROL BUILDING
 RESPONSE SPECTRA**

KWU-SRV
 FIGURE C- 25

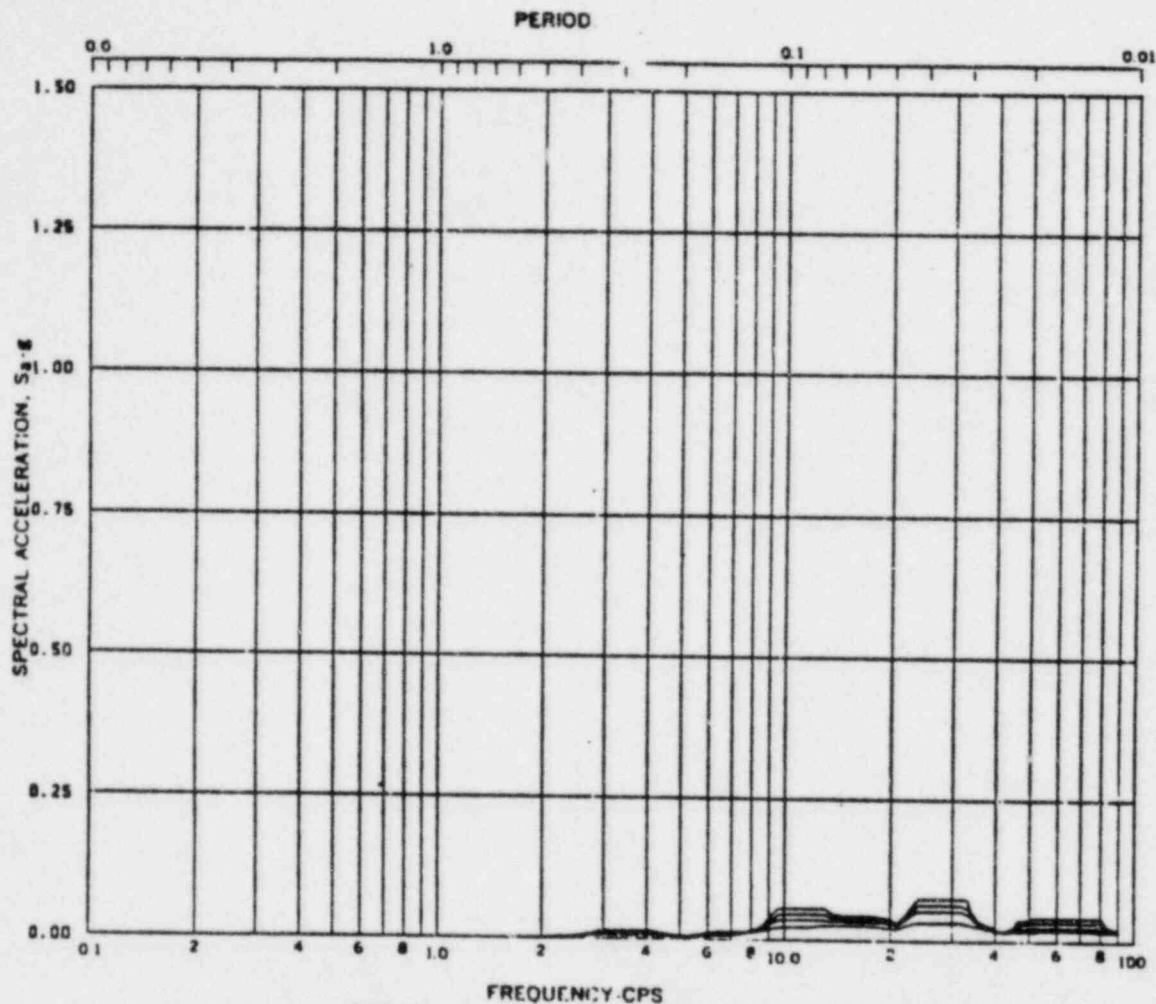


Fig. BE6-3 Acceleration Spectra for REACTOR & CONTROL BLDGS.
 Load Case: Susquehanna SRV
 Mode -, Direction E-W, Elev 709'-0"
 Damping: 0.005, 0.01, 0.02, 0.05

REV. 6, 4/82

**SUSQUEHANNA STEAM ELECTRIC STATION
 UNITS 1 AND 2
 DESIGN ASSESSMENT REPORT**

**REACTOR/CONTROL BUILDING
 RESPONSE SPECTRA**

KWU-SRV

FIGURE C-26

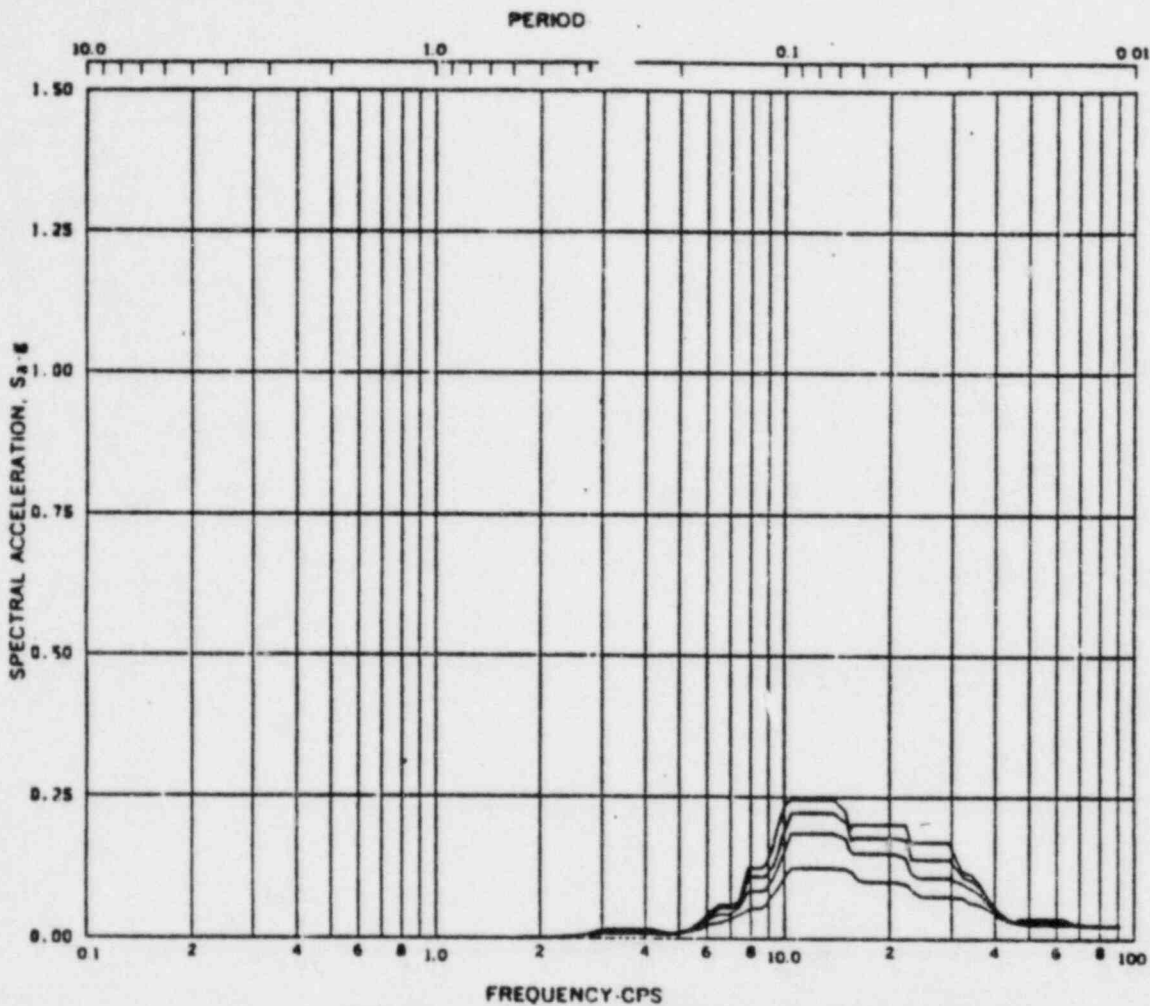


Fig. BE7-3 Acceleration Spectra for REACTOR & CONTROL BLDGS.
 Load Case: Susquehanna SRV
 Mode -, Direction E-W, Elev 719'-1"
 Damping: 0.005, 0.01, 0.02, 0.05

REV. 6, 4/82

**SUSQUEHANNA STEAM ELECTRIC STATION
 UNITS 1 AND 2
 DESIGN ASSESSMENT REPORT**

**REACTOR/CONTROL BUILDING
 RESPONSE SPECTRA**

**KWU-SRV
 FIGURE C-27**

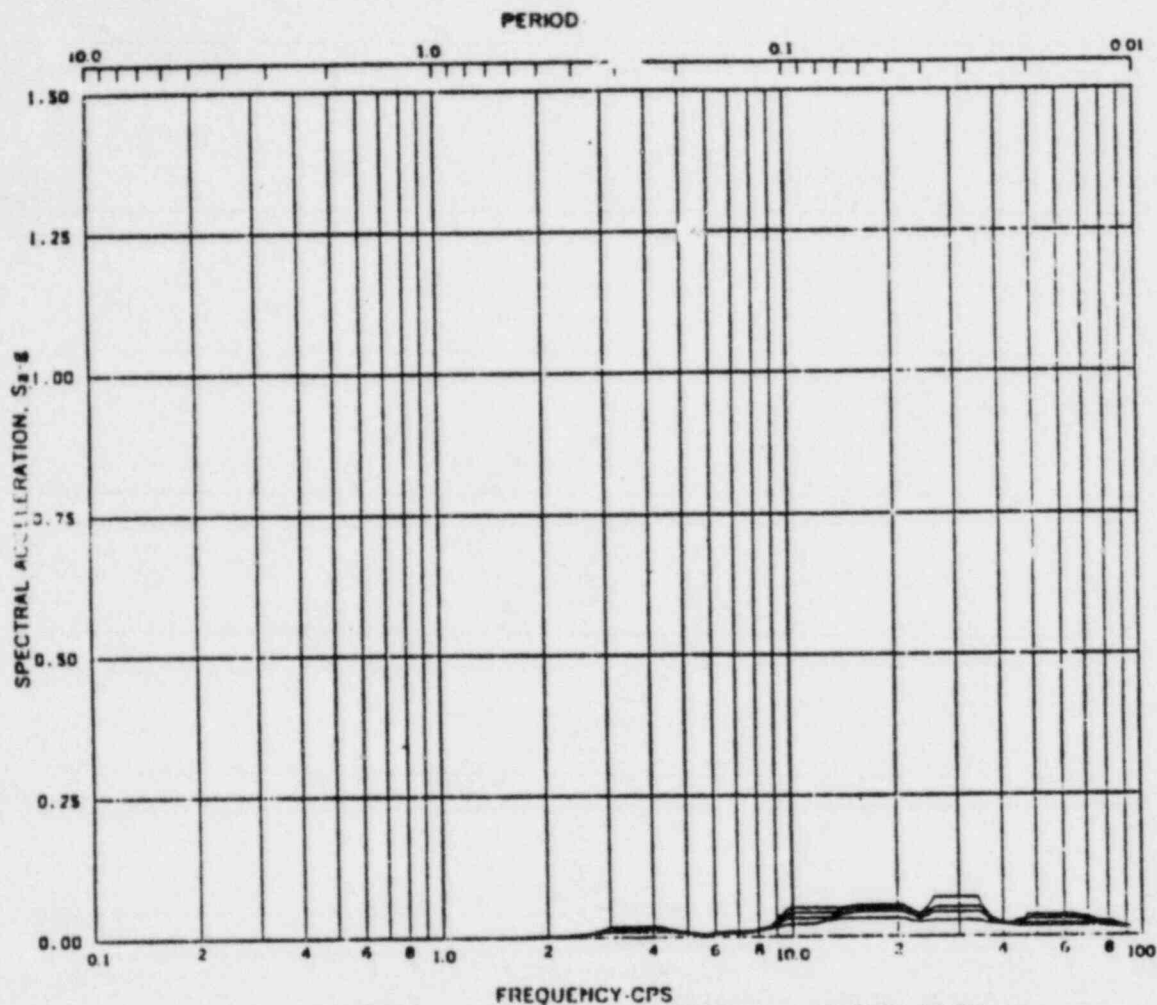


Fig. BE8-3 Acceleration Spectra for REACTOR & CONTROL BLDGS.
 Load Case: Susquehanna SRV
 Mode -, Direction E-W, Elev 728'-0"
 Damping: 0.005, 0.01, 0.02, 0.05

REV. 6, 4/82

**SUSQUEHANNA STEAM ELECTRIC STATION
 UNITS 1 AND 2
 DESIGN ASSESSMENT REPORT**

**REACTOR/CONTROL BUILDING
 RESPONSE SPECTRA**

**KWU-SRV
 FIGURE C- 28**

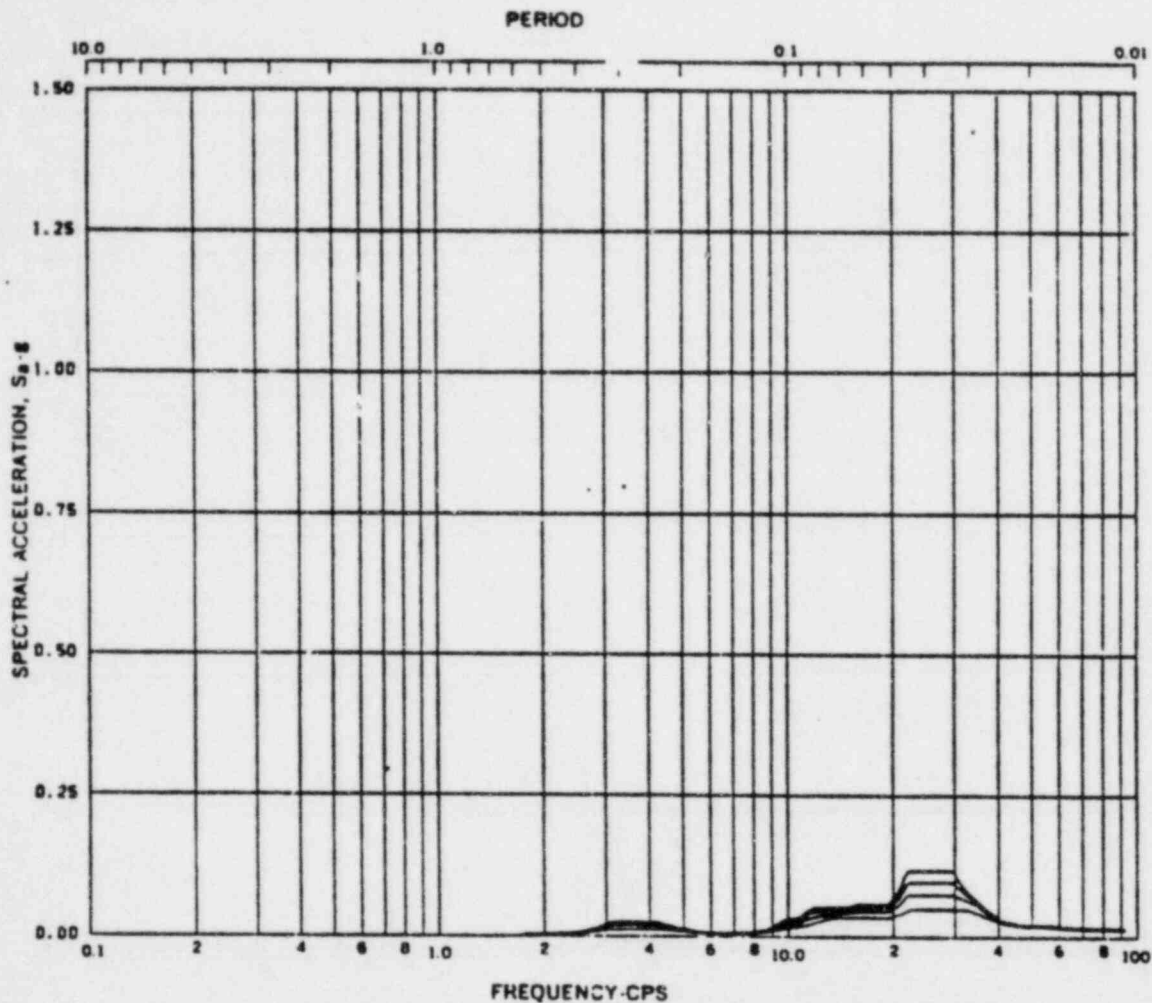


Fig. REQ-3 Acceleration Spectra for REACTOR & CONTROL BLDGS.
 Load Case: Susquehanna SRV
 Mode -, Direction E-W, Elev 749'-1"
 Damping: 0.005, 0.01, 0.02, 0.05

REV. 6, 4/82

**SUSQUEHANNA STEAM ELECTRIC STATION
 UNITS 1 AND 2
 DESIGN ASSESSMENT REPORT**

**REACTOR/CONTROL BUILDING
 RESPONSE SPECTRA**

KWU-SRV

FIGURE C- 29

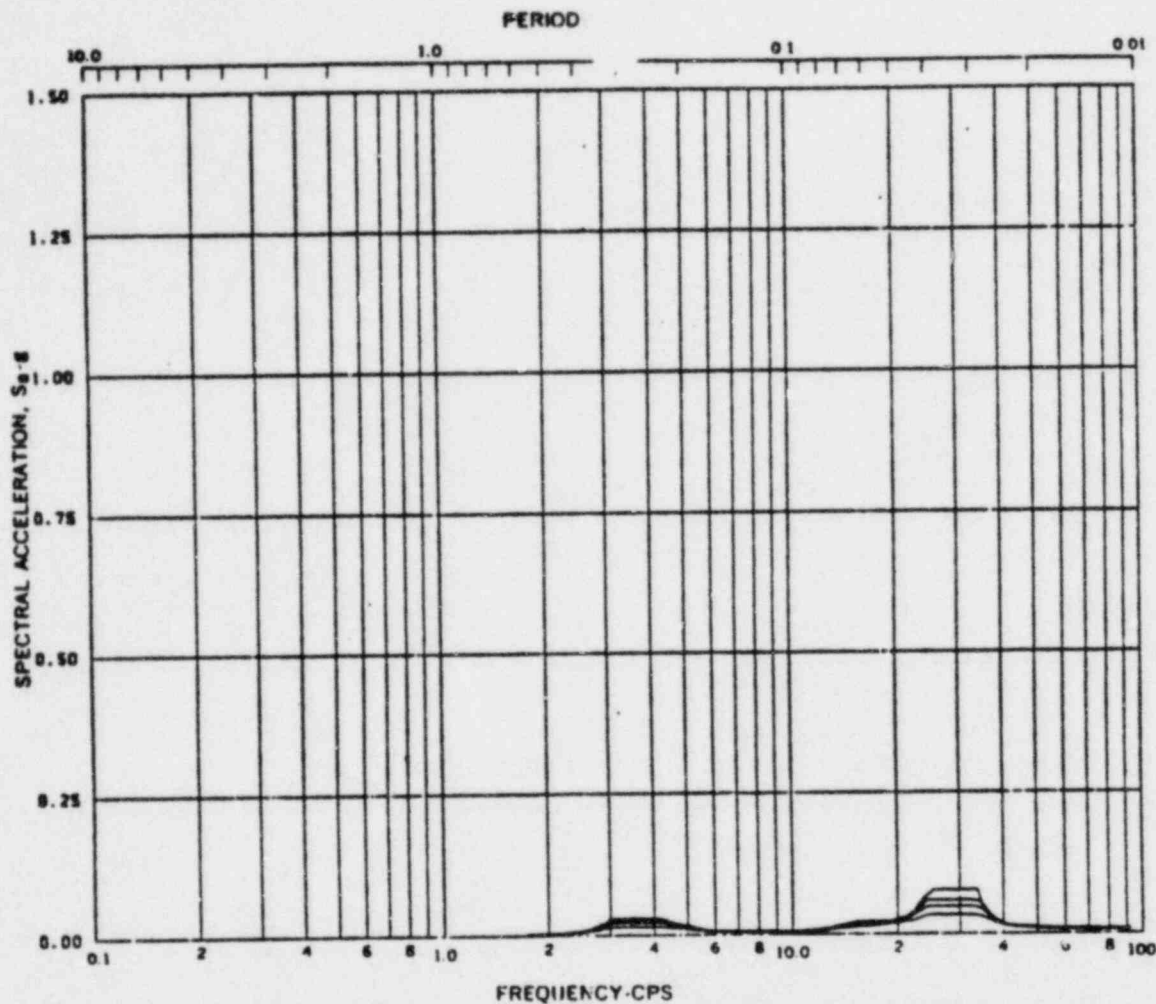


Fig. BE10-3 Acceleration Spectra for REACTOR & CONTROL BLDGS.
 Load Case: Susquehanna SRV
 Mode -, Direction E-W, Elev 771'-0"
 Damping: 0.005, 0.01, 0.02, 0.05

REV. 6, 4/82

**SUSQUEHANNA STEAM ELECTRIC STATION
 UNITS 1 AND 2
 DESIGN ASSESSMENT REPORT**

**REACTOR/CONTROL BUILDING
 RESPONSE SPECTRA**

KWU-SRV

FIGURE C- 30

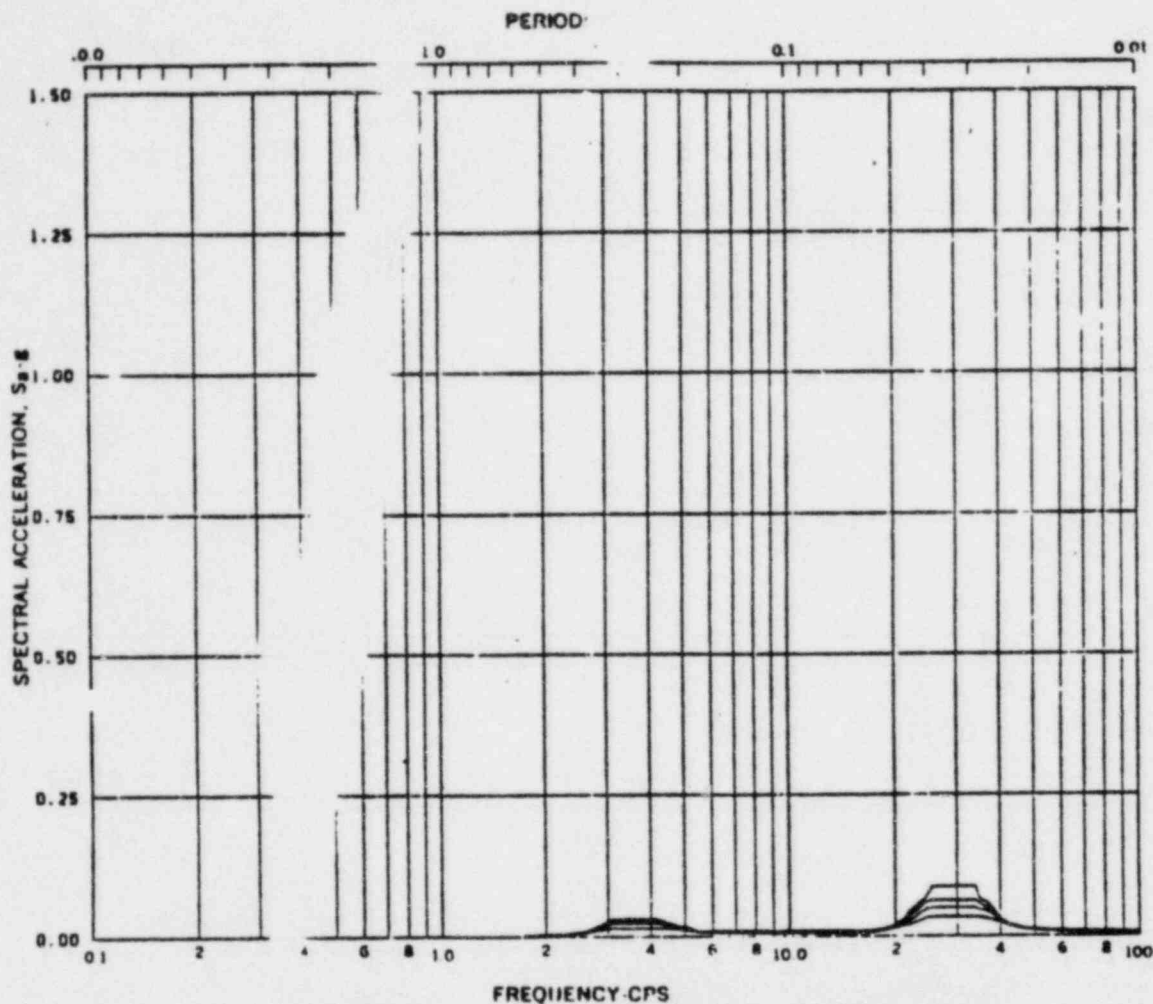


Fig. BE11-3 Acceleration Spectra for REACTOR & CONTROL BLDGS.
 Load Case: Susquehanna SRV
 Mode -, Direction F-W, Elev 779'-1"
 Damping: 0.005, 0.01, 0.02, 0.05

REV. 6, 4/82

**SUSQUEHANNA STEAM ELECTRIC STATION
 UNITS 1 AND 2
 DESIGN ASSESSMENT REPORT**

**REACTOR/CONTROL BUILDING
 RESPONSE SPECTRA**

KWU-SRV
 FIGURE C- 31

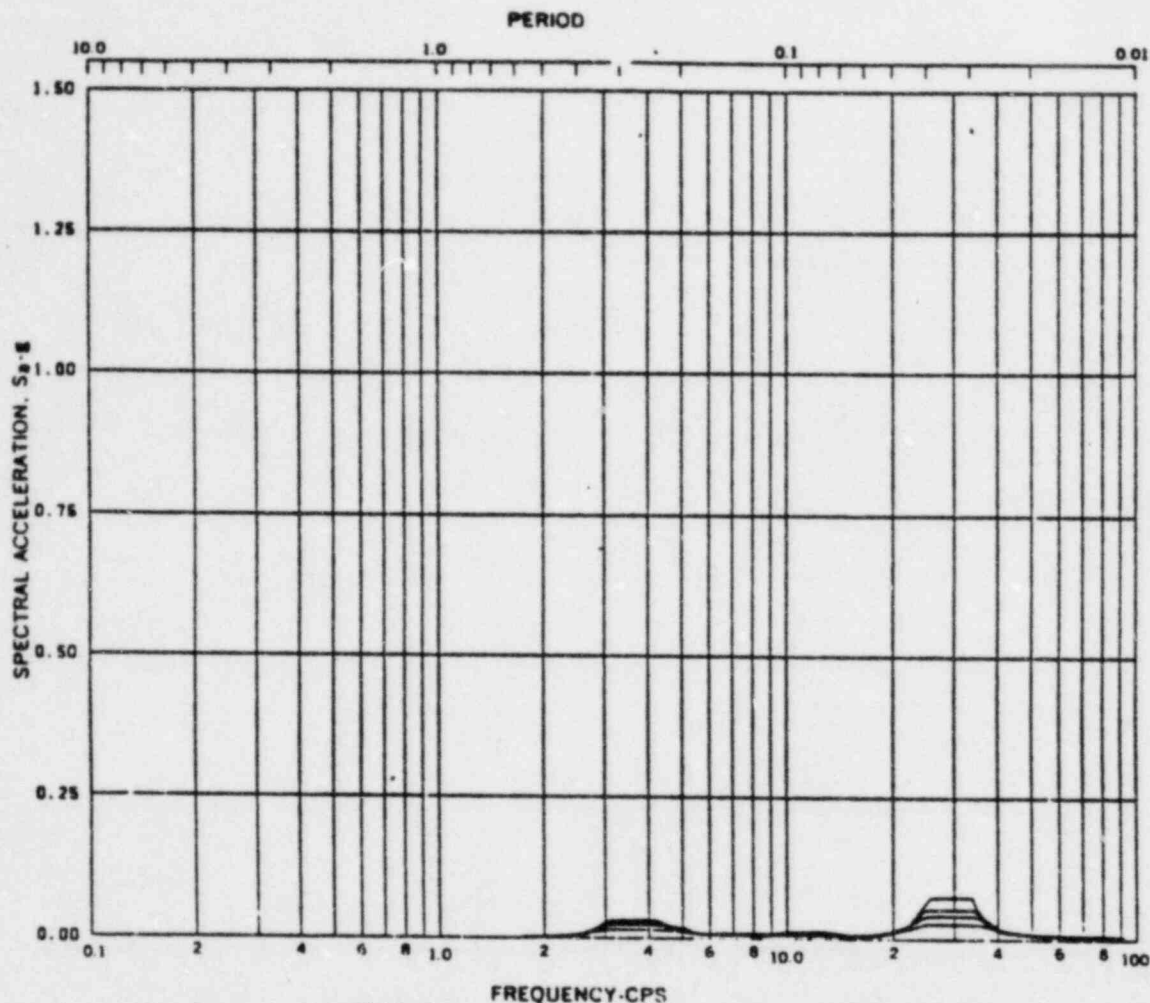


Fig. BE12-3 Acceleration Spectra for REACTOR & CONTROL BLDGS.
 Load Case Busquehanna SRV
 Mode -, Direction E-W, Elev 783'-0"
 Damping: 0.005, 0.01, 0.02, 0.05

REV. 6, 4/82

BUSQUEHANNA STEAM ELECTRIC STATION UNITS 1 AND 2 DESIGN ASSESSMENT REPORT
REACTOR/CONTROL BUILDING RESPONSE SPECTRA
KWU-SRV FIGURE C- 32

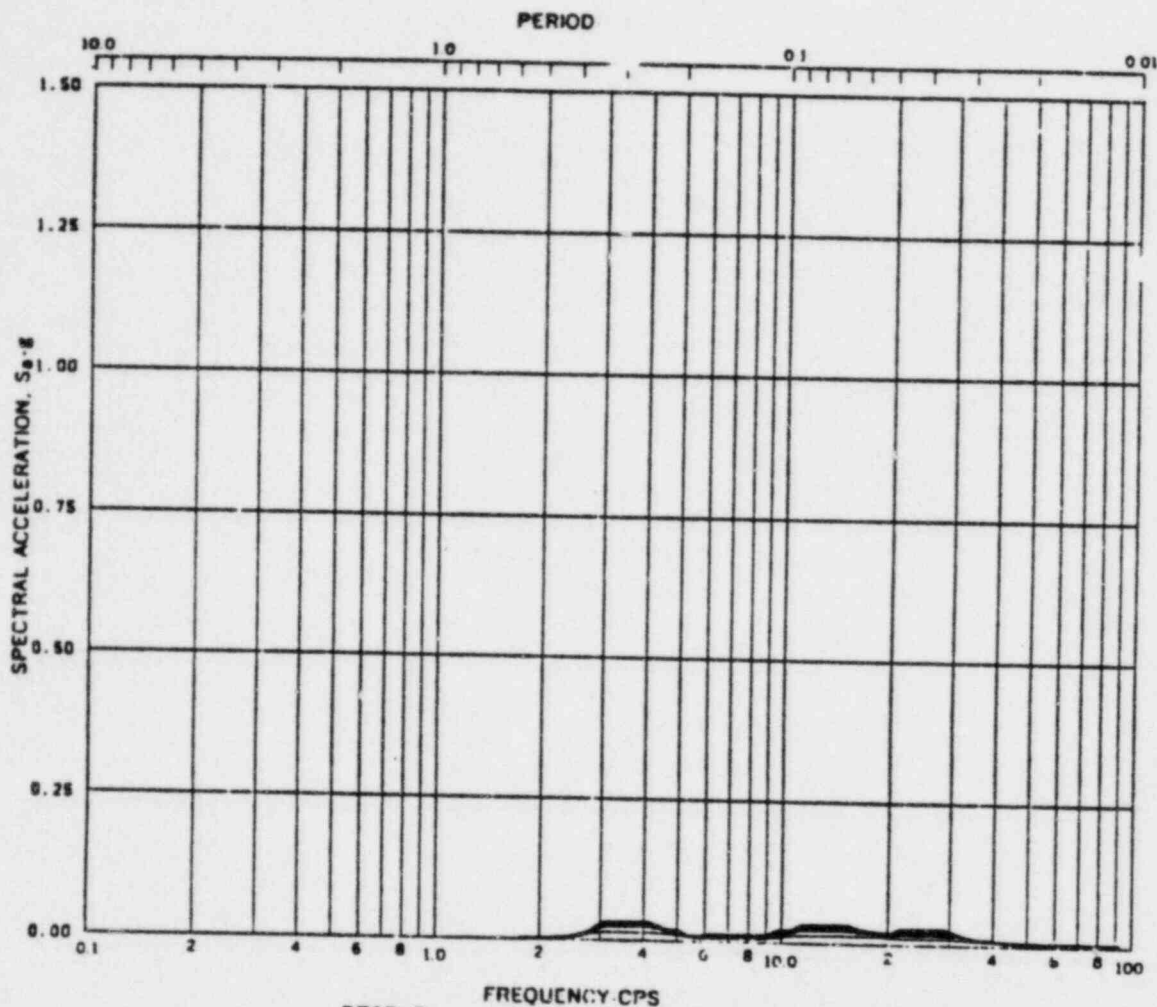


Fig. BE13-3 Acceleration Spectra for REACTOR & CONTROL BLDGS.
 Load Case: Susquehanna SRV
 Mode -, Direction E-W, Elev 799'-1"
 Damping: 0.005, 0.01, 0.02, 0.05

REV. 6, 4/82

SUSQUEHANNA STEAM ELECTRIC STATION UNITS 1 AND 2 DESIGN ASSESSMENT REPORT
REACTOR/CONTROL BUILDING RESPONSE SPECTRA
KWU-SRV FIGURE C- 33

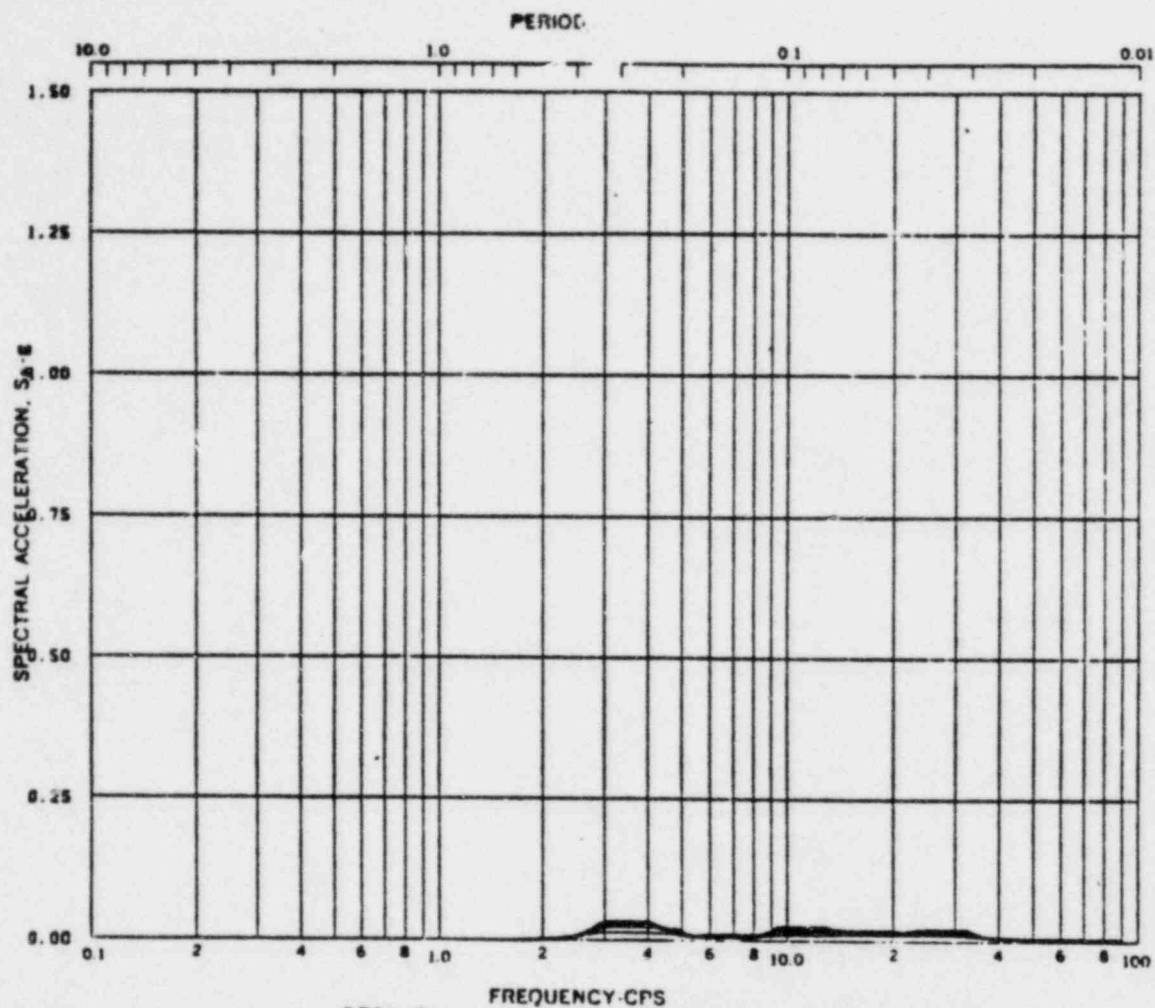


Fig. BE14-3 Acceleration Spectra for REACTOR & CONTROL BLDGS.
 Load Case: Susquehanna SRV
 Mode -, Direction E-W, Elev 806'-0"
 Damping: 0.005, 0.01, 0.02, 0.05

REV. 6, 4/82

**SUSQUEHANNA STEAM ELECTRIC STATION
 UNITS 1 AND 2
 DESIGN ASSESSMENT REPORT**

**REACTOR/CONTROL BUILDING
 RESPONSE SPECTRA**

KWU-SRV

FIGURE C- 34

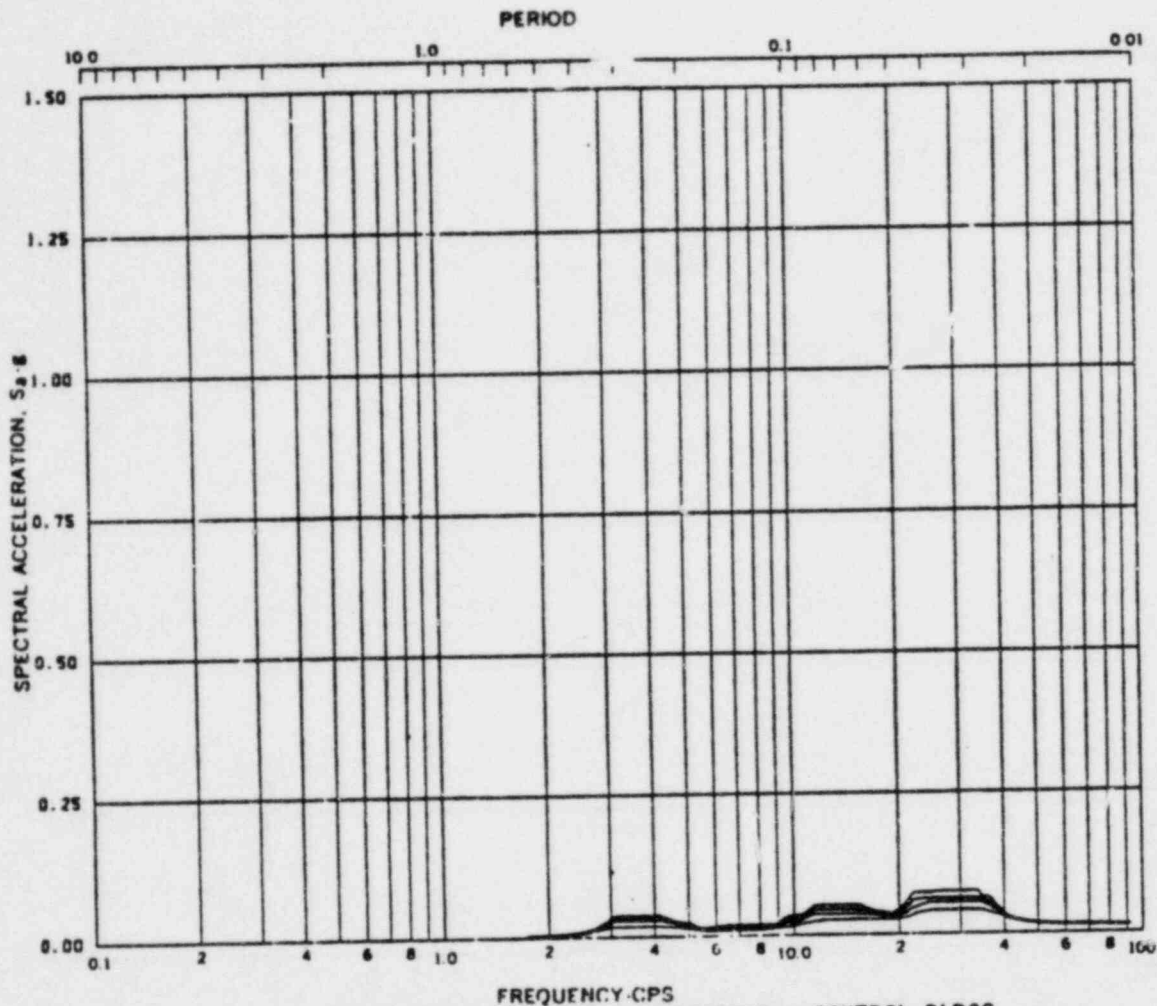


Fig. BE15-3 Acceleration Spectra for REACTOR & CONTROL BLDGS.
 Load Case: Susquehanna SRV
 Mode -, Direction E-W, Elev 818'-1"
 Damping: 0.005, 0.01, 0.02, 0.05

REV. 6, 4/82

**SUSQUEHANNA STEAM ELECTRIC STATION
 UNITS 1 AND 2
 DESIGN ASSESSMENT REPORT**

**REACTOR/CONTROL BUILDING
 RESPONSE SPECTRA**

KWU-SRV
 FIGURE C- 35

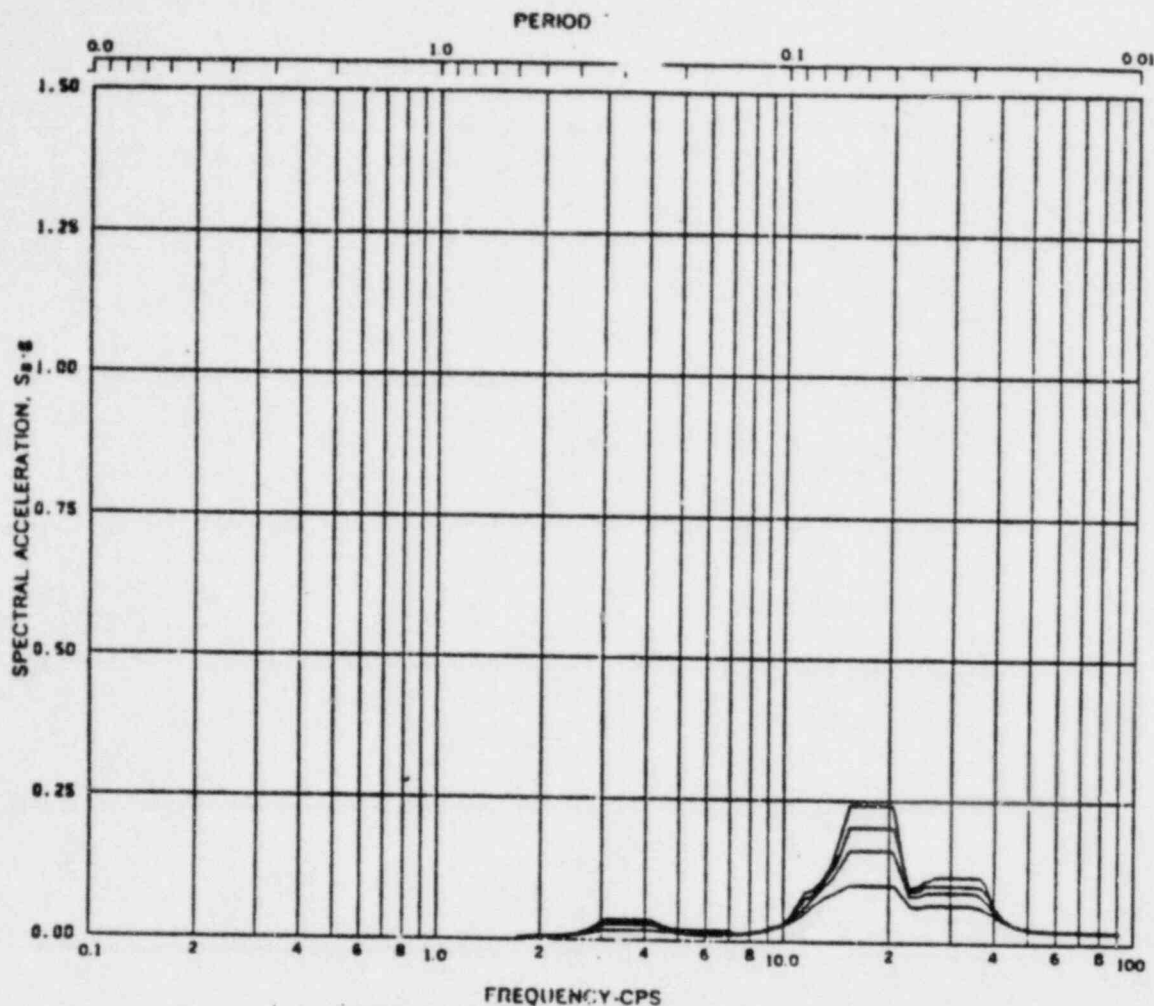


Fig. BE16-3 Acceleration Spectra for REACTOR & CONTROL BLDGS.
 Load Case: Susquehanna SRV
 Node -, Direction E-W, Elev 846'-0"
 Damping: 0.005, 0.01, 0.02, 0.05

REV. 6, 4/82

SUSQUEHANNA STEAM ELECTRIC STATION UNITS 1 AND 2 DESIGN ASSESSMENT REPORT
REACTOR/CONTROL BUILDING RESPONSE SPECTRA
KWU-SRV FIGURE C-36

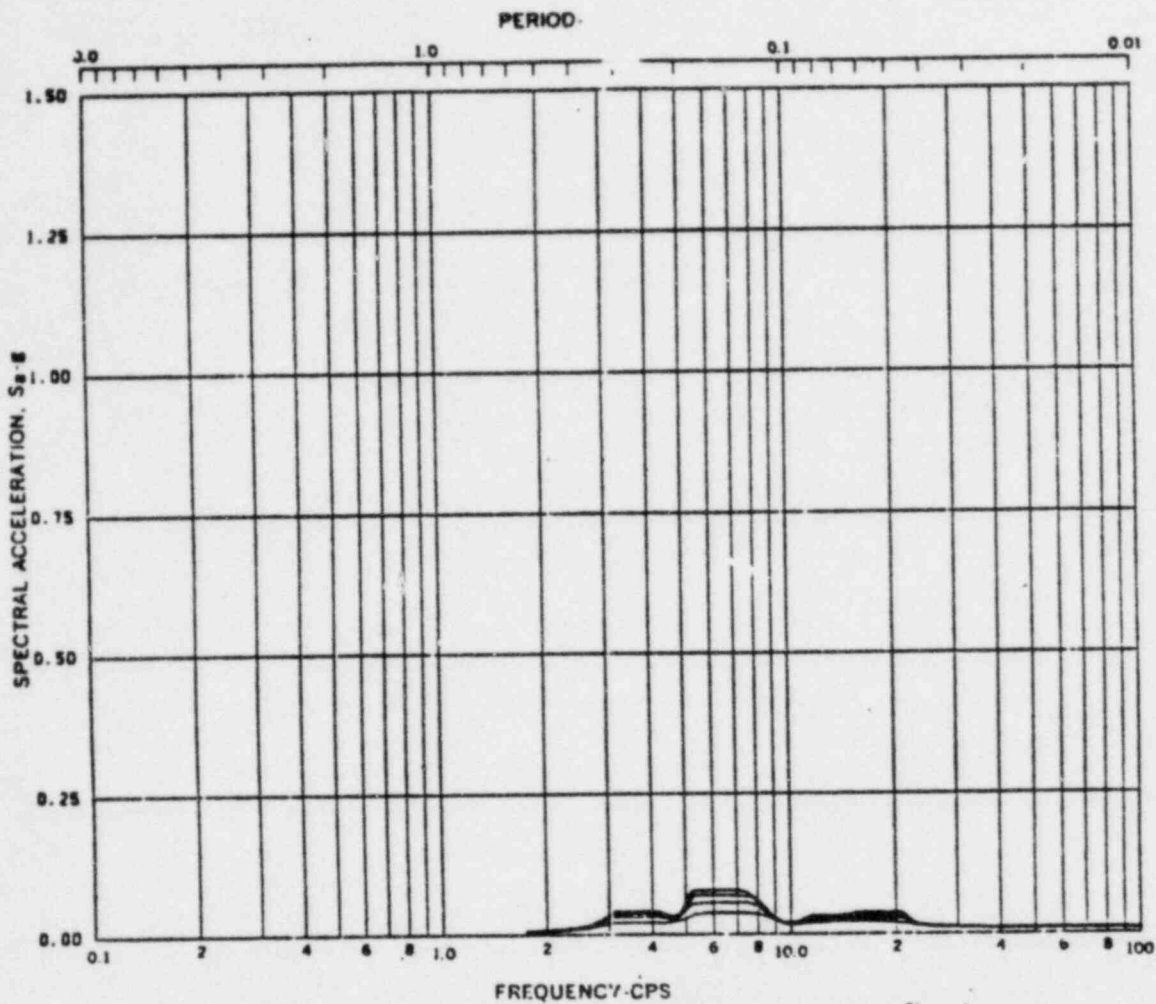


Fig. BF17-3 Acceleration Spectra for REACTOR & CONTROL BLDGS.
 Load Case: Susquehanna SRV
 Mode -, Direction E-W, Elev 870'-0"
 Damping: 0.005, 0.01, 0.02, 0.05

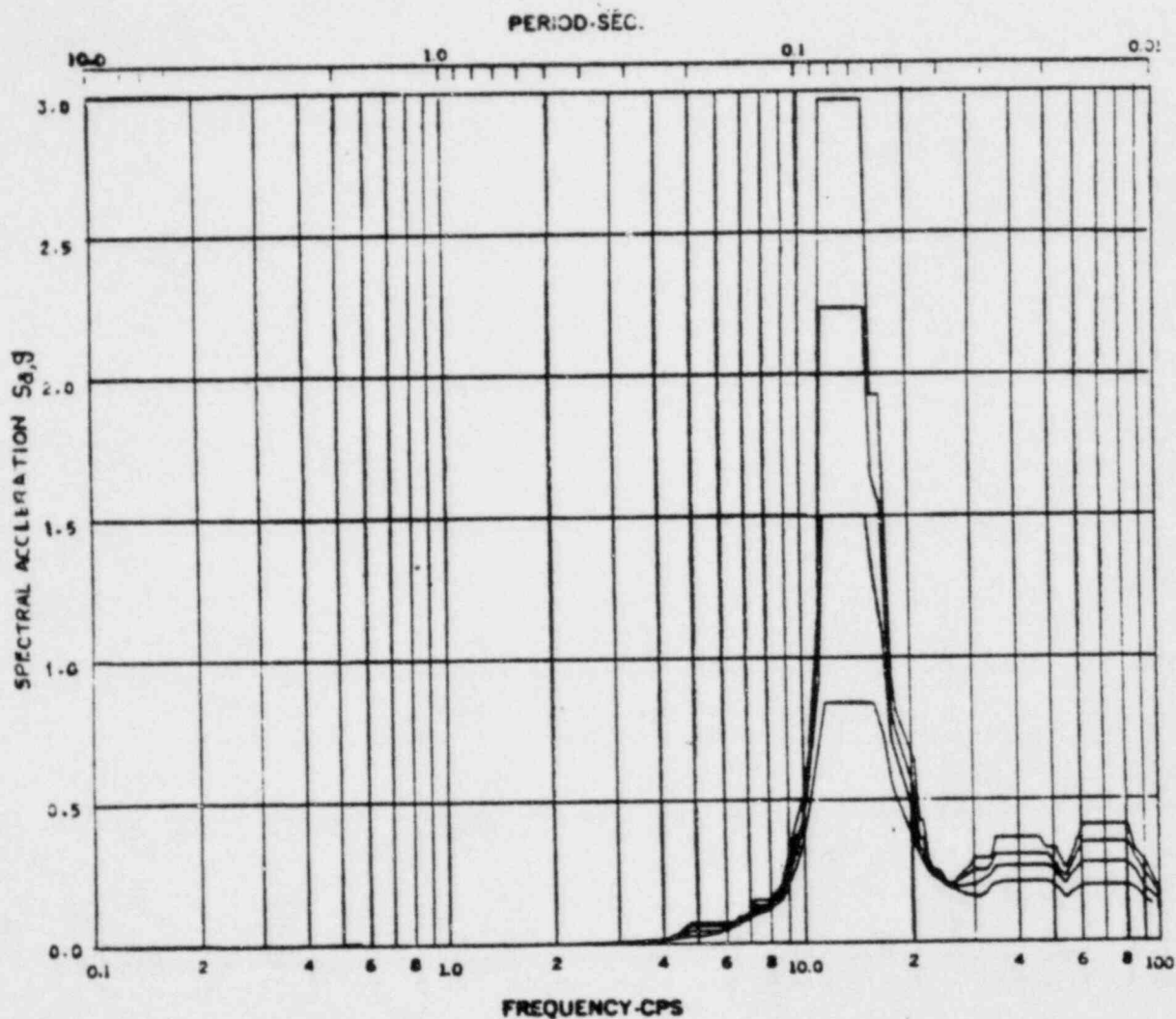
REV. 6, 4/82

SUSQUEHANNA STEAM ELECTRIC STATION
 UNITS 1 AND 2
 DESIGN ASSESSMENT REPORT

REACTOR/CONTROL BUILDING
 RESPONSE SPECTRA

KWU-SRV

FIGURE C- 37



Acceleration Spectra for REACTOR BUILDING
 Load Case: Susquehanna KWU---LOCA
 Mode: --- Direction: VERT., Elev: 670'-2"
 Damping: 0.005, 0.01, 0.02, 0.05

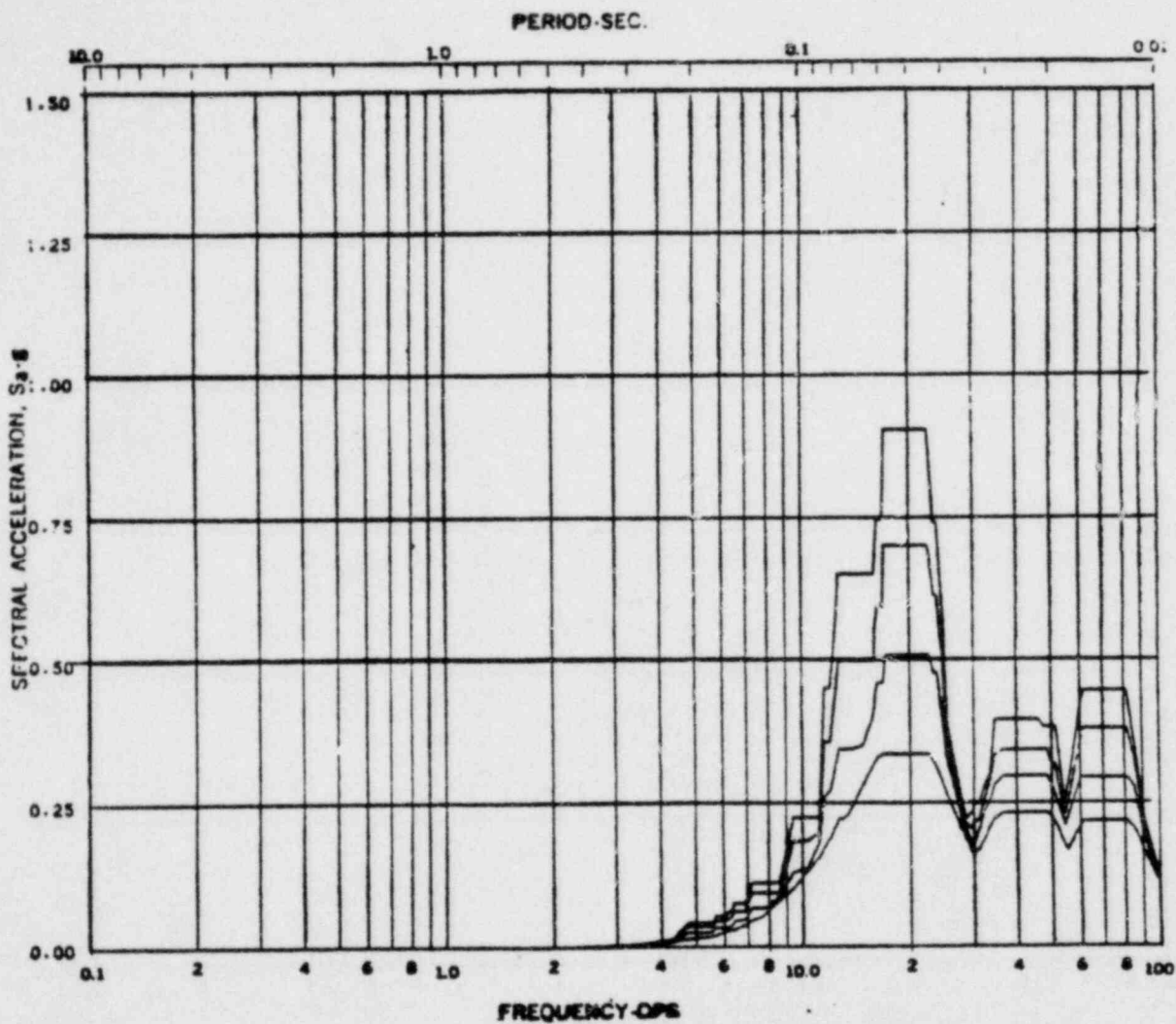
REV. 6, 4/82

SUSQUEHANNA STEAM ELECTRIC STATION
UNITS 1 AND 2
DESIGN ASSESSMENT REPORT

REACTOR/CONTROL BUILDING
 RESPONSE SPECTRA

KWU-LOCA

FIGURE C-38



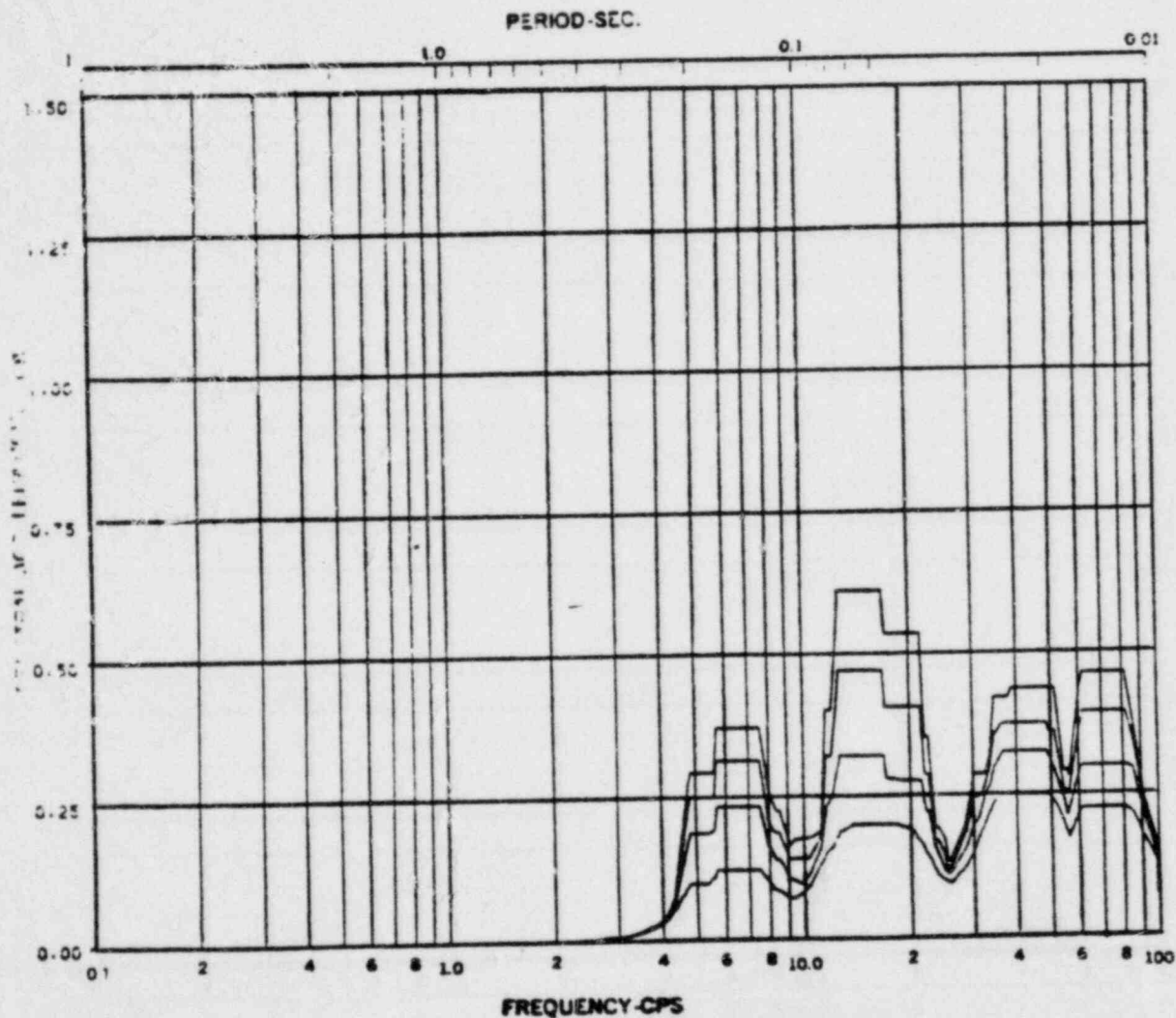
Acceleration System for REACTOR BUILDING
 Load Case: Seismicity KWU-LOCA
 Site ---, Direction VERT., Dir 575'-N
 Sampling: 0.001, 0.01, 0.02, 0.05

REV. 6, 4/82

SUSQUEHANNA STEAM ELECTRIC STATION
 UNITS 1 AND 2
 DESIGN ASSESSMENT REPORT

REACTOR/CONTROL BUILDING
 RESPONSE SPECTRA
 KWU-LOCA

FIGURE C39



FREQUENCY-CPS

Response Spectra for REACTOR BUILDING
 Load Case: Seismicity 1001--- LOCA
 Mode ---, Direction VERT., Elev 683'-3"
 Sampling: 0.010, 0.01, 0.02, 0.05

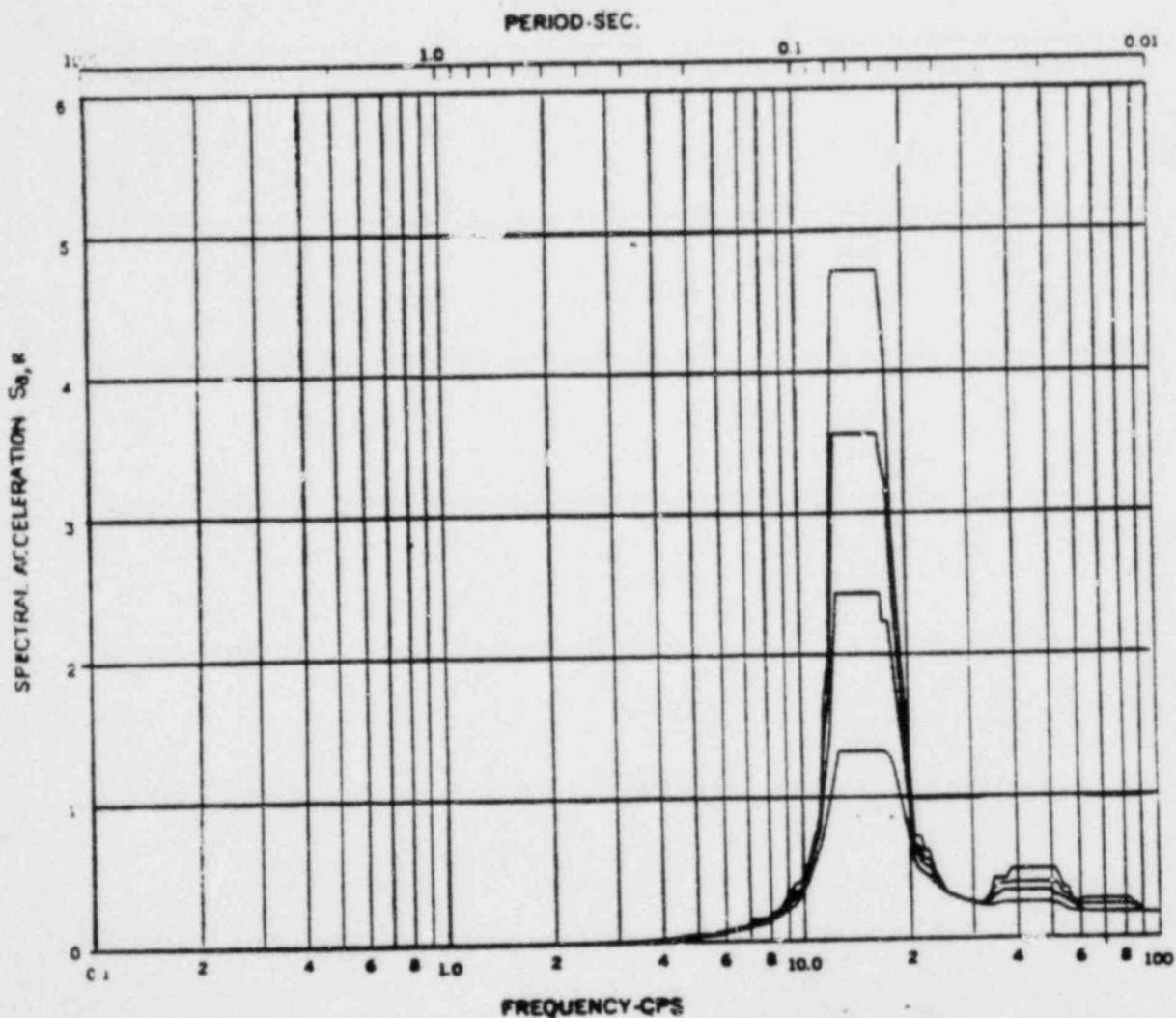
REV. 6, 4/82

SUSQUEHANNA STEAM ELECTRIC STATION
 UNITS 1 AND 2
 DESIGN ASSESSMENT REPORT

REACTOR/CONTROL BUILDING
 RESPONSE SPECTRA

KWU-LOCA

FIGURE C-40



Acceleration Spectra for REACTOR BUILDING
 Load Case: Seismicity KWU-LOCA
 Mode --- Direction VERT. Elev 697'-7"
 Damping: 0.05, 0.01, 0.02, 0.05

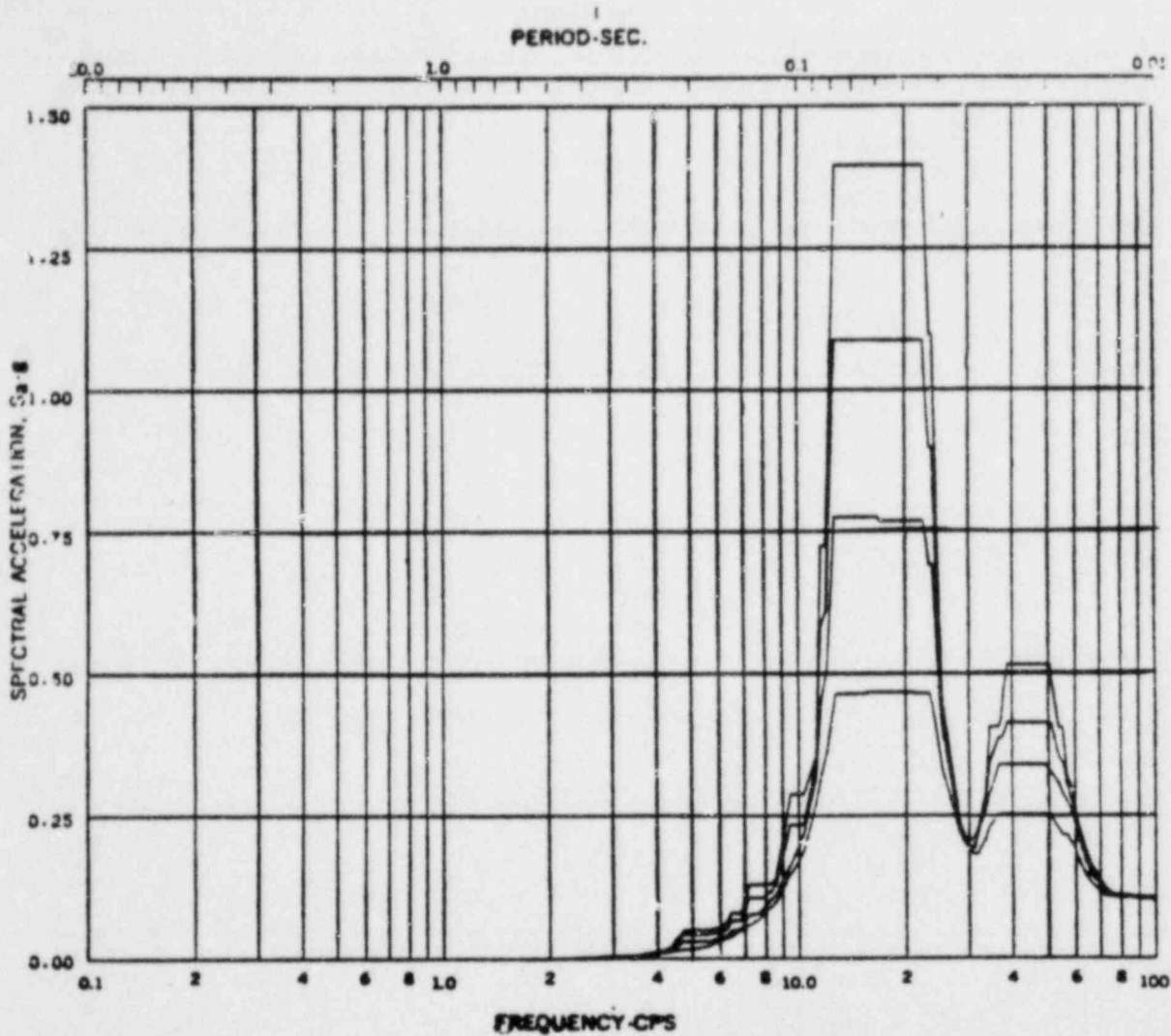
REV. 6, 4/82

BUSQUEHANNA STEAM ELECTRIC STATION
 UNITS 1 AND 2
 DESIGN ASSESSMENT REPORT

REACTOR/CONTROL BUILDING
 RESPONSE SPECTRA

KWU-LOCA

FIGURE C-41



Acceleration 75% for REACTOR BUILDING
 Load Case 2000 KWU-LOCA
 Mode VERT., Dir 79'-J
 Damping 0.005, 0.01, 0.02, 0.05

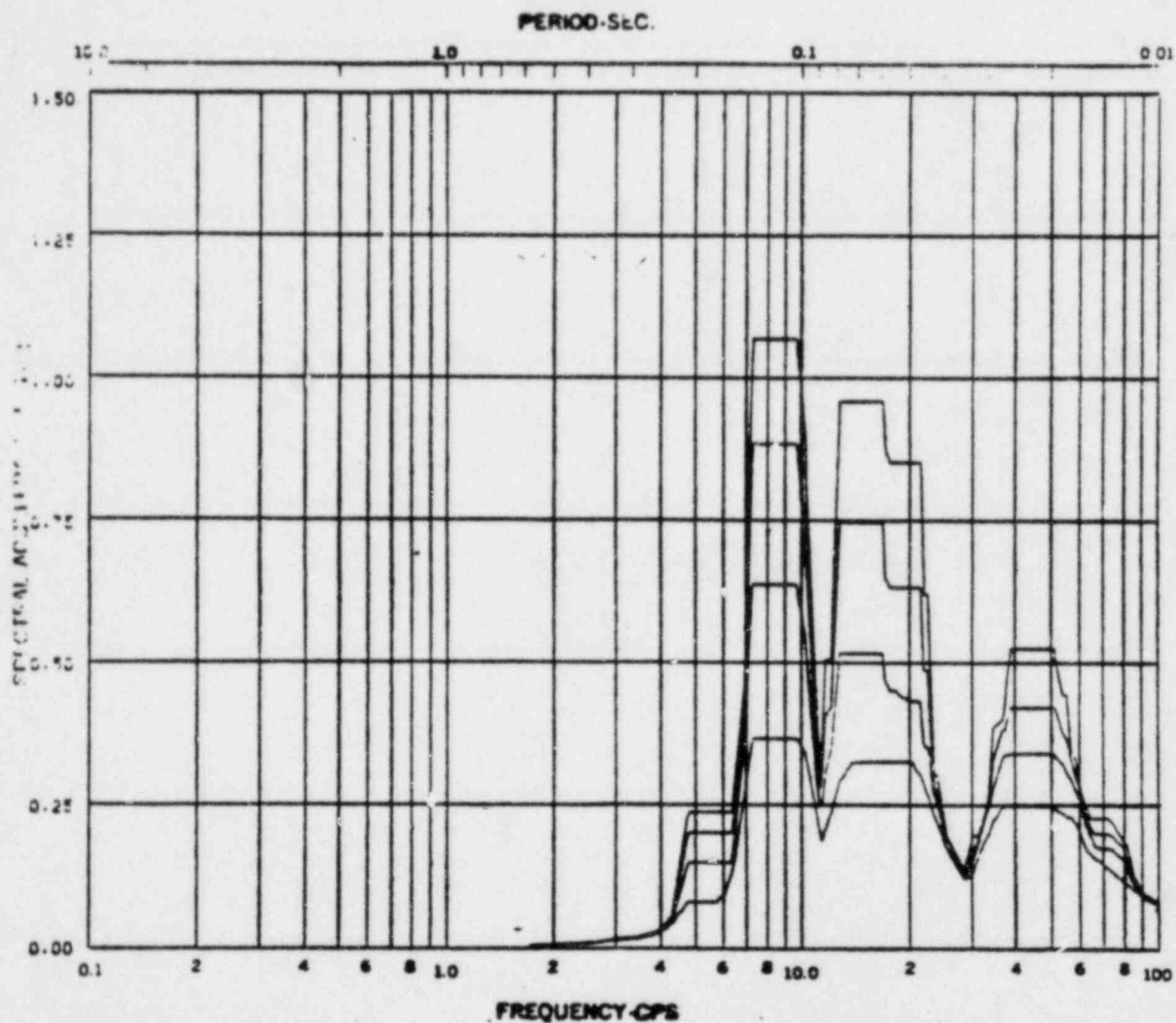
REV. 6, 4/82

SUSQUEHANNA STEAM ELECTRIC STATION
 UNITS 1 AND 2
 DESIGN ASSESSMENT REPORT

REACTOR/CONTROL BUILDING
 RESPONSE SPECTRA

KWU-LOCA

FIGURE C-42



Acceleration Spectra for REACTOR BUILDING
 Load Case: Seismicity KWU--- LOCA
 Mode ---, Direction VERT., Elev 719'-1"
 Sampling: 0.015, 0.01, 0.02, 0.05

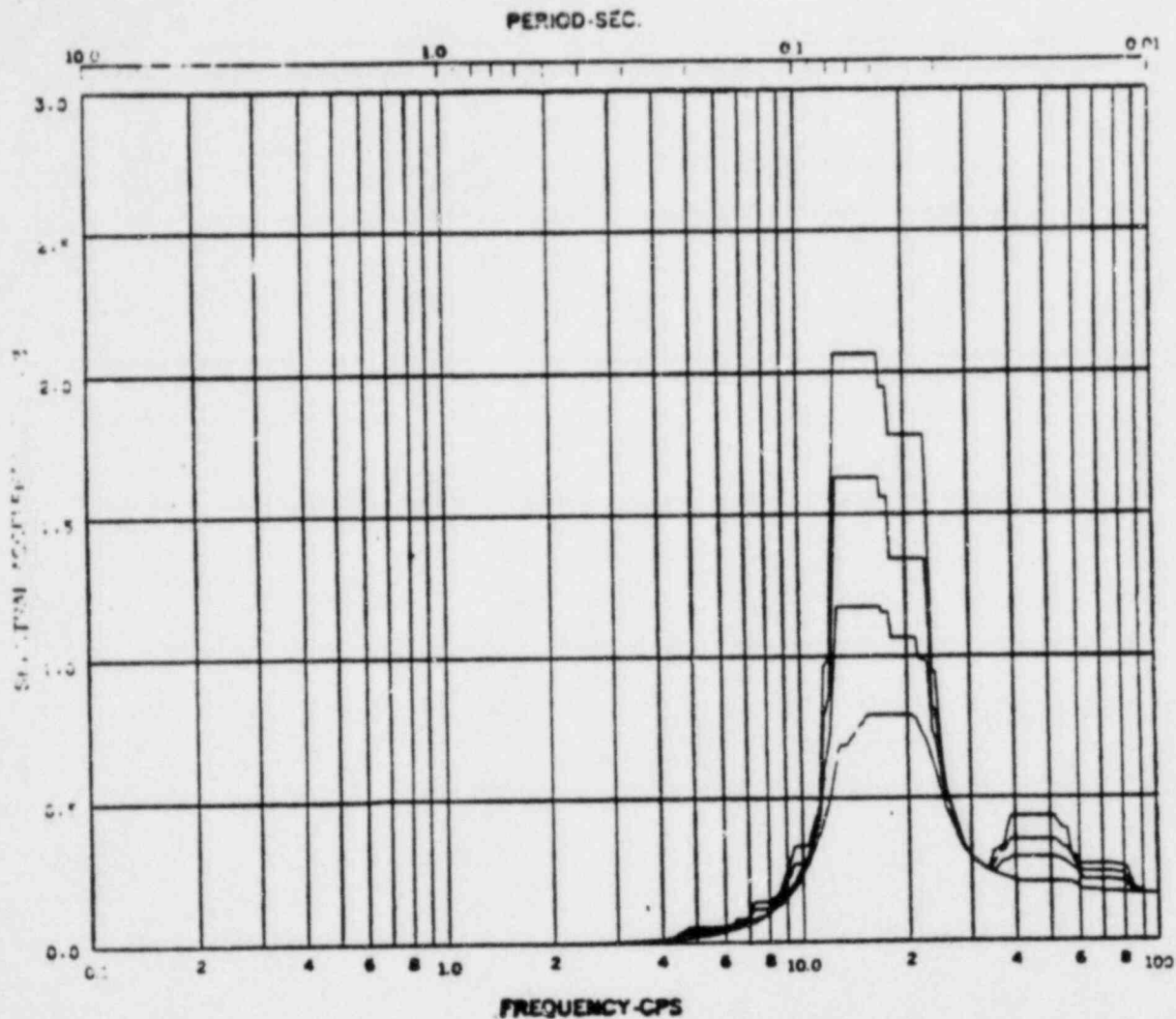
REV. 6, 4/82

SUSQUEHANNA STEAM ELECTRIC STATION
 UNITS 1 AND 2
 DESIGN ASSESSMENT REPORT

REACTOR/CONTROL BUILDING
 RESPONSE SPECTRA

KWU-LOCA

FIGURE C-43



Acceleration Spectra for REACTOR BUILDING
 Load Case: Seismicity 1021 --- LOCA
 Mode --- Direction VERT., 728'-0"
 Sampling: 0.005, 0.01, 0.02, 0.05

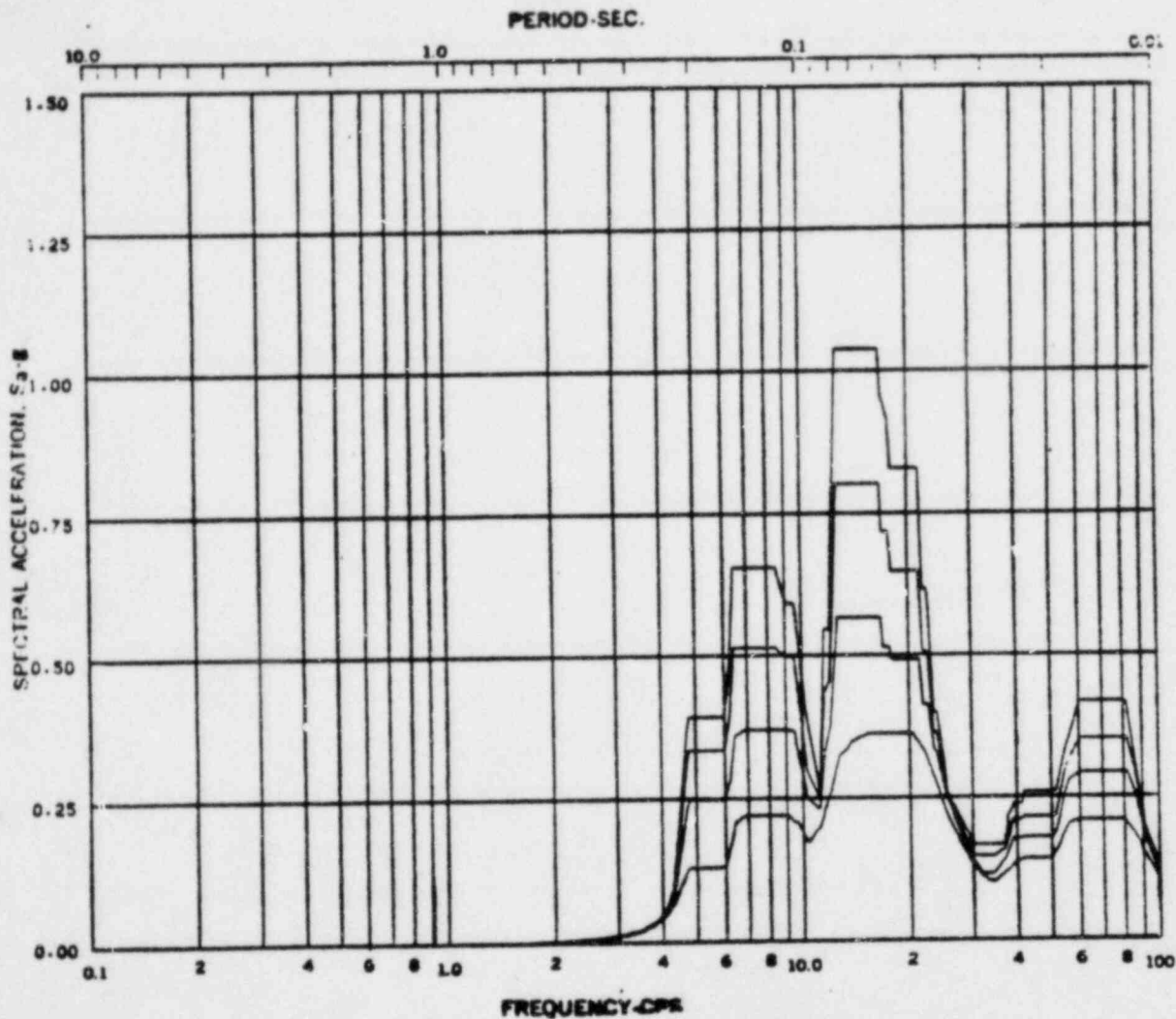
REV. 6, 4/82

SUSQUEHANNA STEAM ELECTRIC STATION
 UNITS 1 AND 2
 DESIGN ASSESSMENT REPORT

REACTOR/CONTROL BUILDING
 RESPONSE SPECTRA

KWU-LOCA

FIGURE C-44



Acceleration Spectra for REACTOR BUILDING
 Load Case: Seismicity KWU --- LOCA
 Site ---, Direction VERT., 789'±1"
 Sampling: 0.001, 0.01, 0.02, 0.05

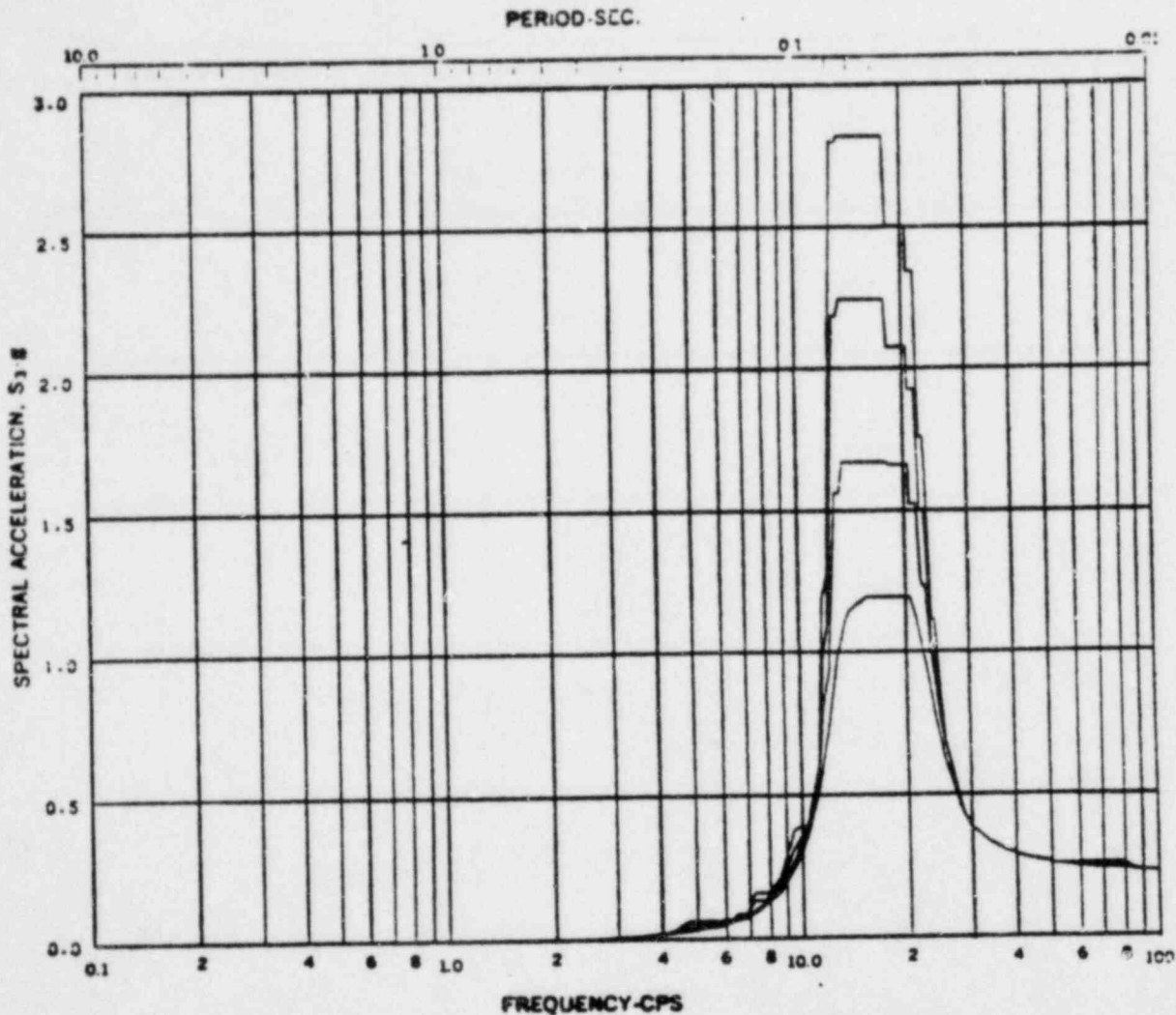
REV. 6, 4/82

BUSQUEHANNA STEAM ELECTRIC STATION
 UNITS 1 AND 2
 DESIGN ASSESSMENT REPORT

REACTOR/CONTROL BUILDING
 RESPONSE SPECTRA

KWU-LOCA

FIGURE C-45



Acceleration Spectra for REACTOR BUILDING
 Load Case: Seismicity KWL --- LOCA
 Mode --- Direction VERT., Elev 753'-0"
 Damping: 0.05%, 0.01%, 0.02%, 0.05%

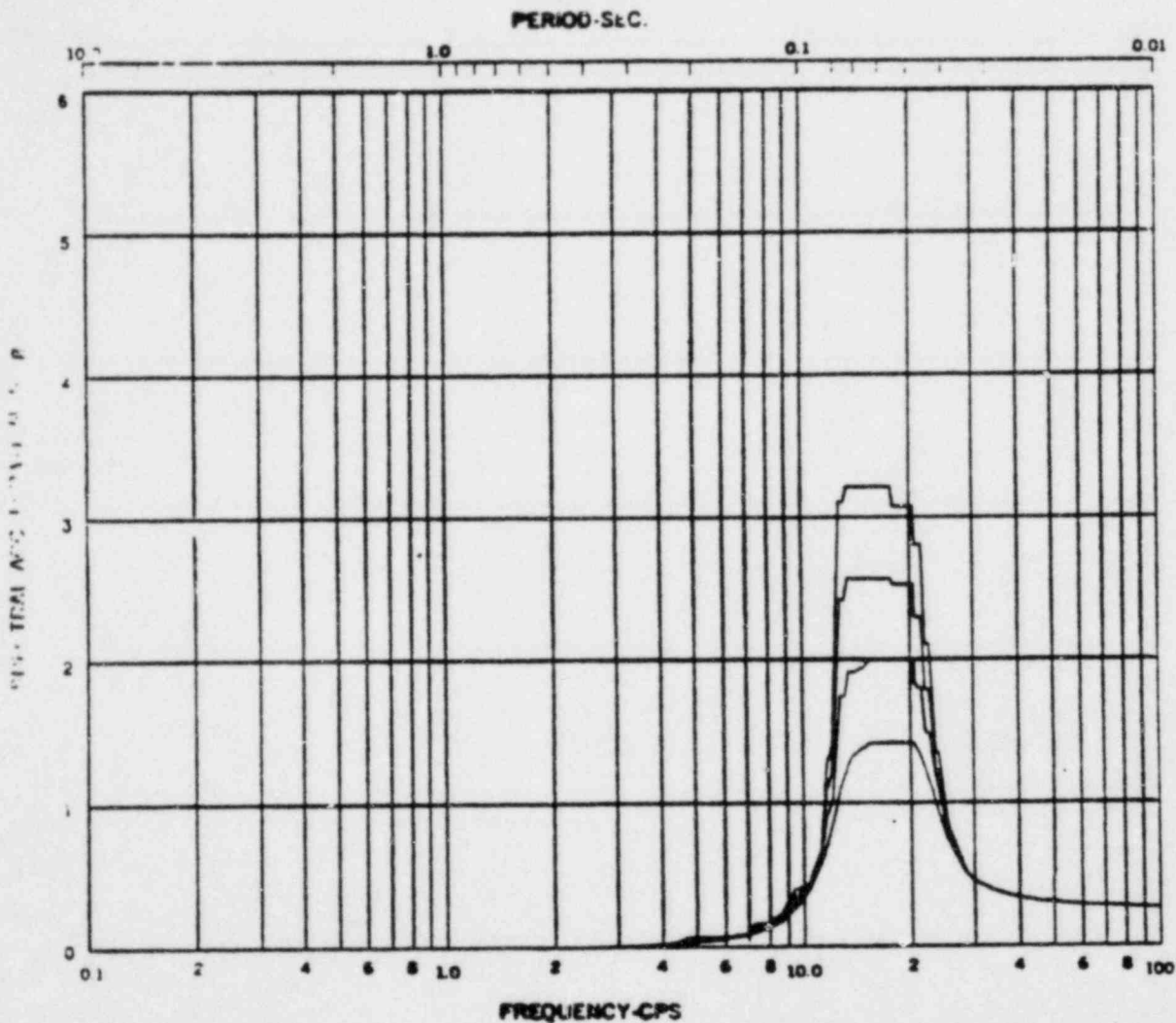
REV. 6, 4/82

SUSQUEHANNA STEAM ELECTRIC STATION
 UNITS 1 AND 2
 DESIGN ASSESSMENT REPORT

REACTOR/CONTROL BUILDING
 RESPONSE SPECTRA

KWL-LOCA

FIGURE C-46



Response Spectra for REACTOR BUILDING
 Load Case: Seismicity KWU-LOCA
 Mode ---, Direction VERT., 180° ZZ1'-0"
 Sampling: 0.001, 0.01, 0.02, 0.05

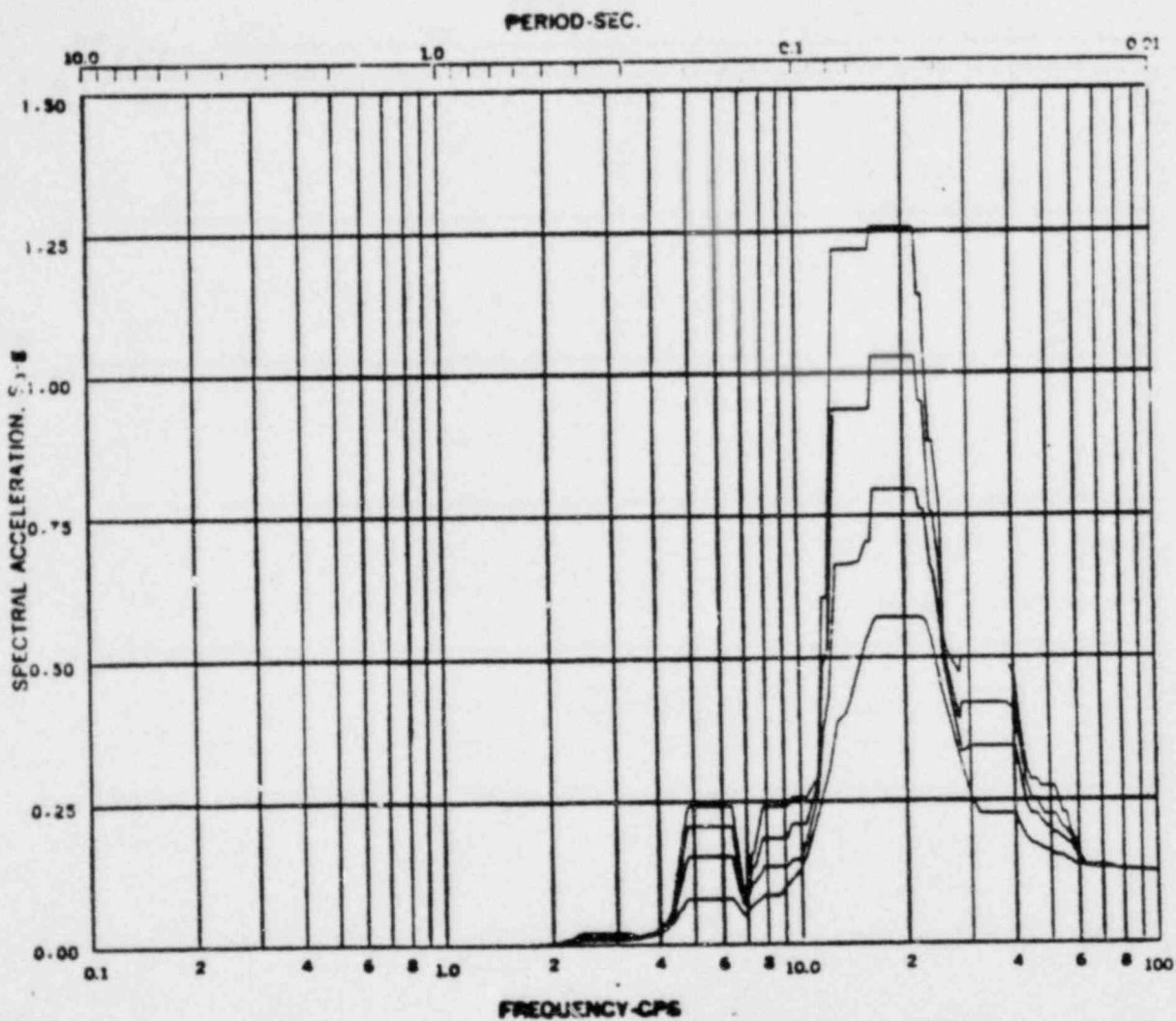
REV. 6, 4/82

BUSQUEHANNA STEAM ELECTRIC STATION
UNITS 1 AND 2
DESIGN ASSESSMENT REPORT

REACTOR/CONTROL BUILDING
RESPONSE SPECTRA

KWU-LOCA

FIGURE C- 47



Acceleration Spectra for REACTOR BUILDING
 Load Case: Normal KWU --- LOCA
 Mode: ---, Direction VERT., 779'-1"
 Damping: 0.05, 0.04, 0.02, 0.01

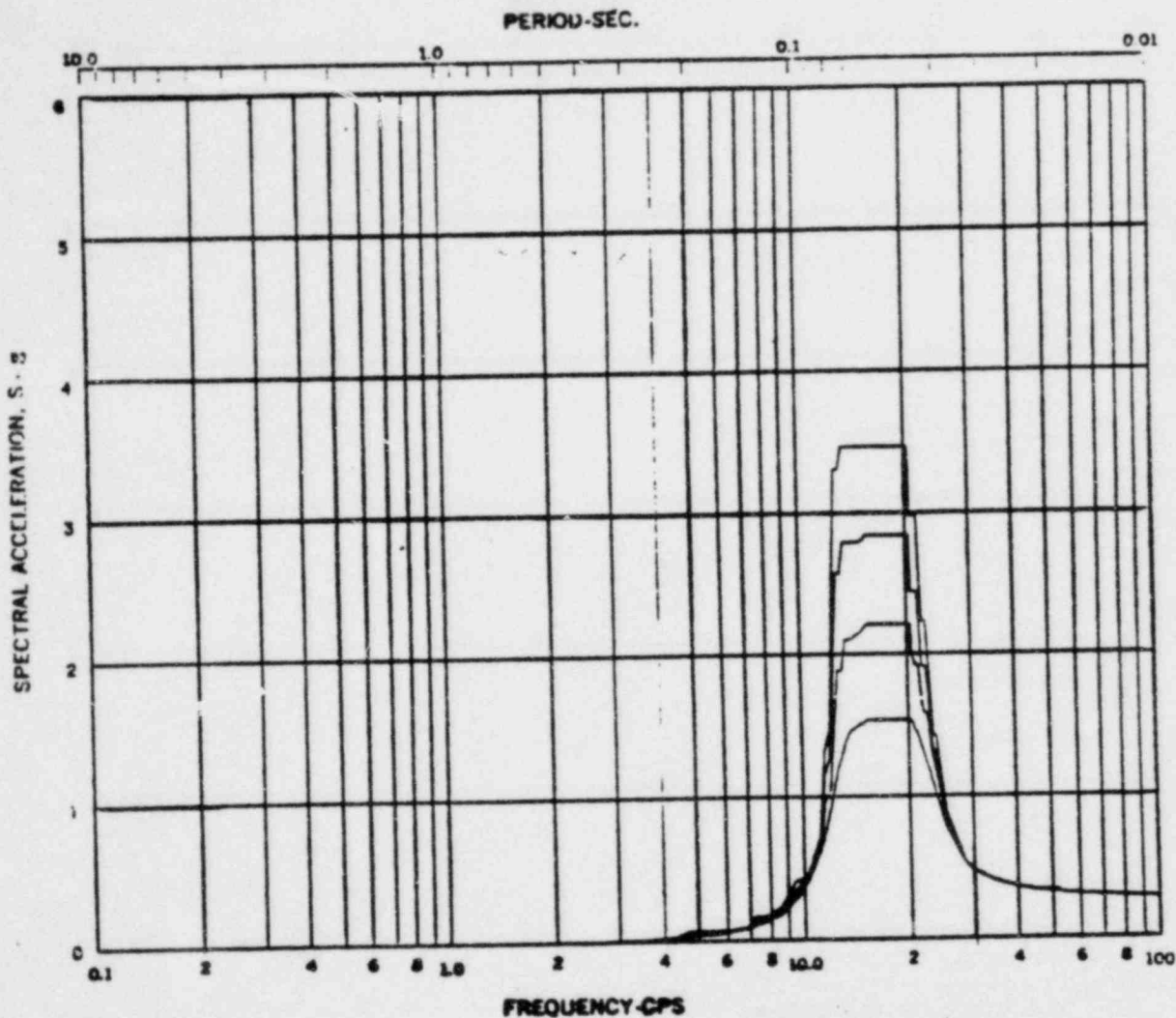
REV. 6, 4/82

**BUSQUEHANNA STEAM ELECTRIC STATION
 UNITS 1 AND 2
 DESIGN ASSESSMENT REPORT**

**REACTOR/CONTROL BUILDING
 RESPONSE SPECTR.**

KWU-LOCA

FIGURE C-48



Acceleration Spectra for REACTOR BUILDING
 Load Case: Seismicity KWU---LOCA
 Mode ---, Direction VERT., Elev 783'-0"
 Damping: 0.05%, 0.04%, 0.02%, 0.01%

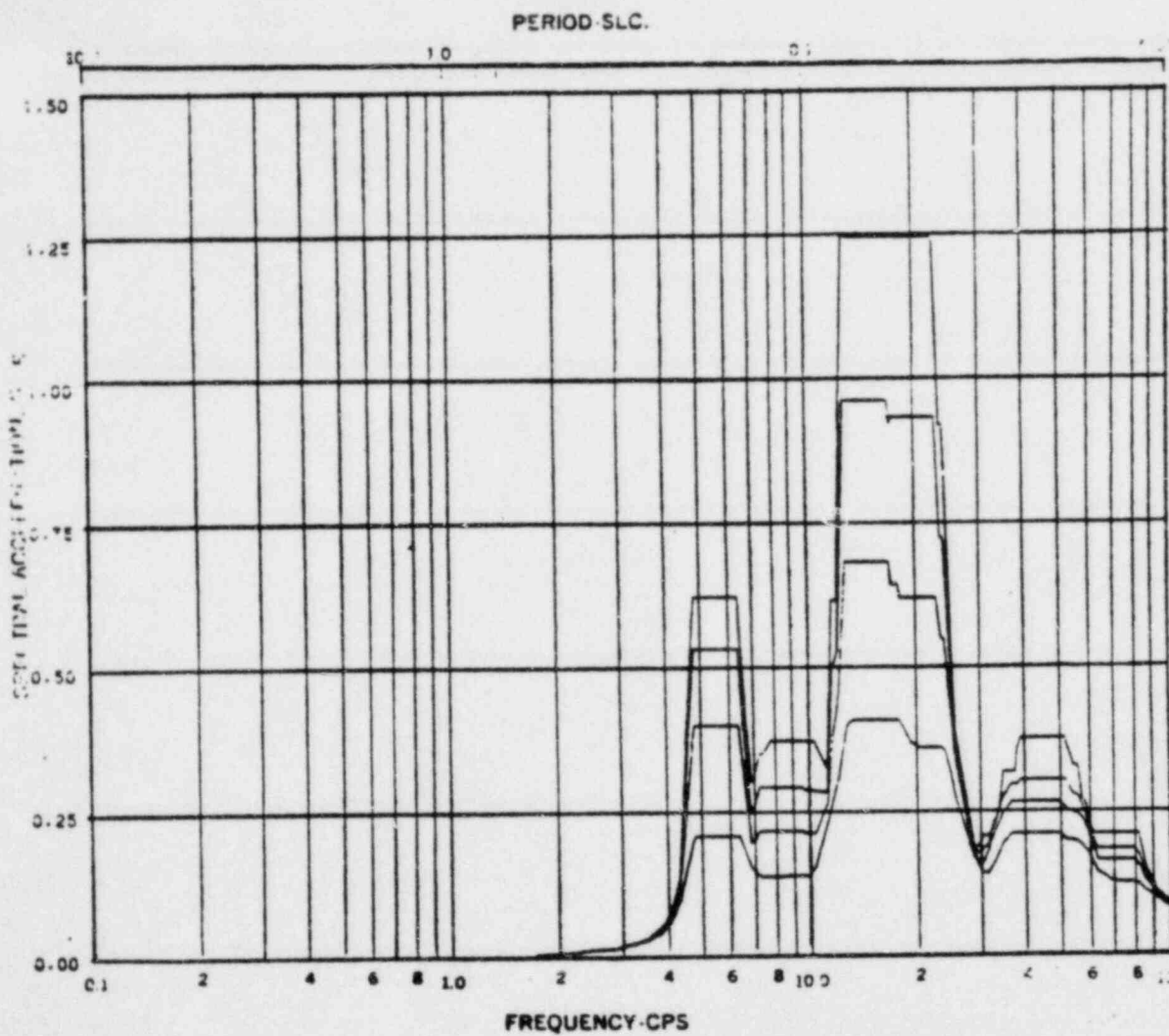
REV. 6, 4/82

SUSQUEHANNA STEAM ELECTRIC STATION
UNITS 1 AND 2
DESIGN ASSESSMENT REPORT

REACTOR/CONTROL BUILDING
 RESPONSE SPECTRA

KWU-LOCA

FIGURE C- 49



Acceleration Spectra for REACTOR BUILDING
 Load Case: Seismicity KWU--- LOCA
 Mode --- Direction VERT., Elev 799'-1"
 Damping: 0.05, 0.01, 0.02, 0.05

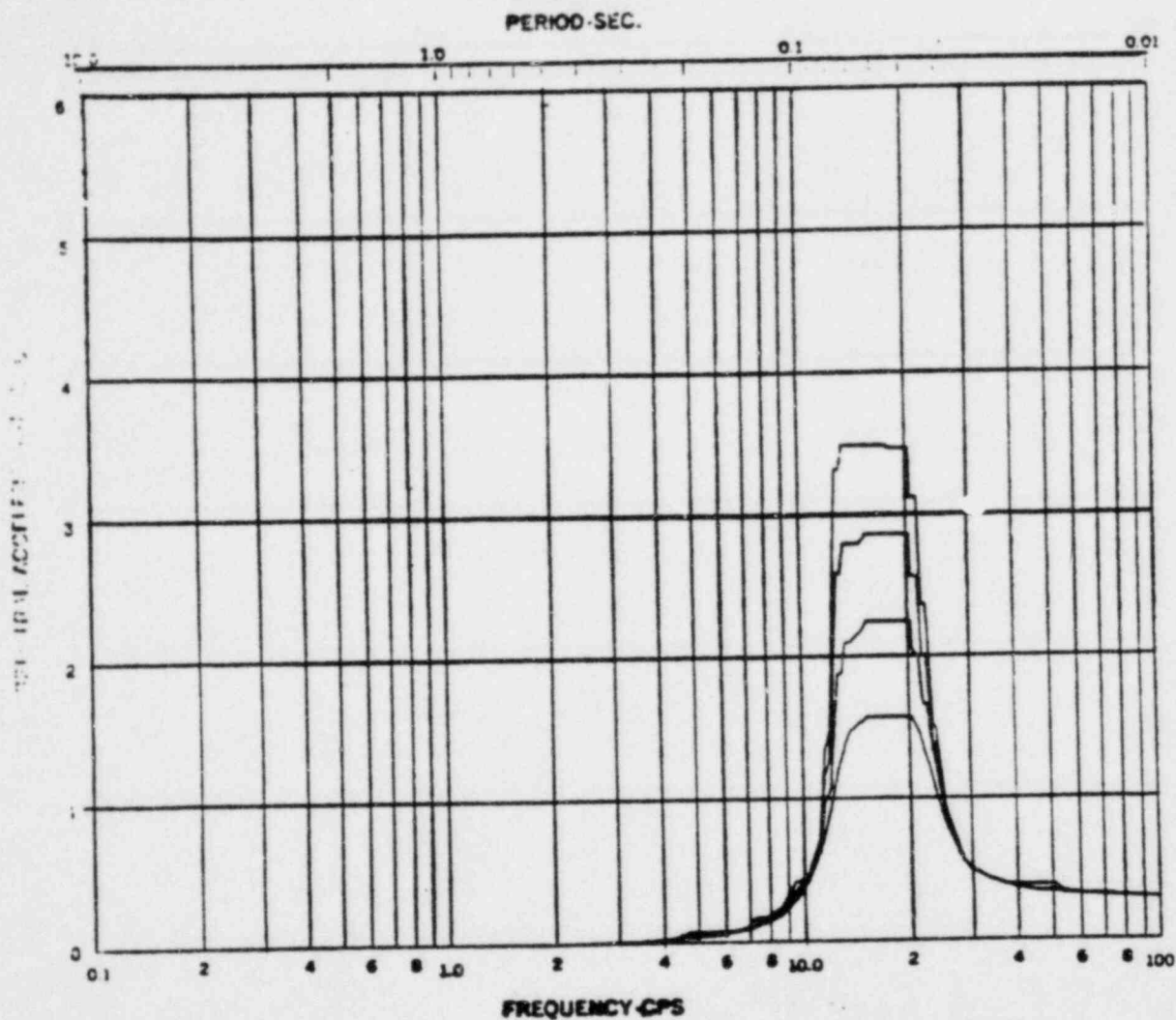
REV. 6, 4/82

**SUSQUEHANNA STEAM ELECTRIC STATION
 UNITS 1 AND 2
 DESIGN ASSESSMENT REPORT**

**REACTOR/CONTROL BUILDING
 RESPONSE SPECTRA**

KWU-LOCA

FIGURE C- 50



Acceleration Spectra for REACTOR BUILDING
 Load Case: Seismicity KWU-LOCA
 Mode: — Direction: VERT. 0°
 Display: 0.001, 0.01, 0.02, 0.05

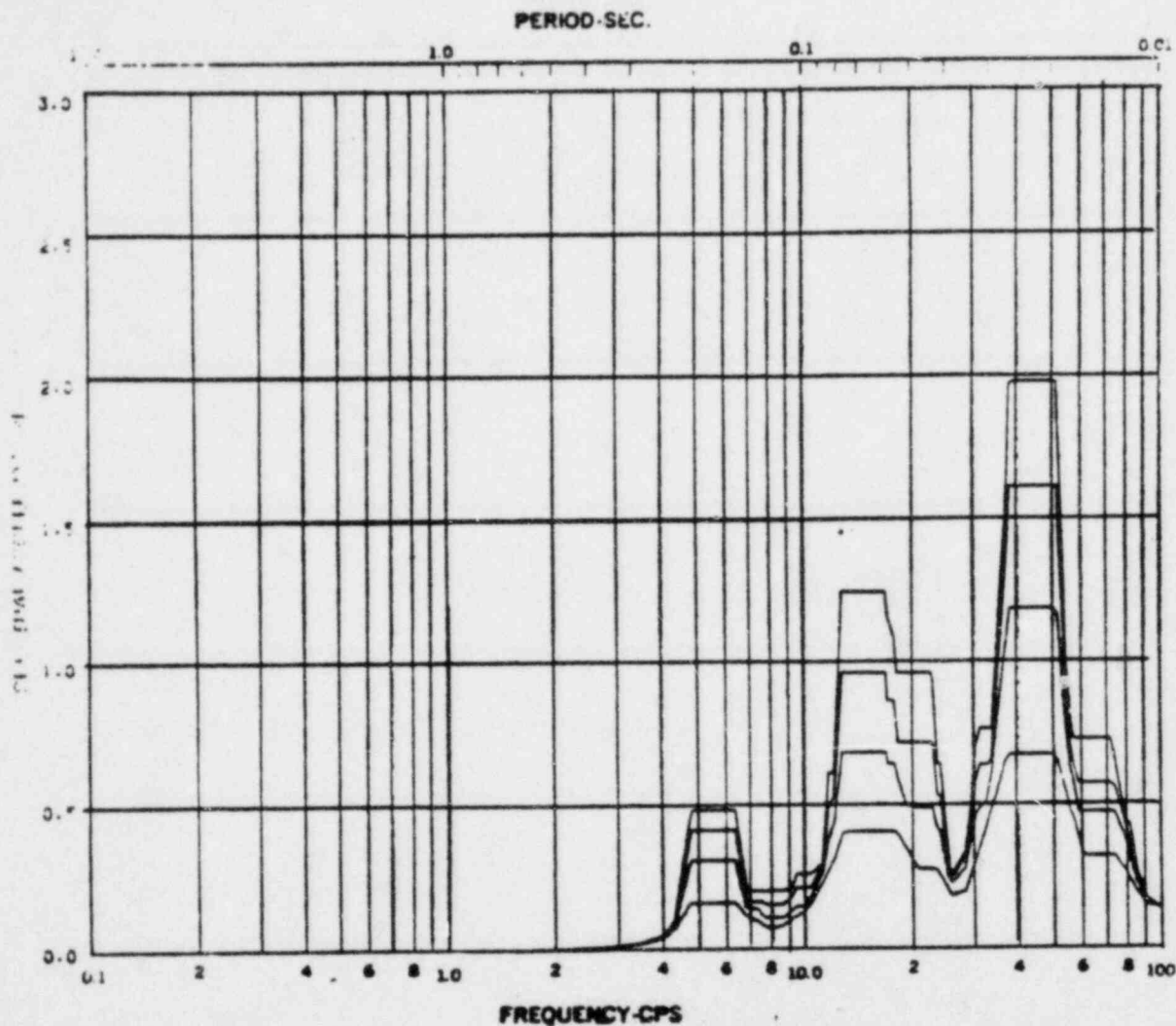
REV. 6, 4/82

SUSQUEHANNA STEAM ELECTRIC STATION
 UNITS 1 AND 2
 DESIGN ASSESSMENT REPORT

REACTOR/CONTROL BUILDING
 RESPONSE SPECTRA

KWU-LOCA

FIGURE C-51



Acceleration Spectra for REACTOR BUILDING
 Load Case: Seismicity KWU --- LOCA
 Mode ---, Direction VERT., Elev 518'-1"
 Damping: 0.001, 0.01, 0.02, 0.05

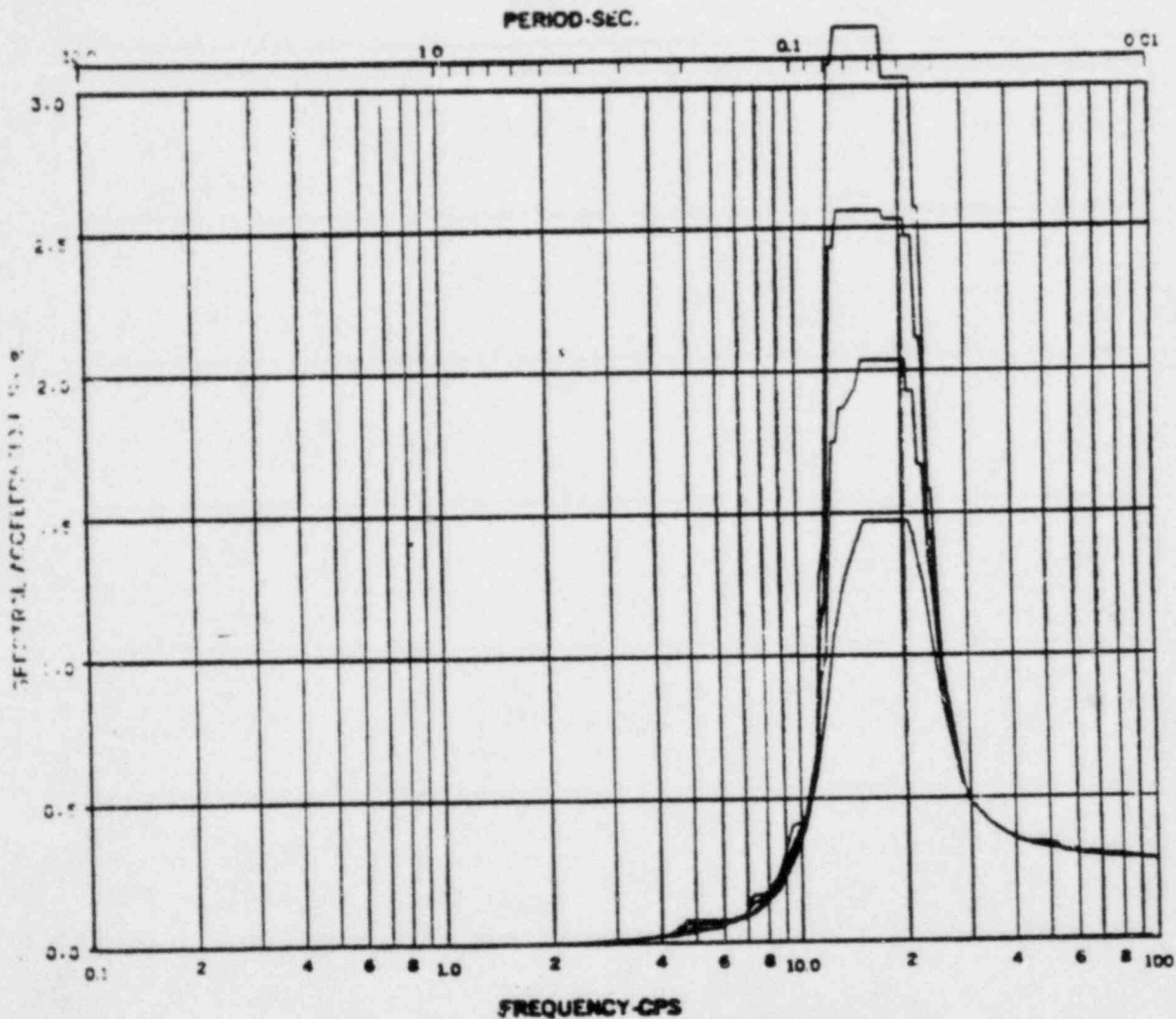
REV. 6, 4/82

SUSQUEHANNA STEAM ELECTRIC STATION
 UNITS 1 AND 2
 DESIGN ASSESSMENT REPORT

REACTOR/CONTROL BUILDING
 RESPONSE SPECTRA

KWU-LOCA

FIGURE C- 52



Acceleration Spectra for REACTOR BUILDING
 Load Case: Seismicity 1001--LOCA
 Mode ---, Direction VERT., 825'-0"
 Sampling: 0.005, 0.01, 0.02, 0.05

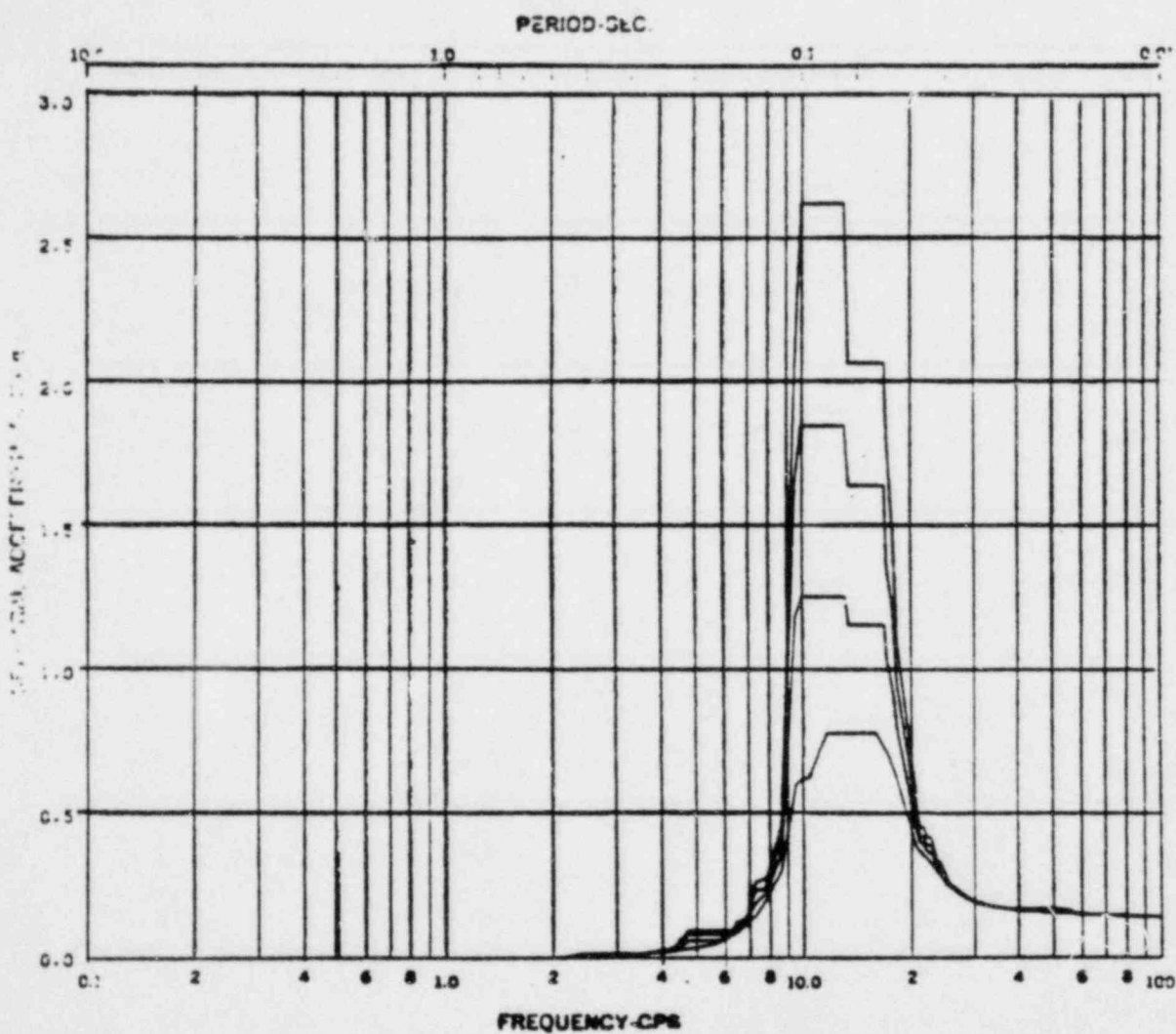
REV. 6, 4/82

SUSQUEHANNA STEAM ELECTRIC STATION
UNITS 1 AND 2
DESIGN ASSESSMENT REPORT

REACTOR/CONTROL BUILDING
 RESPONSE SPECTRA

KWU-LOCA

FIGURE C-53



Acceleration Spectra for REACTOR BUILDING
 Load Case: Seismicity KWU --- LOCA
 Mode ---, Direction VERT., Elev 870'-0"
 Damping: 0.05, 0.01, 0.02, 0.05

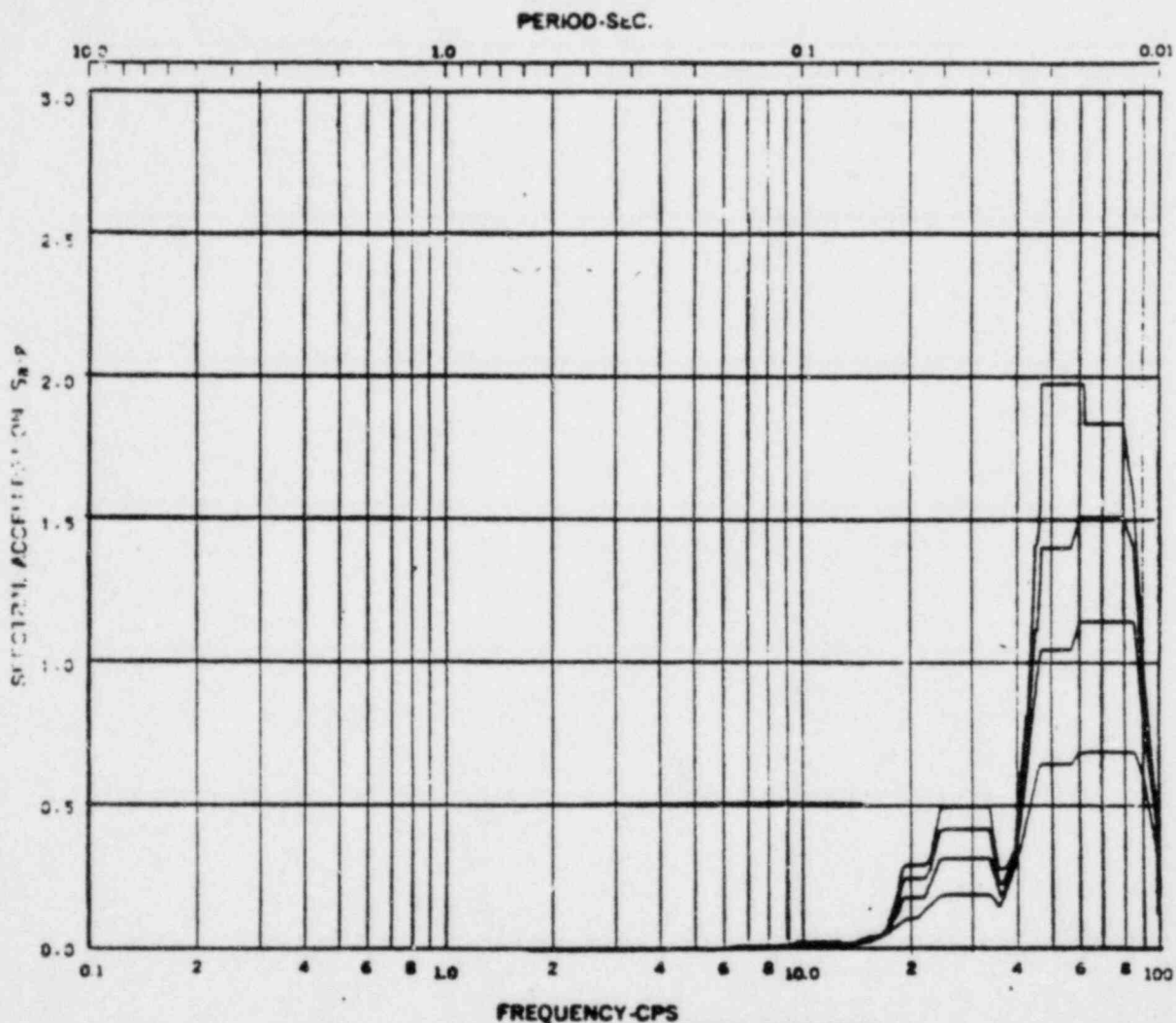
REV. 6, 4/82

BUSQUEHANNA STEAM ELECTRIC STATION
UNITS 1 AND 2
DESIGN ASSESSMENT REPORT

REACTOR/CONTROL BUILDING
 RESPONSE SPECTRA

KWU-LOCA

FIGURE C-54



Acceleration Spectra for REACTOR BUILDING
 Load Case: Susquehanna KWU LOCA
 Mode ---, Direction E-W, 62.6°-1°
 Damping: 0.05, 0.01, 0.02, 0.05

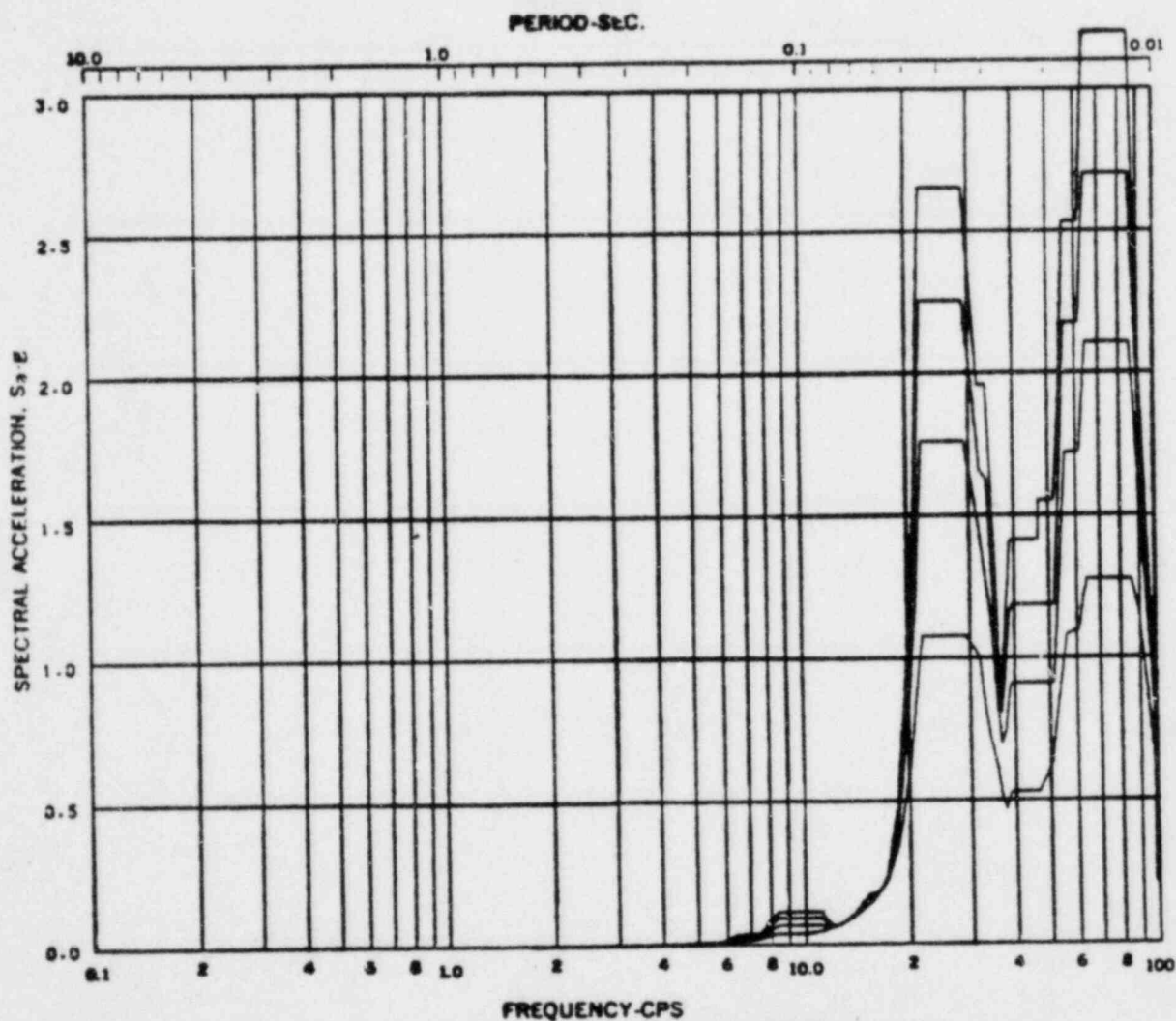
REV. 6, 4/82

**SUSQUEHANNA STEAM ELECTRIC STATION
 UNITS 1 AND 2
 DESIGN ASSESSMENT REPORT**

**REACTOR/CONTROL BUILDING
 RESPONSE SPECTRA**

KWU-LOCA

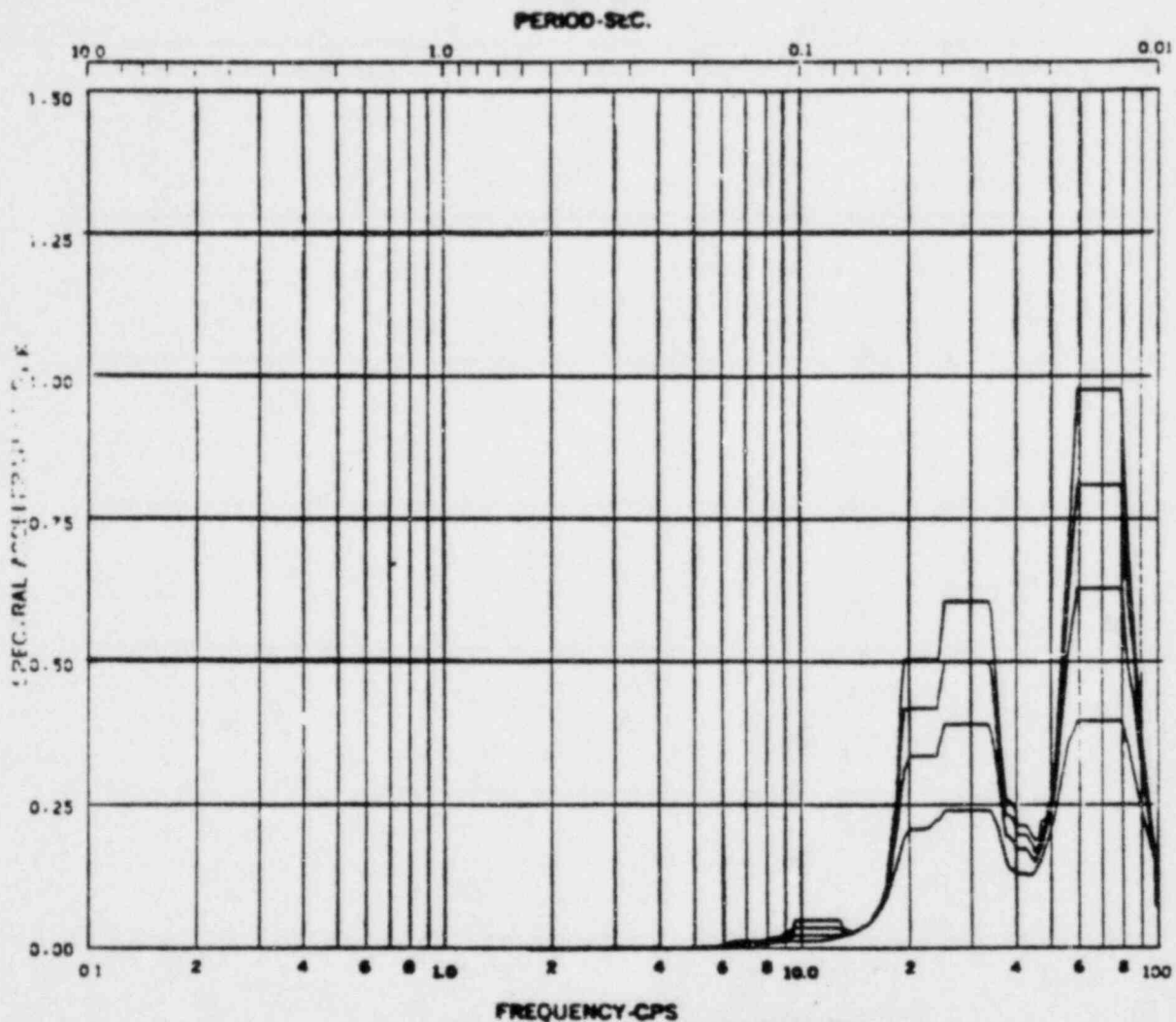
FIGURE C- 55



Acceleration Spectra for REACTOR BUILDING
 Load Case: BUSQUEHANNA KWU LOCA
 Mode ---, Direction E-W, Elev 670'-0"
 Sampling: 0.005, 0.01, 0.02, 0.05

REV. 6, 4/82

BUSQUEHANNA STEAM ELECTRIC STATION UNITS 1 AND 2 DESIGN ASSESSMENT REPORT
REACTOR/CONTROL BUILDING RESPONSE SPECTRA KWU-LOCA
FIGURE C- 56



Acceleration Spectra for REACTOR BUILDING
 Load Case: Susquehanna KWU LOCA
 Mode --- Direction E-W Elev 576'-0"
 Damping: 0.005, 0.01, 0.02, 0.05

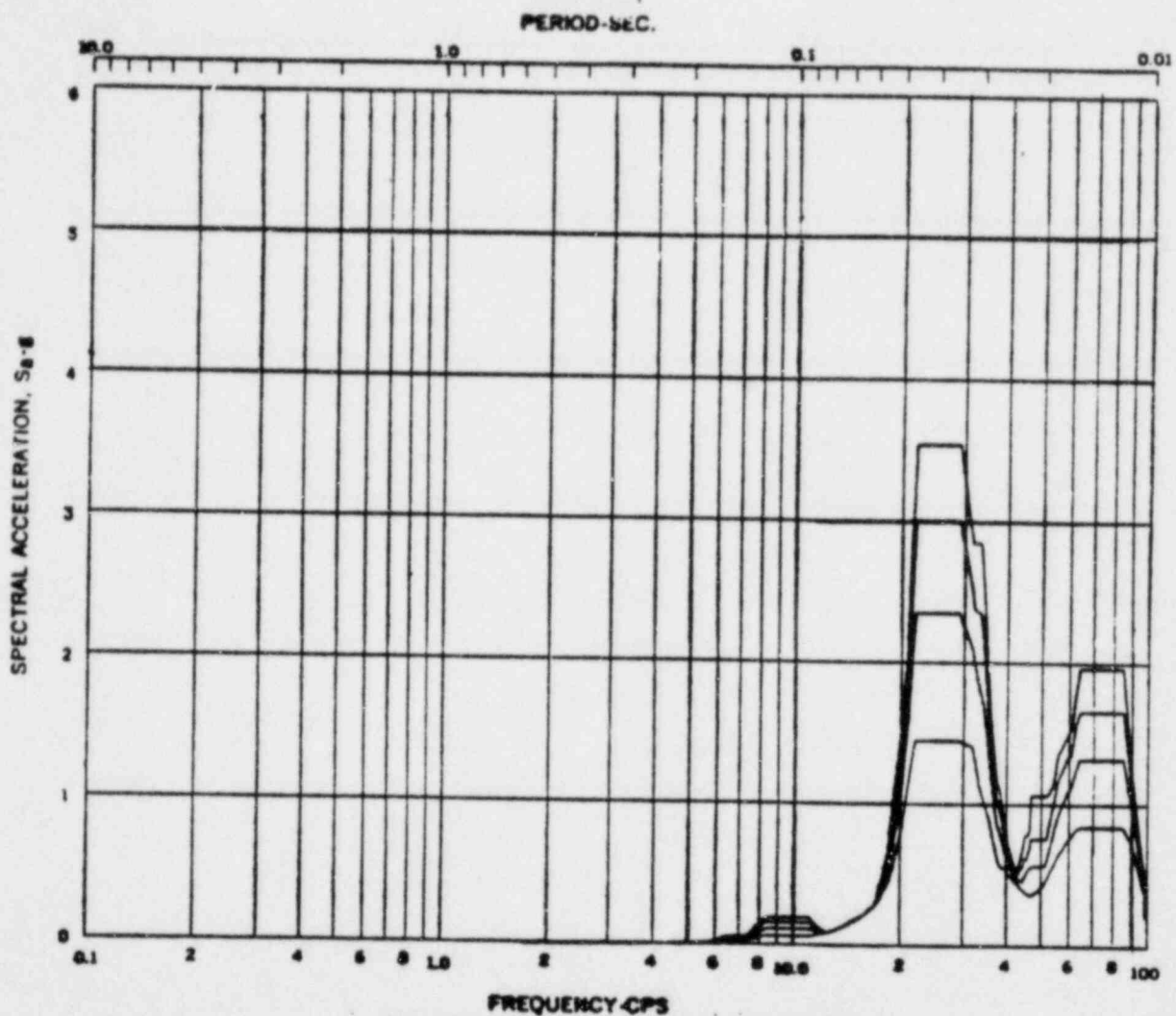
REV. 6, 4/82

SUSQUEHANNA STEAM ELECTRIC STATION
UNITS 1 AND 2
DESIGN ASSESSMENT REPORT

REACTOR/CONTROL BUILDING
 RESPONSE SPECTRA

KWU-LOCA

FIGURE C- 57



FREQUENCY-CPS
 Acceleration Spectra for REACTOR BUILDING
 Load Case: Susquehanna KWU LOCA
 Mode —, Direction E-W, Elev 683'-0"
 Damping: 0.05%, 0.2%, 0.5%, 1.0%

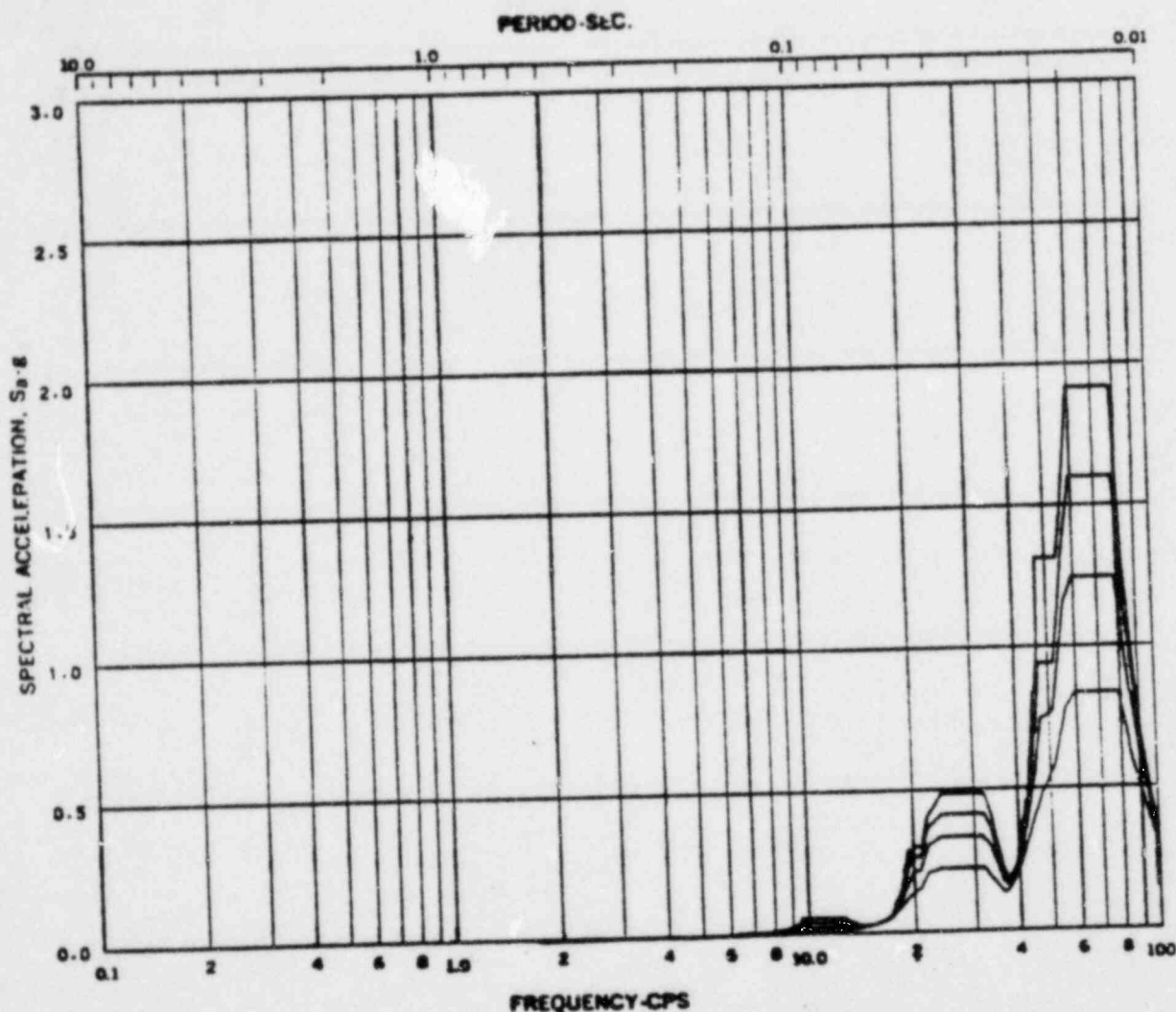
REV. 6, 4/82

SUSQUEHANNA STEAM ELECTRIC STATION
UNITS 1 AND 2
DESIGN ASSESSMENT REPORT

REACTOR/CONTROL BUILDING
RESPONSE SPECTRA

KWU-LOCA

FIGURE C- 58



Acceleration Spectra for REACTOR BUILDING
 Load Case: Resonance KWU LOCA
 Site —, Direction E-W, Elev 697'-0"
 Grouping: 0.001, 0.01, 0.02, 0.05

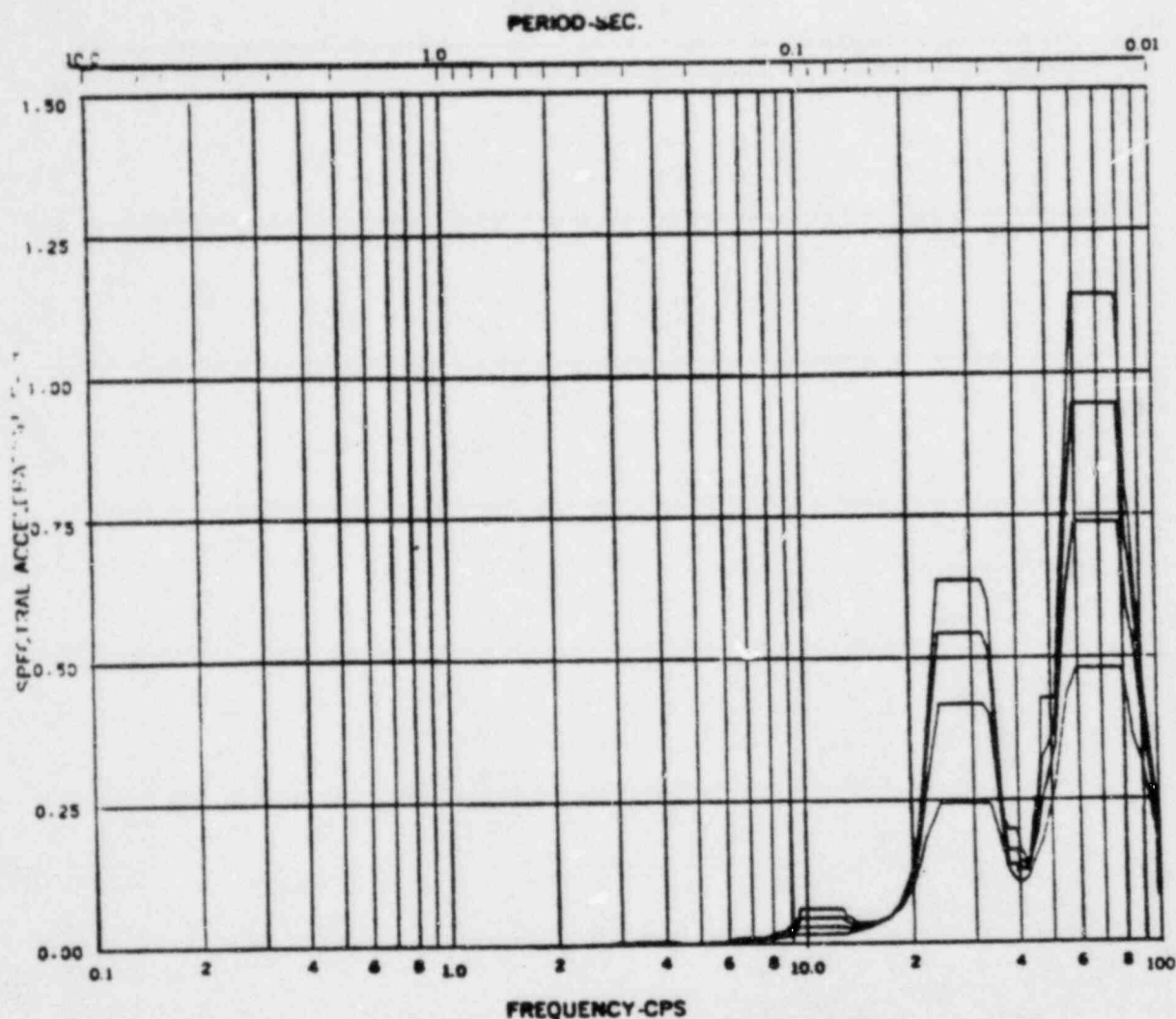
REV. 6, 4/82

BUSQUEHANNA STEAM ELECTRIC STATION
UNITS 1 AND 2
DESIGN ASSESSMENT REPORT

REACTOR/CONTROL BUILDING
RESPONSE SPECTRA

KWU-LOCA

FIGURE C-59



Acceleration Spectra for REACTOR BUILDING
 Load Case: Seismicity - KWU - LOCA
 Fcbr ---, Direction E-W, Elev 709'-0"
 Sampling: 0.025, 0.01, 0.02, 0.05

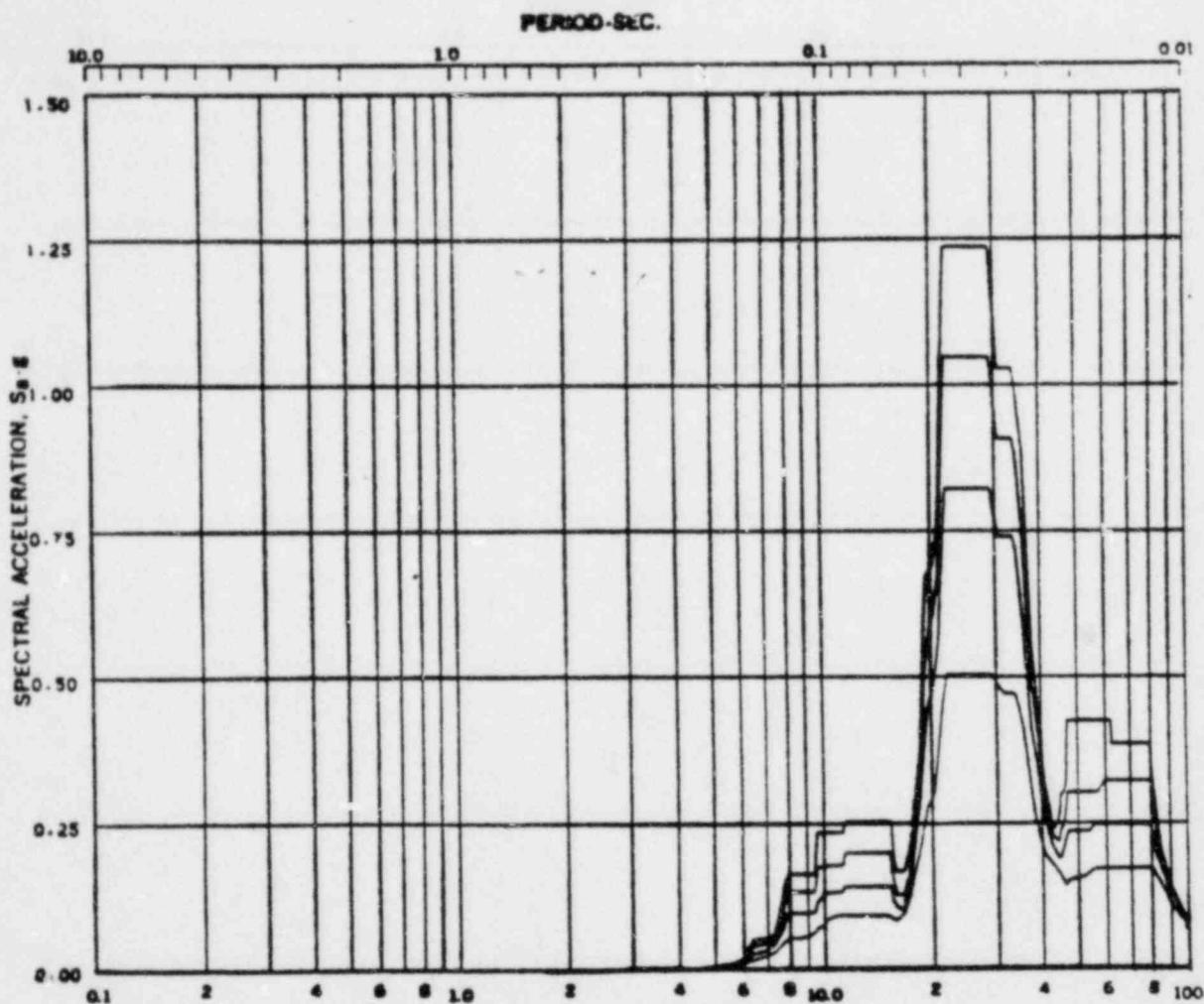
REV. 6, 4/82

BUSQUEHANNA STEAM ELECTRIC STATION
UNITS 1 AND 2
DESIGN ASSESSMENT REPORT

REACTOR/CONTROL BUILDING
RESPONSE SPECTRA

KWU-LOCA

FIGURE C- 60



FREQUENCY-CPS

Acceleration Spectra for REACTOR BUILDING

Load Case: Supersynchronous KWU LOCA

Mode —, Direction E-W, Elev 719'-1"

Damping: 0.005, 0.01, 0.02, 0.05

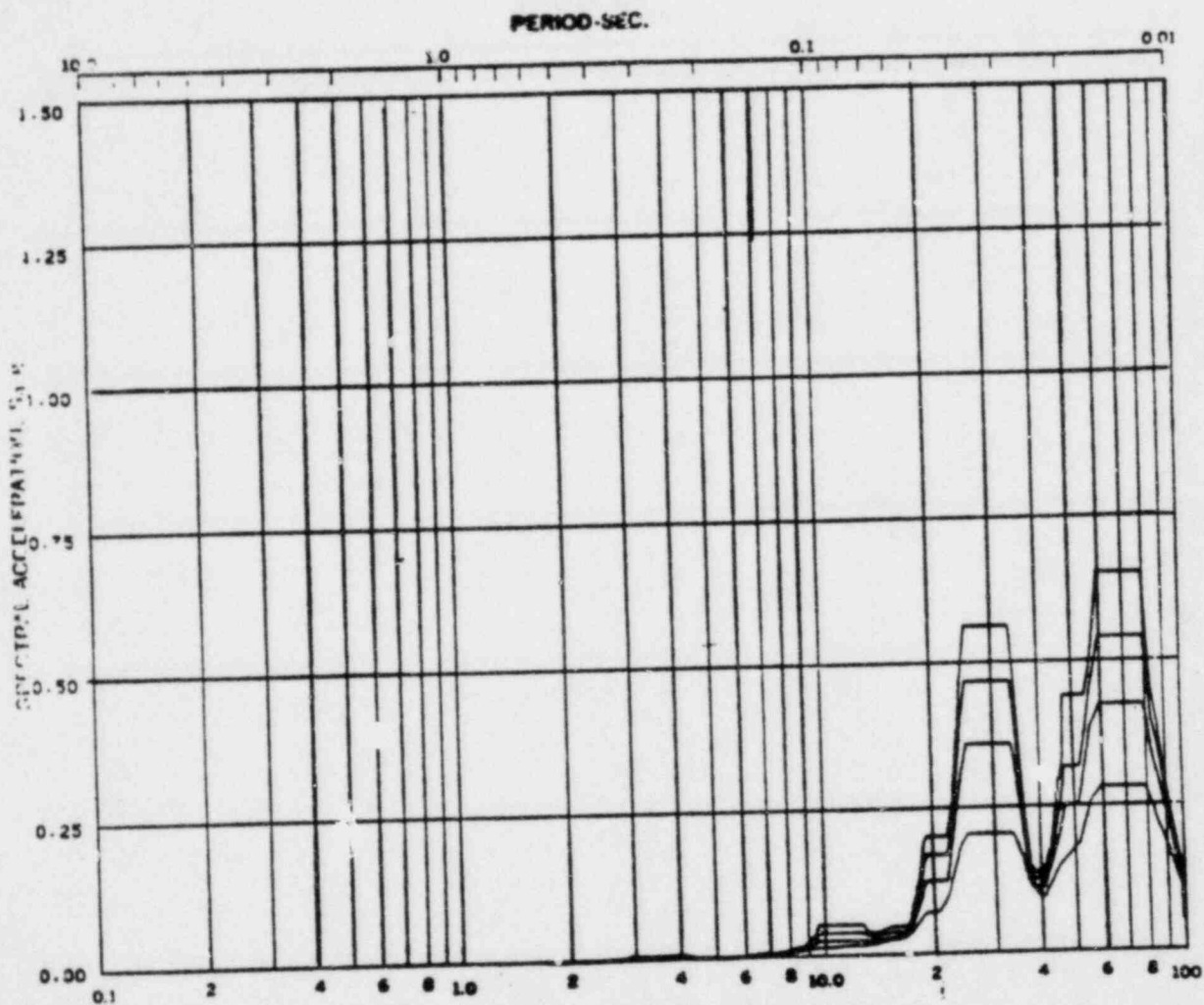
REV. 6, 4/82

**SUSQUEHANNA STEAM ELECTRIC STATION
UNITS 1 AND 2
DESIGN ASSESSMENT REPORT**

**REACTOR/CONTROL BUILDING
RESPONSE SPECTRA**

KWU-LOCA

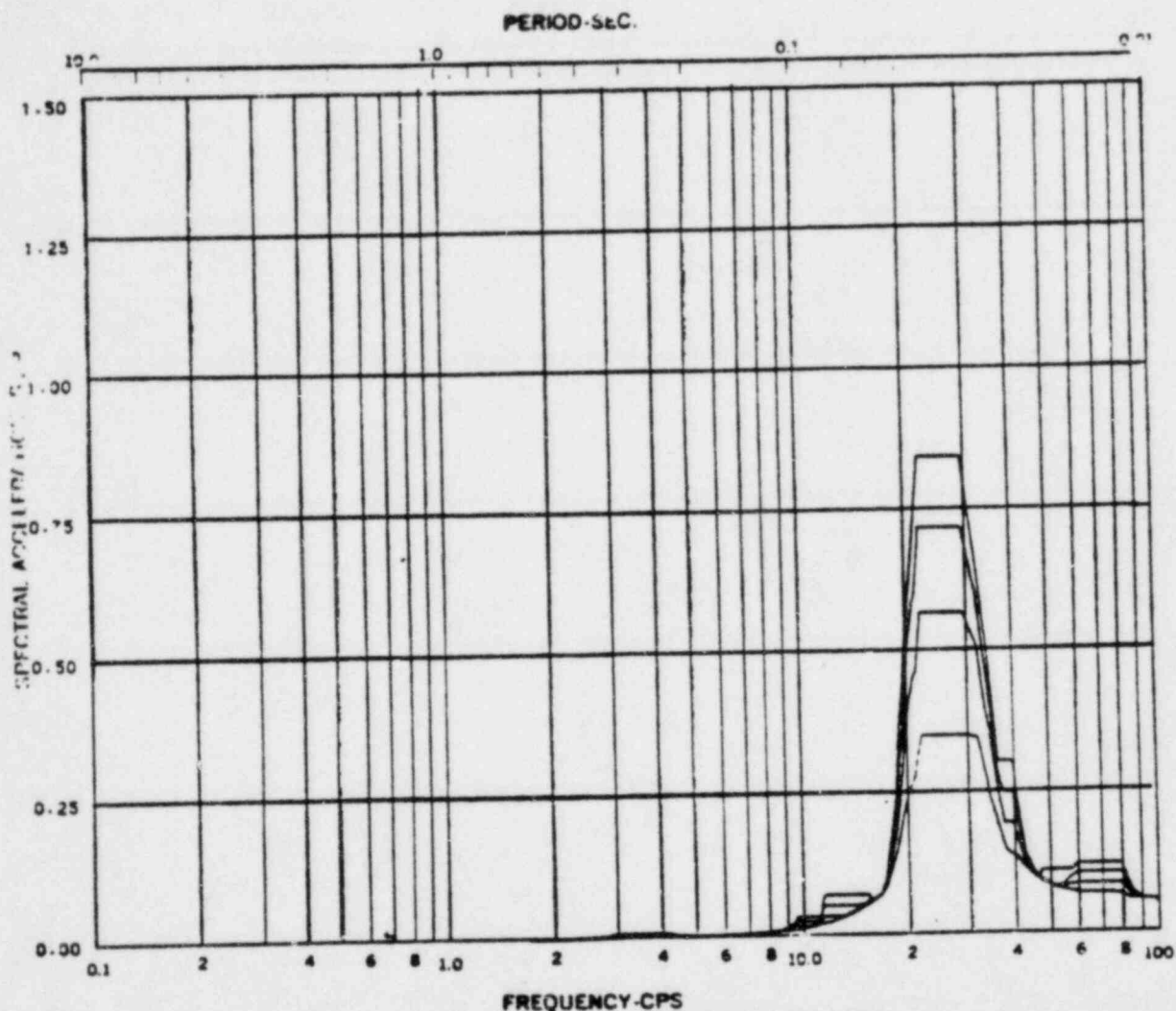
FIGURE C- 61



FREQUENCY-CPS
 Acceleration Spectra for REACTOR BUILDING
 Load Case: Station blackout KWU LOCA
 Mode — Direction E-W Elev 728'-0"
 Damping: 0.005, 0.01, 0.02, 0.05

REV. 6, 4/82

BUSQUEHANNA STEAM ELECTRIC STATION UNITS 1 AND 2 DESIGN ASSESSMENT REPORT
REACTOR/CONTROL BUILDING RESPONSE SPECTRA KWU-LOCA
FIGURE C- 62



Acceleration Spectra for REACTOR BUILDING
 Load Case: Earthquake KWU LOCA
 Mode ---, Direction E-W, Elev 749'-1"
 Damping: 0.05, 0.01, 0.02, 0.05

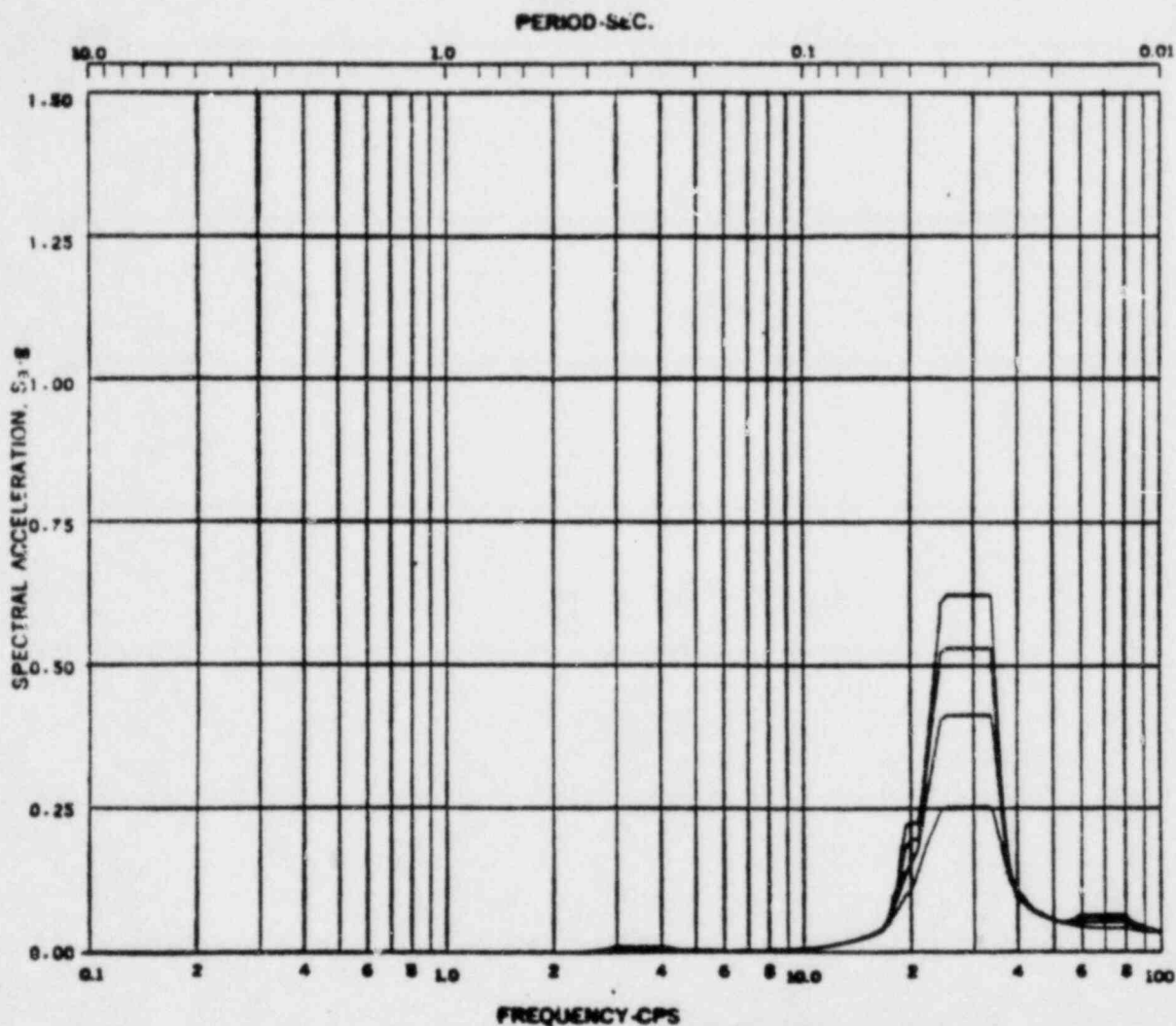
REV. 6, 4/82

SUSQUEHANNA STEAM ELECTRIC STATION
UNITS 1 AND 2
DESIGN ASSESSMENT REPORT

REACTOR/CONTROL BUILDING
RESPONSE SPECTRA

KWU-LOCA

FIGURE C- 63



Acceleration Spectra for REACTOR BUILDING
 Load Case: Supersaturated / E-LOC
 Mode ---, Direction E-W, Elev 771'-0"
 Sampling: 0.005, 0.01, 0.02, 0.05

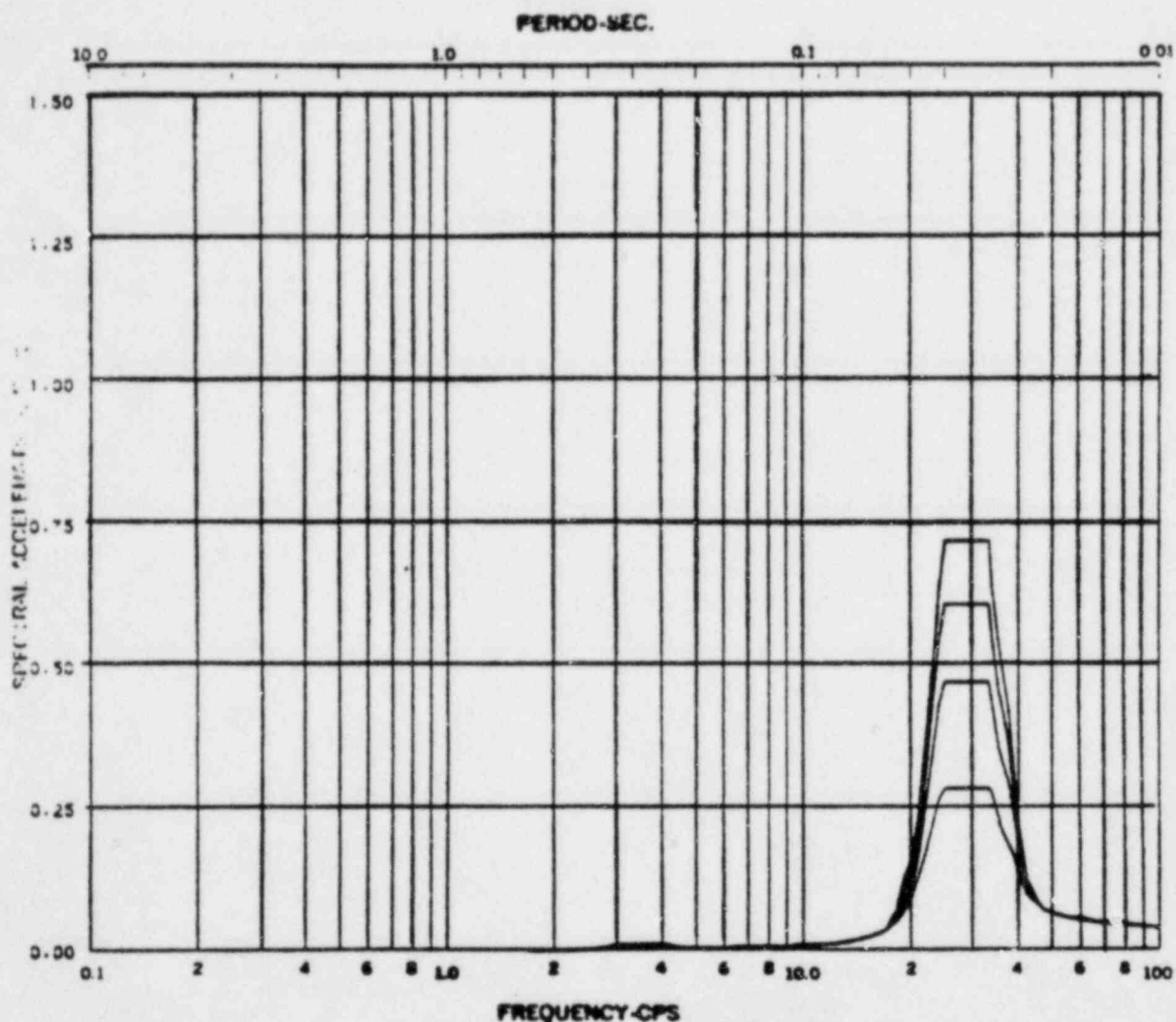
REV. 6, 4/82

SUSQUEHANNA STEAM ELECTRIC STATION
UNITS 1 AND 2
DESIGN ASSESSMENT REPORT

REACTOR/CONTROL BUILDING
 RESPONSE SPECTRA

KWU-LOCA

FIGURE C-64



Acceleration Spectra for REACTOR BUILDING
 Load Case: Seismic LOCA
 Mode --, Direction E-W, Elev 779'-1"
 Damping: 0.05, 0.01, 0.02, 0.05

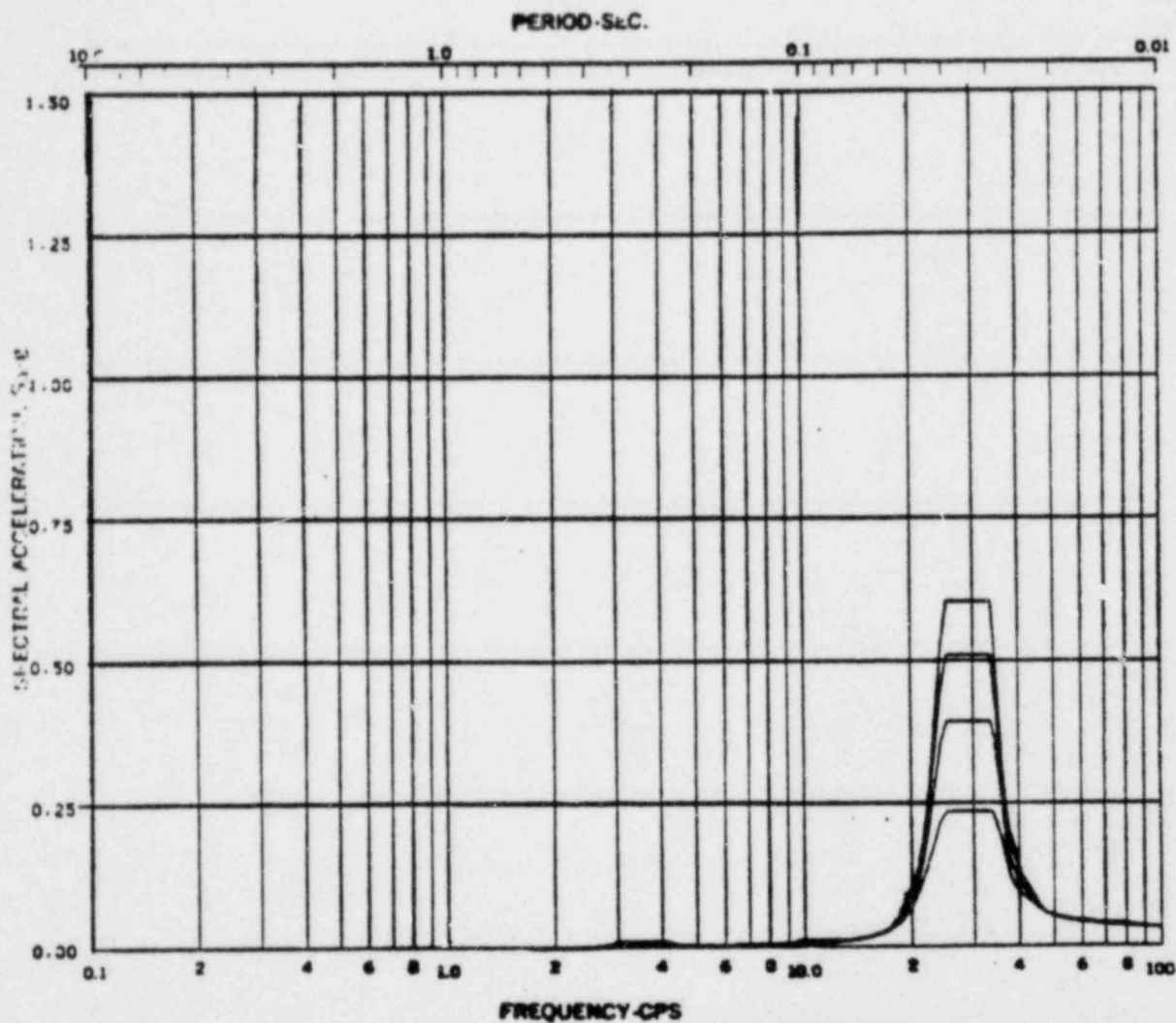
REV. 6, 4/82

**SUSQUEHANNA STEAM ELECTRIC STATION
 UNITS 1 AND 2
 DESIGN ASSESSMENT REPORT**

**REACTOR/CONTROL BUILDING
 RESPONSE SPECTRA**

KWU-LOCA

FIGURE C-65



Acceleration Spectra for REACTOR BUILDING
 Load Case: Supersynchronous KWU LOCA
 Mode —, Direction E-W, Site 783'-0"
 Damping: 0.05, 0.01, 0.02, 0.05

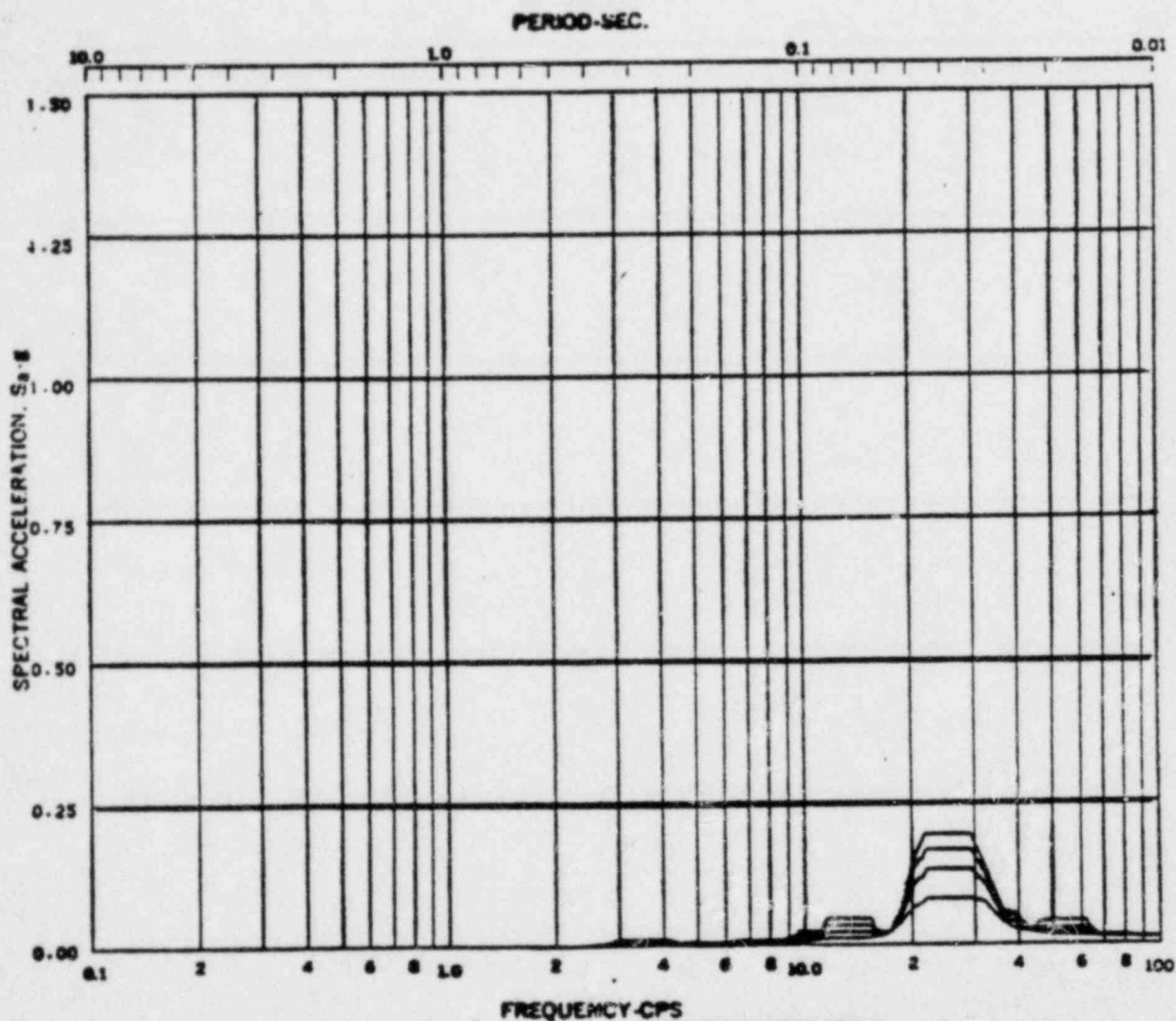
REV. 6, 4/82

**SUSQUEHANNA STEAM ELECTRIC STATION
 UNITS 1 AND 2
 DESIGN ASSESSMENT REPORT**

**REACTOR/CONTROL BUILDING
 RESPONSE SPECTRA**

KWU-LOCA

FIGURE C- 66



Acceleration Spectra for REACTOR BUILDING
 Load Case: Seismicity TWT LOCA
 Mode --- Direction E-W Elev 799'-0"
 Damping: 0.05, 0.01, 0.02, 0.05

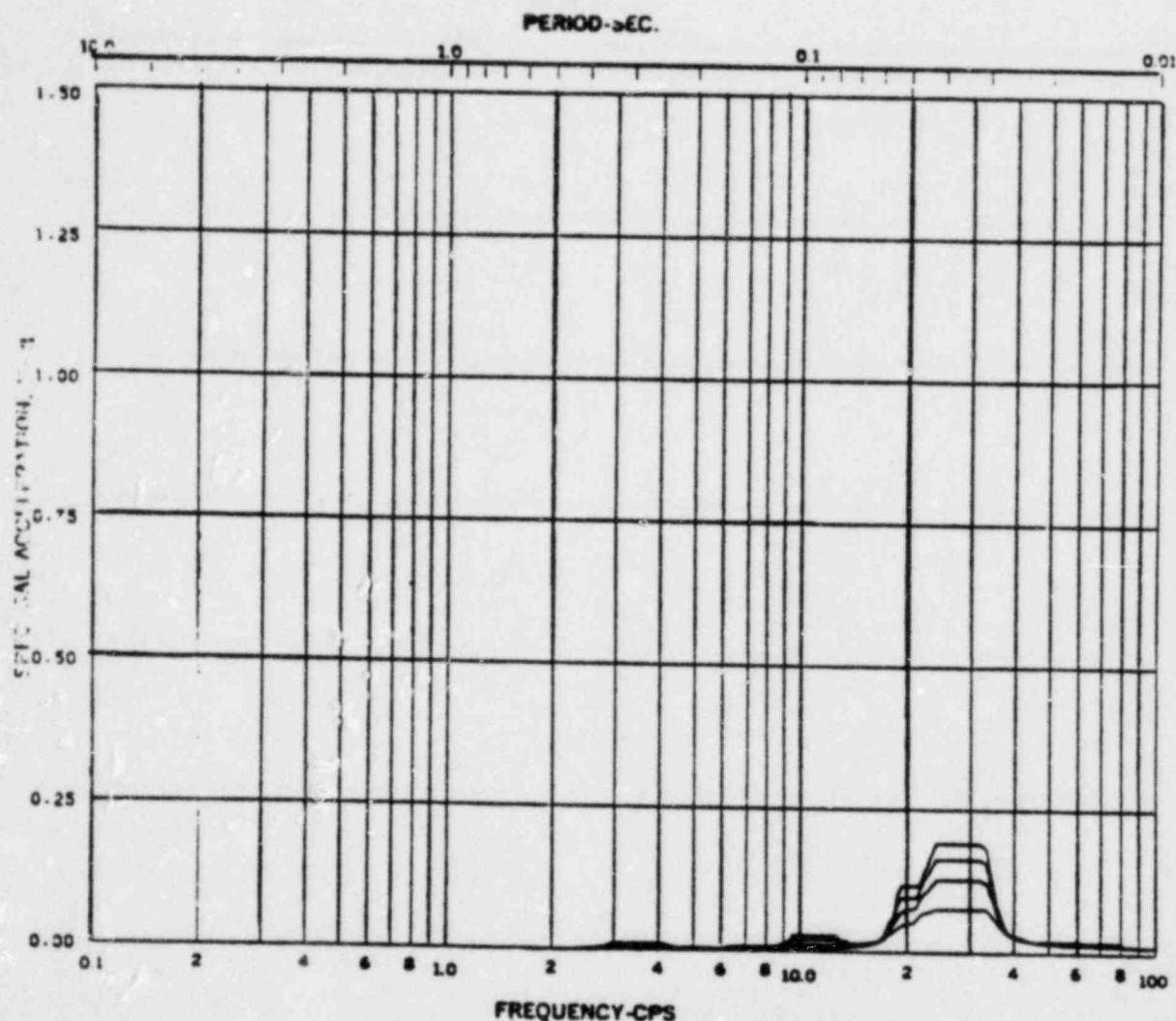
REV. 6, 4/82

**BUSQUEHANNA STEAM ELECTRIC STATION
 UNITS 1 AND 2
 DESIGN ASSESSMENT REPORT**

**REACTOR/CONTROL BUILDING
 RESPONSE SPECTRA**

KWU-LOCA

FIGURE C-67



Acceleration Spectra for REACTOR BUILDING
 Load Case: Seismicity KWU LOCA
 Date ---, Drawn R-M, Size 8.5'-0"
 Damping: 0.05, 0.01, 0.02, 0.05

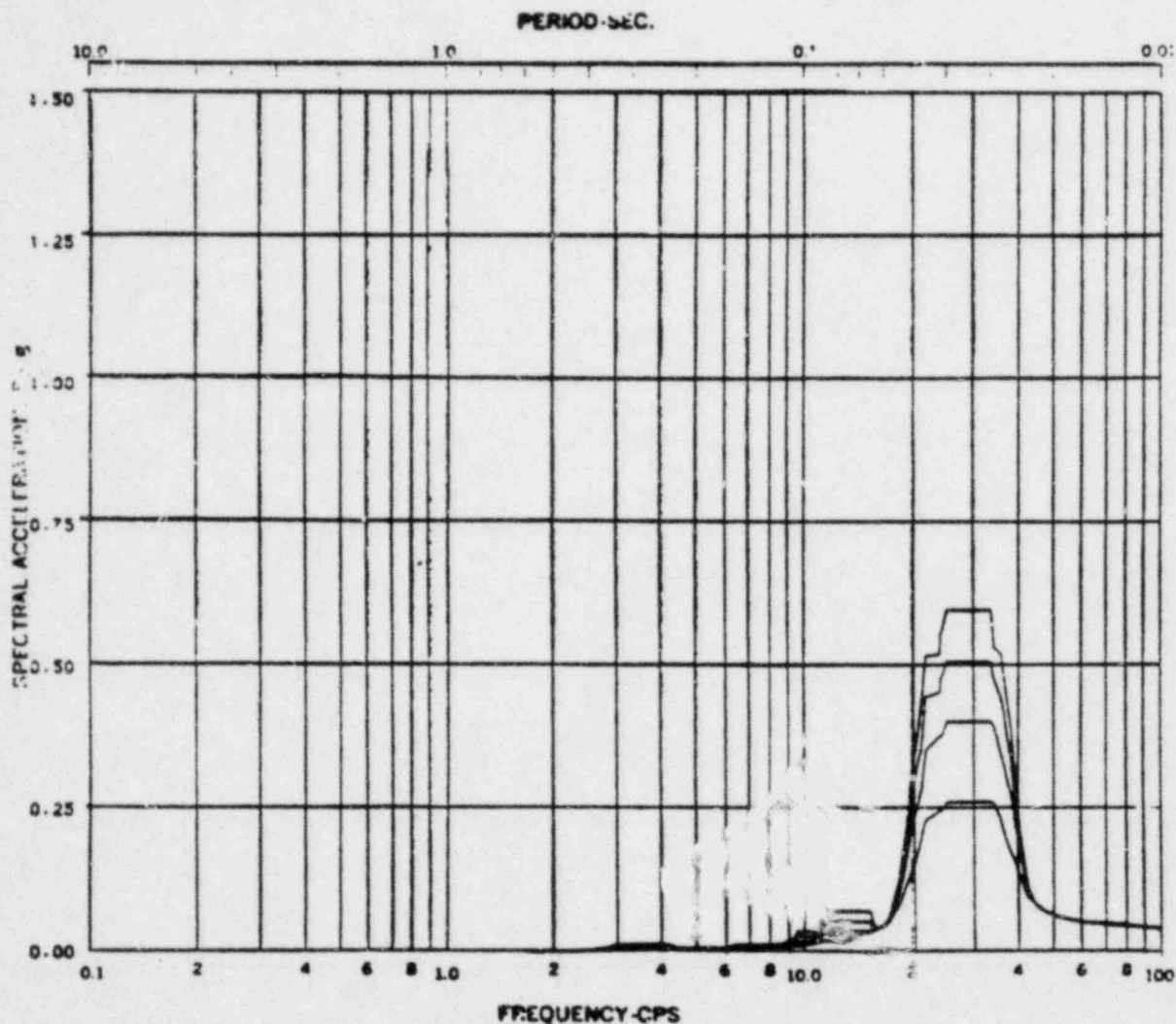
REV. 6, 4/82

BUSQUEHANNA STEAM ELECTRIC STATION
UNITS 1 AND 2
DESIGN ASSESSMENT REPORT

REACTOR/CONTROL BUILDING
 RESPONSE SPECTRA

KWU-LOCA

FIGURE C-68



Acceleration Spectra for REACTOR BUILDING
 Load Case: Surveillance LOCA
 Mode —, Direction E-W, Elev 812'-1"
 Damping: 0.005, 0.01, 0.02, 0.05

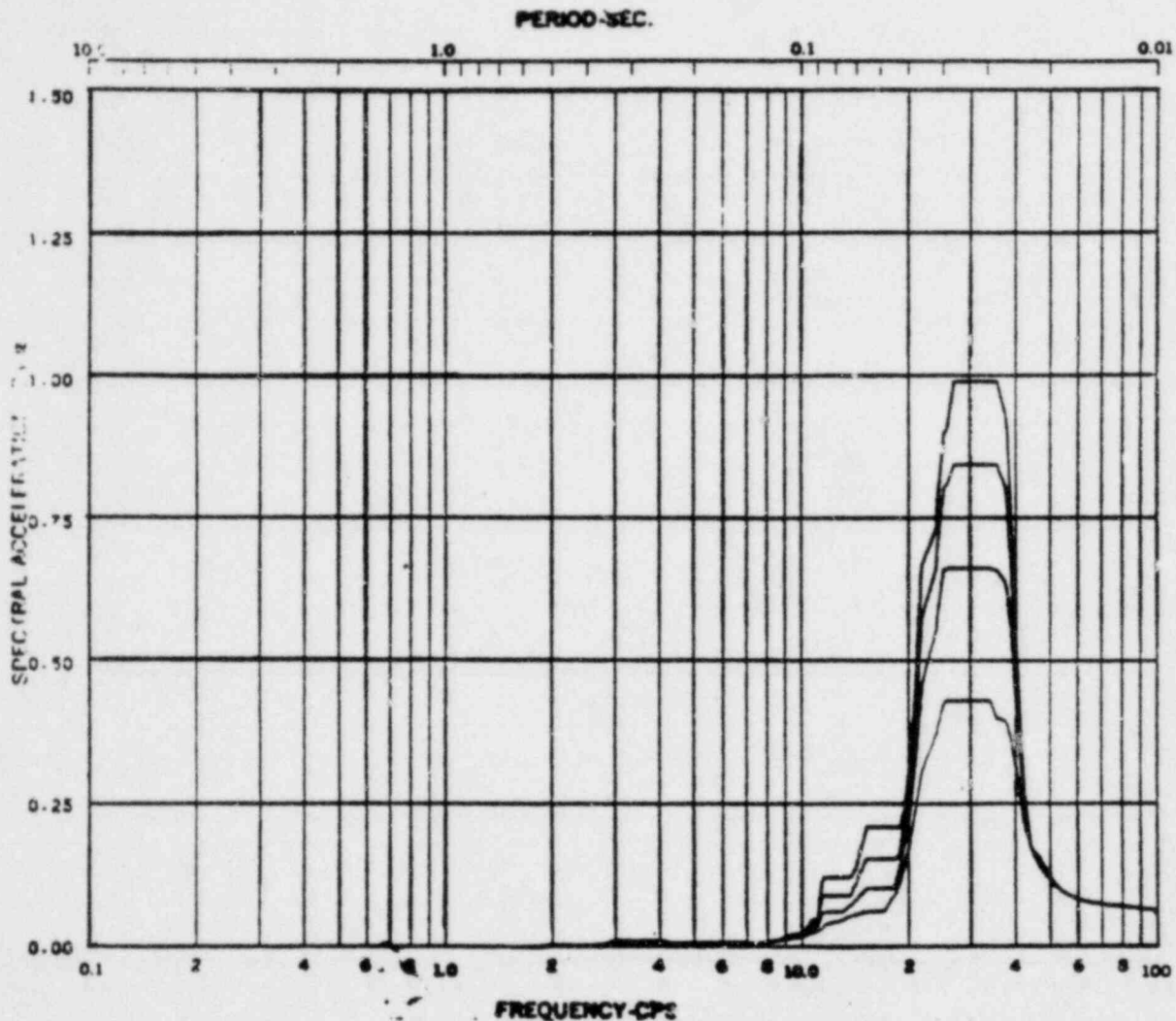
REV. 6, 4/82

SUSQUEHANNA STEAM ELECTRIC STATION
UNITS 1 AND 2
DESIGN ASSESSMENT REPORT

REACTOR/CONTROL BUILDING
 RESPONSE SPECTRA

KWU-LOCA

FIGURE C- 69



FREQUENCY-CPS
 Acceleration Spectra for REACTOR BUILDING
 Unit Case: Susquehanna KWU-LOCA
 Mode , Structure E-W, Elev 846'-0"
 Sampling: 0.005, 0.01, 0.02, 0.05

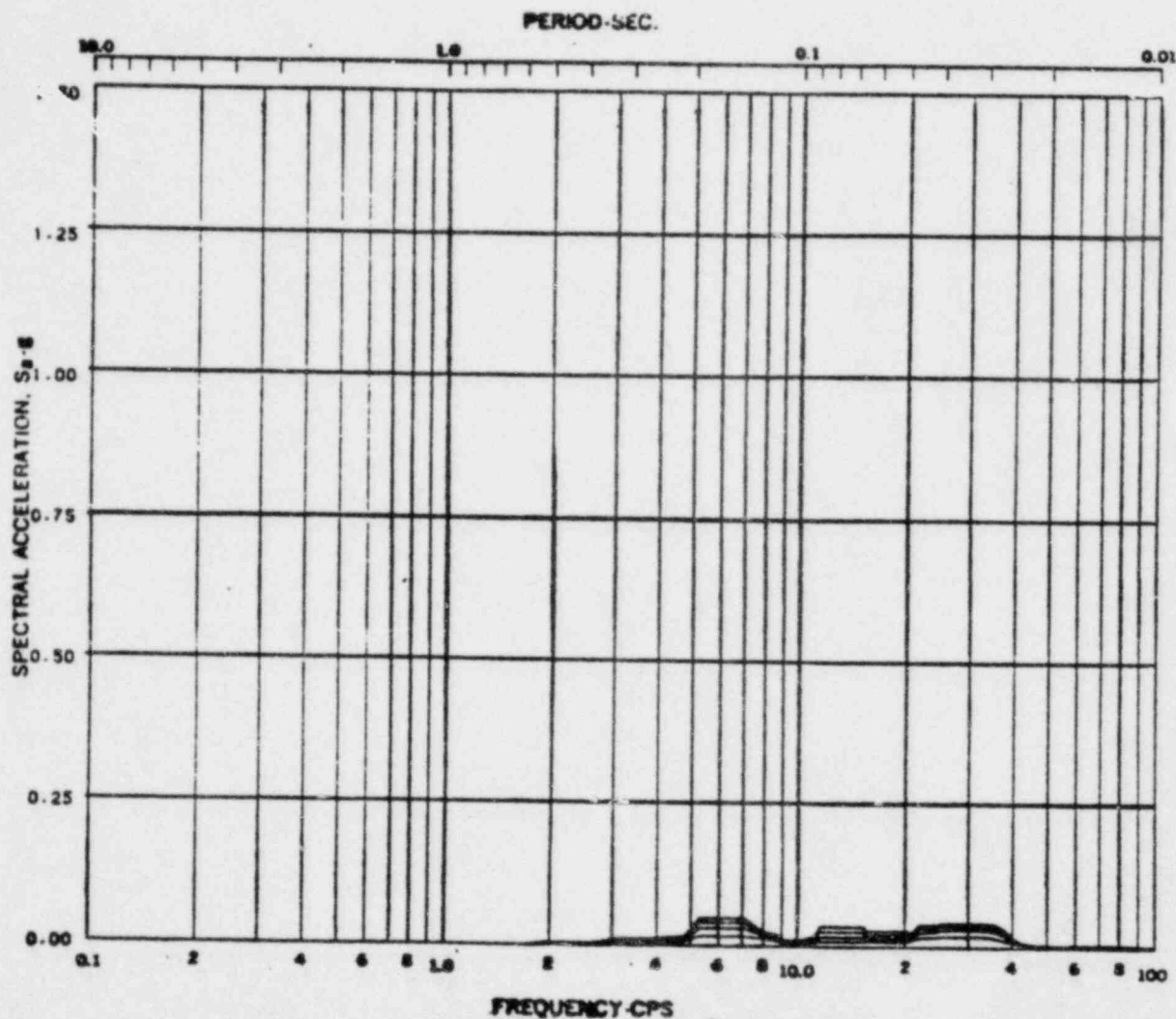
REV. 6, 4/82

SUSQUEHANNA STEAM ELECTRIC STATION
UNITS 1 AND 2
DESIGN ASSESSMENT REPORT

REACTOR/CONTROL BUILDING
 RESPONSE SPECTRA

KWU-LOCA

FIGURE C- 70



Acceleration Spectra for REACTOR BUILDING
 Load Case: Seismicity KWU LOCA
 Mode --- Direction E-W Elev 870'-0"
 Sampling: 0.005, 0.01, 0.02, 0.05

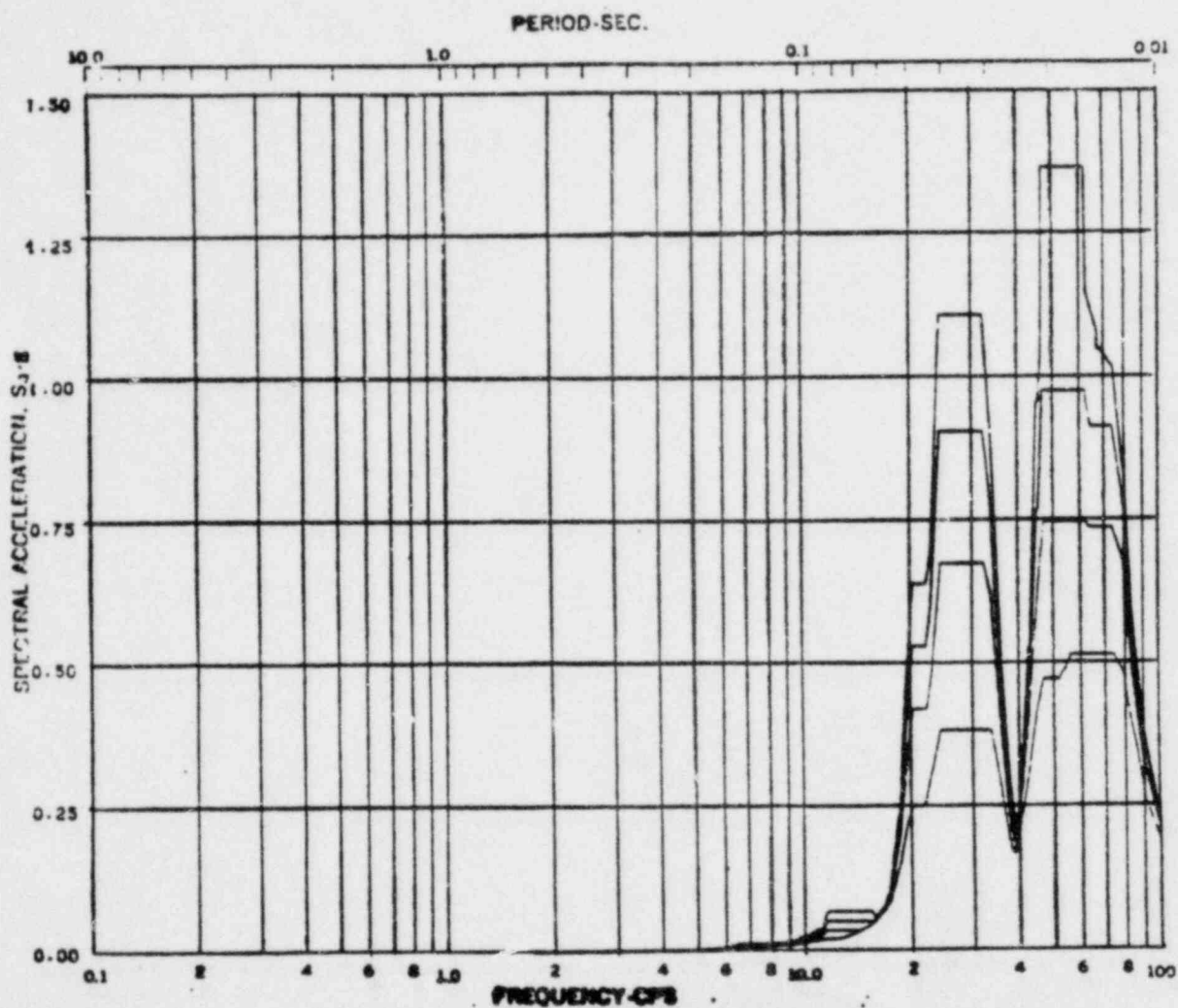
REV. 6, 4/82

**SUSQUEHANNA STEAM ELECTRIC STATION
 UNITS 1 AND 2
 DESIGN ASSESSMENT REPORT**

**REACTOR/CONTROL BUILDING
 RESPONSE SPECTRA**

KWU-LOCA

FIGURE C-71



Acceleration Spectra for REACTOR BUILDING
 Load Case: Seismic LOCA (KWU)
 Mode —, Direction N-S, Rise 676'-0"
 Sampling: 0.005, 0.01, 0.02, 0.05

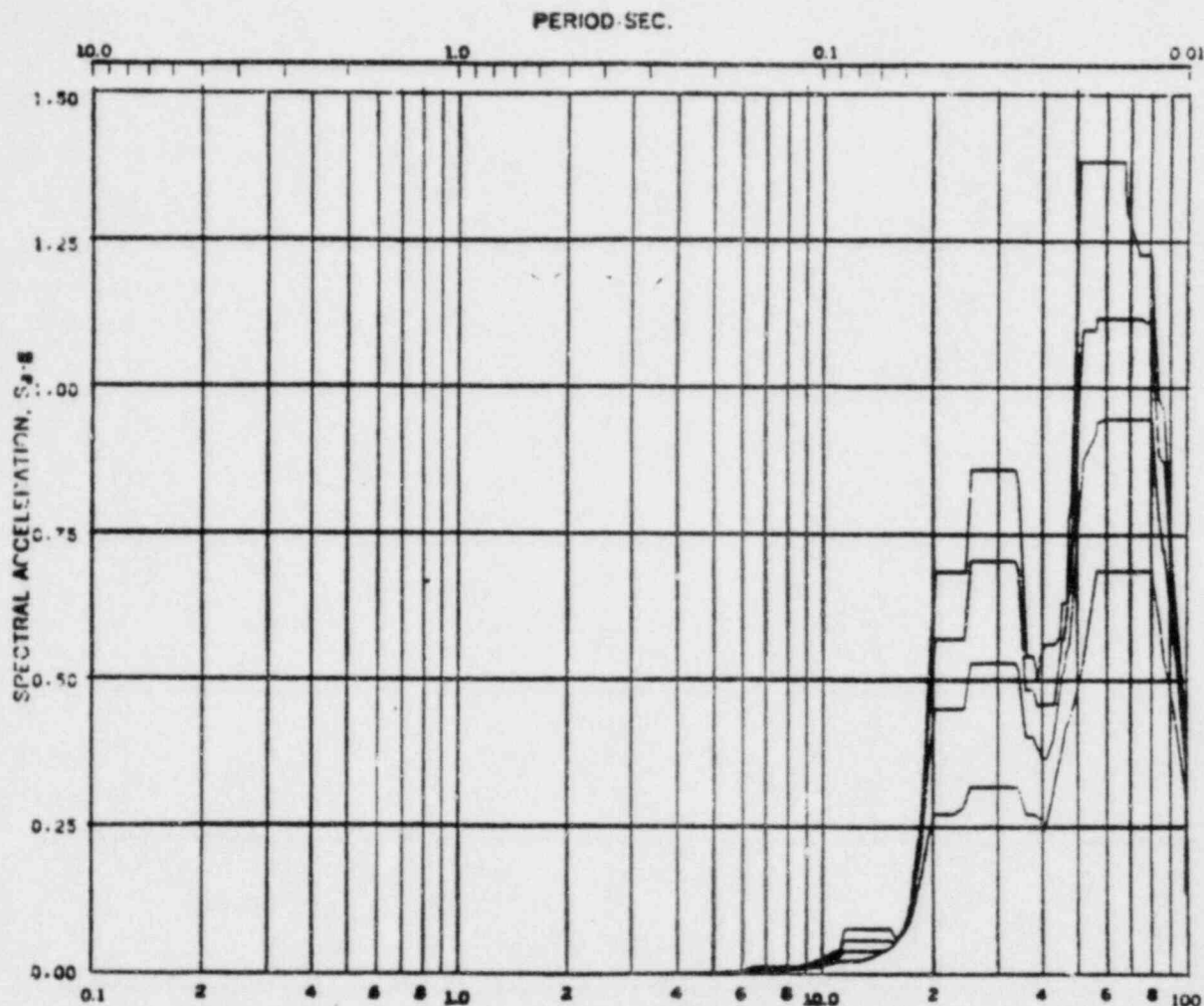
REV. 6, 4/82

SUSQUEHANNA STEAM ELECTRIC STATION
UNITS 1 AND 2
DESIGN ASSESSMENT REPORT

REACTOR/CONTROL BUILDING
RESPONSE SPECTRA

KWU-LOCA

FIGURE C- 72



FREQUENCY - CPS
 Acceleration Spectra for REACTOR BUILDING
 Load Case: LOCN(KWU)
 Site: , Direction: N-S, Elev: 676'-0"
 Damping: 0.05, 0.01, 0.02, 0.05

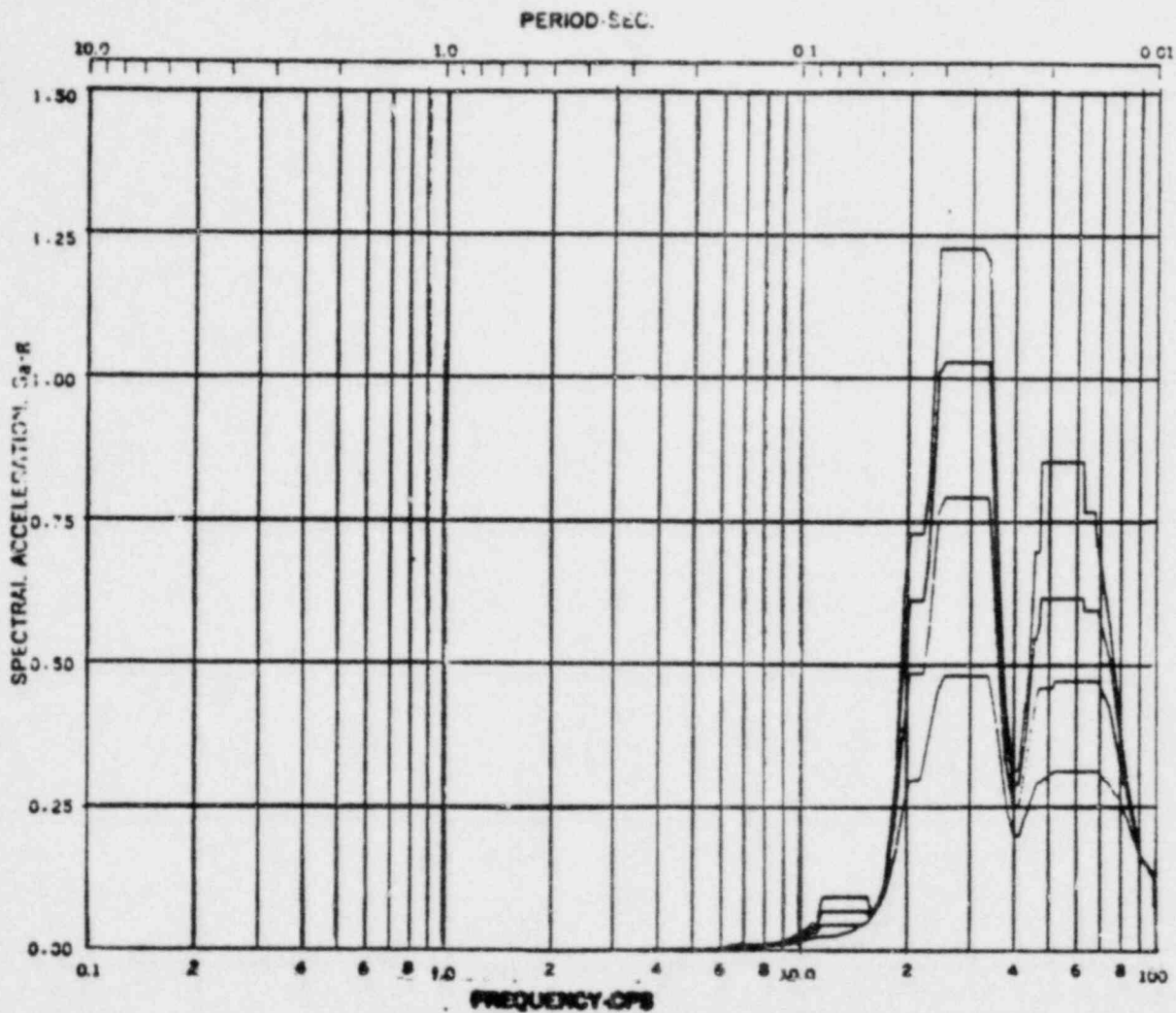
REV. 6, 4/82

SUSQUEHANNA STEAM ELECTRIC STATION
UNITS 1 AND 2
DESIGN ASSESSMENT REPORT

REACTOR/CONTROL BUILDING
 RESPONSE SPECTRA

KWU-LOCA

FIGURE C- 73



Response Spectra for REACTOR BUILDING
 Load Case: Seismicity LOCA(KWU)
 Ref: ---, Division N-S, Elev 683'-0"
 Damping: 0.05, 0.01, 0.02, 0.05

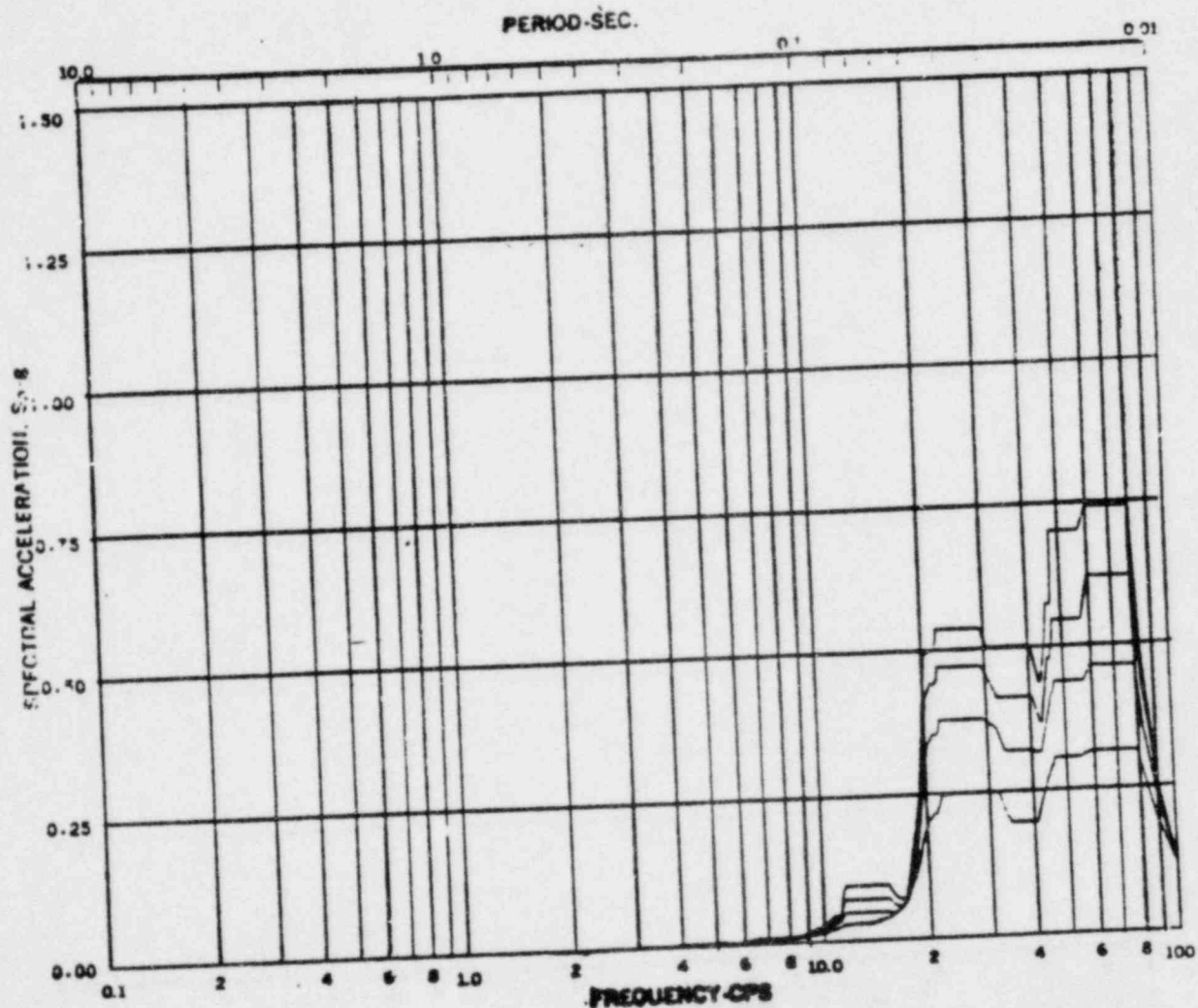
REV. 6, 4/82

SUSQUEHANNA STEAM ELECTRIC STATION
UNITS 1 AND 2
DESIGN ASSESSMENT REPORT

REACTOR/CONTROL BUILDING
 RESPONSE SPECTRA

KWU-LOCA

FIGURE C-74



Acceleration Spectra for REACTOR BUILDING
 Load Case: Seismic LOCA (KWU)
 Mode — Direction N-S Site 697'-8"
 Damping: 0.05, 0.01, 0.02, 0.05

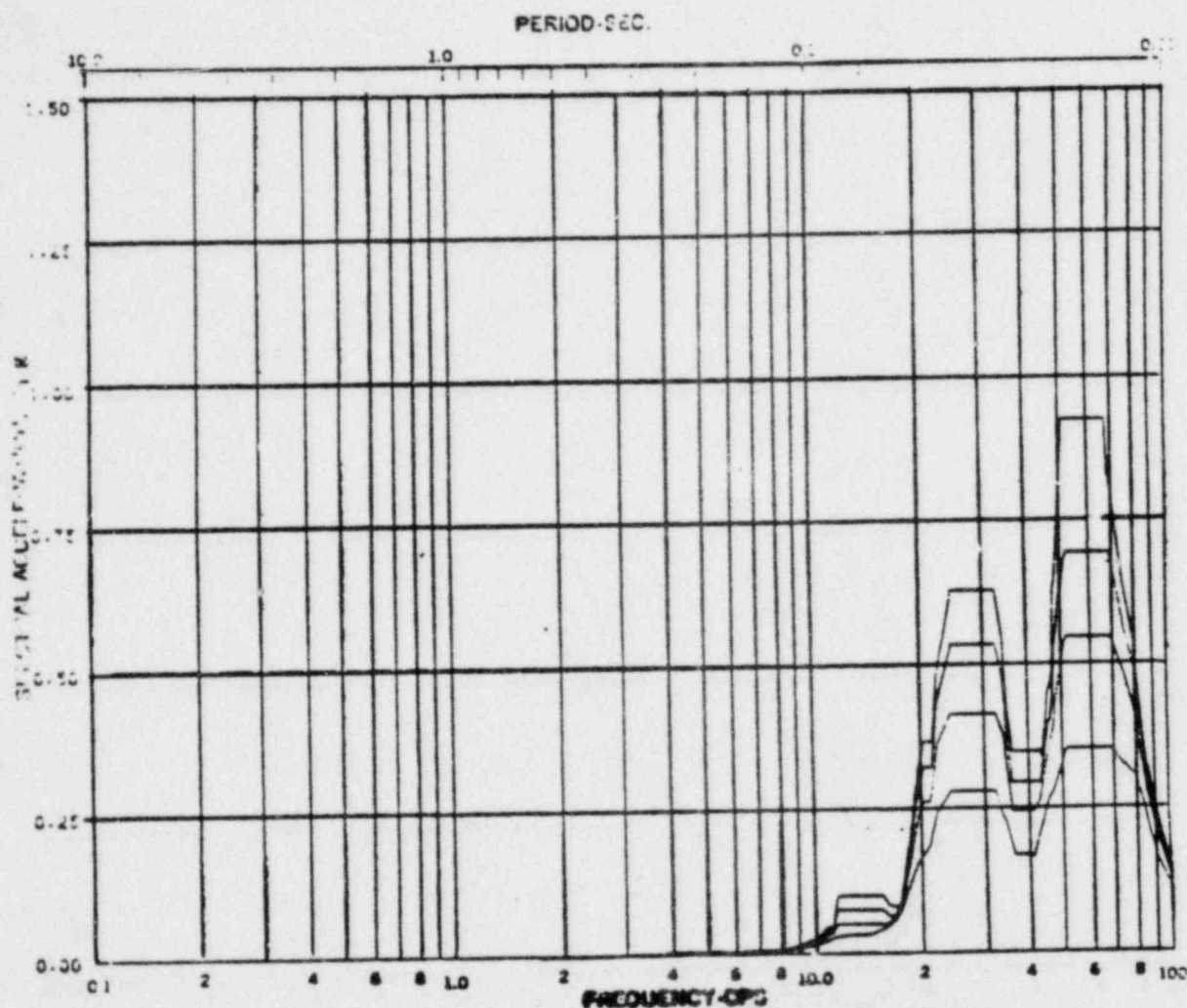
REV. 6, 4/82

BUSQUEHANNA STEAM ELECTRIC STATION
UNITS 1 AND 2
DESIGN ASSESSMENT REPORT

REACTOR/CONTROL BUILDING
 RESPONSE SPECTRA

KWU-LOCA

FIGURE C-75



Acceleration Spectra for REACTOR BUILDING
 Load Case: Seismicity LOCA (KWU)
 Mode --- Direction N-S Site 709'-0"
 Damping: 0.05, 0.01, 0.02, 0.05

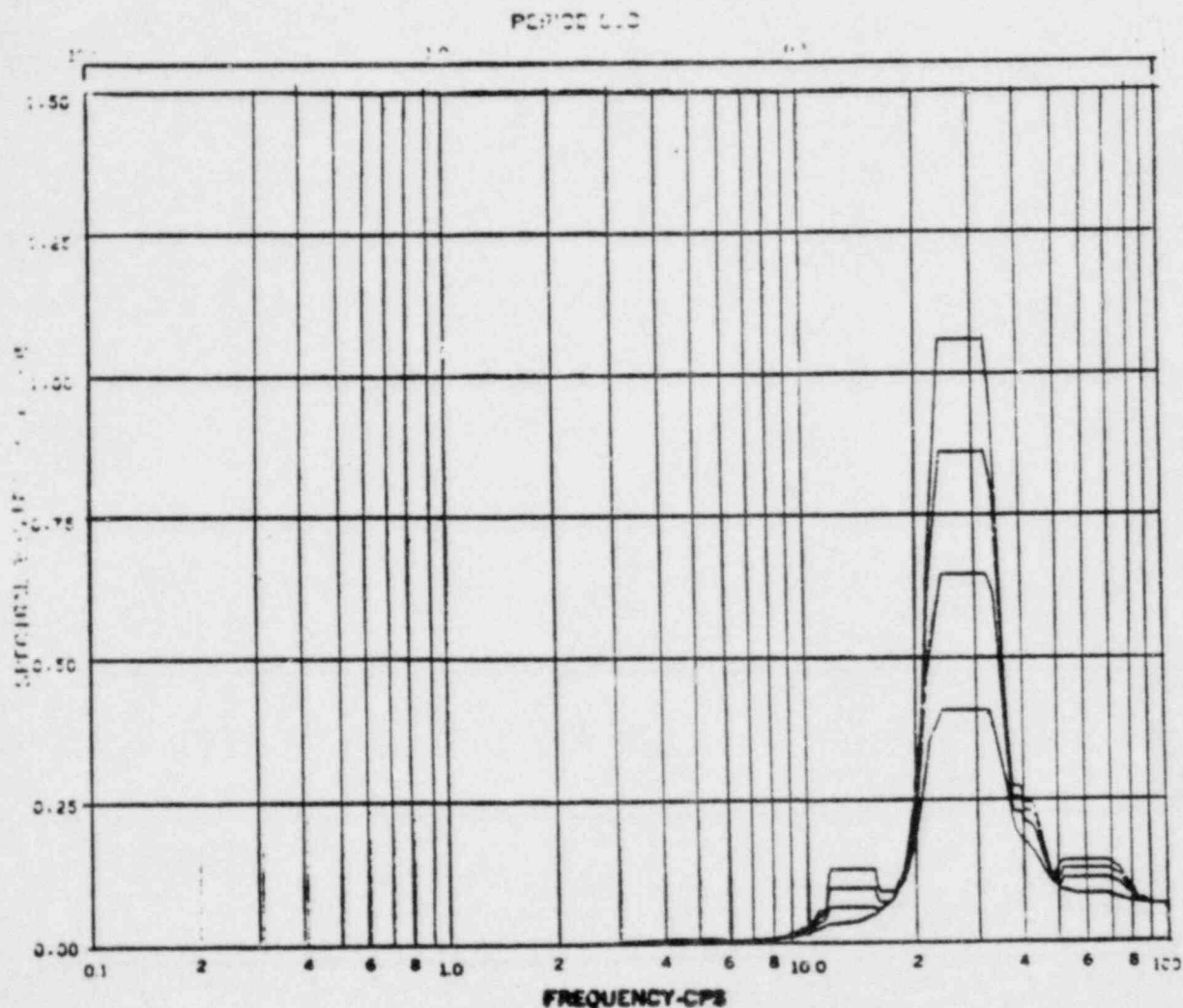
REV. 6, 4/82

**BUSQUEHANNA STEAM ELECTRIC STATION
 UNITS 1 AND 2
 DESIGN ASSESSMENT REPORT**

**REACTOR/CONTROL BUILDING
 RESPONSE SPECTRA**

KWU-LOCA

FIGURE C-76



Acceleration Spectra for REACTOR BUILDING
 Load Case: Seismicity LOCA (KWU)
 Mode ---, Direction N-S, Elav 719'-1"
 Sampling: 0.005, 0.01, 0.02, 0.05

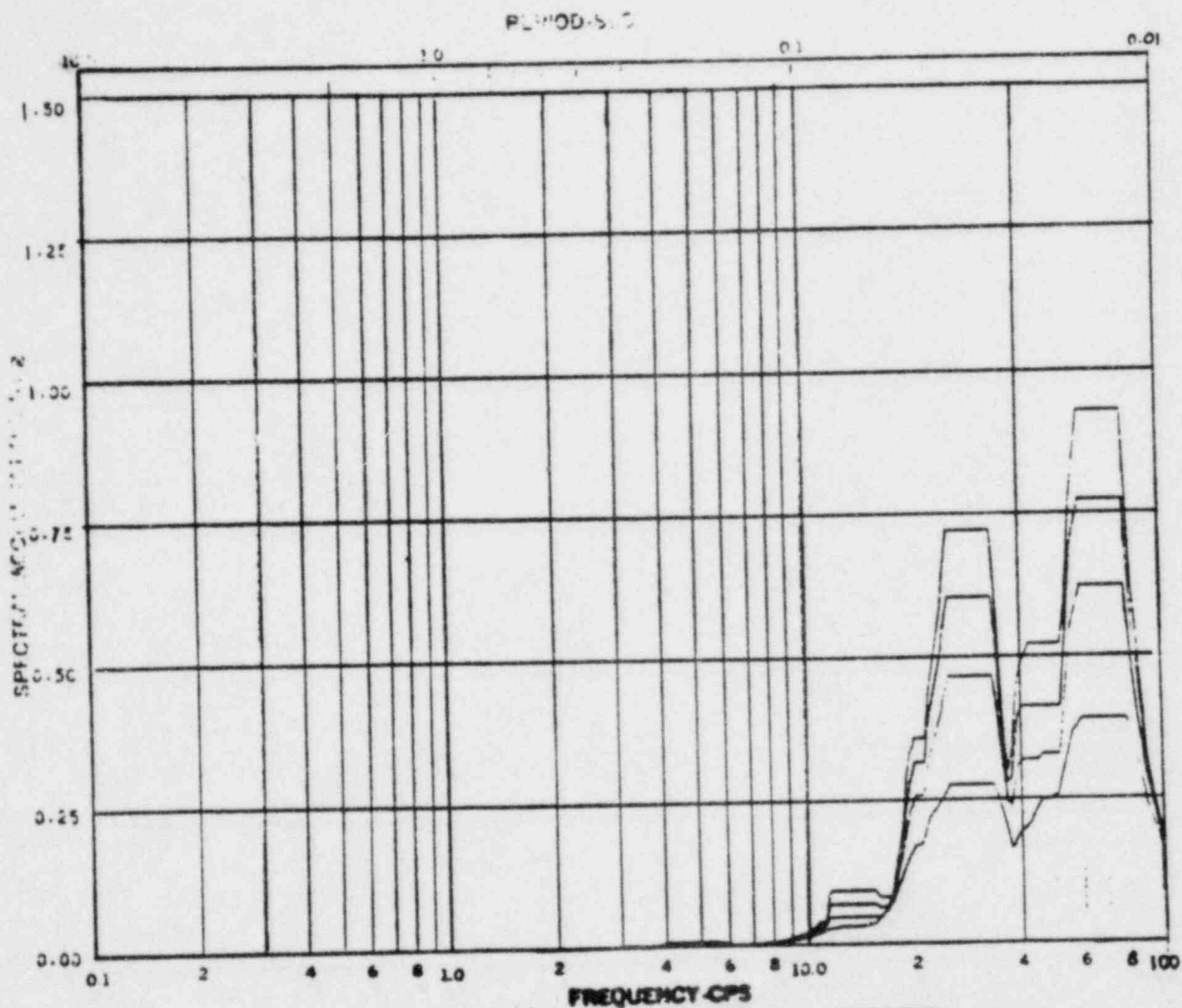
REV. 6, 4/82

**SUSQUEHANNA STEAM ELECTRIC STATION
 UNITS 1 AND 2
 DESIGN ASSESSMENT REPORT**

**REACTOR/CONTROL BUILDING
 RESPONSE SPECTRA**

KWU-LOCA

FIGURE C- 77



Acceleration Spectra for REACTOR BUILDING
 Load Case: Seismic LOCA (KWU)
 Mode —, Direction N-S, Elev 722'-0"
 Damping: 0.005, 0.01, 0.02, 0.05

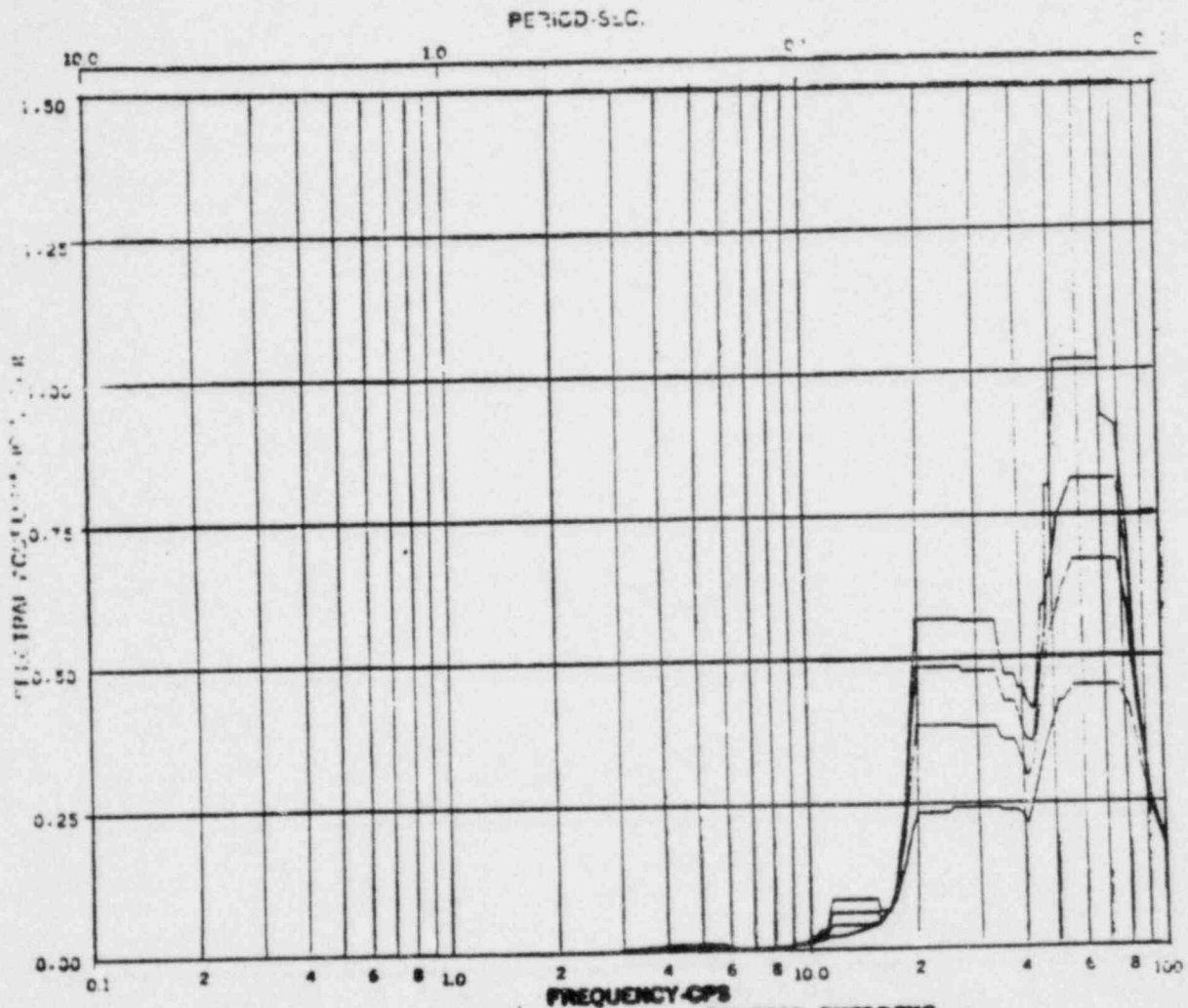
REV. 6, 4/82

**SUSQUEHANNA STEAM ELECTRIC STATION
 UNITS 1 AND 2
 DESIGN ASSESSMENT REPORT**

**REACTOR/CONTROL BUILDING
 RESPONSE SPECTRA**

KWU-LOCA

FIGURE C- 78



Acceleration Spectra for REACTOR BUILDING
 Load Case: Supersession LOCA (KWU)
 Mode 1, Direction N-S, Elev 749'-1"
 Sampling: 0.005, 0.01, 0.02, 0.05

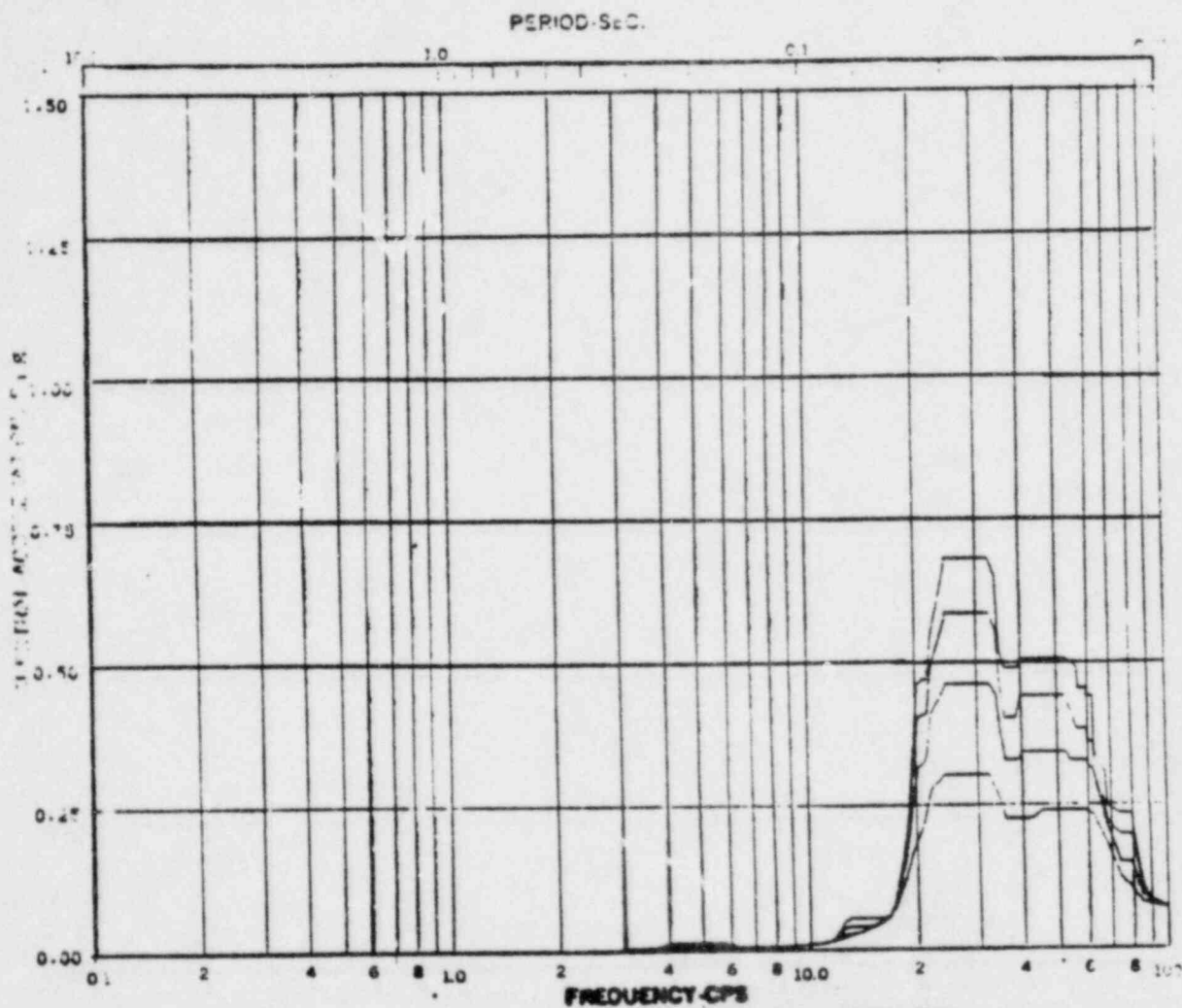
REV. 6, 4/82

SUSQUEHANNA STEAM ELECTRIC STATION
 UNITS 1 AND 2
 DESIGN ASSESSMENT REPORT

REACTOR/CONTROL BUILDING
 RESPONSE SPECTRA

KWU-LOCA

FIGURE C- 79



Acceleration Spectra for REACTOR BUILDING
 Load Case: Seismicity LOCA (KWU)
 Mode --- Direction N-S Elev 771'-0"
 Damping: 0.005, 0.01, 0.02, 0.05

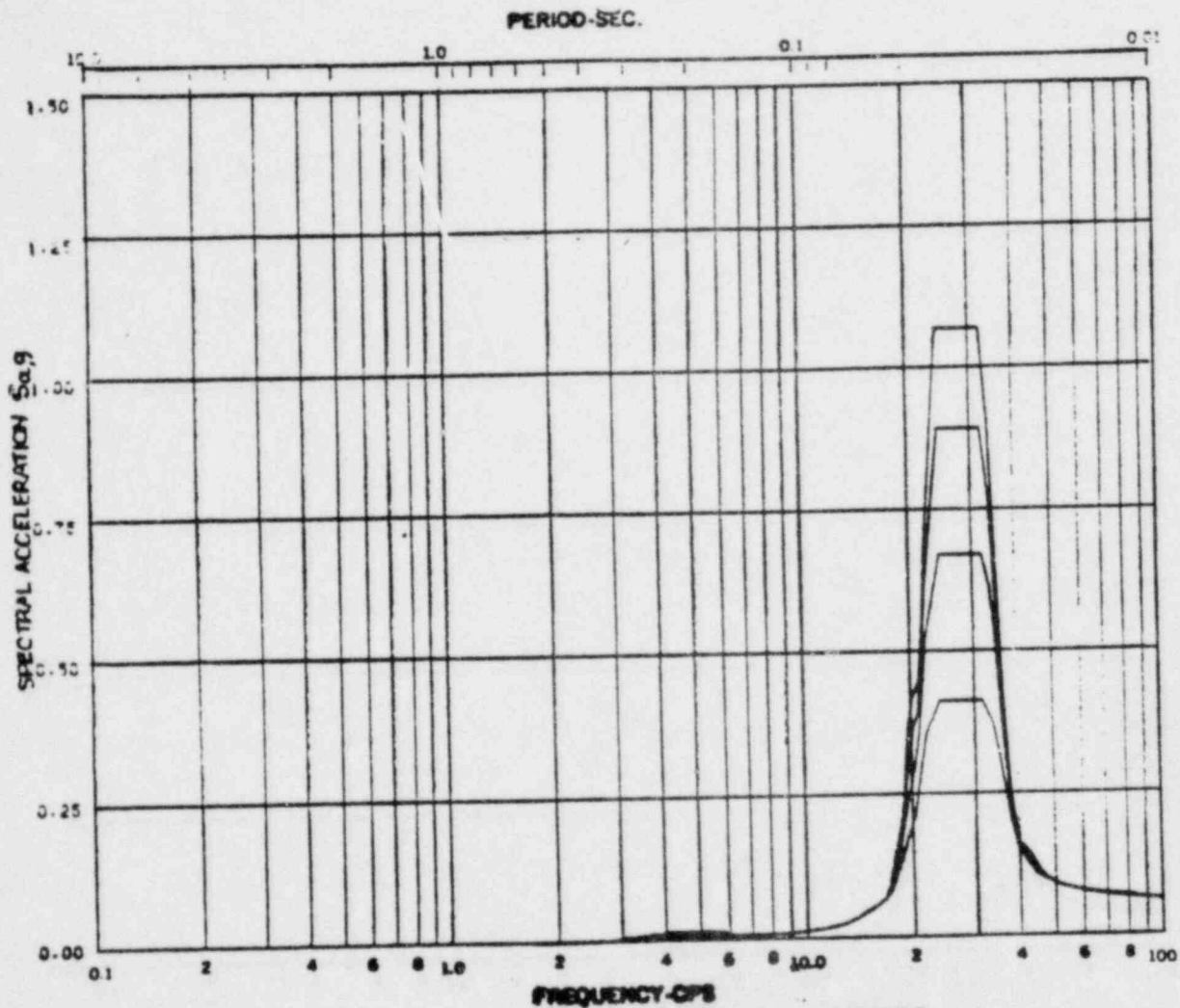
REV. 6, 4/82

SUSQUEHANNA STEAM ELECTRIC STATION
UNITS 1 AND 2
DESIGN ASSESSMENT REPORT

REACTOR/CONTROL BUILDING
RESPONSE SPECTRA

KWU-LOCA

FIGURE C- 80



Acceleration Spectra for REACTOR BUILDING
 Load Case: Seismicity LOCA (KWU)
 Mode — Direction N-S Site 779'-1"
 Sampling: 0.005, 0.01, 0.02, 0.05

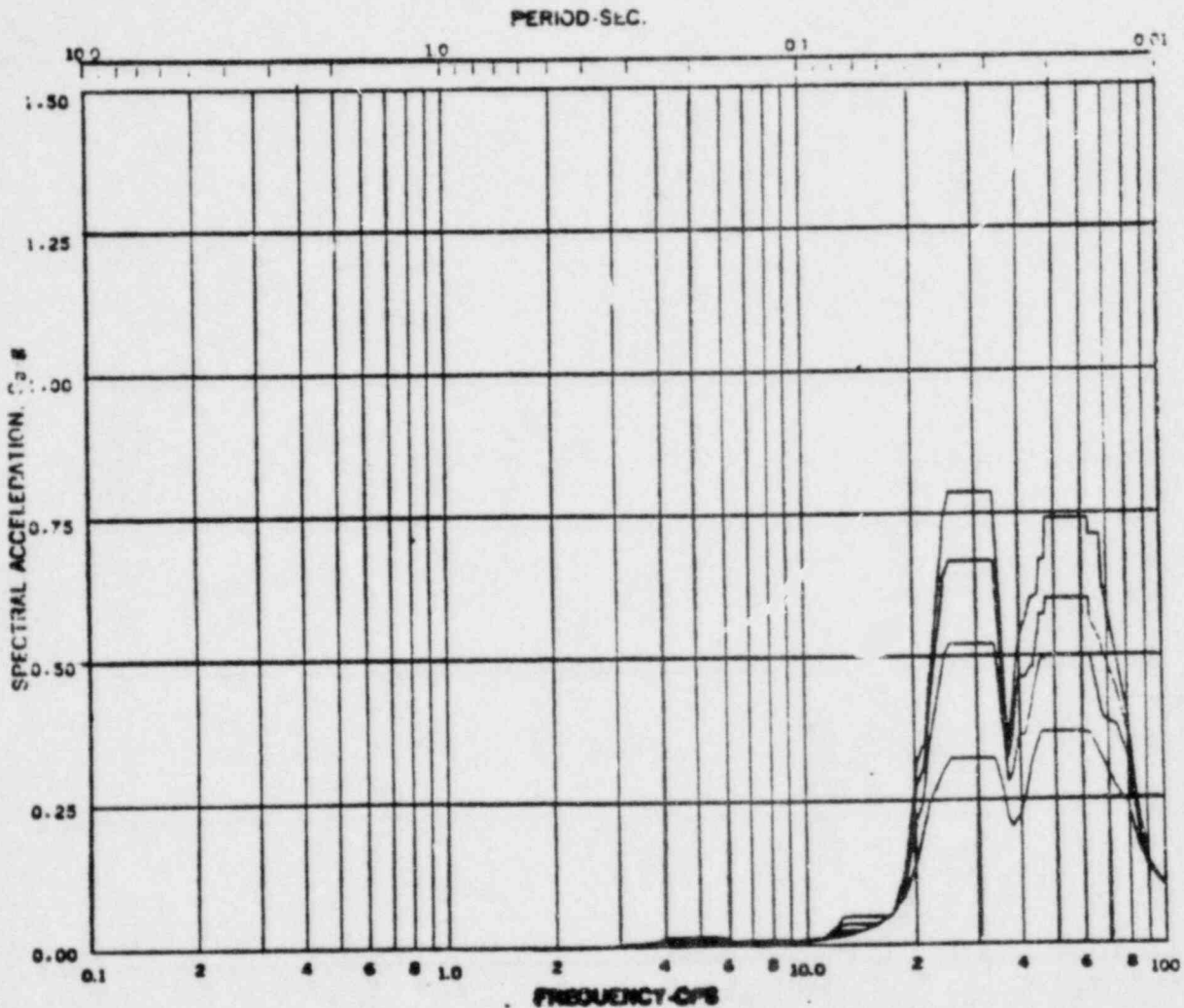
REV. 5, 4/82

BUSQUEHANNA STEAM ELECTRIC STATION
UNITS 1 AND 2
DESIGN ASSESSMENT REPORT

REACTOR/CONTROL BUILDING
RESPONSE SPECTRA

KWU-LOCA

FIGURE C- 81



Acceleration Spectra for REACTOR BUILDING
 Load Case: Supersaturated LOCA (KWU)
 Mode —, Direction N-S, Rise 783°-9°
 Sampling: 0.005, 0.01, 0.02, 0.05

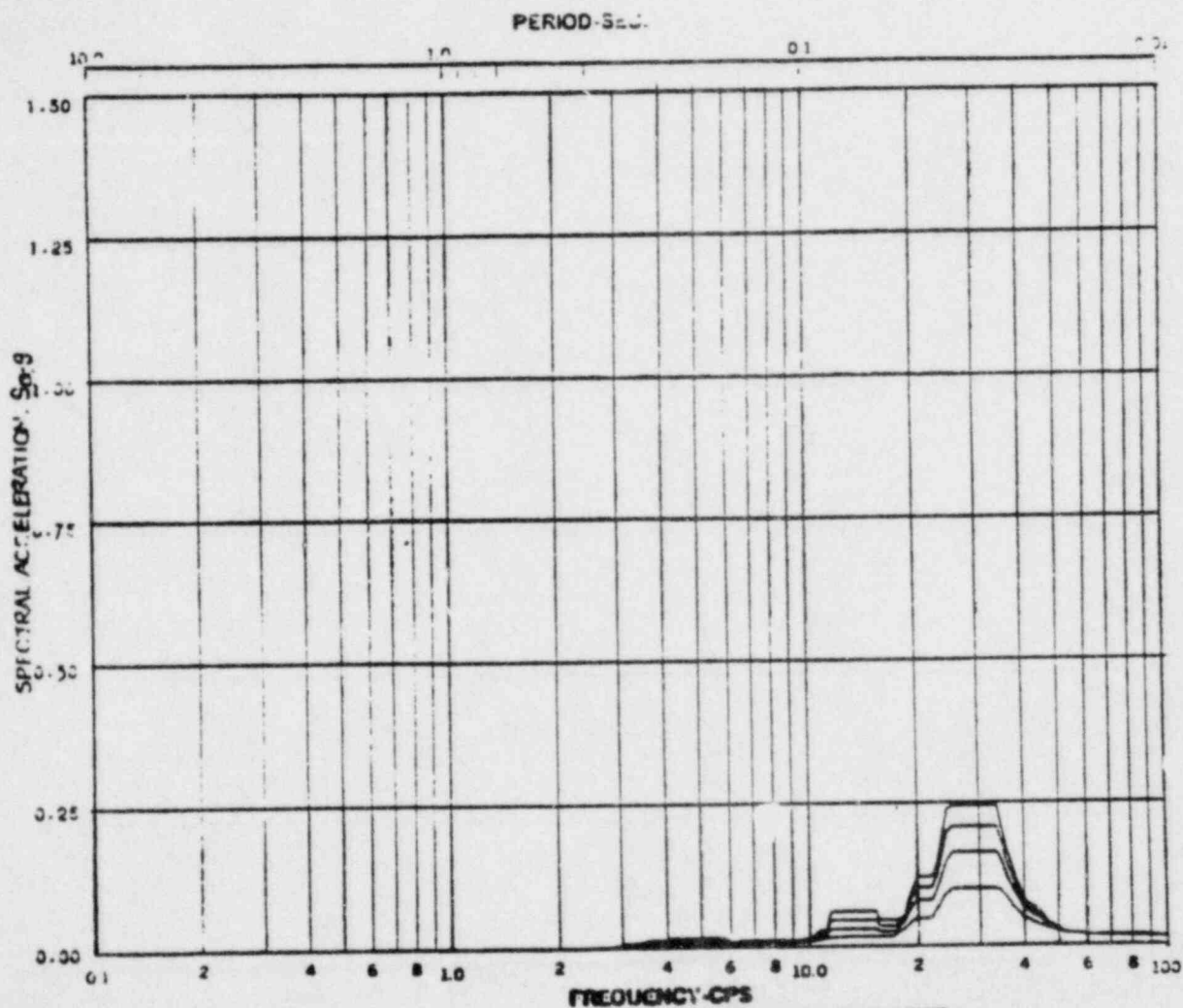
REV. 6, 4/82

EUSQUEHANNA STEAM ELECTRIC STATION
UNITS 1 AND 2
DESIGN ASSESSMENT REPORT

REACTOR/CONTROL BUILDING
 RESPONSE SPECTRA

KWU-LOCA

FIGURE C- 82



Acceleration Spectra for REACTOR BUILDING
 Load Case: Seismicity LOCA (KWU)
 Mode —, Direction N-S, Elev 199'-0"
 Sampling: 0.005, 0.01, 0.02, 0.05

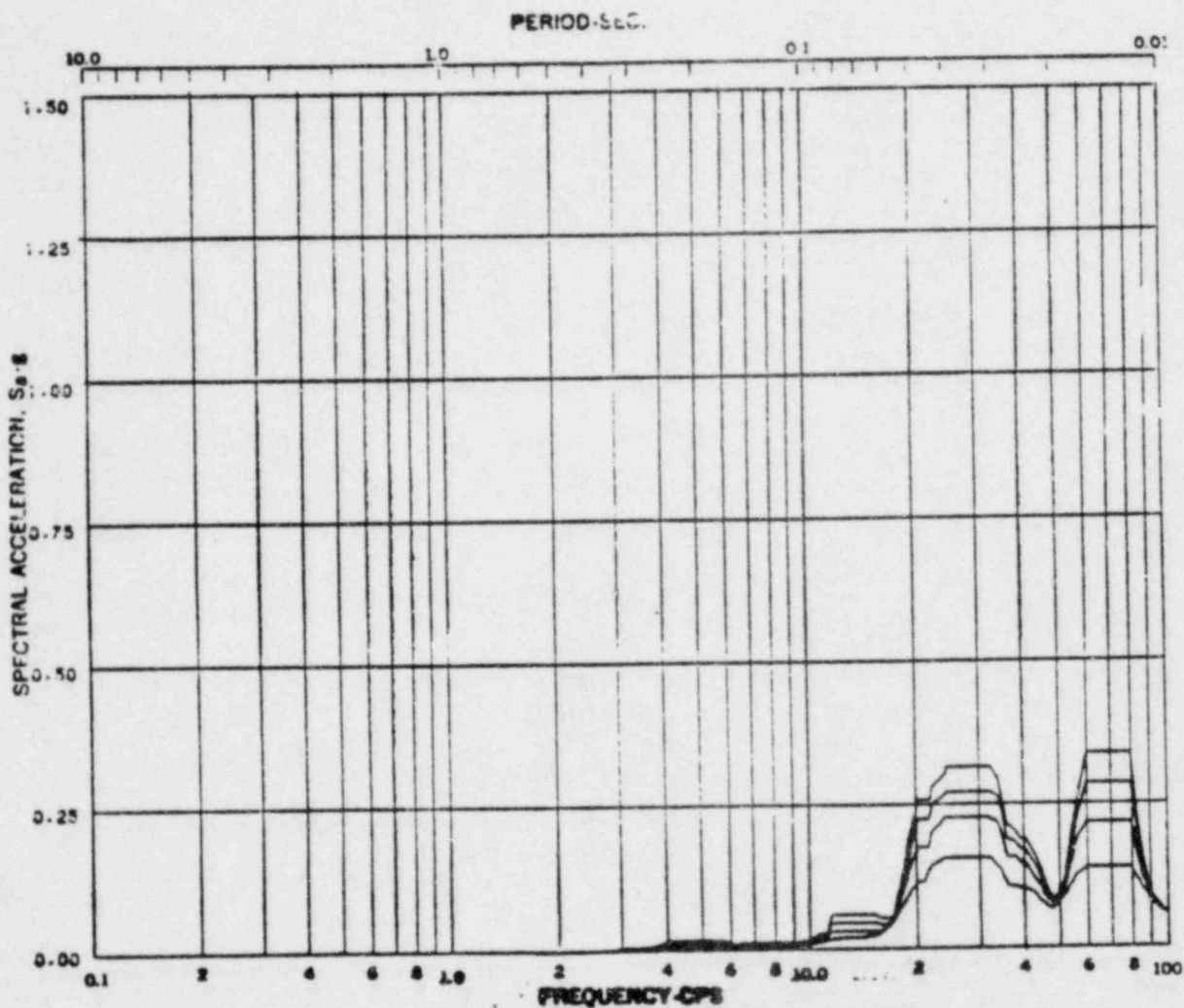
REV. 6, 4/82

SUSQUEHANNA STEAM ELECTRIC STATION
UNITS 1 AND 2
DESIGN ASSESSMENT REPORT

REACTOR/CONTROL BUILDING
 RESPONSE SPECTRA

KWU-LOCA

FIGURE C-83



Acceleration Spectra for REACTOR BUILDING
 Load Case: Seismicity LOCA (KWU)
 Mode ---, Direction N-S, Site RRS'-B"
 Damping: 0.005, 0.01, 0.02, 0.05

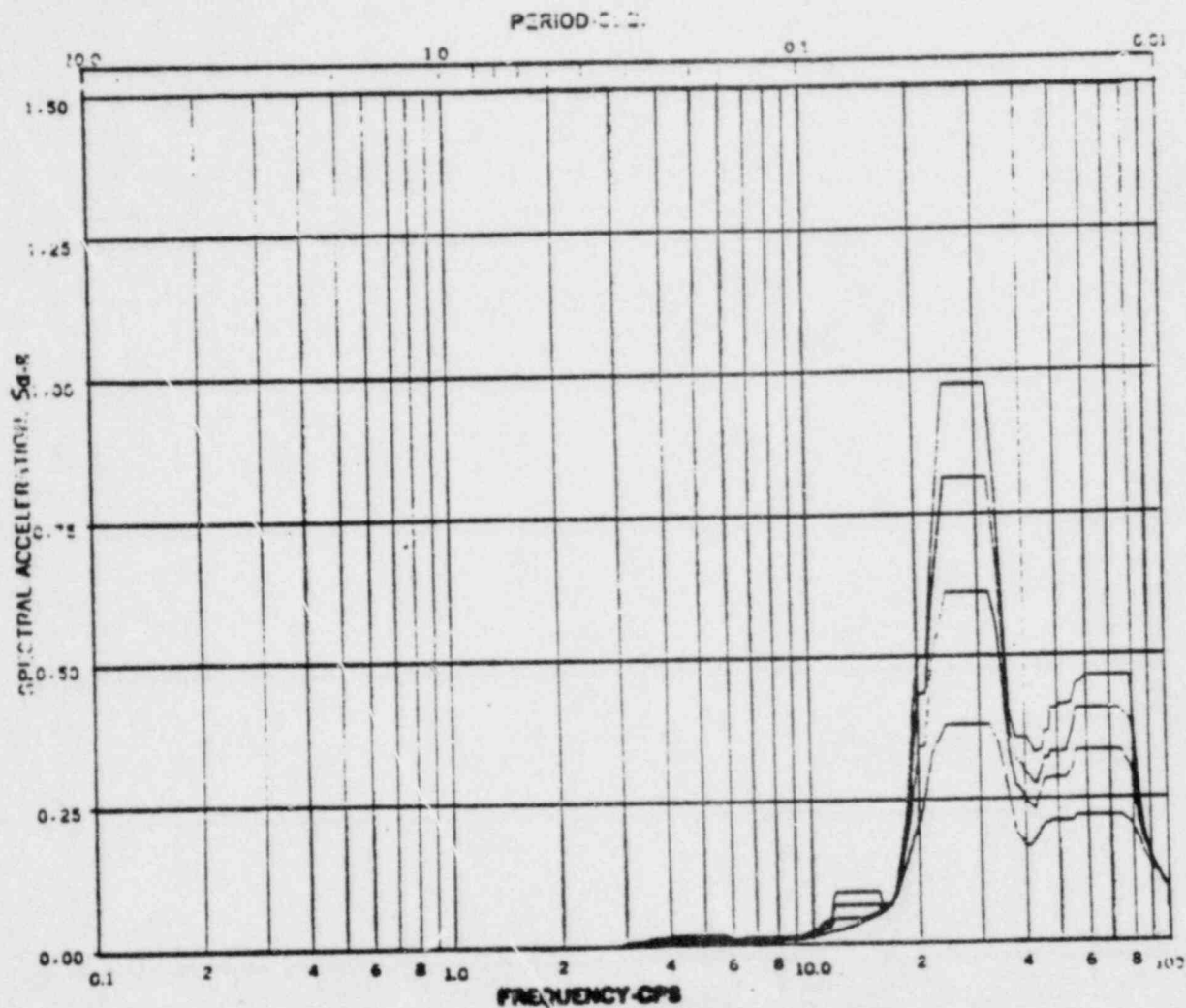
REV. 6, 4/82

**SUSQUEHANNA STEAM ELECTRIC STATION
 UNITS 1 AND 2
 DESIGN ASSESSMENT REPORT**

**REACTOR/CONTROL BUILDING
 RESPONSE SPECTRA**

KWU-LOCA

FIGURE C- 84



Acceleration Spectra (g) REACTOR BUILDING
 Load Case: Seismicity LOCA (KWU)
 Mode —, Direction N-S, Site 818'-1"
 Damping: 0.05, 0.01, 0.02, 0.05

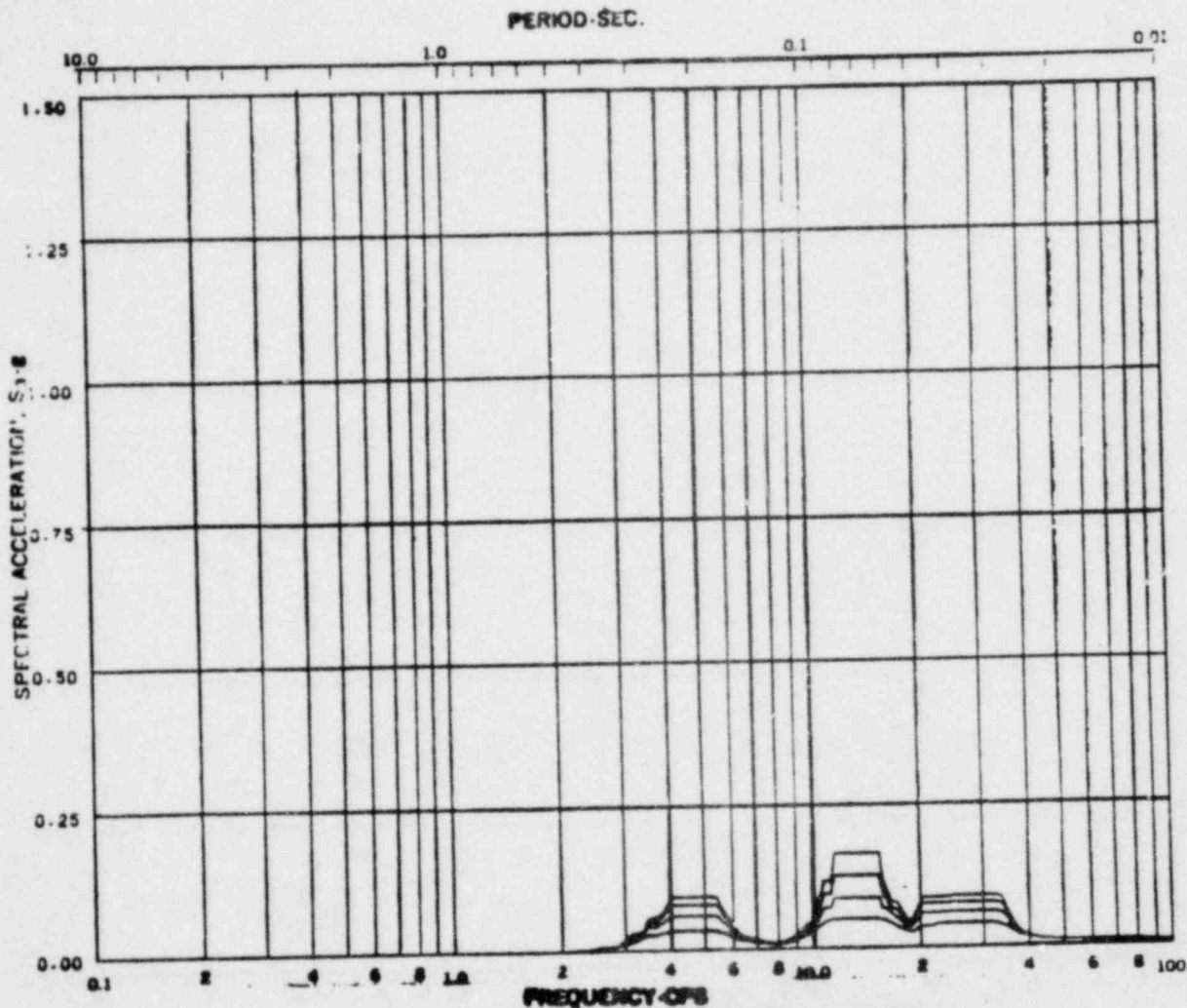
REV. 6, 4/82

BUSQUEHANNA STEAM ELECTRIC STATION
UNITS 1 AND 2
DESIGN ASSESSMENT REPORT

REACTOR/CONTROL BUILDING
RESPONSE SPECTRA

KWU-LOCA

FIGURE C- 85



Acceleration Spectra for REACTOR BUILDING
 Load Case: Seismic LOCA (RWU)
 Mode W-B Direction W-B 045°-0°
 Damping: 0.05, 0.01, 0.05, 0.05

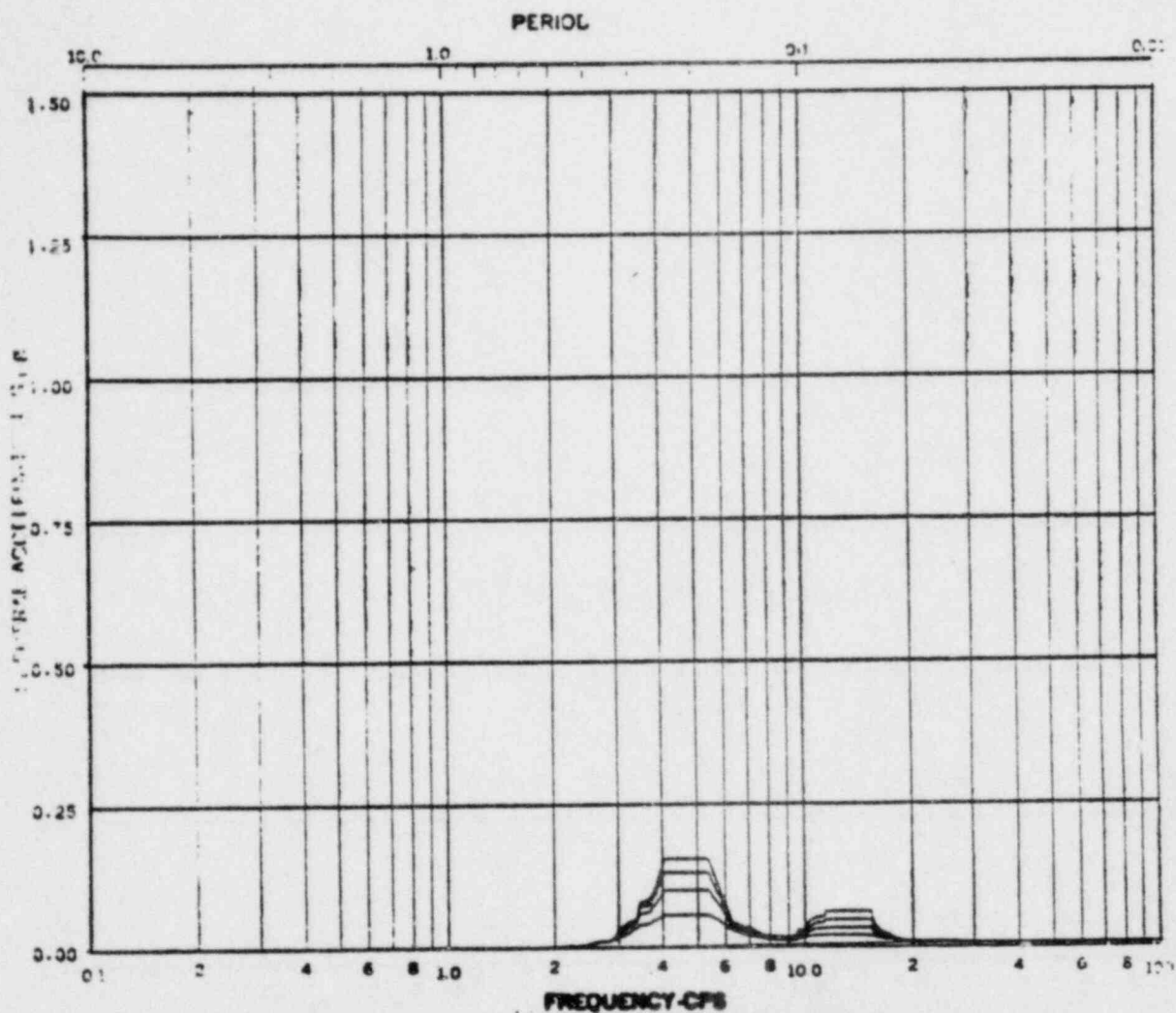
REV. 6, 4/82

SUSQUEHANNA STEAM ELECTRIC STATION
UNITS 1 AND 2
DESIGN ASSESSMENT REPORT

REACTOR/CONTROL BUILDING
RESPONSE SPECTRA

KWU-LOCA

FIGURE C- 86



Acceleration Spectra for REACTOR BUILDING
 Load Case: Earthquake LOCA (KWU)
 Mode —, Direction N-S, Elev 870'-0"
 Sampling: 0.005, 0.01, 0.02, 0.05

REV. 6, 4/82

**SUSQUEHANNA STEAM ELECTRIC STATION
 UNITS 1 AND 2
 DESIGN ASSESSMENT REPORT**

**REACTOR/CONTROL BUILDING
 RESPONSE SPECTRA**

KWU-LOCA

FIGURE C- 87

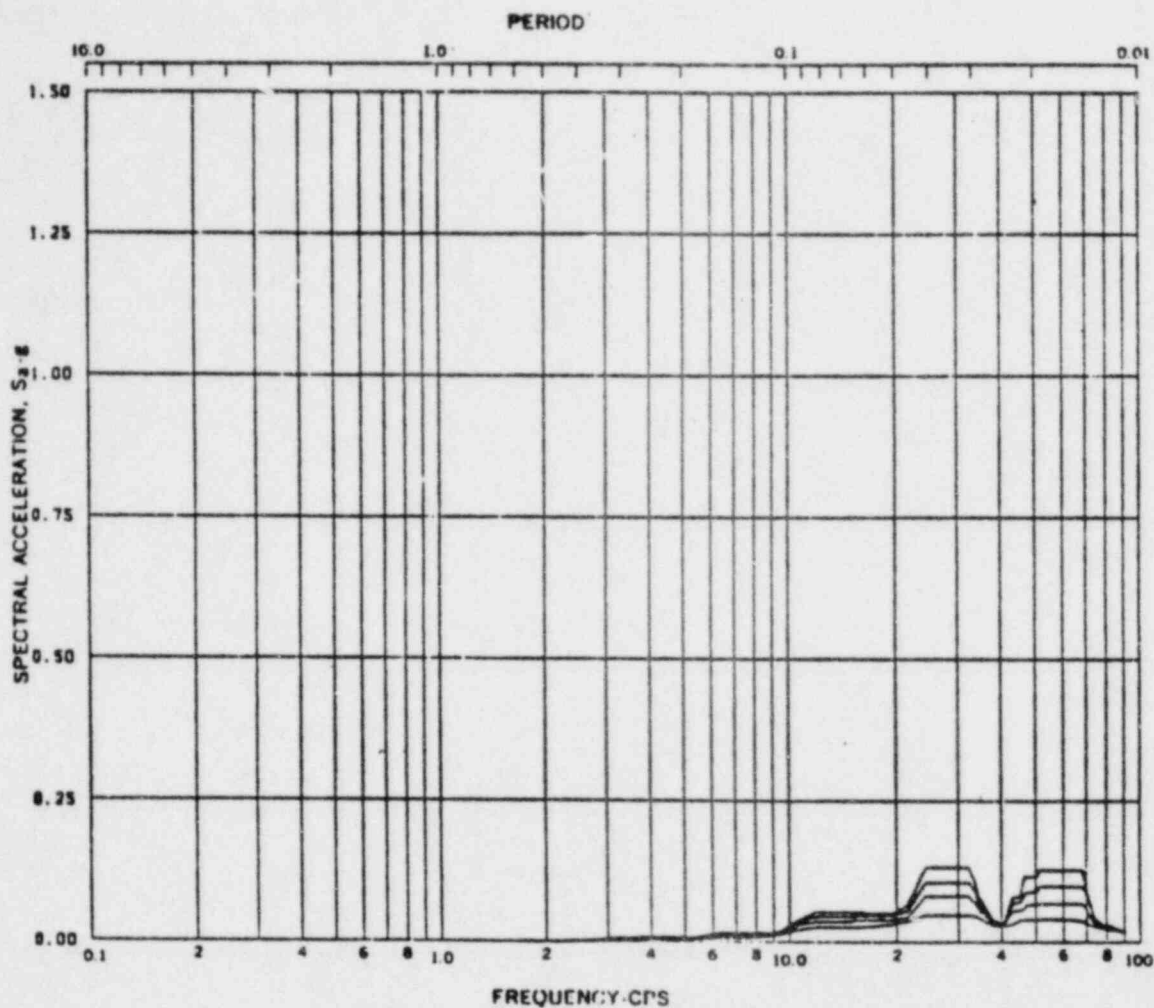


Fig. BH1-3 Acceleration Spectra for REACTOR & CONTROL BLDGS.
 Load Case: Susquehanna SRV
 Mode -, Direction N-S, Elev 670'-0"
 Damping: 0.005, 0.01, 0.02, 0.05

REV. 6, 4/82

**SUSQUEHANNA STEAM ELECTRIC STATION
 UNITS 1 AND 2
 DESIGN ASSESSMENT REPORT**

**REACTOR/CONTROL BUILDING
 RESPONSE SPECTRA**

KWU-SRV

FIGURE C- 88

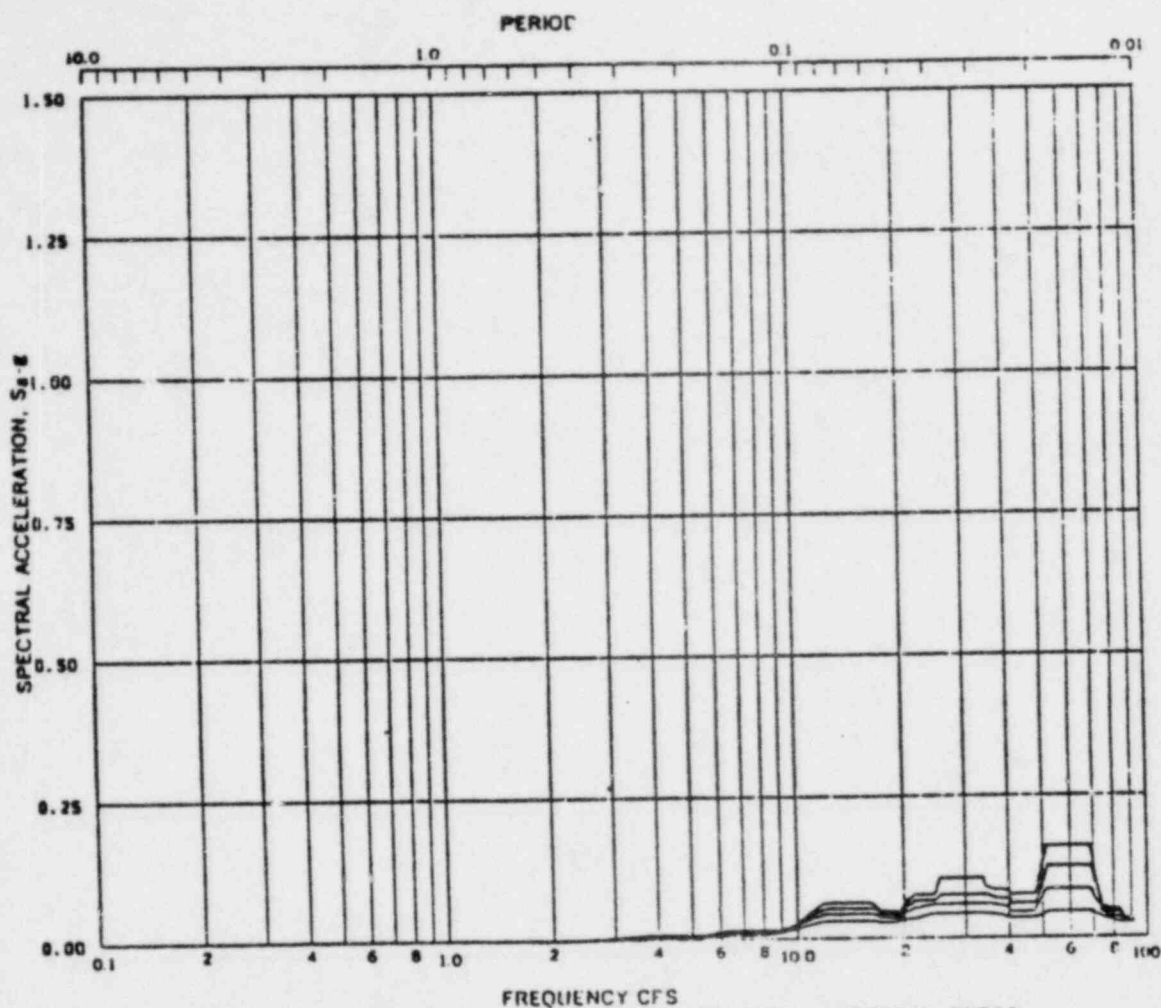


Fig. BN2-3 Acceleration Spectra for REACTOR & CONTROL BLDGS.
 Load Case: Susquehanna SRV
 Node ---, Direction N-S, Elev 676'-0"
 Damping: 0.005, 0.01, 0.02, 0.05

REV. 6, 4/82

**SUSQUEHANNA STEAM ELECTRIC STATION
 UNITS 1 AND 2
 DESIGN ASSESSMENT REPORT**

**REACTOR/CONTROL BUILDING
 RESPONSE SPECTRA**

KWU-SRV

FIGURE C- 89

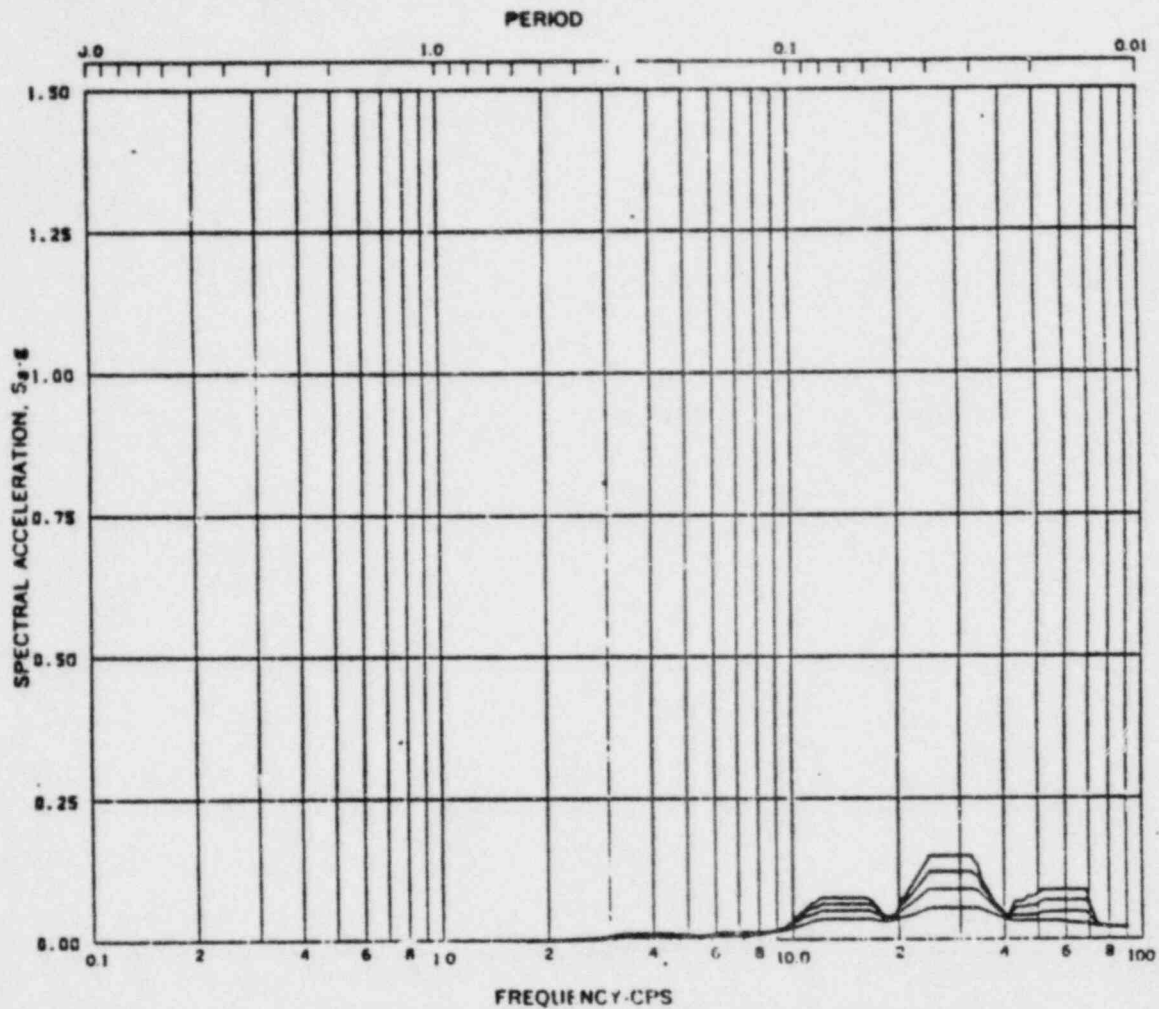


Fig. BN3-3 Acceleration Spectra for REACTOR & CONTROL BLDGS.
 Load Case: Susquehanna SRV
 Mode -, Direction N-S, Elev 683'-0"
 Damping: 0.005, 0.01, 0.02, 0.05

REV. 6, 4/82

SUSQUEHANNA STEAM ELECTRIC STATION
 UNITS 1 AND 2
 DESIGN ASSESSMENT REPORT

REACTOR/CONTROL BUILDING
 RESPONSE SPECTRA

KWU-SRV
 FIGURE C-90

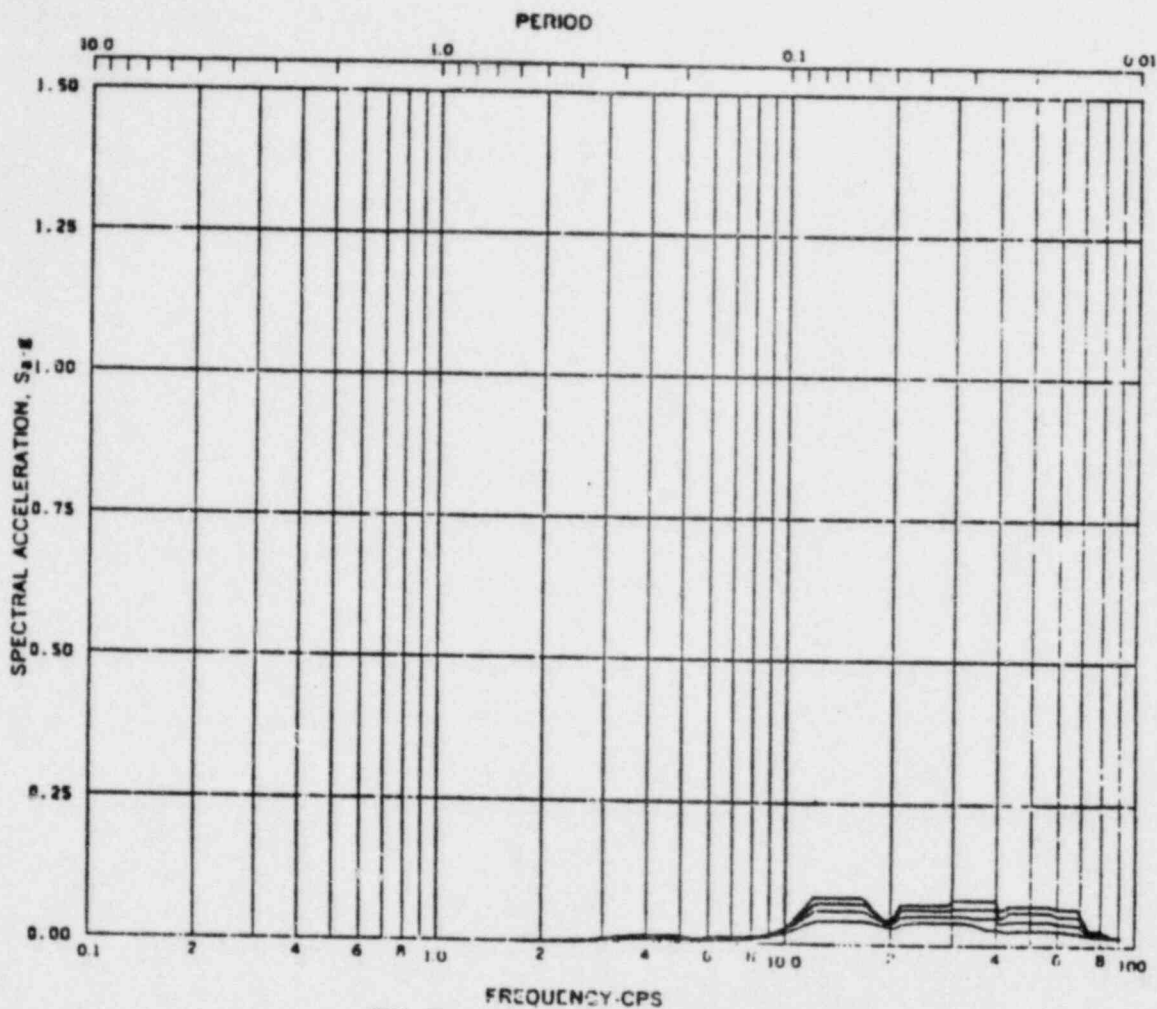


Fig. BN4-3 Acceleration Spectra for REACTOR & CONTROL BLDGS.
 Load Case: Susquehanna SRV
 Mode -, Direction N-S, Elev 597'-0"
 Damping: 0.005, 0.01, 0.02, 0.05

REV. 6, 4/82

**SUSQUEHANNA STEAM ELECTRIC STATION
 UNITS 1 AND 2
 DESIGN ASSESSMENT REPORT**

**REACTOR/CONTROL BUILDING
 RESPONSE SPECTRA**

**KWU-SRV
 FIGURE C- 91**

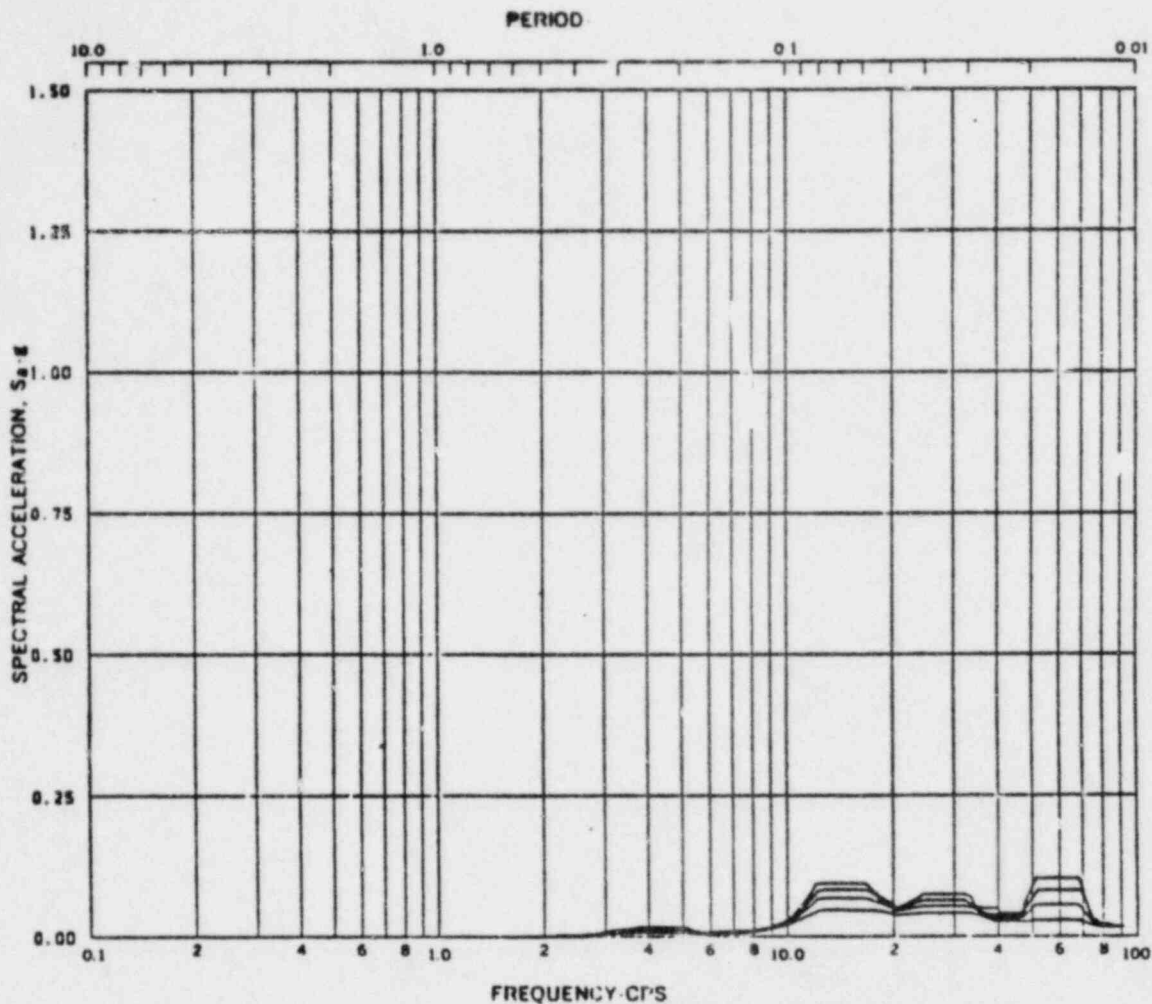


Fig. BNS-3 Acceleration Spectra for REACTOR & CONTROL BLDGS.
 Load Case: Susquehanna SRV
 Node -, Direction N-S, Elev 709'-0"
 Damping: 0.005, 0.01, 0.02, 0.05

REV. 6, 4/82

**SUSQUEHANNA STEAM ELECTRIC STATION
 UNITS 1 AND 2
 DESIGN ASSESSMENT REPORT**

**REACTOR/CONTROL BUILDING
 RESPONSE SPECTRA**

**KWU-SRV
 FIGURE C-92**

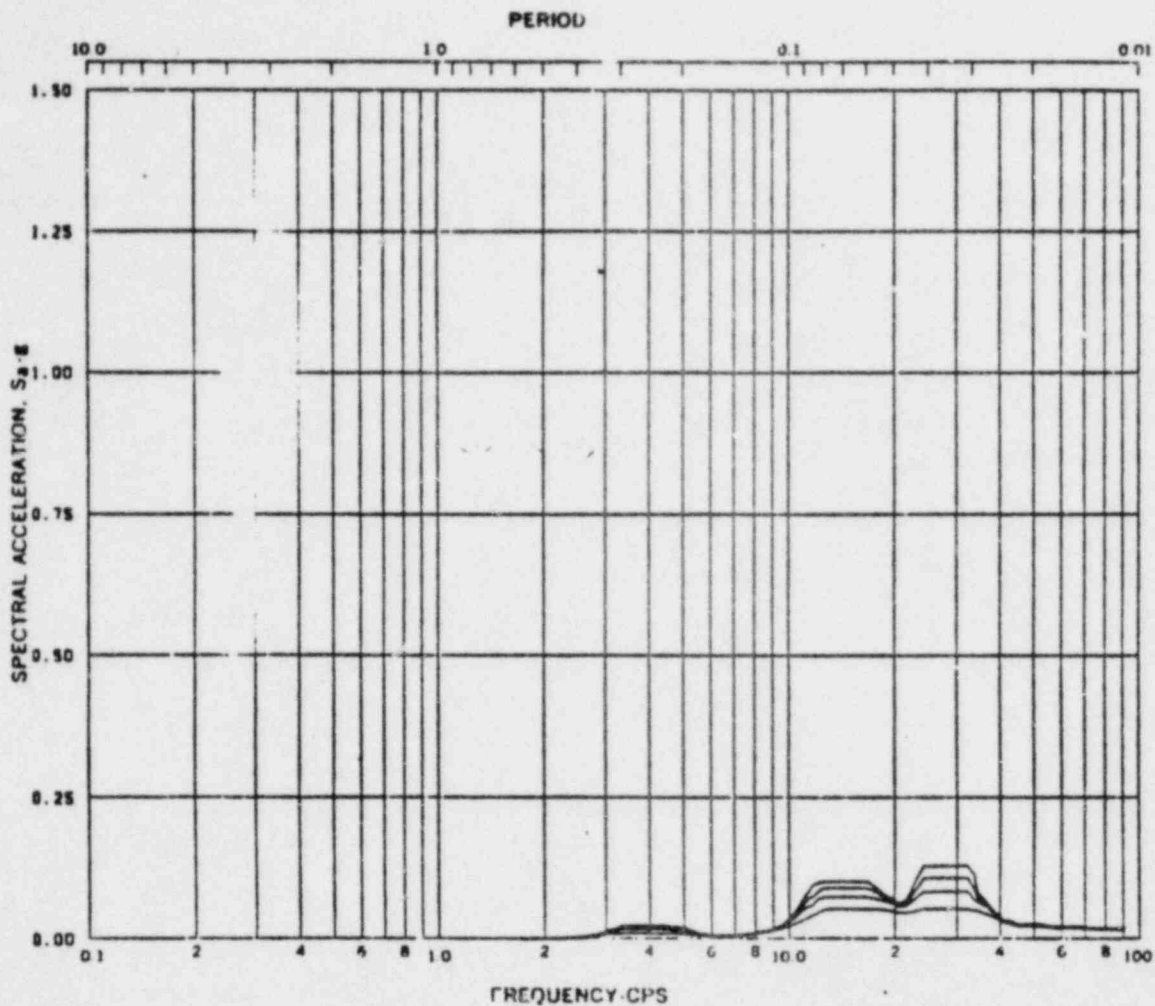


Fig. BNG-3 Acceleration Spectra for REACTOR & CONTROL BLDGS.
 Load Case: Susquehanna SRV
 Mode -, Direction N-S, Elev 719'-1"
 Damping: 0.005, 0.01, 0.02, 0.05

REV. 6, 4/82

SUSQUEHANNA STEAM ELECTRIC STATION
 UNITS 1 AND 2
 DESIGN ASSESSMENT REPORT

REACTOR/CONTROL BUILDING
 RESPONSE SPECTRA

KWU-SRV
 FIGURE C-93

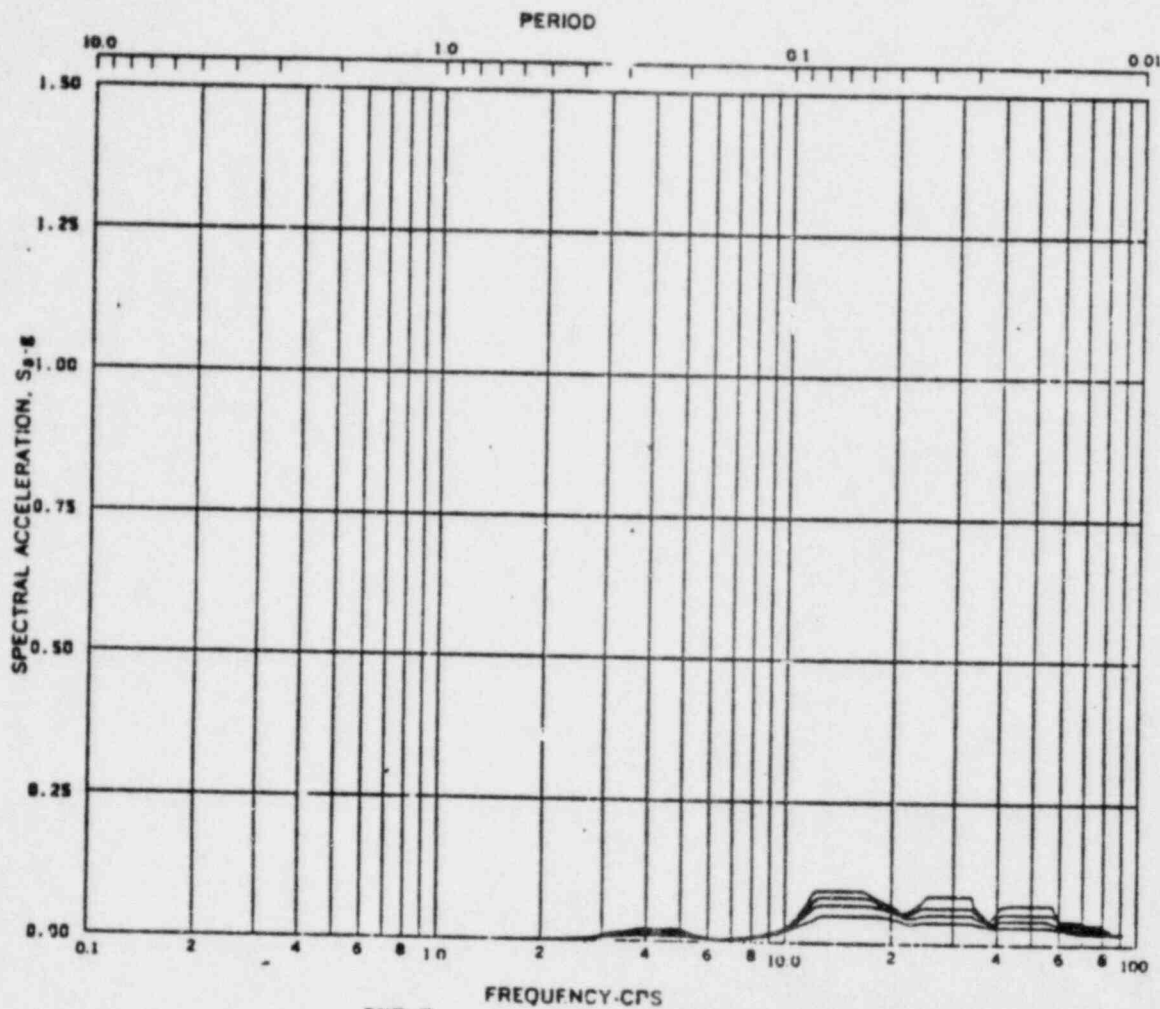


Fig. BN7-3 Acceleration Spectra for REACTOR & CONTROL BLDGS.
 Load Case: Seismicity SRV
 Mode -, Direction: N-S, Elev 728'-0"
 Damping: 0.005, 0.01, 0.02, 0.05

REV. 6, 4/82

**BUSQUEHANNA STEAM ELECTRIC STATION
 UNITS 1 AND 2
 DESIGN ASSESSMENT REPORT**

**REACTOR/CONTROL BUILDING
 RESPONSE SPECTRA**

**KWU-SRV
 FIGURE C- 94**

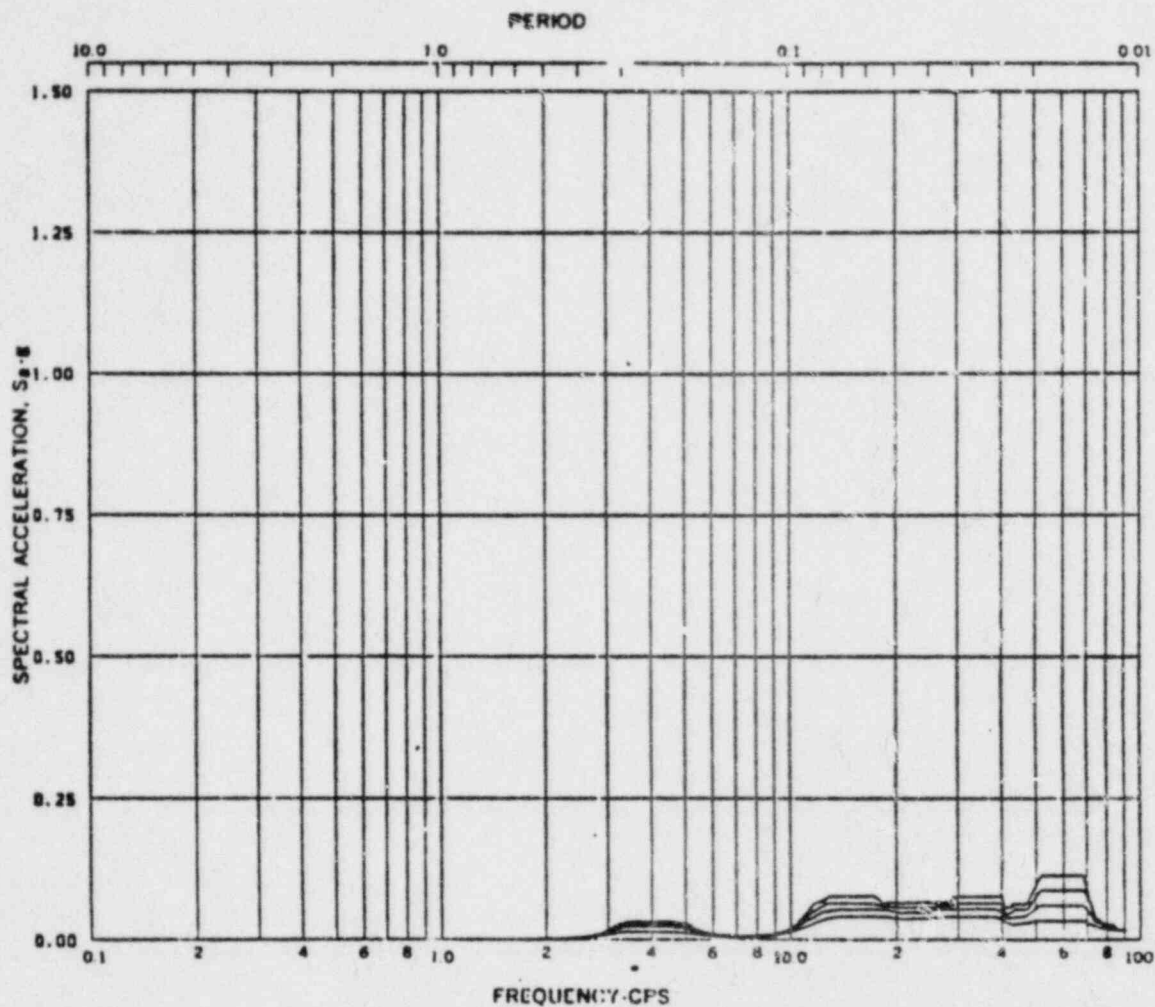


Fig. BN8-3 Acceleration Spectra for REACTOR & CONTROL BLDGS.
 Load Case: Seismic SRV
 Node ~, Direction N-S, Elev 749'-1"
 Damping: 0.005, 0.01, 0.02, 0.05

REV. 6, 4/82

**USQUEHANNA STEAM ELECTRIC STATION
 UNITS 1 AND 2
 DESIGN ASSESSMENT REPORT**

**REACTOR/CONTROL BUILDING
 RESPONSE SPECTRA**

KWU-SRV

FIGURE C- 95

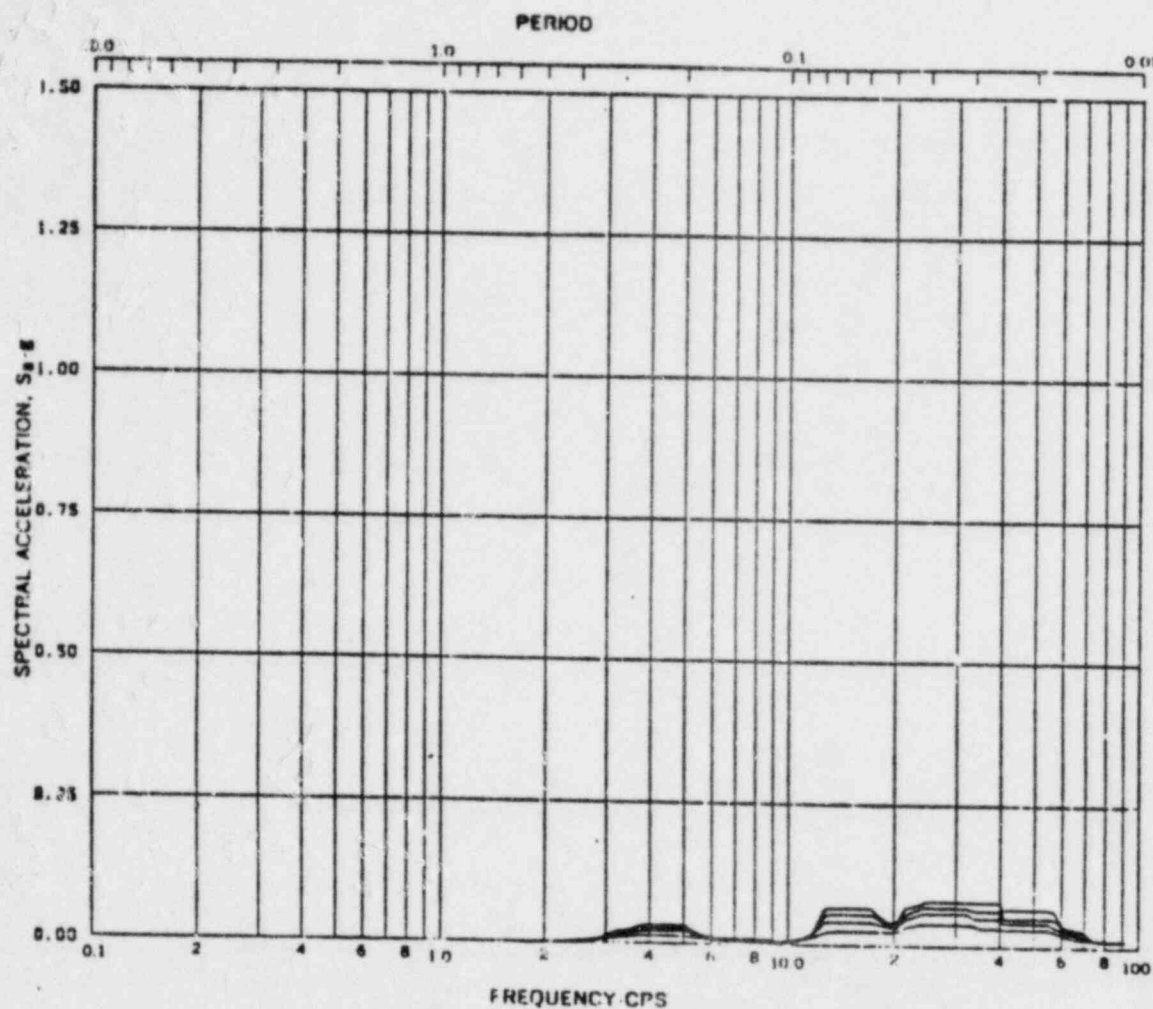


Fig. BN9-3 Acceleration Spectra for REACTOR & CONTROL BLDGS.
 Load Case: Susquehanna SRV
 Node - Direction N-S, Elev 771'-0"
 Damping: 0.005, 0.01, 0.02, 0.05

REV. 6, 4/82

SUSQUEHANNA STEAM ELECTRIC STATION
 UNITS 1 AND 2
 DESIGN ASSESSMENT REPORT

REACTOR/CONTROL BUILDING
 RESPONSE SPECTRA

KWU-SRV
 FIGURE C-96

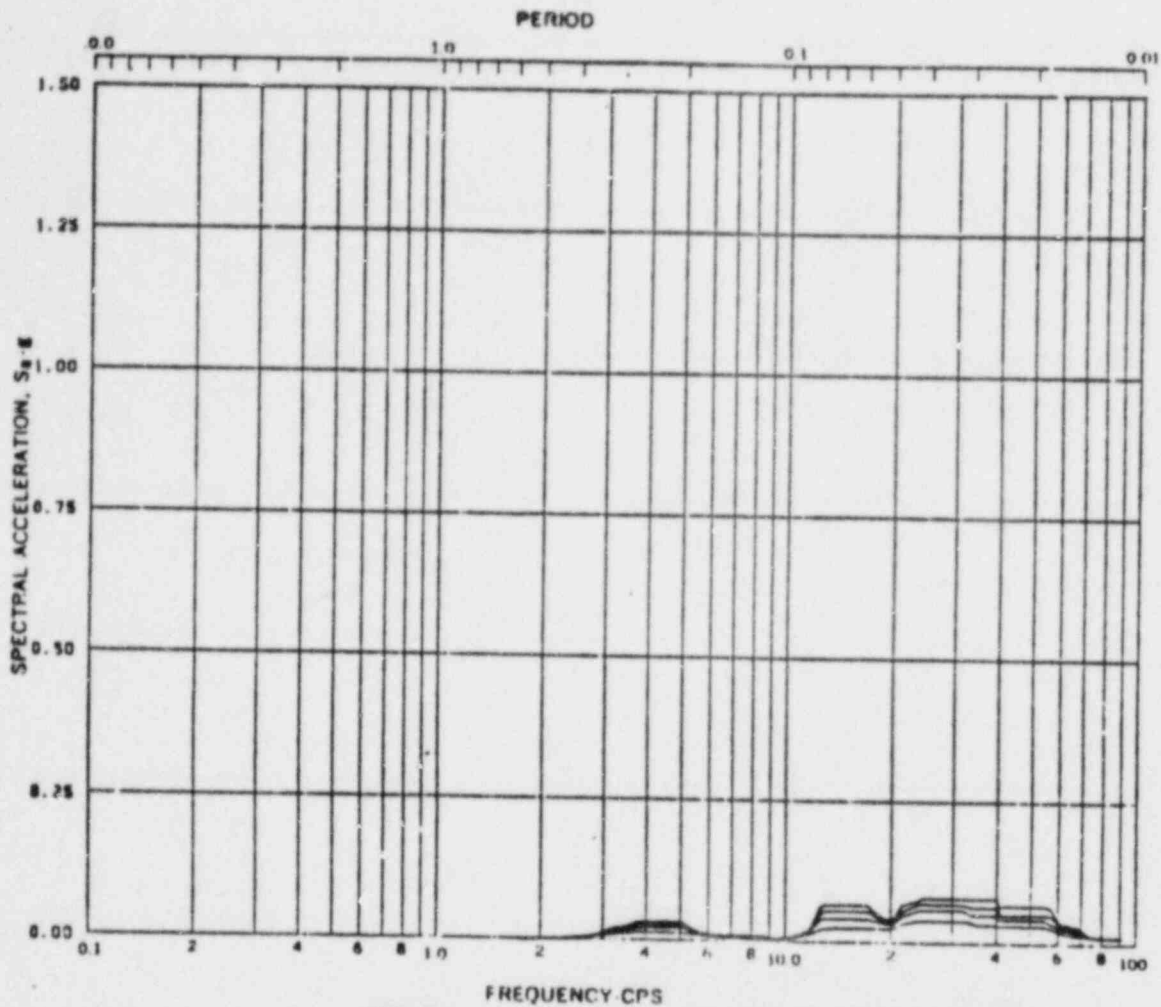


Fig. BN9-3 Acceleration Spectra for REACTOR & CONTROL BLDGS.
 Load Case: Susquehanna SRV
 Mode -, Direction N-S, Elev 771'-0"
 Damping: 0.005, 0.01, 0.02, 0.05

REV. 6, 4/82

SUSQUEHANNA STEAM ELECTRIC STATION
 UNITS 1 AND 2
 DESIGN ASSESSMENT REPORT

REACTOR/CONTROL BUILDING
 RESPONSE SPECTRA

KWU-SRV
 FIGURE C-96

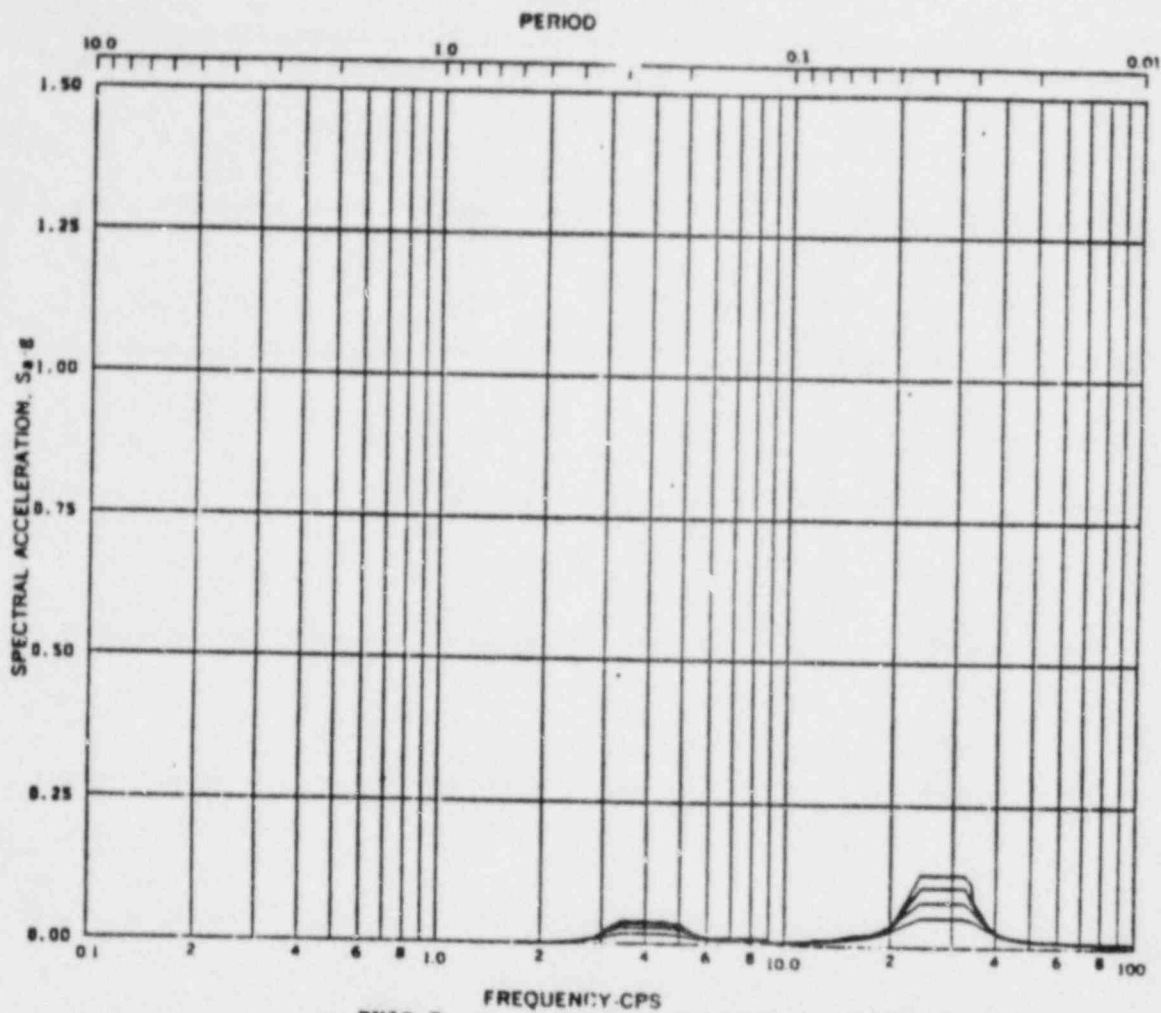


Fig. BN10-3 Acceleration Spectra for REACTOR & CONTROL BLDGS.
 Load Case: Susquehanna SRV
 Mode -, Direction N-S, Elev 779'-1"
 Damping: 0.006, 0.01, 0.02, 0.05

REV. 6, 4/82

SUSQUEHANNA STEAM ELECTRIC STATION
 UNITS 1 AND 2
 DESIGN ASSESSMENT REPORT

REACTOR/CONTROL BUILDING
 RESPONSE SPECTRA

KWU-SRV
 FIGURE C- 97

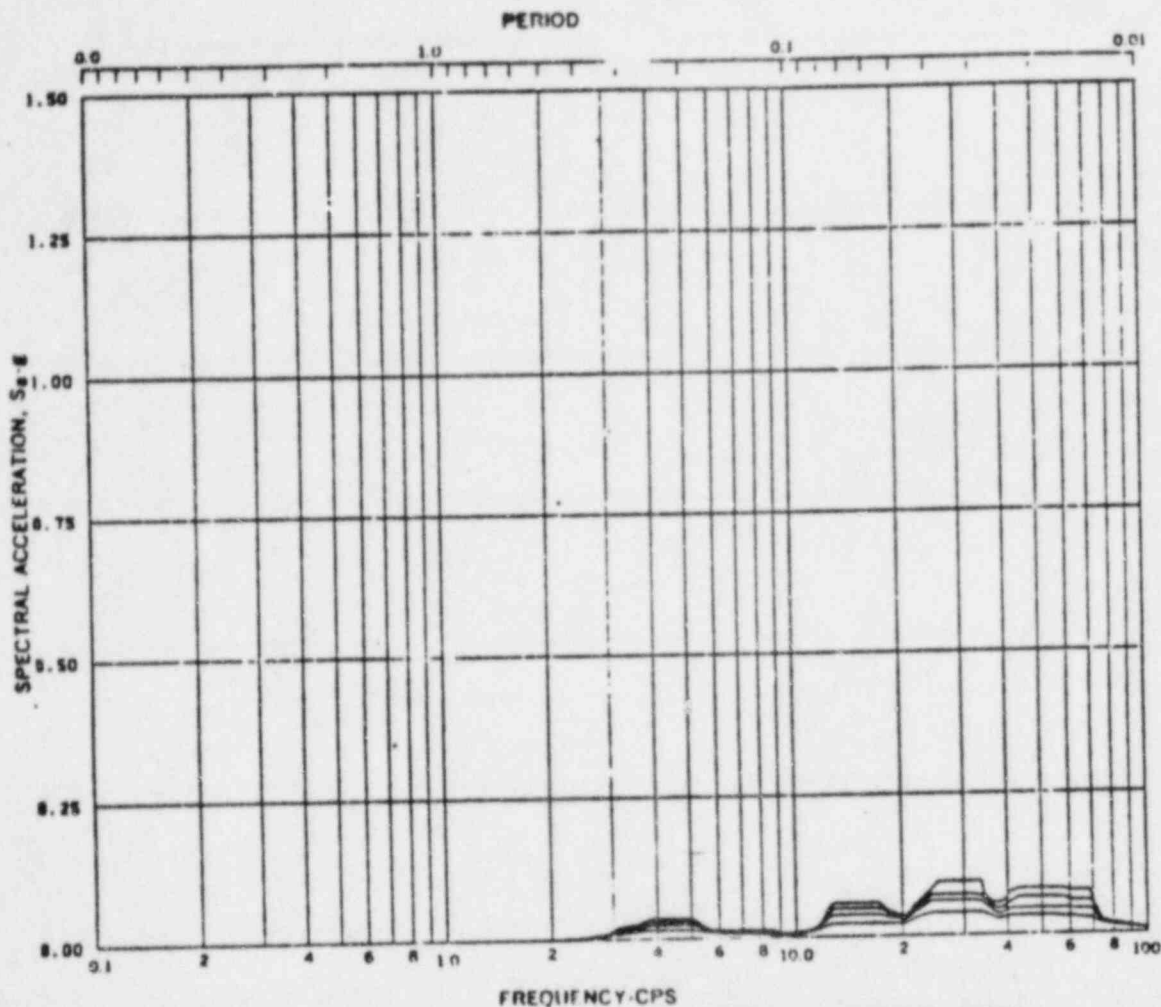


Fig. BN11-3 Acceleration Spectra for REACTOR & CONTROL BLDGS.
 Load Case: Susquehanna SRV
 Mode -, Direction N-S, Elev 783'-0"
 Damping: 0.005, 0.01, 0.02, 0.05

REV. 6, 4/82

**SUSQUEHANNA STEAM ELECTRIC STATION
 UNITS 1 AND 2
 DESIGN ASSESSMENT REPORT**

**REACTOR/CONTROL BUILDING
 RESPONSE SPECTRA**

**KWU-SRV
 FIGURE C- 98**

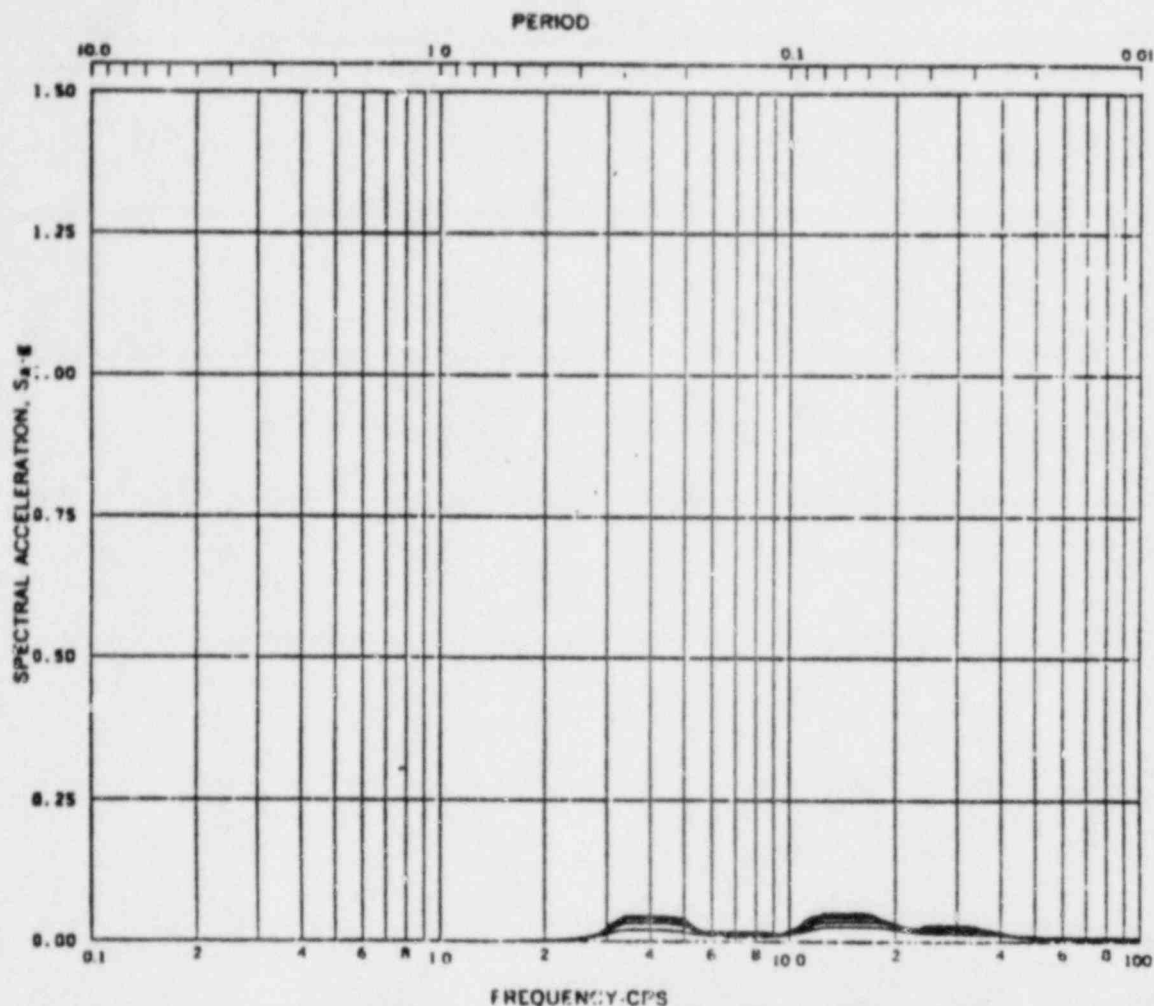


Fig. BN12-3 Acceleration Spectra for REACTOR & CONTROL BLDGS.
 Load Case: Susquehanna SRV
 Mode -, Direction N-S, Elev 799'-1"
 Damping: 0.005, 0.01, 0.02, 0.05

REV. 6, 4/82

**SUSQUEHANNA STEAM ELECTRIC STATION
 UNITS 1 AND 2
 DESIGN ASSESSMENT REPORT**

**REACTOR/CONTROL BUILDING
 RESPONSE SPECTRA**

KWU-SRV

FIGURE C-99

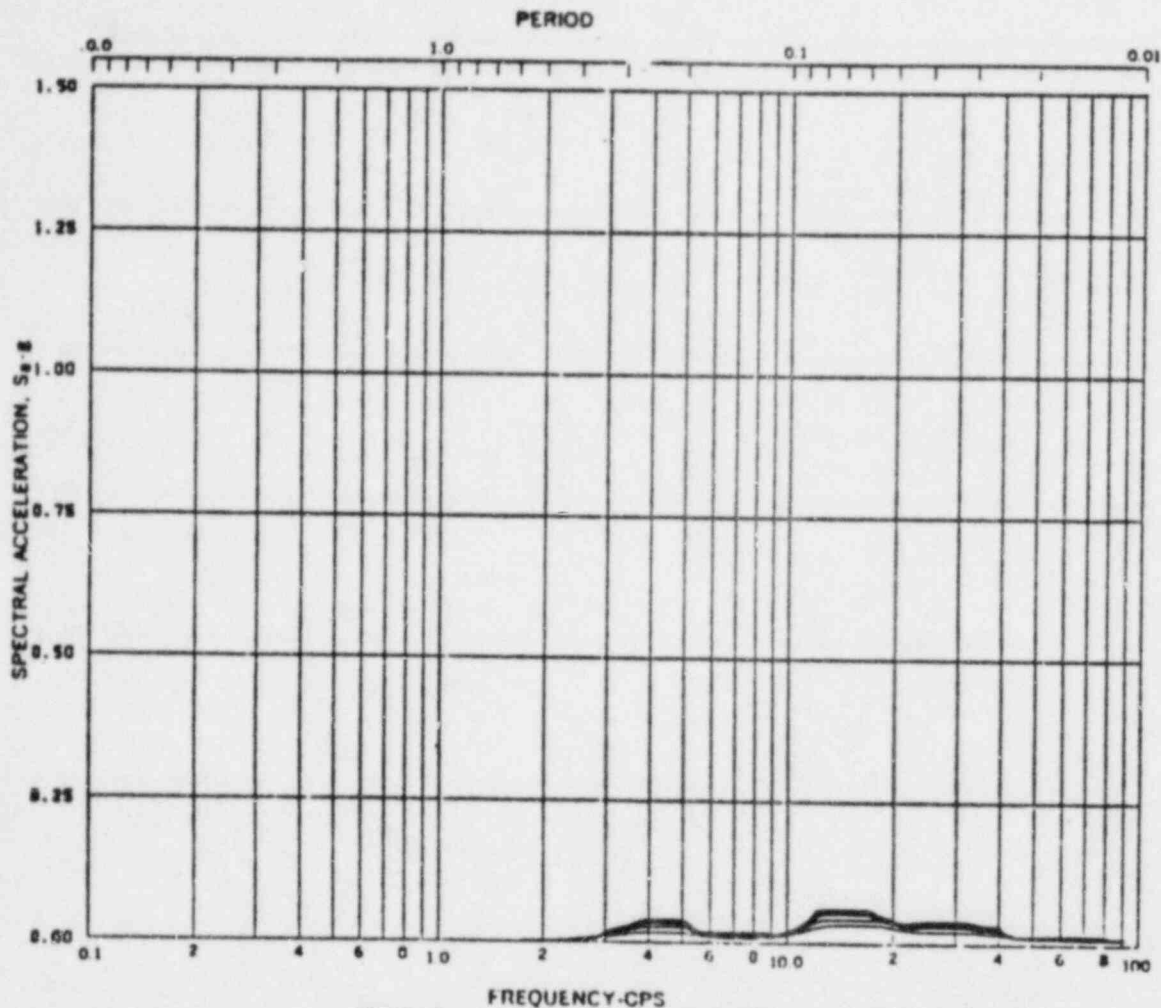


Fig. BN13-3 Acceleration Spectra for REACTOR & CONTROL BLDGS.
 Load Case: Susquehanna SRV
 Mode -, Direction N-S, Elev 806'-0"
 Damping: 0.005, 0.01, 0.02, 0.05

REV. 6, 4/82

**SUSQUEHANNA STEAM ELECTRIC STATION
 UNITS 1 AND 2
 DESIGN ASSESSMENT REPORT**

**REACTOR/CONTROL BUILDING
 RESPONSE SPECTRA**

**KWU-SRV
 FIGURE C-100**

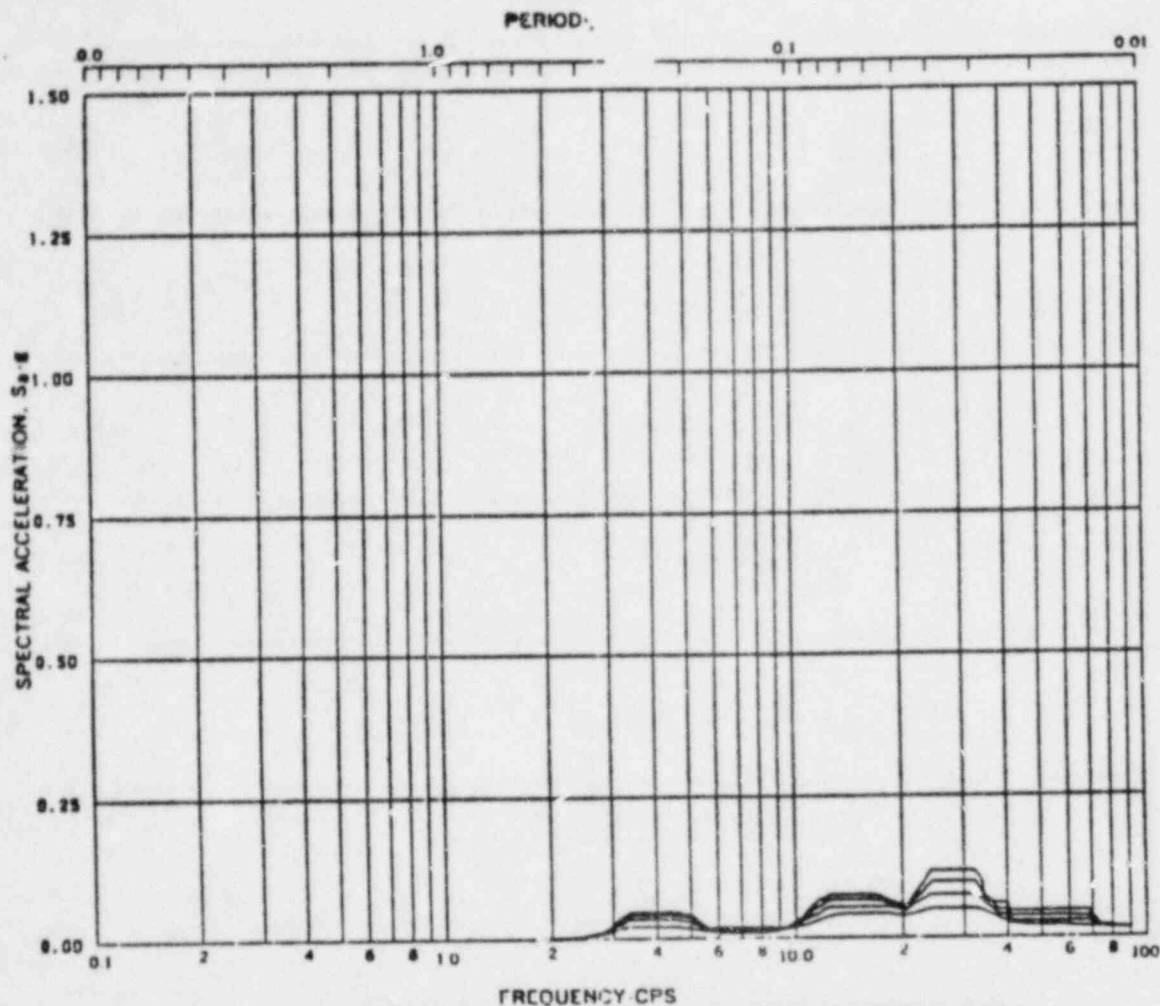


Fig. BN14-3 Acceleration Spectra for REACTOR & CONTROL BLDGS.
 Load Case: Susquehanna SRV
 Mode -, Direction N-S, Elev 818'-1"
 Damping: 0.005, 0.01, 0.02, 0.05

REV. 6, 4/82

SUSQUEHANNA STEAM ELECTRIC STATION
 UNITS 1 AND 2
 DESIGN ASSESSMENT REPORT

REACTOR/CONTROL BUILDING
 RESPONSE SPECTRA

KWU-SRV
 FIGURE C- 101

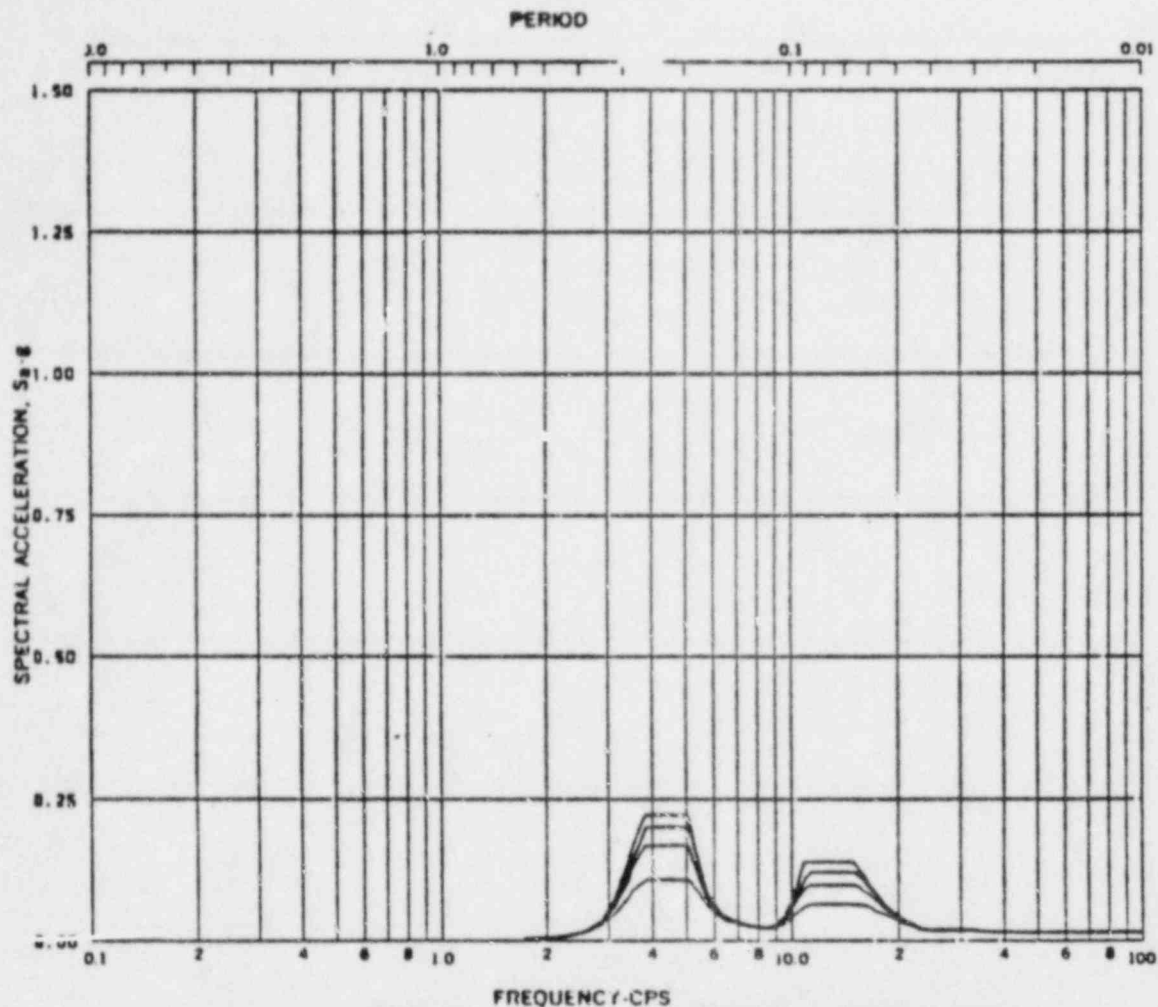


Fig. BN15-3 Acceleration Spectra for REACTOR & CONTROL BLDGS.
 Load Case: Susquehanna SRV
 Mode -, Direction N-S, Elev 846'-0"
 Damping: 0.005, 0.01, 0.02, 0.05

REV. 6, 4/82

**SUSQUEHANNA STEAM ELECTRIC STATION
 UNITS 1 AND 2
 DESIGN ASSESSMENT REPORT**

**REACTOR/CONTROL BUILDING
 RESPONSE SPECTRA**

KWU-SRV

FIGURE C- 102

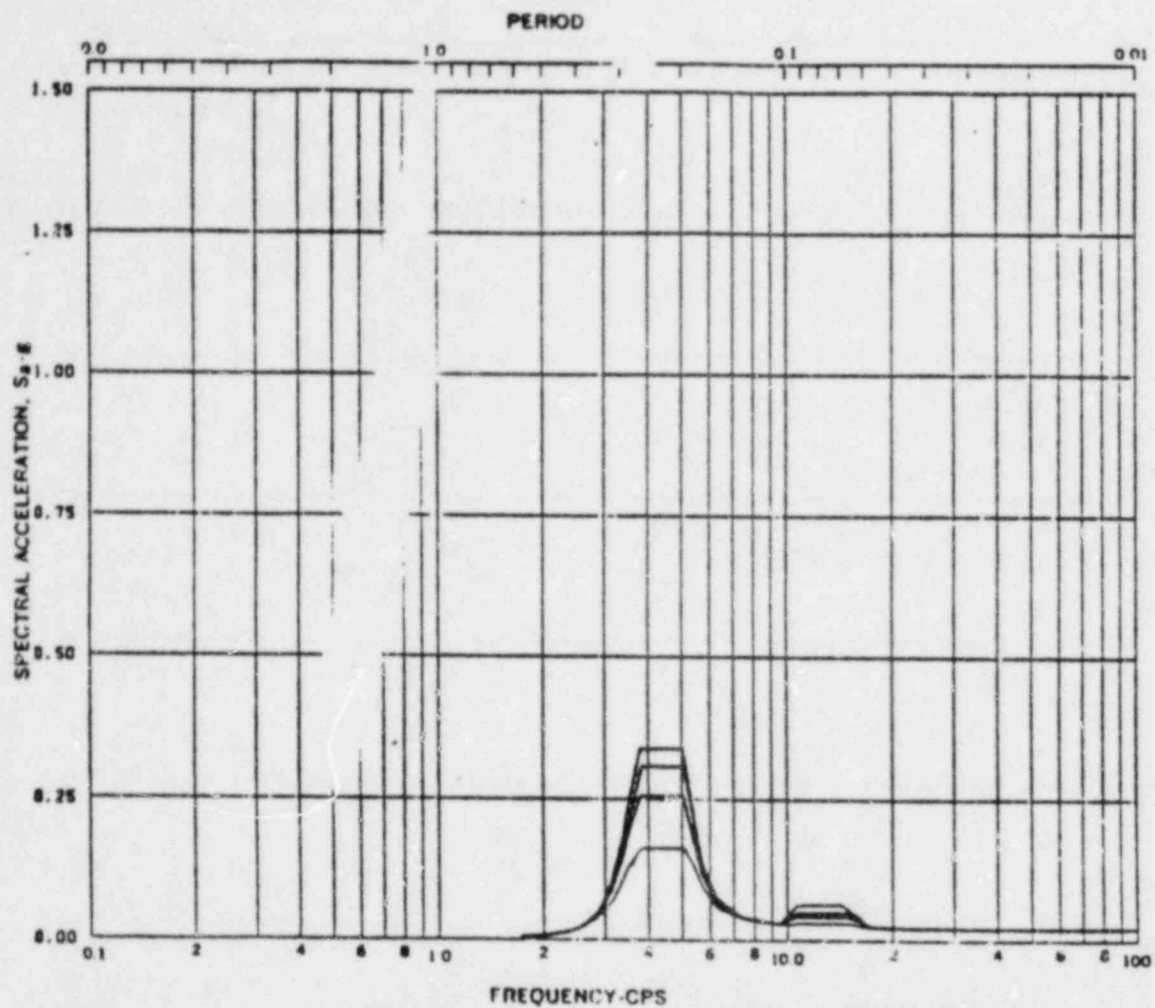


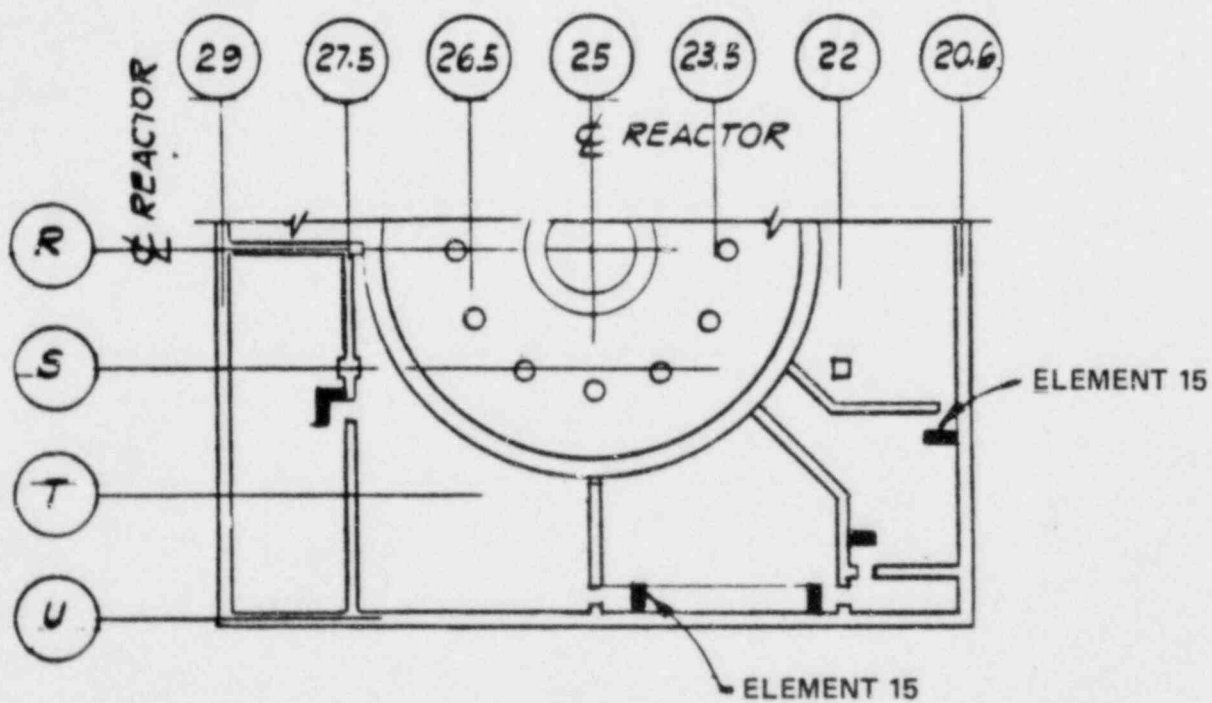
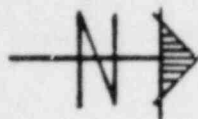
Fig. BN16-3 Acceleration Spectra for REACTOR & CONTROL BLDGS.
 Load Case: Seismicity SRV
 Mode —, Direction N-S, Elev 870'-0"
 Damping: 0.005, 0.01, 0.02, 0.05

REV. 6, 4/82

BUSQUEHANNA STEAM ELECTRIC STATION
 UNITS 1 AND 2
 DESIGN ASSESSMENT REPORT

REACTOR/CONTROL BUILDING
 RESPONSE SPECTRA

KWU-SRV
 FIGURE C-103

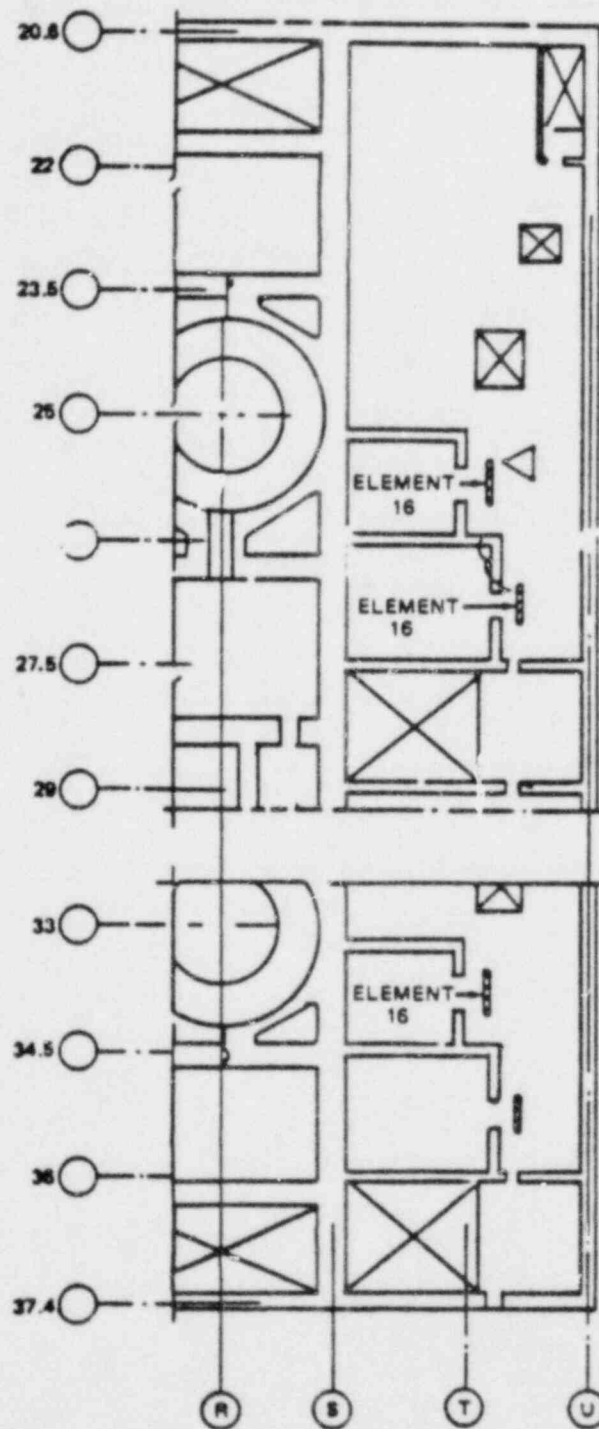


REV. 6, 4/82

SUSQUEHANNA STEAM ELECTRIC STATION
UNITS 1 AND 2
DESIGN ASSESSMENT REPORT

REACTOR BUILDING BLOCKWALL
EL. 645'-0"

FIGURE E-9

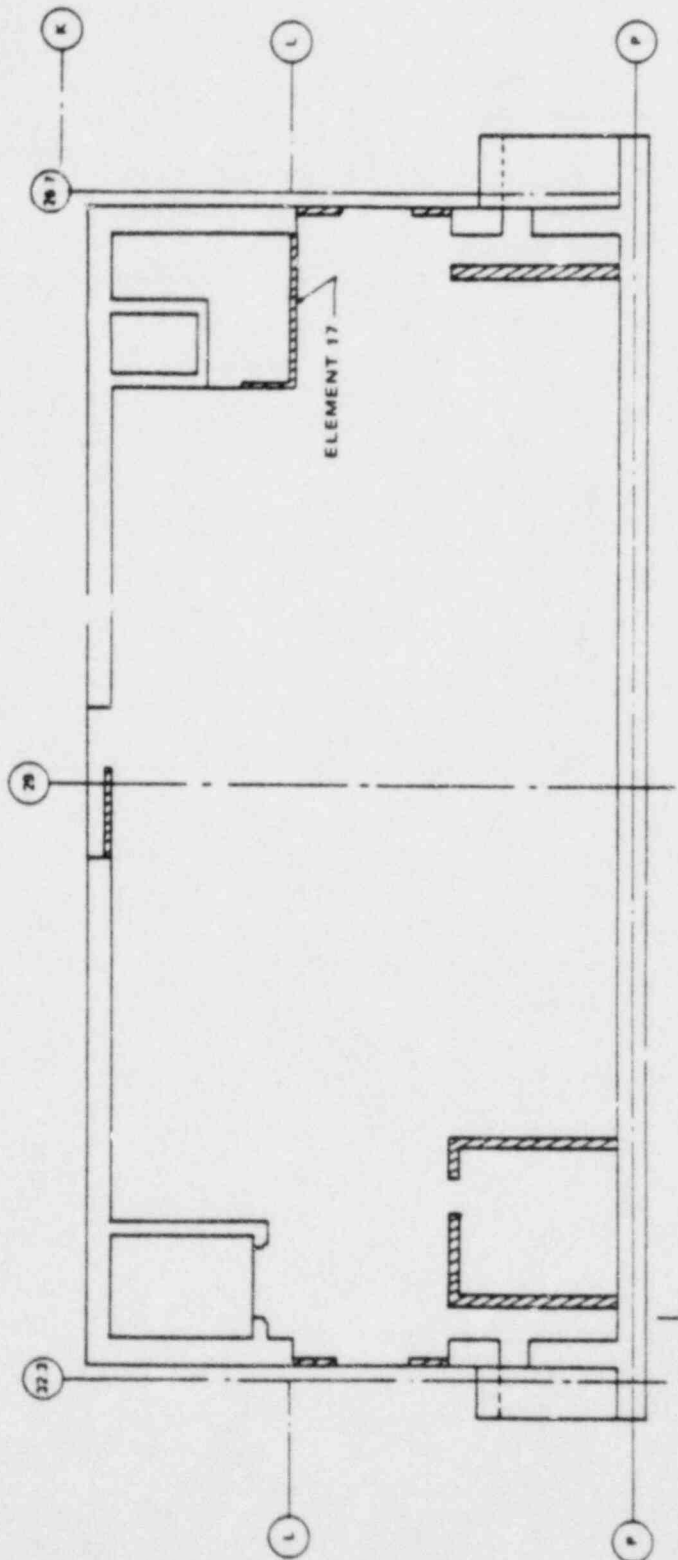


REV. 6, 4/82

SUSQUEHANNA STEAM ELECTRIC STATION
UNITS 1 AND 2
DESIGN ASSESSMENT REPORT

REACTOR BUILDING BLOCKWALLS
EL. 799'-1"

FIGURE E-11

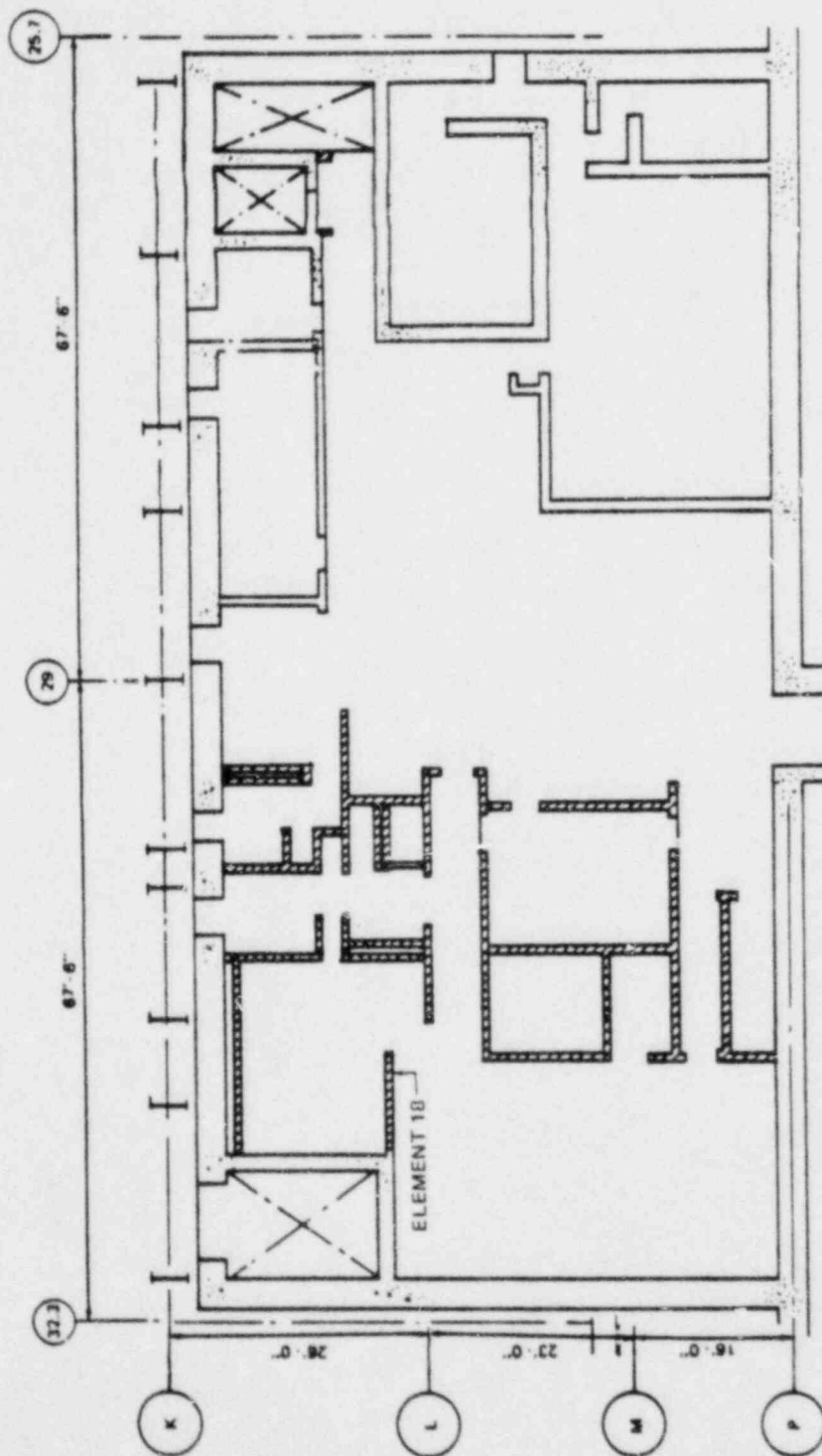


REV. 6, 4/82

SUSQUEHANNA STEAM ELECTRIC STATION
UNITS 1 AND 2
DESIGN ASSESSMENT REPORT

CONTROL BUILDING BLOCKWALL
EL. 656'-0"

FIGURE E-12

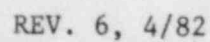


REV. 6, 4/82

SUSQUEHANNA STEAM ELECTRIC STATION
UNITS 1 AND 2
DESIGN ASSESSMENT REPORT

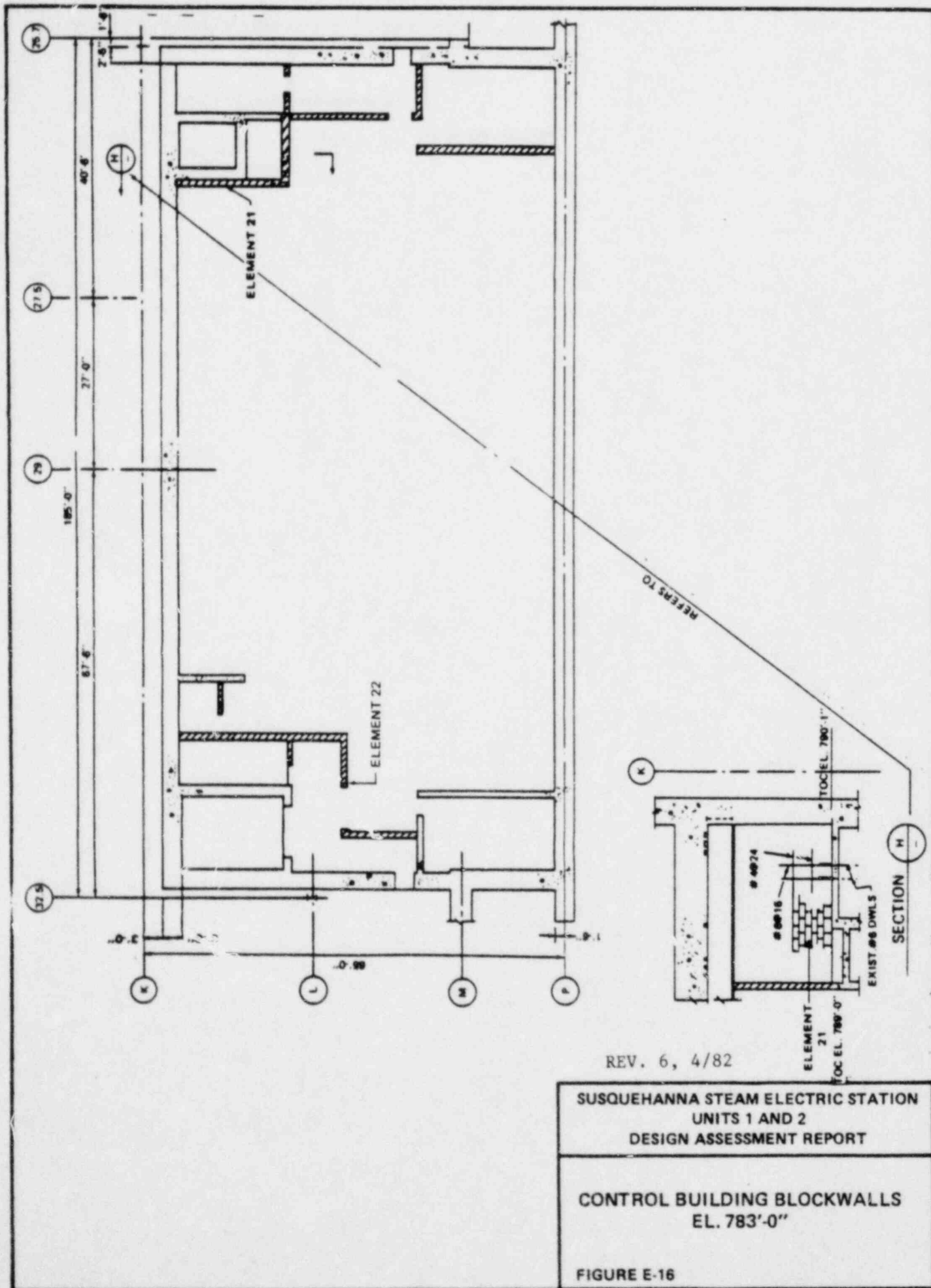
CONTROL BUILDING BLOCKWALLS
EL. 676'-0"

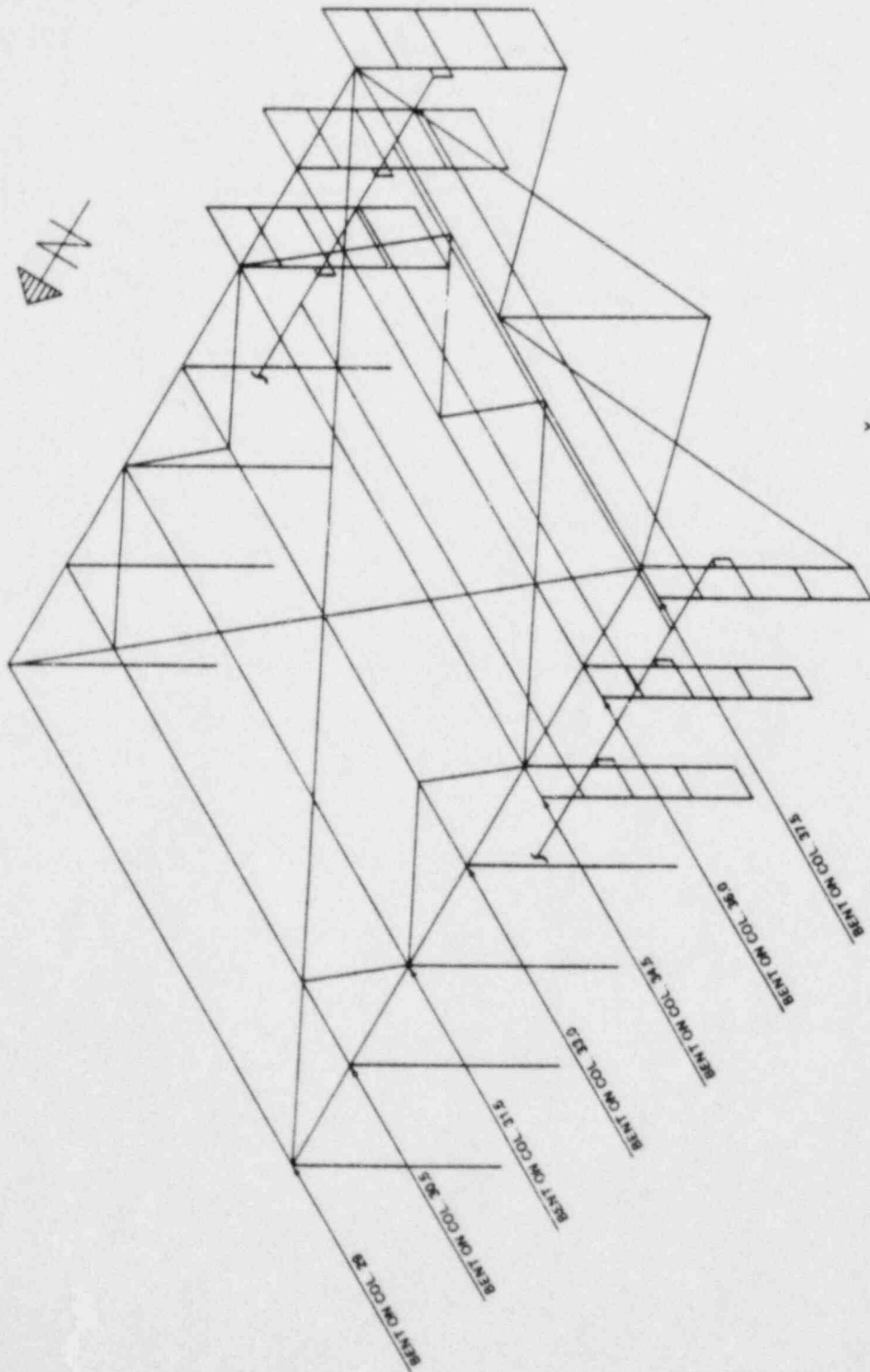
FIGURE E-13



CONTROL BUILDING BLOCKWALLS
EL. 741'-1"

FIGURE E-14



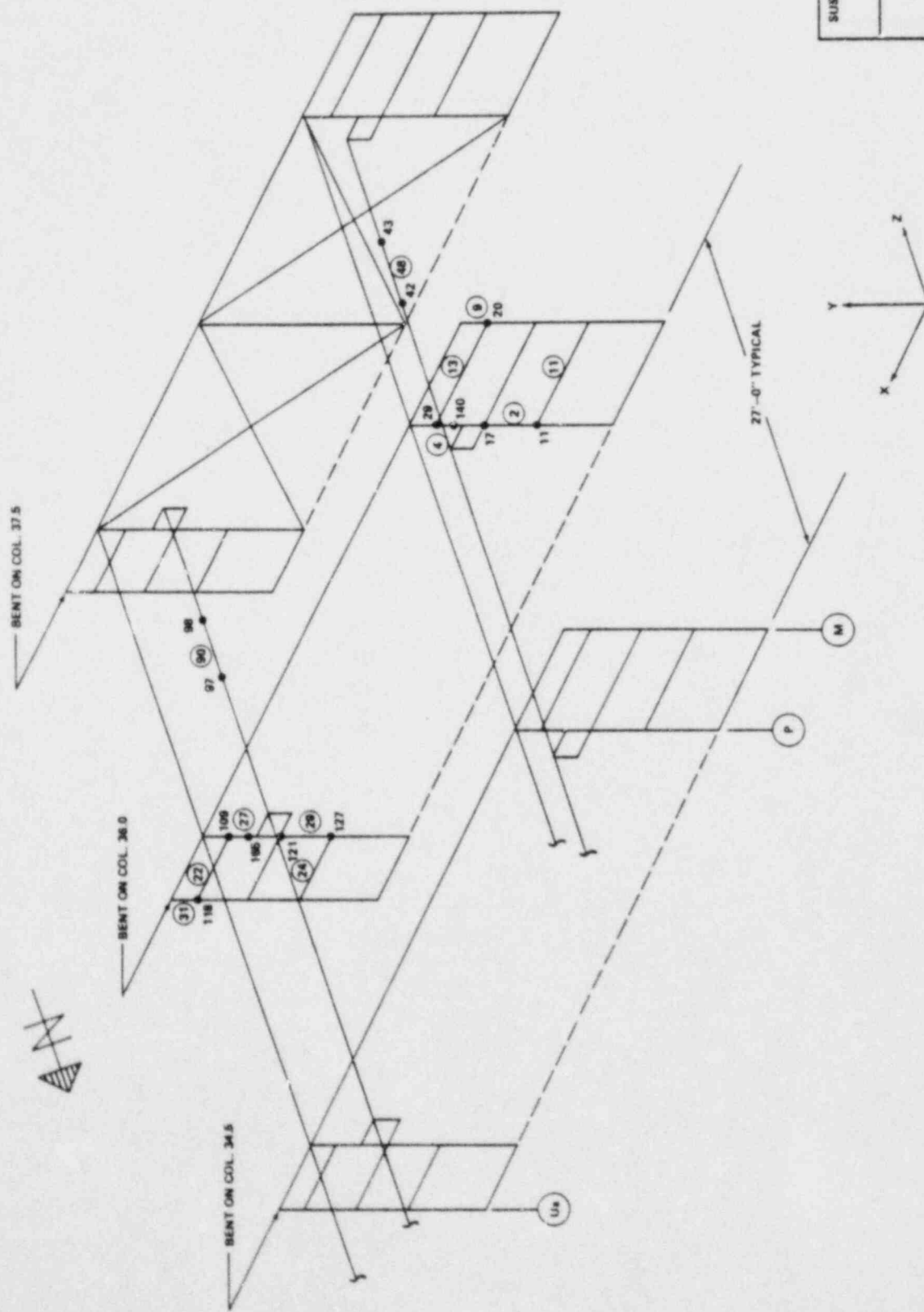


REV. 6, 4/82

SUSQUEHANNA STEAM ELECTRIC STATION
UNITS 1 AND 2
DESIGN ASSESSMENT REPORT

REACTOR BUILDING CRANE
SUPPORTS STRUCTURE

FIGURE E-21

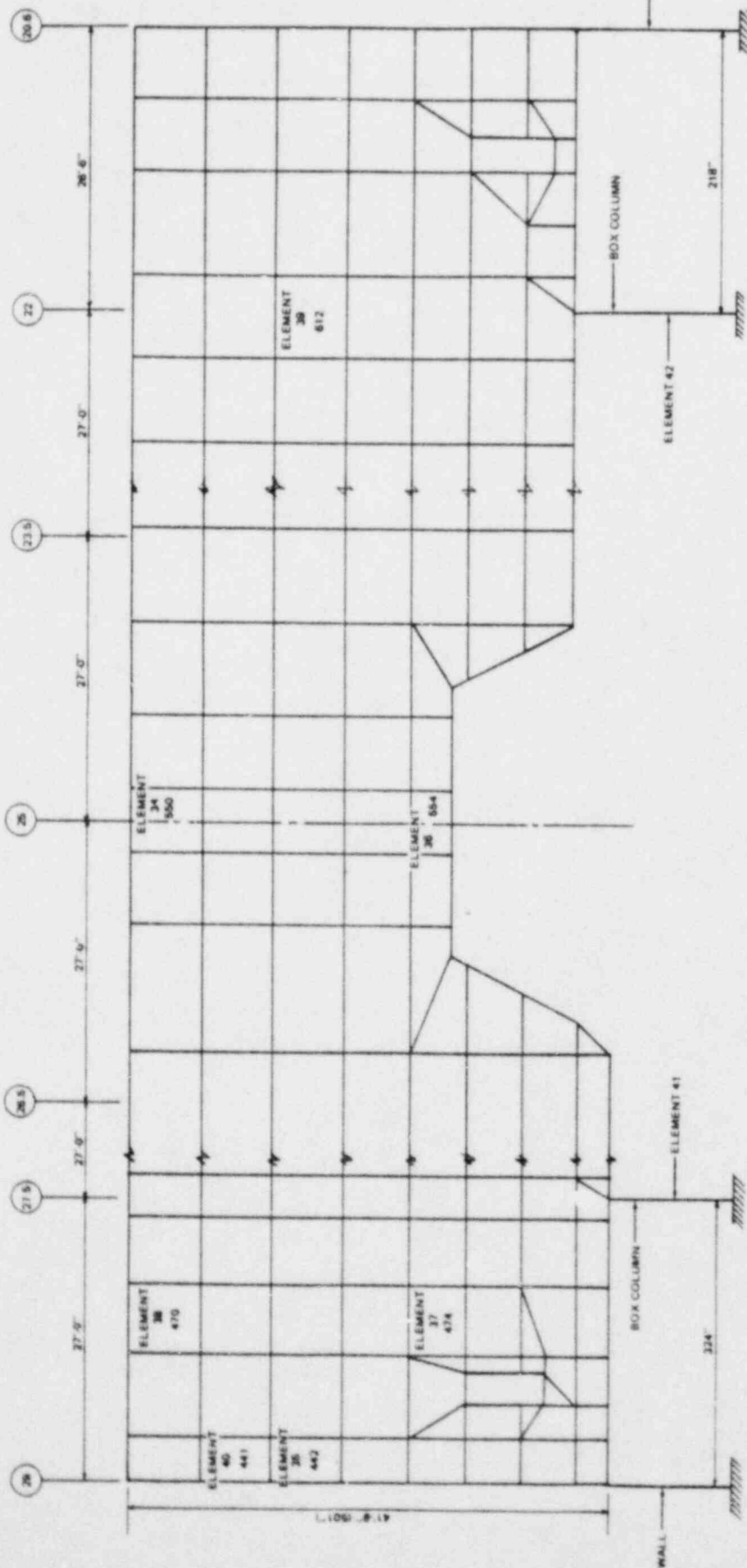


REV. 6, 4/82

SUSQUEHANNA STEAM ELECTRIC STATION
UNITS 1 AND 2
DESIGN ASSESSMENT REPORT

REACTOR BUILDING CRANE
SUPPORT STRUCTURE

FIGURE E-21 b

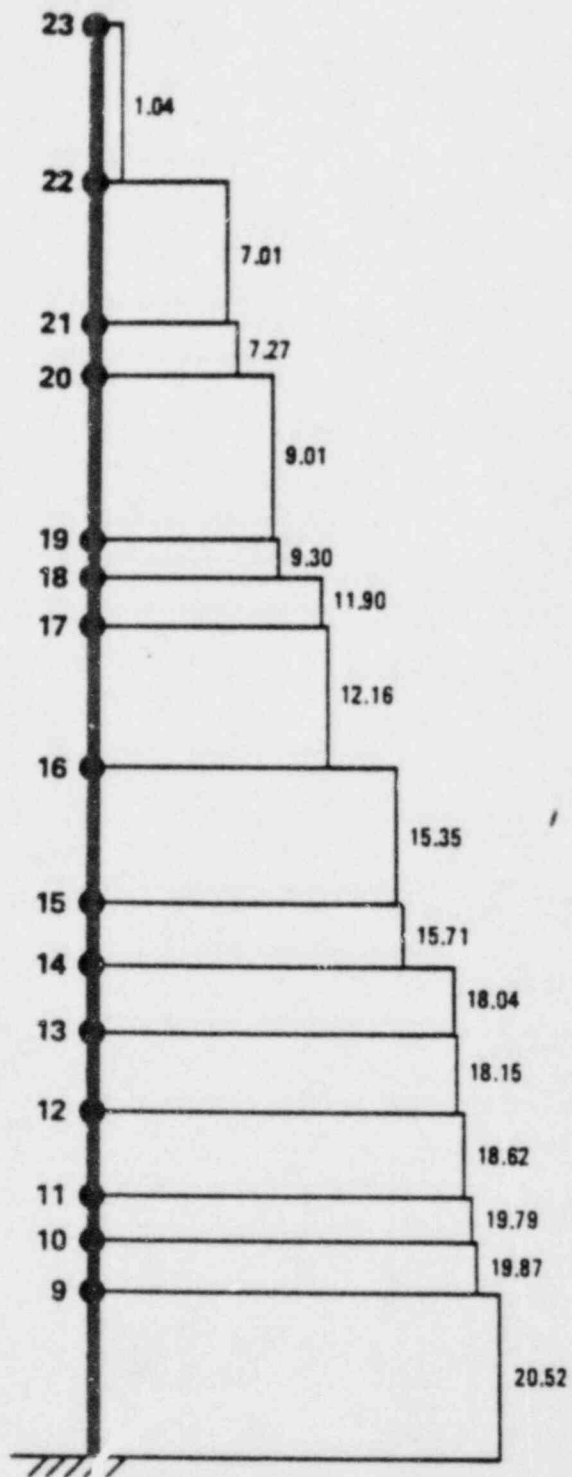
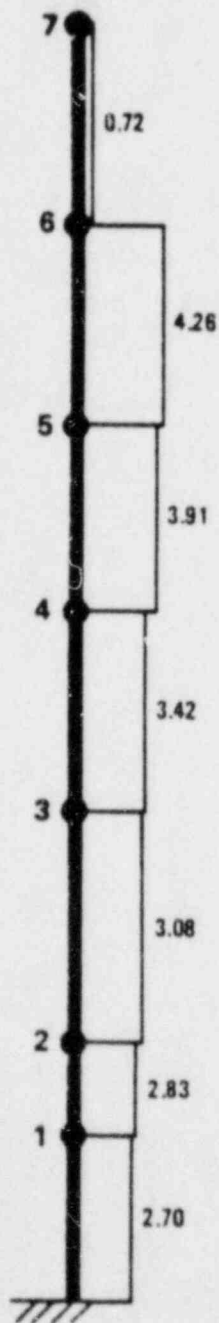


REV. 6, 4/82

SUSQUEHANNA STEAM ELECTRIC STATION
UNITS 1 AND 2
DESIGN ASSESSMENT REPORT

REACTOR BUILDING REFUELING
POOL GIRDER (WEST)

FIGURE E-22

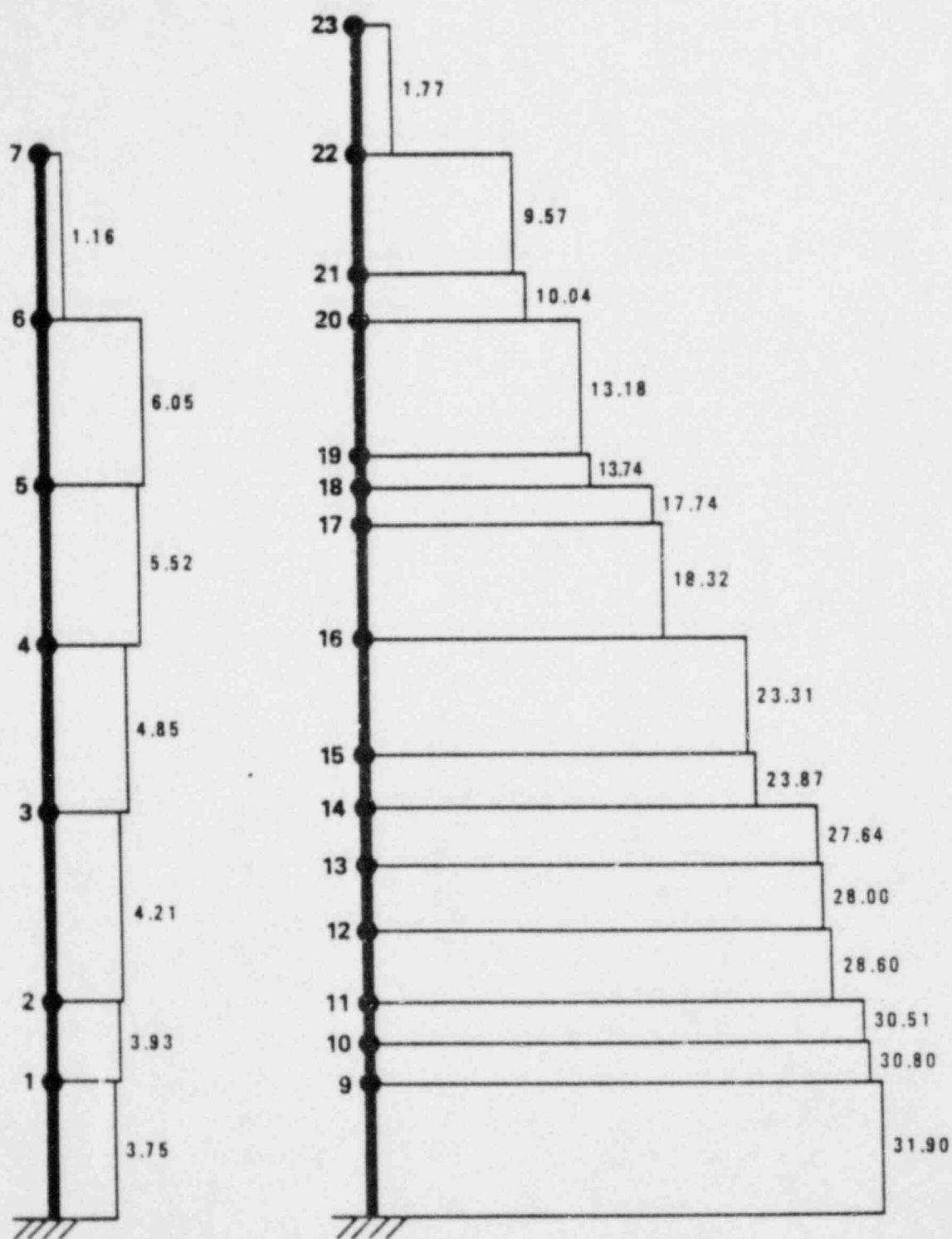


REV. 6, 4/82

SUSQUEHANNA STEAM ELECTRIC STATION
UNITS 1 AND 2
DESIGN ASSESSMENT REPORT

REACTOR BUILDING
VERTICAL AXIAL FORCES (X 10³ KIPS)
OBE + SRV (2% DAMPING)

FIGURE E-23

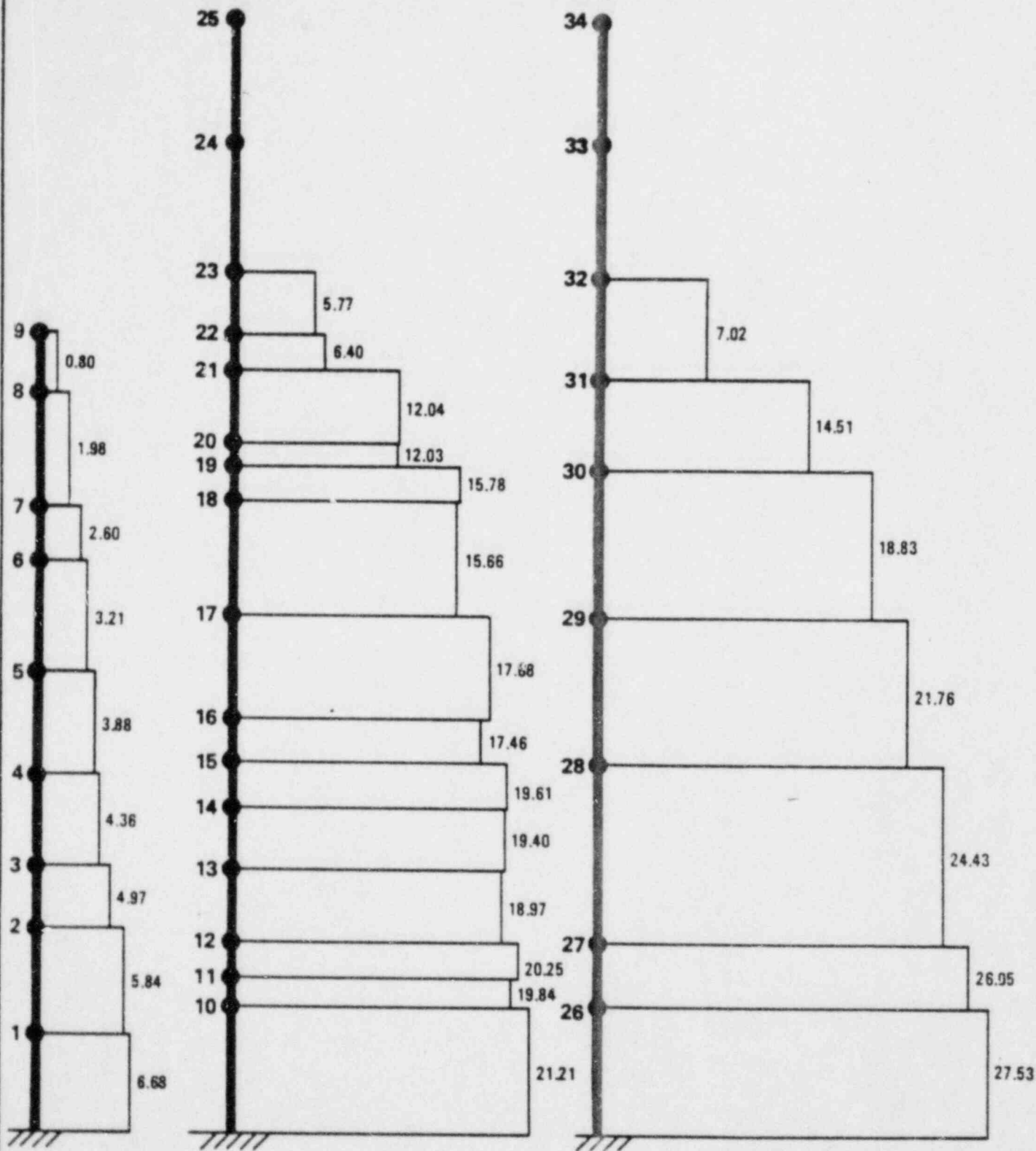


REV. 6, 4/82

SUSQUEHANNA STEAM ELECTRIC STATION
UNITS 1 AND 2
DESIGN ASSESSMENT REPORT

REACTOR BUILDING
VERTICAL AXIAL FORCES ($\times 10^3$ KIPS)
SSE + SRV + LOCA (5% DAMPING)

FIGURE E-24

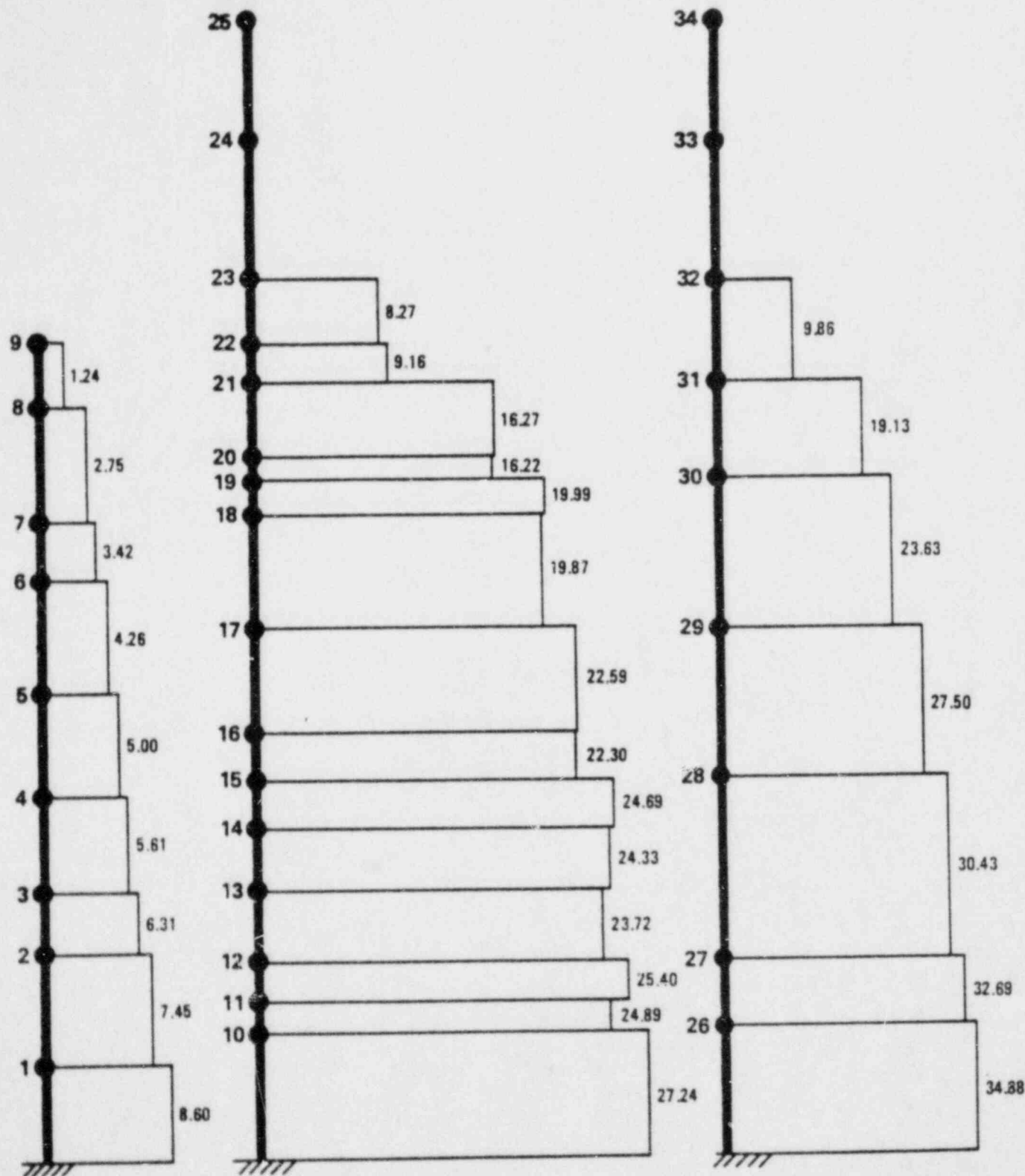


REV. 6, 4/82

SUSQUEHANNA STEAM ELECTRIC STATION
UNITS 1 AND 2
DESIGN ASSESSMENT REPORT

REACTOR BUILDING
N-S SHEAR FORCES (X10³ KIPS)
OBE + SRV (2% DAMPING)

FIGURE E-25

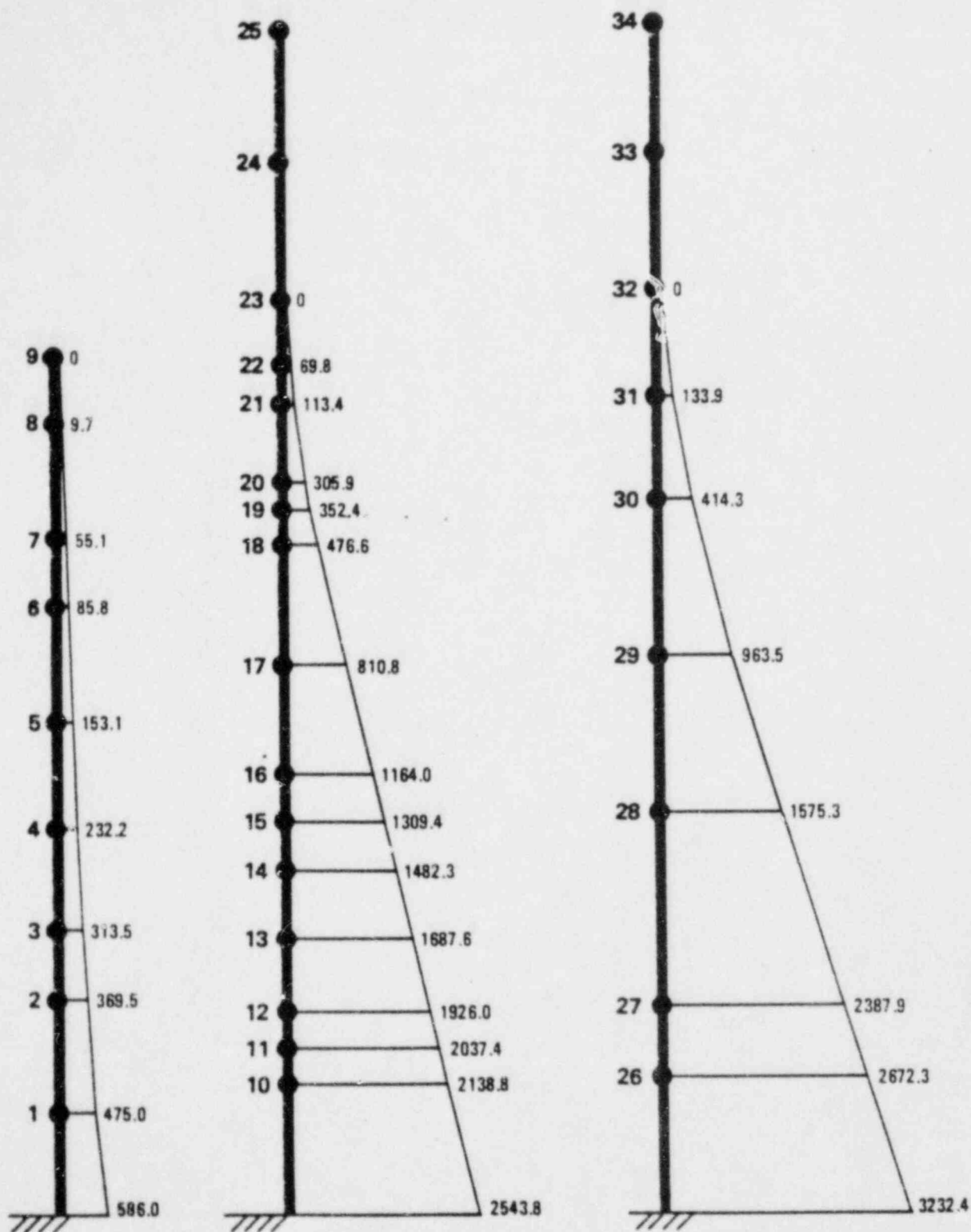


REV. 6, 4/82

SUSQUEHANNA STEAM ELECTRIC STATION
UNITS 1 AND 2
DESIGN ASSESSMENT REPORT

REACTOR BUILDING
N-S SHEAR FORCES (X10³ KIPS)
SSE + SRV + LOCA (5% DAMPING)

FIGURE E-26

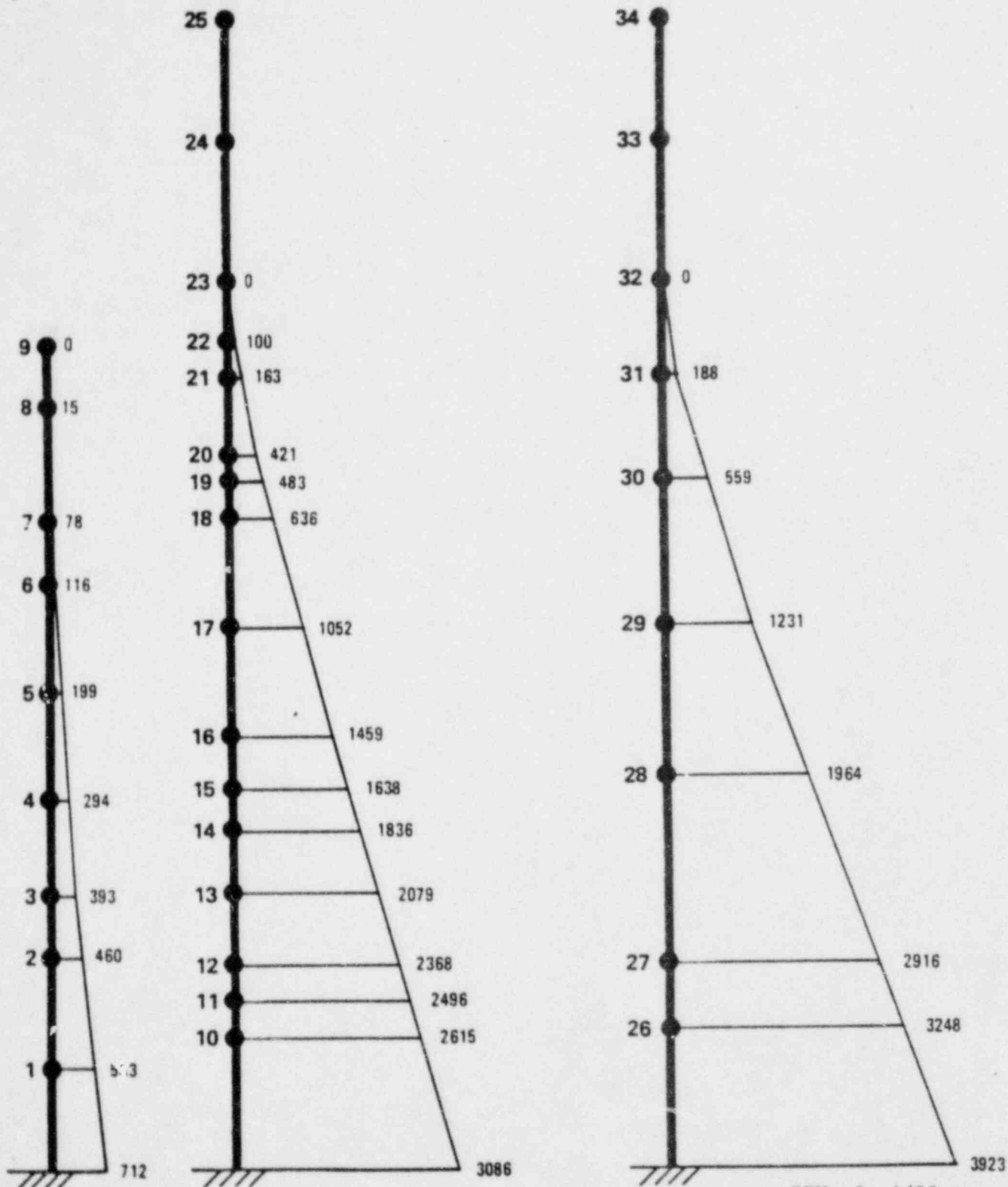


REV. 6, 4/82

SUSQUEHANNA STEAM ELECTRIC STATION
UNITS 1 AND 2
DESIGN ASSESSMENT REPORT

REACTOR BUILDING
N-S MOMENTS (X10³ K-FT)
OBE + SRV (2% DAMPING)

FIGURE E-27



REV. 6, 4/82

SUSQUEHANNA STEAM ELECTRIC STATION
UNITS 1 AND 2
DESIGN ASSESSMENT REPORT

REACTOR BUILDING
N-S MOMENTS ($\times 10^3$ K-FT)
SSE + SRV + LOCA (5% DAMPING)

FIGURE E-28

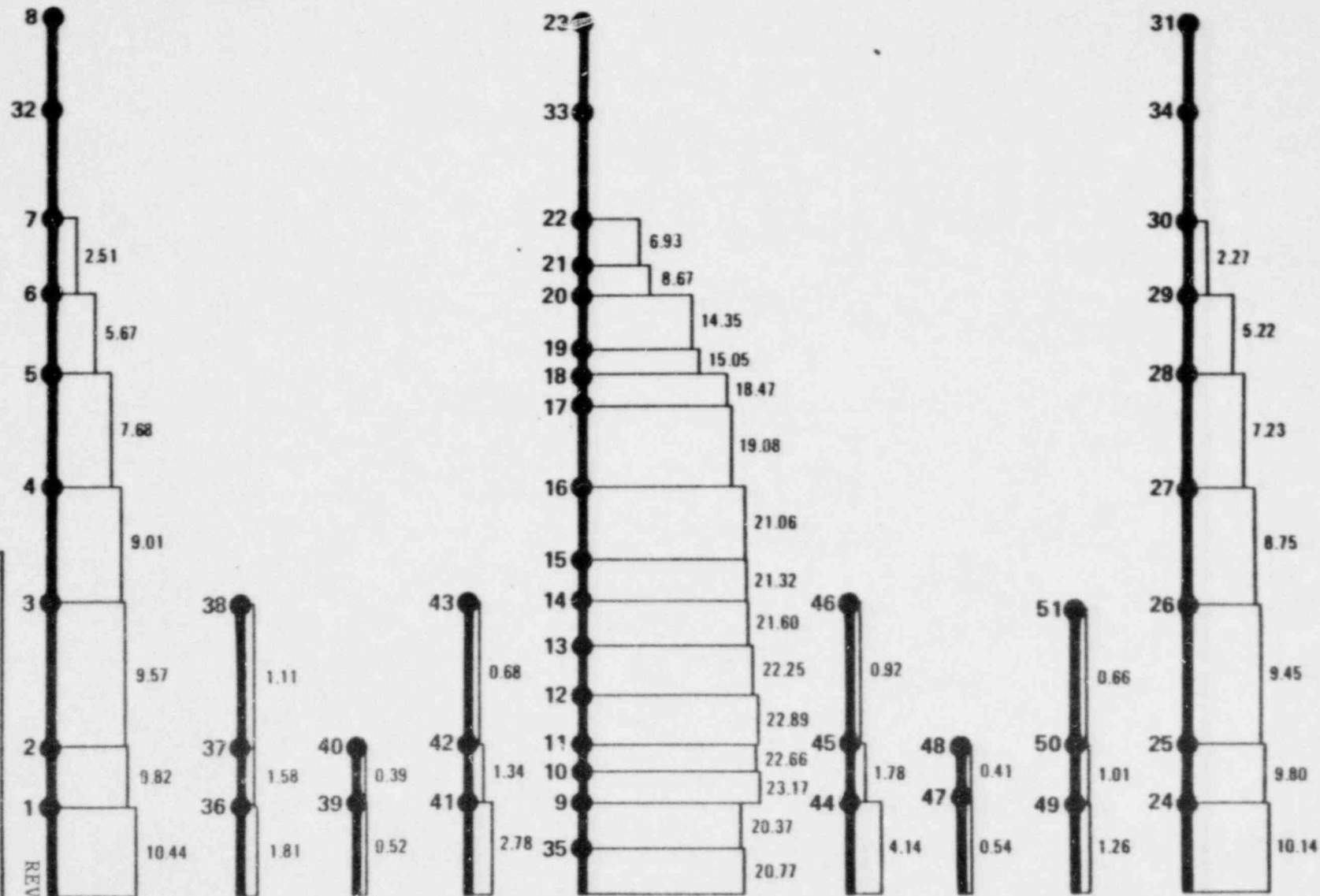
DESIGN ASSESSMENT REPORT

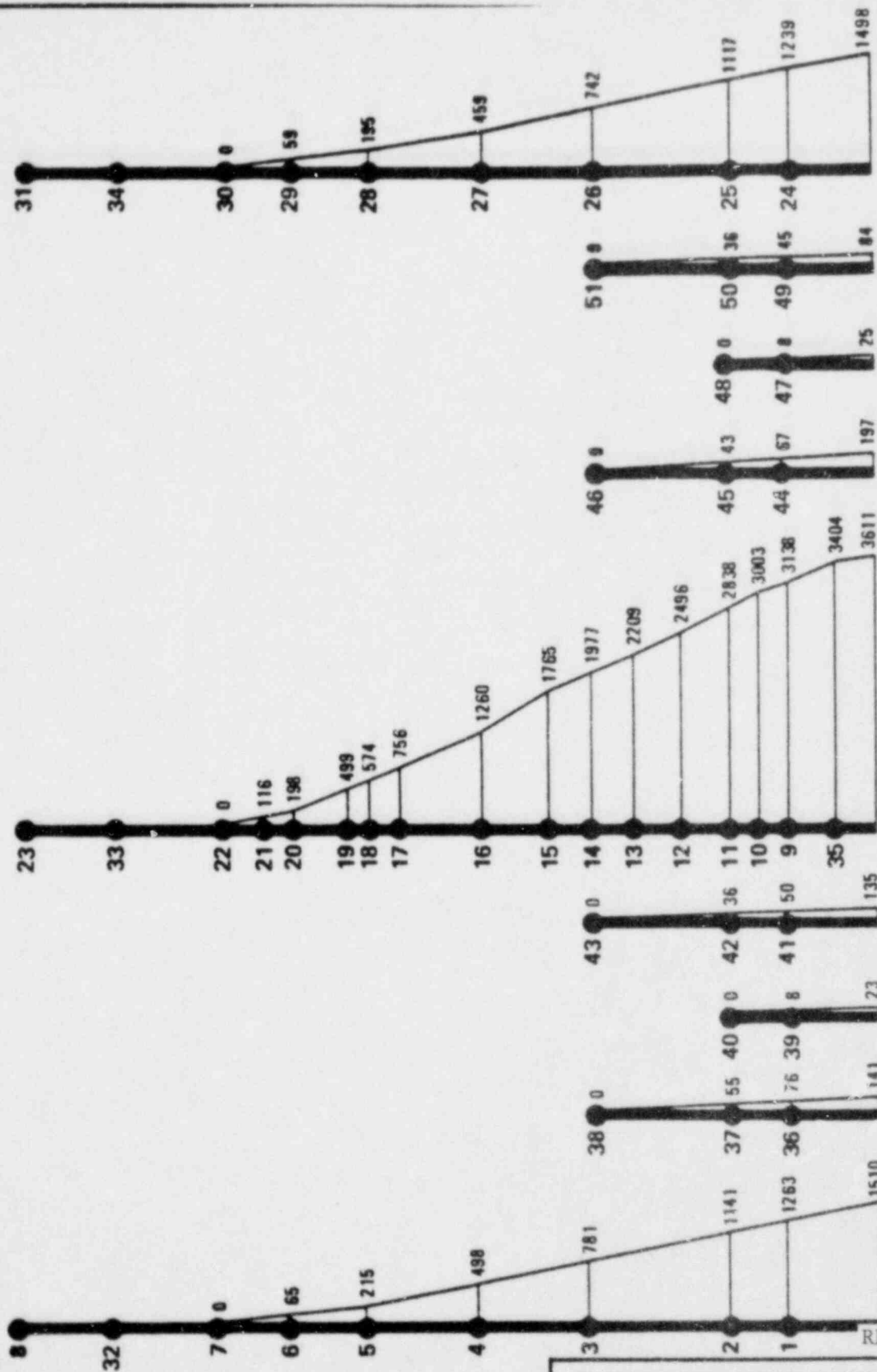
UNITS 1 AND 2

REV. 6, 4/82

REACTOR BUILDING
E-W SHEAR FORCES ($\times 10^3$ KIPS)
OBE + SRV (2% DAMPING)

FIGURE E-29



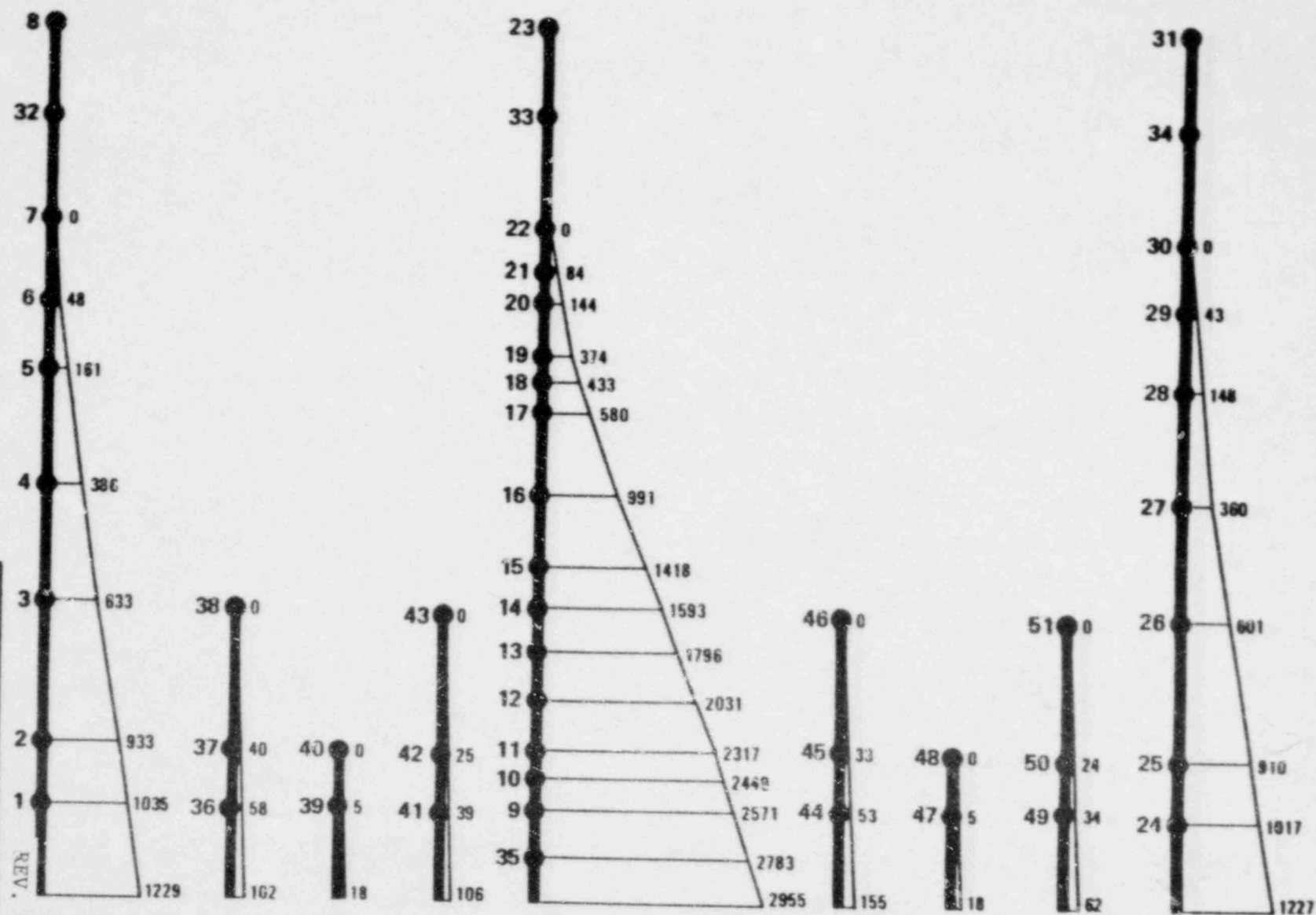


REV. 6, 4/82

SUSQUEHANNA STEAM ELECTRIC STATION
UNITS 1 AND 2
DESIGN ASSESSMENT REPORT

REACTOR BUILDING
E-W MOMENTS (X10³ K-FT)
SSE + SRV + LOCA (5% DAMPING)

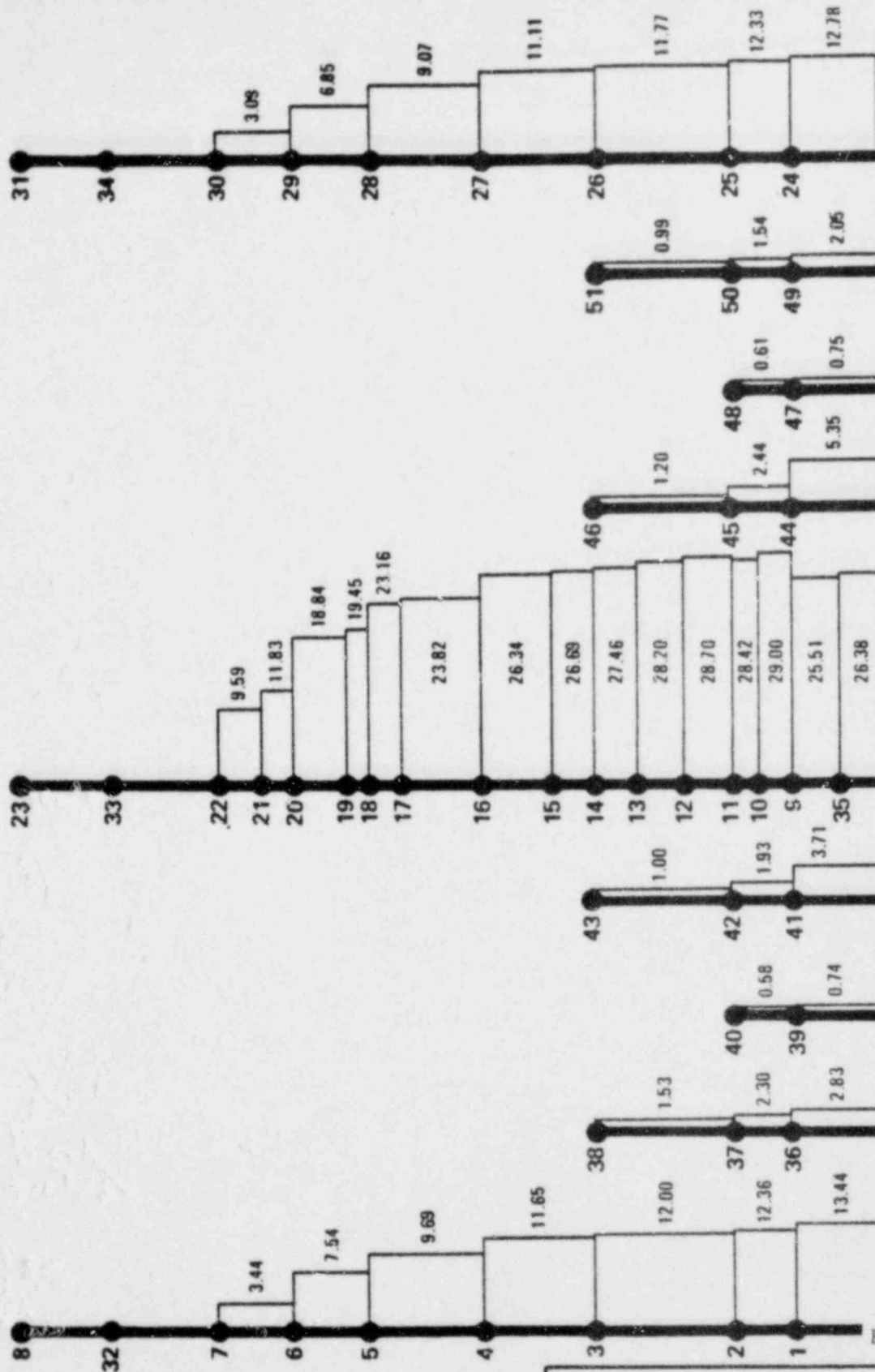
FIGURE E-30



SUSQUEHANNA STEAM ELECTRIC STATION
UNITS 1 AND 2
DESIGN ASSESSMENT REPORT

REACTOR BUILDING
E-W MOMENTS (X10³ K-FT)
OBE + SRV (2% DAMPING)

FIGURE E-31



REV. 6, 4/82

SUSQUEHANNA STEAM ELECTRIC STATION
UNITS 1 AND 2
DESIGN ASSESSMENT REPORT

REACTOR BUILDING
E-W SHEAR FORCES (X10³ KIPS)
SSE + SRV + LOCA (5% DAMPING)

FIGURE E-32

LOAD COMBINATION EQN 1 = 1.4 D + 1.7 L + 1.5 SRV

LOAD COMBINATION EQN 7a = 1.0 D + 1.0 L + 1.0 E_{ss} + 1.0 P_B
+ 1.0 SRV + 1.0 LOCA

SLAB

Section Number	Governing Equation	Elevation (ft)	Rebar Stress* (KSI)	Stress Margin (%)
1	1	645.0	49.79	7.8
2	1	645.0	49.45	8.4
3	1	683.0	1.25	97.7
4	1	719.1	2.43	95.5
5	1	749.1	4.55	91.6
6	1	779.1	3.94	92.7
7	1	818.1	5.52	89.8

* Allowable Reinforcing Steel Stress = 54 KSI

REV. 6, 4/82

SUSQUEHANNA STEAM ELECTRIC STATION
UNITS 1 AND 2
DESIGN ASSESSMENT REPORT

REACTOR AND CONTROL BUILDING
MARGINS
SLAB

FIGURE E-33

LOAD COMBINATION EQN 1 = 1.4 D + 1.7 L + 1.5 SRV

LOAD COMBINATION EQN 7a = 1.0 D + 1.0 L + 1.0 E_{ss} + 1.0 P_B
+ 1.0 SRV + 1.0 LOCA

SHEAR WALLS

Element Number	Governing Equation	Elevation (ft)	Rebar Stress* (KSI)	Stress Margin (%)
8	1	645.0	43.25	20
9	7a	719.1	30.70	43
10	7a	749.1	17.50	68
11	7a	749.1	30.60	43
12	1	645.0	39.91	26
13	7a	645.0	32.40	40

* Allowable Reinforcing Steel Stress = 54 KSI

REV. 6, 4/82

SUSQUEHANNA STEAM ELECTRIC STATION
UNITS 1 AND 2
DESIGN ASSESSMENT REPORT

REACTOR AND CONTROL BUILDING
MARGINS
SHEAR WALLS

FIGURE E-34

LOAD COMBINATION EQN 7a = 1.0 D + 1.0 L + 1.0 E_{SS} + 1.0 P_B + 1.0 SRV
+ 1.0 LOCA

BLOCKWALLS

Element No.	Elevation (ft)	Wall Thickness (in)	Rebar Stress* (Ksi)	Stress Margin (%)	Governing Equation	Concrete Compressive Stress** (Psi)	Stress Margin (%)	Governing Equation
15	645.0	24	14.12	65	7a	202	76	7a
16	799.1	8	24.01	40	7a	633	24	--
17	656.2	8	3.40	92	7a	176	91	7a
18	676.0	8	14.52	64	7a	335	60	7a
19	741.1	8	30.59	24	7a	650	22	--
20	806.0	8	3.89	90	7a	503	40	--
21	783.0	8	15.05	62	7a	522	37	--
22	783.0	8	19.82	50	7a	213	74	--

REV. 6, 4/82

* Allowable Reinforcing Steel Stress = 40 Ksi

** Allowable Compressive Stress For Masonry Concrete = 835 Psi

SUSQUEHANNA STEAM ELECTRIC STATION
UNITS 1 AND 2
DESIGN ASSESSMENT REPORT

REACTOR AND CONTROL BUILDING
MARGINS
BLOCKWALLS

FIGURE E-35

LOAD COMBINATION EQN 7 = D + L + E_{ss} + P_B + SRV + LOCA

STRUCTURAL STEEL

Element Number	Governing Equation	Elevation (ft)	Bending Stress*	Stress Margin (%)	Steel Grade
23	7	683.0	27.9	38	A-588
24	7	683.0	31.9	29	A-588
25	7	719.1	23.0	29	A-36
26	7	719.1	22.5	31	A-36
27	7	739.6	21.5	34	A-36
28	7	818.1	18.5	43	A-36

* Allowable Bending Stress in A-588 Steel = 45 KSI

* Allowable Bending Stress in A-36 Steel = 32.4 KSI

REV. 6, 4/82

SUSQUEHANNA STEAM ELECTRIC STATION
UNITS 1 AND 2
DESIGN ASSESSMENT REPORT

REACTOR AND CONTROL BUILDING
MARGINS
STRUCTURAL STEEL

FIGURE E-36

LOAD COMBINATION EQN 7 = D + L + E_{ss} + SRV + LOCA + P + R + (T_O + T_a)

CRANE SUPPORT STRUCTURE

Member*	Joint*	Governing Equation	Interaction Formula	Stress Margin (%)
4	140	7	1.00	0
22	109	7	1.00	0
90	97	7	1.00	0
27	165	7	0.92	8
13	29	7	1.00	0
13	20	7	0.90	10
11	11	7	0.89	11
2	17	7	0.88	12
27	109	7	0.85	15
31	118	7	0.88	12
48	42	7	1.00	0
29	121	7	0.85	15

* See Fig. E-21 for model.

REV. 6, 4/82

BUSQUEHANNA STEAM ELECTRIC STATION
UNITS 1 AND 2
DESIGN ASSESSMENT REPORT

REACTOR-AND CONTROL BUILDING
MARGINS
CRANE SUPPORT STRUCTURE

FIGURE E-37

LOAD COMBINATION EQN 7a = 1.0 D + 1.0 L + 1.0 E_{ss} + 1.0 P_B + 1.0 SRV
+ 1.0 LOCA

REFUELING POOL GIRDER

Governing Equation	Element Number	Rebar Stress* (KSI)	Stress Margin (%)
7a	550	50.9	5
7a	442	51.7	4
7a	554	12.8	76
7a	474	38.2	29
7a	470	43.9	13
7a	612	34.9	35
7a	441	51.7	4

* Allowable Reinforcing Steel Stress = 54 KSI

REV. 6, 4/82

BUSQUEHANNA STEAM ELECTRIC STATION
UNITS 1 AND 2
DESIGN ASSESSMENT REPORT

REACTOR AND CONTROL BUILDING
MARGINS
REFUELING POOL GIRDER

FIGURE E-38

Load Combination Eqn. 6 = 1.0D + 1.0L + 1.0 E_O + 1.0 P_B + 1.0SRV

SUPPORTING COLUMNS

Element Number	Governing Equation	Supporting Column At Node	Interaction Formula	Stress Margin (%)
41	6	399	0.72	38
42	6	517	0.49	51

Allowable Reinforcing Steel Stress = 54 KSI

REV. 6, 4/82

SUSQUEHANNA STEAM ELECTRIC STATION
UNITS 1 AND 2
DESIGN ASSESSMENT REPORT

REACTOR-AND CONTROL BUILDING
MARGINS
BOX SECTION COLUMNS

FIGURE E-38a

APPENDIX F

BOP AND NSSS PIPING DESIGN ASSESSMENT

All Seismic Category I balance of plant (BOP) and NSSS piping systems inside the containment and Reactor Building are analyzed for seismic and hydrodynamic loads per the load combinations given in Subsection 5.5 and 5.6.

Table J-1 summarizes the stresses and stress margins for selected BOP piping systems.

The stress reports for the evaluation of the BOP and NSSS piping are available for NRC review.

Table F-1 Summary of Piping Stresses

Piping System	I.C. / O.C.	Maximum Stress (psi)			Max. Stress Allowable Stress			Reference Stress Calc. with Rev. #
		Normal/ Upset	Emergency	Faulted	Normal/ Upset	Emergency	Faulted	
Reactor Water Clean Up	O.C.	8007	8016	8024	0.445	0.297	0.223	938 Rev. 2
	O.C.	7596	7606	7701	0.422	0.282	0.214	966-1 Rev. 3
	I.C.	2736	4801	4884	0.152	0.178	0.136	875 Rev. 2
Residual Heat Removal	I.C.	10501	16598	16600	0.479	0.504	0.378	840-11 Rev. 1
	O.C.	14735	15520	15520	0.819	0.575	0.431	843 Rev. 1
	O.C.	17652	18229	18229	0.981	0.675	0.506	846 Rev. 1
	I.C.	6839	21802	22251	0.380	0.807	0.618	868 Rev. 1
Core Spray	O.C.	7246	7260	7260	0.403	0.269	0.202	835-1 Rev. 2
	O.C.	5577	18107	18107	0.251	0.542	0.407	878-1 Rev. 1
	I.C.	2624	3481	3481	0.146	0.129	0.097	879-11 Rev. 1
	O.C.	9823	23367	23367	0.546	0.865	0.649	882 Rev. 1
Fuel Pool Cooling & Clean Up	O.C.	11624	13339	13339	0.646	0.494	0.371	842-3 Rev. 1
	O.C.	8584	9324	9324	0.457	0.331	0.248	997-2 Rev. 1
	O.C.	1337	1667	1567	0.074	0.062	0.046	997-3 Rev. 1

I.C. = Inside Containment

O.C. = Outside Containment

Design Margin = $1 - \frac{\text{Max. Stress}}{\text{Allowable Stress}}$

Table F-1 Summary of Piping Stresses (Con't.)

Piping System	I.C. O.C.	Maximum Stress (psi)			Max. Stress Allowable Stress			Reference Stress Calc. with Rev. #
		Normal/ Upset	Emergency	Faulted	Normal/ Upset	Emergency	Faulted	
Fuel Pool Cooling & Clean Up	O.C.	10578	10593	10593	0.563	0.376	0.282	1018-2 Rev. 1
High Pressure Coolant Injection	O.C.	13707	13885	13885	0.762	0.514	0.386	838-2 Rev. 1
	O.C.	7722	26002	26002	0.429	0.963	0.722	852-1 Rev. 1
	O.C.	9332	22220	22220	0.518	0.823	0.617	899 Rev. 1
	I.C.	4860	7147	7148	0.270	0.265	0.199	899-11 Rev. 1

APPENDIX G

NSSS DESIGN ASSESSMENT

This Appendix has been deleted.

6

APPENDIX H

EQUIPMENT DESIGN ASSESSMENT

This appendix has been deleted.

|6

APPENDIX I

SUPPRESSION POOL TEMPERATURE RESPONSE TO SRV DISCHARGE

TABLE OF CONTENTS

I.1	Introduction
I.2	Analyzed Scenarios
I.3	Assumptions
	I.3.1 General
	I.3.2 Available Equipment
	I.3.3 Operator Actions
I.4	Analysis Method
I.5	Analysis Results & Conclusions
I.6	Figures
I.7	Tables

I.2 Analyzed Scenarios

Three (3) different initiating events have been considered in the analysis with two (2) different single failures each, resulting in six (6) different analysis cases:

- Stuck Open Relief Valve (SORV) at Power (Initiating Event)

A safety relief valve is assumed to open spuriously when the reactor is operating at full power and to stick open throughout the transient.

A stuck open relief valve will be indicated by two (2) independent safety grade systems on the front row panels of the control room. First, the flow noise generated by the steam flowing through an open SRV will be picked up by an acoustic sensor and provide positive indication as to which SRV opened. Secondly, the suppression pool temperature monitoring system will indicate a temperature rise in the suppression pool and alarm the operator to initiate corrective action.

In accordance with the emergency procedure guidelines, the operator will manually scram the reactor by turning the mode switch to "shutdown" if the SRV cannot be reclosed immediately. For analysis purposes, it is conservatively assumed that scram does not occur until the technical specification limit on pool temperature for power operation (110°F) is reached.

Case 1.a Single Failure: One (1) RHR System Unavailable

Following scram the turbine control valves will gradually close, thus isolating the turbine from the reactor. The steam jet air ejectors will continue to maintain vacuum in the main condenser. The operator will then enhance the depressurization of the reactor vessel through the SORV by manually opening the turbine bypass valves to the main condenser. In the analysis, this is assumed not to occur until twenty (20) minutes after scram.

Case 1.b Single Failure: Spurious Main Steam Line Isolation at Scram

Main steam line isolation is assumed to occur simultaneously with manual scram following a SORV as described above. As a result of the isolation reactor pressure will rise causing additional SRVs to open and discharge steam into the suppression pool until the operator initiates manual depressurization.

- Isolation/Scram (Initiating Event)

5 The main steam line isolation valves are assumed to spuriously close, thus causing automatic reactor scram.

Case 2.a Single Failure: One (1) RHR System Unavailable
Following isolation SRVs will automatically open to maintain reactor pressure until the operator initiates manual depressurization.

Case 2.a.1 Single Failure: One (1) RHR System Unavailable and Shutdown Cooling Unavailable

As documented in Response 6 of Subsection 10.2.3, a complete Loss of Offsite Power (LOOP) coincident with a failure of the OG501C diesel generator will disable one loop of the RHR pool cooling mode and both loops of the shutdown cooling mode. This case used the same assumptions as Case 2.a, except for the following:

- 6
- One RHR is placed in pool cooling mode 10 minutes after high pool temperature alarm and stays in pool cooling mode
 - Shutdown cooling is not initiated
 - Complete Loss of Offsite Power (Loop)
 - No CRD flow
 - Due to feedwater pump coastdown, feedwater is available for only the first 60 seconds following scram.
 - Reactor coolant makeup is provided by the HPCI pump after 60 seconds with suction from the condensate storage tank until the pool temperature reaches 100°F and from the suppression pool thereafter.

Case 2.b Single Failure: Stuck Open Relief Valve (SORV)

The SORV is assumed to occur simultaneously with main steam line isolation.

5 - Small Break Accident (Initiating Event)

A small break in the primary reactor system is assumed to occur, thus causing automatic reactor scram. In addition a spurious main steam line isolation is assumed to occur simultaneously with scram.

Case 3.a Single Failure: One (1) RHR System Unavailable
Case 3.b Single Failure: Shutdown Cooling Unavailable

This single failure does not have an immediate impact on peak suppression pool temperature since the operator will not attempt to switch from RHR pool cooling to shutdown cooling before the peak is reached. The operator will ultimately reach cold shutdown by establishing the alternate shutdown cooling path as outlined in Subsection 15.2.9 of the SSES PSAR.

This page has been intentionally
left blank.

suppression pool cooling within ten (10) minutes following LPCI initiation.

NOTE: No LPCI discharge into the reactor will actually occur since the "low reactor pressure" setpoint is higher than the RHR pump shutoff head.

- fast switchover from RHR pool cooling to shutdown cooling

This applies to Cases 1.a, 2.a and 3.a only (1 RHR train available). As soon as the reactor pressure drops below the permissive pressure for RHR shutdown cooling, the operator is assumed to perform a fast switchover (without flush) from pool cooling to shutdown cooling. It is assumed that the RHR system is unavailable for the duration of the switchover (approximately sixteen (16) minutes).

NOTE: No switchover is assumed to be performed for cases 1.b, 2.b and 3.b (2 RHR trains available).

I.4 Analysis Method

The analysis uses the Stone & Webster computer code CONTORT which calculates both reactor pressure and suppression pool temperature.

The reactor coolant is represented by volumes of steam and liquid in thermal equilibrium. The total volume of the coolant (steam and liquid) in the reactor system is assumed constant. The reactor water level is maintained by feedwater and CRD flow throughout the transient. Heat is added to the reactor coolant from thermal mixing with feedwater/CRD flow, decay heat, fuel sensible heat, fission energy and the reactor vessel and internals metal mass. At the beginning of the transient, reactor vessel, internals and coolant are assumed to be in thermal equilibrium. With the depressurization of the reactor vessel the coolant temperature decreases. This establishes a heat flow from the reactor vessel and internals to the coolant.

Steam can flow from the reactor coolant steam volume to the main condenser or through SRVs into the suppression pool which is modeled as a homogeneously mixed water volume. For SBA steam is directly added to the suppression pool. SRV and SBA flows are calculated using the Moody frictionless flow model.

The computer model assumes that the reactor vessel, feedwater system and suppression pool are surrounded by adiabatic walls not allowing any enthalpy flow from these systems other than to the main condenser or the RHR service water. The model, as discussed, is schematically outlined in Figure I-1.

I.5 Analysis Results and Conclusions

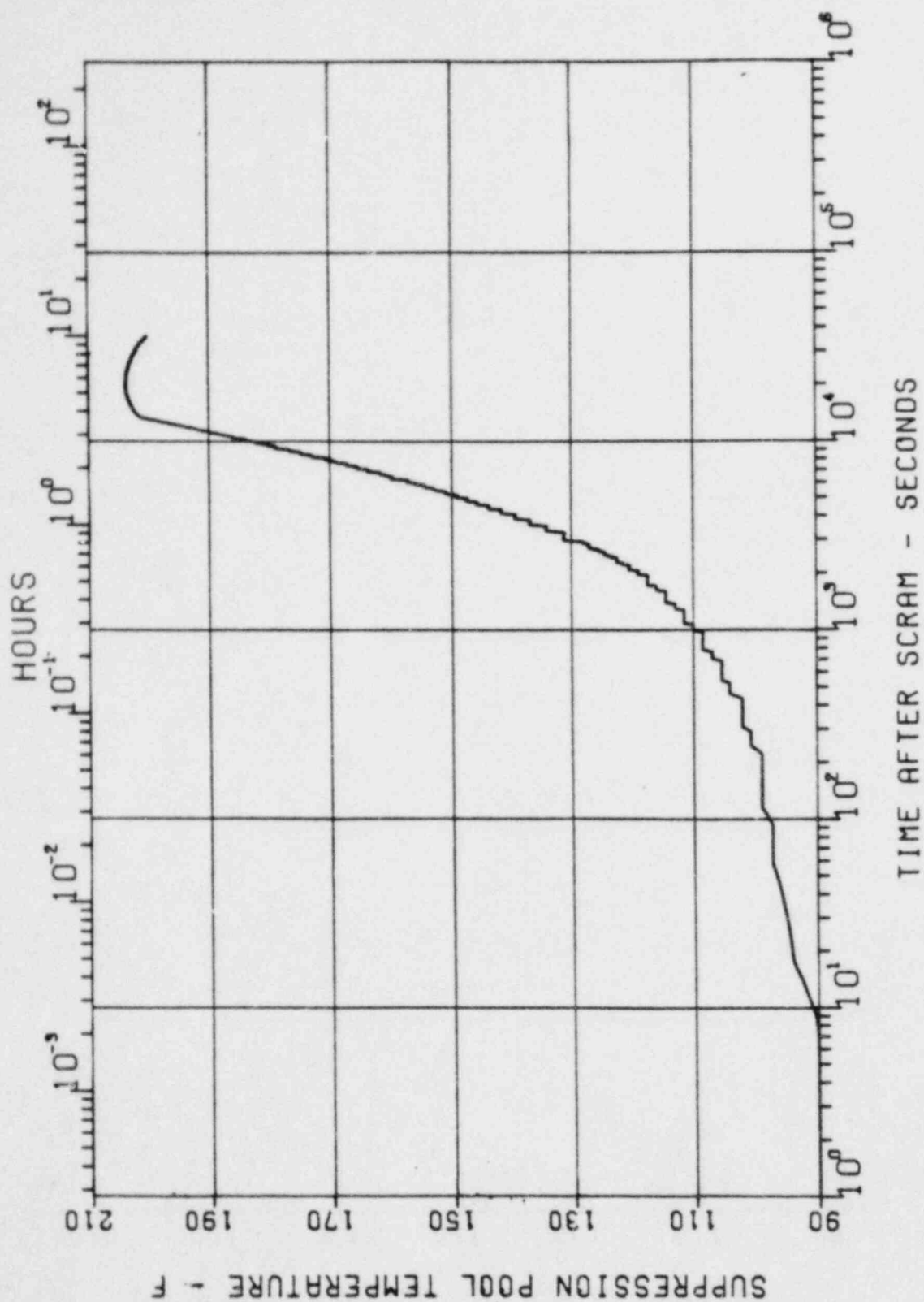
5 Table I-2 lists the peak suppression pool temperatures that were calculated using the CONTORT computer code for the scenarios described in Subsection I.2. These temperatures are "bulk" temperatures, i.e., they were calculated assuming a homogeneously mixed suppression pool. In reality pool mixing will not be perfect and differences will exist between the "local" temperature of the water in the immediate neighborhood of the quencher and the calculated "bulk" temperature. However, because of the special design features of quenchers and their orientation in the suppression pool (as discussed in Subsection 8.5.5) these differences are expected to be small and not exceed the value which was previously derived for ramhead discharge devices in Mark I plants (10°F). It is intended to verify this number using data from in-plant tests which are presently under preparation for the lead plants LaSalle and Zimmer.

6 Figures I-2 through I-15 show plots of the suppression pool
5 temperature and the respective reactor pressure vs. time. For Case 1.a and 1.b only the portion of the transient following manual scram (assumed at 110°F suppression pool temperature) is shown.

5 The sharp pressure fluctuations at full reactor pressure in
6 Figures I-7, I-11, I-13 and I-15 are due to the opening and reclosing of SRVs before the operator manually initiates depressurization.

5 Fluctuations in pool temperature and reactor pressure towards the end of the transient in Figures I-4, I-5, I-8 and I-9 (indicated by a slightly heavier line) are due to numerical instabilities and are insignificant for the analysis results.

Also insignificant is the step-like appearance of the depressurization portion in the reactor pressure vs. time plots which is a result of the model used for adding feedwater.



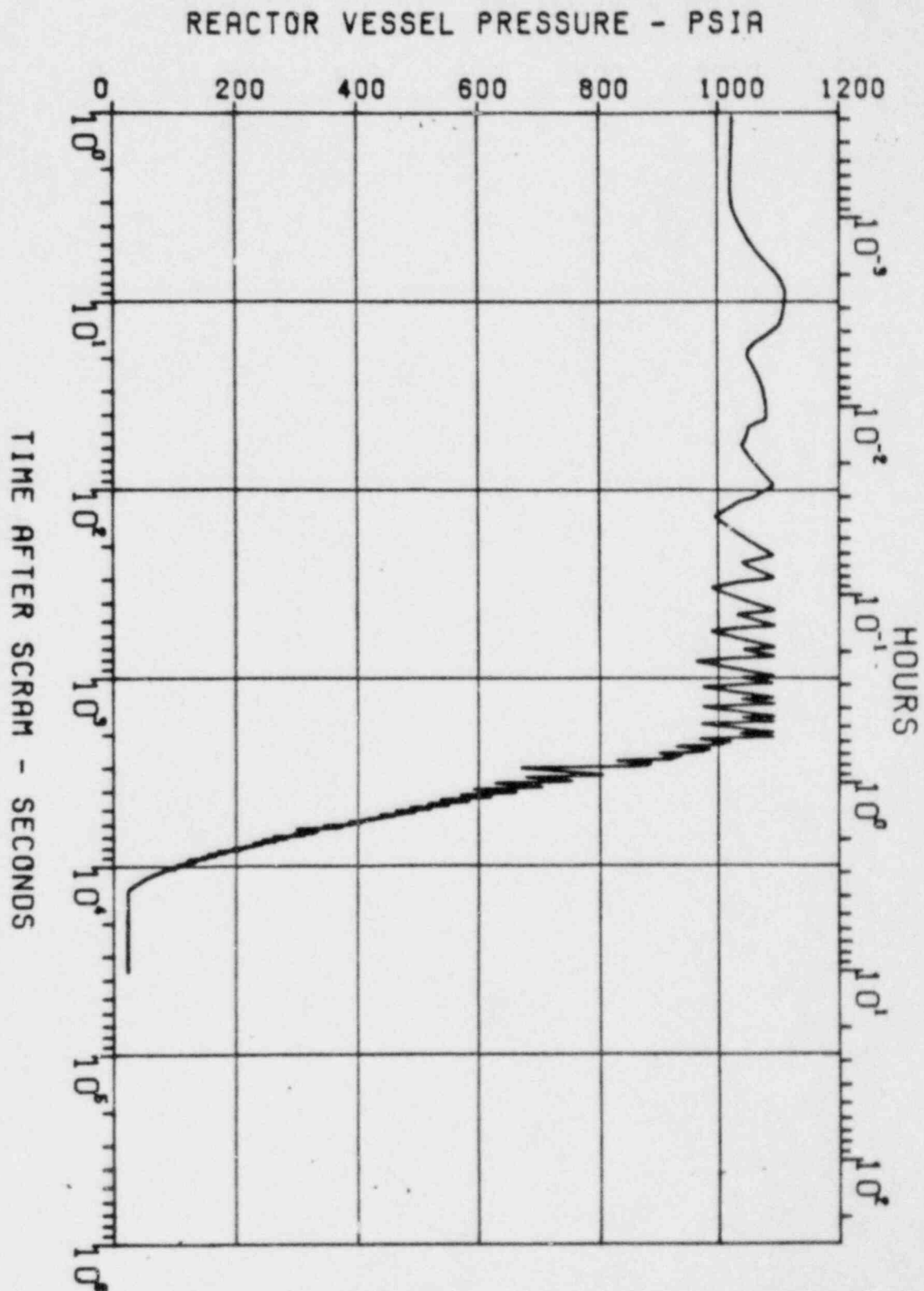
REV. 6, 4/82

SUSQUEHANNA STEAM ELECTRIC STATION
UNITS 1 AND 2
DESIGN ASSESSMENT REPORT

SUPPRESSION POOL TEMPERATURE
(ASE 2.A.1)

FIGURE I-14

REV. 6, 4/82



Closure Time (sec) (Scram at t=0; 0.5 sec instrument delay and 3 sec linear decrease of steam flow to zero; all valves assumed to close simultaneously)			
11. Turbine Control Valve Closure Time (sec) (for Case 1.a only, scram at t=0)	15.1		5
12. SRV Flow Rate (lbm/sec) (122.5% ASME rated, body flow)	298 at 1,215 psia		
13. Break Size (ft) (for Cases 3.a and 3.b only)	0.01		
14. CRD Flow Rate (lbm/sec)	16.3		
15. CRD Flow Enthalpy (btu/lbm)	68		6
16. Feedwater Flow Rate	as required to maintain RPV level		
17. Feedwater Mass/Enthalpy			
	Mass (lbm)	Enthalpy (btu/lbm)	
	169,000	347	
	292,400	261	
	360,400	175	
	10 E6	175	
18. SRV Setpoints (Relief Function)	See DAR Table 1-3		
19. Pressure Difference for SRV Reclosure (psi)	50		
20. RHR Pump Power Consumption (hp) (fully added to RHR system enthalpy)	2,000		5
21. Suppression Pool Water Mass (lbm) (at low suppression pool water level, w/o water mass inside pedestal)	7.19 x 10 ⁶		
22. Wetwell Airspace Pressure (psia)	15.45		
23. Suppression Pool Temperature Technical Specification Limits for:			
a. continuous operation without suppression pool cooling	90°F		
b. power operation	110°F		
c. hot standby	120°F		
24. RHR Service Water Temperature (°F)	95		

TABLE I-2

Peak Suppression Pool Temperatures

SORV at Power

Case 1.a	164°F
Case 1.b	184°F

5

Isolation/Scram

Case 2.a	192°F
Case 2.b	178°F
Case 2.a.1	204°F

6

SBA

Case 3.a	193°F
Case 3.b	182°F

5

To update your proprietary copy of the SSES DAR remove and insert the following pages, figures and tables.

REMOVE

INSERT

BOOK 2

Pages 9P-2a/2b
Pages 9P-15/15a
Pages 9P-71/72
Pages 9P-73/74
Pages 9P-77/78
....
....
....
....

New Pages 9P-2a/2b
New Pages 9P-15/15a
New Pages 9P-71/72
New Pages 9P-73/74
New Pages 9P-77/78
New Pages 9P-85/86
New Pages 9P-87/88
New Pages 9P-89/90
New Figure 9-270

PROPRIETARY INFORMATION

(T-QUENCHER)

Pages 4P-15/16
....
....
....
Table 4-14
Table 4-15
....
....
....
....

New Pages 4P-15/16
New Pages 4P-17 to 4P-20
New Figure 4-65
New Figure 4-66
New Table 4-14
New Table 4-15
New Table 4-15.1
New Table 4-15.2
New Table 4-15.3
New Appendix J Tab,
Pages J-1 to J-12,
Figures J-1 to J-82,
and Table J-1 after
existing Appendix D

This page has been intentionally left blank

9P-2a

Rev. 5, 3/81

	9.6.1.1	Containment Acceleration Response Spectra Comparison
	9.6.1.1.1	LOCA(DPFR) vs. LOCA(KWU) Acceleration Response Spectra Comparison
	9.6.1.1.2	SSE + SRV(ADS) + LOCA(DPFR) vs. SSE + SRV(ADS) + LOCA(KWU) Acceleration Response Spectra comparison
	9.6.1.2	Evaluation of the Containment Response Spectra Comparison
	9.6.1.2.1	Load Reduction Assessment
	9.6.1.2.1.1	Reduction of Load Amplitude Factor
	9.6.1.2.1.2	Re-Selection of Pressure Time Histories
	9.6.1.2.1.3	Adoption of Mark II Owner's Group Load Methodology
	9.6.1.2.1.4	Development of a New Chugging Load Methodology
5	9.6.1.2.2	Plant Reassessment
	9.6.1.3	Summary
	9.6.2	Verification of the Mark II Single Vent Dynamic Lateral Load Specification
	9.6.2.1	Theoretical Determination of the Bracing Force at GKM II-M
	9.6.2.1.1	Finite Element Model
	9.6.2.1.2	Model Assumptions
	9.6.2.1.3	Fluid Representation
	9.6.2.1.4	Structural Model
	9.6.2.1.5	Loading
	9.6.2.1.6	Analysis Results
	9.6.2.2	Bracing Force Data at GKM II-M
	9.6.2.2.1	Measurement of the Bracing Forces
	9.6.2.2.2	Resultant Bracing Forces
	9.6.2.3	Comparison of the Theoretical and Measured Maximum Resultant Bracing Force
	9.6.3	Statistical Evaluation of the GKM II-M Resultant Bracing Force Data
	9.6.3.1	Introduction
6	9.6.3.2	Derivation of a Probability Density Function from the measured Resultant Bracing Forces from the 1/6 MSL Tests
	9.6.3.2.1	General Considerations
	9.6.3.2.2	Application to the 1/6 MSL Tests
	9.6.3.3	Determination of the Extrapolated Mark II Impulse

- 9-206 Comparison of PTH No. 14 (P 6.8) and the Pressure
Output From IWECS
- 9-207 Comparison of the PSD of PTH No. 14 (P 6.8) and the PSD
of the Pressure Output From IWECS
- 9-208 IWECS/MARS Coordinate System
- 9-209 Comparison of Horizontal Acceleration Response Spectra
thru Due to LOCA(DPFR) vs. LOCA(KWU)
9-218
- 9-219 Comparison of Vertical Acceleration Response Spectra
thru Due to LOCA(DPFR) vs. LOCA(KWU)
9-227
- 9-228 Comparison of Horizontal Acceleration Response Spectra
thru for the combination SSE + SRV + LOCA(DPFR) vs.
9-237 SSE + SRV + LOCA(KWU)
- 9-238 Comparison of Vertical Acceleration Response Spectra
thru for the Combination SSE + SRV + LOCA(DPFR) vs.
9-246 SSE + SRV + LOCA(KWU)
- 9-247 Schematic View of Finite Element Model
- 9-248 Schematic View of Structural Model
- 9-249 Schematic View of Fluid Elements
- 9-250 Amplitudes of the Resultant Force at the Bracing
- Frequency Range: 0.5...200Hz - Test No. 3 & 4
- 9-251 Amplitudes of the Resultant Force at the Bracing
- Frequency Range: 0.5...200Hz - Test No. 5 & 6
- 9-252 Amplitudes of the Resultant Force at the Bracing
- Frequency Range: 0.5...200Hz - Test No. 7 & 8
- 9-253 Amplitudes of the Resultant Force at the Bracing
- Frequency Range: 0.5...200 HZ - Test No. 9 & 10
- 9-254 Amplitudes of the Resultant Force at the Bracing
- Frequency Range: 0.5...200Hz - Test No. 11 & 12
- 9-255 Amplitudes of the Resultant Force at the Bracing
- Frequency Range: 0.5...200Hz - Test No. 13 & 14
- 9-256 Amplitudes of the Resultant Force at the Bracing
- Frequency Range: 0.5...200Hz - Test No. 15 & 16

PROPRIETARY

- 9-257 Amplitudes of the Resultant Force at the Bracing
- Frequency Range: 0.5...200Hz - Test No. 17 & 18
- 9-258 Amplitudes of the Resultant Force at the Bracing
- Frequency Range: 0.5...200Hz - Test No. 19 & 20
- 9-259 Frequency Distribution of the Resultant Bracing Forces
- Test No. 3..10
- 9-260 Frequency Distribution of the Resultant Bracing Forces
- Test No. 11 & 12
- 9-261 Frequency Distribution of the Resultant Bracing Forces
- Test No. 13...18
- 9-262a&b CO Pressure Traces From Various Test Break Sizes
- 5 9-263 Dependence of Largest Mean CO Amplitude
on Steam Mass Flux
- 9-264 Comparison of the Envelope of the PSD's of PTH No. 14
with the Mean of the PSD Envelope of Test No. 1 & 2
- 9-265 PSD's of PTH No. 14 with the time expansion and contraction
factors
- 9-266 Comparison of Chug Strengths Observed in the JAERI
- 9-267 JAERI Geometry- Actual and the One Used in the Acoustic Mode
- 9-268 Comparison of the SSES Chugging Load Definition with
the JAERI Test 0002 Data at 1800 mm Elevation
- 9-269¹ Comparison of the SSES Chugging Load Definition with
the JAERI Test 0002 Data at 3600 mm Elevation
- 6 9-270 Comparison of the Theoretical Frequency Distribution
of the Resultant Bracing Forces with the Test Data -
Test Nos. 13-18

geometry and the geometry used in the acoustic model is shown in Figure 9-267. The acoustic model of the JAERI facility closely follows the acoustic model developed in the Task A.16 Generic Mark II Acoustic Methodology (see Reference 65). Briefly, the inhomogeneous wave equation is solved for the annular 20° wedge by means of the Green's function method.

A JAERI acoustic run involves applying the selected source at each of the 7 vents one at a time. The pressure histories due to the sources applied at each individual vents at each of the sensor locations are then computed. A set of start times of a particular time trial is selected from a 50msec uniform probability desynchronization window. Having obtained the start times for individual vents, the pressure time history at each sensor location is then synthesized with the appropriate start times. As described in the next subsection, a total of 160 time trials were run for each of the four chug sources which constitute the chugging load definition.

9.5.3.5.1.2.4 Comparison Basis

As described in Subsection 9.5.3.5.1.2.1, the comparison is made with eight chugs from JAERI Tests 0002. To make the comparison on a statistically meaningful basis, a simulation was made in the same manner as that used for obtaining the envelope of the actual eight JAERI chugs. That is, eight time trials or "chugs" were run in the JAERI acoustic model and a PSD* envelope of the eight trials was constructed. To make the envelope of the computed pressure time histories insensitive to the random statistics of the eight time trials selected, this procedure was repeated 20 times (i.e., $8 \times 20 = 160$ time trials). This results in 20 PSD envelopes (one PSD envelope for a set of eight time trials). These PSD envelopes were then averaged to obtain an average PSD envelope for a particular source. Such an average envelope was then constructed for each of the four sources.

For the four sources, the average envelopes for each source were enveloped and this envelope is then compared against the envelope of the eight chugs in the JAERI tests. In addition, the symmetric amplitude factor (see Subsection 9.5.3.2) was not applied to the wall loads calculated by the SSES load definition for comparison with JAERI. Thus, the comparison represents mean value chugs at GKM II-M.

However, the PSD's generated by the SSES chugging load definition reflect the use of the time expansion and contraction factors (see Figures 9-157 to 9-170).

The comparison basis described above is identical to that used by the Mark II Generic Program.

9.5.3.5.1.3 Results and Discussion

* The PSD's generated by the SSES sources were normalized to account for their difference in time duration when compared to the time duration of the JAERI chugs.

The results of the comparison are shown in Figures 9-268 and 9-269 at the two elevations in JAERI. As described earlier in Subsection 9.5.3.5.2.4, the envelope for the sources excludes the source for the CO period in the GKM II tests as well as the symmetric amplitude factor.

Figures 9-268 and 9-269 show the comparisons at the 1800mm and the 3600mm elevations, respectively. From these figures it is seen that the SSES load definition bounds the JAERI data by a substantial margin over the entire range from 0-100 Hz.

In conclusion, a comparison between our chugging load definition and the eight large chugs observed in JAERI Test 0002 has been presented. The comparison has been made on a basis which is statistically meaningful and shows that the current SSES chugging load definition developed from GKM II-M is very conservative.

5 9.5.3.5.2 Verification of the 50 msec Time Window

Verification of the 50 msec desynchronization time window will be documented in the Generic Mark II Load Definition Report scheduled for submittal in April of 1981.

9.6 VERIFICATION OF THE DESIGN SPECIFICATION

This section provides information verifying the conservatism of the DFFR steam condensation load definition (see Subsection 4.2.2) and the MK II single vent lateral load definition (see Reference 47).

9.6.1 Evaluation of the DFFR CO and Chugging Load Specification

6 Currently, all SSES plant design assessment for LOCA steam condensation loads employ the DFFR CO and chugging load specification developed from the original 4T test program (see Appendix A of Reference 21 and Reference 16).

5 However, the NRC in NUREG 0487 expressed concern about the conservatism of the DFFR specification because of the non-prototypical vent length used in the 4T test facility. As a result, PP&L initiated the GKM II-M test program to resolve the NRC's concerns. Subsection 9.4 documents the results of the GKM II-M tests and Subsection 9.5 presents the SSES LOCA load definition resulting from the GKM II-M data base.

In this subsection, a comparison of the DFFR LOCA load and the SSES LOCA load definition is provided. This evaluation is accomplished by comparing the DFFR containment acceleration response spectra (ARS) curves with the containment ARS curves generated by the SSES specification. This comparison study is made for LOCA (DFFR) vs. LOCA (KWU), as well as the combination

LOCA (DPFR) + SSE + SRV vs. LOCA(KWU) + SSE + SRV. Subsection 9.6.1.1 presents the results of the two comparison cases. Subsection 9.6.1.2 provides an evaluation the ARS comparison. Finally, Subsection 9.6.1.3 summarizes the LOCA loads comparison.

9.6.1.1 Containment Acceleration Response Spectra Comparison

9.6.1.1.1 LOCA(DPFR) vs. LOCA(KWU) Acceleration Response Spectra Comparison

Figures 9-209 through 9-218 compare the containment horizontal ARS curves due to the DPFR LOCA load definition (LOCA(DPFR)) with the containment horizontal ARS curves generated by the SSES LOCA load definition (LOCA(KWU)) for 2% spectral damping. Figures 9-219 through 9-227 compare the vertical LOCA(DPFR) ARS curves with the vertical LOCA(KWU) ARS curves for 2% spectral damping.

The LOCA(DPFR) curves represent enveloping spectra and were generated as follows:

- o The DPFR LOCA load consisting of chugging and CO (see Appendix A of Reference 21 and Reference 16), each of which contain three (3) frequencies, were inputed to the 3-D ANSYS structural model (see Figure B-1) to calculate ARS curves at the required node points. Both an asymmetric and symmetric load case were considered for chugging, while only a symmetric load case was considered for CO.
- o These individual LOCA(DPFR) ARS curves were then enveloped into one (1) ARS curve at each nodal point. This was done for both horizontal and vertical responses.
- o The ARS curves for nodal points at approximately the same elevation were then further enveloped to give one (1) ARS curve for each required elevation. Table 9-14 gives the nodal points enveloped at each elevation for the LOCA(DPFR) spectra and 3-D ANSYS model. Additionally, the peak frequencies of the spectra were broadened by 15% to account for any uncertainties in the modeling techniques and material properties.

Similarly, the LOCA(KWU) curves represent enveloping spectra and were obtained as follows:

- o The SSES LOCA load definition was used to calculate fifteen (15) sets of symmetric wall loads and twelve (12) sets of asymmetric wall loads (see Subsections 9.5.3.4.1 and 9.5.3.4.2, respectively) for input to the ANSYS model. The ANSYS model then generated ARS curves at the required nodes for each set of pressure time histories.

- o These individual LOCA(KWU) ARS curves were then enveloped into one (1) ARS curve at each nodal point. This was done for both horizontal and vertical responses.
- o The ARS curves for nodal points at approximately the same elevation were then enveloped to form a representative curve for each elevation. Table 9-14 gives the nodal points enveloped at each elevation for the LOCA(KWU) curves and 3-D ANSYS model. The LOCA(KWU) curves were then broadened by 15% at the peak frequencies.

9.6.1.1.2 SSE + SRV(ADS) + LOCA(DFFR) vs. SSE + SRV(ADS) + LOCA(KWU) Acceleration Response Spectra Comparison

Figure 9-228 through 9-237 compare the containment horizontal ARS curves for the combination SSE + SRV(ADS) + LOCA(DFFR) with the containment horizontal ARS curves for the combination SSE + SRV(ADS) + LOCA(KWU) for 2% spectral damping. Figures 9-238 through 9-246 compare the vertical containment ARS curves for the same combination with 2% spectral damping. These combination curves were obtained by combining the individual spectra by the absolute sum method (SSE + SRV + LOCA).

The LOCA(DFFR) and LOCA(KWU) spectra combined with the remaining spectra were generated as described in Subsection 9.6.1.1.1.

The SRV ARS curves combined with the other spectra were obtained as follows:

- o The three original KWU traces (see Subsection 4.1.3.5) were contracted and expanded in time to give five different traces between 55% and 110% of the frequency of the original trace. This gives fifteen sets of pressure time histories for input to the 3-D ANSYS model.
- o The ADS load case is considered for combination with LOCA and SSE. However, the azimuth distribution on the containment boundary as discussed in Subsection 4.1.3 indicates that the all valve case governs the ADS case for symmetric loading. Therefore, for the combination SSE + SRV + LOCA, the all valve load case (see Subsection 4.1.3.1) was used to calculate the SRV spectra.
- o The 3-D ANSYS model then produced fifteen sets of spectra at the required nodal points. This was done for the horizontal and vertical spectra.
- o The fifteen spectra were then enveloped to give one spectra for each node and then further enveloped with the spectra for nodes at approximately the same elevation. This yielded one ARS curve for each elevation. Table 9-14 indicates the node points enveloped at each elevation for the 3-D ANSYS

The selection of these amplitude factors was based on a probability calculation. An exceedance probability of 10^{-5} per chugging event was selected. If one assumed the probability of a LOCA occurring as 10^{-6} , then the combined probability of having a LOCA and exceeding the specified load definition is 10^{-11} . We believe a high degree of conservatism will still be retained in the load definition if a reasonable reduction in the specified exceedance probability is taken. As can be seen in Figures 9-190 & 9-191, the following amplitude factors result with the indicated change in exceedance probability:

Exceedance Probability ($w_T = 1$)	Symmetric Amplitude Factor	Asymmetric Amplitude Factor
10^{-5}	1.3	.37
10^{-4}	1.27	.35
10^{-3}	1.23	.31
10^{-2}	1.17	.25

9.6.1.2.1.2 Re-Selection of Pressure Time Histories

As described in Subsection 9.5.3.1.2, the selected chugging pressure time histories were to be selected as representative of the mean value events. The selection basis was an evaluation of peak over pressure and observed oscillation frequency. As a check of the selected pressure time histories, a Power Spectral Density (PSD) evaluation was performed. This evaluation is described in Subsection 9.5.3.1.3.1. Figure 9-178a shows the final PSD comparison. As can be seen the selected mean value events substantially bound the mean value PSD for Tests 3/4, 9/10, 11/12, 13/14 and 19/20. This indicates that the selected chugging events are actually representative of events substantially above the mean. If this proves to be true, the application of amplitude factors would not be appropriate for these selected pressure time histories. A re-selection of new mean value events based on power will be performed.

9.6.1.2.1.3 Adoption of Mark II Owners Group Load Methodology

Another option for potential load reduction would be use of the load methodology developed by GE for the Mk II Owners Group. This methodology uses a different selection bases for design chugs. These design chugs are the average of the seven largest chugs observed in the 4TCO data with their largest neighbor chug. This methodology could be used with the GKM IIM data base to develop an alternate load definition.

9.6.1.2.1.4 Development of a New Chugging Load Methodology

As a further option, the basis for a new chugging load methodology exists. This new methodology would consist of the development of a series of design sources from GKM IIM tests

5 which represent bounding blowdown conditions. These sources would be developed from the actual chugs which occur during the selected time segments for each test. These sources would then be applied randomly to an acoustic model of the Susquehanna suppression pool. In addition random source start times would be employed. This load definition would give the most realistic overall load input for plant assessment.

9.6.1.2.2 Plant Re-Assessment

6 As a result of the comparison documented in Subsection 9.6.1 and Bechtel's opinion that a re-assessment of SSES based on the GKM II-M load definition would not significantly impact our projected fuel load date, PP&L on April 1, 1981 decided to terminate the assessment of SSES based on the DFPR chugging and CO specification and re-evaluate SSES based on the GKM II-M load specification.

Section 7.0 provides the results of this re-assessment.

9.6.1.3 Summary

5 The new SSES LOCA load definition results in containment responses which exceed, in many frequencies, the responses obtained from the DFPR chugging and condensation oscillation load.

5 We are presently reviewing the degree of conservatism which exists in the SSES LOCA load. There are several areas where load reduction could be obtained. In addition, several other options exist for general load reduction.

6 On April 1, 1981, PP&L opted to terminate the re-evaluation of SSES with the DFPR load definition, and instead performed a re-evaluation of the plant based on the GKM II-M load specification.

9.6.3 Statistical Evaluation of the GKM II-M Resultant Bracing Force Data

9.6.3.1 Introduction

DAR Subsection 9.6.2 compares the maximum calculated resultant bracing force at GKM II-M, using the Mark II single vent lateral load, with the maximum measured resultant bracing force at GKM II-M. This comparison reveals that the theoretical value bounds the measured value and indicates the conservatism of the Mark II single vent lateral load. However, the NRC performed a re-evaluation of the Mark II lateral tip load based on a statistical analysis of the original 4T bracing force data. They now conclude that the Mark II impulse should be extrapolated to 65 Kips while preserving the 3 msec impulse duration. This corresponds to a lateral load which will be exceeded once in 10^5 bracing force events or once in ten LOCAs, if one assumes 100 chugs at 100 vents per LOCA.

To provide additional confirmation of the conservatism of using an extrapolated Mark II lateral load at 10^{-5} exceedance probability, a statistical analysis of the GKM II-M bracing force data has been performed. This gave a relation for determining the resultant bracing force as a function of the exceedance probability. From this relation, the GKM II-M resultant bracing force required for a 10^{-5} exceedance probability was then determined. The lateral load impulse which predicts this bracing force at GKM II-M was then determined and compared to the revised Mark II tip impulse. The following subsections document this effort.

9.6.3.2 Derivation of a Probability Density Function from the Measured Resultant Bracing Forces from the 1/6 MSL Tests

The mean and maximum resultant bracing force values for the 1/6 MSL tests envelop the mean and maximum values for the full and 1/3 MSL tests. Thus, to maximize the statistically determined resultant bracing force, the present statistical analysis is restricted to only the 1/6 MSL bracing force data.

9.6.3.2.1 General Consideration

To derive an expression for the probability density function, we assume the function follows an exponential decay. Thus, the

PROPRIETARY

following probability density function is selected for the 1/6 MSL resultant bracing force data:

$$f(u) = u \cdot e^{-u} \quad (1)$$

where: $u = C \cdot x$
 $C =$ constant to be determined
 $x =$ resultant bracing force, kN

Integrating Eq. (1) and evaluating the interval yields:

$$\int_0^{\infty} f(u) du = \int_0^{\infty} u \cdot e^{-u} du = e^{-u}(-u-1) \Big|_0^{\infty} = 1$$

Thus, this function satisfies the basic condition imposed on the probability density function; namely, that the total probability = 1.

To determine the constant, C, the mean value of the distribution, \bar{u} , is defined as the first-order moment of the probability density function described by Eq. (1). Thus

$$\bar{u} = \int_0^{\infty} u^2 \cdot e^{-u} \cdot du = e^{-u}(-u^2-2u-2) \Big|_0^{\infty} = 2$$

This is used to determine the constant, C, as:

$$C = \frac{2}{\bar{x}}$$

and u from Eq. (1) as:

$$u = \frac{2}{\bar{x}} \cdot x \quad (2)$$

where: \bar{x} is the mean value of the 1/6 MSL resultant bracing force data.

PROPRIETARY

The exceedance probability based on the probability density function of Eq. (1) is:

$$F'(u) = \int_0^{\infty} f(u) du = (1+u)e^{-u} \quad (3)$$

The probability that the resultant lies in the interval $a \leq x \leq b$ is:

$$F(a \leq u \leq b) = (a+1)e^{-a} - (b+1)e^{-b} \quad (4)$$

9.6.3.2.2 Application to the 1/6 MSL Tests

The range of mass fluxes to be used in evaluating the resulting bracing forces from Tests 13 to 18 is:

$$11 \leq \frac{\dot{m}}{A} \leq 33 \quad (\text{kg/m}^2\text{s})$$

Tests 19 and 20 were omitted since they are bounded by the remaining 1/6 MSL tests.

Table 9B shows the frequency distribution for Tests 13 to 18. The numbers in parenthesis designate the number of occurrences per test.

TABLE 9B

Bracing Forces kN	Number of Events

0 - 10	36 (6)
10 - 20	212 (35.3)
20 - 30	237 (39.5)
30 - 40	110 (18.3)
40 - 50	52 (8.6)
50 - 60	25 (4.16)
60 - 70	6 (1)
70 - 80	1 (1/6)
80 - 90	1 (1/6)

Listed in Table 9B are a total of 680 events, or 111.3 events per test.

The mean value of the frequency distribution is:

PROPRIETARY

$$\bar{x} = 25.6 \text{ kN}$$

Thus, Eq. (2) becomes

$$u = \frac{2 \cdot x}{25.6} = 0.078 \cdot x \quad (5)$$

Now Eq. (4) and (5) can be used to determine the interval probability. A comparison of the theoretically determined interval probability (Eq. 4 and Eq. 5) with the relative frequencies obtained from Table 9B (test data) is shown in Table 9C.

TABLE 9C

Bracing Forces kN	Relative Frequency (Test Data)	Interval Probability
0 - 10	0.053	0.184
10 - 20	0.31	0.2784
20 - 30	0.35	0.216
30 - 40	0.16	0.14
40 - 50	0.026	0.0826
50 - 60	0.037	0.0465
60 - 70	8.8×10^{-3}	0.025
70 - 80	1.5×10^{-3}	0.013
80 - 90	1.5×10^{-3}	6.8×10^{-3}

Figure 9-270 compares the theoretical with the measured relative frequencies. Thus, the function $f(u) = ue^{-u}$ predicts a conservative distribution.

From Eq. (3) the exceedance probability is:

$$F'(u) = (1 + u) e^{-u} \quad (6)$$

with $u = 0.078 \cdot x$

Thus, the bracing force x which is exceeded with a probability F' can be determined.

From Eq. (6) with an exceedance probability of 10^{-5} the resultant bracing force x is:

$$182 \text{ kN} = 40.9 \text{ Kips}$$

9.6.3.3 Determination of the Extrapolated Mark II Impulse

To determine the Mark II impulse required to produce a bracing force of 182 kN at GKM II-M, we assume that the bracing force is linearly proportional to the impulse. This yields the following relation:

PROPRIETARY

$$\frac{I_m}{F_m} = \frac{I_1}{P_1} \quad (7)$$

where: I_m = impulse of present Mark II single vent lateral load definition

F_m = bracing force at GKM II-M produced by I_m

I_1 = impulse required to produce bracing force at GKM II-M corresponding to a 10^{-5} exceedance probability

P_1 = statistical determined bracing force at GKM II-M for a 10^{-5} exceedance probability.

Subsection 9.6.2.1.6 calculates a maximum bracing force of 22.8 Kips with lateral load of 30,000 lbs and 3 msec impulse duration. Thus, $F_m = 22.8$ Kips and the Mark II impulse, I_m , is the area under the half sine wave impulse curve calculated with the following relation:

$$I_m = 2 F t_D / \pi \quad (8)$$

where: F = amplitude of Mark II impulse
 t_D = time duration of Mark II impulse

Substituting $F = 30,000$ lbs. and $t_D = 3$ msec gives:

$$\begin{aligned} I_m &= (2) (30,000) (.003) / \pi \\ I_m &= 57.3 \text{ #-sec} \end{aligned}$$

Substituting $P_1 = 182 \text{ kN} = 40.9$ Kips, $I_m = 57.3$ #-sec and $F_m = 22.8$ Kips into Eq. (7) gives:

$$\frac{57.3}{22.8} = \frac{I_1}{40.9}$$

$$I_1 = 102.8 \text{ #-sec}$$

To determine the extrapolated Mark II force required to give an impulse of 102.8 #-sec, we assume the impulse duration of 3 msec remains the same and solve for F in Eq. (8). Thus, for $I_1 = 102.8$ #-sec

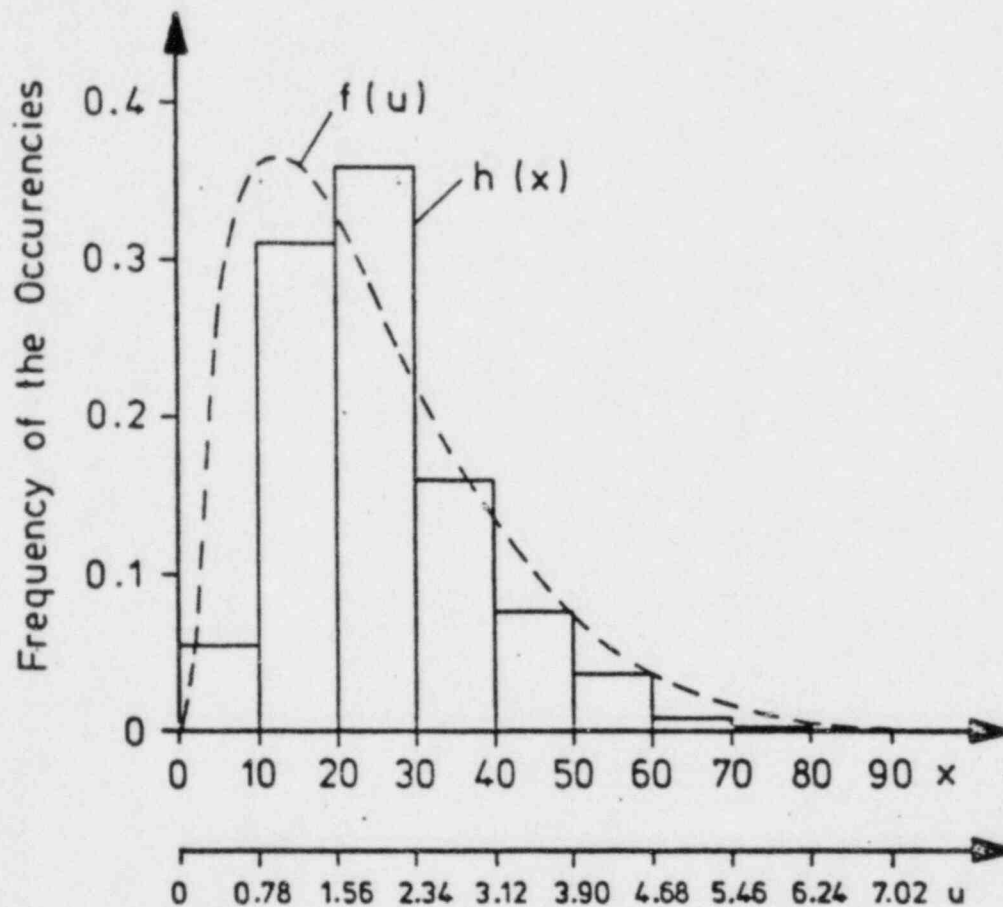
$$F = \frac{(102.8) (\pi)}{(2) (.003)}$$

$$F = 54.8 \text{ Kips}$$

PROPRIETARY

Thus, an extrapolated half-sine wave impulse of 54 Kips with a 3 msec time duration produces a bracing force in GKM II-M corresponding to an exceedance probability of 10^{-5} . This compares to the Mark II impulse magnitude of 65 Kips.

For SSES, the Mark II impulse of 65 Kips with a 3 msec time duration, as required by the NRC, will be used for a single vent lateral load definition (see Subsection 4.2.2.3).



REV. 6, 4/82

**SUSQUEHANNA STEAM ELECTRIC STATION
UNITS 1 AND 2
DESIGN ASSESSMENT REPORT**

COMPARISON OF THE THEORETICAL
FREQUENCY DISTRIBUTION OF THE
RESULTANT BRACING FORCES WITH
THE TEST DATA-TEST NOS 13..18

FIGURE 9-270

32 and 4-33). When the rapid damping of the oscillation as shown in Figure 4-28 is taken into account, a unique bubble oscillation can be presumed to have occurred.

In addition to the most important first 0.6 seconds of each trace, Figures 4-34 to 4-36 show the power spectral density functions during longer periods of the same traces. The bubble frequency remains the dominant frequency even though the pressure amplitudes are in practice damped out before the analyzer trace ends. This prevailing frequency shows that the traces do not contain geometrical effects or are affected by the eigenfrequencies of the structure. Therefore, the pressure time histories are used as pure forcing functions. It should be added that the pressure transducers used were fastened to a stiff sandwich wall structure to minimize interaction effects.

In order to obtain a conservative frequency content, the variation in air mass between the Susquehanna SRV discharge lines and those used for Brunsbittel were taken into consideration. The longest SSES discharge line has a conservatively estimated enclosed air volume of 3.1 m^3 (109.5 ft^3) (refer to Table 1-3) while the Brunsbittel discharge lines have an enclosed air volume of 1.45 m^3 (51.2 ft^3) (refer to Reference 2). The ratio of these volumes is 2.14 to 1.

Assuming a spherical air bubble, the air bubble frequency is inversely proportional to the cube root of the air volume ratio as can be seen in Reference 4. If a flat bubble with a constant cross sectional area is assumed, the air bubble frequency will be inversely proportional to the square root of the volume ratio as can be seen in Reference 5. This analysis assumes the real bubble shape to be between these two limits, and the resulting frequency shift to be between the two models' prediction of the air-volume ratio proportionality.

In order to obtain a conservative frequency content range, the three traces (see Figures 4-28 to 4-30) which were used as normalized forcing functions were expanded in time by a factor 1.8 (an expansion) and reduced in time by a factor 0.9 (a contraction). Within a given frequency range one of the three traces affects an individual location in the containment structure more adversely than the others.

The SSES quencherers were designed to compensate for the fact that some of the Susquehanna parameters were different from those of the Brunsbittel plant. To adjust for lower values of steam mass flux per SRV, and for the greater initial enclosed air mass, the exit area of the Susquehanna quencher was reduced to approximately one half of that of existing KWU power plants. Any further reduction in quencher discharge area, regardless of its desirability, is unfeasible due to design limitations imposed on SRV discharge line internal pressures as well as SRV backpressures. Based on the experience obtained during the subscale testing phase of KWU's quencher development program (refer to Reference 1), it is unlikely the maximum SSES pressure amplitudes will ever exceed a normalized value of 1.5 when

applied to the Brunsbuttel pressure amplitudes. Therefore, this evaluation is based on a conservative normalized value of 1.5; this value was verified during the SSES unique unit cell testing program, which is explained in Subsection 8.5.3, and has been used in conjunction with pressure-time histories (see Figures 4-28 through 4-30) for the suppression pool wall, pedestal, and basemat adequacy assessments.

4.1.3.7 Loads on Submerged Structures due to SRV Actuation

Two methodologies can be used for calculating the SRV air bubble loads on submerged structures. The first one is a simple pressure differential methodology which was introduced by KWU in 1977. This was used for analyzing most submerged structures. The second method uses potential flow method-of-image technique for determining the drag force. The second method was primarily used in generating the loads for the assessment of the bracing system of the LOCA downcomers (see Subsection 7.1.2.1). Both methods are described below.

4.1.3.7.1 Submerged Structure Load Simple Pressure Differential Method

The normalized pressure time histories presented in Figures 4-28, 4-29, and 4-30 (refer to Subsection 4.1.3.5) are also used for the analysis of loads on submerged structures. The vertical pressure distribution of Figure 4-24 is adopted. The loads are calculated using the pressure values and the submerged structure projected area. The computed loads were assumed to be acting in the lateral direction except for the downcomer bracing and the downcomer stiffener ring loads.

The downcomer bracing loads are assumed to be acting in the lateral and vertical directions simultaneously. The lateral load is calculated using the reduced pressure value according to Figure 4-24. The vertical load is calculated using the absolute pressure value. The downcomer ring plate loads are assumed to be acting in the vertical direction. This vertical load is also calculated using the full pressure value.

Similar to the loads on the suppression pool wetted walls, a multiplier was adopted when applying the normalized pressure time histories to account for differences between SSES and Brunsbuttel quenchers. The value of the multiplier was taken differently depending on the size (diameter) of the submerged structure. Discussions pertaining to the choice of this multiplier are provided below.

For the case of a single spherical oscillating gas bubble, the pressure amplitudes relative to the surrounding water pressure can be calculated by the simple relation:

PROPRIETARY

$$\text{Pressure differential attenuation} = \frac{R_0}{R}$$

where

R_0 = bubble radius

R = distance from point under consideration to the bubble center

If the bubble diameter is assumed to be equivalent to the overall quencher dimensions as shown in Reference 1 (approximately 3M), the bubble radius is then 1.5m (4.92 ft). The pressure difference between the front and rear of a submerged body may be calculated by assuming that the body presence does not influence the bubble dynamics. Since the largest pressure gradient occurs when the submerged body is in contact with the bubble, the relative reduction in the pressure at the front and rear of the body may be calculated for several object sizes (diameter d) from the above relation, with $R = R_0 + d$. These factors are referred to as "Calculated P_{SHAPE} " in Table 4-14. To be conservative, they were rounded off to the higher values shown in Table 4-14 as "Specified P_{SHAPE} ".

Based on the "specified P_{SHAPE} " in Table 4-14 and the 1.5 multiplier, the pressure time history multipliers for various submerged structures sizes are specified in the second to last column of Table 4-15. Verification of the conservatism of this approach for a typical submerged structure was made in the single cell test described in Subsection 8.5.7.

It should be noted that for a cylindrical body, the maximum pressure gradient occurs between the front and the rear; as one moves to the sides the gradient is reduced (see Figure 4-37). Also, with the exception of the 42 in. diameter wetwell columns which are located only a small distance from certain quenchers, submerged structures do not touch the discharged quencher gas bubbles. As the distance from the bubble increases, the pressure gradient is reduced.

The above mentioned multipliers were developed by KWU from analytical pressure differential across an object with some added conservatism. In subsequent SRV air bubble simulation Susquehanna in-plant tests (Reference 78) conducted in 1979, SRI International formulated an upper bound for the pressure differential across an object from the measured data:

$$\Delta P/P = 0.07 + 0.1555 \Delta R \quad (\text{Reference 78})$$

where ΔR is the difference in distance from the bubble center to the front and rear of the object (in feet), ΔP is the differential pressure, and P is peak incident pressure.

PROPRIETARY

The maximum value of ΔR for any object is its diameter, d . This formulation yields higher pressure differentials than those calculated by KWU, yet smaller than those specified by KWU (see Table 4-14). With the inclusion of the factor of 1.5, the pressure time history multipliers for various submerged structure sizes based on the SRI formulation are listed in the last column of Table 4-15. Note that the SRI multipliers are smaller than the original KWU specified multipliers. However, these multipliers were conservatively determined from actual in-plant test data (Reference 78). This is demonstrated further in the following section.

4.1.3.7.2 Submerged Structure Load Potential Flow Drag Force Method

This method calculates acceleration and standard drag forces on a submerged structure due to an oscillating air bubble in a water pool using method-of-images (MOI) technique for solution of potential flow. It accounts for the pool boundary effects on the flow. The method and assumptions are documented in Reference 13 (NEDE-21730). The essential equations are reproduced in Table 4-15.1.

In order to calculate the load on a submerged structure from the equations listed in Table 4-15.1, it is necessary to determine the air bubble source strength (PAT and PST in Table 4-15.1) and the location of the bubble versus time. The location of the bubble can be determined by assuming it is at the quencher center initially and stays there for a small amount of time (t_r) before rising to the pool water surface at an average velocity (V_{rise}). Figure 4-65 shows the rising source relative to a location where pressure is measured. V_{rise} and t_r can either be determined analytically from bubble dynamics or from test data. Examination of the Karlstein test data yielded average values for t_r and V_{rise} to be about 0.1 sec and 8.2 ft/sec (2.5 m/sec), respectively. To determine the bubble source strength, PAT, the normalized pressure time histories (allowing for the 1.5 pressure amplitude multiplier) presented in Figures 4-28, 4-29, and 4-30 are used, assuming they were measured at the basemat directly below the quencher center. The other source strength parameter, PST, can be calculated by integrating PAT time history.

The source strengths thus determined can then be used in the drag force equations shown in Table 4-15.1. The forces are calculated in three directions.

For multiple SRV actuation, the load contributions from each of the sources are calculated by using the above methodology. Components in each direction for all these sources are then summed algebraically. Table 4-15.2 outlines the procedure described above.

PROPRIETARY

This method has been verified against SRI balloon Susquehanna in-plant tests and Karlstein unit cell tests. The results are presented in Appendix J. It was demonstrated that this methodology predicted the test data accurately.

Table 4-15.3 presents a comparison between the SRV loads on various submerged structures considering SSES typical quencher/object relative locations using the three approaches described in this section. These loads were based on Trace #76 (see Figure 4-29), assumed acting at a node closest to the quencher. The method-of-images approach yields much lower loads than the differential pressure approach.

The MOI technique used is similar to the one documented in NEDE-21730 (Reference 13), which has been evaluated by NRC staff in NUREG-0487 and Supplement 1 (References 46 and 79). Below, the criteria affecting this methodology are summarized; their consideration is also discussed.

Standard Drag

For SRV air bubble, standard drag was found to be insignificant as compared to acceleration drag. The NUREG requires that this has to be demonstrated before the standard drag can be neglected. In addition, values of standard drag coefficient under unsteady flow are recommended instead of the steady values in Reference 13. For SSES it has been demonstrated that the standard drag on typical submerged structures due to SRV air clearing is small as compared to acceleration drag and therefore can be neglected.

Segmentation

To calculate the forces acting on a long submerged structure, the structure should be divided into segments such that the ratio of segment length to the structure diameter is between 1.0 and 1.5, as specified by the NUREG criterion, and the velocity and acceleration (or drag force) should be calculated at the center of the segments.

Interference

The interference effects for structures that are close together (within three characteristic diameters of the larger one) should be evaluated. For downcomers, columns, and SRV discharge lines in the SSES pool, this effect was found to be small as evidenced by the SRI in-plant test data (see Appendix J). This was demonstrated further by numerical evaluations using equations outlined in Reference 51. This is because the distances between these structures are at the upper bound of the specified separation. Therefore, interference effects for these structures can be neglected.

4.1.3.7.3 Submerged Structural Load for Downcomer Bracing System Assessment

For downcomer bracing assessment, the MOI technique was used to generate the forces on downcomers and SRV discharge lines.

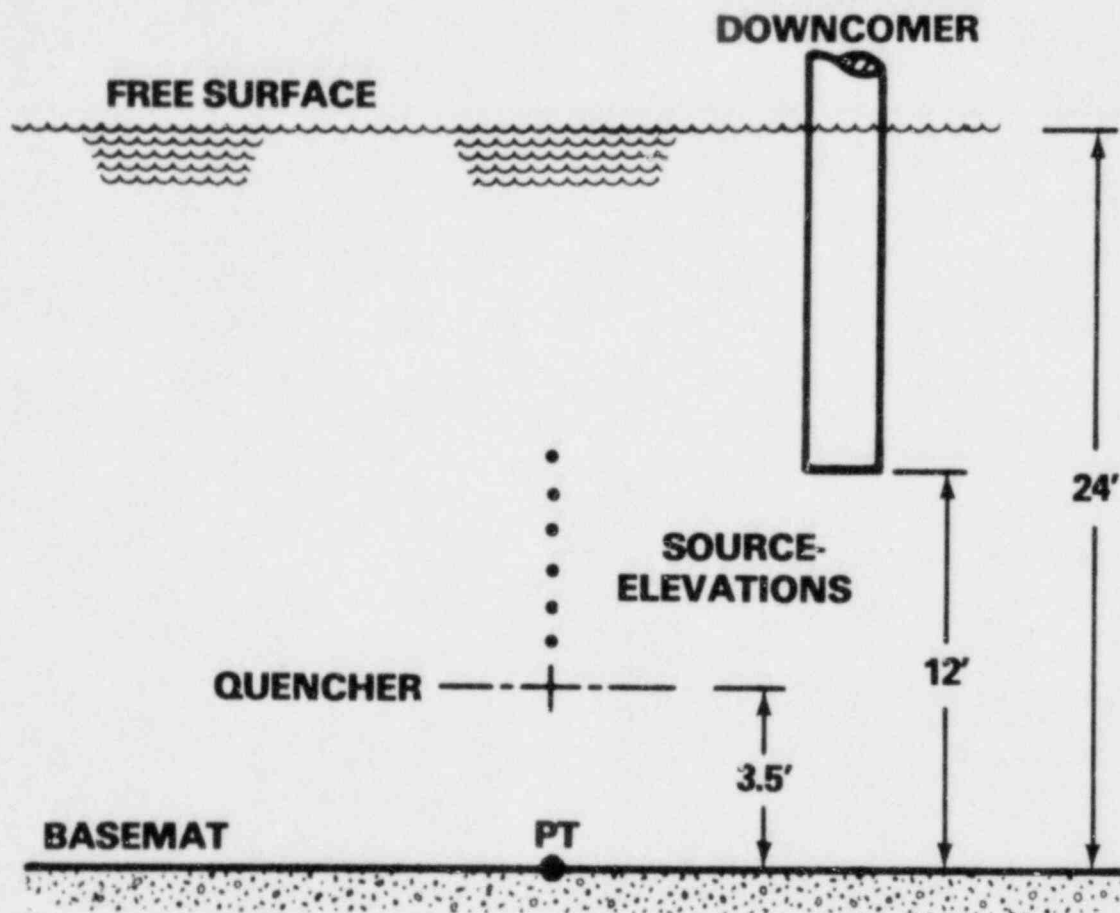
In the SSES suppression pool, the downcomer bracing system is divided into four independent quadrants. Figure 4-66 shows one typical quadrant as related to the whole suppression pool. In order to assess the adequacy of the bracing system, it is necessary to calculate the SRV air bubble loads on all downcomers connected by the bracing and combine these loads with other loads, such as seismic load, LOCA load, and thermal load, etc. (see Table 5-2). It was determined that the SRV actuation under ADS constitutes the worst load combination. Therefore, it was assumed that all six ADS valves actuated simultaneously. For comparison, loads were also generated with only one ADS valve actuation (SRV "G"), and with six ADS valves actuation with one valve (SRV "G") actuating 180° out of phase, which was based on the findings of SRI in-plant tests (Reference 78) that two-bubble in phase yielded smaller loads than those caused by single bubble or two-bubble out-of-phase discharge for certain objects.

The acceleration drag forces were calculated on the downcomers in one of the four quadrants (see Figure 4-66). The standard drag was demonstrated to be negligible. Each downcomer was divided into three vertical segments of 4 ft. (1.2 m) length and the force was calculated at the bottom of each segment. This segmentation was demonstrated to be conservative with respect to the nodding shear specified earlier.

The forces for bracing system assessment were generated before the methodology was verified against test data. A factor of 4.25 was applied to the forces generated so that the calculated force matched the force calculated for a downcomer using the KWU specification with the SRI downcomer shape factor (see Subsection 4.1.2.7.1). The verification effort (Appendix J) showed that this calibration multiplier provided a substantial margin in the loads used in the bracing system assessment.

Loads on bracing members were evaluated using the simple differential pressure methodology documented in Subsection 4.1.3.7.1. They are applied simultaneously with loads on the downcomers.

KWU PRESSURE TRACE LOCATION IN RELATIONSHIP TO THE AIR BUBBLE

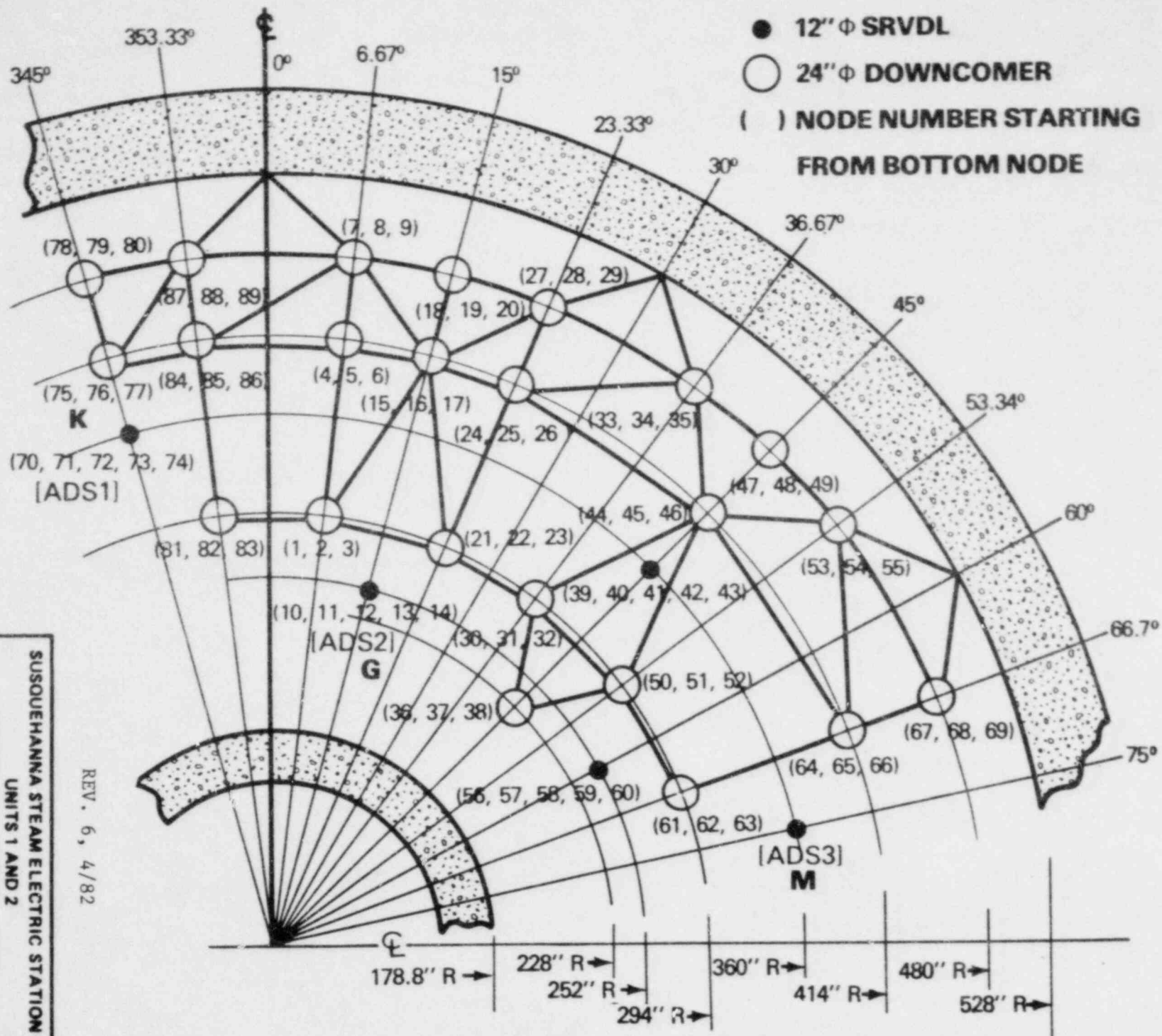


REV. 6, 4/82

SUSQUEHANNA STEAM ELECTRIC STATION
UNITS 1 AND 2
DESIGN ASSESSMENT REPORT

KWU PRESSURE TRACE LOCATION

FIGURE 4-65



SUSQUEHANNA STEAM ELECTRIC STATION
 UNITS 1 AND 2
 DESIGN ASSESSMENT REPORT

PLAN VIEW -
 DOWNCOMER BRACING

FIGURE 4-66

REV. 6, 4/82

PROPRIETARY

TABLE 4-14

SUBMERGED STRUCTURE
PRESSURE DIFFERENCE AS A FUNCTION OF BODY DIMENSION

ITEM	DIMENSION	<u>KWU</u>		<u>SRI</u>
		CALCULATED $P_{\text{SHAPE}} \frac{R_o}{1 - \frac{R_o}{R_o + D}}$	SPECIFIED P_{SHAPE} FACTOR	SRI SHAPE FACTOR (0.07 + 0.155D)
Columns	1.1m (3.61ft)	0.43	1.0	0.63
Downcomers and ECCS Suction Lines	0.6m (1.97ft)	0.29	0.5	0.38
Quencher and SRV Lines	0.4m (1.3ft)	0.22	0.33	0.28

PROPRIETARY

TABLE 4-15

SUBMERGED STRUCTURE MULTIPLIERS

<u>Item</u>	<u>Rough Dimension</u>	<u>KWU Specifid Multiplier</u>	<u>SRI Multiplier</u>
Columns	1.1m (3.61 ft)	1.5	0.95
LOCA Vents and ECCS Suction Lines	0.6m (1.97 ft)	0.75	0.57
Quenchers and SRV Discharge Lines	0.4m (1.31 ft)	0.5	0.41

PROPRIETARY

TABLE 4-15.1

EQUATION FOR CALCULATING SEV SUBMERGED STRUCTURE DRAG FORCE

$$P(r,t) = PAT(t) - XXI(r,t)$$

$$P(r,t) = P_A(r,t) + P_S(r,t)$$

$$P_A(r,t) = \text{acceleration drag force} = C_m \frac{\pi d^2 L}{4 g_c} \rho \dot{U}_{\infty N}$$

$$P_S(r,t) = \text{standard drag force} = C_D \frac{dL}{2 g_c} \rho U_{\infty N} |U_{\infty N}|$$

$$U_{\infty} = PST (XI\vec{i} + YI\vec{j} + ZI\vec{k})$$

$$\dot{U}_{\infty} = PAT (XI\vec{i} + YI\vec{j} + ZI\vec{k})$$

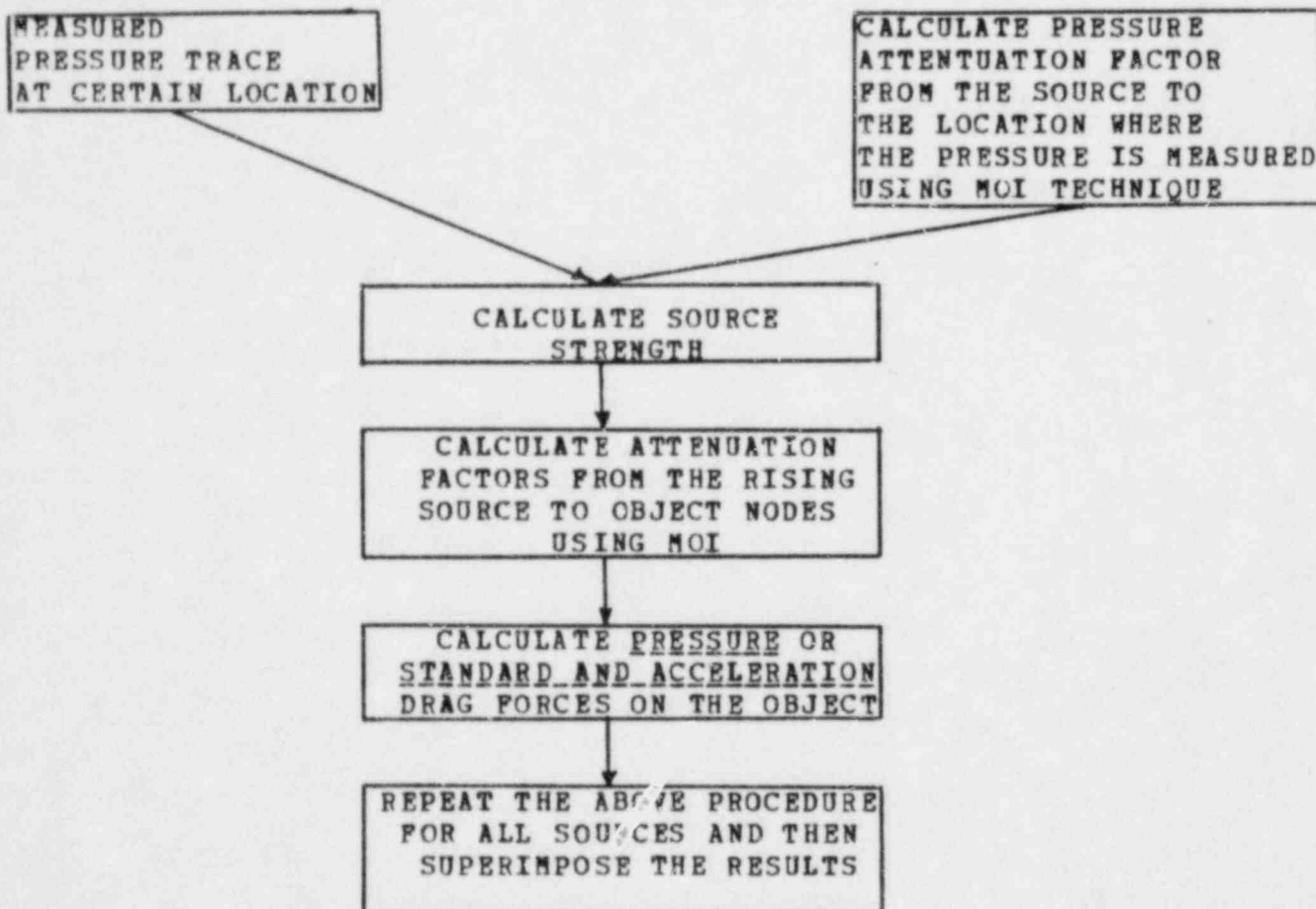
where:

P	is pressure
P	is total drag force
r	designate any location r
t	is time
d	is object diameter
L	is object length
ρ	is pool medium density
$U_{\infty N}$	is free stream velocity normal to the object
$\dot{U}_{\infty N}$	is free stream acceleration normal to the object
XI, YI, ZI	are attenuation factors in X, Y, and Z direction
XXI	is pressure attenuation factor
PAT	is bubble source strength = $R^2 \ddot{R} + 2 \dot{R} \ddot{R}$
PST	is bubble source strength = $R^2 \dot{R}$
C_m	is inertia coefficient (= 2 for cylindrical structure. To interference effect it may be larger)
C_D	is standard drag coefficient (should to 3 times the values listed in Ref. 13)
R	is the spherical bubble radius

PROPRIETARY

TABLE 4-15.2

GENERAL APPROACH FOR SRV SUBMERGED STRUCTURE LOAD CALCULATION



PROPRIETARY

TABLE 4-15.3

SRV LOAD COMPARISON ON SUBMERGED STRUCTURES USING DIFFERENT METHODOLOGIES

	MAXIMUM FORCE (LBP/FT) *				
	<u>MOI</u>	<u>KWU</u>	<u>SRI</u>	<u>KWU/</u> <u>MOI</u>	<u>SRI/</u> <u>MOI</u>
SRVDL	50	626	514	12	10.3
COLUMN	1758	6577	4166	3.7	2.4
BRACING MEMBER	15	626	626	41.7	41.7
DOWNCOMER	223	1253	952	5.6	4.3

* Based on KWU Trace 76 Source

PROPRIETARY

APPENDIX J

VERIFICATION OF POTENTIAL FLOW METHODOLOGY
USED FOR CALCULATING SRV SUBMERGED STRUCTURE LOADS

TABLE OF CONTENTS

J.1	SRI Test Comparison
J.1.1	SRI Test Description
J.1.2	Simulation of SRI Tests for Verification
J.1.2.1	SRI Source Strengths
J.1.2.2	SRI Pressure Comparisons
J.1.2.3	SRI Pressure Differential Comparisons
J.1.2.4	SRI Force Comparisons
J.1.2.5	SRI Strain Comparisons
J.2	KWU Karlstein Test Comparison
J.2.1	Karlstein Unit Cell Test Description
J.2.2	Simulation of Karlstein Tests for Verification
J.2.2.1	Karlstein Unit Cell Source Strengths
J.2.2.2	Karlstein Unit Cell Pressure Comparisons
J.3	Figures
J.4	Tables

PROPRIETARY

APPENDIX J

FIGURES

<u>Number</u>	<u>Title</u>
J-1	Sensor Locations
J-2	Comparison of Source Strengths - Sensor P1A, P5A, and P14
J-3	Comparison of Source Strengths - Sensor P12 and P14
J-4	Source Strength - Sensor P14 - Test S3
J-5	Comparison of Predicted Pressure Time History with Test Data - Sensor P1A - Test S1
J-6	Comparison of Predicted Pressure Time History with Test Data - Sensor P1B - Test S1
J-7	Comparison of Predicted Pressure Time History with Test Data - Sensor P2A - Test S1
J-8	Comparison of Predicted Pressure Time History with Test Data - Sensor P3B - Test S1
J-9	Comparison of Predicted Pressure Time History with Test Data - Sensor P5A - Test S1
J-10	Comparison of Predicted Pressure Time History with Test Data - Sensor P5B - Test S1
J-11	Comparison of Predicted Pressure Time History with Test Data - Sensor P6A - Test S1
J-12	Comparison of Predicted Pressure Time History with Test Data - Sensor P6B - Test S1
J-13	Comparison of Predicted Pressure Time History with Test Data - Sensor P7A - Test S1
J-14	Comparison of Predicted Pressure Time History with Test Data - Sensor P7B - Test S1
J-15	Comparison of Predicted Pressure Time History with Test Data - Sensor P1A - Test S3
J-16	Comparison of Predicted Pressure Time History with Test Data - Sensor P1B - Test S3
J-17	Comparison of Predicted Pressure Time History with Test Data - Sensor P2A - Test S3

PROPRIETARY

APPENDIX J

- J-18 Comparison of Predicted Pressure Time History with Test Data - Sensor P3B - Test S3
- J-19 Comparison of Predicted Pressure Time History with Test Data - Sensor P5A - Test S3
- J-20 Comparison of Predicted Pressure Time History with Test Data - Sensor P5B - Test S3
- J-21 Comparison of Predicted Pressure Time History with Test Data - Sensor P7A - Test S3
- J-22 Comparison of Predicted Pressure Time History with Test Data - Sensor P7B - Test S3
- J-23 Comparison of Predicted Pressure Time History with Test Data - Sensor P1A - Test S5
- J-24 Comparison of Predicted Pressure Time History with Test Data - Sensor P1B - Test S5
- J-25 Comparison of Predicted Pressure Time History with Test Data - Sensor P2A - Test S5
- J-26 Comparison of Predicted Pressure Time History with Test Data - Sensor P3B - Test S5
- J-27 Comparison of Predicted Pressure Time History with Test Data - Sensor P5A - Test S5
- J-28 Comparison of Predicted Pressure Time History with Test Data - Sensor P5B - Test S5
- J-29 Comparison of Predicted Pressure Time History with Test Data - Sensor P7A - Test S5
- J-30 Comparison of Predicted Pressure Time History with Test Data - Sensor P7B - Test S5
- J-31 Comparison of Predicted Differential Time History with Test Data - Sensor P1A-P1B - Test S1
- J-32 Comparison of Predicted Differential Pressure Time History with Test Data - Sensor P5A-P5B - Test S1
- J-33 Comparison of Predicted Differential Pressure Time History with Test Data - Sensor P6A-P6B - Test S1
- J-34 Comparison of Predicted Differential Pressure Time History with Test Data - Sensor P7A-P7B - Test S1

PROPRIETARY

APPENDIX J

- J-35 Comparison of Predicted Differential Pressure Time History with Test Data - Sensor P1A-P1B - Test S3
- J-36 Comparison of Predicted Differential Pressure Time History with Test Data - Sensor P5A-P5B - Test S3
- J-37 Comparison of Predicted Differential Pressure Time History with Test Data - Sensor P6A-P6B - Test S3
- J-38 Comparison of Predicted Differential Pressure Time History with Test Data - Sensor P7A-P7B - Test S3
- J-39 Comparison of Predicted Force Time History with Test Data - P1AB - Test S1
- J-40 Comparison of Predicted Force Time History with Test Data - P5AB - Test S1
- J-41 Comparison of Predicted Force Time History with Test Data - P6AB - Test S1
- J-42 Comparison of Predicted Force Time History with Test Data - P7AB - Test S1
- J-43 Comparison of Predicted Force Time History with Test Data - P1AB - Test S3
- J-44 Comparison of Predicted Force Time History with Test Data - P5AB - Test S3
- J-45 Comparison of Predicted Force Time History with Test Data - P6AB - Test S3
- J-46 Comparison of Predicted Force Time History with Test Data - P7AB - Test S3
- J-47 Comparison of Predicted Force Time History with Test Data - P1AB - Test S5
- J-48 Comparison of Predicted Force Time History with Test Data - P5AB - Test S5
- J-49 Comparison of Predicted Force Time History with Test Data - P6AB - Test S5
- J-50 Comparison of Predicted Force Time History with Test Data - P7AB - Test S5
- J-51 Comparison of Predicted Force Time History with Test Data Filtered above 30 Hz - P5AB - Test S3

PROPRIETARY

APPENDIX J

J-52 NASTRAN Downcomer Model

J-53 Comparison of the Predicted Strain with Measured Data - Strain Gage S5A - Test S1

J-54 Comparison of the Predicted Strain with Measured Data - Strain Gage S5B - Test S1

J-55 Comparison of the Predicted Strain with Measured Data - Strain Gage S7A - Test S1

J-56 Comparison of the Predicted Strain with Measured Data - Strain Gage S7B - Test S1

J-57 Comparison of the Predicted Strain with Measured Data - Strain Gage S5A - Test S3

J-58 Comparison of the Predicted Strain with Measured Data - Strain Gage S5B - Test S3

J-59 Comparison of the Predicted Strain with Measured Data - Strain Gage S7A - Test S3

J-60 Comparison of the Predicted Strain with Measured Data - Strain Gage S7B - Test S3

J-61 Comparison of the Predicted Strain with Measured Data - Strain Gage S5A - Test S5

J-62 Comparison of the Predicted Strain with Measured Data - Strain Gage S5B - Test S5

J-63 Comparison of the Predicted Strain with Measured Data - Strain Gage S7A - Test S5

J-64 Comparison of the Predicted Strain with the Test Data - Strain Gage S7B - Test S5

J-65 Comparison of the Predicted Strain with the Test Data - Strain Gage S1 - Test S1

J-66 Comparison of the Predicted Strain with the Test Data - Strain Gage S2 - Test S1

J-67 Comparison of the Predicted Strain with the Test Data - Strain Gage S1 - Test S3

J-68 Comparison of the Predicted Strain with the Test Data - Strain Gage S2 - Test S3

J-69 Comparison of the Predicted Strain with the Test Data - Strain

PROPRIETARY

APPENDIX J

Gage S1 - Test S5

- J-70 Comparison of the Predicted Strain with the Test Data - Strain Gage S2 - Test S5
- J-71 Pressure Transducer and Strain Gage Locations - Karlstein T-Quencher Test Tank
- J-72 Source Strength Comparison - Test 5.1.4
- J-73 Comparison of the Predicted Pressure Time History with the Test Data - P5.1 - Test 5.1.4
- J-74 Comparison of the Predicted Pressure Time History with the Test Data - P5.5 - Test 5.1.4
- J-75 Comparison of the Predicted Pressure Time History with the Test Data - P5.9 - Test 5.1.4
- J-76 Comparison of the Predicted Pressure Time History with the Test Data - P5.10 - Test 5.1.4
- J-77 Comparison of the Predicted Pressure Time Histories with the Test Data - P5.1 to P5.5 - Test 5.1.4
- J-78 Comparison of the Predicted Pressure Time Histories with the Test Data - P5.6 to P5.10 - Test 5.1.4
- J-79 Comparison of the Predicted Pressure Time Histories with the Test Data - P5.1 to P5.5 - Test 4.1.5
- J-80 Comparison of the Predicted Pressure Time Histories with the Test Data - P5.6 to P5.10 - Test 4.1.5
- J-81 Comparison of the Predicted Pressure Time Histories with the Test Data - P5.1 to P5.5 - Test 15.1.6
- J-82 Comparison of the Predicted Pressure Time Histories with the Test Data - P5.6 to P5.10 - Test 15.1.6

PROPRIETARY

APPENDIX J

TABLES

Number

Title

J-1

Sensor Locations - SRI Submerged Structure Bubble Tests

VERIFICATION OF POTENTIAL FLOW METHODOLOGY
USED FOR CALCULATING SRV SUBMERGED STRUCTURE LOADS

The methodology used for calculating SRV submerged structure loads based on potential flow technique (Subsection 4.1.3.7.2) was verified against KWU Karlstein unit cell test data (Chapter 8) and SRI inplant test data (Reference 78). Results of the verification are presented in this Appendix.

Karlstein unit cell tests were performed by KWU in 1978 to support the SSES T-quencher load specifications provided by KWU in late 1977. Specifications of loads on submerged structures due to SRV bubble dynamics were based on theoretical calculations which were demonstrated to be conservative by measured results in the tests. To obtain a more realistic definition of SRV submerged structure loads, SRI performed inplant tests at SSES in late 1979. The results of these two tests provide the data base for the SRV submerged structure load comparison.

Section J.1 presents comparison with SRI tests and Section J.2 presents comparison with Karlstein tests.

J.1 SRI Test Comparison

This section presents comparisons of SRV submerged structure loads calculated by the method described in Subsection 4.1.3.7.2 with the SRI test results. The description of the SRI test is given in Subsection J.1.1 and comparison results are given in Subsection J.1.2.

J.1.1 SRI Test Description

SRI measured loads on submerged structures in the SSES suppression pool using balloon sources that simulated SRV air clearing. The balloon sources were calibrated in the Karlstein tank, in which the SRV blowdown tests for the verification of SSES quencher loads were performed, such that the pressures in the pool measured during the blowdown tests were reproduced. Details of the source calibration can be found in Reference 78. Eight tests were performed in the SSES pool with the SRI balloon sources. Five tests were performed with one balloon source, and three were performed with two balloon sources. The main purpose of the tests with two sources was to investigate the loads resulting from multiple SRV actuations.

Pressure sensors and strain gages were installed at various locations near the sources in the SSES suppression pool to measure pressure, differential pressure across objects, and strain time histories. Figure J-1 and Table J-1 present the locations of all the test sensors. Details of tests performed as

well as instrumentation, hardware, and results obtained are presented in Reference 78.

J.1.2 Simulation of SRI Tests

To verify the methodology presented in Subsection 4.1.3.7.2, three SRI tests were simulated. These tests were:

- (a) Test S_1 (one source)
- (b) Test S_3 (two sources in-phase)
- (c) Test S_5 (two sources out-of-phase by 180°)

For each of the three tests the source strength was first developed from the measured pressure time histories. The calculated source strength was then used to determine the pressure, differential pressure across objects, and drag forces for comparison with the measured data. Refer to Subsection 4.1.3.7.2 for the calculation procedures.

J.1.2.1 SRI Source Strengths

For Test S_1 (one bubble), bubble source strengths were calculated from the measured pressure time history data of sensors P1A, P5A, P12 and P14 (see Figure C-1 for sensor locations). A bubble rise time of 4.0 sec. was used based on SRI's evaluation of the test data. Figure J-2 shows the close comparison between source strengths based on P1A, P5A and P14. Figure J-3 presents the comparison between source strengths based on P12 and P14. The source strength based on P12 is lower than P14, probably due to the proximity of P12 to the bubble (P12 is about 2 ft. below the source center). The results shown in Figures J-2 and J-3 demonstrate that any measured trace can be used to determine source strength, provided that the measuring location is not too close to the source. In the following analyses, P14 will be used for sourcing.

For Test S_3 (two bubbles in-phase), the source strength was calculated from the P14 pressure time history. Figure J-4 shows the S_3 source strength. For simplicity, the source strength of S_3 was utilized to generate the pressure and loads for Test S_5 .

J.1.2.2 SRI Pressure Comparisons

Pressure comparisons were made between calculated (see Subsection 4.1.3.7.2) and measured data at all sensor locations for which the digitized data were available for the three tests. Figures J-5 to J-14 present this comparison for Test S_1 .

PROPRIETARY

APPENDIX J

Figures J-15 to J-22 show this comparison for Test S₃. Test S₅ pressure comparisons are presented in Figures J-23 to J-30.

The calculated pressure time histories agree well with the test data except for Test S₅, where the phasing is off. This is due to the approximation that the Test S₅ source was the same as the Test S₃ source. However, the pressure magnitude was well predicted.

J.1.2.3 SRI Pressure Differential Comparison

For Tests S₁ and S₃, a differential pressure comparison between calculated and measured data was made at selected location across a downcomer and a column. Figures J-31 to J-34 show this comparison for Test S₁. Comparison for Test S₃ is shown in Figures J-35 to J-38.

For differential pressure across the column, P1A-1B (Figure J-31 and J-35), the measured values were slightly under-predicted. For differential pressure across the downcomers, the measured data exhibit high frequency fluctuation. This is due to movements of the pressure transducer associated with the downcomer vibration. Further discussion of this effect will be presented in the following subsection.

In general, the differential pressures were under-predicted. This can be attributed to the effect of presence of the object in the flow field. In the calculation the objects were assumed to be nonexistent. For calculating the force time history, this effect is accounted for by the inclusion of the inertia coefficient.

J.1.2.4 SRI Force Comparison

Calculated acceleration drag forces (see Subsection 4.1.3.7.2) were compared with forces calculated from measured differential pressure by the following formulation:

$$F_{\text{test}} = \Delta P_{\text{test}} \cdot \frac{\pi r^2}{2}$$

where ΔP_{test} = measured differential pressure across an object

r = the object radius

This formulation was given by Reference 78 based on the cosine pressure distribution around the structure's cross section. This cosine distribution was demonstrated to be realistic through measured pressure data in Reference 78. The calculated forces were based on an inertia coefficient, C_m , of 2.0, and were resolved into the directions in which the differential pressures were measured.

PROPRIETARY

APPENDIX J

Figures J-39 to J-42 present the comparisons for Test S_1 . The comparisons for Tests S_3 and S_5 are shown in Figures J-43 to J-46 and J-47 to J-50, respectively.

As mentioned in Subsection J.1.2.3, the excitation of the downcomers caused high frequency fluctuations in the measured data. In Figure J-51 the measured data of Figure J-44 (force on downcomer) were filtered above 30 Hz, and this comparison is more reasonable.

The calculated drag forces are comparable to the forces based on the measured differential pressures.

J.1.2.5 SRI Strain Comparison

The calculated drag forces on column 1 and downcomer 3 (Figure (J-1) were used as input to the NASTRAN program to calculate the moment and strains at the locations where strain gages were installed. A beam model was adopted.

Figure J-52 shows the beam model used for the downcomer. The strains were compared with measured data. They are shown in Figures J-53 to J-70. For the strain comparison on the column, the calculated strains always overpredicted the test data (Figure J-65 to J-70). For the downcomer, the calculated strains, in general, overpredicted the test data at the rigid location near the diaphragm (strain gage S7) for all the three tests. For the location 8 ft. (2.4 m) above the downcomer exit (strain gage S5) the calculated strain, in general, underpredicted the test data. This underprediction is probably caused by the influence of the localized effect of the downcomer bracing. It can therefore be concluded that the strains calculated using the calculated drag force overpredicted the test data.

J.2 KWU Karlstein Test Comparison

Karlstein unit cell tests were performed by KWU to support the design of SSES T-quencher. Nineteen tests were performed with the long discharge line and thirteen with the short discharge line. Section 8 presents the comprehensive test matrix for the tests performed.

J.2.1 Karlstein Unit Cell Test Description

The pressure sensors installed at various locations to measure the wall loading in the pool are shown in Figure J-71. A dummy vent was also installed to represent a SSES downcomer. Strain gages were installed on the vent to measure SRV loads. Figure J-71 shows the locations of the dummy vent and strain gages. Details of the tests performed, instrumentation, hardware, and data obtained are presented in Section 8.

PROPRIETARY

APPENDIX J

J.2.2 Simulation of Karlstein Tests for Verification

To verify the methodology presented in Subsection 4.1.3.7.2, three of the Karlstein long line tests were chosen based on availability of digitized test data. These tests were:

- (a) Test 4.1.5
- (b) Test 5.1.4
- (c) Test 15.1.6

For each of the test simulated, the source strength was first developed from a measured pressure time history. From the calculated source strength pressures at sensor locations were calculated for comparison with test data. Drag forces were also calculated on the dummy vent for subsequent strain calculation.

J.2.2.1 Karlstein Unit Cell Source Strengths

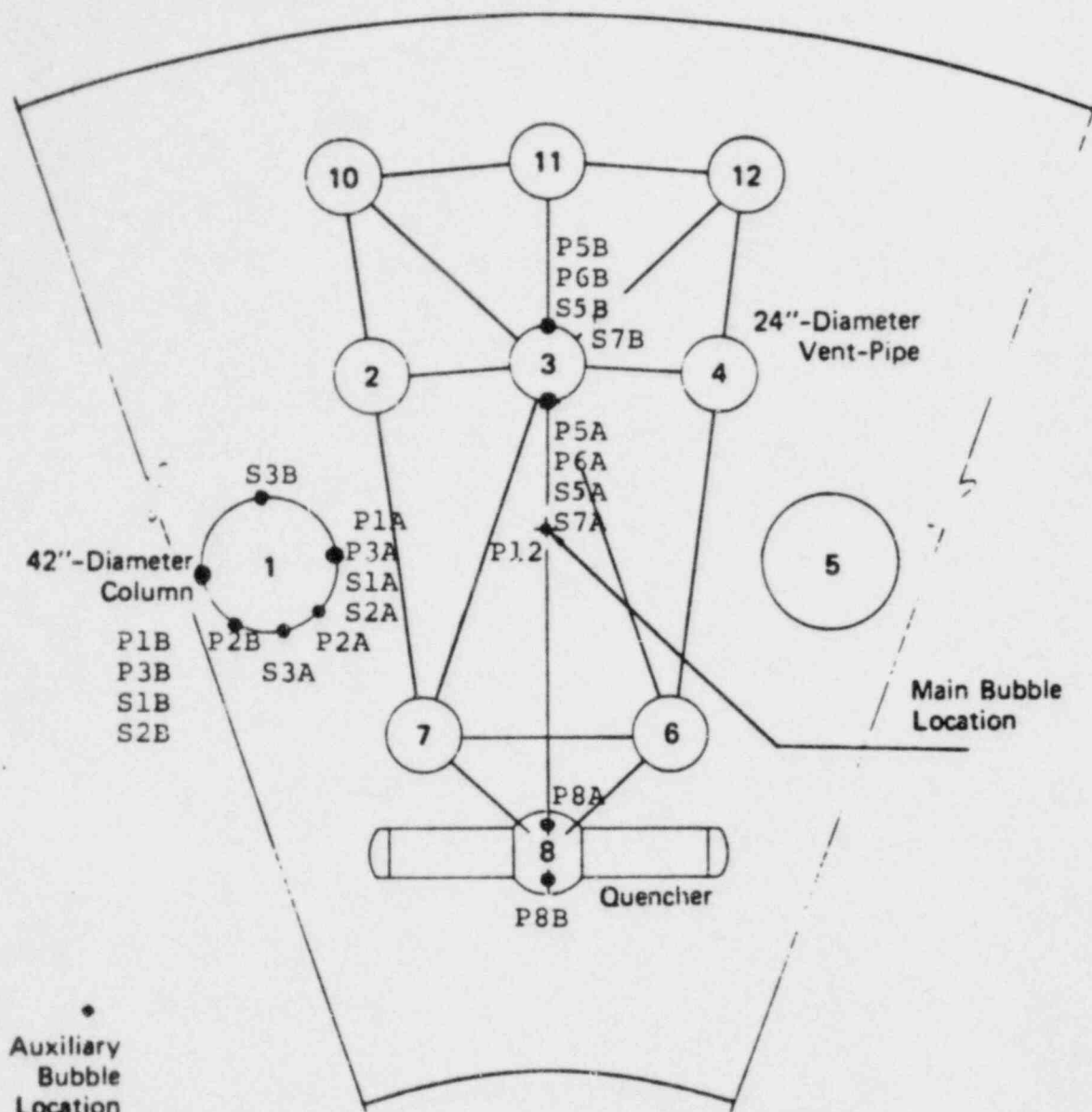
For Test 5.1.4 source strengths were generated from the measured pressure time histories of sensors P5.1, P5.9 and P5.10 using a bubble rise time of 2.5 sec. observed from the test data. Figure J-72 shows a source strength comparison based on these pressure time histories. A good comparison is observed between the three traces up to about 0.7 sec., after which P5.10 source exhibits a more erratic behavior. This is due to the steam condensation effect, since the P5.10 sensor is very close to the quencher. The P5.9 source strength was used for calculating the pressures and drag forces for Test 5.1.4. For Tests 4.1.5 and 15.1.6, the source strengths based on P5.10 were used for calculating the pressures and drag forces, because they were the only digitized data available.

J.2.2.2 Karlstein Unit Cell Pressure Comparison

Pressure comparisons were made between calculated and measured data at all sensor locations.

For Test 5.1.4, Figures J-73 to J-78 present the comparison between calculated and measured pressures. Figures J-79 and J-80 present the comparison between calculated and measured pressures for Test 4.1.5. For Test 15.1.6, the comparison between calculated and measured pressures is presented in Figures J-81 and J-82.

The calculated pressure time histories agree well with the test data.



SSes POOL SEGMENT

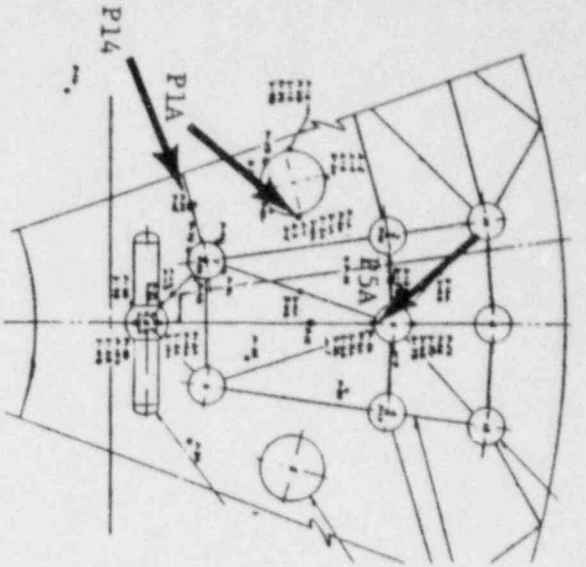
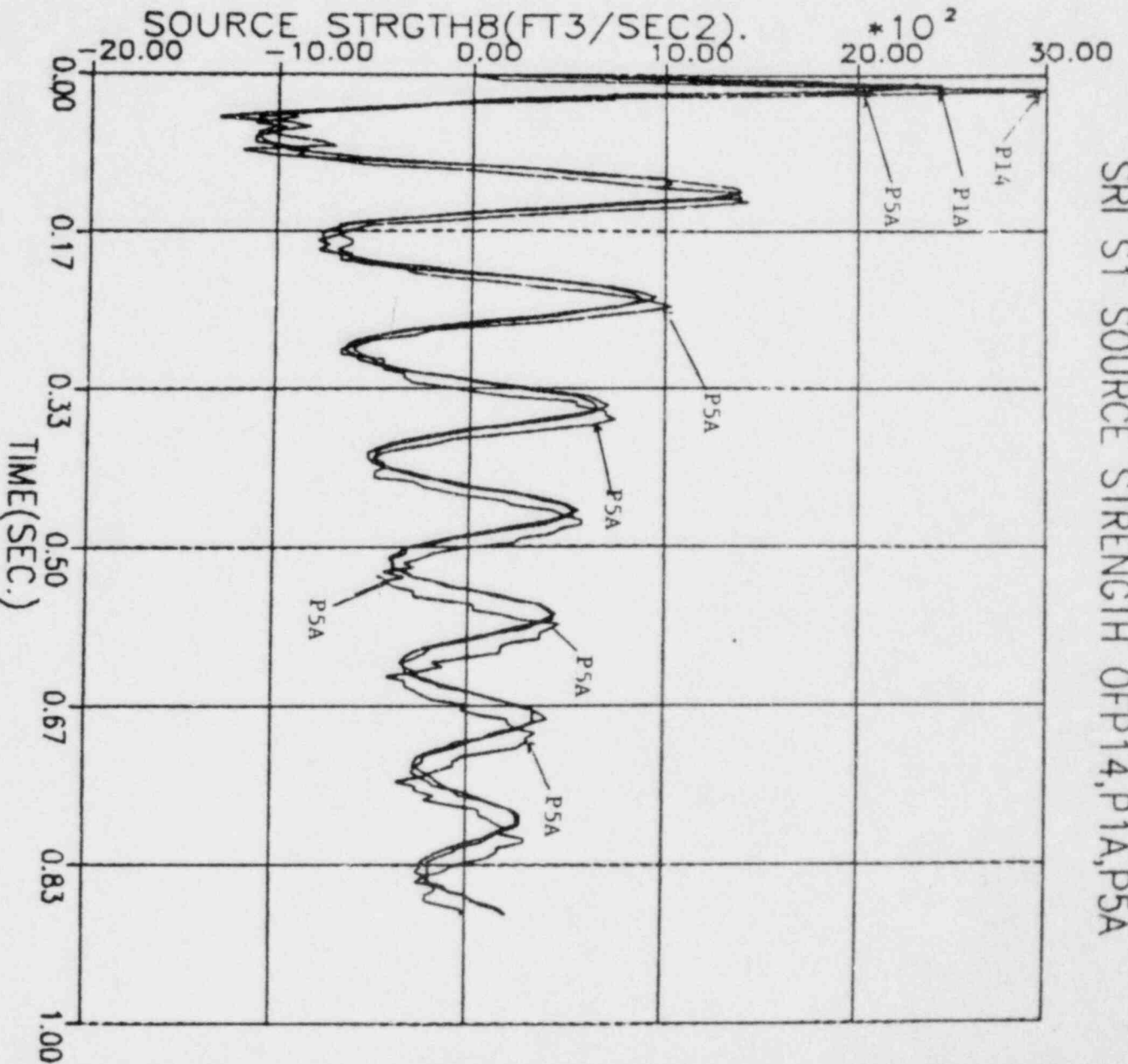
REV. 6, 4/82

SUSQUEHANNA STEAM ELECTRIC STATION
UNITS 1 AND 2
DESIGN ASSESSMENT REPORT

SENSOR LOCATIONS

FIGURE J-1

SRI S1 SOURCE STRENGTH OF P14, P1A, PSA



Elevation	
P1A	3.6'
PSA	13.88'
P14	0.42'

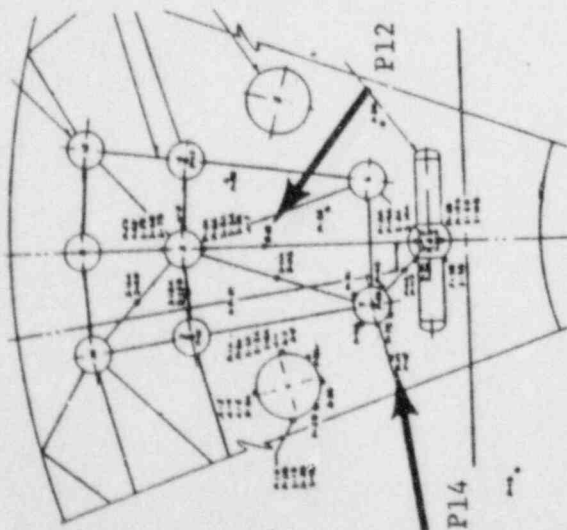
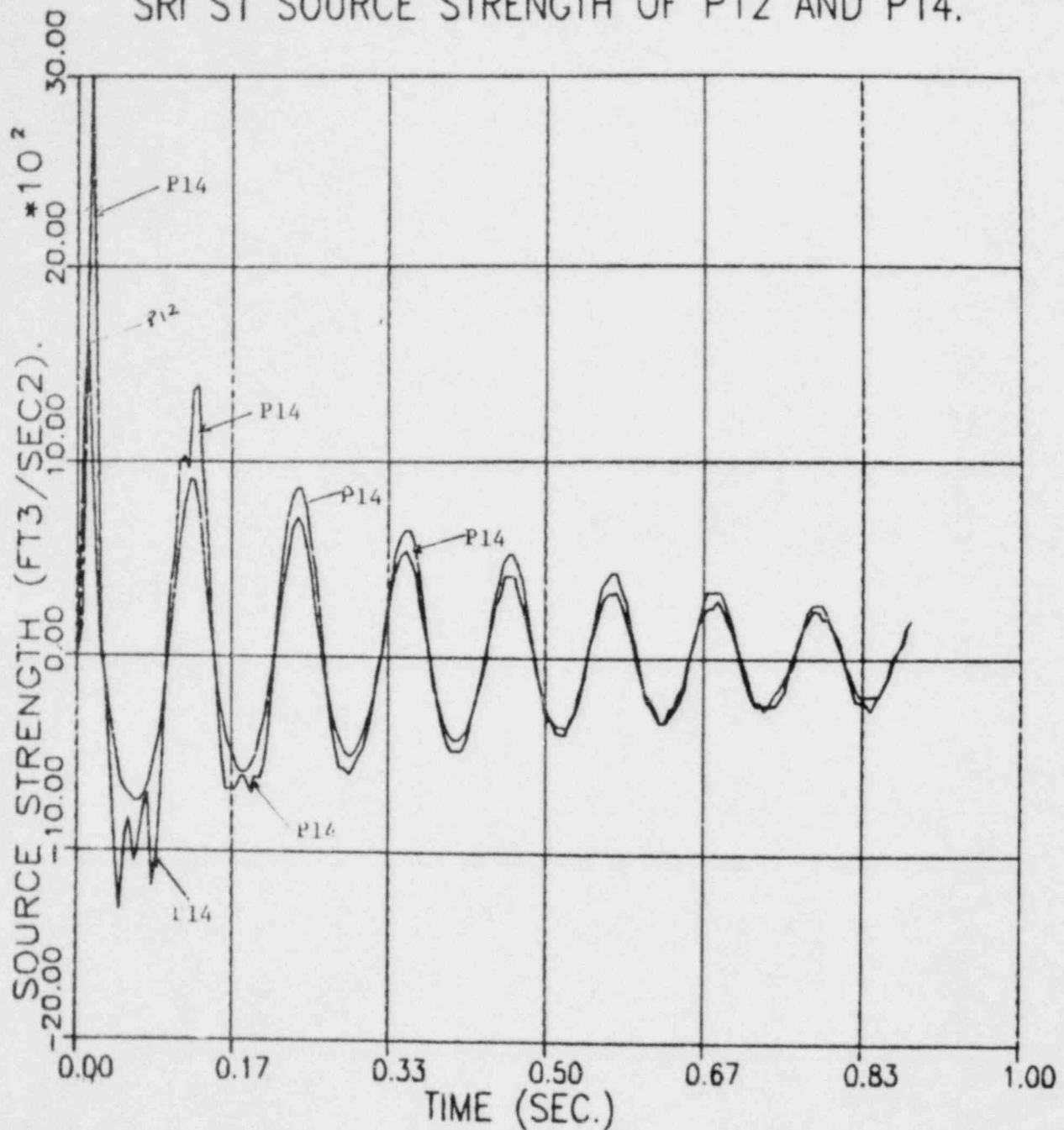
REV. 6, 4/82

SUSQUEHANNA STEAM ELECTRIC STATION
UNITS 1 AND 2
DESIGN ASSESSMENT REPORT

COMPARISON OF SOURCE STRENGTHS -
SENSOR P1A, PSA, AND P14

FIGURE J-2

SRI S1 SOURCE STRENGTH OF P12 AND P14.



Elevation	
P12	1.46'
P14	0.42'

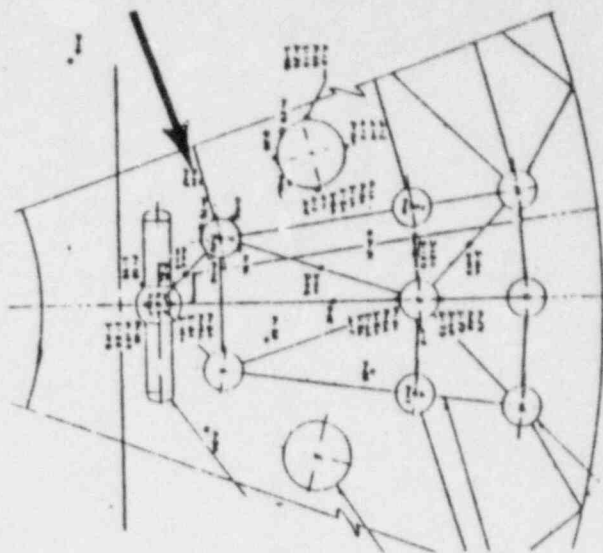
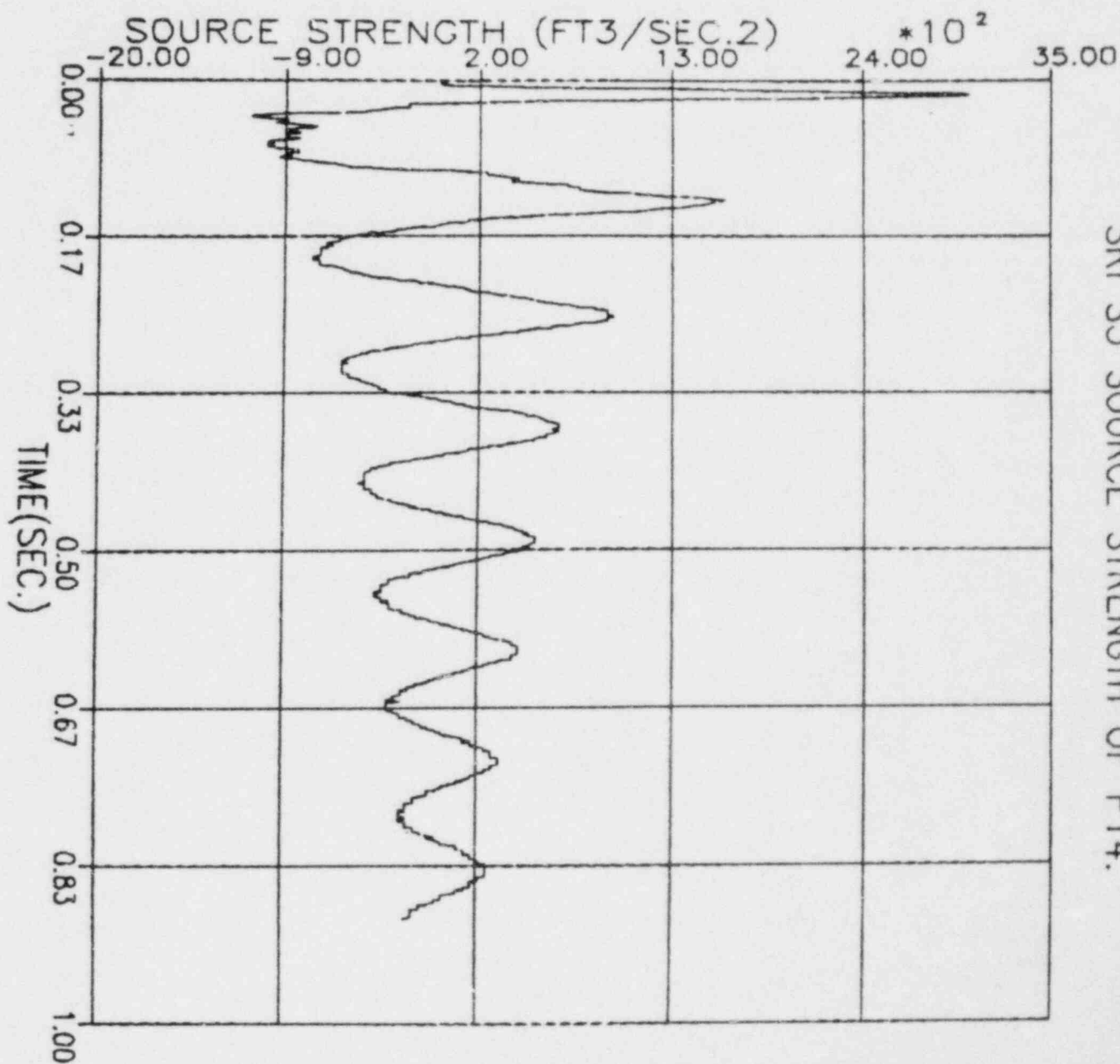
REV. 6, 4/82

**SUSQUEHANNA STEAM ELECTRIC STATION
UNITS 1 AND 2
DESIGN ASSESSMENT REPORT**

COMPARISON OF SOURCE STRENGTHS -
SENSOR P12 AND P14

FIGURE J-3

SRI S3 SOURCE STRENGTH OF P14.



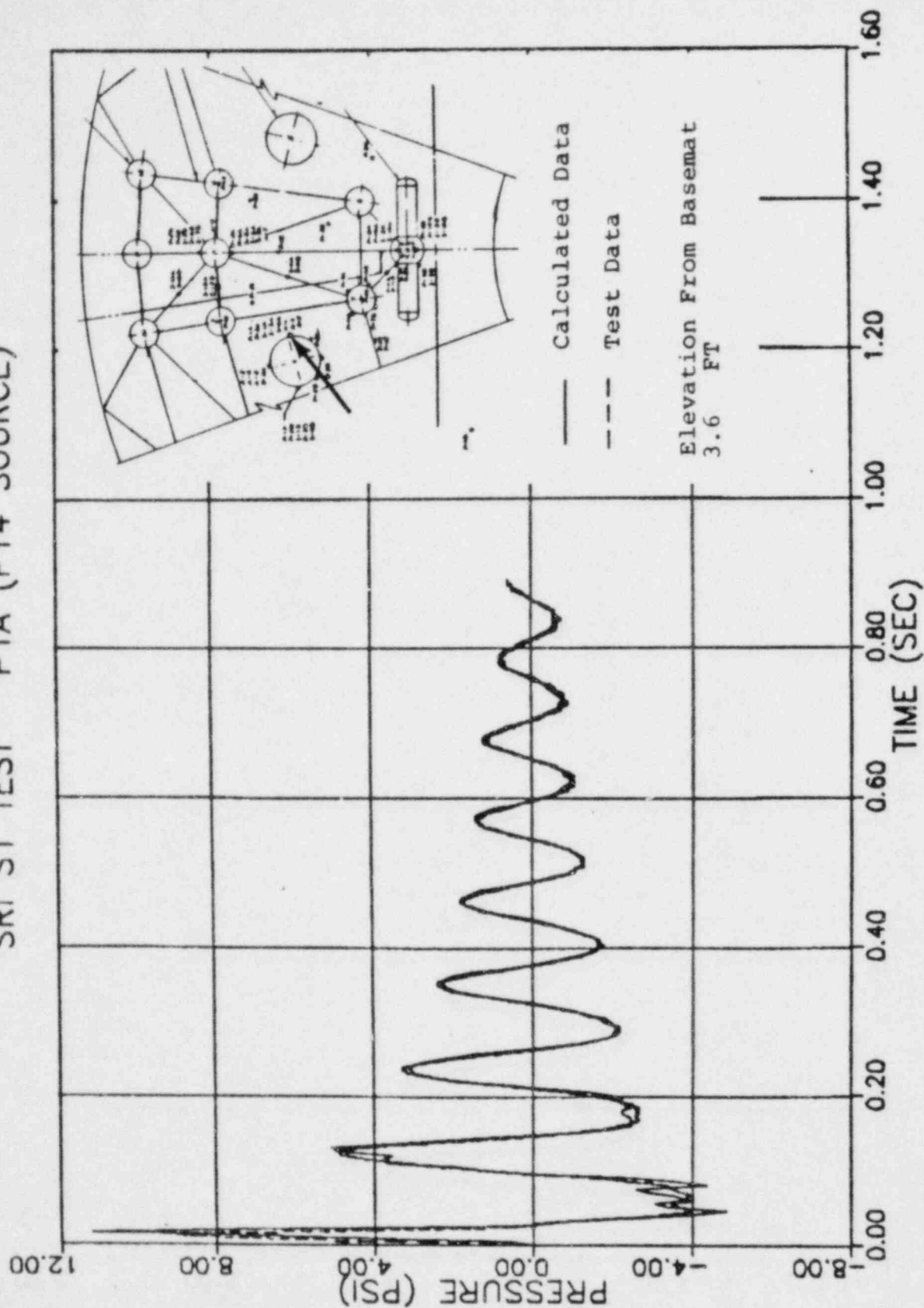
SUSQUEHANNA STEAM ELECTRIC STATION
UNITS 1 AND 2
DESIGN ASSESSMENT REPORT

REV. 6, 4/82

SENSOR P14 - TEST S3

FIGURE J-41

SRI S1 TEST P1A (P14 SOURCE)



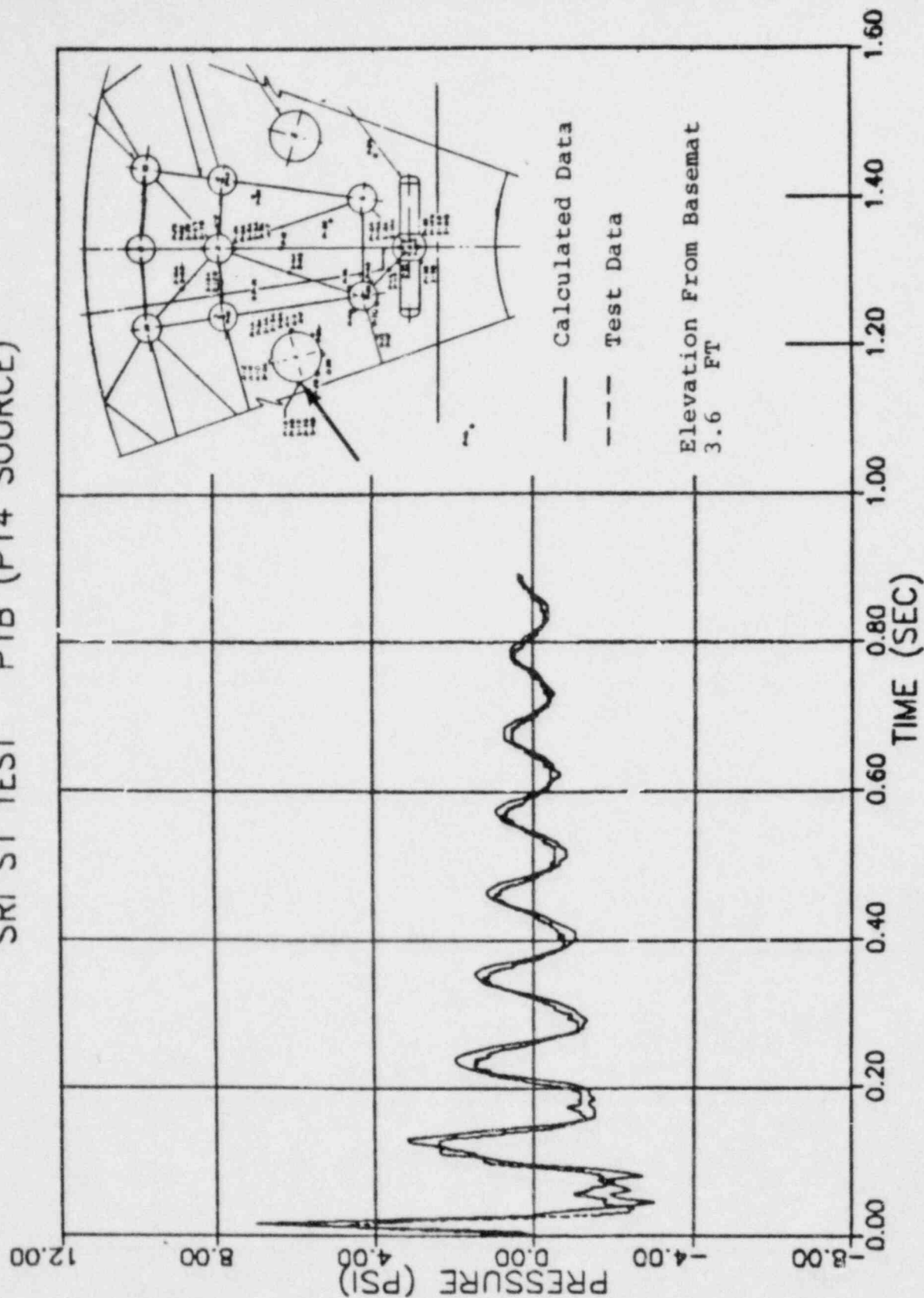
REV. 6, 4/82

SUSQUEHANNA STEAM ELECTRIC STATION
UNITS 1 AND 2
DESIGN ASSESSMENT REPORT

COMPARISON OF PREDICTED PRESSURE
TIME HISTORY WITH TEST
DATA - SENSOR P1A - TEST S1

FIGURE J-5

SRI S1 TEST P1B (P14 SOURCE)



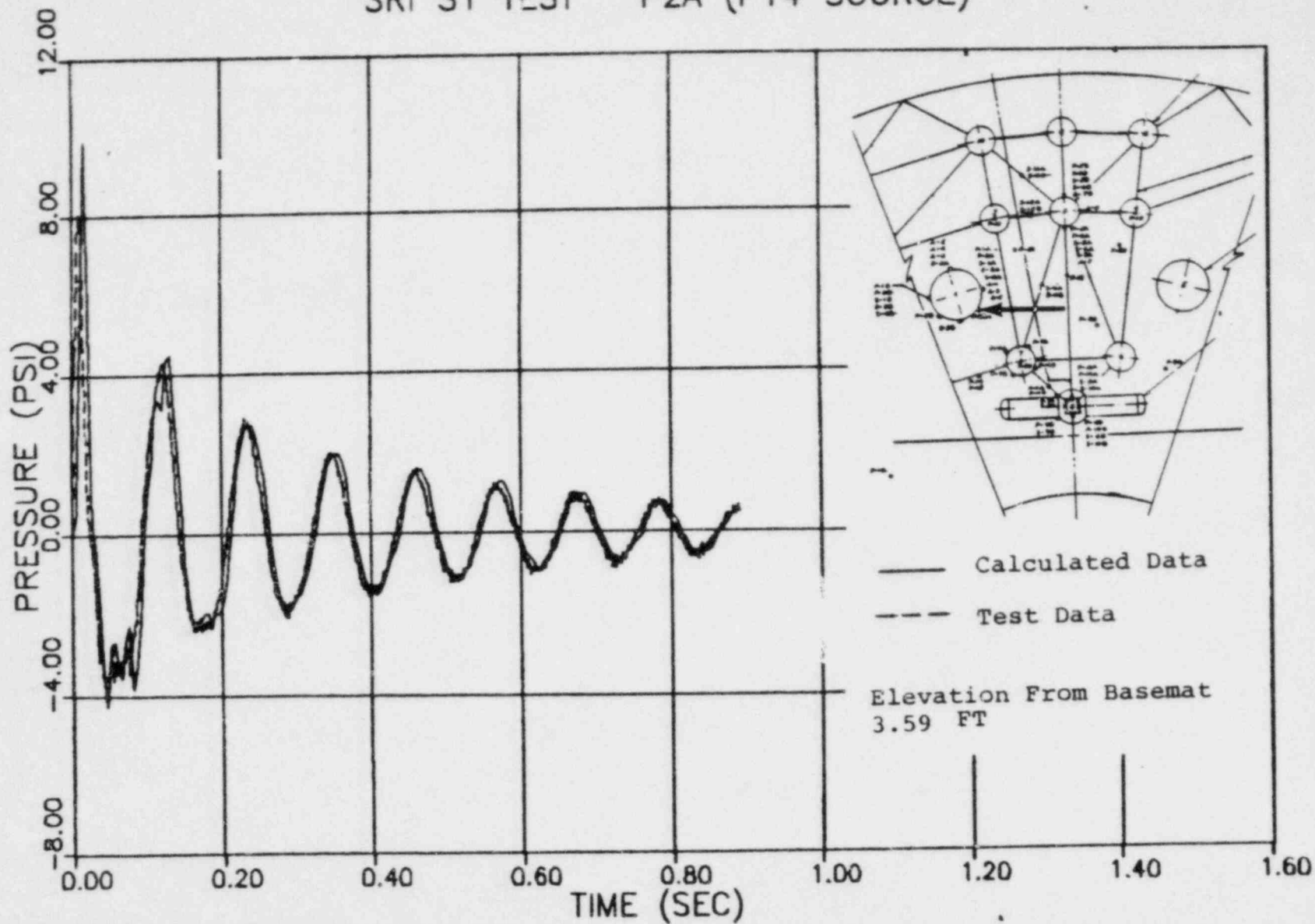
REV. 6, 4/82

SUSQUEHANNA STEAM ELECTRIC STATION UNITS 1 AND 2 DESIGN ASSESSMENT REPORT

COMPARISON OF PREDICTED PRESSURE
TIME HISTORY WITH TEST
DATA - SENSOR P1B - TEST S1

FIGURE J-6

SRI S1 TEST P2A (P14 SOURCE)



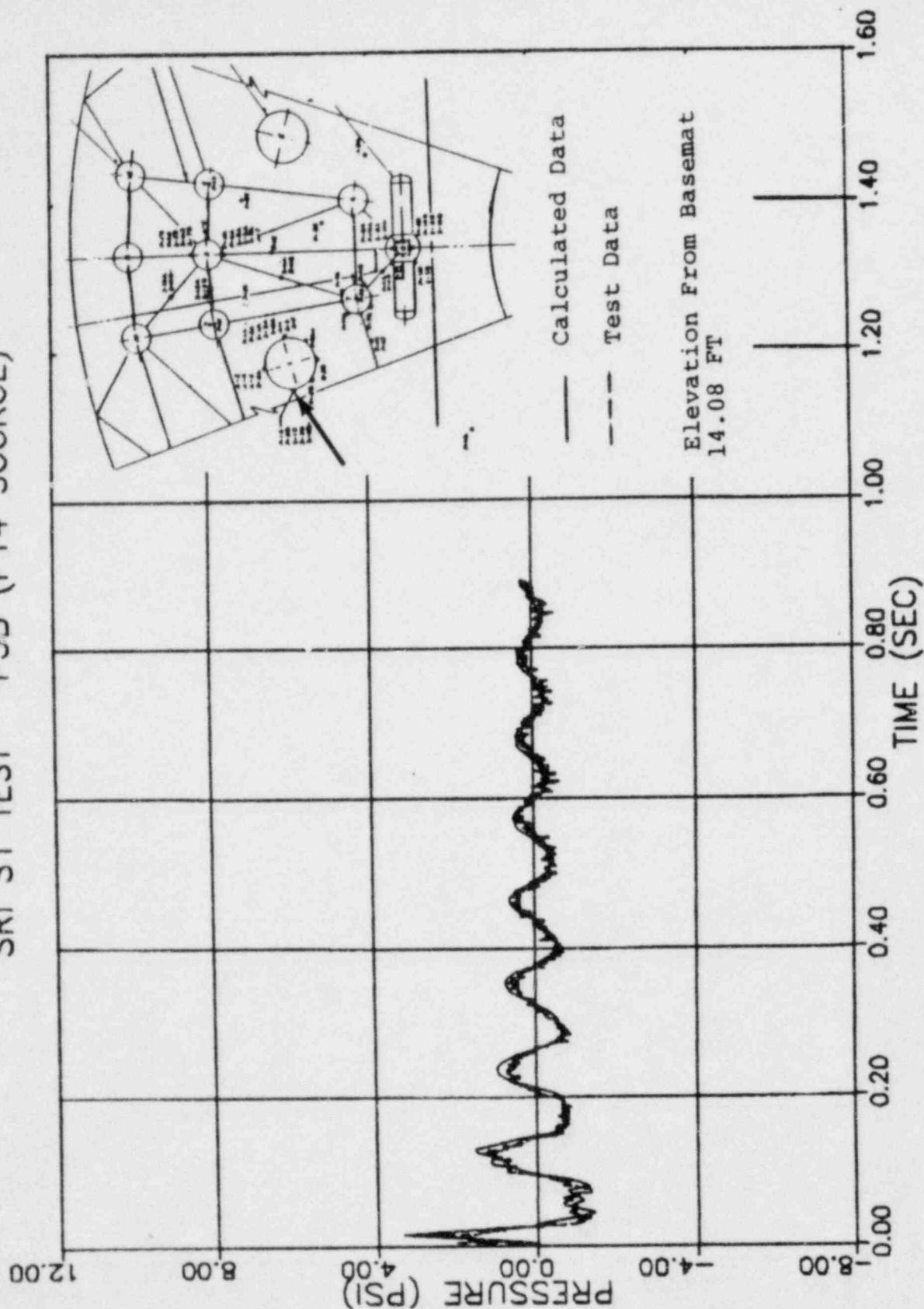
SUSQUEHANNA STEAM ELECTRIC STATION
UNITS 1 AND 2
DESIGN ASSESSMENT REPORT

REV. 6, 4/82

COMPARISON OF PREDICTED PRESSURE
TIME HISTORY WITH TEST
DATA - SENSOR P2A - TEST S1

FIGURE J-7

SRI S1 TEST P3B (P14 SOURCE)



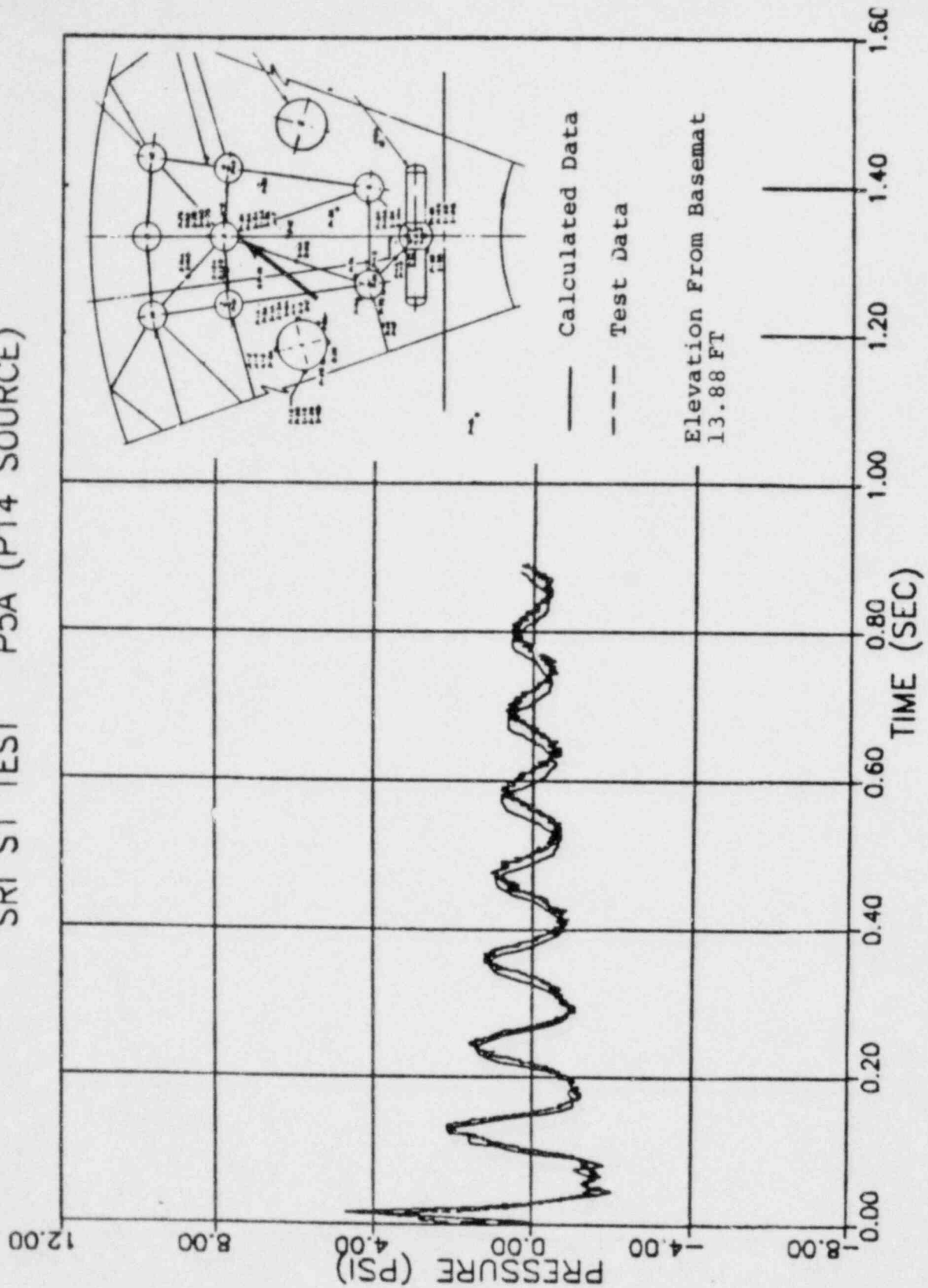
REV. 6, 4/82

SUSQUEHANNA STEAM ELECTRIC STATION UNITS 1 AND 2 DESIGN ASSESSMENT REPORT

COMPARISON OF PREDICTED PRESSURE
TIME HISTORY WITH TEST
DATA - SENSOR P3B - TEST S1

FIGURE J-8

SRI S1 TEST P5A (P14 SOURCE)



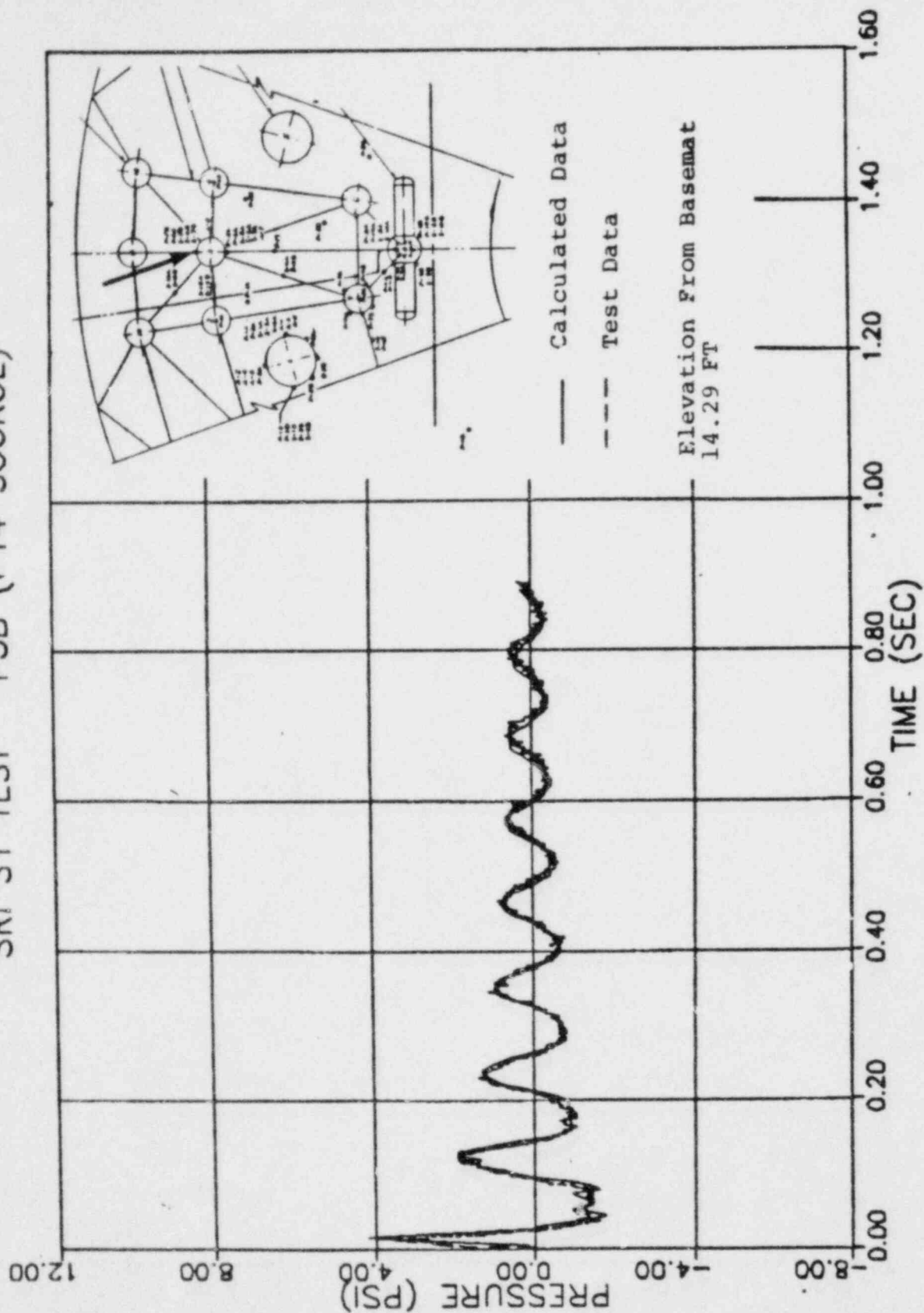
REV. 6, 4/82

SUSQUEHANNA STEAM ELECTRIC STATION UNITS 1 AND 2 DESIGN ASSESSMENT REPORT

COMPARISON OF PREDICTED PRESSURE
TIME HISTORY WITH TEST
DATA - SENSOR P5A - TEST S1

FIGURE J-9

SRI S1 TEST P5B (P14 SOURCE)



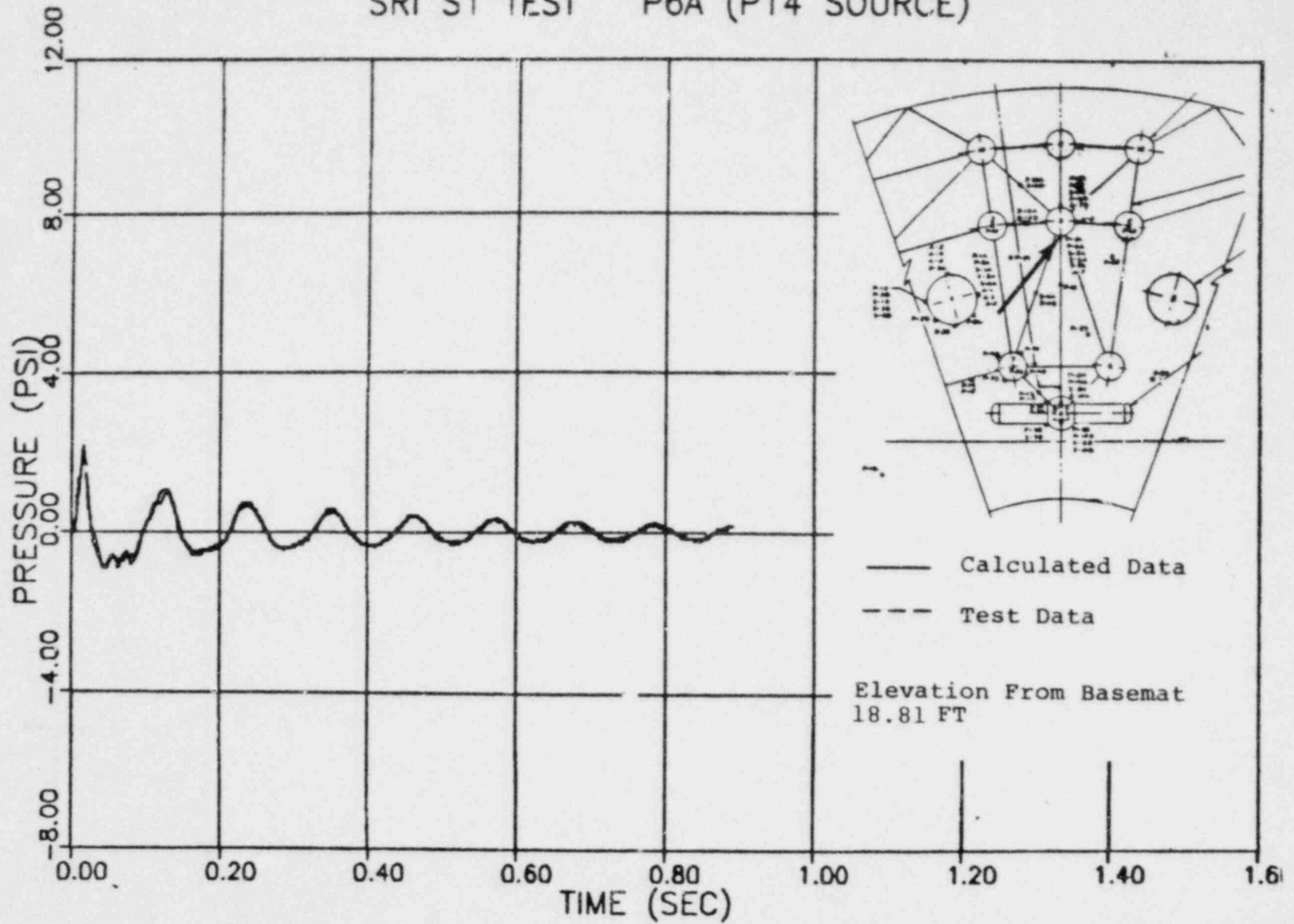
REV. 6, 4/82

SUSQUEHANNA STEAM ELECTRIC STATION
UNITS 1 AND 2
DESIGN ASSESSMENT REPORT

COMPARISON OF PREDICTED PRESSURE
TIME HISTORY WITH TEST
DATA - SENSOR P5B - TEST S1

FIGURE J-10

SRI S1 TEST P6A (P14 SOURCE)

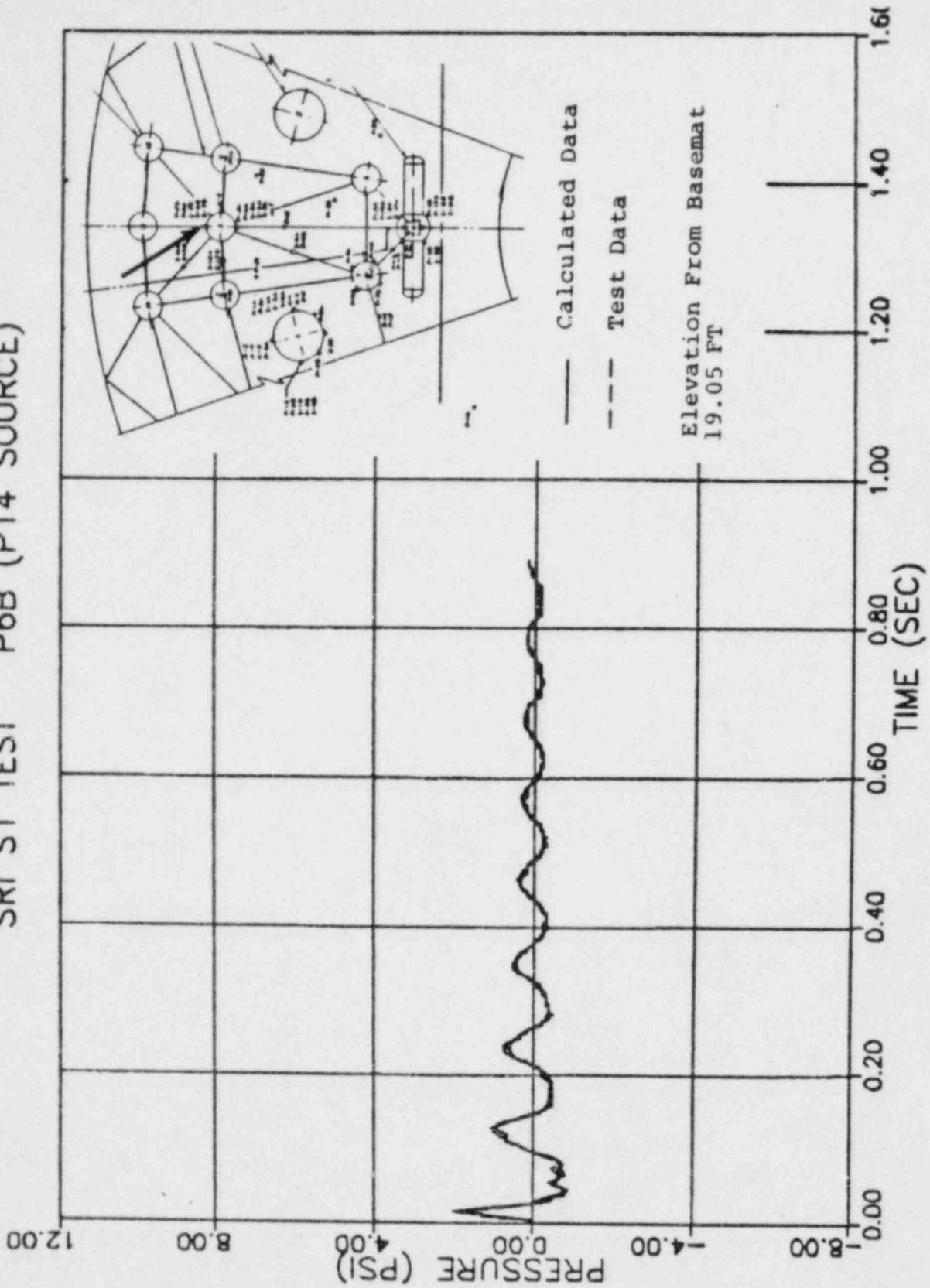


REV. 6, 4/82

SUSQUEHANNA STEAM ELECTRIC STATION
UNITS 1 AND 2
DESIGN ASSESSMENT REPORT

COMPARISON OF PREDICTED PRESSURE
TIME HISTORY WITH TEST
DATA - SENSOR P6A - TEST S1
FIGURE 1-11

SRI S1 TEST P6B (P14 SOURCE)



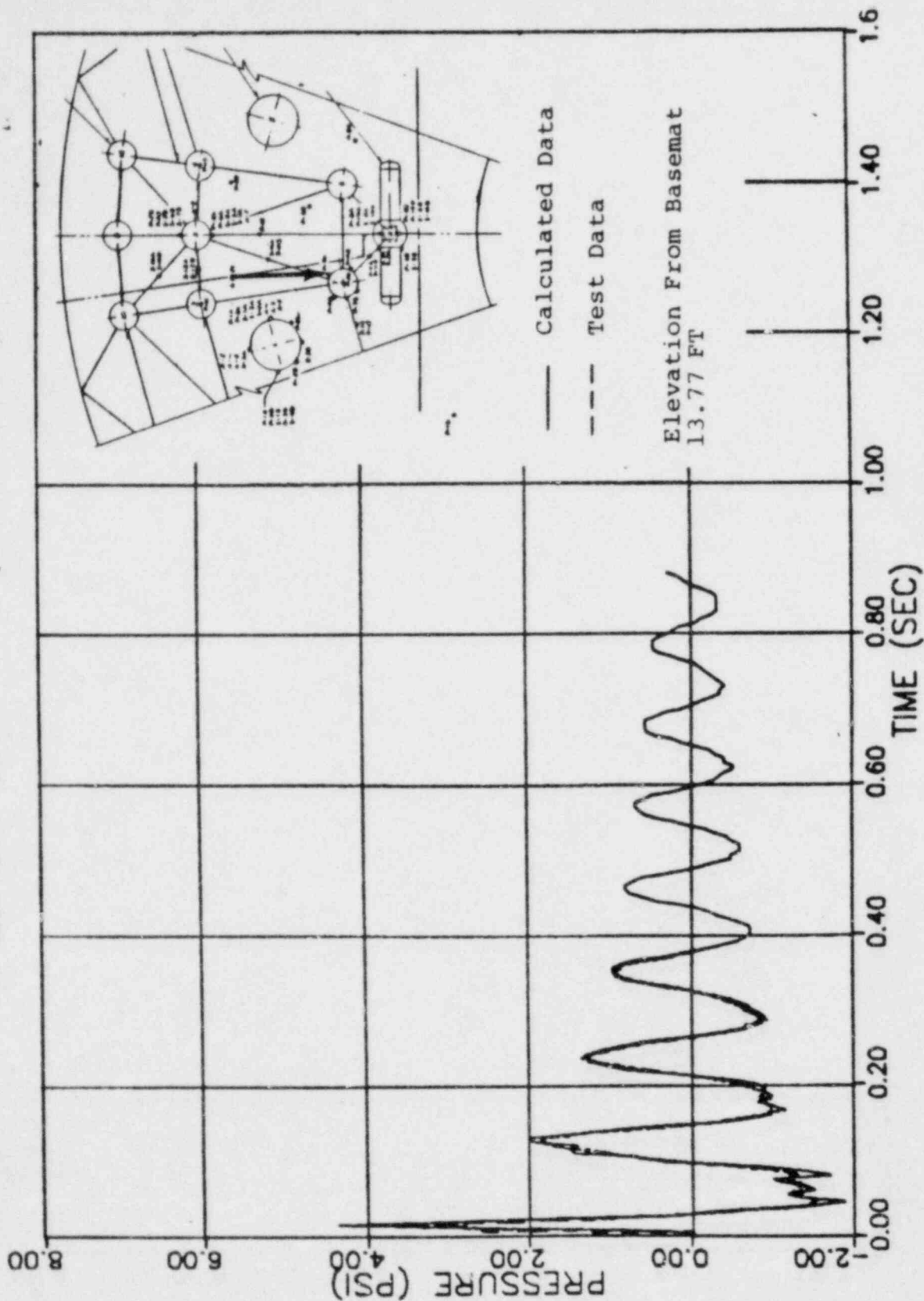
REV. 6, 4/82

SUSQUEHANNA STEAM ELECTRIC STATION
UNITS 1 AND 2
DESIGN ASSESSMENT REPORT

COMPARISON OF PREDICTED PRESSURE
TIME HISTORY WITH TEST
DATA - SENSOR P6B - TEST S1

FIGURE J-12

SRI S1 TEST P7A (P14 SOURCE)



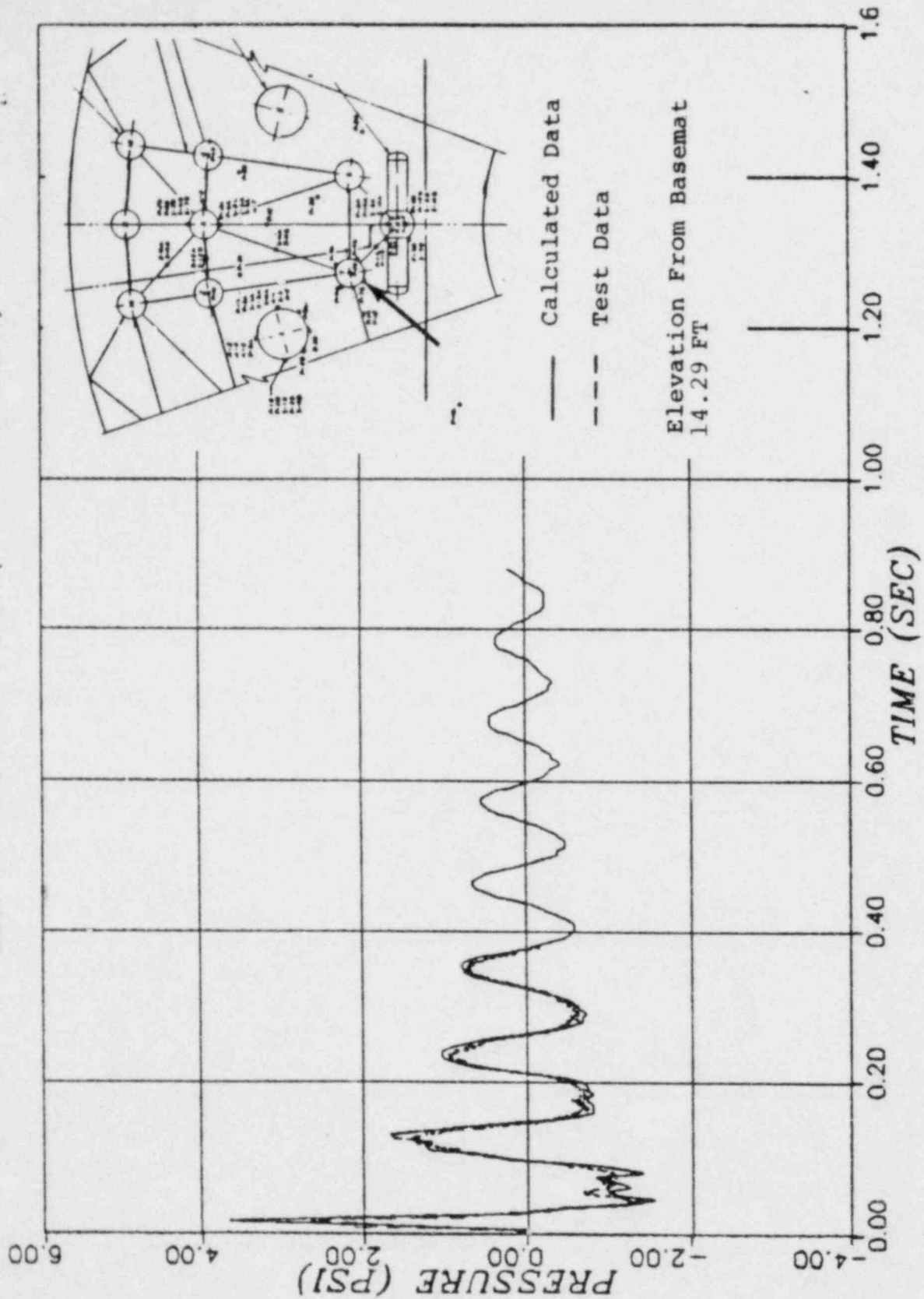
REV. 6, 4/82

SUSQUEHANNA STEAM ELECTRIC STATION
UNITS 1 AND 2
DESIGN ASSESSMENT REPORT

COMPARISON OF PREDICTED PRESSURE
TIME HISTORY WITH TEST
DATA - SENSOR P7A - TEST S1

FIGURE J-13

SRI S1 TEST P7B (P14 SOURCE)



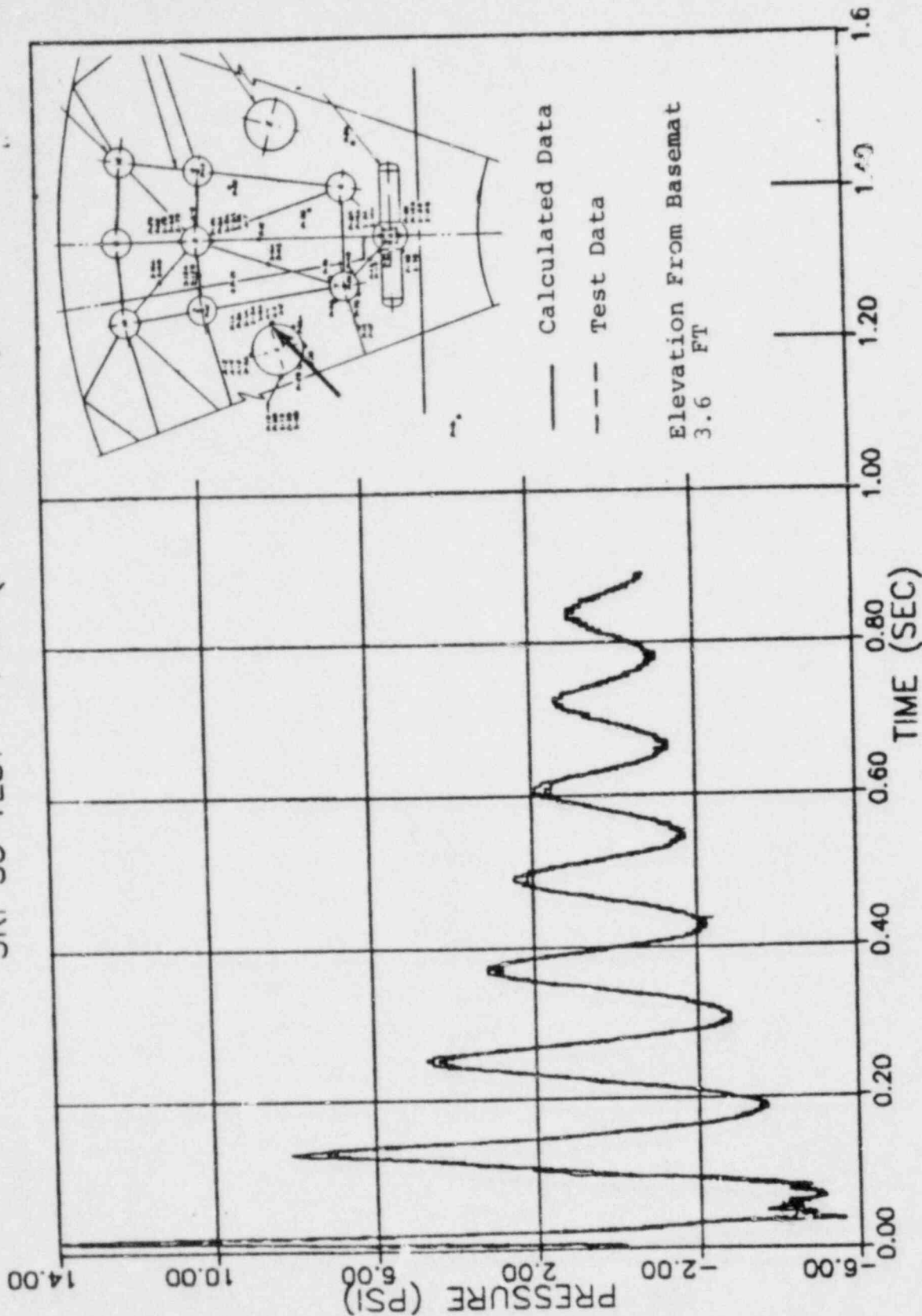
REV. 6, 4/82

SUSQUEHANNA STEAM ELECTRIC STATION
UNITS 1 AND 2
DESIGN ASSESSMENT REPORT

COMPARISON OF PREDICTED PRESSURE
TIME HISTORY WITH TEST
DATA - SENSOR P7B - TEST S1

FIGURE J-14

SRI S3 TEST P1A (P14 SOURCE)



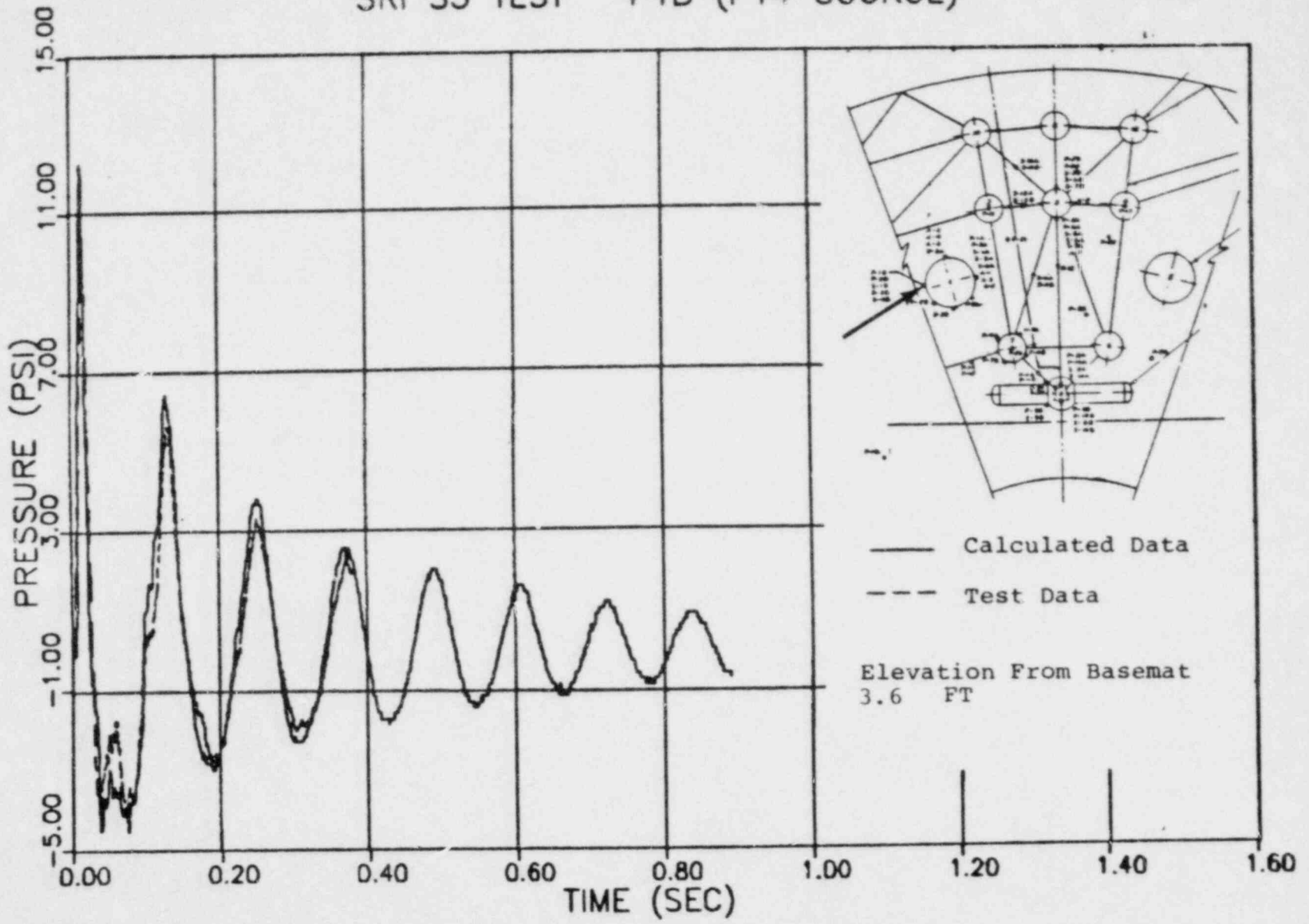
REV. 6, 4/82

SUSQUEHANNA STEAM ELECTRIC STATION UNITS 1 AND 2 DESIGN ASSESSMENT REPORT

COMPARISON OF PREDICTED PRESSURE
 TIME HISTORY WITH TEST
 DATA - SENSOR P1A - TEST S3

FIGURE J-15

SRI S3 TEST P1B (P14 SOURCE)



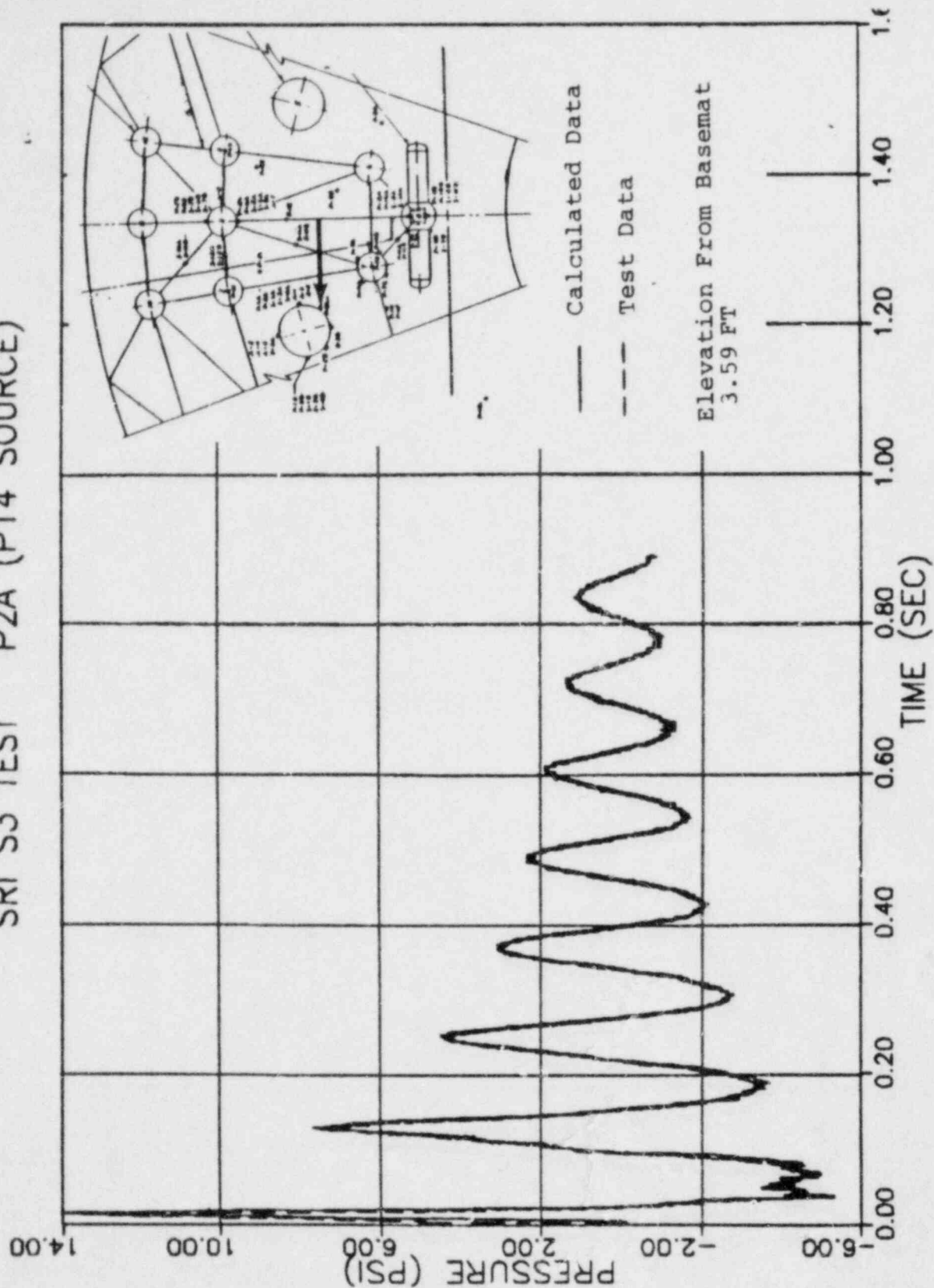
REV. 6, 4/82

SUSQUEHANNA STEAM ELECTRIC STATION
UNITS 1 AND 2
DESIGN ASSESSMENT REPORT

COMPARISON OF PREDICTED PRESSURE
TIME HISTORY WITH TEST
DATA - SENSOR P1B - TEST S3

FIGURE J-16

SRI S3 TEST P2A (P14 SOURCE)



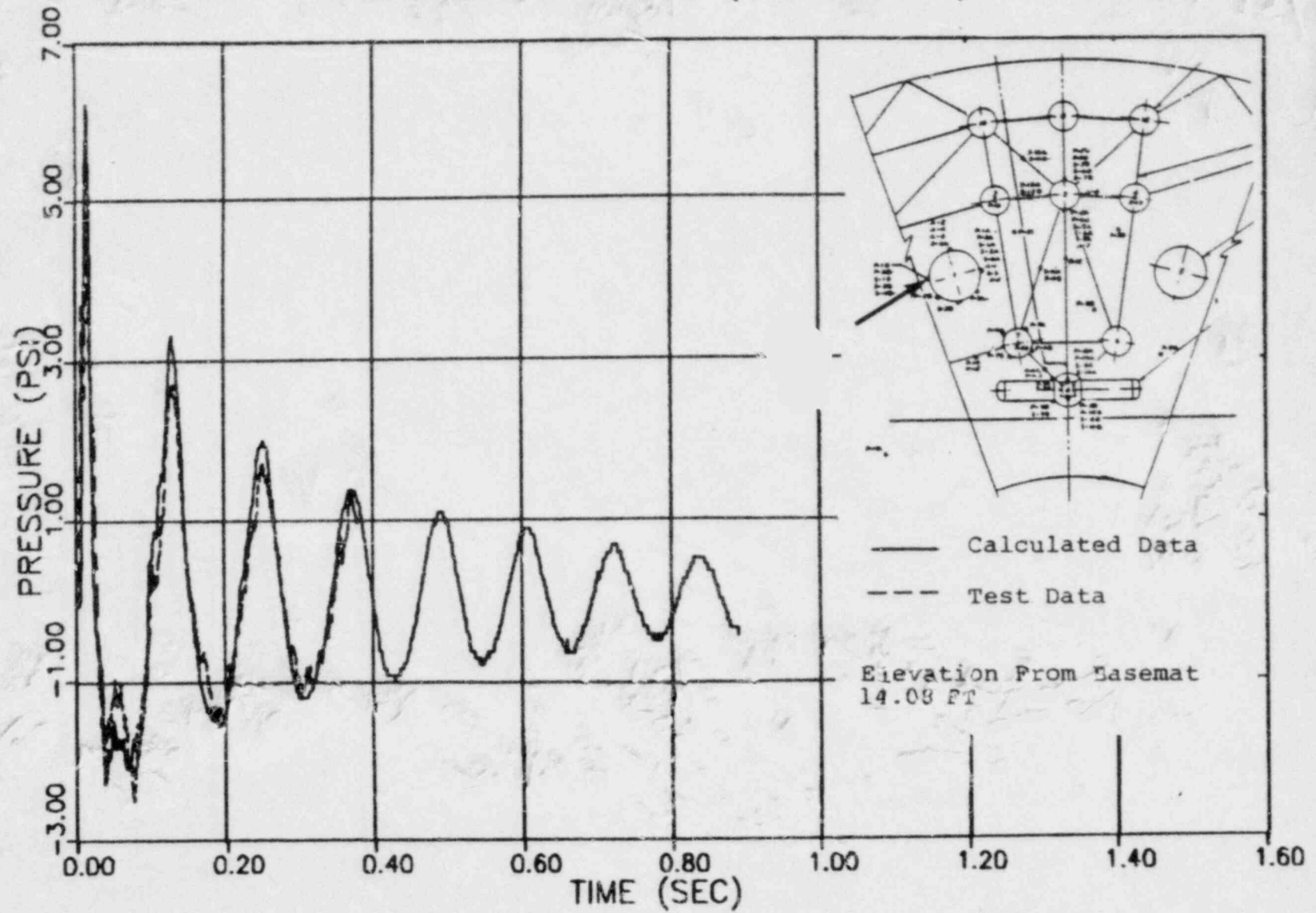
REV. 6, 4/82

SUSQUEHANNA STEAM ELECTRIC STATION
UNITS 1 AND 2
DESIGN ASSESSMENT REPORT

COMPARISON OF PREDICTED PRESSURE
TIME HISTORY WITH TEST
DATA - SENSOR P2A - TEST S3

FIGURE J-17

SRI S3 TEST P3B (P14 SOURCE)



REV. 5, 4/82

SUSQUEHANNA STEAM ELECTRIC STATION

UNITS 1 AND 2

DESIGN ASSESSMENT REPORT

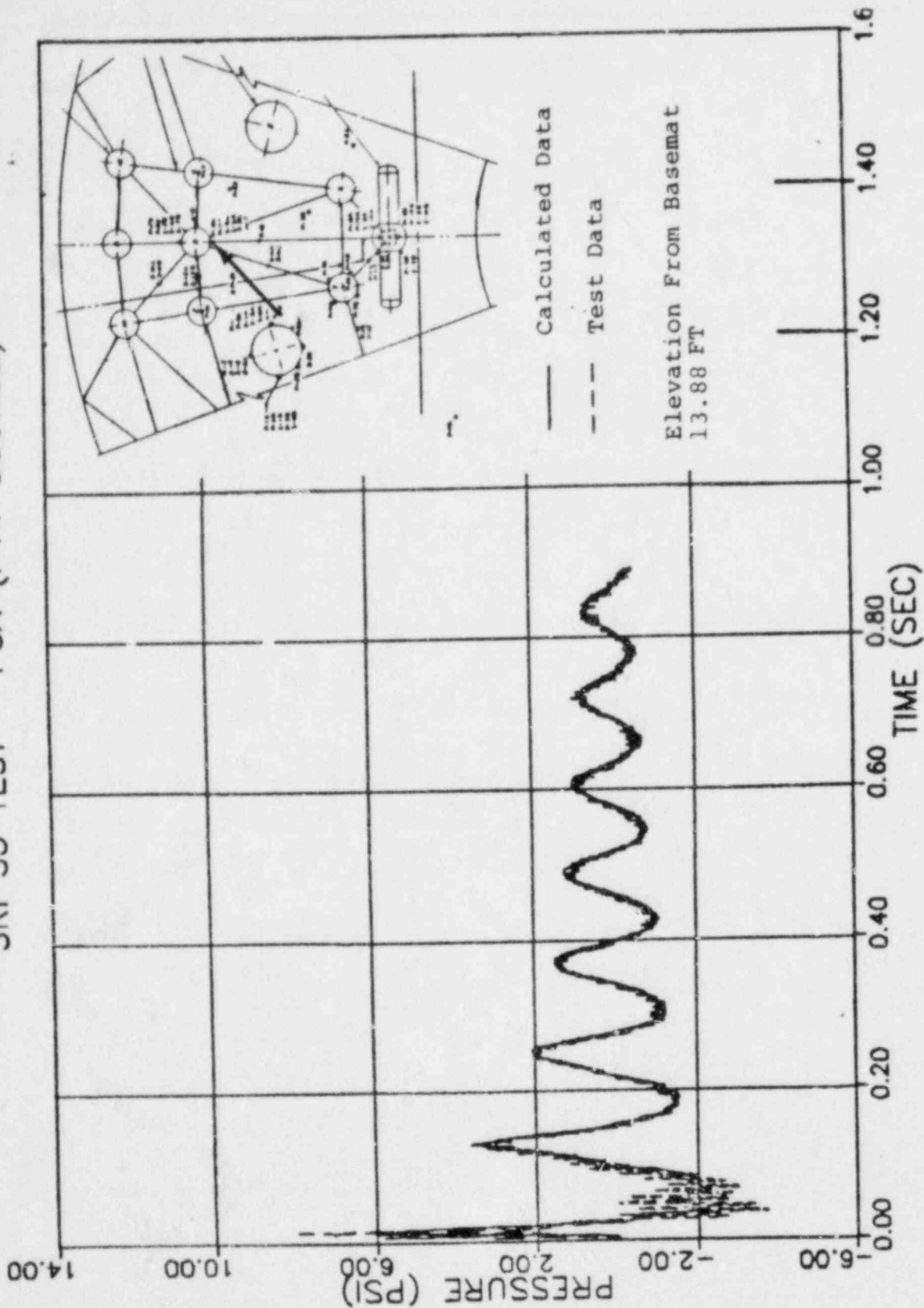
COMPARISON OF PREDICTED PRESSURE

TIME HISTORY WITH TEST

DATA - SENSOR P3B - TEST S3

FIGURE J-18

SRI S3 TEST PGA (P14 SOURCE)

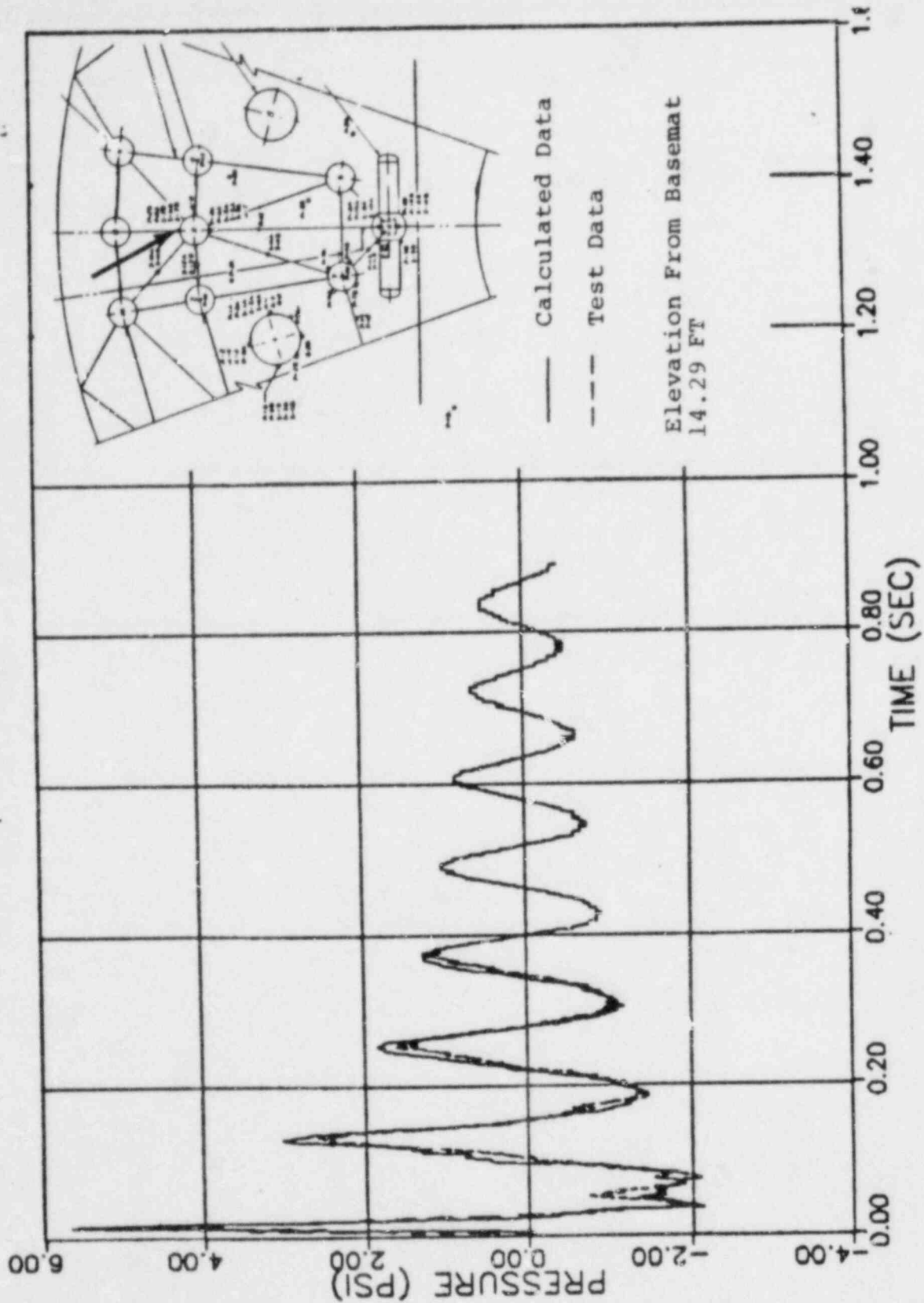


REV. 6, 4/82

SUSQUEHANNA STEAM ELECTRIC STATION
UNITS 1 AND 2
DESIGN ASSESSMENT REPORT

COMPARISON OF PREDICTED PRESSURE
TIME HISTORY WITH TEST
DATA - SENSOR P5A - TEST S3
FIGURE J-19

SRI S3 TEST P5B (P14 SOURCE)

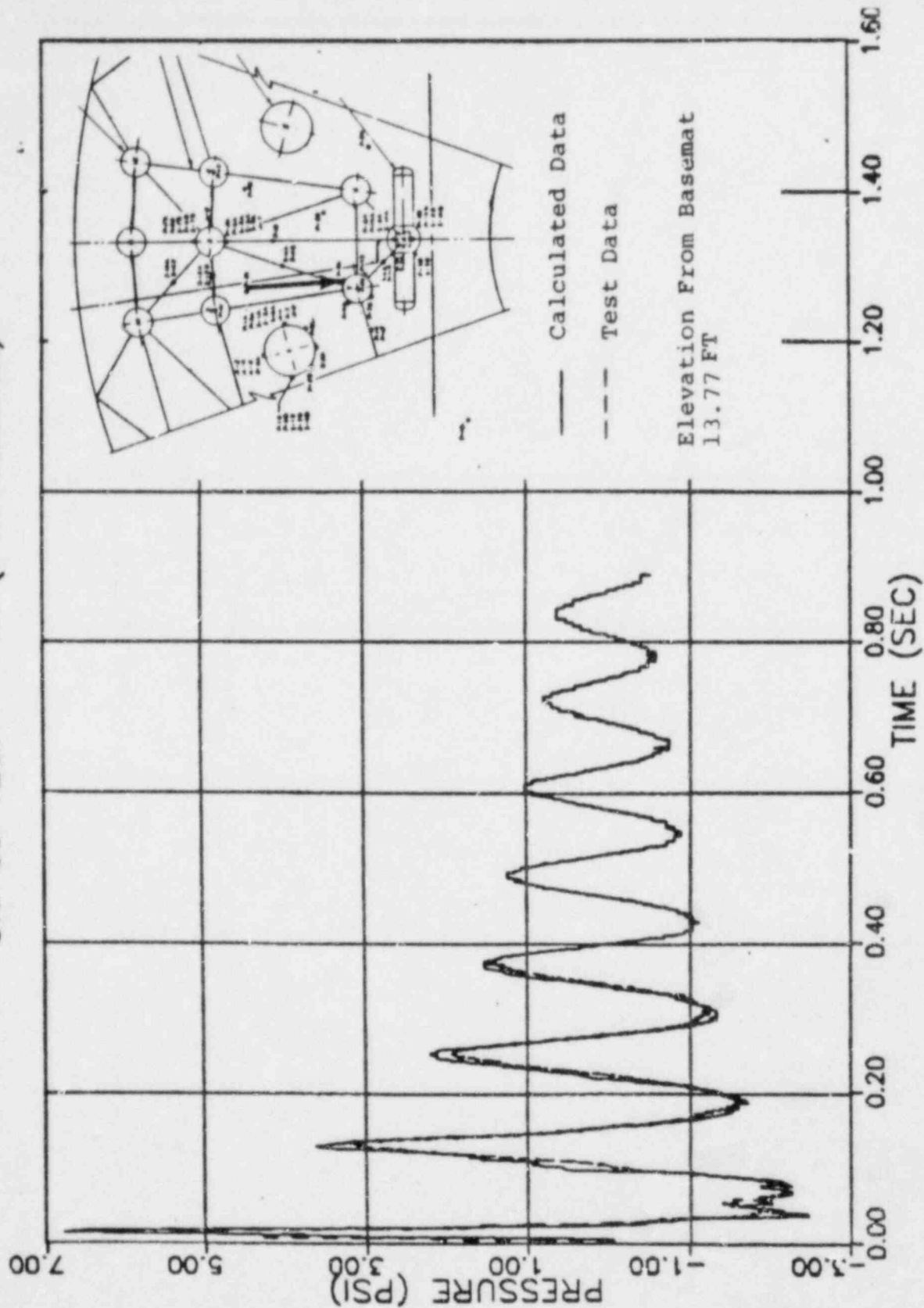


REV. 6, 4/82

SUSQUEHANNA STEAM ELECTRIC STATION
UNITS 1 AND 2
DESIGN ASSESSMENT REPORT

COMPARISON OF PREDICTED PRESSURE
TIME HISTORY WITH TEST
DATA - SENSOR P5B - TEST S3
FIGURE J-20

SRI S3 TEST P7A (P14 SOURCE)



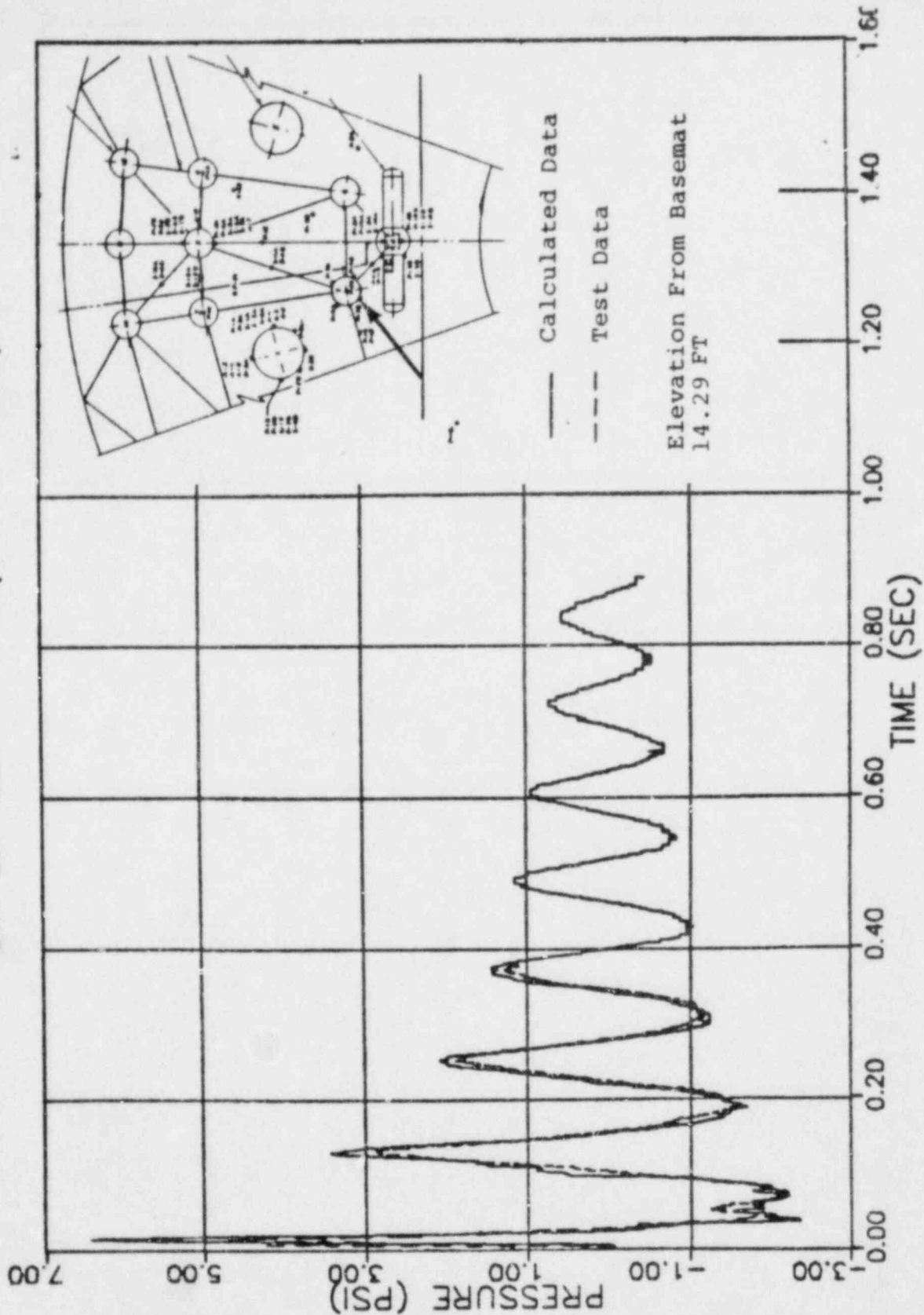
REV. 6, 4/82

SUSQUEHANNA STEAM ELECTRIC STATION
UNITS 1 AND 2
DESIGN ASSESSMENT REPORT

COMPARISON OF PREDICTED PRESSURE
TIME HISTORY WITH TEST
DATA - SENSOR P7A - TEST S3

FIGURE J-21

SRI S3 TEST P7B (P14 SOURCE)



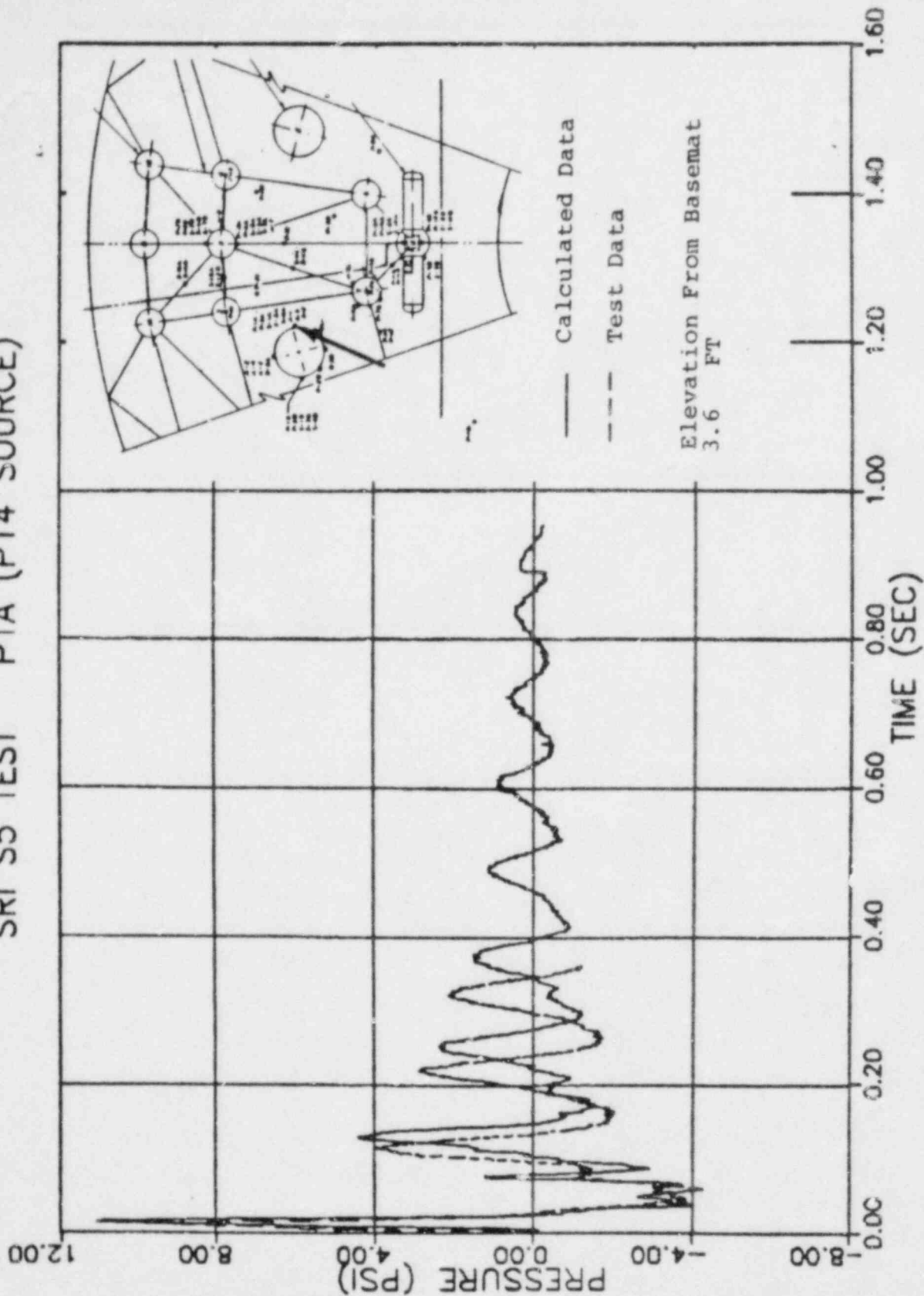
REV. 6, 4/82

SUSQUEHANNA STEAM ELECTRIC STATION
UNITS 1 AND 2
DESIGN ASSESSMENT REPORT

COMPARISON OF PREDICTED PRESSURE
TIME HISTORY WITH TEST
DATA - SENSOR P7B - TEST S3

FIGURE J-22

SRI S5 TEST P1A (P14 SOURCE)



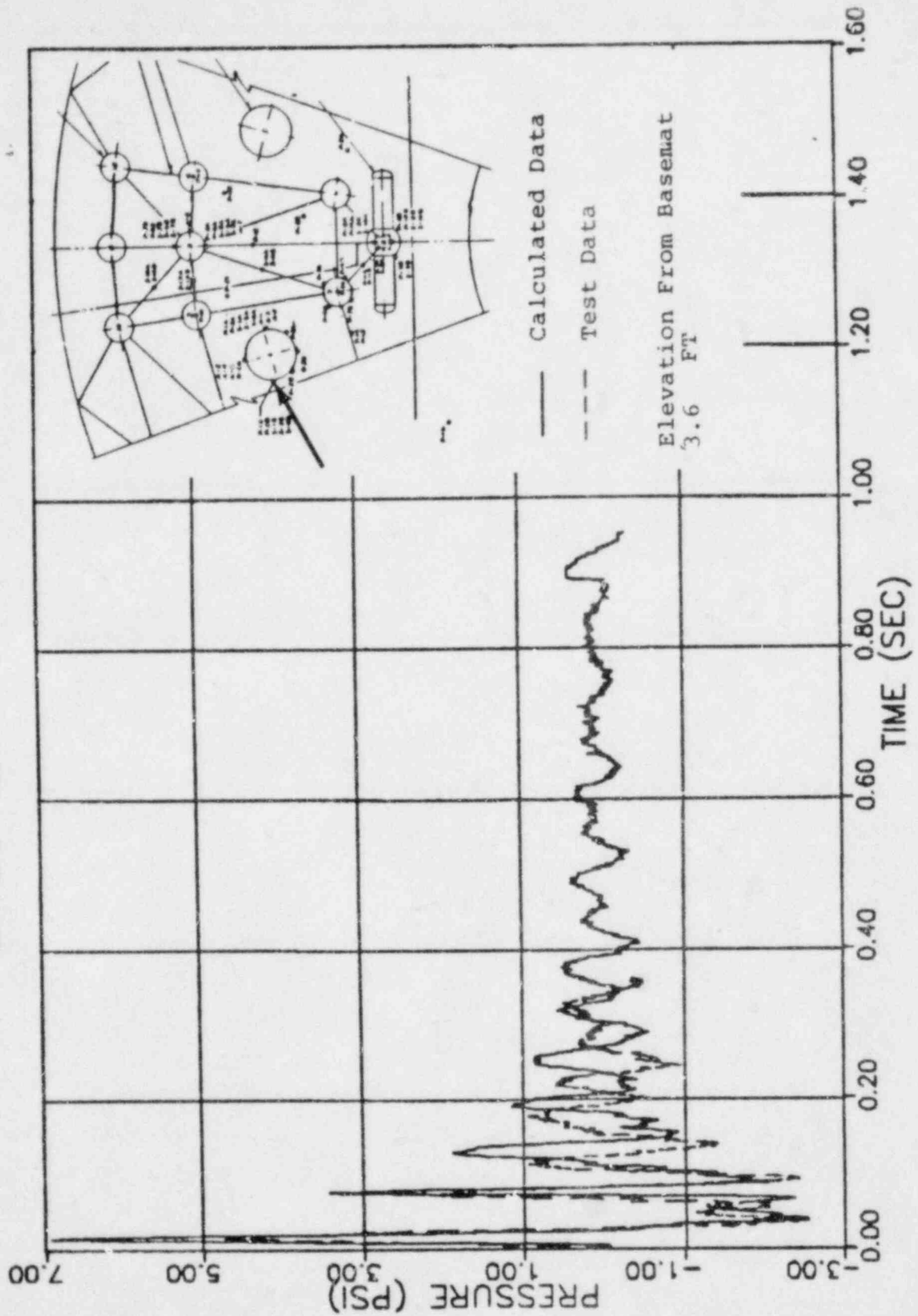
REV. 6, 4/82

SUSQUEHANNA STEAM ELECTRIC STATION
UNITS 1 AND 2
DESIGN ASSESSMENT REPORT

COMPARISON OF PREDICTED PRESSURE
TIME HISTORY WITH TEST
DATA - SENSOR P1A - TEST S5

FIGURE J-23

SRI S5 TEST P1B (P14 SOURCE)



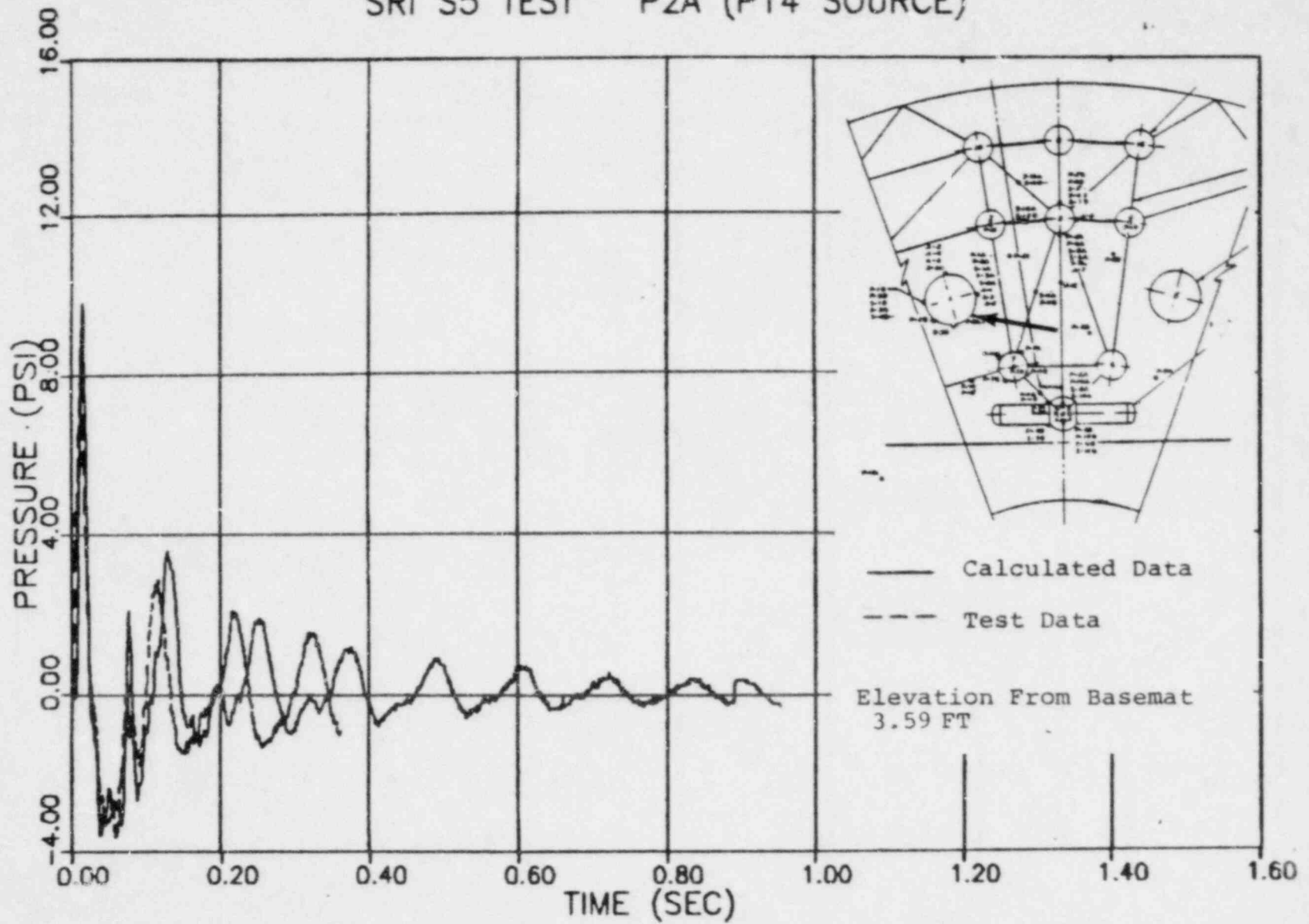
REV. 6, 4/82

SUSQUEHANNA STEAM ELECTRIC STATION
UNITS 1 AND 2
DESIGN ASSESSMENT REPORT

COMPARISON OF PREDICTED PRESSURE
TIME HISTORY WITH TEST
DATA - SENSOR P1B - TEST S5

FIGURE J-24

SRI S5 TEST P2A (P14 SOURCE)



REV. 6, 4/82

SUSQUEHANNA STEAM ELECTRIC STATION
 UNITS 1 AND 2
 DESIGN ASSESSMENT REPORT

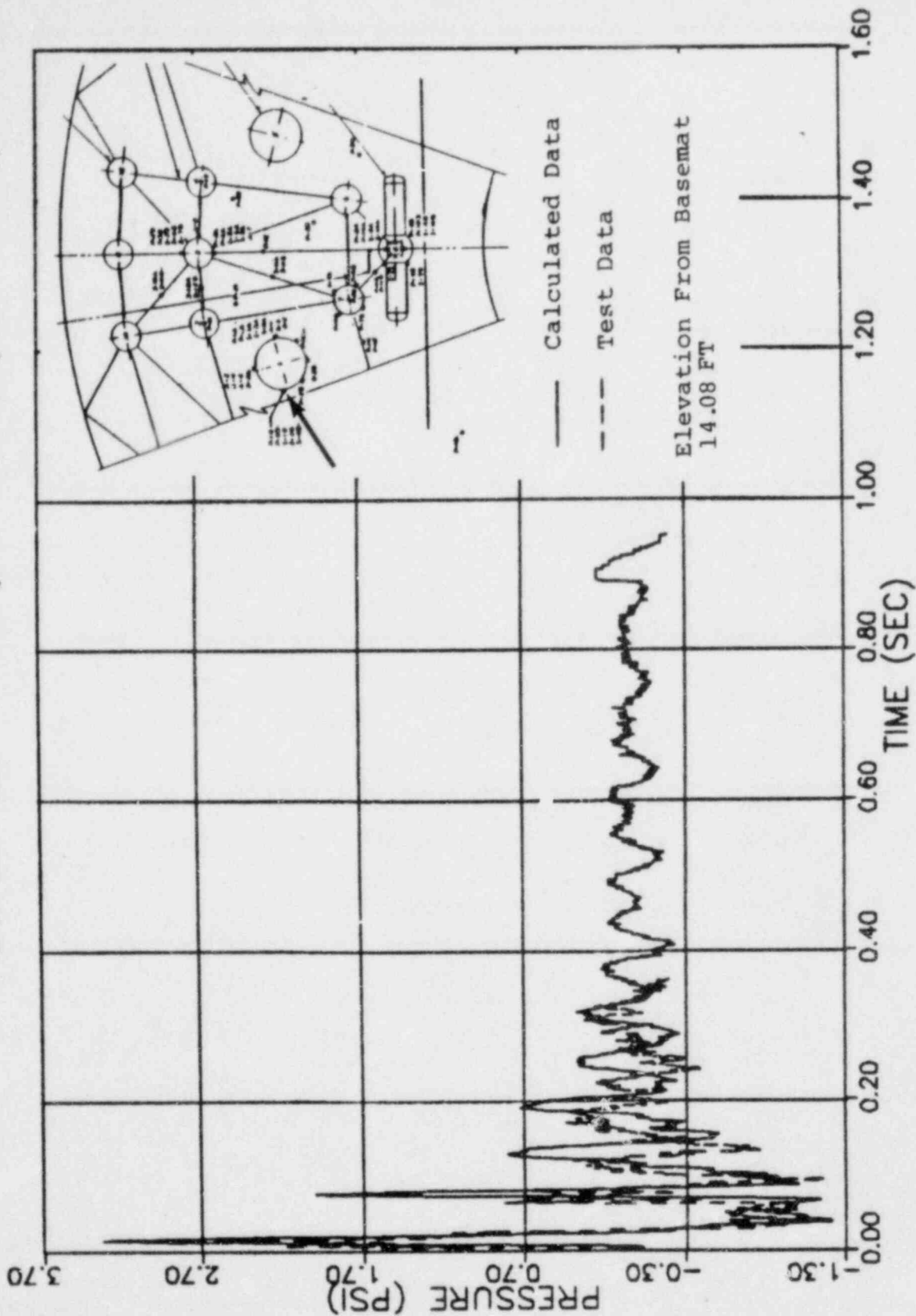
COMPARISON OF PREDICTED PRESSURE

TIME HISTORY WITH TEST

DATA - SENSOR P2A - TEST S5

FIGURE J-25

SRI S5 TEST P3B (P14 SOURCE)



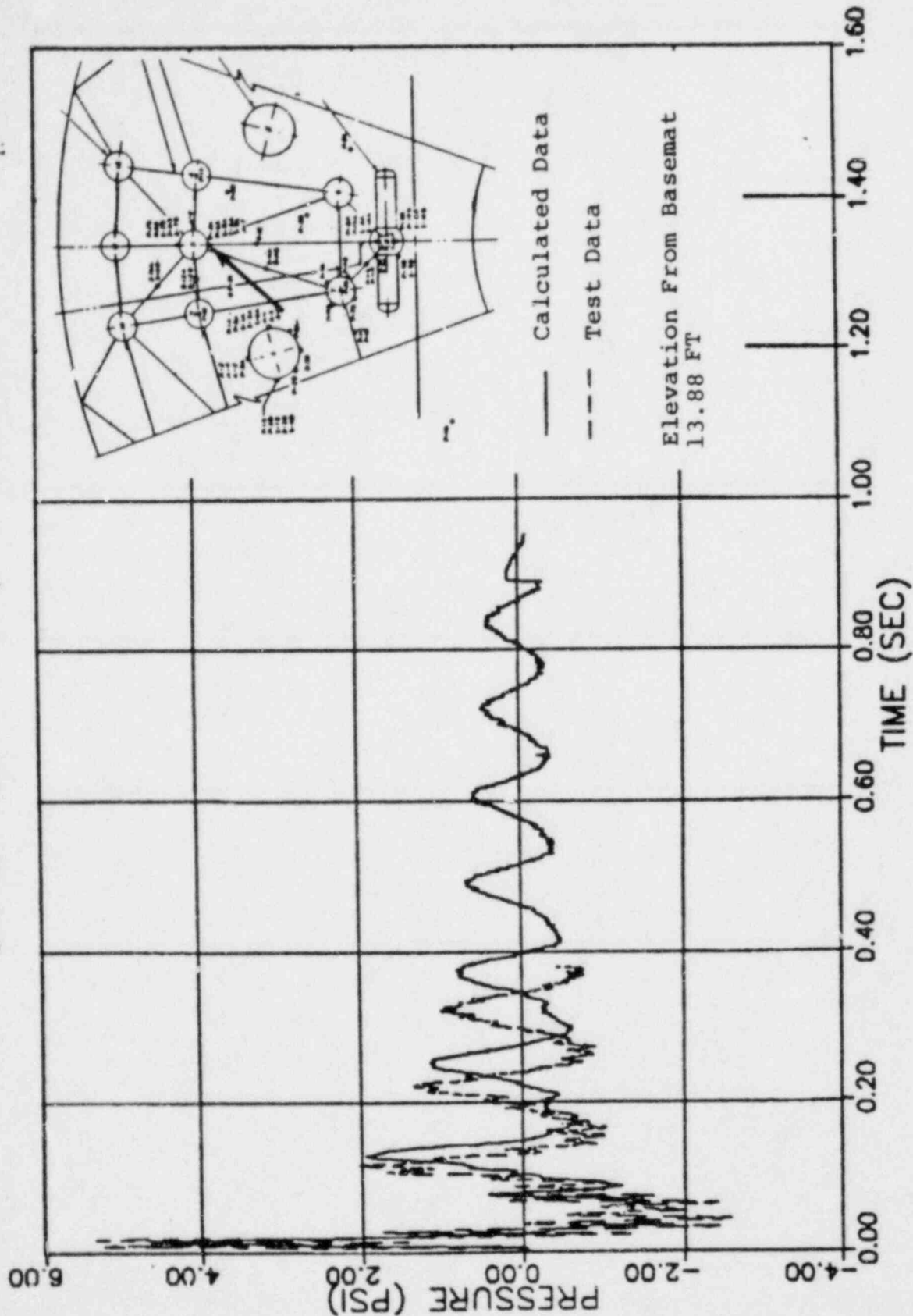
REV. 6, 4/82

SUSQUEHANNA STEAM ELECTRIC STATION
UNITS 1 AND 2
DESIGN ASSESSMENT REPORT

COMPARISON OF PREDICTED PRESSURE
TIME HISTORY WITH TEST
DATA - SENSOR P3B - TEST S5

FIGURE J-26

SRI S5 TEST P5A (P14 SOURCE)

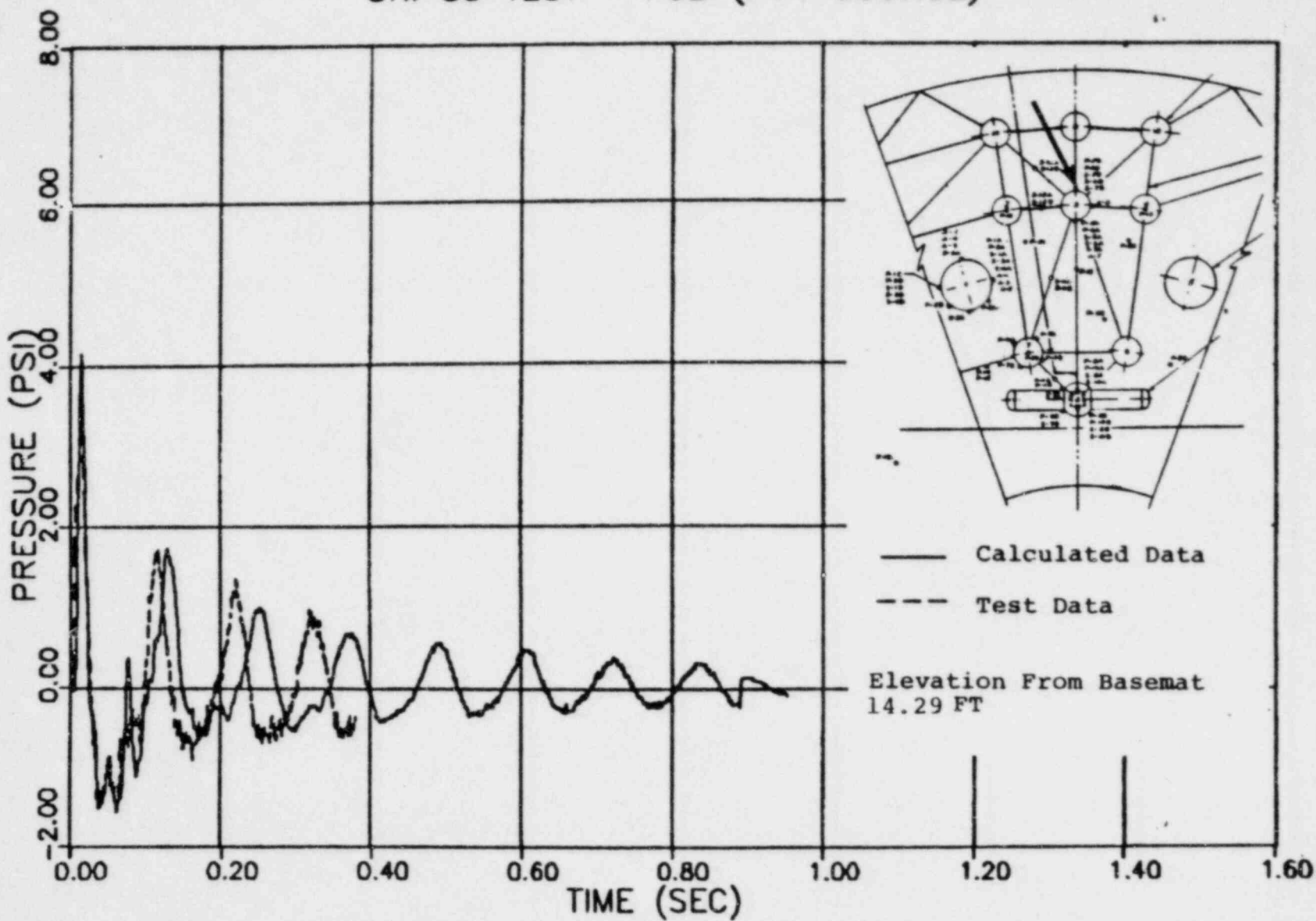


REV. 6, 4/82

SUSQUEHANNA STEAM ELECTRIC STATION
UNITS 1 AND 2
DESIGN ASSESSMENT REPORT

COMPARISON OF PREDICTED PRESSURE
TIME HISTORY WITH TEST
DATA - SENSOR P5A - TEST S5
FIGURE J-27

SRI S5 TEST P5B (P14 SOURCE)



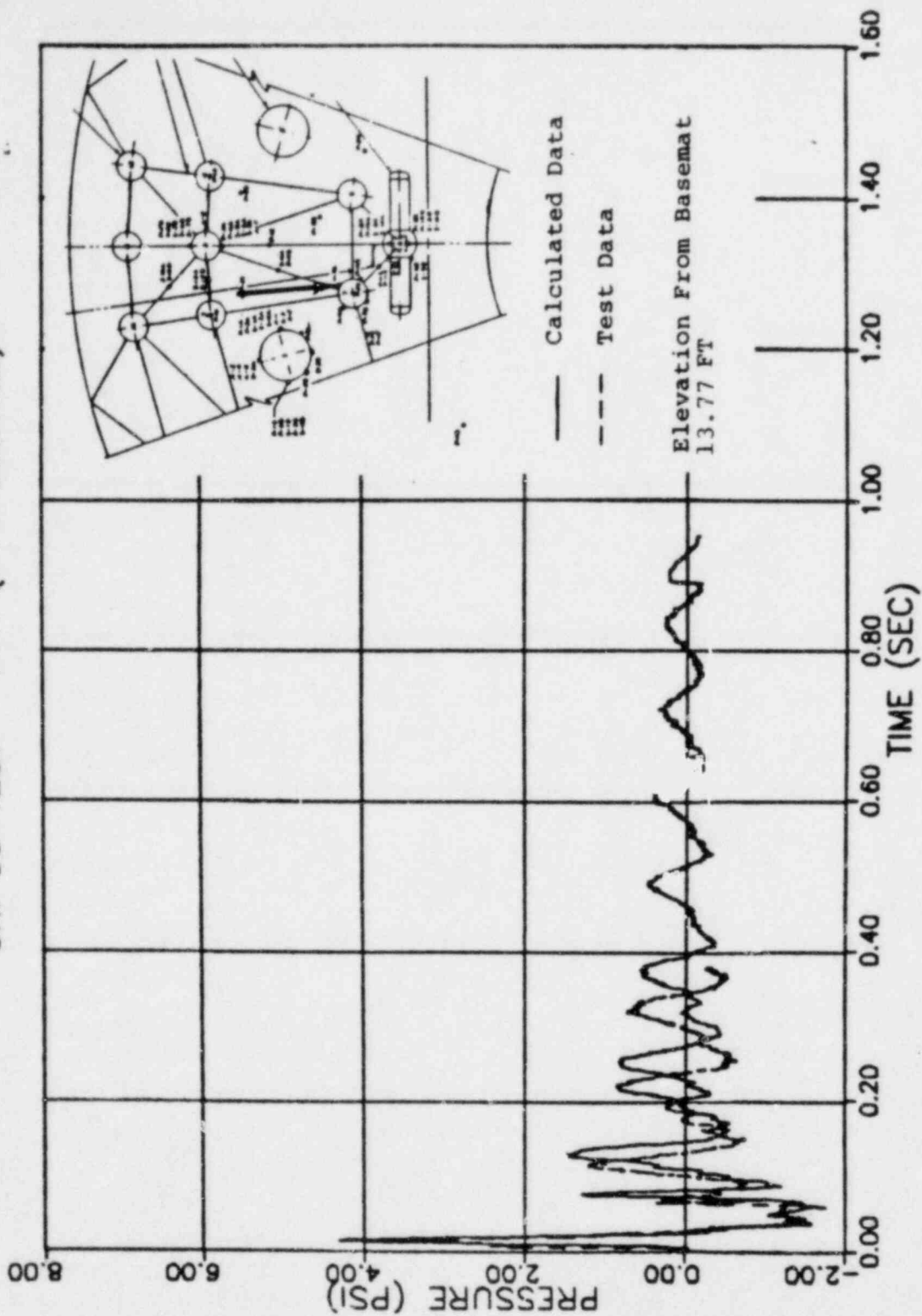
REV. 6, 4/82

SUSQUEHANNA STEAM ELECTRIC STATION
UNITS 1 AND 2
DESIGN ASSESSMENT REPORT

COMPARISON OF PREDICTED PRESSURE
TIME HISTORY WITH TEST
DATA - SENSOR P5B - TEST S5

FIGURE J-23

SRI S5 TEST P7A (P14 SOURCE)

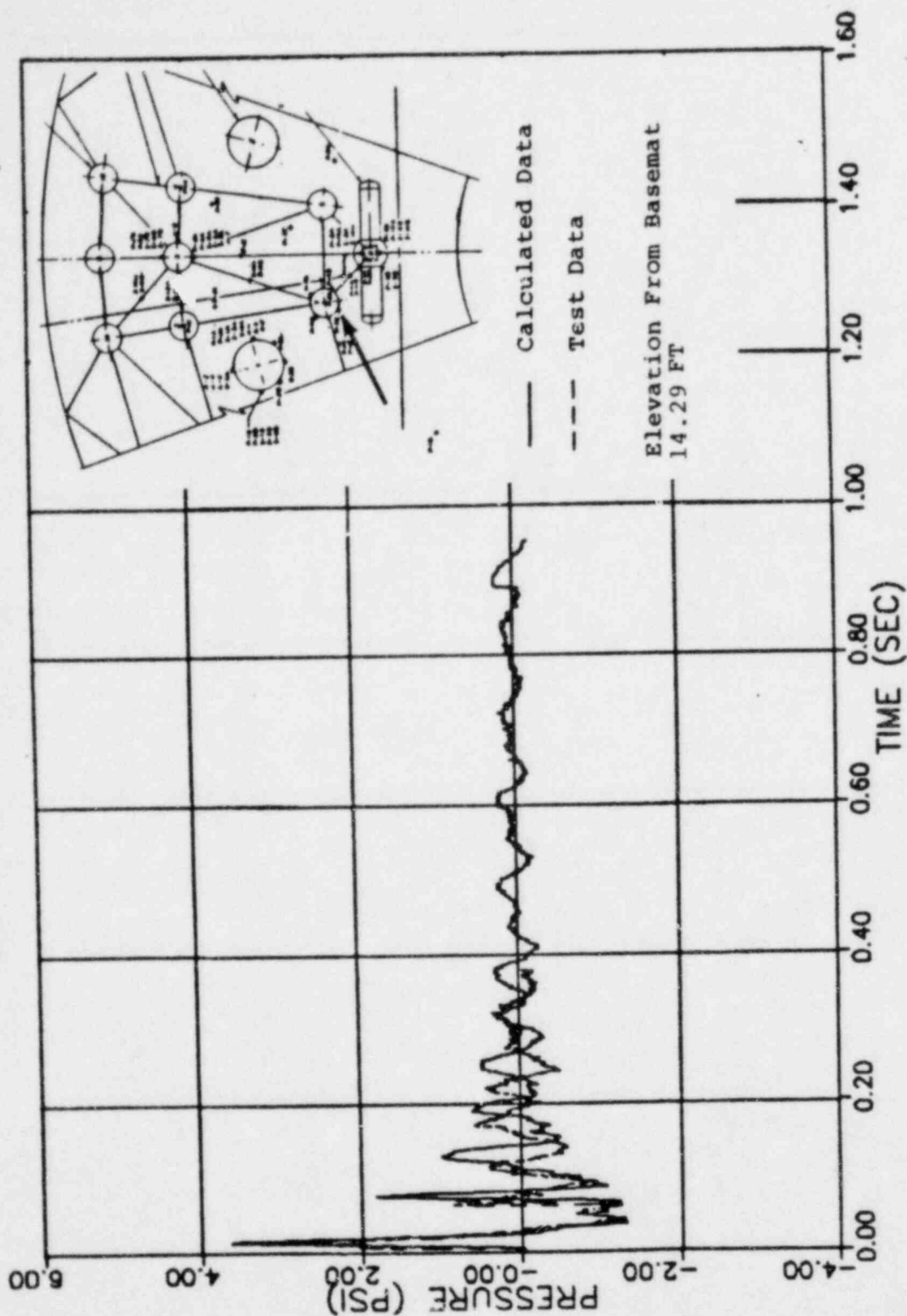


REV. 6, 4/82

SUSQUEHANNA STEAM ELECTRIC STATION
 UNITS 1 AND 2
 DESIGN ASSESSMENT REPORT

COMPARISON OF PREDICTED PRESSURE
 TIME HISTORY WITH TEST
 DATA - SENSOR P7A - TEST S5
 FIGURE J-29

SRI S5 TEST P7B (P14 SOURCE)



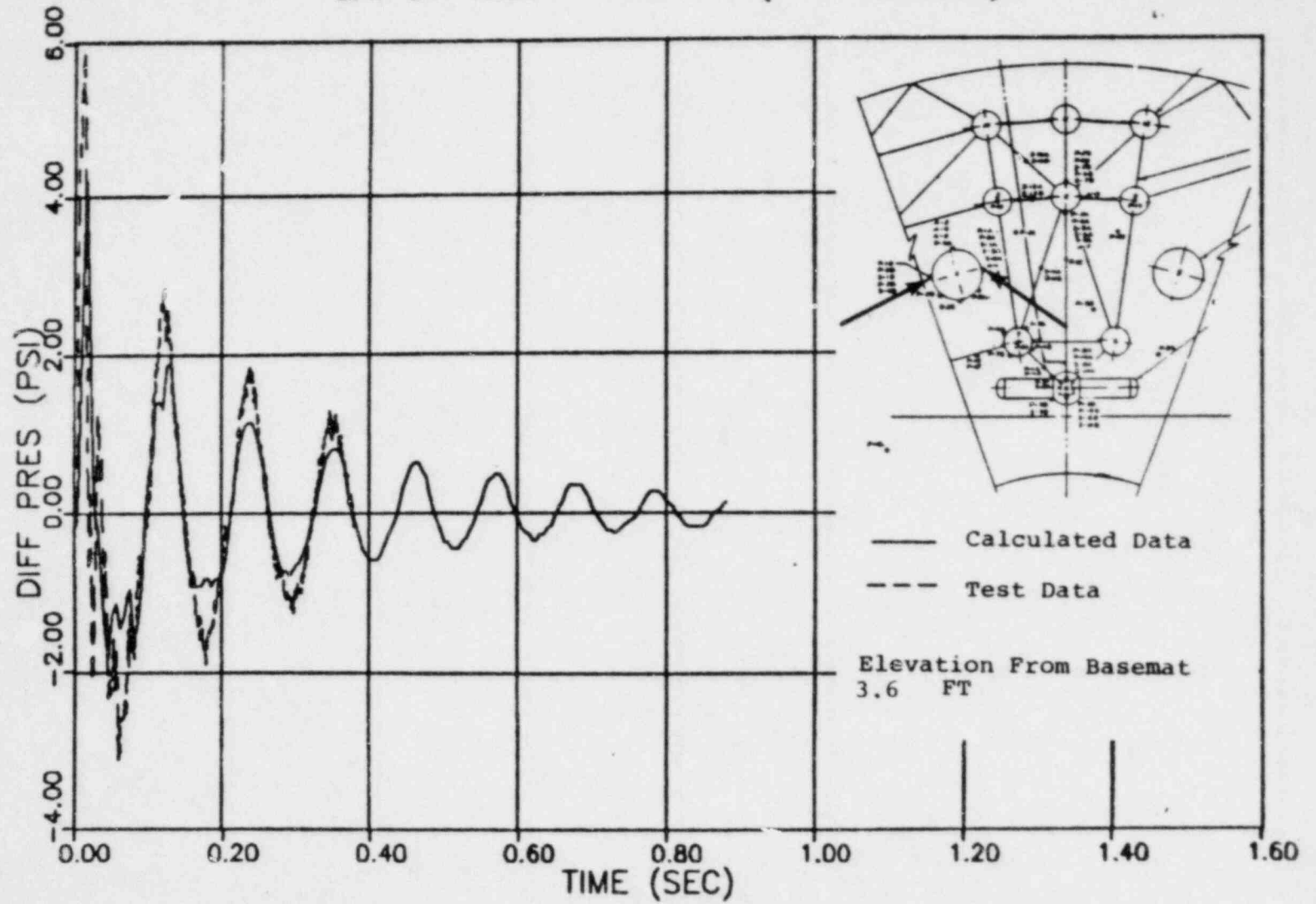
REV. 6, 4/82

**SUSQUEHANNA STEAM ELECTRIC STATION
UNITS 1 AND 2
DESIGN ASSESSMENT REPORT**

COMPARISON OF PREDICTED PRESSURE
TIME HISTORY WITH TEST
DATA - SENSOR P7B - TEST S5

FIGURE J-30

SRI S1 TEST P1A-1B (P14 SOURCE)

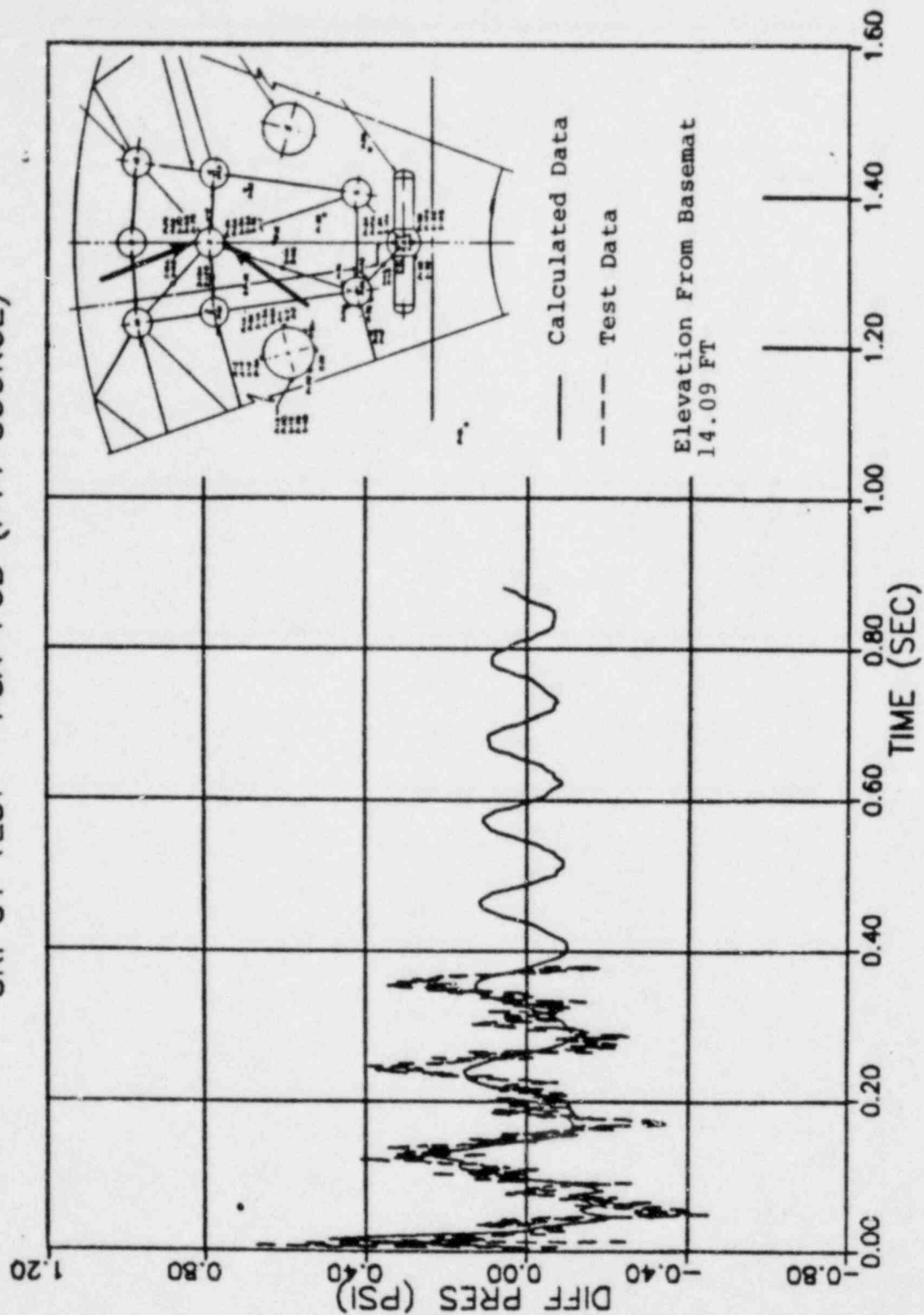


REV. 6, 4/82

SUSQUEHANNA STEAM ELECTRIC STATION
UNITS 1 AND 2
DESIGN ASSESSMENT REPORT

COMPARISON OF PREDICTED
DIFFERENTIAL PRESSURE TIME HISTORY
WITH TEST
DATA - SENSOR P1A-1B - TEST S1
FIGURE J-31

SRI S1 TEST P5A-P5B (P14 SOURCE)

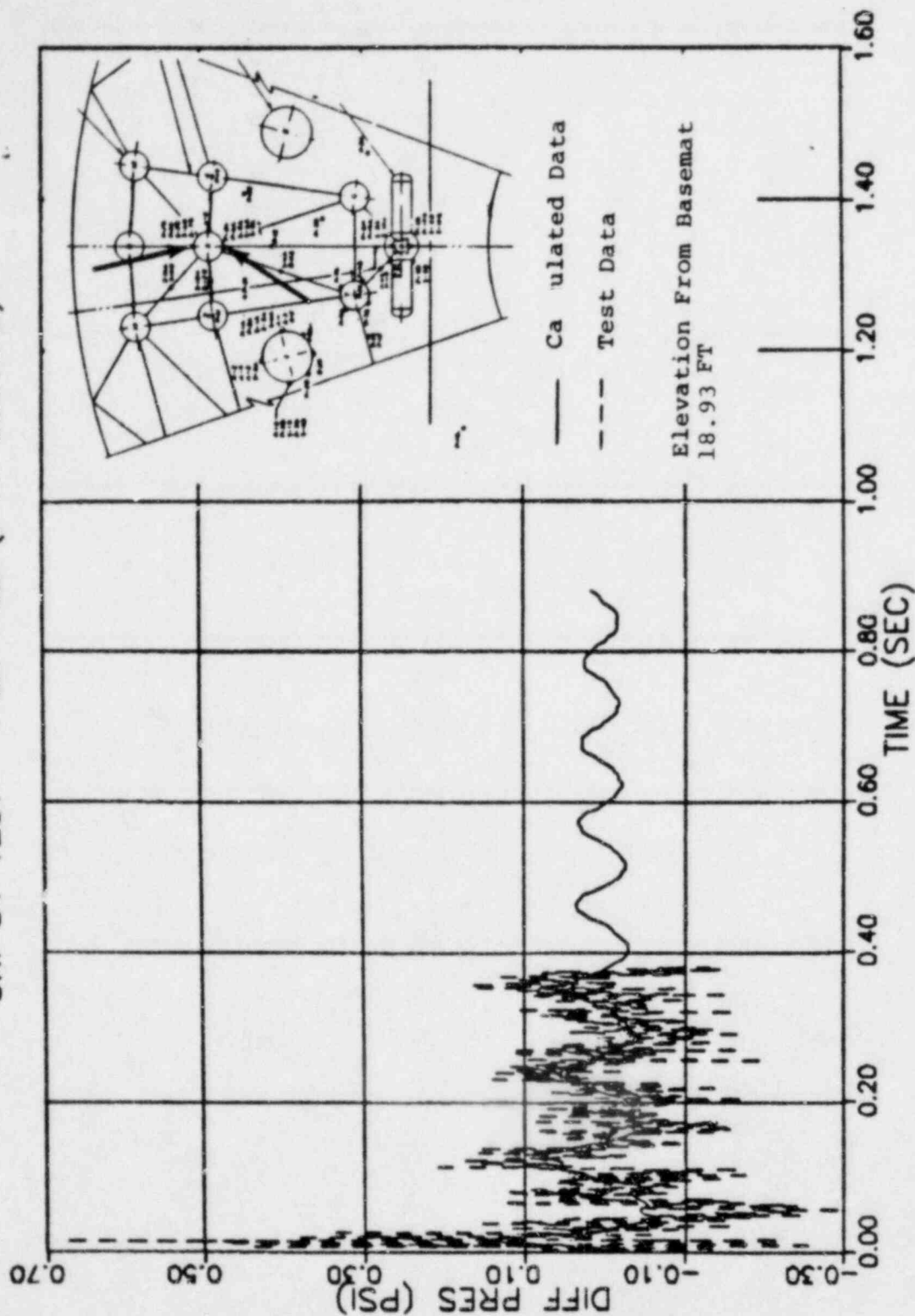


REV. 6, 4/82

SUSQUEHANNA & TEAM ELECTRIC STATION
UNITS 1 AND 2
DESIGN ASSESSMENT REPORT

COMPARISON OF PREDICTED
DIFFERENTIAL PRESSURE TIME HISTORY
WITH TEST
DATA - SENSOR P5A-P5B - TEST S1
FIGURE J-32

SRI S1 TEST P6A-P6B (P14 SOURCE)

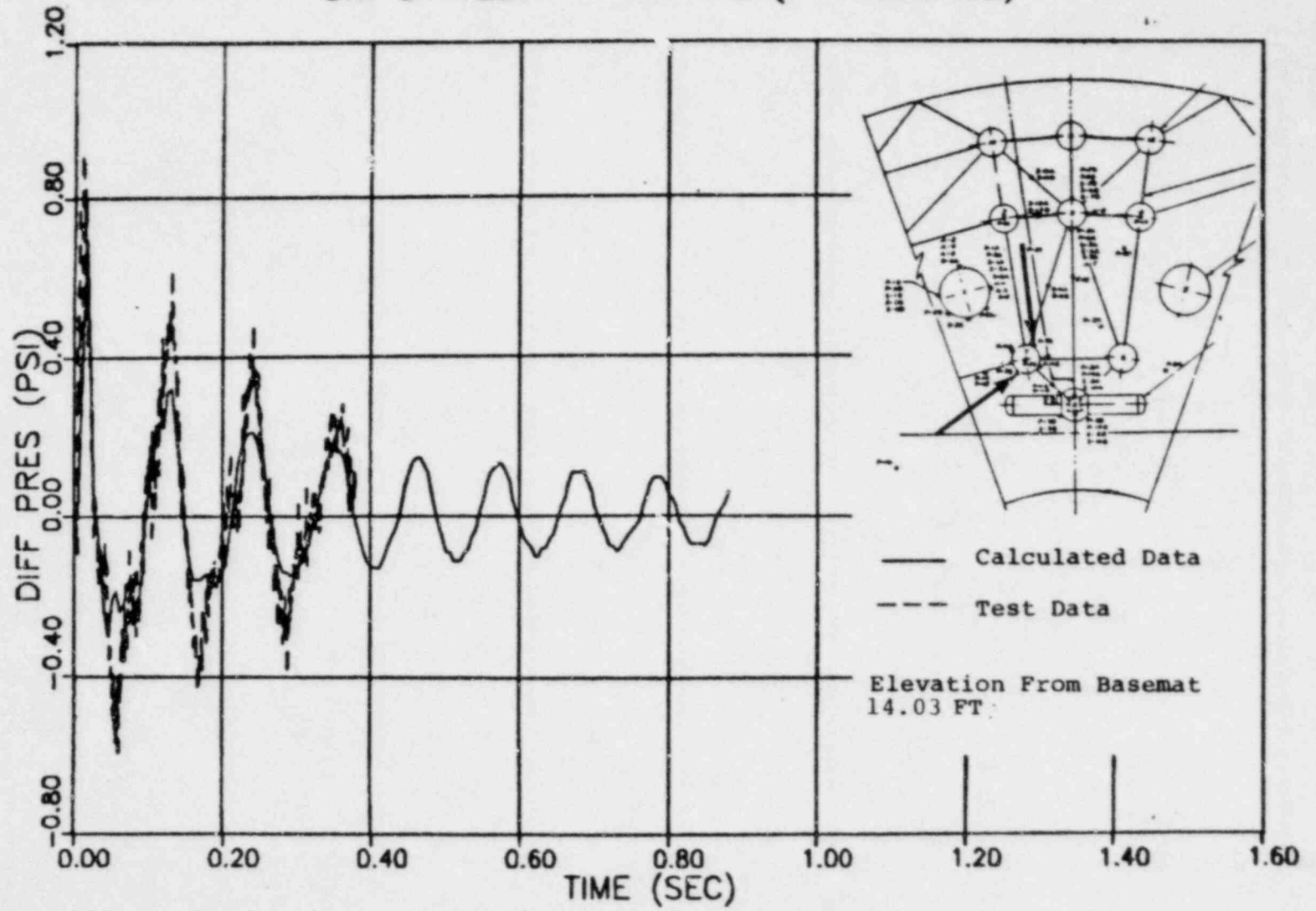


REV. 6, 4/82

SUSQUEHANNA STEAM ELECTRIC STATION
UNITS 1 AND 2
DESIGN ASSESSMENT REPORT

COMPARISON OF PREDICTED
DIFFERENTIAL PRESSURE TIME HISTORY
WITH TEST
DATA - SENSOR P6A-P6B - TEST S1
FIGURE J-33

SRI S1 TEST P7A-P7B (P14 SOURCE)

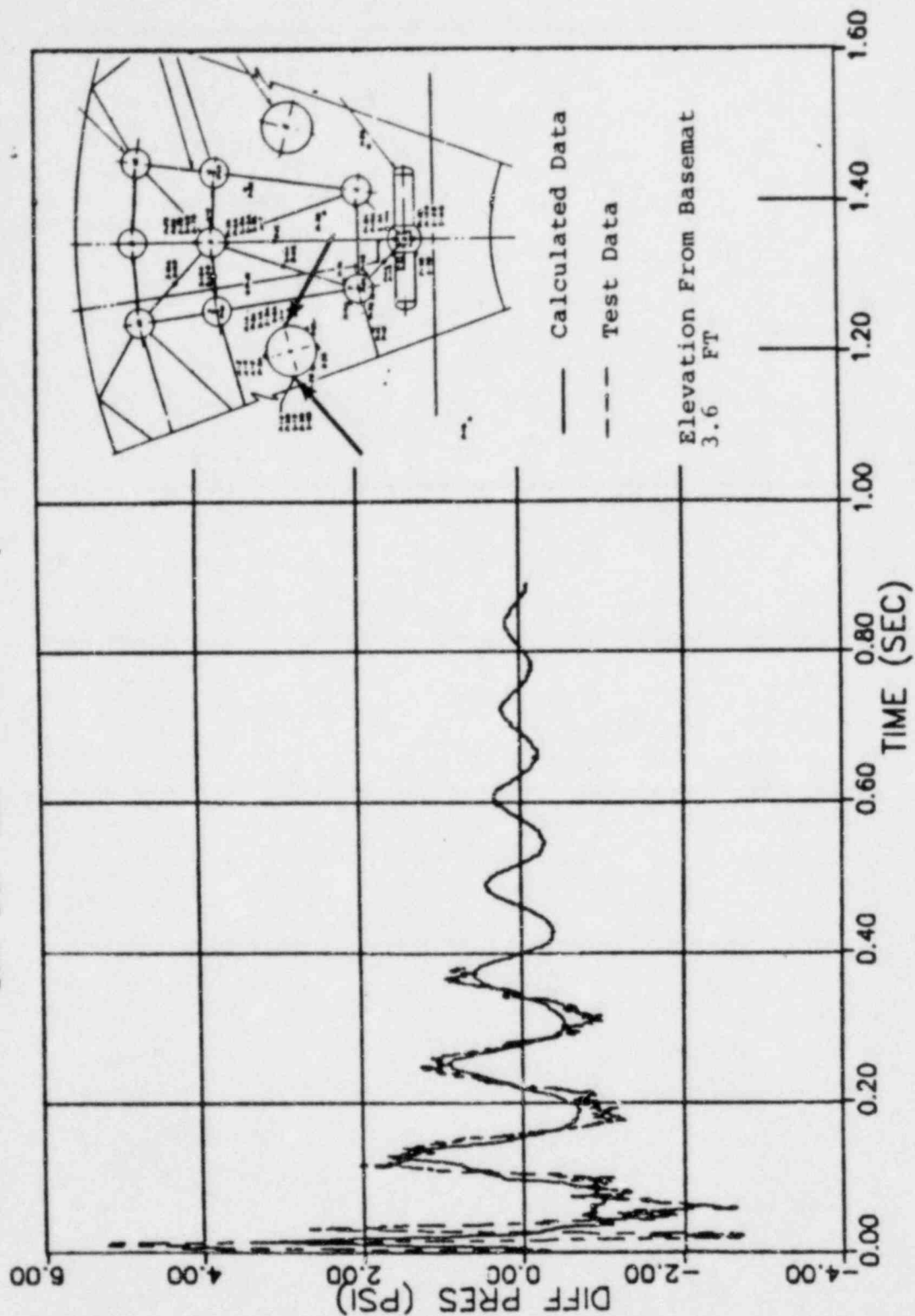


REV. 6, 4/82

SUSQUEHANNA STEAM ELECTRIC STATION
 UNITS 1 AND 2
 DESIGN ASSESSMENT REPORT

COMPARISON OF PREDICTED
 DIFFERENTIAL PRESSURE TIME
 HISTORY WITH TEST DATA-SENSOR
 P7A-P7B-TEST 81
 FIGURE J-34

SRI S3 TEST P1A-1B (P14 SOURCE)

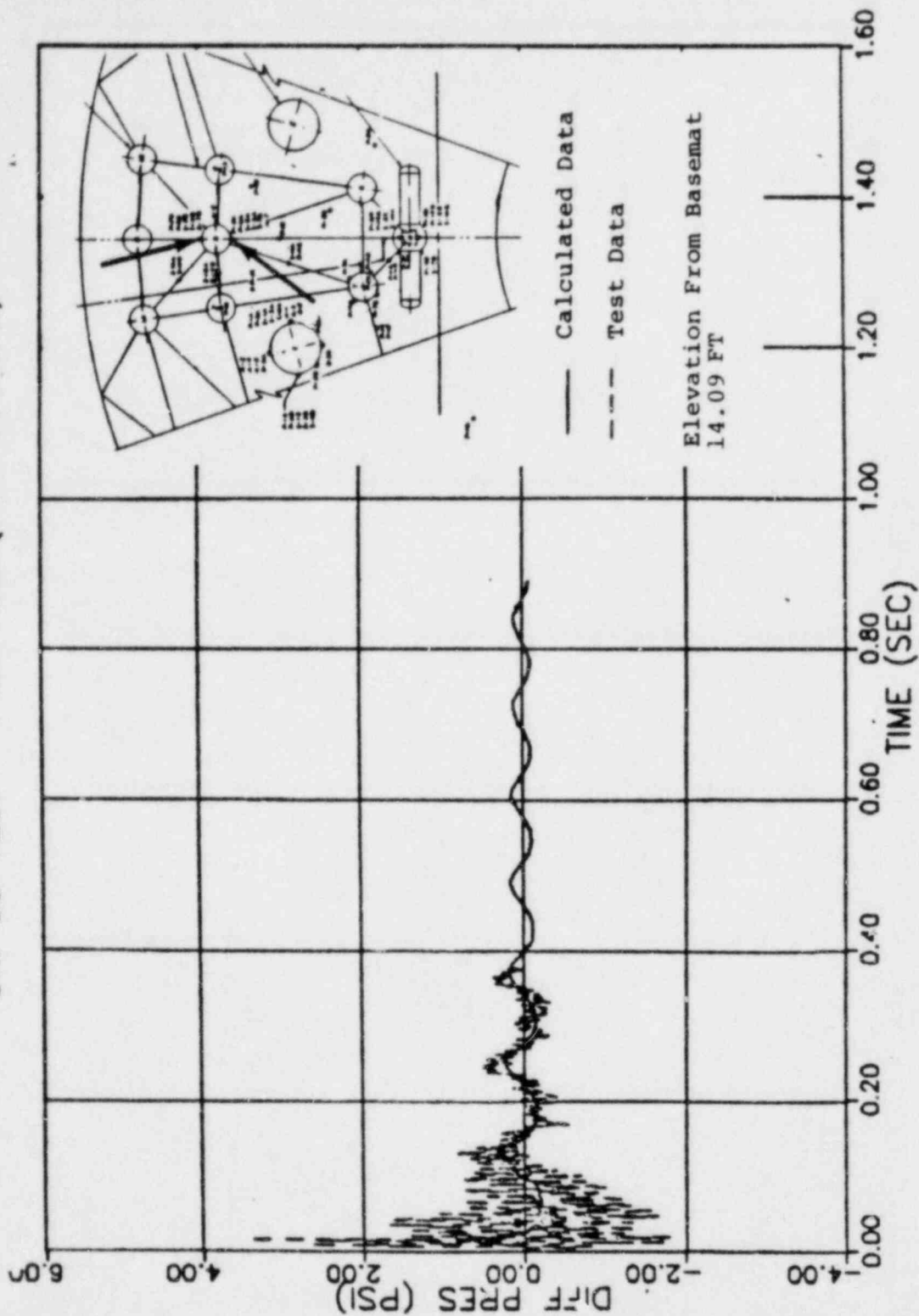


REV. 6, 4/82

SUSQUEHANNA STEAM ELECTRIC STATION
UNITS 1 AND 2
DESIGN ASSESSMENT REPORT

COMPARISON OF PREDICTED
DIFFERENTIAL PRESSURE TIME HISTORY
WITH TEST
DATA - SENSOR P1A-P1B - TEST S3
FIGURE J-35

SRI S3 TEST P5A-P5B (P14 SOURCE)

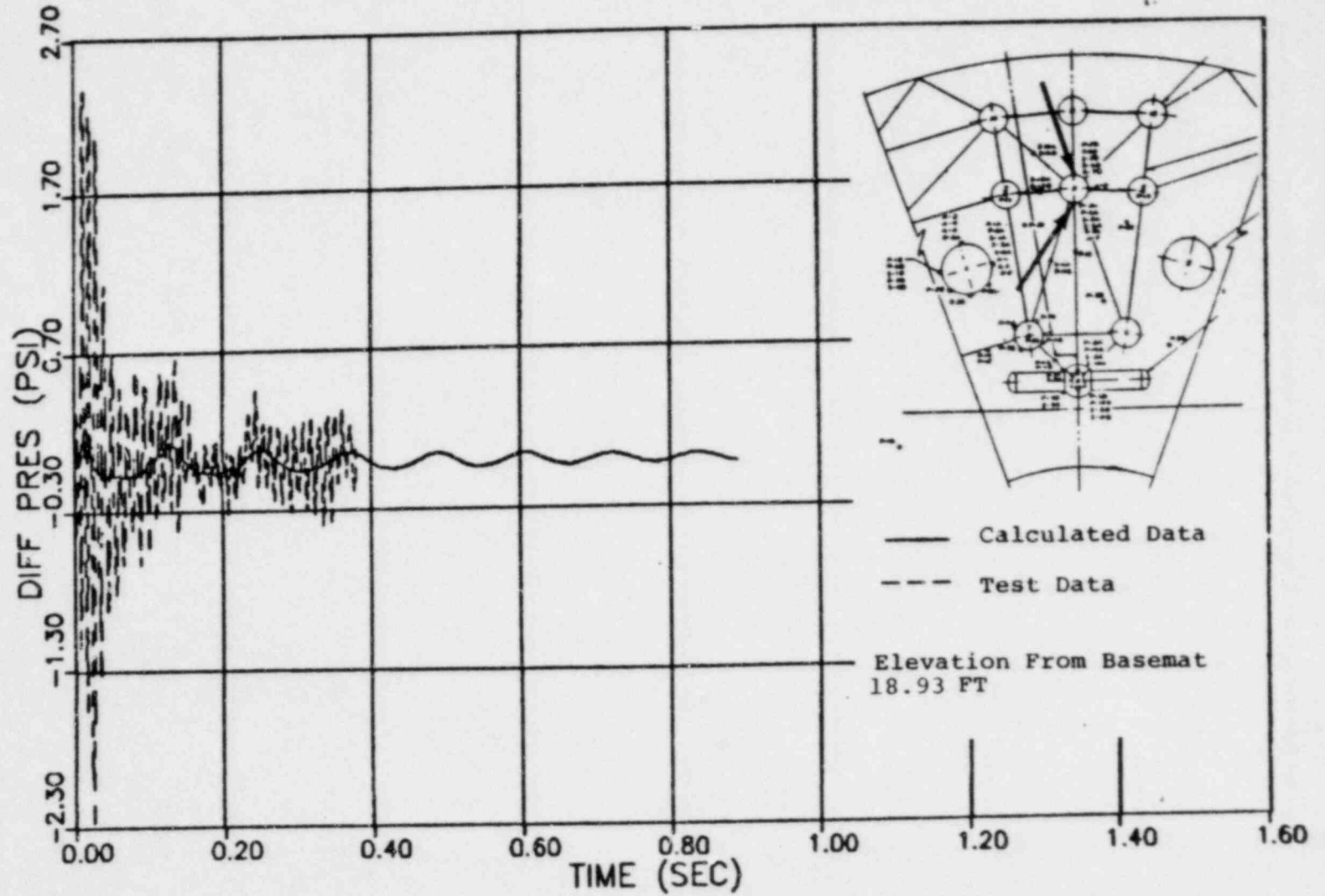


REV. 6, 4/82

SUSQUEHANNA STEAM ELECTRIC STATION
UNITS 1 AND 2
DESIGN ASSESSMENT REPORT

COMPARISON OF PREDICTED
DIFFERENTIAL PRESSURE TIME HISTORY
WITH TEST
DATA - SENSOR P5A-P5B - TEST S3
FIGURE J-36

SRI S3 TEST P6A-P6B (P14 SOURCE)

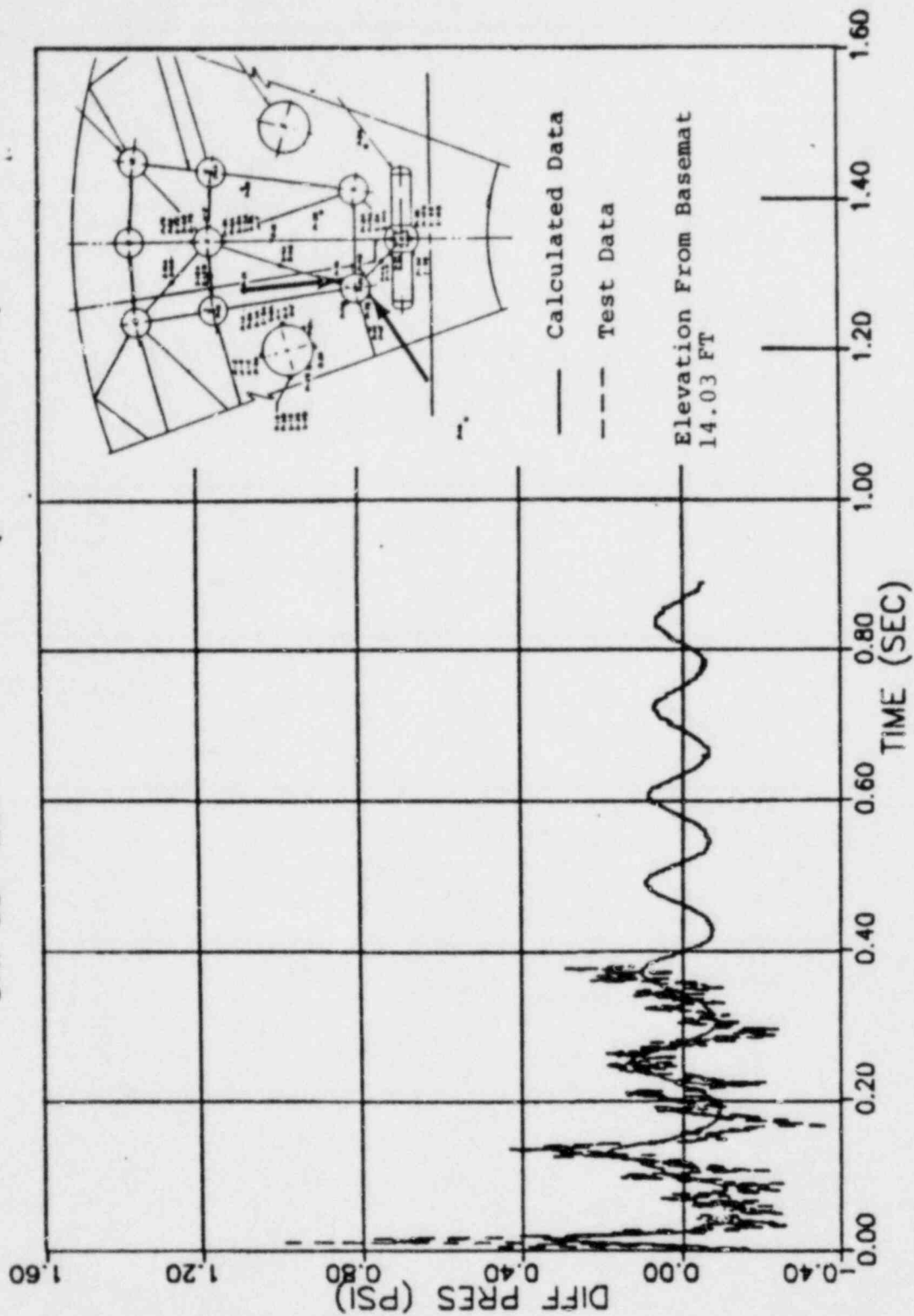


REV. 6, 4/82

SUSQUEHANNA STEAM ELECTRIC STATION
UNITS 1 AND 2
DESIGN ASSESSMENT REPORT

COMPARISON OF PREDICTED
DIFFERENTIAL PRESSURE TIME HISTORY
WITH TEST
DATA - SENSOR P6A-P6B - TEST S3
FIGURE J-37

SRI S3 TEST P7A-P7B (P14 SOURCE)

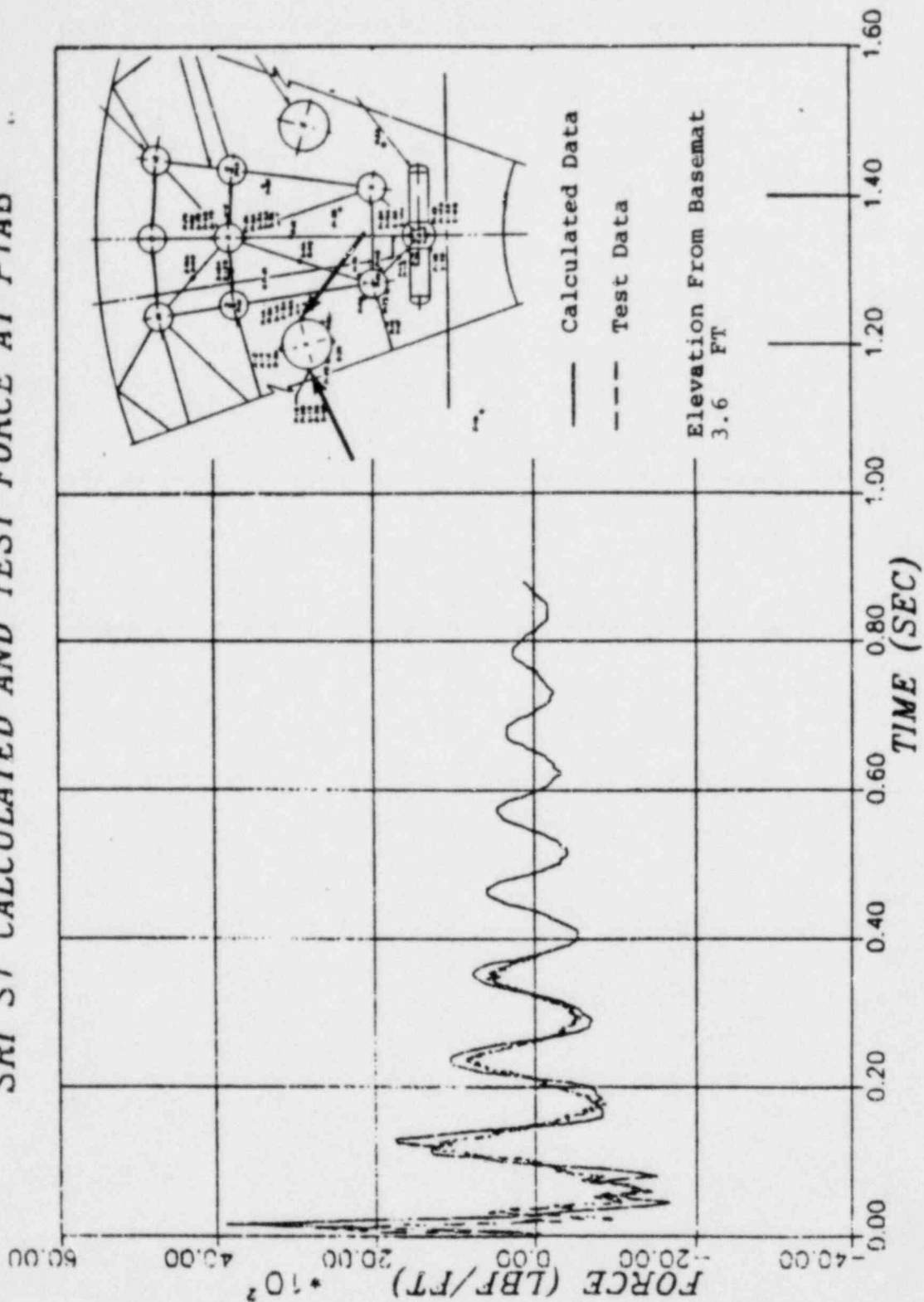


REV. 6, 4/82

SUSQUEHANNA STEAM ELECTRIC STATION
UNITS 1 AND 2
DESIGN ASSESSMENT REPORT

COMPARISON OF PREDICTED
DIFFERENTIAL PRESSURE TIME HISTORY
WITH TEST
DATA - SENSOR P7A-P7B - TEST S3
FIGURE J-38

SRI S1 CALCULATED AND TEST FORCE AT P1AB



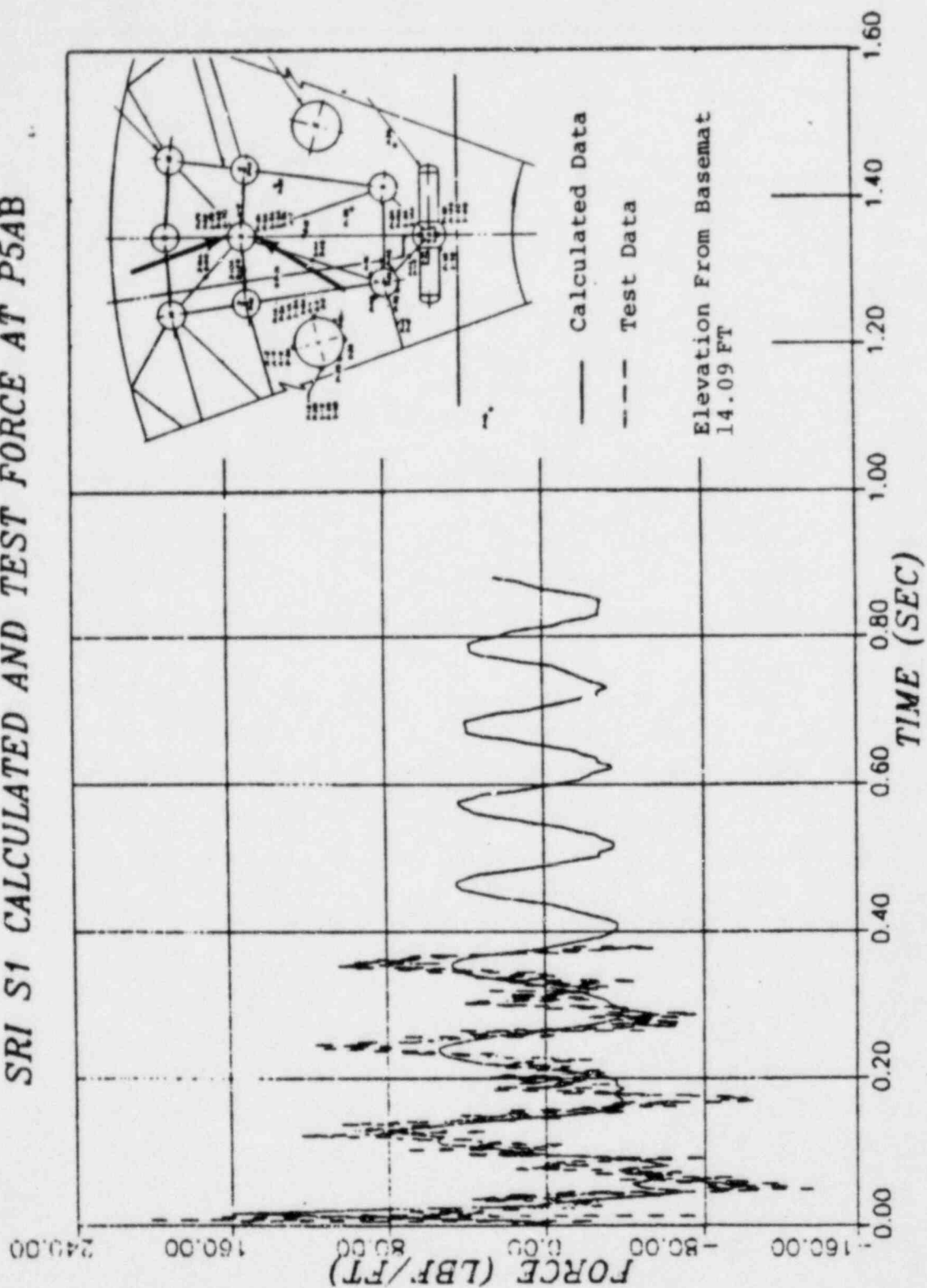
REV. 6, 4/82

SUSQUEHANNA STEAM ELECTRIC STATION
UNITS 1 AND 2
DESIGN ASSESSMENT REPORT

COMPARISON OF PREDICTED FORCE
TIME HISTORY WITH TEST
DATA - P1AB - TEST S1

FIGURE J-39

SRI S1 CALCULATED AND TEST FORCE AT P5AB



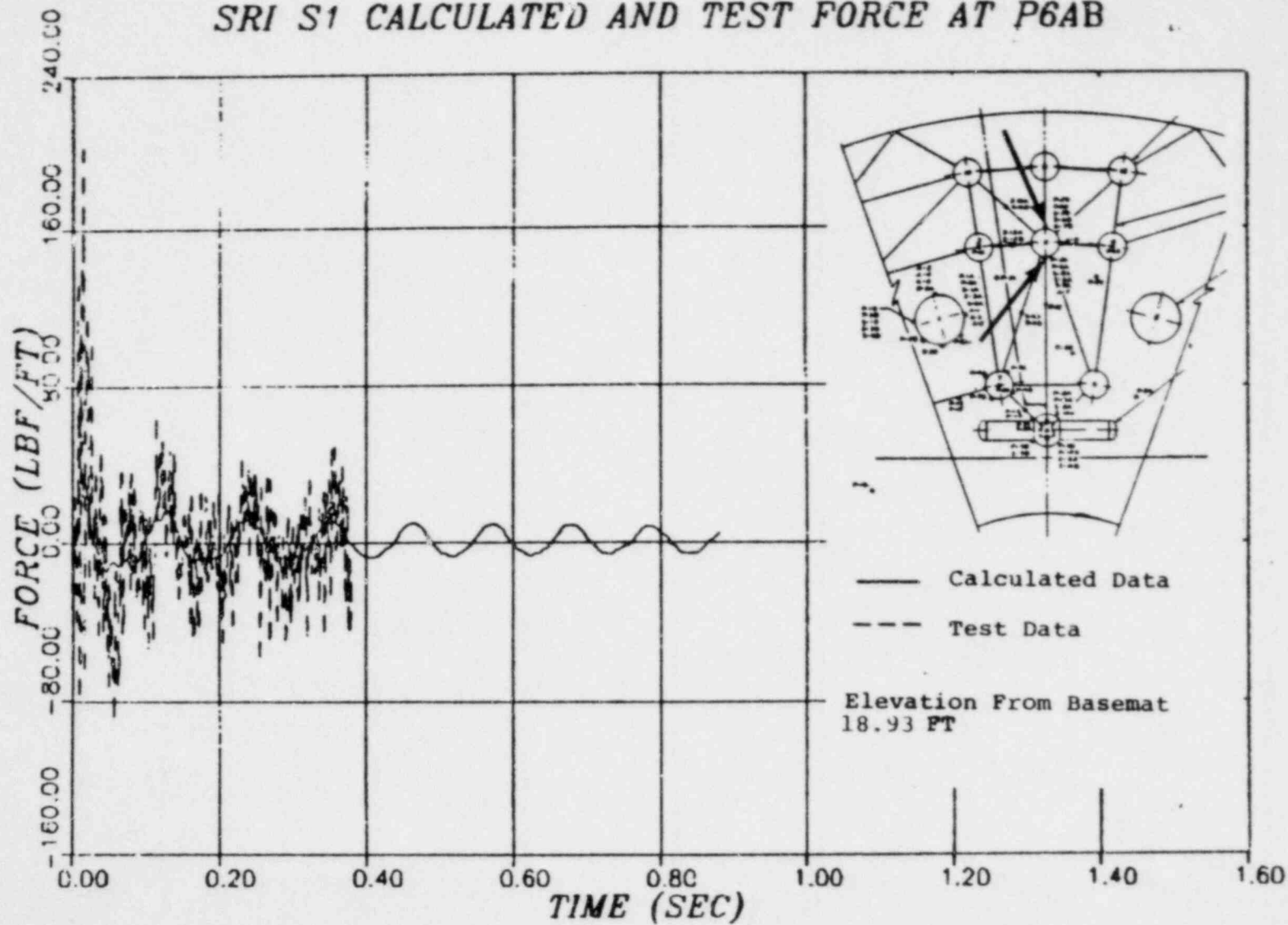
REV. 6, 4/82

SUSQUEHANNA STEAM ELECTRIC STATION
UNITS 1 AND 2
DESIGN ASSESSMENT REPORT

COMPARISON OF PREDICTED FORCE
TIME HISTORY WITH TEST
DATA - P5AB - TEST S1

FIGURE J-40

SRI S1 CALCULATED AND TEST FORCE AT P6AB

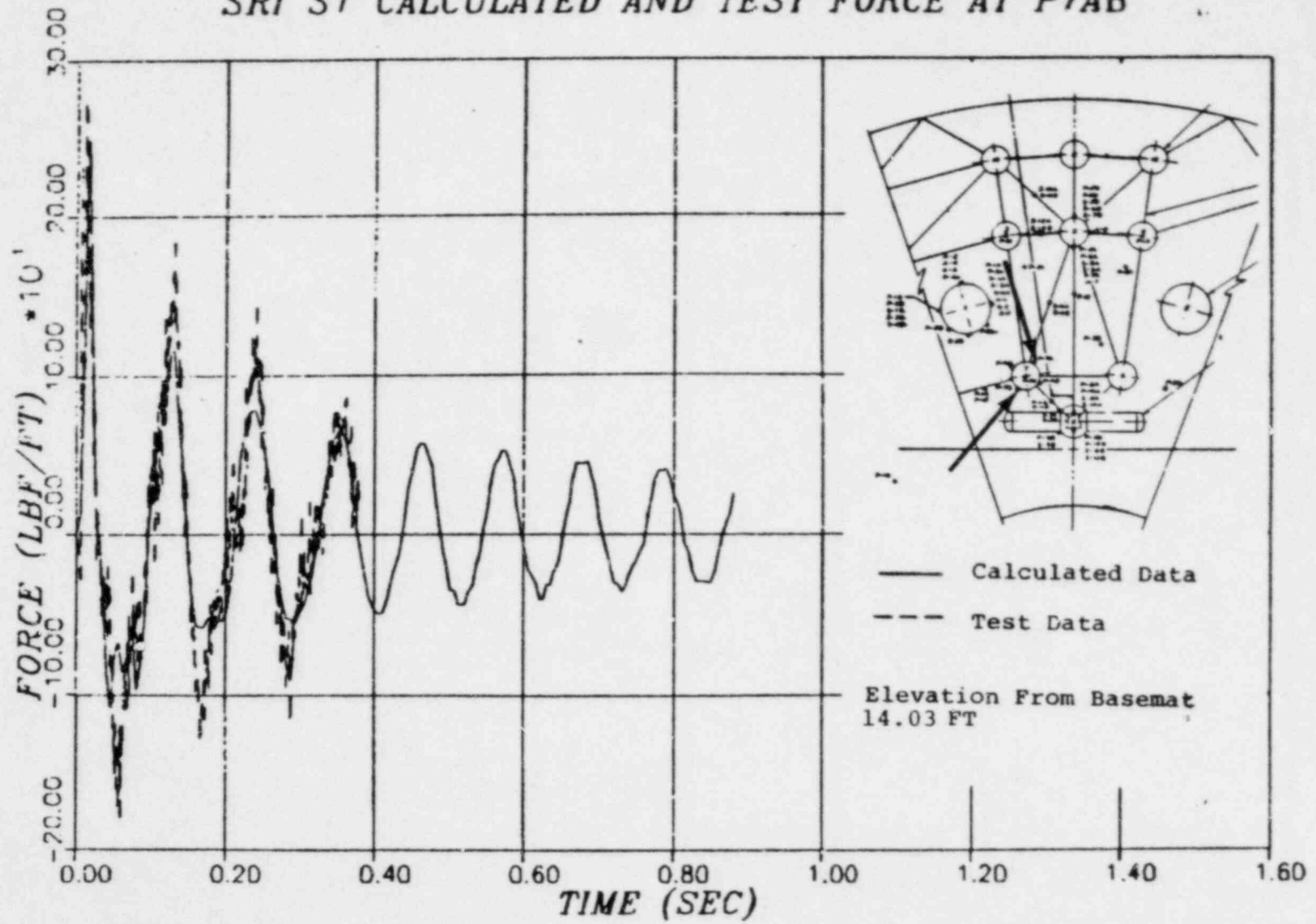


REV. 6, 4/82

SUSQUEHANNA STEAM ELECTRIC STATION
 UNITS 1 AND 2
 DESIGN ASSESSMENT REPORT

COMPARISON OF PREDICTED FORCE
 TIME HISTORY WITH TEST
 DATA - P6AB - TEST S1
 FIGURE J-41

SRI S1 CALCULATED AND TEST FORCE AT P7AB

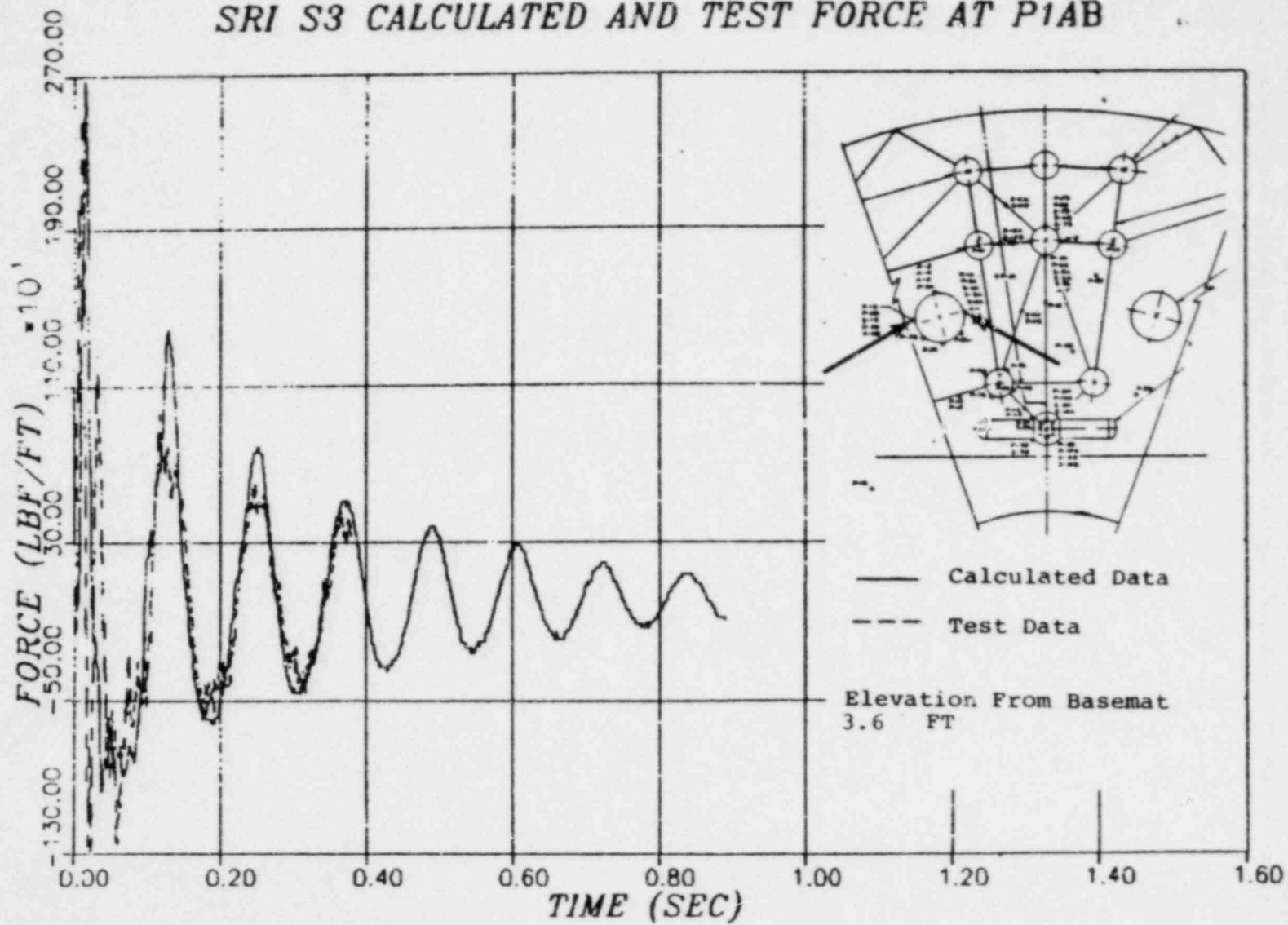


REV. 6, 4/82

SUSQUEHANNA STEAM ELECTRIC STATION
UNITS 1 AND 2
DESIGN ASSESSMENT REPORT

COMPARISON OF PREDICTED FORCE
TIME HISTORY WITH TEST
DATA - P7AB - TEST S1
FIGURE J-42

SRI S3 CALCULATED AND TEST FORCE AT P1AB



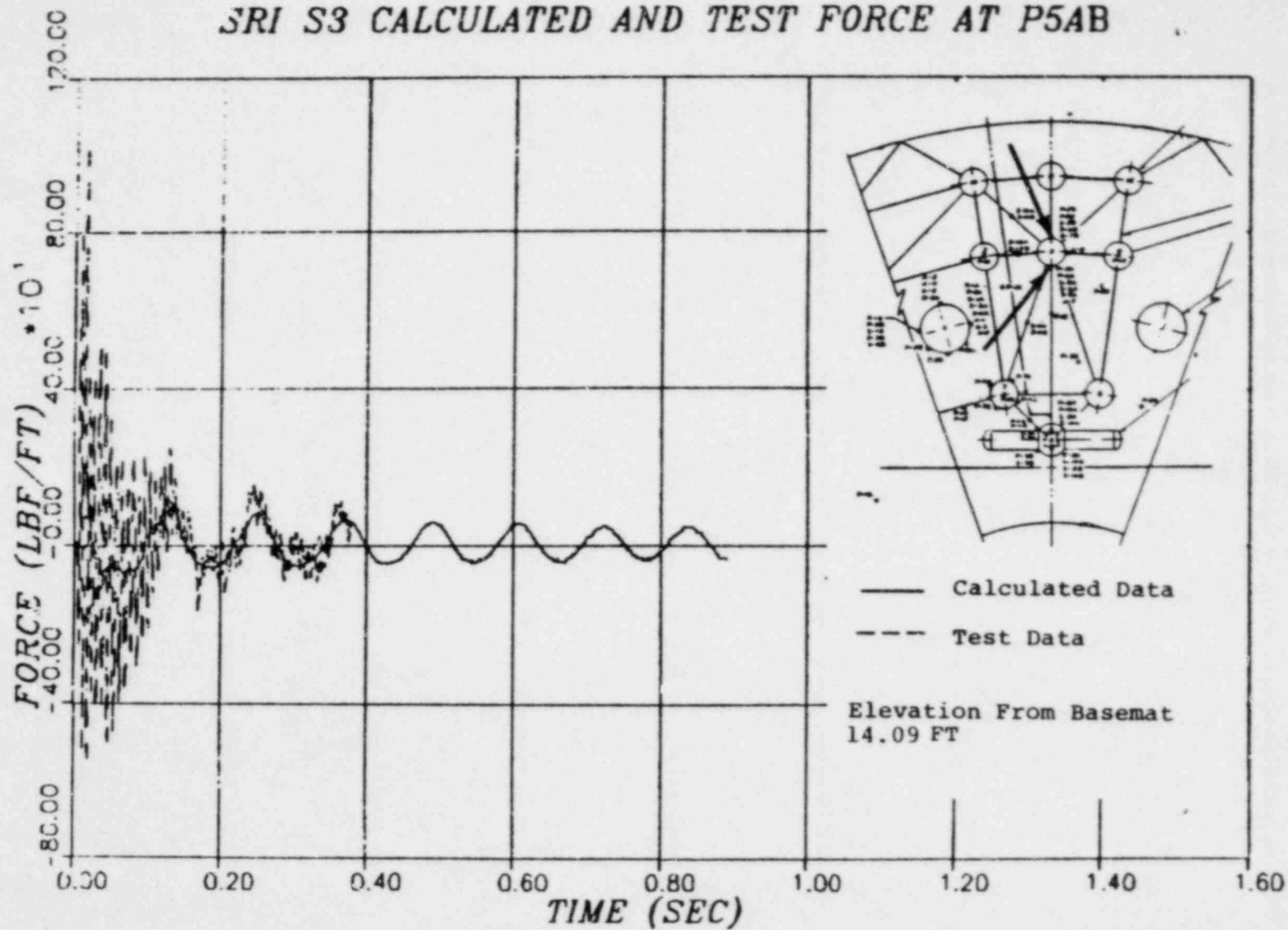
REV. 6, 4/82

SUSQUEHANNA STEAM ELECTRIC STATION
UNITS 1 AND 2
DESIGN ASSESSMENT REPORT

COMPARISON OF PREDICTED FORCE
TIME HISTORY WITH TEST
DATA - P1AB - TEST S3

FIGURE J-43

SRI S3 CALCULATED AND TEST FORCE AT P5AB



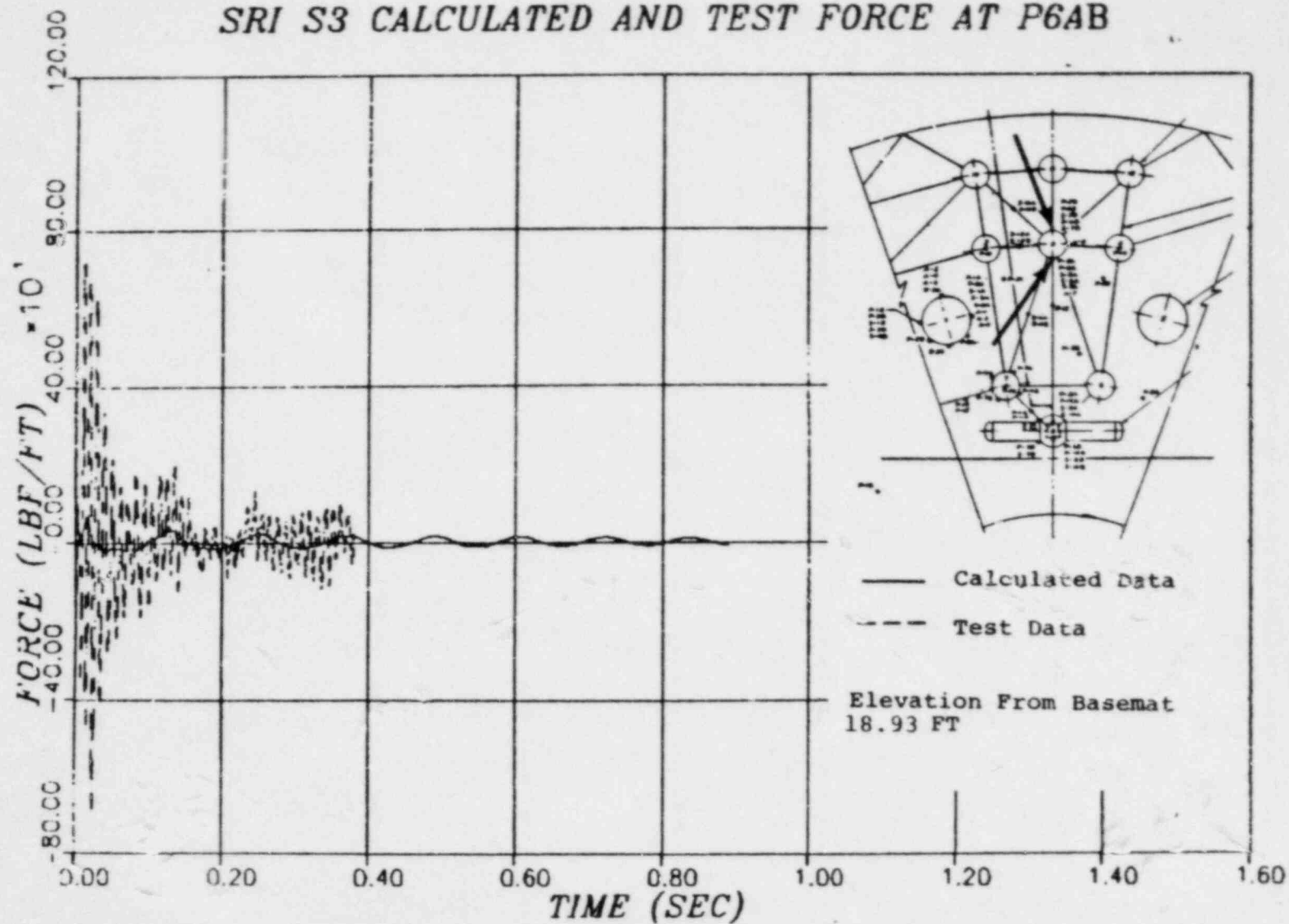
REV. 6, 4/82

SUSQUEHANNA STEAM ELECTRIC STATION
UNITS 1 AND 2
DESIGN ASSESSMENT REPORT

COMPARISON OF PREDICTED FORCE
TIME HISTORY WITH TEST
DATA - P5AB - TEST S3

FIGURE J-44

SRI S3 CALCULATED AND TEST FORCE AT P6AB

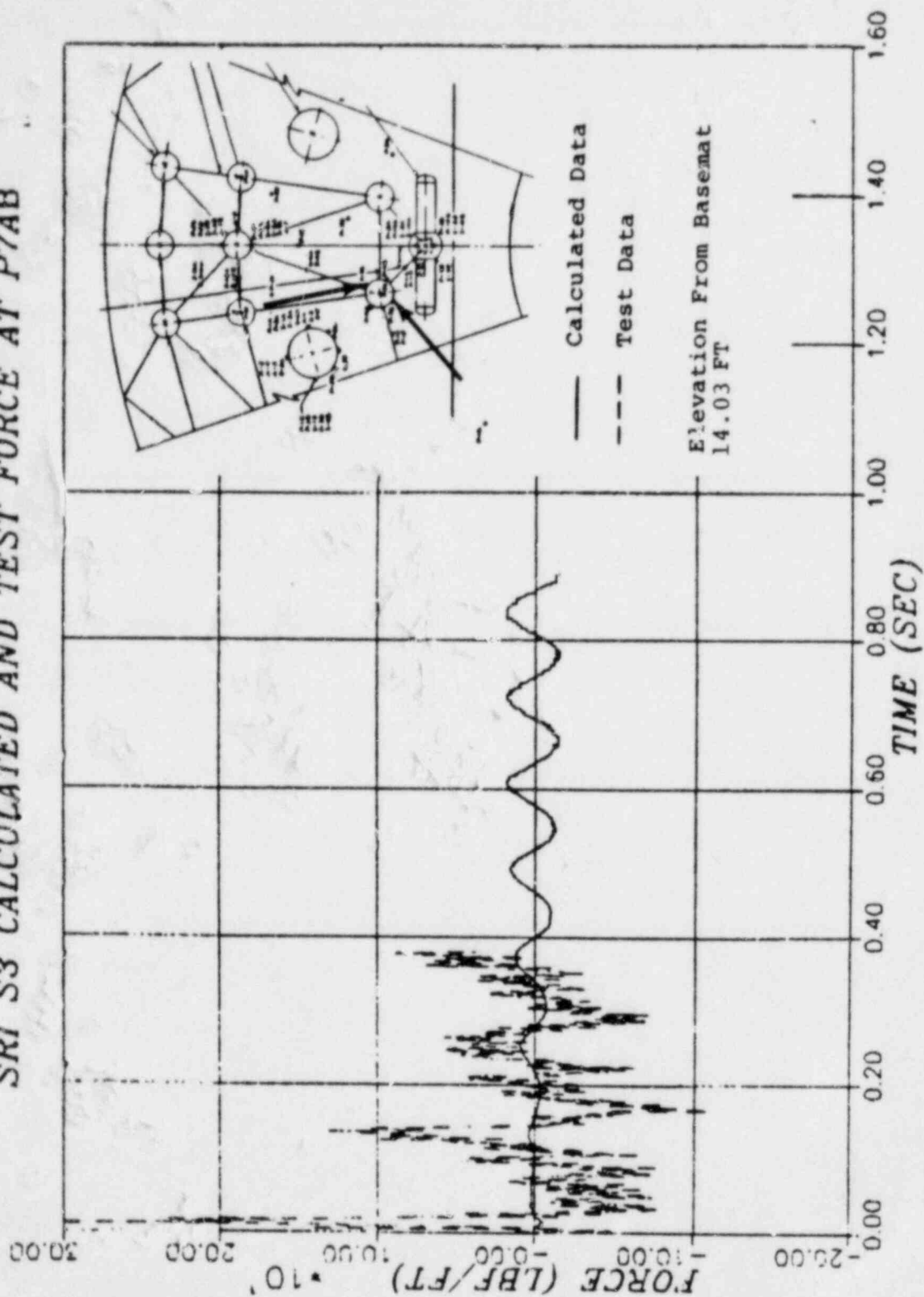


REV. 6, 4/82

SUSQUEHANNA STEAM ELECTRIC STATION
UNITS 1 AND 2
DESIGN ASSESSMENT REPORT

COMPARISON OF PREDICTED FORCE
TIME HISTORY WITH TEST
DATA - P6AB - TEST S3
FIGURE J-45

SRI S3 CALCULATED AND TEST FORCE AT P7AB



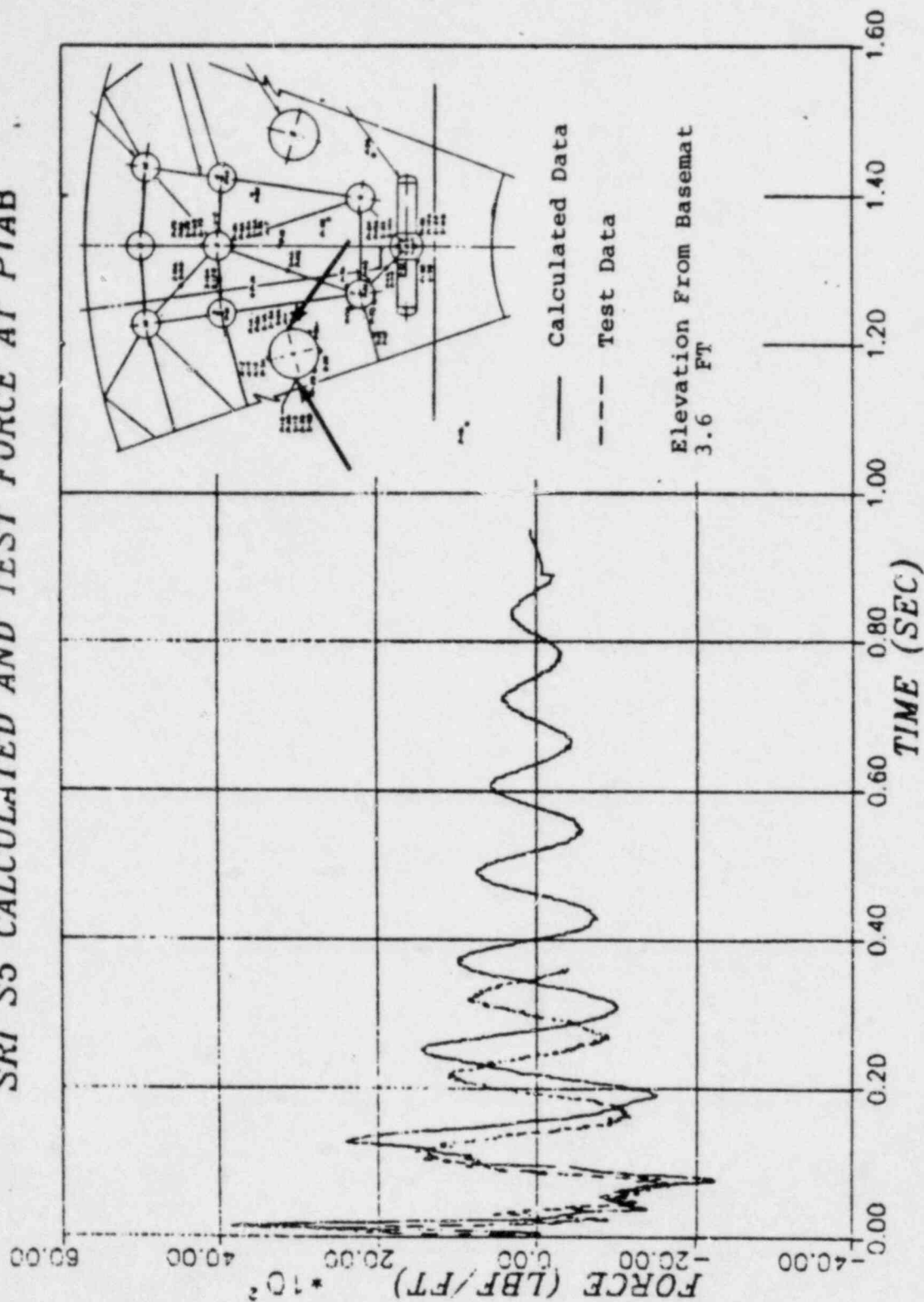
REV. 6, 4/82

SUSQUEHANNA STEAM ELECTRIC STATION
UNITS 1 AND 2
DESIGN ASSESSMENT REPORT

COMPARISON OF PREDICTED FORCE
TIME HISTORY WITH TEST
DATA - P7AB - TEST S3

FIGURE J-46

SRI S5 CALCULATED AND TEST FORCE AT P1AB



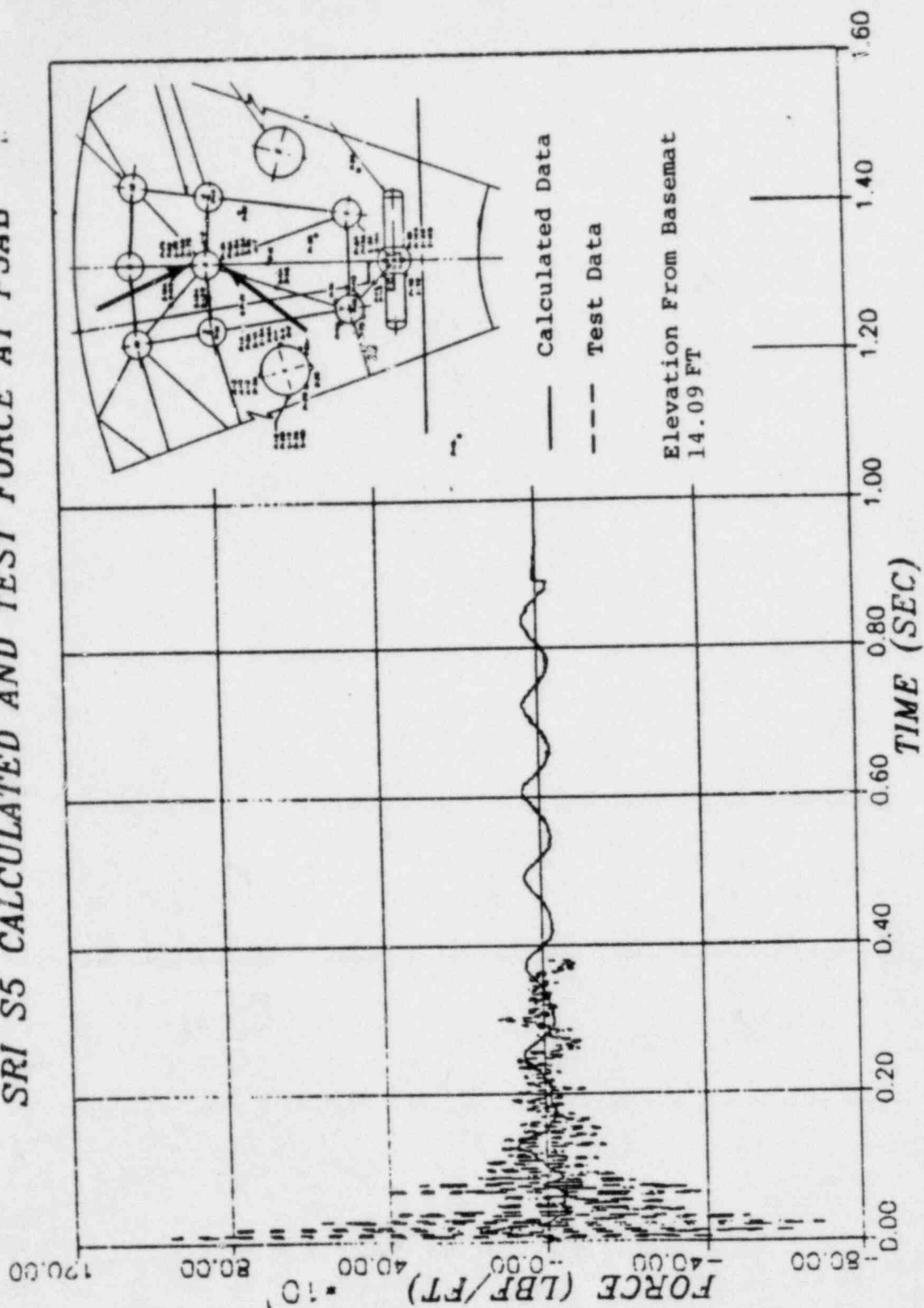
REV. 6, 4/82

SUSQUEHANNA STEAM ELECTRIC STATION
UNITS 1 AND 2
DESIGN ASSESSMENT REPORT

COMPARISON OF PREDICTED FORCE
TIME HISTORY WITH TEST
DATA - P1AB - TEST S5

FIGURE 1-47

SRI S5 CALCULATED AND TEST FORCE AT P5AB



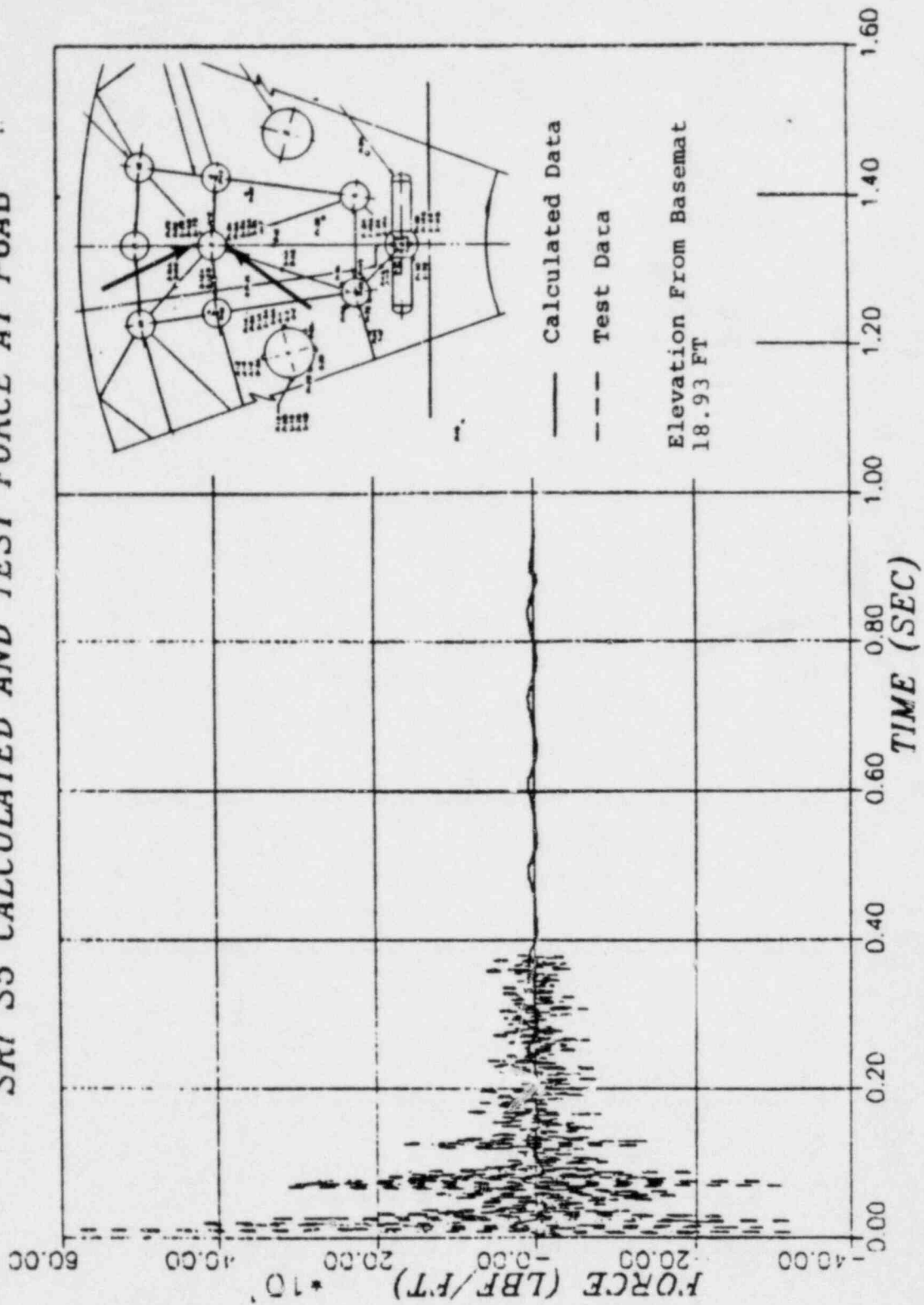
REV. 6, 4/82

SUSQUEHANNA STEAM ELECTRIC STATION
UNITS 1 AND 2
DESIGN ASSESSMENT REPORT

COMPARISON OF PREDICTED FORCE
TIME HISTORY WITH TEST
DATA - P5AB - TEST S5

FIGURE J-14

SRI S5 CALCULATED AND TEST FORCE AT P6AB



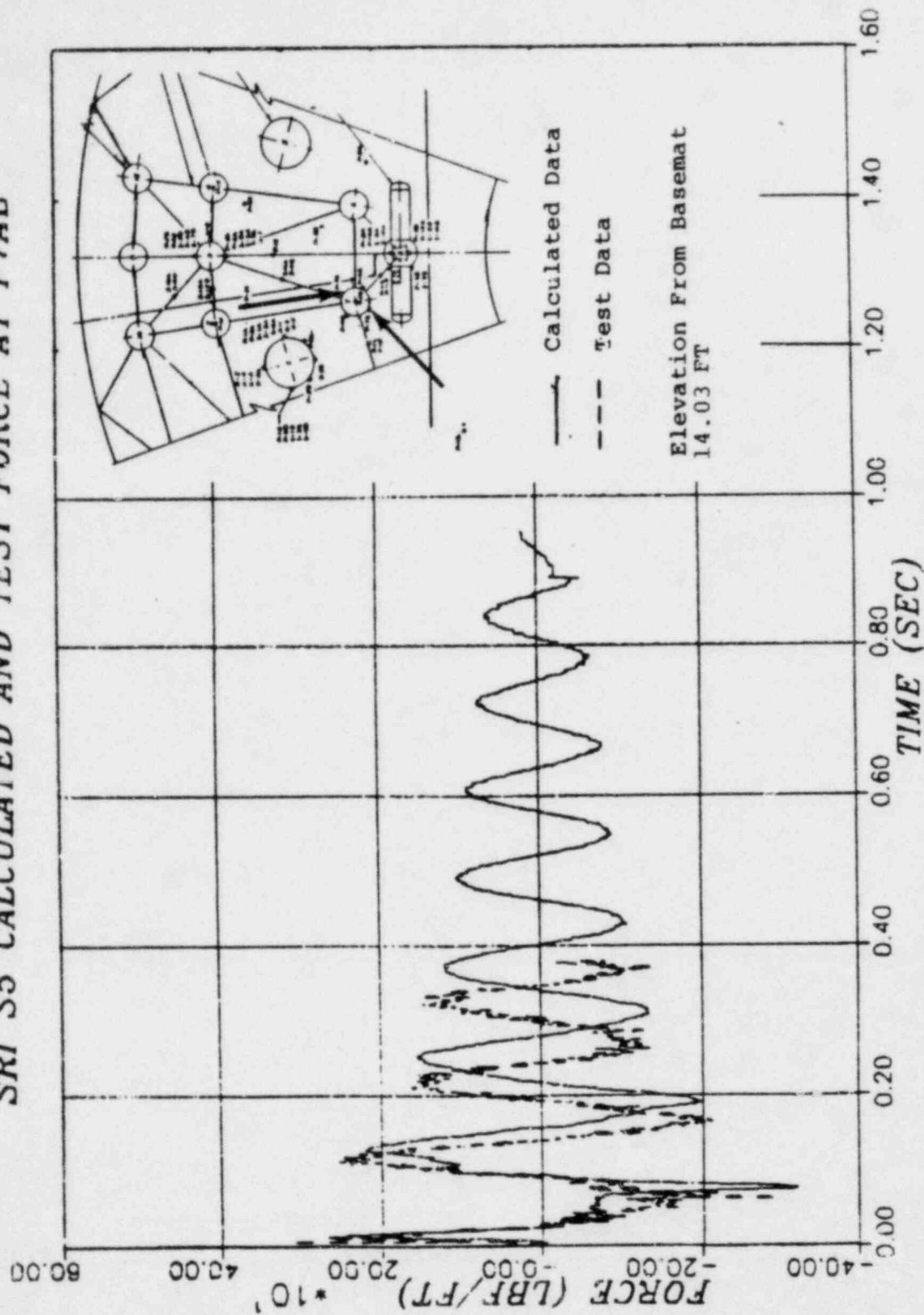
REV. 6, 4/82

SUSQUEHANNA STEAM ELECTRIC STATION
UNITS 1 AND 2
DESIGN ASSESSMENT REPORT

COMPARISON OF PREDICTED FORCE
TIME HISTORY WITH TEST
DATA - P6AB - TEST S5

FIGURE 1-44

SRI S5 CALCULATED AND TEST FORCE AT P7AB



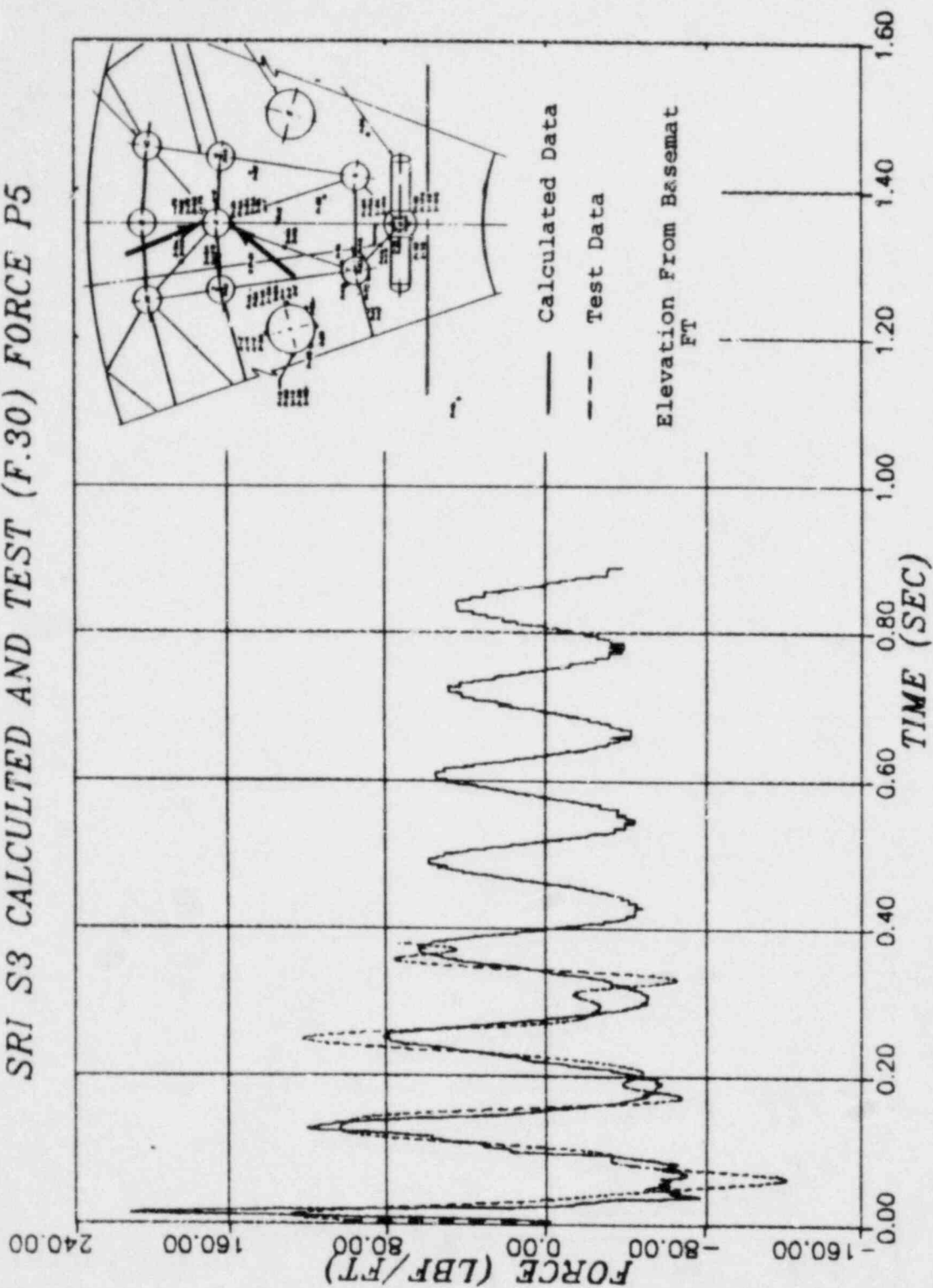
REV. 6, 4/82

SUSQUEHANNA STEAM ELECTRIC STATION
UNITS 1 AND 2
DESIGN ASSESSMENT REPORT

COMPARISON OF PREDICTED FORCE
TIME HISTORY WITH TEST
DATA - P7AB - TEST S5

FIGURE J-50

SRI S3 CALCULATED AND TEST (F.30) FORCE P5



#TEST DATA FILTERED AT 30 HZ

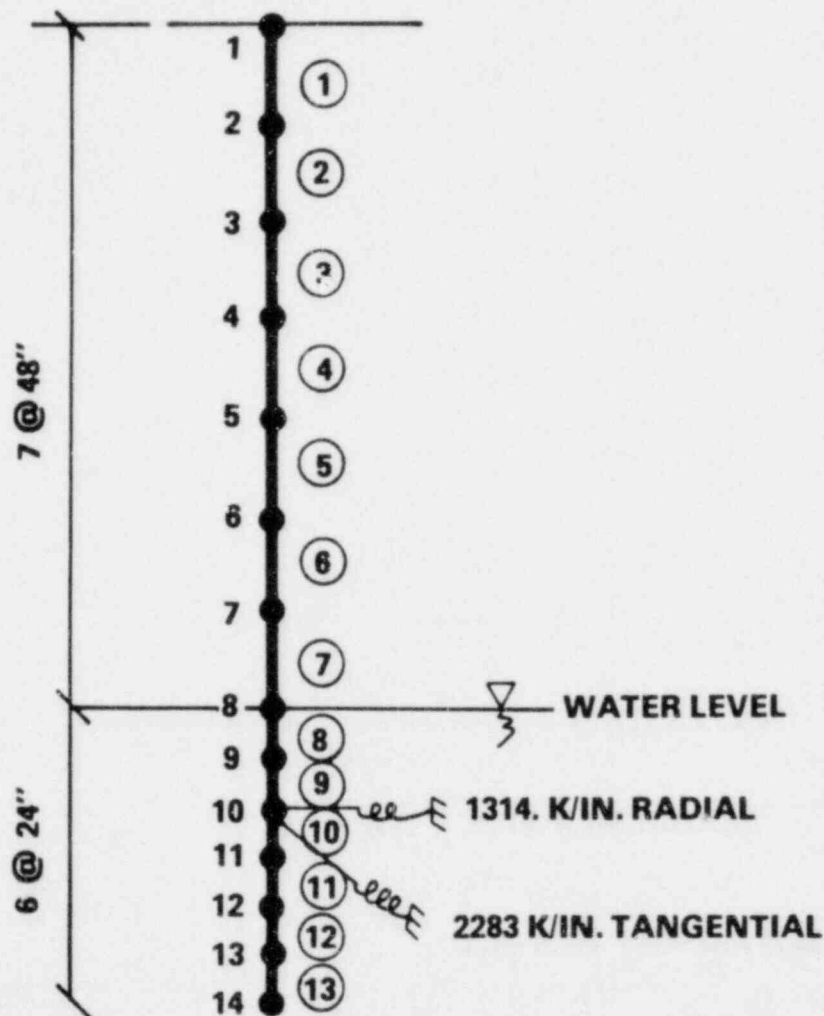
REV. 6, 4/82

SUSQUEHANNA STEAM ELECTRIC STATION
UNITS 1 AND 2
DESIGN ASSESSMENT REPORT

COMPARISON OF PREDICTED FORCE LINE
HISTORY WITH TEST
DATA FILTERED ABOVE 30 HZ - DAB -
TEST S3

FIGURE J-51

NASTRAN—DOWNCOMER MODEL (SSES) BEAM ELEMENTS



**DYNAMIC NODAL LOADS
APPLIED @ NODES 9-14**

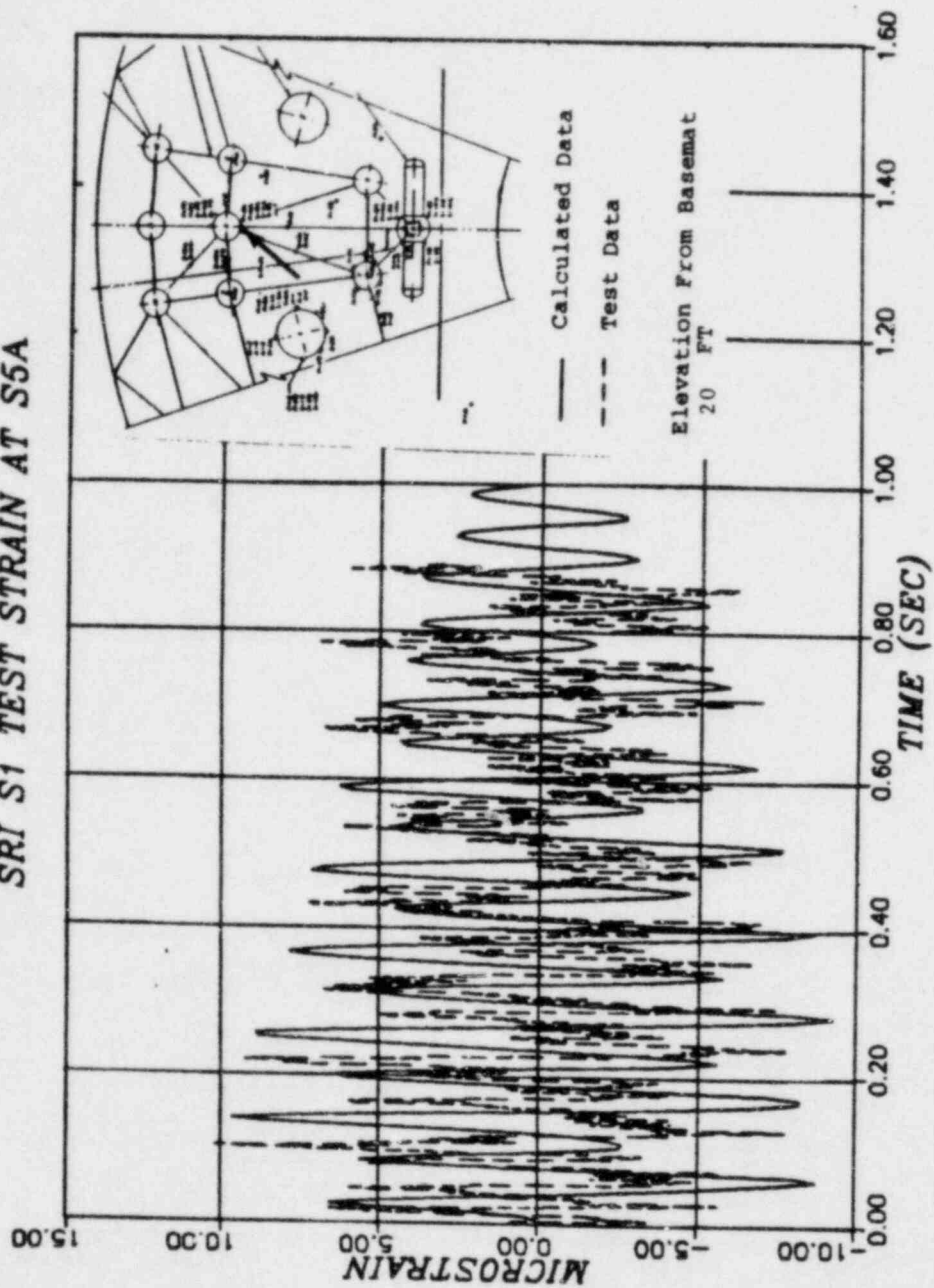
REV. 6, 4/82

SUSQUEHANNA STEAM ELECTRIC STATION
UNITS 1 AND 2
DESIGN ASSESSMENT REPORT

NASTRAN DOWNCOMER MODEL

FIGURE J-52

SRI S1 TEST STRAIN AT S5A

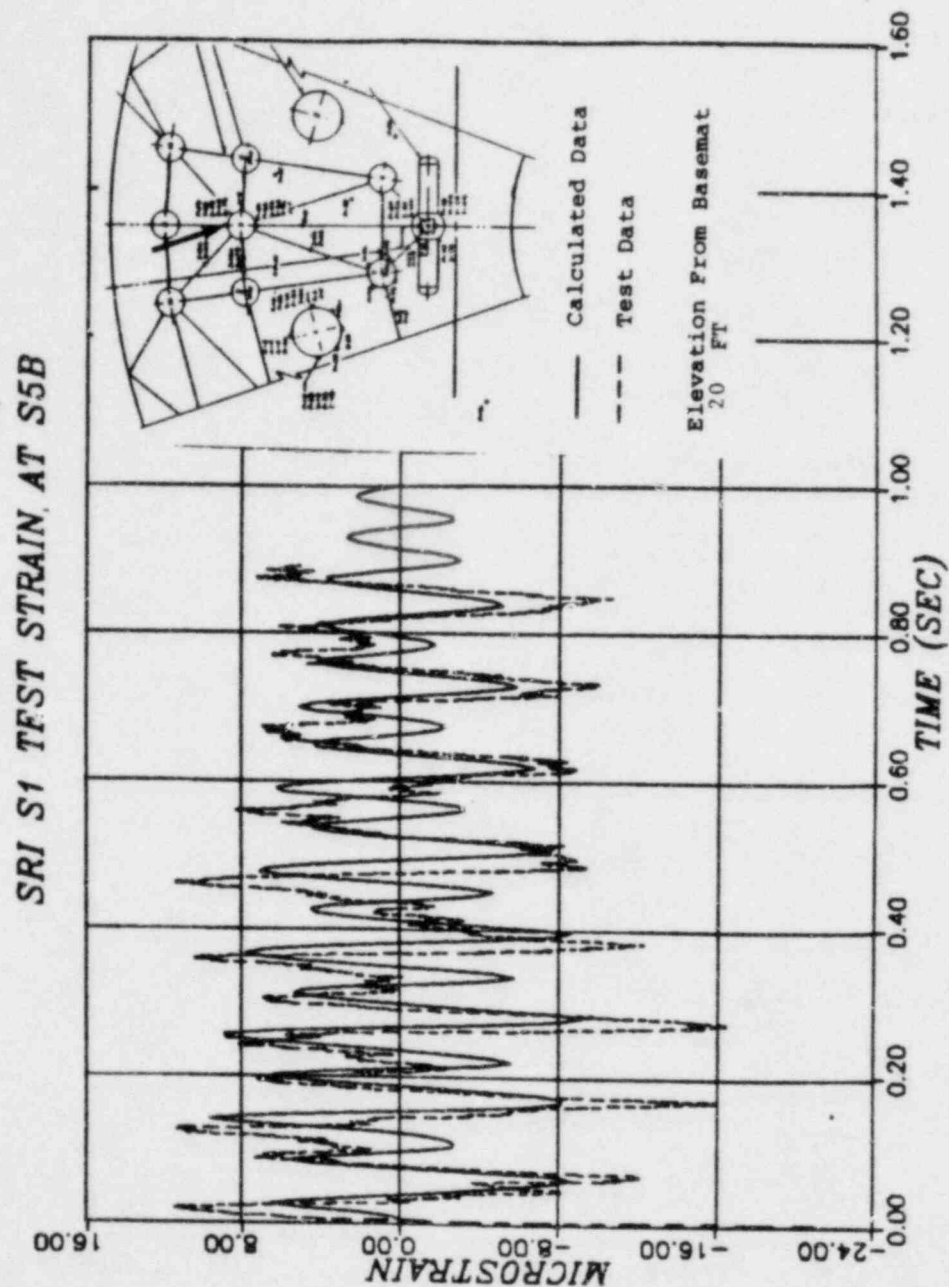


REV. 6, 4/82

SUSQUEHANNA STEAM ELECTRIC STATION
UNITS 1 AND 2
DESIGN ASSESSMENT REPORT

COMPARISON OF THE PREDICTED
STRAIN WITH MEASURED DATA -
STRAIN
GAGE S5A - TEST S1

FIGURE J-53

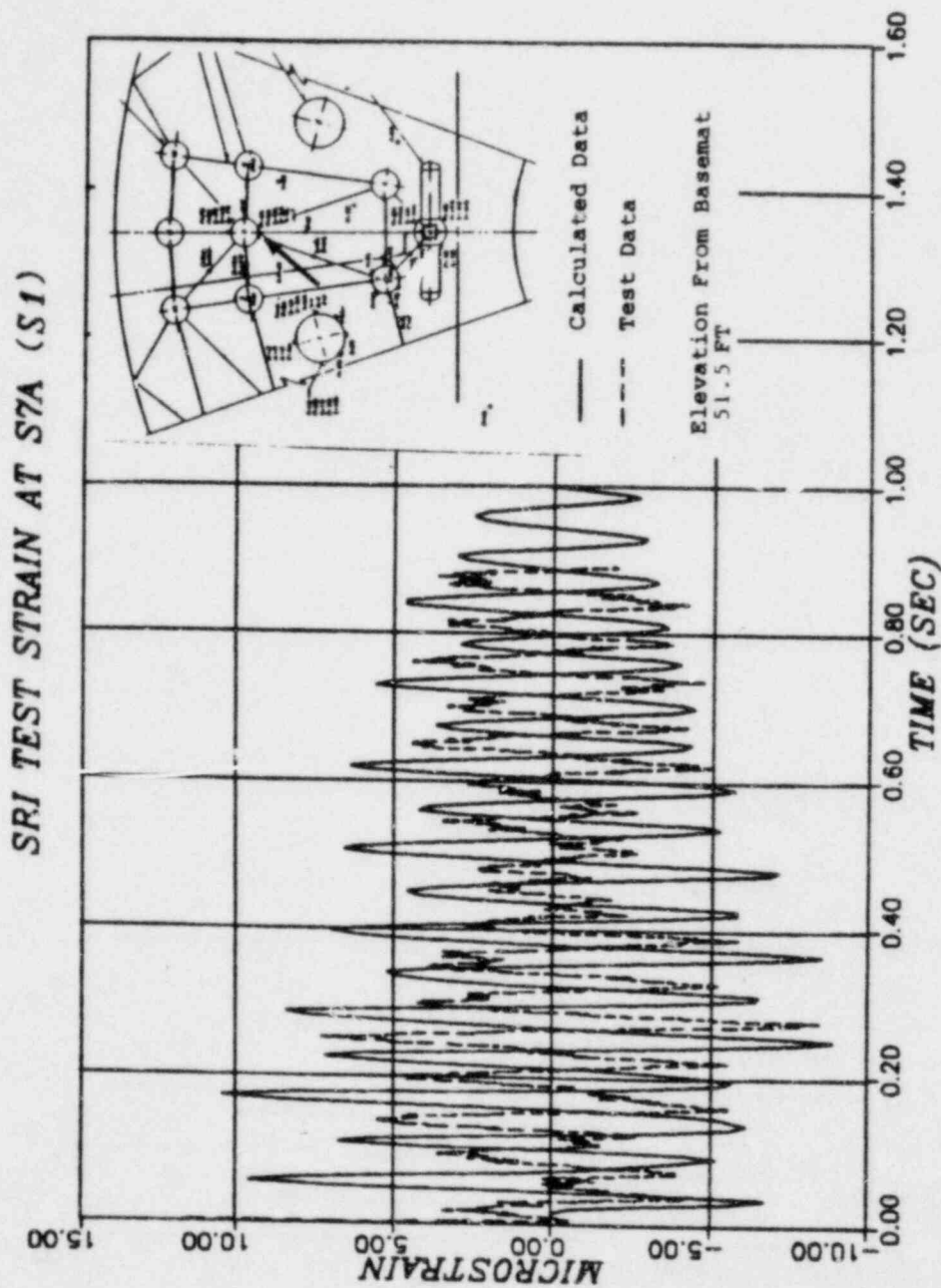


REV. 6, 4/82

**SUSQUEHANNA STEAM ELECTRIC STATION
UNITS 1 AND 2
DESIGN ASSESSMENT REPORT**

COMPARISON OF THE PREDICTED STRAIN
WITH MEASURED DATA - STRAIN
GAGE S5B - TEST S1

FIGURE J-54



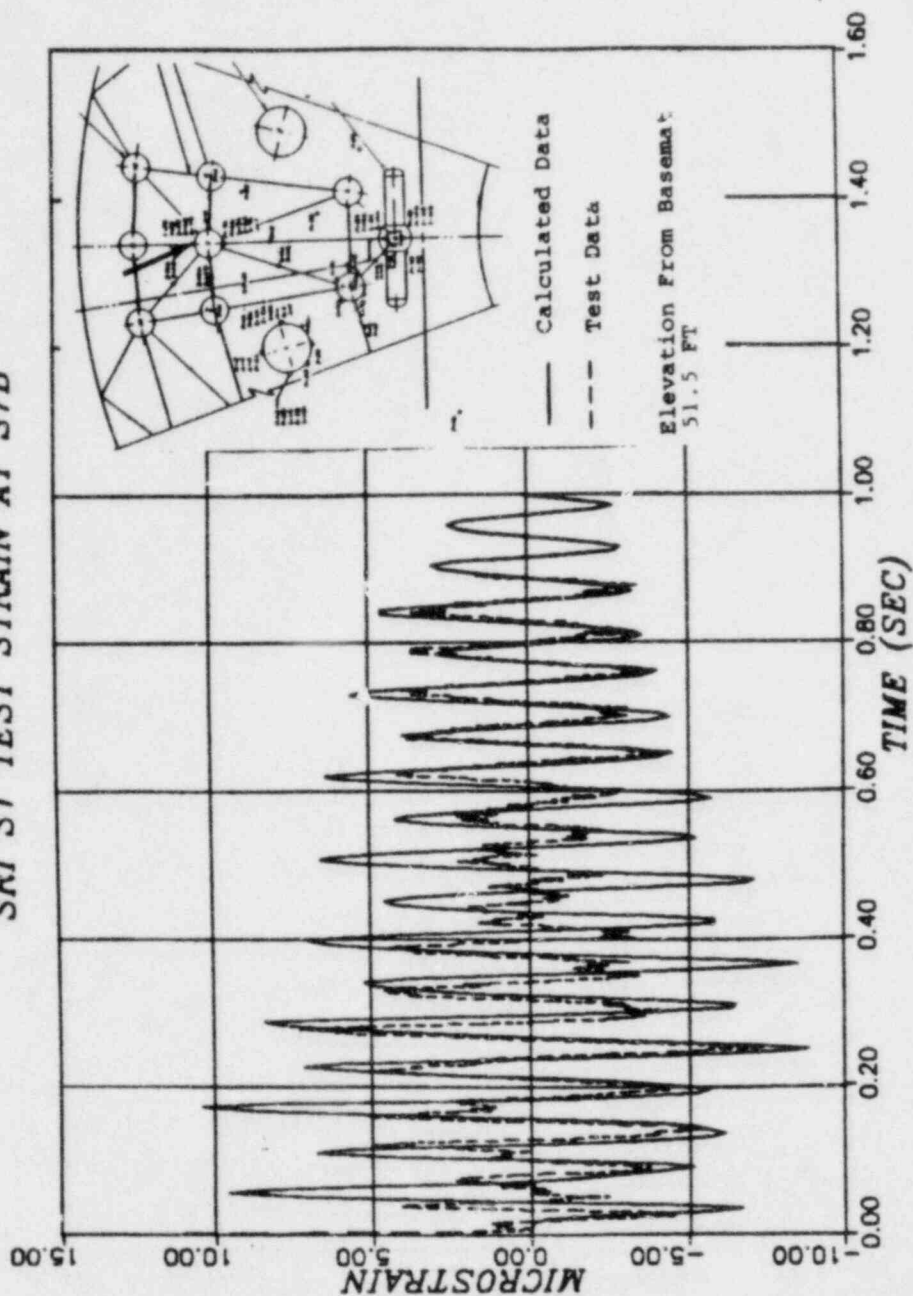
REV. 6, 4/82

**SUSQUEHANNA STEAM ELECTRIC STATION
UNITS 1 AND 2
DESIGN ASSESSMENT REPORT**

COMPARISON OF THE PREDICTED STRAIN
WITH MEASURED DATA - STRAIN
GAGE S7A - TEST S1

FIGURE L-55

SRI S1 TEST STRAIN AT S7B



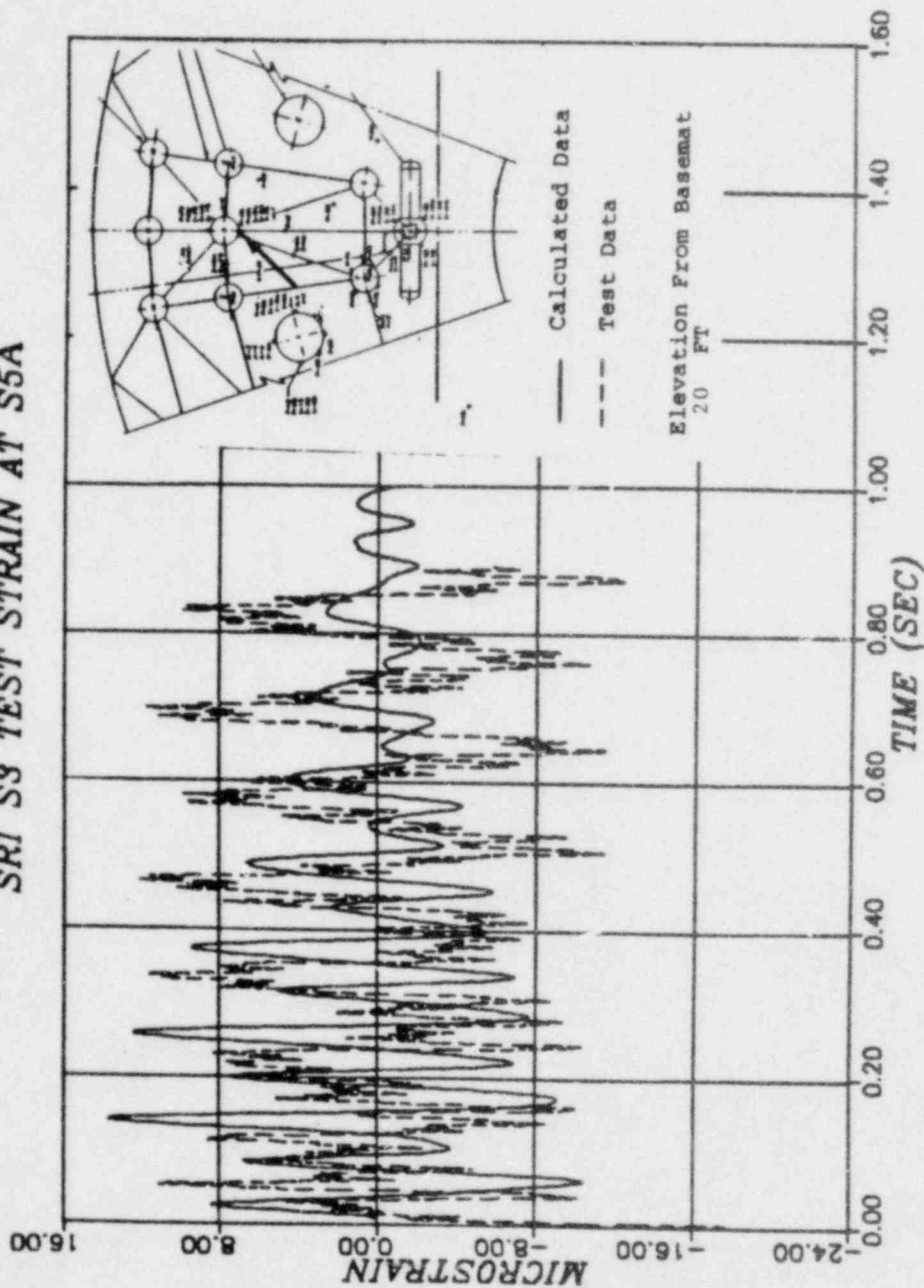
REV. 6, 4/82

SUSQUEHANNA STEAM ELECTRIC STATION
UNITS 1 AND 2
DESIGN ASSESSMENT REPORT

COMPARISON OF THE PREDICTED STRAIN
WITH MEASURED DATA - STRAIN
GAGE S7B - TEST S1

FIGURE J-56

SRI S3 TEST STRAIN AT S5A



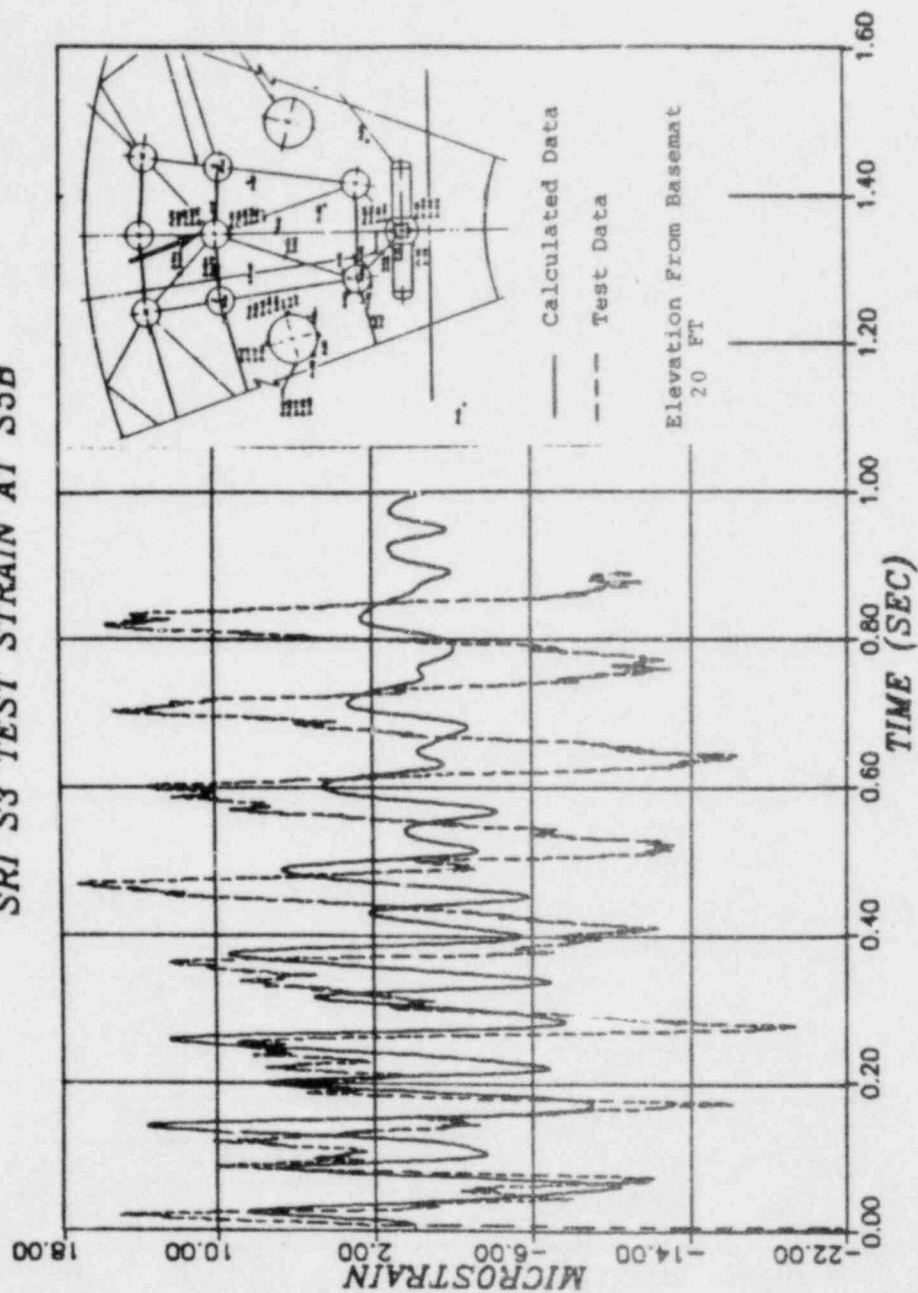
REV. 6, 4/82

SUSQUEHANNA STEAM ELECTRIC STATION
UNITS 1 AND 2
DESIGN ASSESSMENT REPORT

COMPARISON OF THE PREDICTED STRAIN
WITH MEASURED DATA - STRAIN
GAGE S5A - TEST S3

FIGURE J-57

SRI S3 TEST STRAIN AT S5B



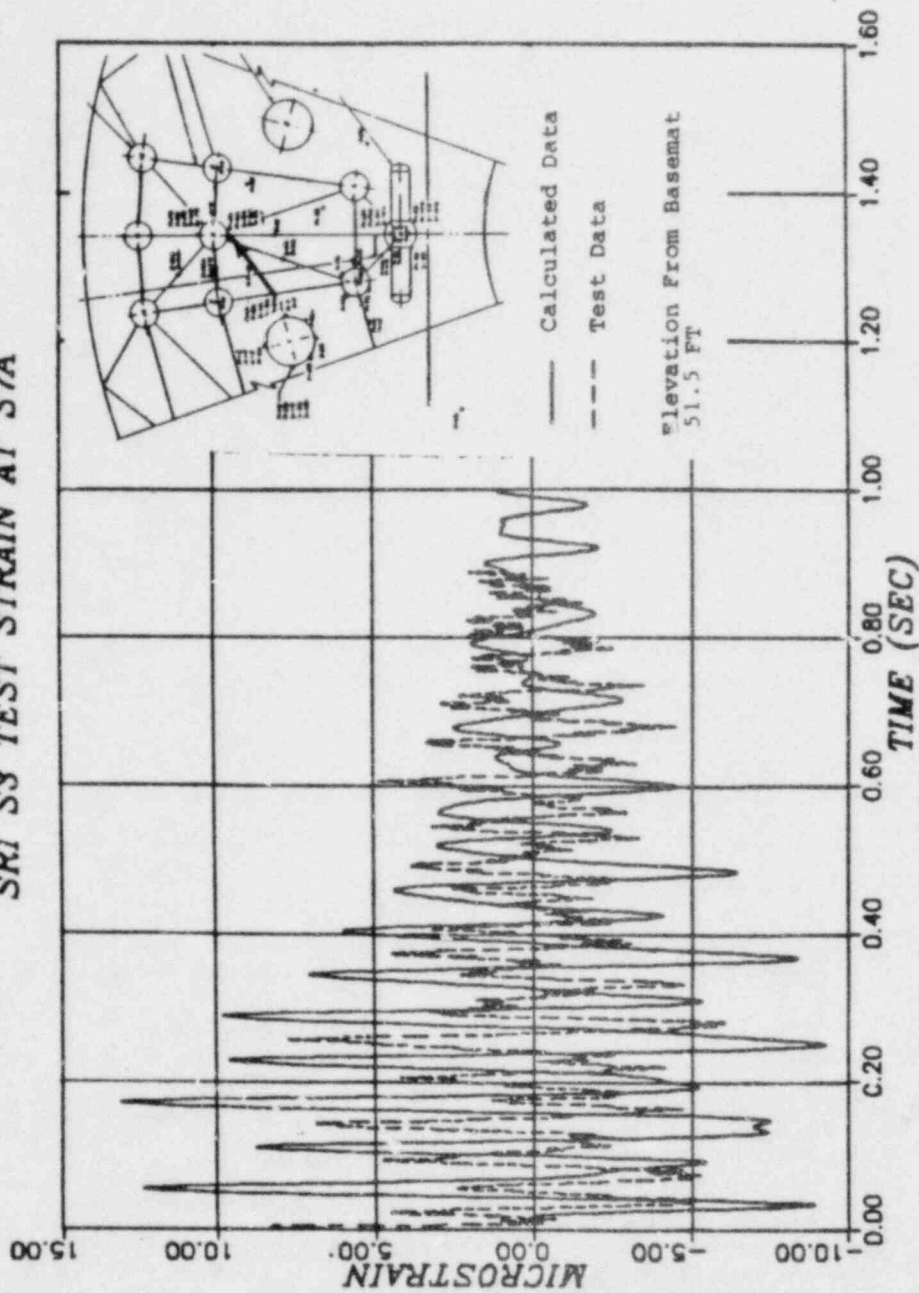
REV. 6, 4/82

SUSQUEHANNA STEAM ELECTRIC STATION
UNITS 1 AND 2
DESIGN ASSESSMENT REPORT

COMPARISON OF THE PREDICTED STRAIN
WITH MEASURED DATA - STRAIN
GAGE S5B - TEST S3

FIGURE J-53

SRI S3 TEST STRAIN AT S7A

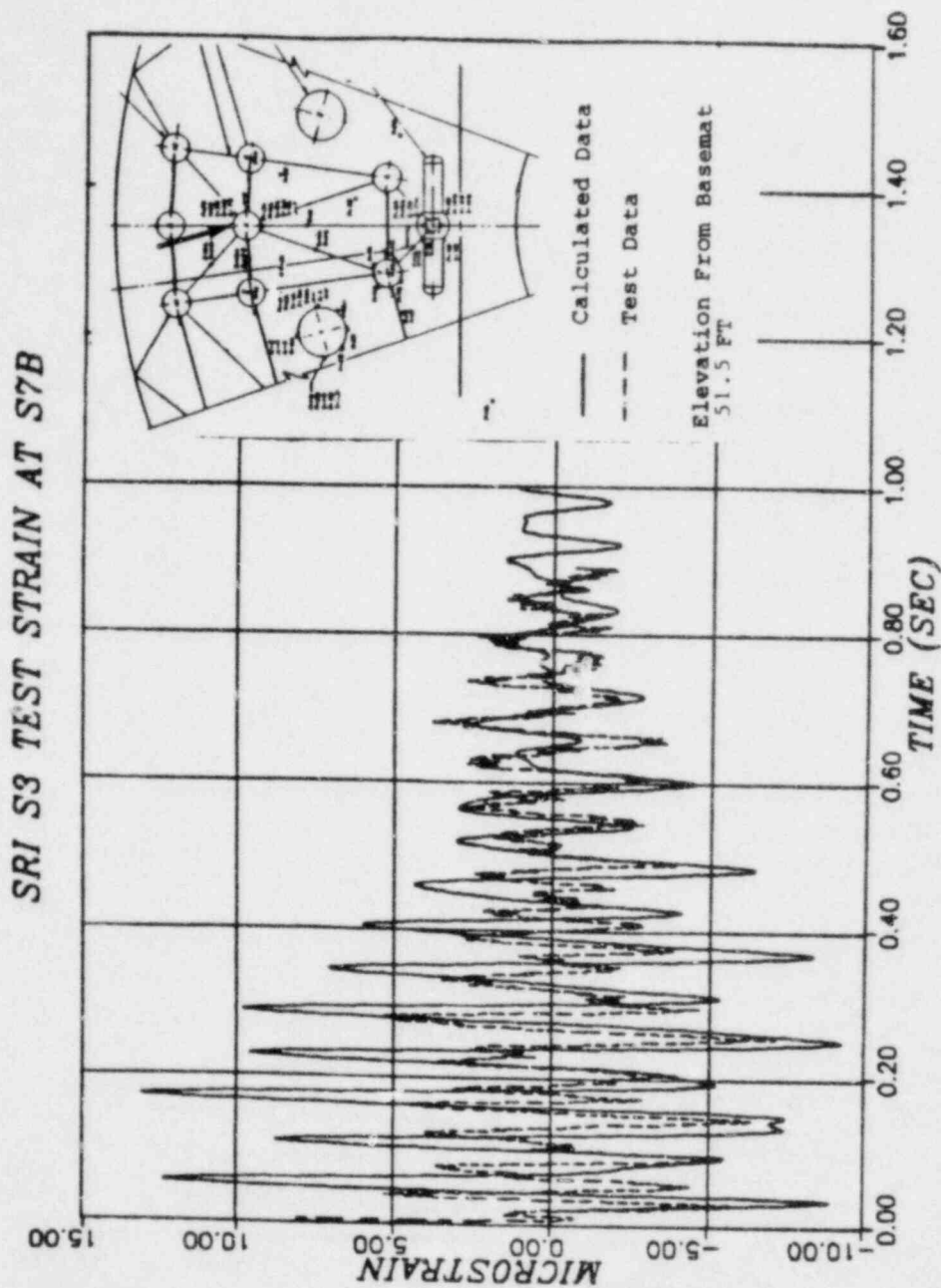


REV. 6, 4/82

SUSQUEHANNA STEAM ELECTRIC STATION
UNITS 1 AND 2
DESIGN ASSESSMENT REPORT

COMPARISON OF THE PREDICTED STRAIN
WITH MEASURED DATA - STRAIN
GAGE S7A - TEST S3

FIGURE J-59



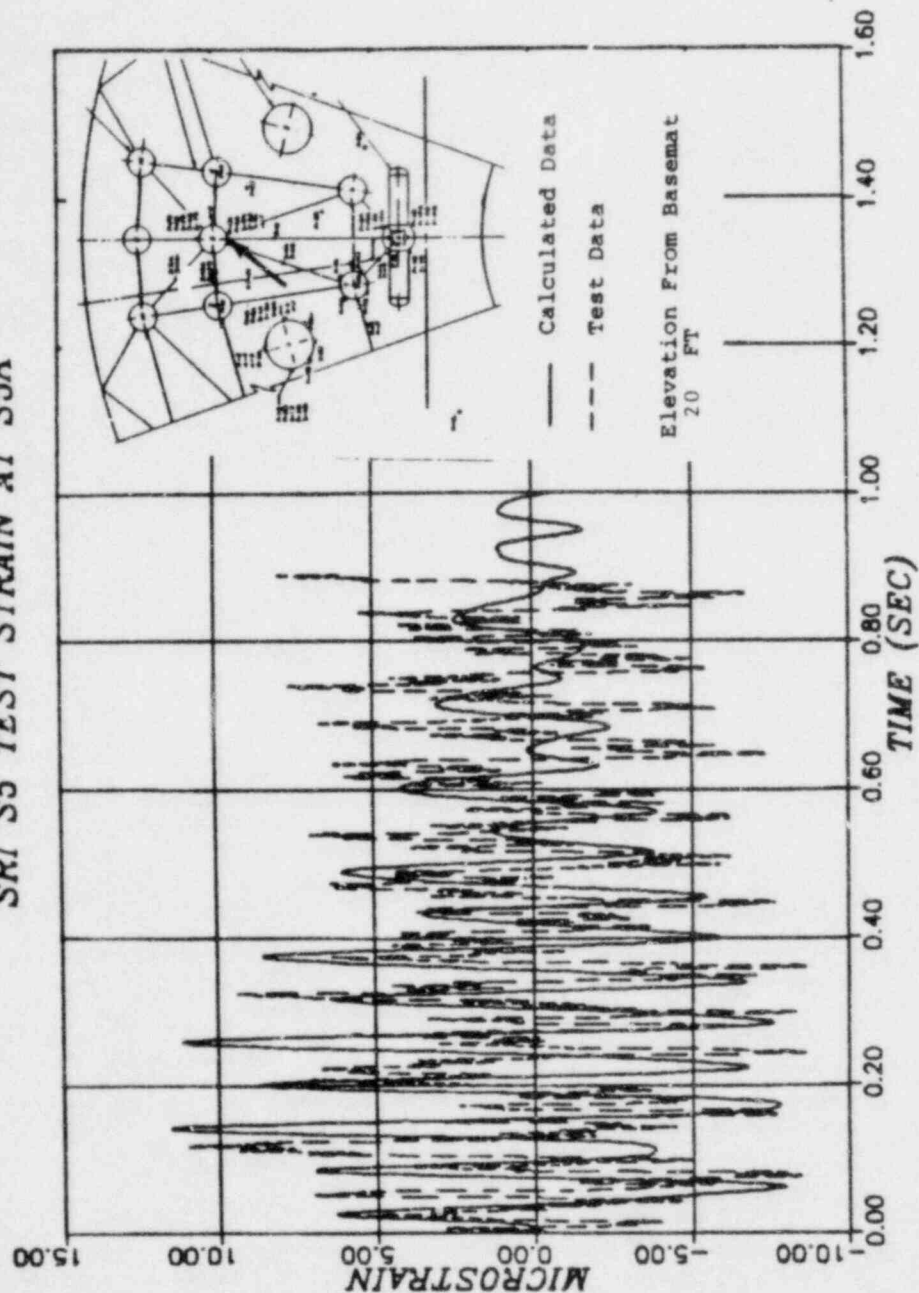
REV. 6, 4/82

**SUSQUEHANNA STEAM ELECTRIC STATION
UNITS 1 AND 2
DESIGN ASSESSMENT REPORT**

COMPARISON OF THE PREDICTED STRAIN
WITH MEASURED DATA - STRAIN
GAGE S7B - TEST S3

FIGURE J-60

SRI S5 TEST STRAIN AT S5A



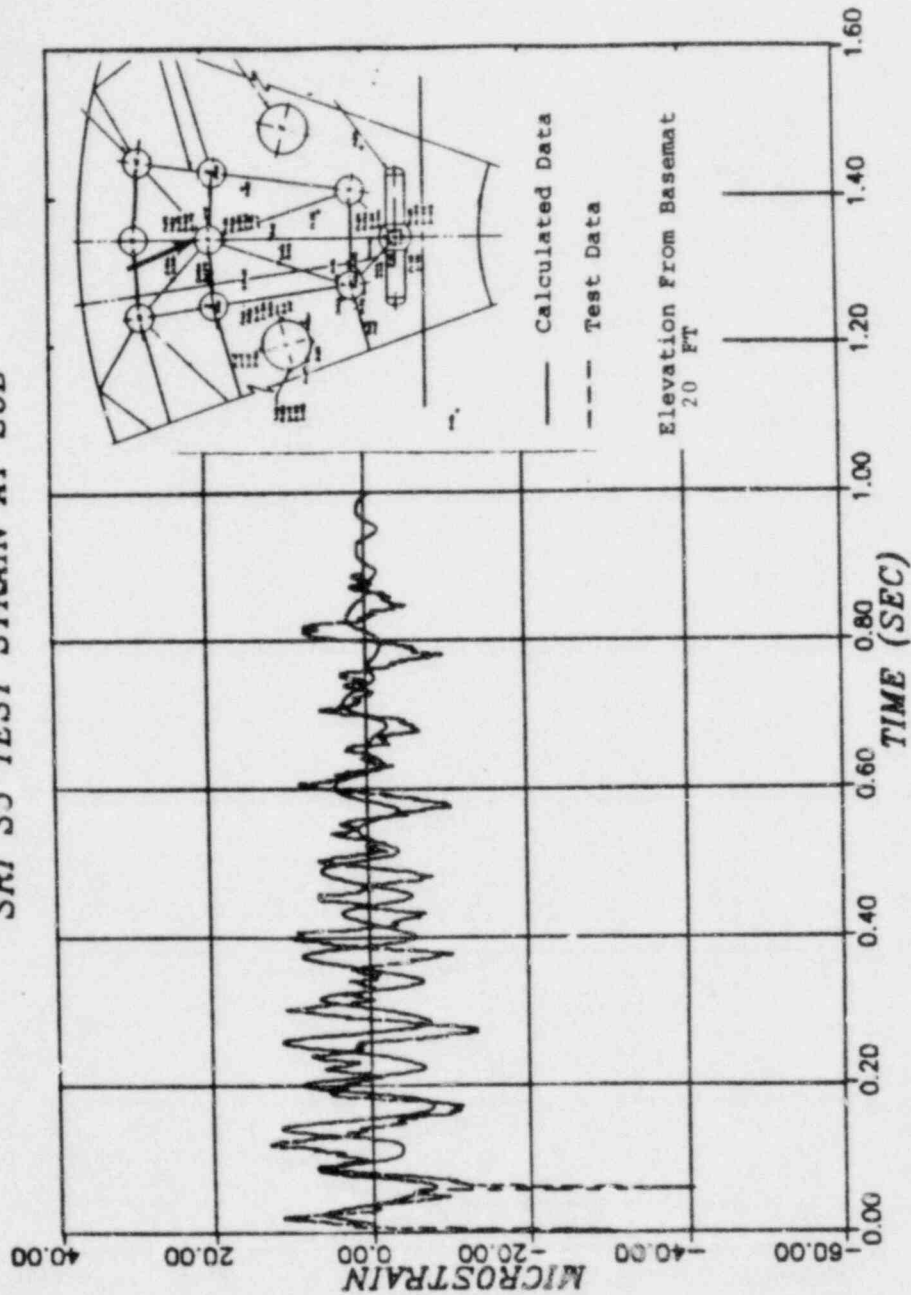
REV. 6, 4/82

SUSQUEHANNA STEAM ELECTRIC STATION
UNITS 1 AND 2
DESIGN ASSESSMENT REPORT

COMPARISON OF THE PREDICTED STRAIN
WITH MEASURED DATA - STRAIN
GAGE S5A - TEST S5

FIGURE 1-61

SRI S5 TEST STRAIN AT S5B



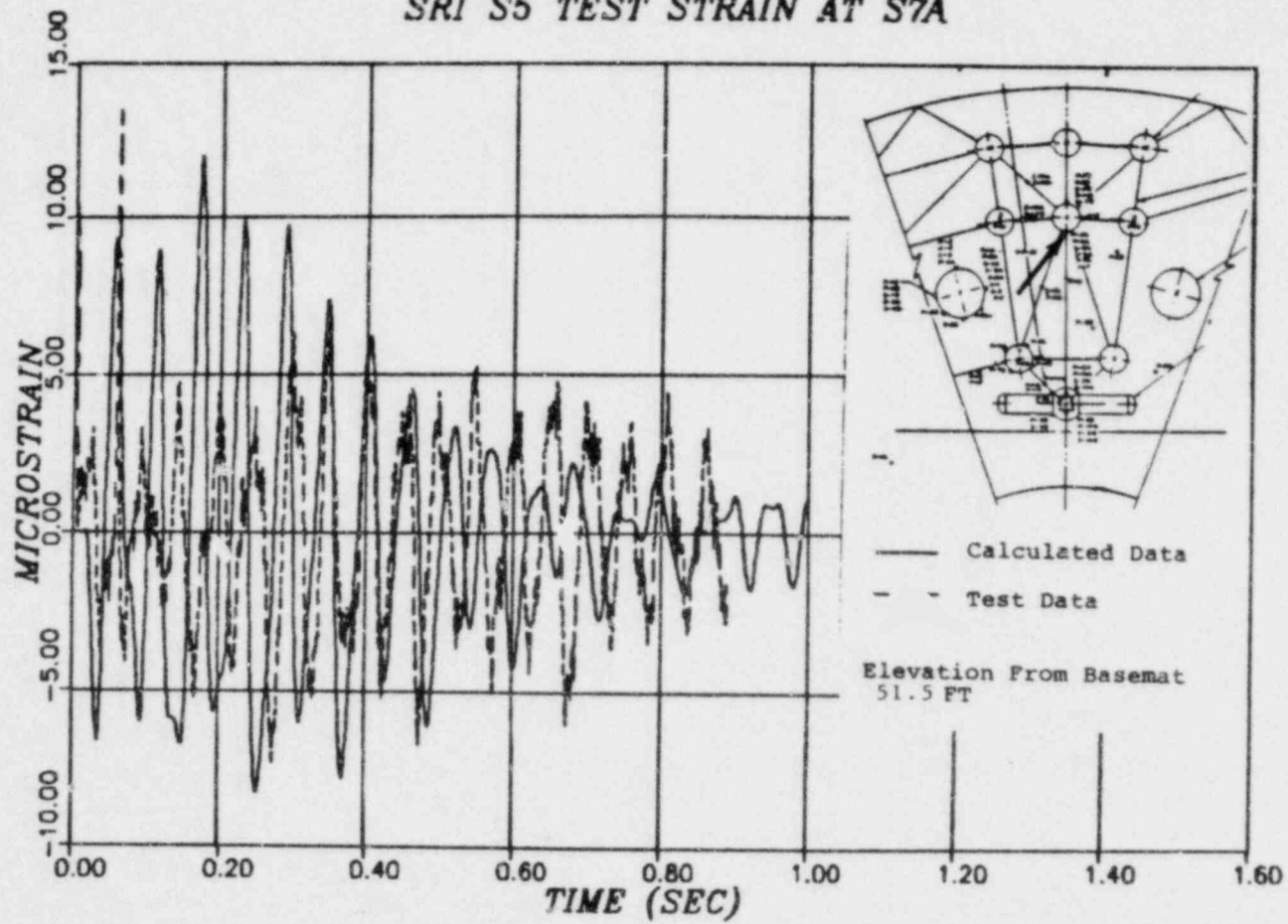
REV. 6, 4/82

SUSQUEHANNA STEAM ELECTRIC STATION
UNITS 1 AND 2
DESIGN ASSESSMENT REPORT

COMPARISON OF THE PREDICTED STRAIN
WITH MEASURED DATA - STRAIN
GAGE S5B - TEST S5

FIGURE J-62

SRI S5 TEST STRAIN AT S7A

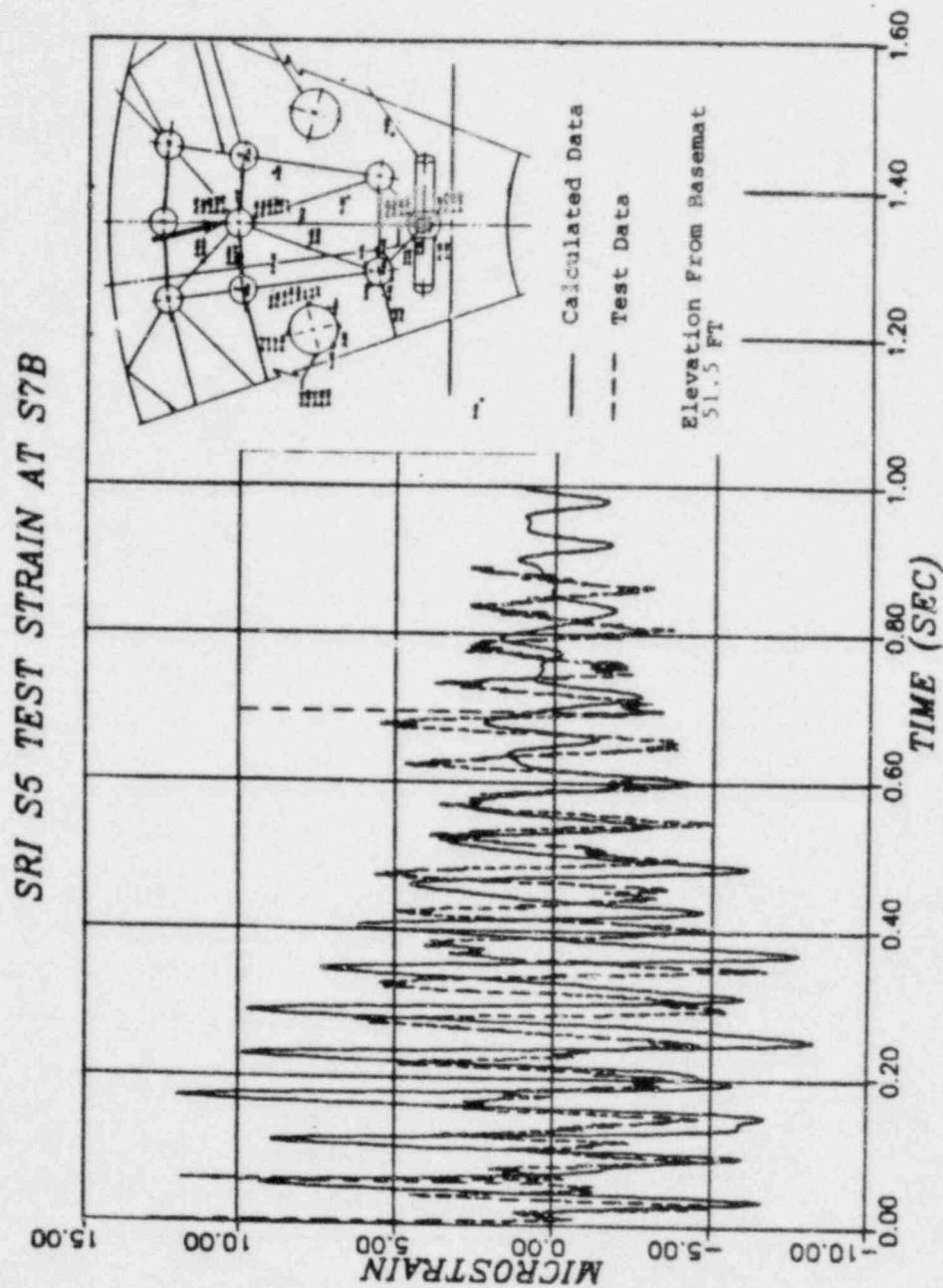


REV. 6, 4/82

SUSQUEHANNA STEAM ELECTRIC STATION
UNITS 1 AND 2
DESIGN ASSESSMENT REPORT

COMPARISON OF THE PREDICTED STRAIN
WITH MEASURED DATA - STRAIN
GAGE S7A - TEST S5

FIGURE 1-63

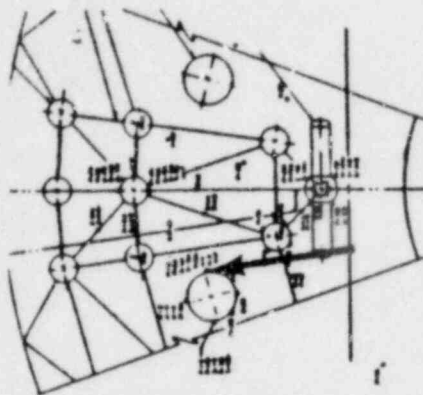


REV. 6, 4/82

**SUSQUEHANNA STEAM ELECTRIC STATION
UNITS 1 AND 2
DESIGN ASSESSMENT REPORT**

COMPARISON OF THE PREDICTED STRAIN
WITH THE TEST DATA - STRAIN
GAGE S7B - TEST S5

FIGURE J-64

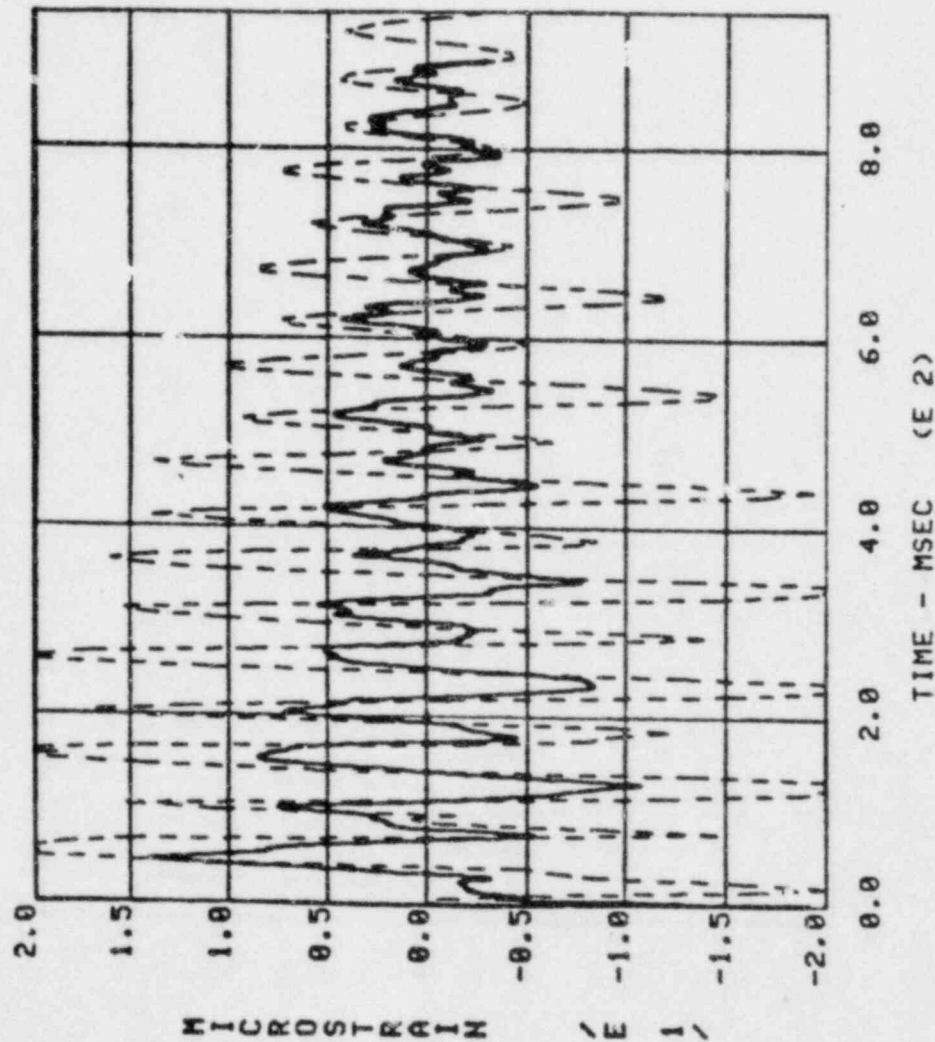


--- Calculated Data

— Test Data

Elevation From Basement
1 Pt

SRI S1 TEST STRAIN AT S1



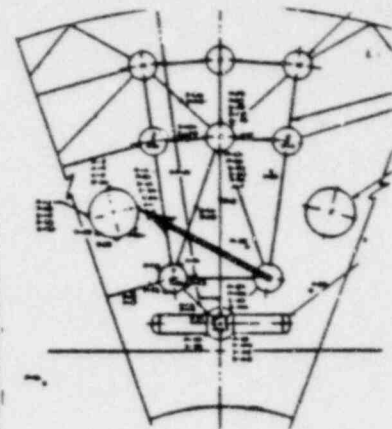
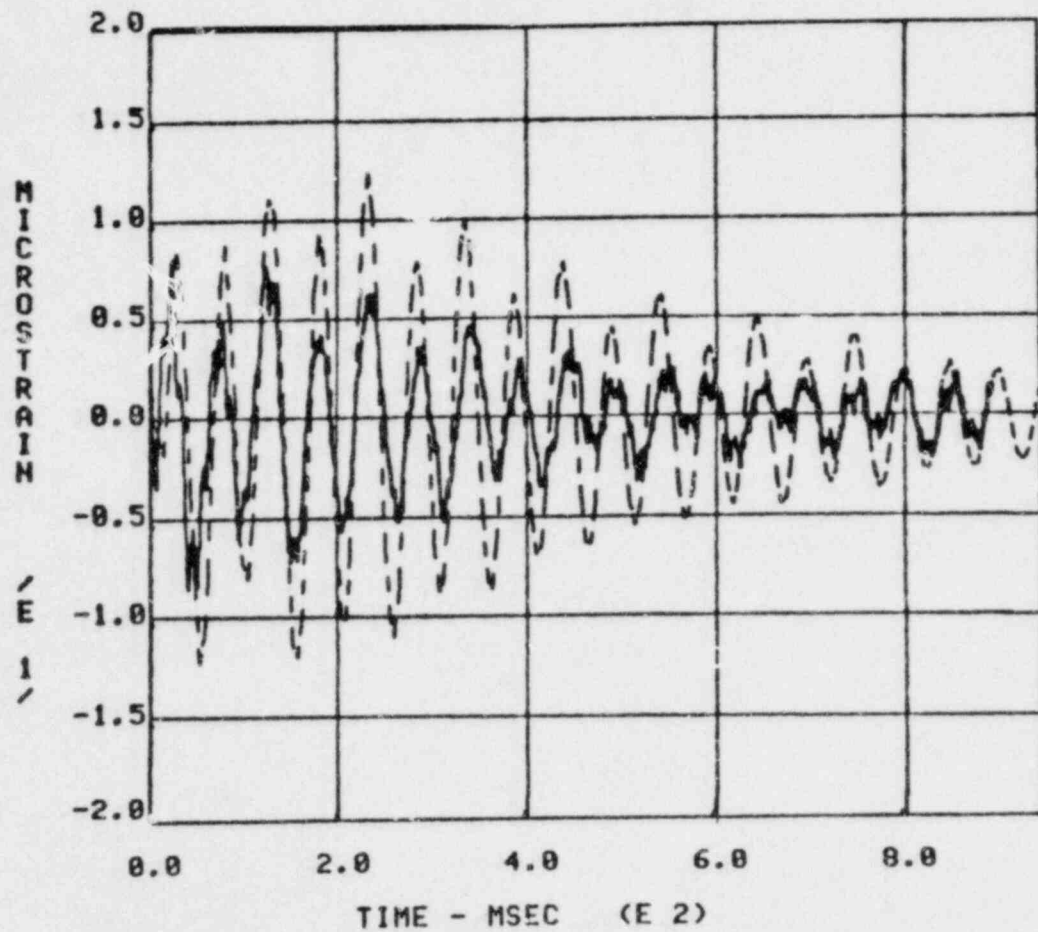
REV. 6, 4/82

SUSQUEHANNA STEAM ELECTRIC STATION
UNITS 1 AND 2
DESIGN ASSESSMENT REPORT

COMPARISON OF THE PREDICTED STRAIN
WITH THE TEST DATA - STRAIN
GAGE S1 - TEST S1

FIGURE J-65

SRI S1 TEST STRAIN AT S2



--- Calculated Data
 — Test Data

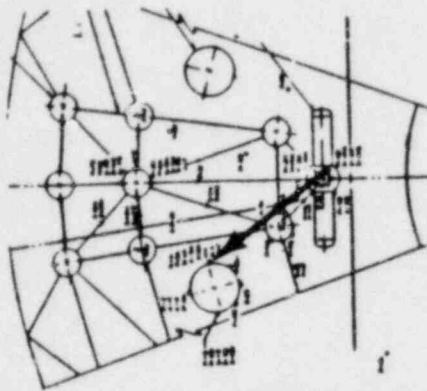
Elevation From Basemat
 24 FT

REV. 6, 4/82

SUSQUEHANNA STEAM ELECTRIC STATION
 UNITS 1 AND 2
 DESIGN ASSESSMENT REPORT

COMPARISON OF THE PREDICTED STRAIN
 WITH THE TEST DATA - STRAIN
 GAGE S2 - TEST S1

FIGURE J-65

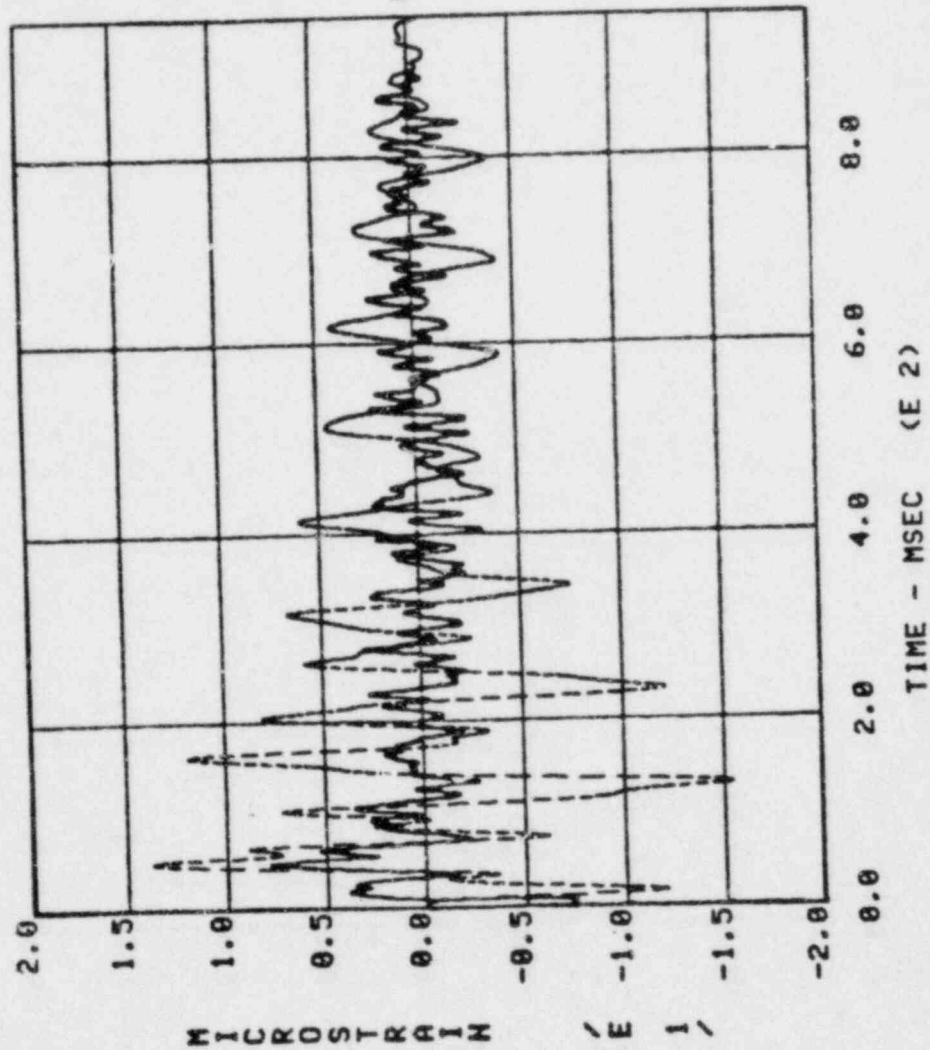


--- Calculated Data

— Test Data

Elevation From Basement
1 FT

SRI S3 TEST STRAIN AT S1

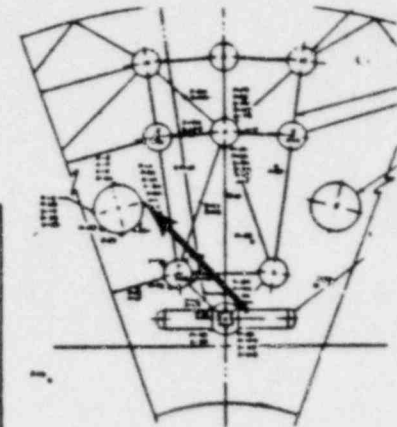
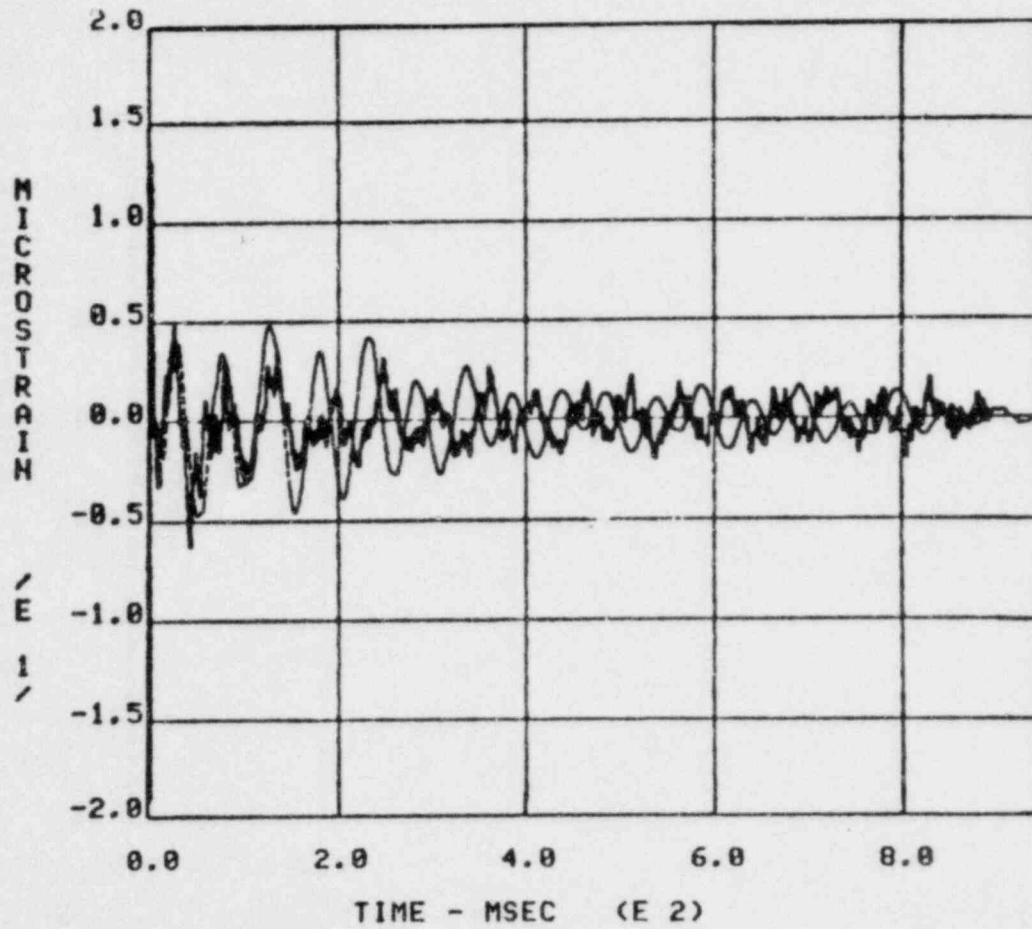


REV. 6, 4/82

SUSQUEHANNA STEAM ELECTRIC STATION
UNITS 1 AND 2
DESIGN ASSESSMENT REPORT

COMPARISON OF THE PREDICTED STRAIN
WITH THE TEST DATA - STRAIN
GAGE S1 - TEST S3
FIGURE J-67

SRI S3 TEST STRAIN AT S2



--- Calculated Data
 — Test Data

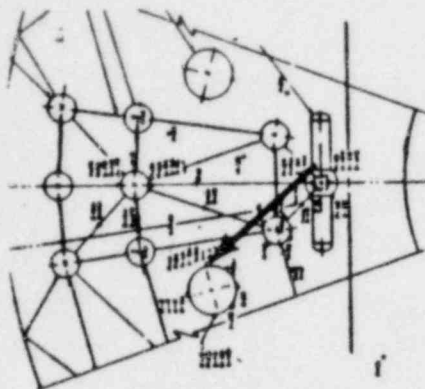
Elevation From Basemat
 24 FT

REV. 6, 4/82

SUSQUEHANNA STEAM ELECTRIC STATION
 UNITS 1 AND 2
 DESIGN ASSESSMENT REPORT

COMPARISON OF THE PREDICTED STRAIN
 WITH THE TEST DATA - STRAIN
 GAGE S2 - TEST S3

FIGURE J-68

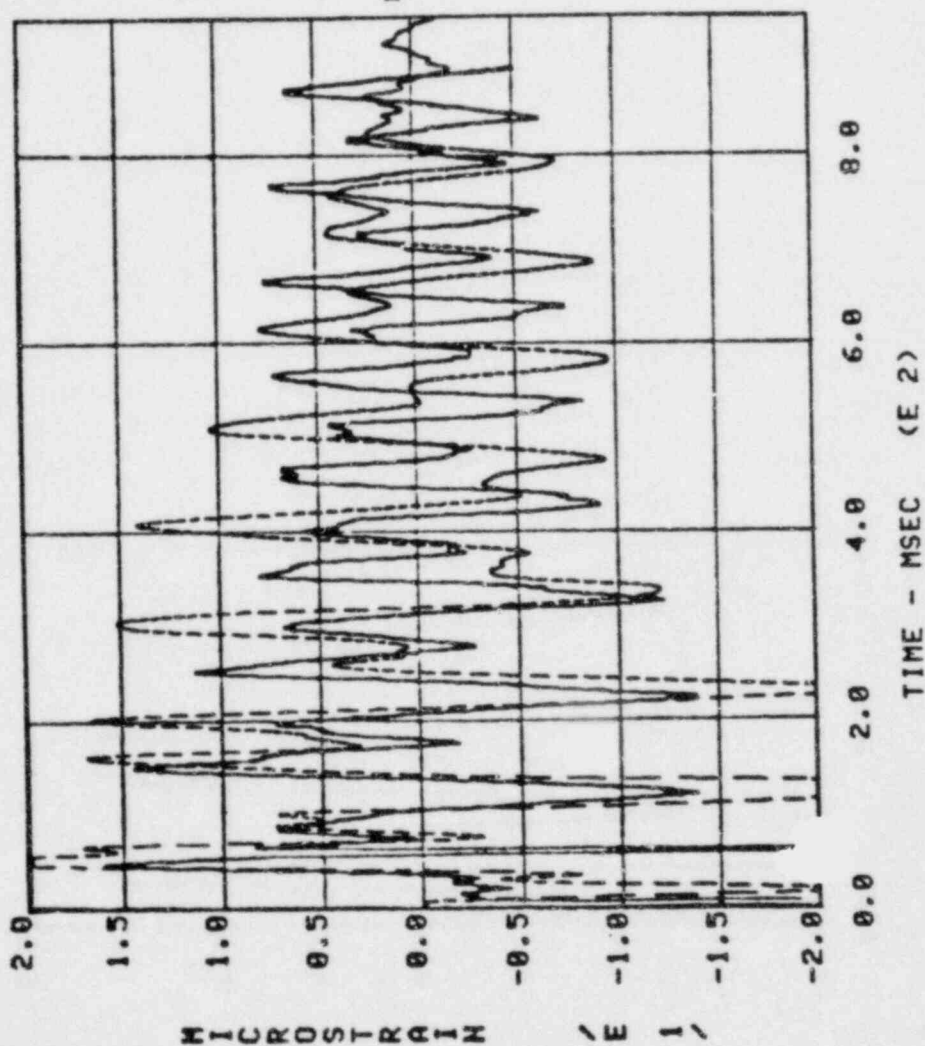


--- Calculated Data

— Test Data

Elevation From Basemat
1 Ft

SRI S5 TEST STRAIN AT S1



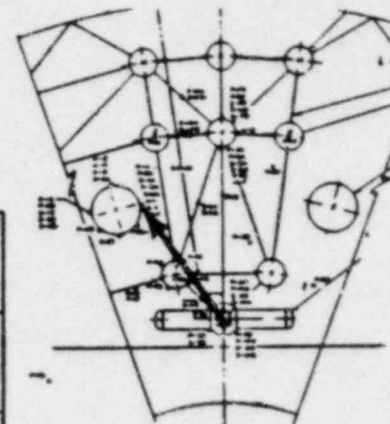
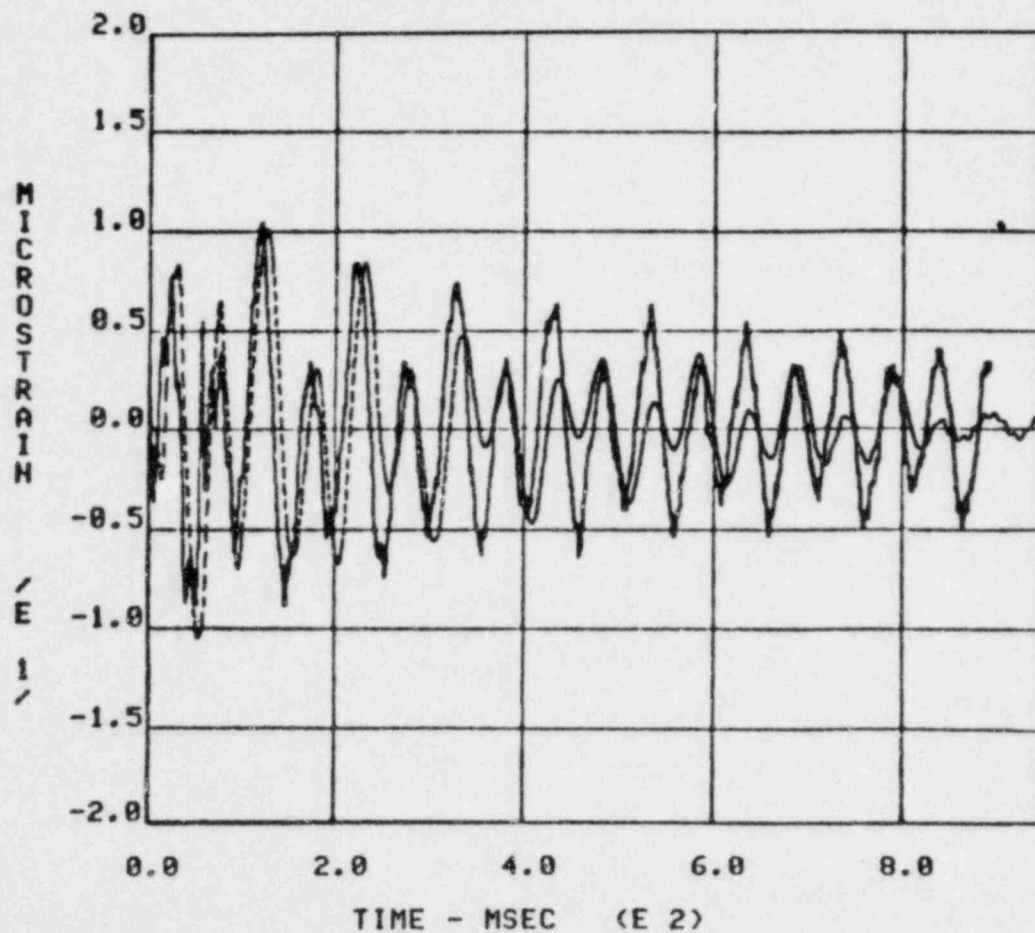
REV. 6, 4/82

SUSQUEHANNA STEAM ELECTRIC STATION
UNITS 1 AND 2
DESIGN ASSESSMENT REPORT

COMPARISON OF THE PREDICTED STRAIN
WITH THE TEST DATA - STRAIN
GAGE S1 - TEST S5

FIGURE J-69

SRI S5 TEST STRAIN AT S2



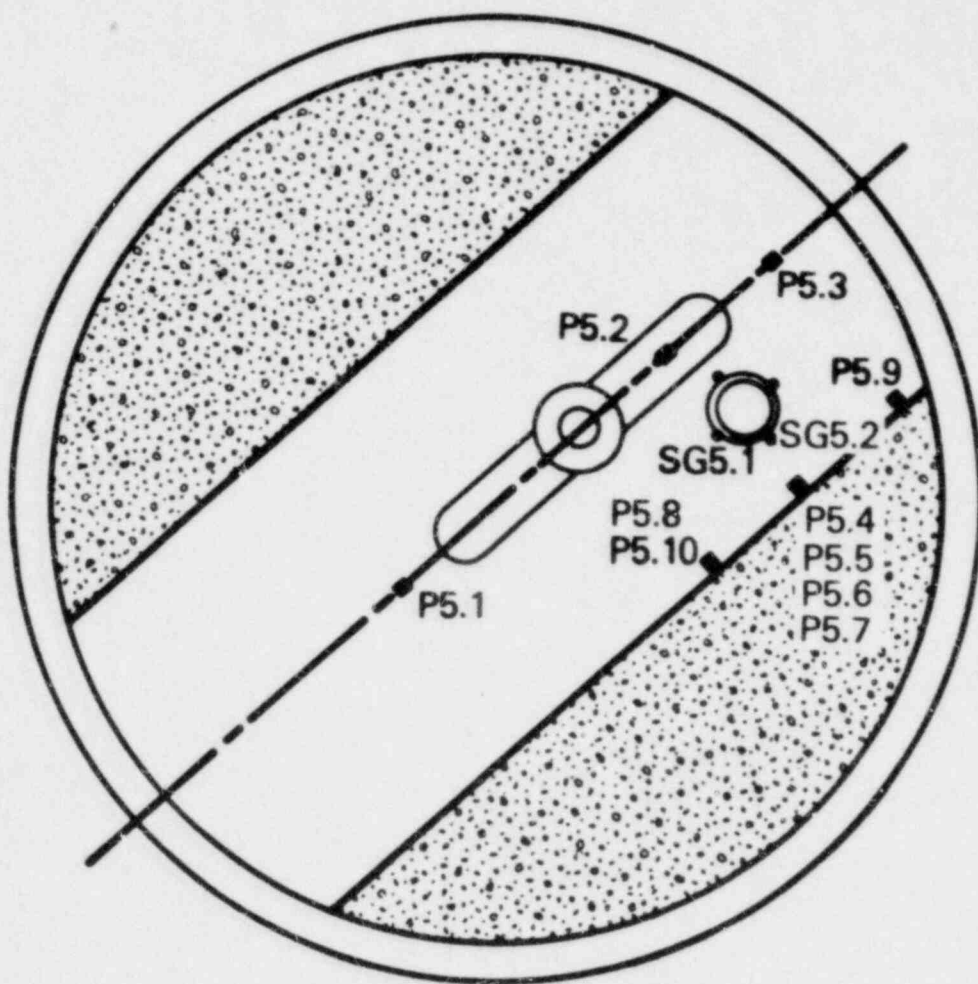
--- Calculated Data
 — Test Data

Elevation From Basemat
 24 FT

REV. 6, 4/82

SUSQUEHANNA STEAM ELECTRIC STATION
 UNITS 1 AND 2
 DESIGN ASSESSMENT REPORT

COMPARISON OF THE PREDICTED STRAIN
 WITH THE TEST DATA - STRAIN
 GAGE S2 - TEST S5
 FIGURE 1-70



ELEVATION

P5.1	0.
P5.2	0.
P5.3	0.
P5.4	0.
P5.5	3.5' (1.07m)
P5.6	9.19' (2.8m)
P5.7	16.41' (5.0m)
P5.8	9.19' (2.8m)
P5.9	9.19' (2.8m)
P5.10	3.5' (1.07m)

REV. 6, 4/82

SUSQUEHANNA STEAM ELECTRIC STATION

UNITS 1 AND 2

DESIGN ASSESSMENT REPORT

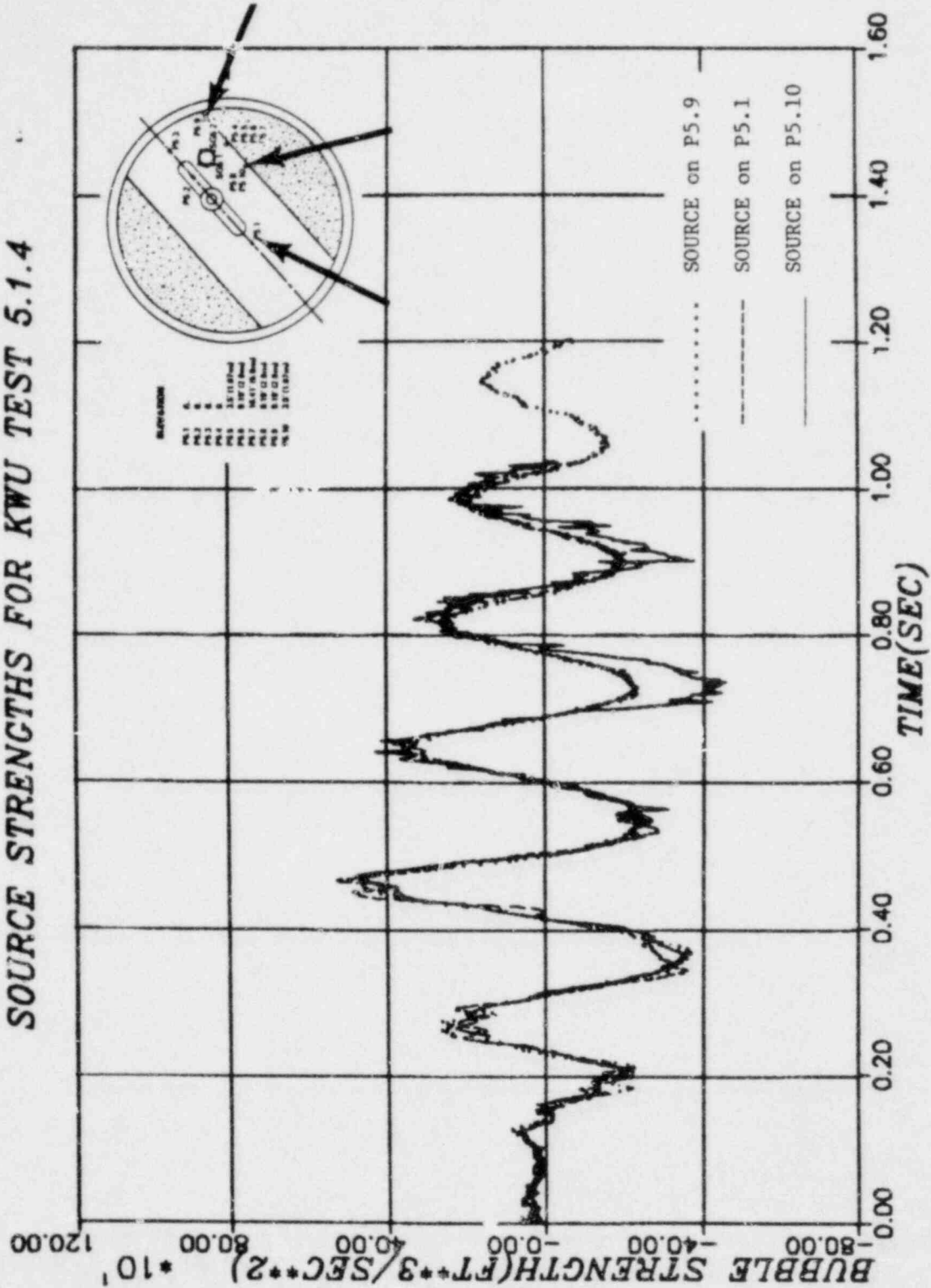
PRESSURE TRANSDUCER AND STRAIN

GAGE LOCATIONS -

KARLSTEIN T-QUENCHER TEST TANK

FIGURE J-71

SOURCE STRENGTHS FOR KWU TEST 5.1.4



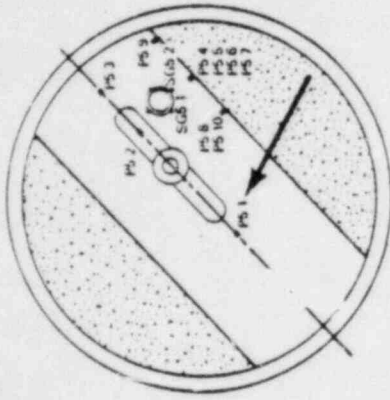
REV. 6, 4/82

SUSQUEHANNA STEAM ELECTRIC STATION
UNITS 1 AND 2
DESIGN ASSESSMENT REPORT

SOURCE STRENGTH COMPARISON
TEST 5.1.4

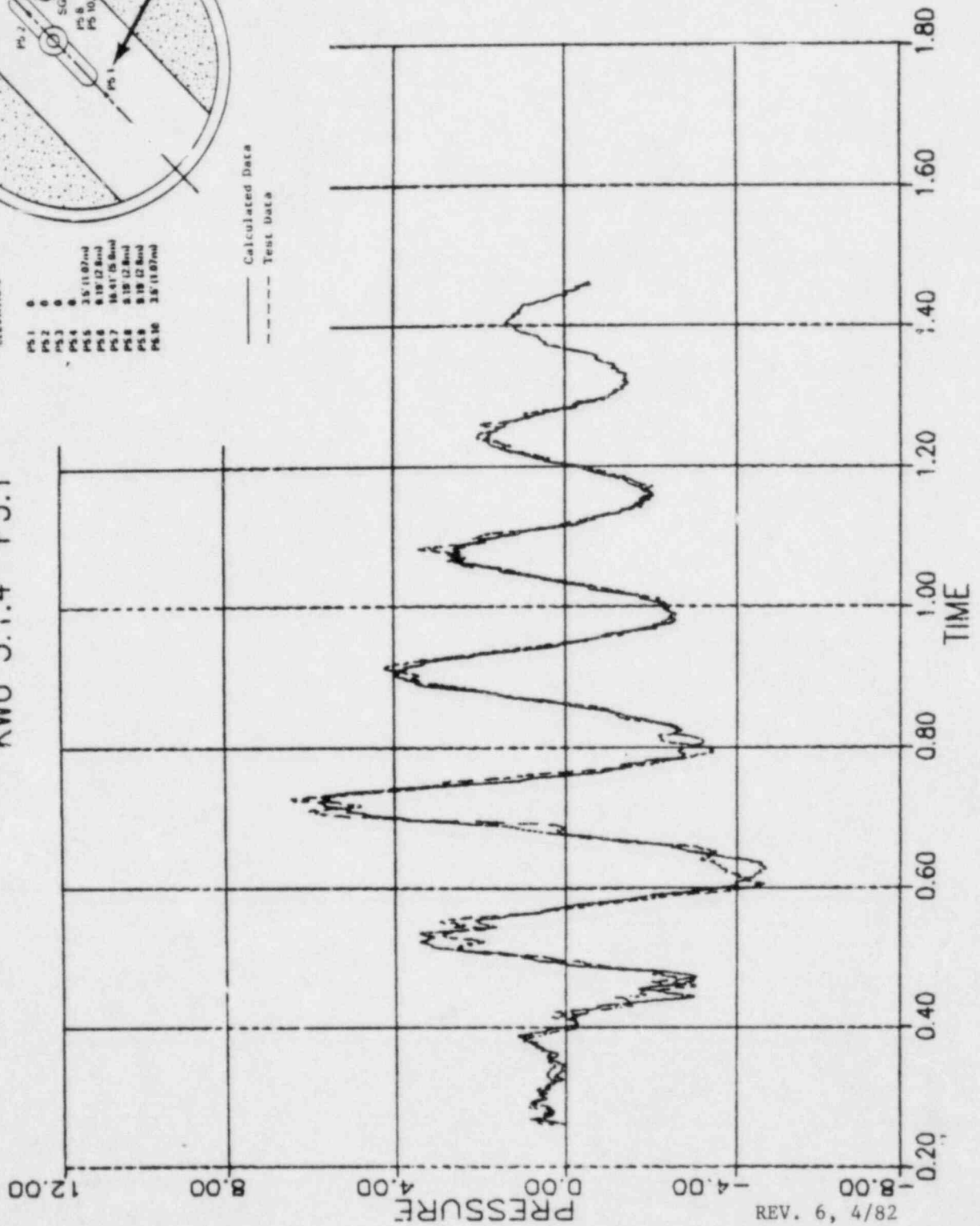
FIGURE J-72

KWU 5.1.4 P5.1*



ELEVATION	
P5.1	0
P5.2	0
P5.3	0
P5.4	0
P5.5	3.5' (1.07m)
P5.6	8.18' (2.50m)
P5.7	16.41' (5.00m)
P5.8	2.15' (0.65m)
P5.9	8.18' (2.50m)
P5.10	3.5' (1.07m)

— Calculated Data
 - - - Test Data



REV. 6, 4/82

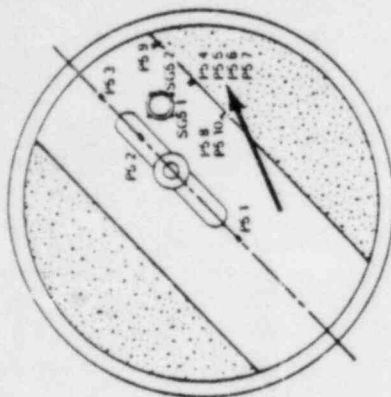
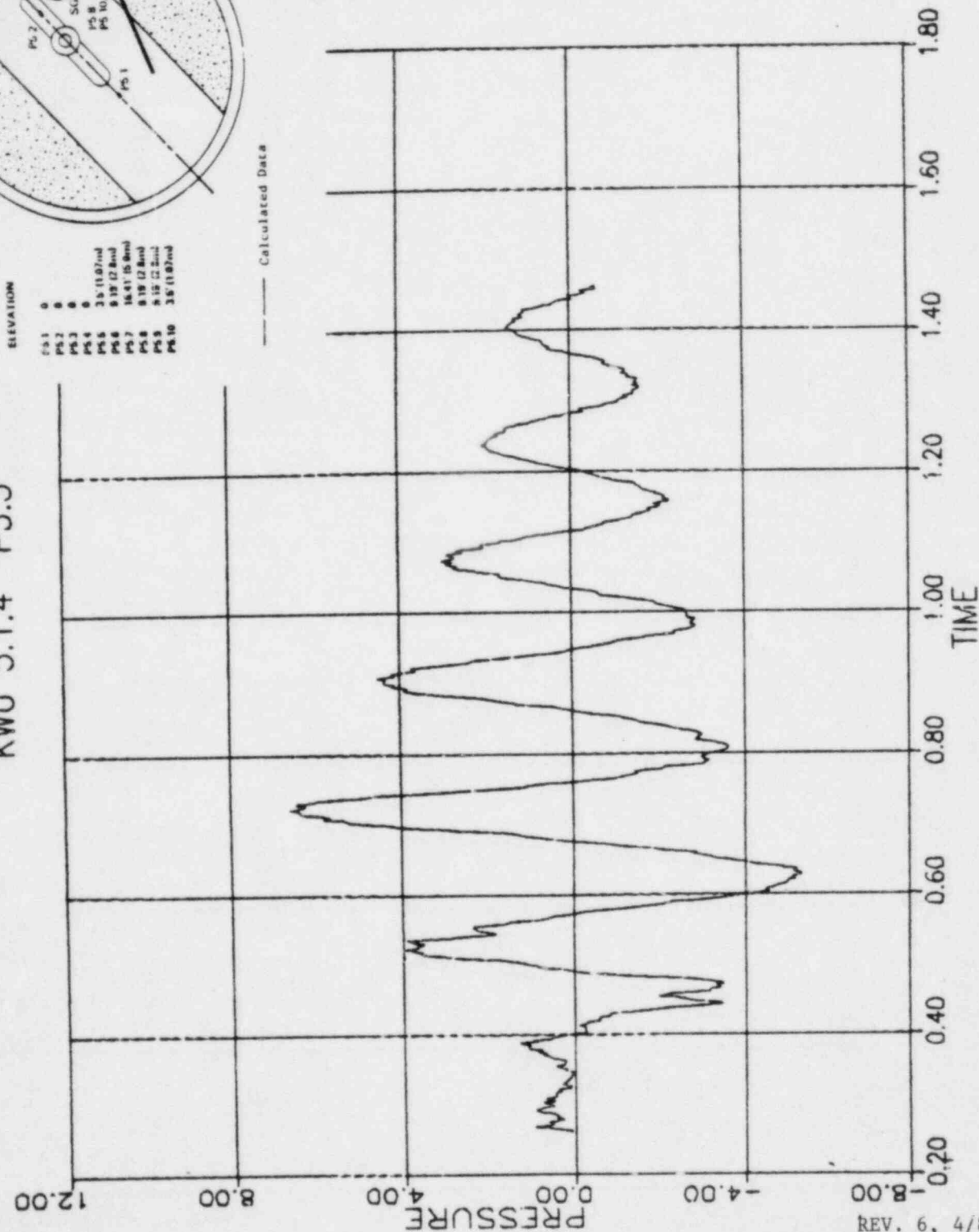
**SUSQUEHANNA STEAM ELECTRIC STATION
 UNITS 1 AND 2
 DESIGN ASSESSMENT REPORT**

COMPARISON OF THE PREDICTED
 PRESSURE TIME HISTORY WITH THE
 TEST
 DATA - P5.1 - TEST 5.1.4

FIGURE J-73

*SOURCE BASED ON P5.9

KWU 5.1.4 P5.5*



ELEVATION	
P5.1	0
P5.2	0
P5.3	0
P5.4	0
P5.5	3.5 (10.7)nd
P5.6	9.15 (28.0)nd
P5.7	16.41 (50.8)nd
P5.8	9.15 (28.0)nd
P5.9	9.15 (28.0)nd
P5.10	3.5 (10.7)nd

Calculated Data

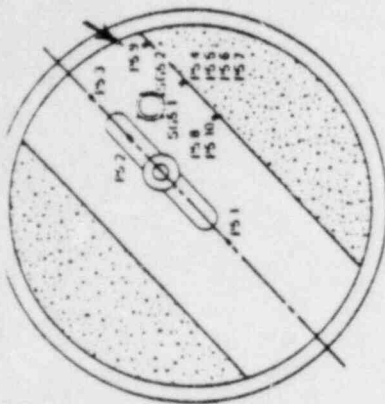
REV. 6, 4/82

<p>SUSQUEHANNA STEAM ELECTRIC STATION UNITS 1 AND 2 DESIGN ASSESSMENT REPORT</p>
<p>COMPARISON OF THE PREDICTED PRESSURE TIME HISTORY WITH THE TEST DATA - P5.5 - TEST 5.1.4</p>
<p>FIGURE J-74</p>

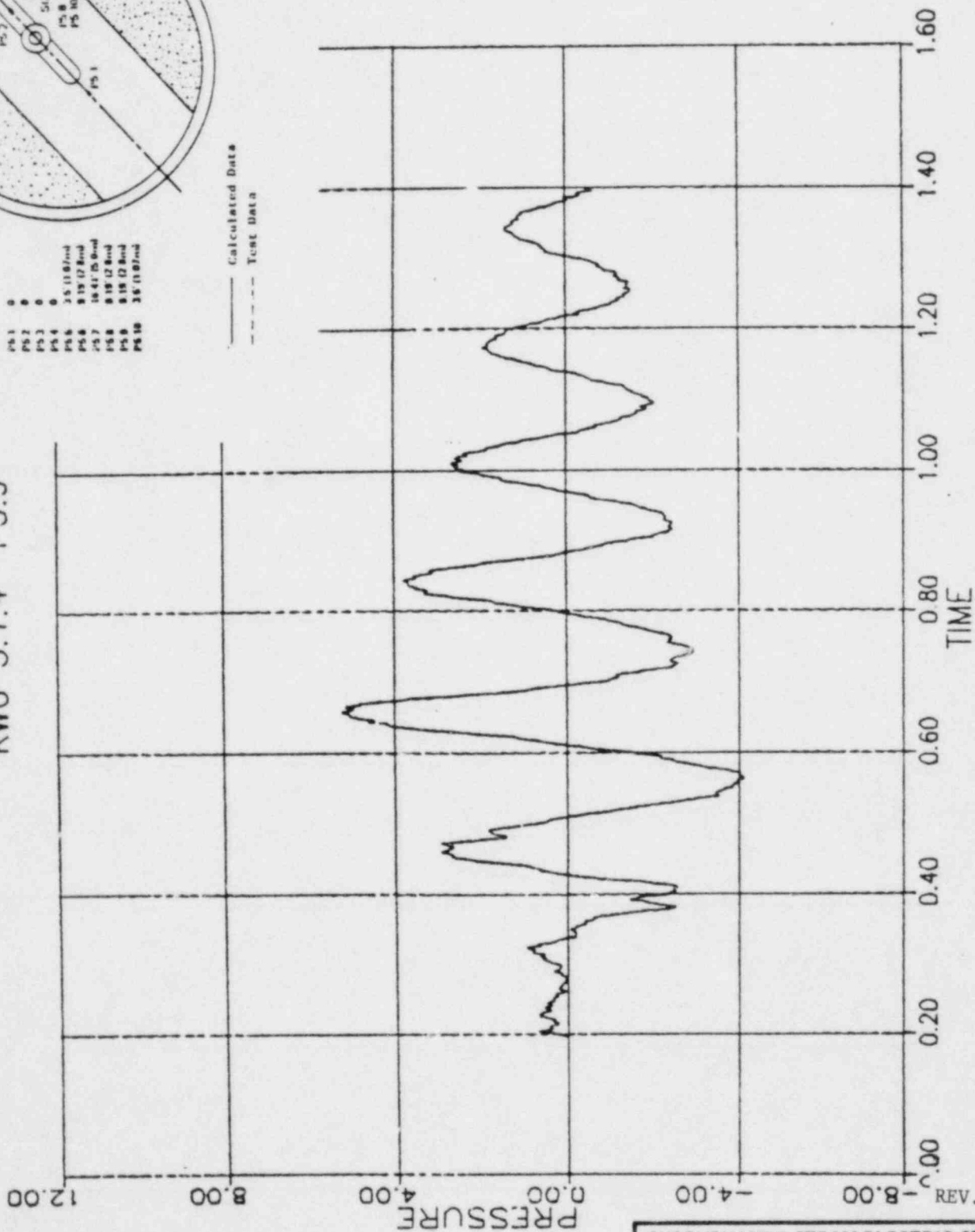
*SOURCE BASED ON P5.9

KWU 5.1.4 P5.9*

ELEVATION	
P5.1	0
P5.2	0
P5.3	0
P5.4	0
P5.5	3.5 (11.8)ft
P5.6	9.35 (28.4)ft
P5.7	16.41 (50.7)ft
P5.8	8.15 (24.8)ft
P5.9	8.15 (24.8)ft
P5.10	3.8 (11.6)ft



— Calculated Data
 --- Test Data



*SOURCE BASED ON P5.9

SUSQUEHANNA STEAM ELECTRIC STATION
 UNITS 1 AND 2
 DESIGN ASSESSMENT REPORT

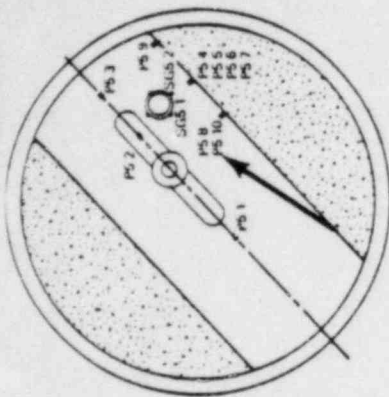
COMPARISON OF THE PREDICTED
 PRESSURE TIME HISTORY WITH THE
 TEST
 DATA - P5.9 - Test 5.1.4
 FIGURE J-75

REV. 6, 4/82

KWU 5.1.4 P5.10*

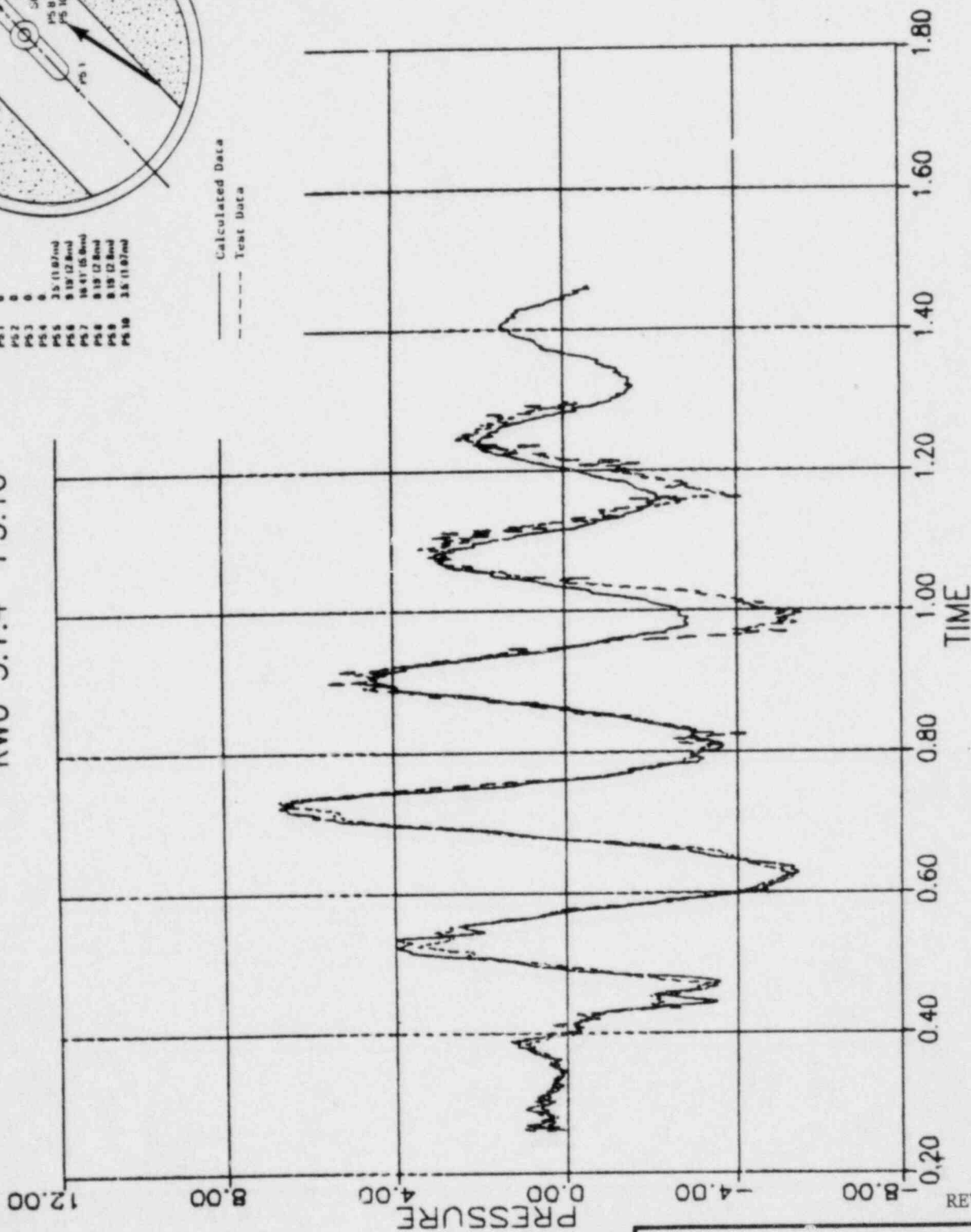
ELEVATION

P5.1	0
P5.2	0
P5.3	0
P5.4	0
P5.5	25 (11.87m)
P5.6	9.19 (12.8m)
P5.7	16.41 (15.8m)
P5.8	9.19 (12.8m)
P5.9	9.19 (12.8m)
P5.10	3.8 (11.87m)



— Calculated Data

- - - - - Test Data



*SOURCE BASED ON P5.9

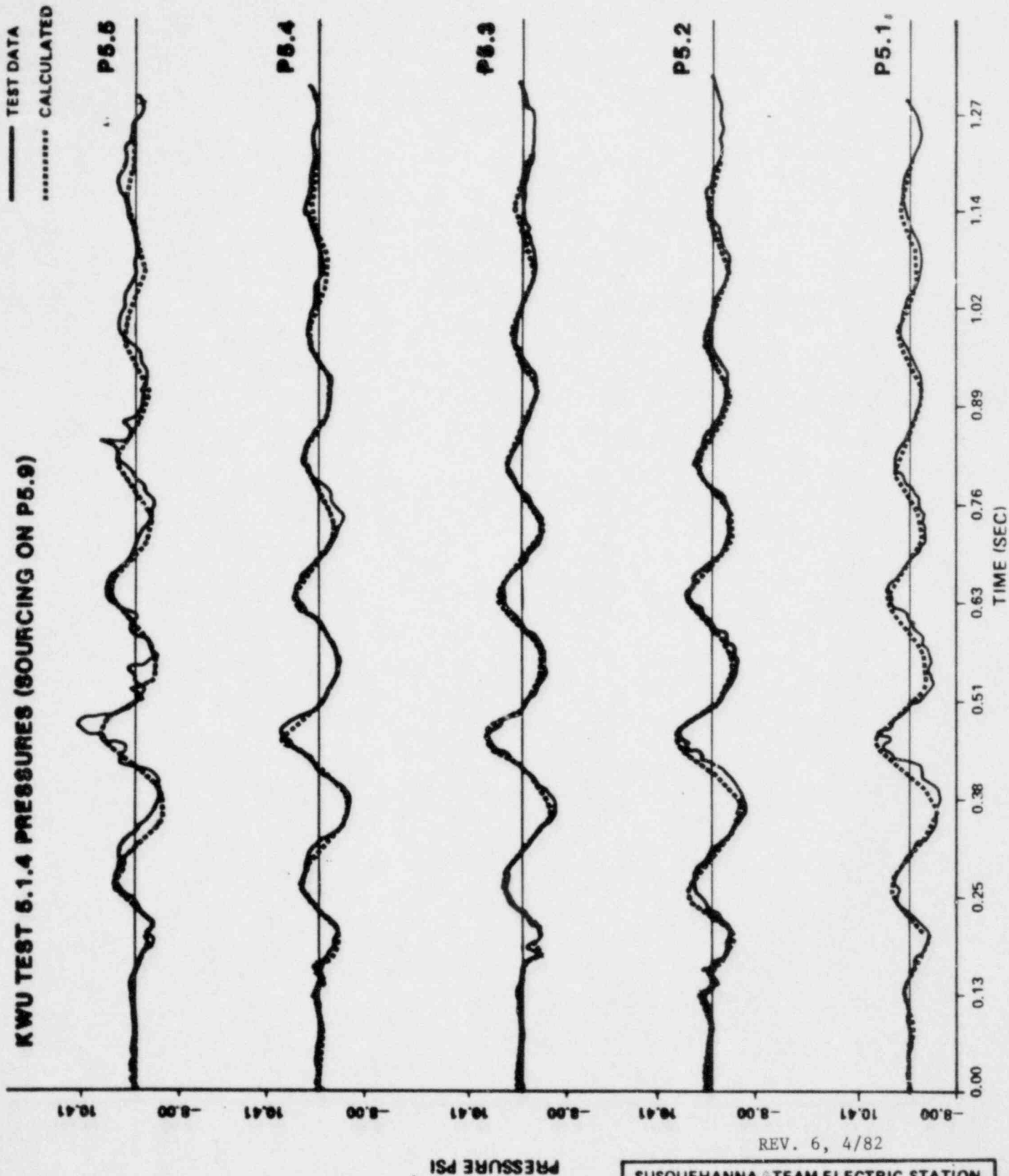
REV. 6, 4/82

**SUSQUEHANNA STEAM ELECTRIC STATION
UNITS 1 AND 2
DESIGN ASSESSMENT REPORT**

COMPARISON OF THE PREDICTED
PRESSURE TIME HISTORY
WITH THE TEST
DATA - P5.10 - TEST 5.1.4

FIGURE J-76

KWU TEST 5.1.4 PRESSURES (SOURCING ON P5.9)

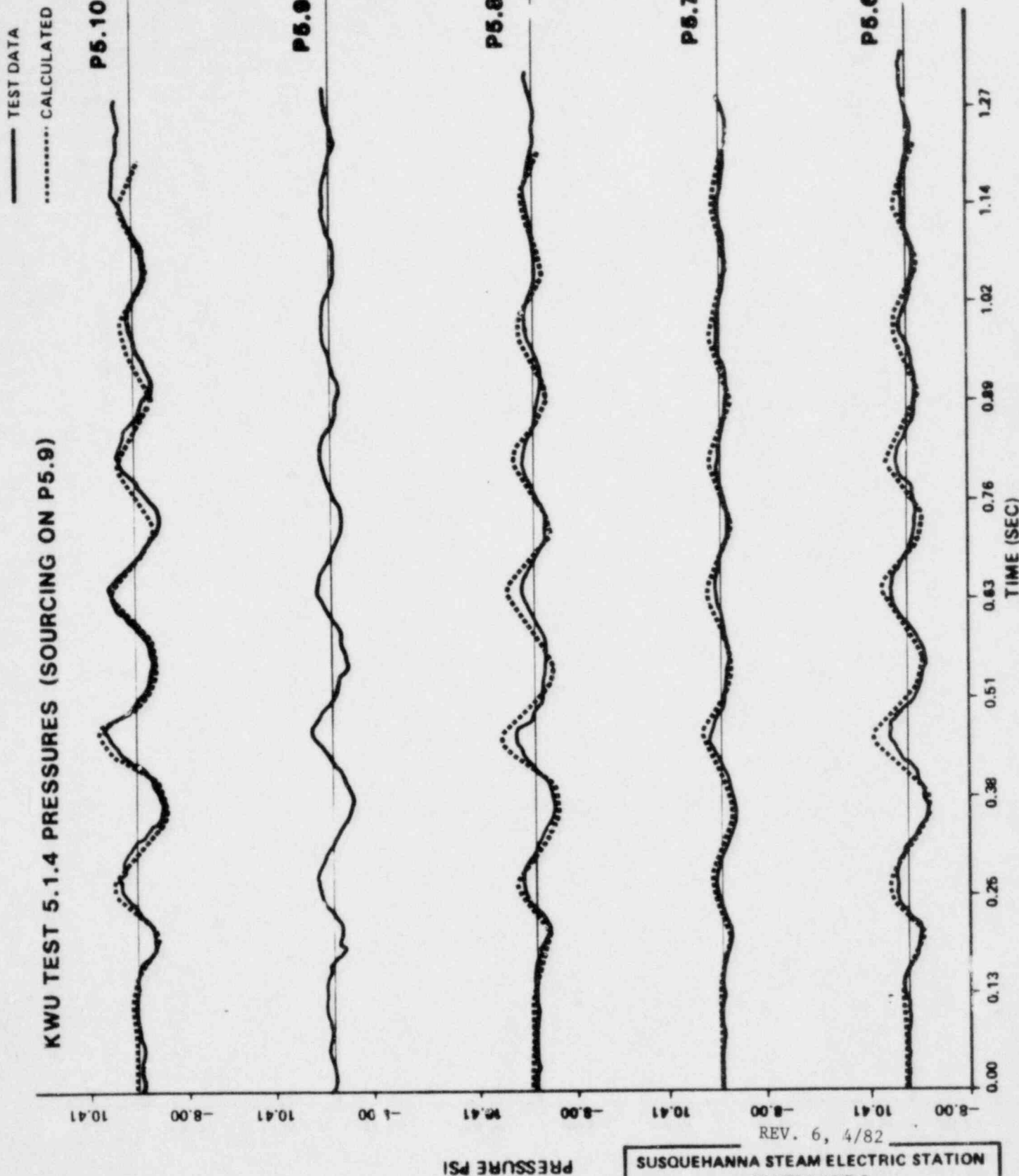


REV. 6, 4/82

SUSQUEHANNA STEAM ELECTRIC STATION
UNITS 1 AND 2
DESIGN ASSESSMENT REPORT

COMPARISON OF THE PREDICTED
PRESSURE TIME HISTORIES
WITH THE TEST
DATA - P5.1 TO P5.5 - TEST 5.1.4
FIGURE J-77

KWU TEST 5.1.4 PRESSURES (SOURCING ON P5.9)



REV. 6, 4/82

SUSQUEHANNA STEAM ELECTRIC STATION
 UNITS 1 AND 2
 DESIGN ASSESSMENT REPORT

COMPARISON OF THE PREDICTED
 PRESSURE TIME HISTORIES
 WITH THE TEST
 DATA - P5.6 TO P5.10 - Test 5.1.4
 FIGURE J-73

KWU TEST 4.1.5 PRESSURES (SOURCING ON P5.10)

— TEST DATA
 CALCULATED

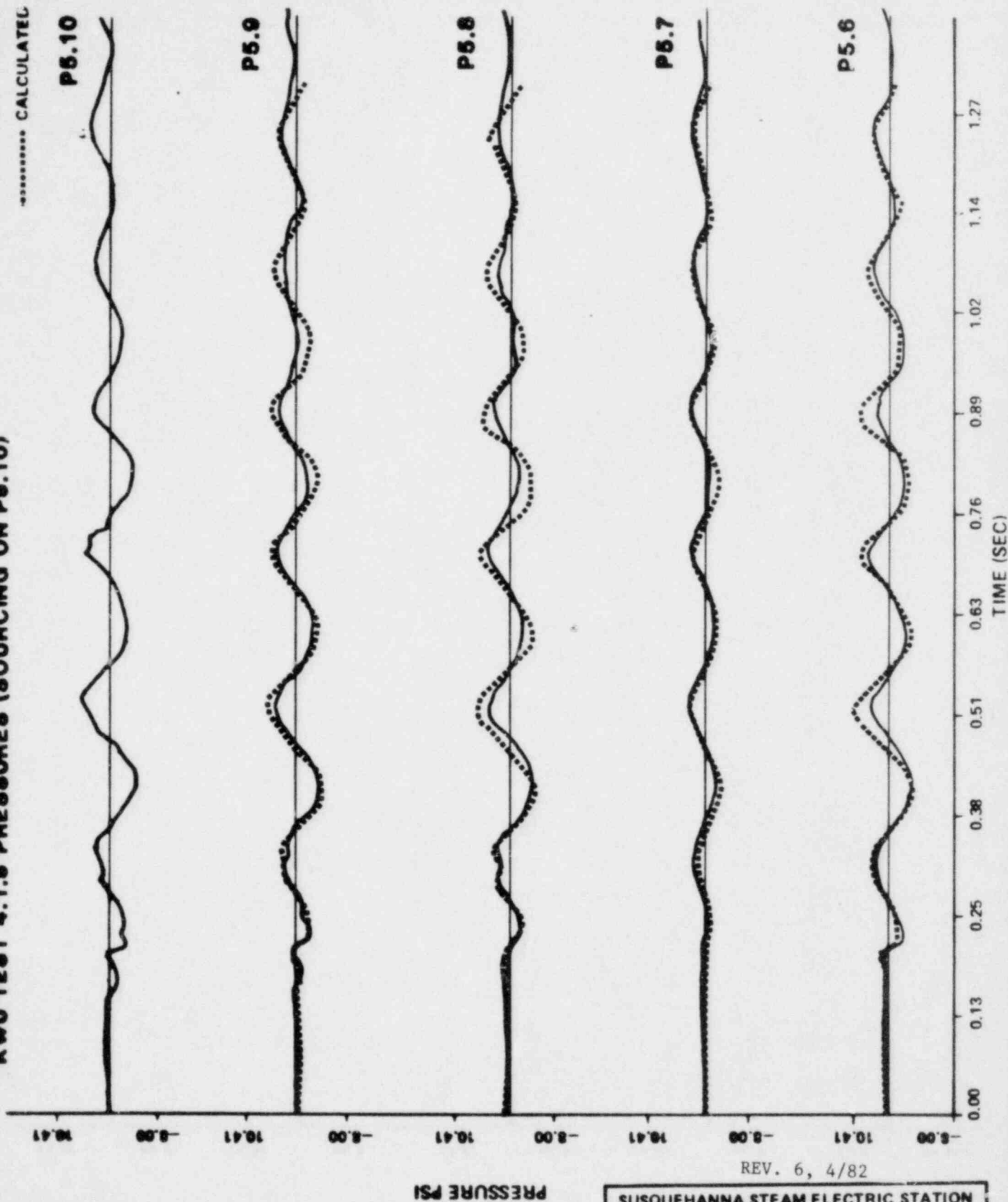
P5.10

P5.9

P5.8

P5.7

P5.6



REV. 6, 4/82

SUSQUEHANNA STEAM ELECTRIC STATION
 UNITS 1 AND 2
 DESIGN ASSESSMENT REPORT

COMPARISON OF THE PREDICTED
 PRESSURE TIME HISTORIES
 WITH THE TEST
 DATA - P5.6 TO P5.10 - TEST 4.1.5
 FIGURE J-30

KWU TEST 15.1.6 PRESSURES (SOURCING ON P5.10)

— TEST DATA
 CALCULATED

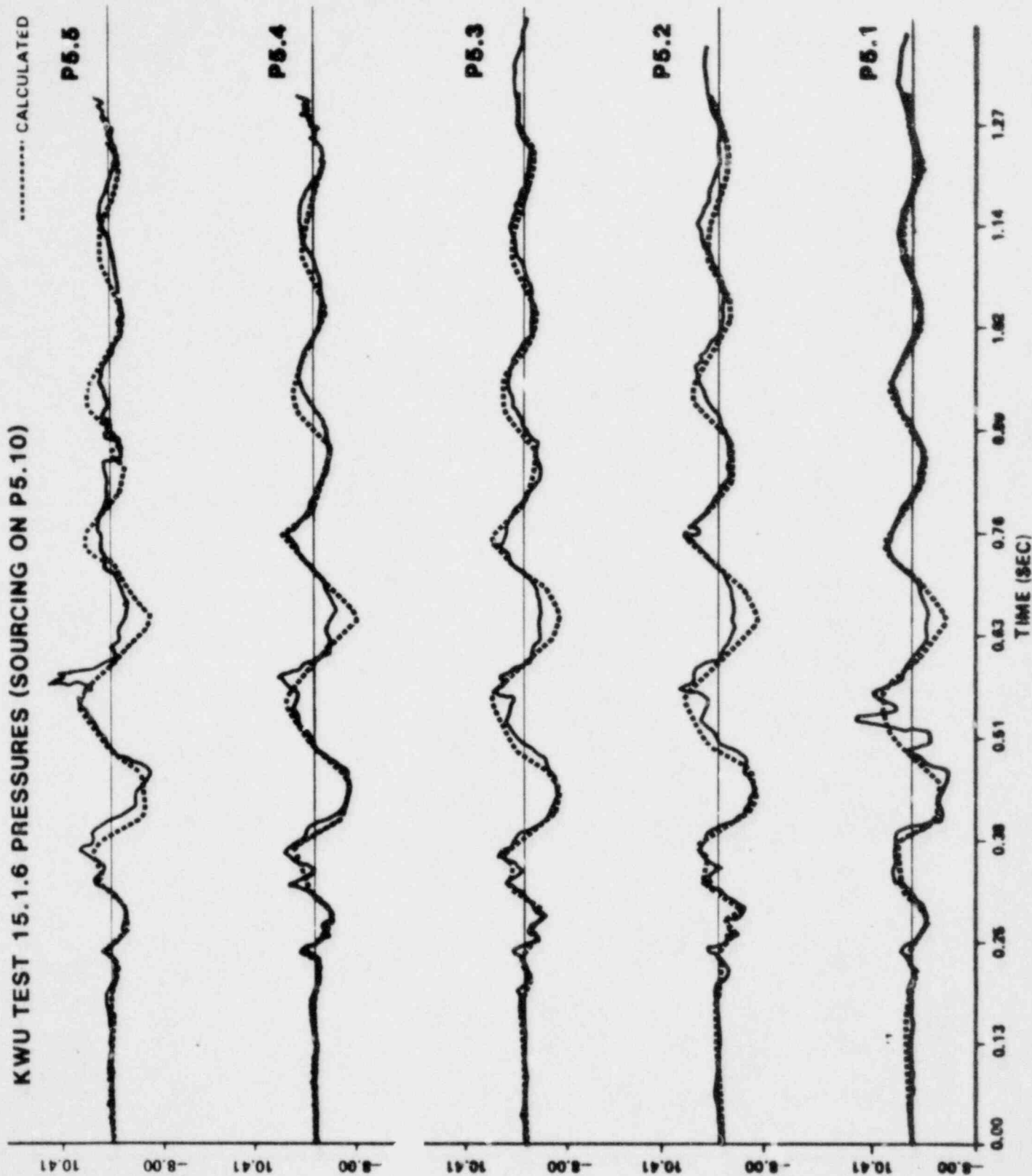
P5.5

P5.4

P5.3

P5.2

P5.1



PRESSURE PSI

REV. 6, 4/82

SUSQUEHANNA STEAM ELECTRIC STATION
 UNITS 1 AND 2
 DESIGN ASSESSMENT REPORT

COMPARISON OF THE PREDICTED
 PRESSURE TIME HISTORIES
 WITH THE TEST
 DATA - P5.1 TO P5.5 - TEST 15.1.6
 FIGURE J-81

KWU TEST 15.1.6 PRESSURES (SOURCING ON P5.10)

— TEST DATA
 CALCULATED

P5.10

P5.9

P5.8

P5.7

P5.6

10.41

-8.00

10.41

-8.00

10.41

-8.00

10.41

-8.00

10.41

-8.00

PRESSURE PSI

TIME (SEC)

1.27

1.14

1.02

0.89

0.76

0.63

0.51

0.38

0.25

0.13

0.00

REV. 6, 4/82

SUSQUEHANNA STEAM ELECTRIC STATION
 UNITS 1 AND 2
 DESIGN ASSESSMENT REPORT

COMPARISON OF THE PREDICTED
 PRESSURE TIME HISTORIES
 WITH THE TEST
 DATA - P5.6 TO P5.10 - TEST 15.1.6
 FIGURE J-32

TABLE J-1
SENSOR LOCATIONS - SRI
SUBMERGED STRUCTURE
BUBBLE TESTS

Sensor	Parameter and Location	Elevation (ft)	Sensor	Parameter and Location	Elevation (ft)
P-1A	Pressure on lower front of column 1	3.60	P-10A	Pressure on front of SRV Line	13.75
P-1B	Pressure on lower back of column 1	3.60	P-10B	Pressure on back of SRV Line	14.15
P-2A	Pressure on lower side of column 1	3.59	P-11A	Pressure on bottom surface of I-beam bracing halfway between vent pipe 7 and 8 SRV line 10	19.58
P-2B	Pressure on lower side of column 1	3.60	P-11B	Pressure on top surface of I-beam bracing halfway between vent pipe 7 and 8 SRV line 10	21.21
P-3A	Pressure on middle front of column 1	13.75	P-12	Pressure below main bubble	1.46
P-3B	Pressure on middle back of column 1	14.08	P-13	Pressure below auxiliary bubble	1.46
P-4A*	Pressure on lower front of vent pipe 7	14.08	P-14	Pressure on pool floor between two bubbles	0.42
P-4B	Pressure on lower back of vent pipe 7	14.10	P-15†	Pressure on pool floor between two bubbles	0.42
P-5A	Pressure on lower front of vent pipe 3	13.88	P-16	Pressure inside main bubble	NA
P-5B	Pressure on lower back of vent pipe 3	14.29	P-17	Pressure inside auxiliary bubble	NA
P-6A	Pressure on front of vent pipe 3 just below bracing	18.81	P-18	Free-field pressure below vent pipe 2	3.50
P-6B	Pressure on back of vent pipe 3 just below bracing	19.05	P-19	Free-field pressure below vent pipe 4	3.50
P-7A	Pressure on lower front of vent pipe 7	13.77	P-20	Free-field pressure below vent pipe 7	3.50
P-7B	Pressure on lower back of vent pipe 7	14.29	P-21**	Free-field pressure halfway between column 1 and vent pipe 3	13.38
P-8A	Pressure on front of quencher 8 support leg	1.84	P-22	Free-field pressure halfway between vent pipes 3 and 5	13.33
P-8B	Pressure on back of quencher 8 support leg	1.67	P-23	Free-field pressure halfway between vent pipes 5 and 7	13.81
P-9A	Pressure on front of quencher 8 arm joint	3.50	P-24	Pressure on floor opposite P-14 with respect to pool radius passing thru test bubble	0.42
P-9B	Pressure on back of quencher 8 arm joint	3.50			

* Gage P-4A failed prior to the tests.

† Reserve transducer.

** P21 was disconnected prior to the tests in order to accommodate a recording channel for a velocity gage.

TABLE J-1 (CONT'D)

Sensor	Parameter and Location	Elevation (ft)	Sensor	Parameter and Location	Elevation (ft)
S-1A	Strain in lower front of column 1	1.00	S-9B	Strain in back of quencher 8 arm joint	3.50
S-1B	Strain in lower back of column 1	1.13	S-10A	Strain in front of SRV line at water level	24.02
S-2A	Strain in middle front of column 1	24.17	S-10B	Strain in back of SRV line at water level	24.02
S-2B	Strain in middle back of column 1	24.13	S-11A	Strain on the bottom of bracing halfway between vent pipes 3 and 7	19.81
S-3A	Strain in middle front of column 1	24.13	S-11B	Strain on the top of bracing halfway between vent pipes 3 and 7	20.36
S-3B	Strain in middle back of column 1	24.13	S-12A	Strain on the bottom of bracing halfway between vent pipes 3 and 2	19.81
S-4A	Strain in top front of column 1	51.71	S-12B	Strain on the top of bracing halfway between vent pipes 3 and 2	20.36
S-4B	Strain in top back of column 1	51.71	S-13A	Strain on the bottom of bracing halfway between vent pipes 3 and SRV line 10	19.81
S-5A	Strain in lower front of vent pipe 3 just below bracing	19.75	S-13B	Strain on the top of bracing halfway between vent pipes 3 and SRV line 10	20.36
S-5B	Strain in lower back of vent pipe 3 just below bracing	19.79	A-1	Acceleration at lower front of column 1	2.98
S-6A	Strain in front of vent pipe 3 at water level	24.08	A-2	Acceleration at lower side of column 1	3.02
S-6B	Strain in back of vent pipe 3 at water level	24.08	A-3	Acceleration at middle front of column 1	43.58
S-7A	Strain in top front of vent pipe 3	51.44	A-4	Acceleration at middle side of column 1	43.58
S-7B	Strain in top back of vent pipe 3	51.42	A-5	Acceleration at top front of column 1	51.21
S-8A	Strain in front of quencher 8 support leg	2.27	A-6	Acceleration at top side of column 1	51.21
S-8B	Strain in back of quencher 8 support leg	2.27	A-7	Acceleration at lower front of vent pipe 3	13.56
S-9A	Strain in front of quencher 8 arm joint	3.50	A-8	Acceleration at lower side of vent pipe 3	13.57